Dissertation submitted to the Combined Faculties for the Natural Sciences and for Mathematics of the Ruperto-Carola University of Heidelberg, Germany for the degree of Doctor of Natural Sciences

Presented by:
M.Sc. Sara Mahmoud Hegy Ahmed
Born in: Cairo
Oral-examination: 28.07.2020

# Inter-organ control of gut sexual dimorphism by steroid hormone signaling in *Drosophila*

Referees: 1st examiner (Erstgutachter) Prof. Dr. Sylvia Erhardt

2nd examiner (Zweitgutachter)- Wissenschaftler Betreuer Prof. Dr. Aurelio Teleman

بِسۡمِ ٱللَّهِ ٱلرَّحۡمَـٰنِ ٱلرَّحِيمِ

وَاعْبُدْ رَبَّكَ حَتَّىٰ يَأْتِيَكَ الْيَقِينُ

مَنْ عَمِلَ صَالِحًا مِّن ذَكَرٍ أَوْ أُنثَىٰ وَهُوَ مُؤْمِنٌ فَلَنُحْيِيَنَّهُ حَيَاةً طَيِّبَةً ۖ وَلَنَجْزِيَنَّهُمْ أَجْرَهُم بِأَحْسَنِ مَا كَانُوا يَعْمَلُونَ

رَبِّ أَوْزِعْنِي أَنْ أَشْكُرَ نِعْمَتَكَ الَّتِي أَنْعَمْتَ عَلَيَّ وَعَلَىٰ وَالِدَيَّ وَأَنْ أَعْمَلَ صَالِحًا تَرْضَاهُ وَأَدْخِلْنِي بِرَحْمَتِكَ فِي عِبَادِكَ الصَّالِحِينَ

يا ربّ بالمصطفى بلّغ مقاصدنا..واغفر لنا ما مضى يا واسعَ الكرَم

اللهم أحسن لوالدي في الدنيا والآخرة كما أحسنوا إلي

# Summary

Suggestive evidence points that exogenous exposure to steroid hormones has detrimental consequences that are not well explored specifically in the gut, where nutrient uptake occurs. The human gastrointestinal (GI) tract expresses endogenous steroid hormone receptors in the crypts and the enterocytes but their functions are not well understood. Accumulating epidemiological data suggest that GI tumor progression in most cases maybe endocrine dependent. Given the complexity of the mammalian gut yet, the genetic amenability of cell-type specific gene manipulation in *Drosophila melanogaster*, I studied the effect of exogenously fed or endogenous steroid hormone signaling on the gut and its implications during homeostasis and disease.

In this PhD thesis, I discover the gut to be a sexually dimorphic organ that is regulated by steroid sex hormone: 20-hydroxyecdysone (20HE), which binds EcR•Usp receptor complex and activates downstream target gene transcription during aging and after mating, but not after stress (the receptors have non-overlapping functions). 20HE stimulates intestinal stem cell (ISC) division in a biphasic manner when fed for 16-20hrs, with males being insensitive to the 1$^{st}$ peak and both sexes competent to divide at the 2$^{nd}$ peak of ISC division. EcR functions in the ISCs cell autonomously and in enteroblasts (EBs) non-autonomously to regulate the ISC division. Females have higher levels of circulating 20HE than the males and I identified the ovaries as an endogenous ecdysone source to control mating-induced ecdysone-dependent ISC mitoses and post-mating-dependent gut growth to promote optimal egg-laying. This reproductive advantage given by the highly active female gut comes at the expense of a faster aging epithelium and higher propensity to tumors. Interestingly, exogenous 20HE feeding to males overrides the restricted ability of male ISCs to divide and abolishes the sex differences in ISC division accompanied by transcriptional regulation of metabolic and cell-cycle related genes and subsequent gut growth.

All in all, this study identifies sexually dimorphic 20HE levels as a regulator of ISC behavior and intestinal growth at the expense of gut deterioration and aging.

# Zusammenfassung

Hinweise deuten darauf hin, dass eine exogene Exposition mit Steroidhormonen nachteilige Folgen hat, die speziell im Darm, wo die Nährstoffaufnahme auftritt, nicht gut erforscht sind. Der menschliche Magen-Darm-Trakt (GI) exprimiert endogene Steroidhormonrezeptoren in den Krypten und den Enterozyten, aber ihre Funktionen sind nicht gut verstanden. Akkumulierende epidemiologische Daten legen nahe, dass das Fortschreiten des GI-Tumors in den meisten Fällen möglicherweise endokrinabhängig ist. Angesichts der Komplexität des Säugetierdarms und der genetischen Eignung zur zelltypspezifischen Genmanipulation bei Drosophila melanogaster untersuchte ich die Wirkung von exogen gefütterten oder endogenen Steroidhormonsignalen auf den Darm und ihre Auswirkungen während der Homöostase und Krankheit. In dieser Doktorarbeit entdecke ich, dass der Darm ein sexuell dimorphes Organ ist, das durch das Steroid-Sexualhormon reguliert wird: 20-Hydroxyecdyson (20HE), das den EcR-Usp-Rezeptorkomplex bindet aktiviert die nachgeschaltete Transkription von Zielgenen während des Alterns und nach der Paarung aber nicht nach Stress (die Rezeptoren haben nicht überlappende Funktionen). 20HE stimuliert die Teilung von Darmstammzellen (ISC) zweiphasig, wenn es 16 bis 20 Stunden lang gefüttert wird, wobei Männechen unempfindlich gegenüber dem 1. Peak sind und beide Geschlechter faehig sind, sich am 2. Peak der ISC-Teilung zu teilen. EcR funktioniert in der ISC-Zelle autonom und in Enteroblasten (EBs) nicht autonom, um deren ISC-Teilung zu regulieren. Weibchen haben einen höheren zirkulierenden 20HE-Spiegel als die Männchen. Ausserdem identifiziere ich die Eierstöcke als endogene Ecdysonquelle zur Kontrolle der durch Paarung induzierten Ecdyson-abhängigen ISC-Mitosen und des nach der Paarung abhängigen Darmwachstums, was eine optimale Eiablage zu fördert. Dieser Fortpflanzungsvorteil des hochaktiven weiblichen Darms geht zu Lasten eines schneller alternden Epithels und einer höheren Neigung zu Tumoren. Interessanterweise überschreibt die exogene 20HE-Fütterung von Männern die eingeschränkte Fähigkeit männlicher ISCs, sich zu teilen, und hebt die Geschlechtsunterschiede bei der ISC-Teilung auf, begleitet von der Transkriptionsregulation von metabolischen und zellzyklusbezogenen Genen und dem anschließenden Darmwachstum. Insgesamt identifiziert diese Studie sexuell dimorphe 20HE-Spiegel als Regulator des ISC-Verhaltens und des Darmwachstums auf Kosten der Darmverschlechterung und des Alterns.

# Declaration

I, Sara Mahmoud Hegy Ahmed, hereby declare that the work in this thesis represents my original research results. The thesis has been written by myself using the references and resources indicated. Any work of others has been appropriately marked. The work has been conducted under the supervision of Prof. Dr. Aurelio Teleman. This thesis is being submitted for the degree of Doctor of Natural Sciences at Heidelberg University, Germany, and has not been presented to any other university as part of an examination or degree.

_____ _____

Place & Date Sara Mahmoud Hegy Ahmed

# Acknowledgements

To my supervisors Aurelio and Bruce, thank you so incredibly much for giving me this honor of being taught by you. It is with great pleasure and gratitude that I admit that my long search for mentors has not failed me. I have enjoyed a lot knocking on either of your doors every time during the last 5 years. Even during tough times, I still learned a lot! It is with a lot of thankfulness that I take every bit you taught me both personally and intellectually hoping that I can continue to pass it onto the many lives I am meant to touch. A special extra thank you to Aurelio for being THE person who taught how to do many things properly!

My TAC committee, Prof.Dr. Bernd Bukau for your incredible advice and support ever since I stepped feet in Heidelberg 8 years ago, Prof.Dr. Sylvia Erhardt for your encouraging support and feedback and for meeting me everytime with a smile, Prof.Dr. Ingrid Lohmann for your prompt agreement to evaluate my thesis.

Behind every good story, there is “behind the scenes” and it is no secret that mine was eventful and as I write these words today, I acknowledge being incredibly thankful to everyone who brought joy to my heart during my rough times and especially my anchors, my parents Mahmoud and Howaida. To my siblings, the shining stars, Ahmed, Marwa (my better half), Yousr and Jana, may you shine brighter, everyday! To my Uncle Mohamed, one of the kindest hearts I ever met, thank you for every bit..thank you for being you! To my most incredible best friends Jonathan and Sandra Bohlen, I thank my stars everyday that I have you in my life! To my Nanna, aunties Shimaa and Eman, uncle Ashraf, thank you for always having faith in me when I was all weary!

It is with a lot of mounting strength that I gratefully and thankfully made it through! To every who passed by or is in my life, who lit my candle with support, love and hope, Thank you!

To Marwa Mahmoud Hegy Ahmed, a lot of this would not have happened without you.. Thank you for your dedication to help and support me whenever I was going crazy.. You’re awesome..

To Mohamed Noseir, you are the best friend any person can ask for.. Thank you for being mine..

To Sanja, the kind heart I met that changed my life forever, you are my savior and I cannot thank you enough for your kindness..

To Ehab Allam, Thank you for making my heart laugh, every time! Thank you for supporting me unconditionally during my roughest times..

To Federica, Omneya and Nadja, some of my deepest most unique friendships, I am so blessed you light my candle so bright..

To Ehab El Agamy, thank you for bringing absolute pure joy to my heart when I did not think anyone could..

To Samaa, Thank you for the many laughs I had and for the good company you've given me as I wrote my thesis..

To Islam Mohamed, Thank you for your unparalleled support and kindheartedness, as I am closing the Heidelberg chapter, knowing you has made me realize that the best is yet to come..

To Omar Hany, Thank you for being a great friend and for helping me create such a fancy model for my paper.

To Mohamed Assem, Thank you for your prompt help in drawing the 20HE structure on such a short notice.

To Saioa, Thank you for always being one of the first people to help me when I needed any help and for nice breaks I had with you when everything was so hectic..

To the rest of the Teleman Lab, who endured many years of boastful and passionate lab meetings with about sex hormones, ecdysone feeding and stem cells. Thank you for the brilliantly intellectual atmosphere and positive advice.

# List of abbreviations:

| | |
|---|---|
| 20Eoic | 20-hydroxyecdysonoic acid |
| 20HE | 20-hydroxyecdysone |
| 24-methylE | 24-methylecdysone |
| Apc | *Adenomatous polyposis coli* |
| AR | Androgen receptor |
| Atoh1 | atonal homolog 1 |
| BMP | bone morphogenetic protein |
| *BR-C* | *Broad Complex* |
| *C. elegans* | *Caenorhabditis elegans* |
| C2 | cysteine |
| CBC stem cells | crypt base columnar stem cells |
| CDK | cyclin-dependent kinase |
| CK1α | casein kinase 1α |
| CK1α | casein kinase 1α |
| CNVs | copy number variants |
| DBD | DNA-binding domain |
| dFOXO | *Drosophila* Foxo |
| Dhh | desert hedgehog |
| dhMaA | 24(28)-dehydromakisterone |
| Diap1 | Death-associated inhibitor of apoptosis 1 |
| Dilp3 | *Drosophila* insulin-like peptide3 |
| DLL | Delta-like ligand |
| *Dmrt1* | Doublesex and Mab3 Related Transcription factor 1 |
| Dome | Domeless |
| dpERK | diphospho-ERK |
| Dpp | *Drosophila* homolog Decapentaplegic |
| Dpp | Decapentaplegic |
| dS6k or S6K | ribosomal S6 kinase |
| DSS | Dextran sulfate sodium |
| dsx | doublesex |
| dTOR | *Drosophila* Tor |
| DVL | dishevelled |
| E1 | estrone |
| E2 | 17β-estradiol |
| E3 | estriol |
| E4 | estetrol |
| EBs | enteroblasts |
| EcR | ecdysone receptor gene |
| ECs | enterocytes |
| EEs/ees | Enteroendocrine cells |

| | |
|---|---|
| EFG | epidermal growth factor |
| EGFR | epidermal growth factor receptor |
| *Eip75B* | *ecdysone-inducible puff 75B* |
| eQTLs | expression quantitative trait loci |
| ER | Estrogen receptor |
| ER | estrogen receptor |
| EREs | estrogen response elements |
| ERα | Estrogen receptor alpha |
| ERβ | Estrogen receptor beta |
| ESD | environmental sex determination |
| esg | escargot |
| FGF9 | fibroblast growth factor 9 |
| FGF9 | fibroblast growth factor 9 |
| FKHR | Forkhead-related transcription factor ( |
| FLP | Flippase |
| FOXO | forkhead transcription factor |
| fru | fruitless |
| FXR | farnesoid X receptors |
| Fz | Frizzled |
| Fz2 | Frizzled 2 |
| FZD | Frizzled |
| FZD | frizzled |
| Gbb | Glass bottom boat |
| GCK | germinal center protein kinase |
| GH | Growth hormone |
| GI | gastrointestinal tract |
| GPER1 | G protein-coupled estrogen receptor 1 |
| GR | glucocorticoid receptor |
| GSD | genetic sex determination |
| GSK3β | glycogen synthase kinase 3β |
| GWAS | genome-wide association studies |
| H2 | histidine |
| $H_2O_2$ | hydrogen peroxide |
| HDACs | histone deacetylases |
| Hep | Hemipterous |
| *hpo* | hippo |
| Hr3 | *Drosophila* Hormone Receptor 3 |
| Hr96 | *Drosophila* Hormone Receptor 96 |
| IGF1 | insulin-like growth factor 1 |
| IGF2 | insulin-like growth factor 2 |
| IGFs | Insulin-like growth factors |
| IL-22 | interleukin-22 |
| ILC | innate lymphoid cells |
| IPCs | insulin-producing cells |
| IRS | insulin receptor substrate |
| ISC | intestinal stem cell |
| JAG | Jagged |

| | |
|---|---|
| JAK | Janus kinase |
| Jak-Stat | Janus Kinas-Signal Transducer and activato of Transcription pathway |
| JNK | c-Jun N-terminal kinase |
| Krn | keren |
| LATS1/2 | large tumour suppressor 1/2 |
| LBD | ligand-binding domain |
| LRCs | label-retaining cells |
| Lrp5/6 | low-density lipoprotein receptor-related protein 5/6 |
| LXR | liver X receptors |
| LXR | liver X receptor |
| M | Microfold |
| MaA | 20-hydroxylated derivative makisteroneA |
| Mad | Mothers-against-Dpp |
| Mad | Mothers against dpp |
| MAPK | mitogen-activated protein kinase |
| MARCM | mosaic analysis with a repressible cell marker |
| Mats | Mob as a tumour suppressor |
| mCD8-GFP | Gal4-driven membrane-targeted green fluorescent protein |
| Med | Co-Smad Medea |
| MOB1A/B | Mps one binder kinase activator-like 1A and 1B |
| msl-2 | male specific lethal 2 |
| Msn | Mishapen |
| MST1/2 | mammalian sterile 20-like kinase 1/2 |
| NCs | nuclear receptors |
| NICD | Notch intracellular domain |
| NICD | Notch intracellular domain |
| *npr1* | non-pupariating |
| *P.e.* | *Pseudomonas entomophila* |
| PDGF | platelet-derived growth factor |
| PDGF | platelet-derived growth factor |
| PDK-1 | Phosphatidylinositol dependent kinase 1 |
| PI3K | phosphatidyl- inositol 3-kinase |
| PKC | protein kinase C |
| PLC | phospholipase C |
| PM | peritrophic membrane or matrix |
| PNR | photoreceptor-specific nuclear receptor |
| PPAR | peroxisome proliferator activated receptors |
| PPAR | peroxisome proliferator activated receptors |
| PTEN | lipid phosphatase |

| | |
|---|---|
| ptgds | prostaglandin D2 synthase |
| RAR | retinoic acid receptor |
| rbp | *reduced bristles on palpus* |
| Rho | Rhomboid |
| ROR | retinoid-related orphan receptor |
| RXR | retinoid X receptor |
| SAV1 | Salvador |
| Sax | Saxophone |
| Sd | Scalloped |
| shaggy or GSK-3 | Glycogen synthase kinase-3 |
| SNPs | single- nucleotide polymorphisms |
| Spi | Spitz |
| sQTLs | splicing quantitative trait loci |
| Sry | sex determining region Y |
| stat | signal transducer of activation |
| TA | Transit amplifying cells |
| TAZ | WW domain-containing transcription regulator 1 |
| TCF/LEF | T-cell factor/lymphoid enhancer factor |
| TGF-β | transforming growth factor-β |
| Tkv | type-I receptors Thickvein |
| TR | thyroid hormone receptor |
| tra | transformer |
| unf/Hr51 | Hormone Receptor 51 or unfulfilled |
| Usp | Ultraspiracle |
| VM | visceral muscle |
| Vn | Vein |
| *wg* | *Drosophila* WNT ligand *wingless* |
| Wts | Warts |
| Yki | Yorkie |
| β -TrCP E3 | β-transducin repeat-containing protein, an E3 ubiquitin ligase |

# Introduction

### 1.1. *Drosophila* and mammalian midgut morphology

The *Drosophila* gut is analogous to the mammalian gut. They are both tubes with distinctive compartments where different steps of food utilization take place. They both undergo continuous homeostatic turnover across the organism's lifetime by a stem cell compartment that reside basally. Both have a microbiome which are commensal bacterial species populating the gut which are essential for the health of the organism[1].

The *Drosophila* and mammalian gastrointestinal (GI) tracts share a high degree of similarity in their structures, their overall physiology, and the signaling pathways directing tissue turnover[1]. Both *Drosophila* and mammalian digestive systems comprise an upper region where food uptake occurs, followed by a middle region where food digestion takes place then, and a last region where nutrient absorption occurs. In mammals, the GI tract evolved into complex structures composed of histologically distinct regions. But in *Drosophila*, regionalization is achieved through physical separation by major constrictions referred to as anatomical boundaries. The upper region in the mammalian GI tract consists of the mammalian mouth, pharynx, and esophagus while in *Drosophila* it comprises the esophagus, the crop and the cardia. The middle region consists of a mammalian stomach and duodenum, and it is analogous to the *Drosophila* middle acidic copper cell and iron region[2]. The final region of the digestive tract consists of the mammalian small intestine and colon that are the functional equivalents of the *Drosophila* midgut and hindgut respectively. The anatomical boundaries in the midgut alone divide it into 6 histologically different regions with distinct gene expression patterns: R0-R5. R4-R5 is the region where most nutrient absorption takes place [1,3]. At the cellular level the two GI tracts are organized similarly and the relative position of the ISCs within the epithelium is also highly alike, even though the mammalian intestine has a more complex ISC lineage. The mammalian intestine consists of layered crypt-villi structures whereby the gastrointestinal stem cells reside at the bottommost positions of the stomach, small intestine, and colon crypts[4].

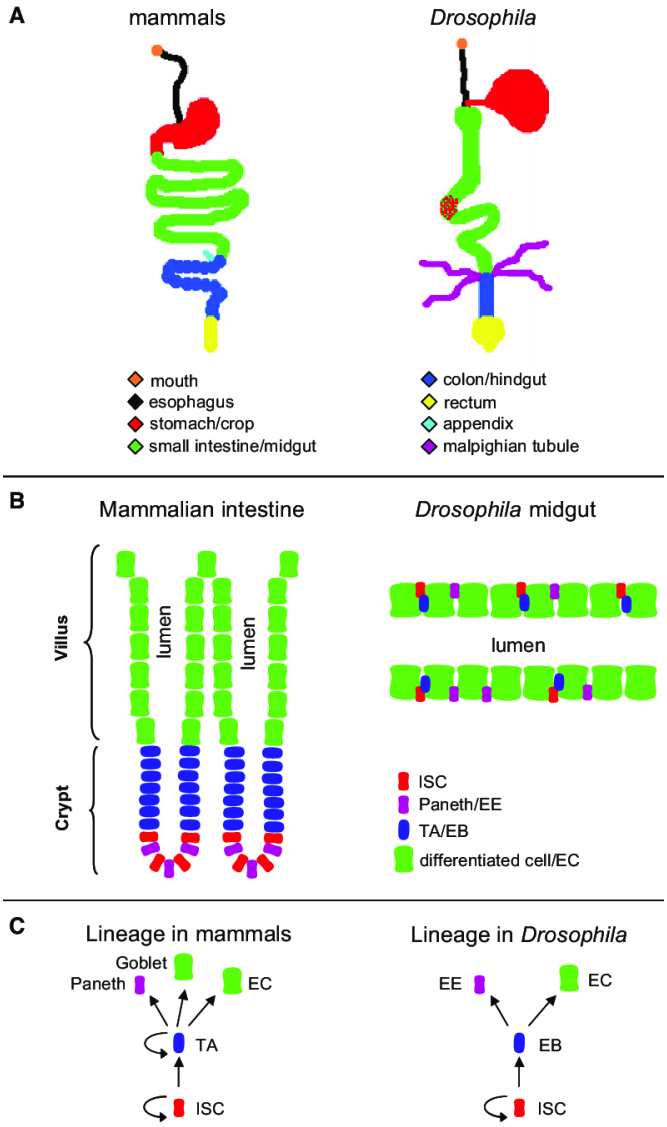


**Figure 1.1: Comparison of the physiological resemblance between the mammalian and *Drosophila* Digestive Tracts.** (A) Anatomy of the gut. The upper region of the gut is comprised of mouth and esophagus in mammals and esophagus, crop and cardia in *Drosophila.* The middle region consists of the stomach in mammals and copper cell region in *Drosophila*. The final region consists of the small intestine and the colon in mammals and the midgut and hindgut in *Drosophila*. Excrement elimination takes place via the rectum. Malpighian tubules are the functional analogs of the mammalian kidney and they branch at the midhindgut junction (shown in purple). (B) Cellular composition of the gut. The mammalian gut is organized in crypts and villi. The crypt base columnar (CBC) stem cells reside at the bottom of the crypt together with Paneth cells. *Drosophila* gut is organized in a simple epithelial monolayer where ISCs basally reside, situated between other differentiated cells. (C) ISC lineage in mammals and *Drosophila.* Actively cycling stem cells asymmetrically divide to give rise to transit amplifying (TA) cells that divide and terminally differentiate into all secretory and absorptive epithelial lineages of the villus in mammals. In *Drosophila*, ISCs asymmetrically divide to self-renew and give rise to an enteroblast (EB) daughter cell. The EB differentiates into either an enterocyte (EC) or enteroendocrince (ee) cell. Adopted from Pitsouli et al,2009.

Similarly the adult *Drosophila* ISCs reside basally within the simple epithelial monolayer of the gut[5].The mammalian ISCs divide to give rise to transient amplifying cells (TAs) that expand and differentiate into epithelial cells as they migrate upwards from the crypt. Mammalian epithelial cells are either absorptive enterocytes, mucus-secreting goblet cells, secretory enteroendocrine cells or paneth cells that secrete antimicrobial peptides and essential factors for stem cell maintenance. Additionally, the mammalian intestine

has two more rare cell populations: secretory mechanosensing Tuft cells that sense the intestinal luminal contents and M (microfold) cells that are located above Peyer's patches of lymphatic tissue to communicate with the gut's immune system and monitor intestinal microflora (reviewed in[6]). The nutrient-absorbing enterocytes constitute most of the villi lining. Those enterocytes have microvilli projections that form the striated or brush border, providing a greater surface area for nutrient absorption. The mammalian gastrointestinal tract is profusely innervated along its entire length and is surrounded by longitudinal and circular muscles that initiate peristaltic contractions. When *Drosophila* ISCs divide, they self-renew and give rise to daughter cells that turn into transient but committed progenitor cells, called enteroblasts. *Drosophila* midgut enteroblasts directly differentiate into large absorptive polyploid enterocytes (ECs) or diploid enteroendocrine cells (EEs), with secretory properties. The structure of the *Drosophila* gut is organized in a simple monolayer, yet it remains quite complex because it is extensively regionalized into six regions with their major constrictions referred to as anatomical boundaries. Each region has its specific histological and cellular features (villi length, lumen width), nutrient content, physical properties (e.g., luminal pH), and gene expression profiles[2,3]. The *Drosophila* intestine is ensheathed along its length by circular and longitudinal layers of mesodermally derived visceral muscle (VM). Within the epithelium, the ISCs are located just above the extracellular matrix-rich basement membrane, which separates the epithelium from the underlying visceral muscle cells. Inside the intestinal lumen, a glycoprotein-based chitinous membrane, called the peritrophic membrane or matrix (PM), lines the epithelium, isolating it from the ingested food and serves as a structural barrier against the gut bacteria. An extensively branched network of intestinal trachea is present in close proximity to the VM and reaches the epithelium to deliver oxygen to the cells. Neuronal innervations are present around parts of the anterior midgut: (esophagus and cardia), the midgut-hindgut boundary and the rectum, whereas most of the midgut has no neuronal innervations (reviewed in [7]).

### 1.2. ISC behavior during homeostasis or regenerative damage

The intestinal epithelial lining of the digestive system represents one of the most intensively self-replenishing organs whereby self-renewal occurs through the intestinal

stem cells (ISCs) to replenish dead or lost cells. Normally, the entire epithelium gets replaced every 5-7 days in both *Drosophila*[8] and mammals[6]. In both systems, the ISCs integrate extracellular cues, provided by neighboring niche cells through a multitude of local, paracrine, and systemic signals and signaling pathways. Collectively, these decisions direct the ISC behavior to meet the homeostatic function or regenerative demands upon insult of the organ.

Both mammalian and *Drosophila* guts contain sub-populations of stem cells that display distinct behavioral characteristics. In the mammalian small intestine, there are two different ISC populations: a predominant population (crypt base columnar cells, or CBCs) which are the only cell type with long-term self-renewing ability and a slow dividing, Bmi1+ 'reserve stem cell' population, also called position 4/+4 cells or label-retaining cells (LRCs) which are located four cell diameters above the base of the crypt and are directly adjacent to the CBC/Paneth region[9]. Also in the *Drosophila* midgut, ISCs of the different morphological regions divide at different rates[2] however there are no known subpopulations of ISCs with varying cycling rhythmicity defined within a region.

Stem cells cycle between two modes of cell division: symmetric whereby two identical daughter cells are produced, both of which are stem cells, and asymmetric division which results in only one stem cell and a committed progenitor cell. Asymmetric division is associated with unequal segregation of proteins or RNA within the daughters, resulting in different genetic programs to direct the fate of the newly formed progenitor. In the mammalian intestine, symmetric cell divisions occur during continuous homeostatic renewal of the gut epithelium, however during inflammation asymmetric stem cell divisions are enforced [9]. Similarly, in the *Drosophila* midgut, expansion of stem cell populations during early feeding-induced organ growth[10] or during clonal competition[11,12] occurs mainly via symmetric ISC divisions. Upon acute regenerative stress response, asymmetric ISC division occurs[13]. Hence, strikingly, both digestive systems follow a pattern of neutral drift dynamics during homeostasis in which stem cell-derived clones expand and contract at random until they either take over the crypt or they are lost. Interestingly, under extreme instances of extensive tissue damage, mammalian progenitor or early enterocyte populations can de-differentiate and revert to stem-like cells to

replenish the crypt[6]. In *Drosophila*, physical or functional loss of ISCs during starvation or aging likewise induces amitotis: a process through which polyploid enterocytes dedifferentiate leading to a depolyploidization to give rise to functional ISCs[14].

### 1.3. ISC niche in mammals vs *Drosophila*

The ISC niche is a complex cellular structure of several cell types that supports and regulates the ISC functions. The mammalian and *Drosophila* niche share some similarity in their organization and in the signaling ligands that the niche provides to ISCs. The mammalian ISC niche consists of the neighboring epithelial Paneth cells and sub-epithelial mesenchymal myofibroblasts, fibroblasts, telocytes, neuronal and smooth muscle cells surrounding the crypt base basal lamina[15]. The physical proximity of the niche cells with ISCs enables the supply of essential factors for ISC division and maintenance[6]. The mesenchymal part of the niche provides the ISCs with various Wnt ligands and R-spondins (Wnt agonists) bone morphogenetic protein (BMP) inhibitors to repress BMP-mediated differentiation, and epidermal growth factor (EGF) to maintain the ISCs and trigger their division. The intestinal integrity is disrupted and ISCs are lost when the functions of the neighboring epithelial Paneth cells or mesenchymal component are compromised respectively though Paneth cells seem to have a more redundant role *in-vivo*[16-18]. Similarly, the *Drosophila* ISC niche consists of mesodermally-derived visceral muscle, the neighboring enteroblasts and enterocytes. VM expresses the EGFR ligand: vein[19], a JAK-STAT ligand: upd1[20], *Drosophila* insulin-like peptide3 (Dilp3)[10], and *Drosophila* WNT ligand *wingless* (*wg*)[21], which contribute to the ISC proliferation, long-term ISC maintenance or both. Additionally, muscle-derived bone morphogenetic proteins (BMPs) *Drosophila* homolog Decapentaplegic (Dpp) limits over-expansion of ISCs through regulating EGF and Jak-Stat signaling[22,23]. Most studies focused on the requirement of EBs or ECs as niche components during regenerative ISC responses[24] Fewer homeostatic epithelial components of the niche have been identified, except for EB-derived wg and EGF signaling which contribute to the homeostatic ISC renewal[25] and division[26] respectively and the requirement of Notch or restrictive Hippo signaling in EBs to keep the ISCs in check, avoiding accumulation of hyper-dividing ISCs[27,28].

## 1.4 Signaling Pathways controlling intestinal stem cell division during homeostasis and stress.

Both the *Drosophila* and mammalian adult intestine displays a remarkable regenerative response to many stressors or damaging agents, which disrupt epithelial integrity. In *Drosophila,* subjecting the flies to stress-inducing agents such as Dextran sulfate sodium (DSS), bleomycin[29], ROS producing agents such as paraquat and hydrogen peroxide ($H_2O_2$)[30]. Examples of bacterial infections that stimulate host immune responses include infection with the Gram-negative lethal bacteria *Pseudomonas entomophila* (*P.e.*)[31], and non-pathogenic *Erwinia carotovora* carotovora 15[32].

Below is a summary of the most important pathways governing the ISC division during intestinal homeostasis and damage.

### a. Wnt/wingless signaling:

Wnt signaling promotes ISC division and maintenance in both the *Drosophila* and mammals GI tracts. Wnt ligands are produced in mammals by Paneth cells[33] and mesenchymal cells[34] which bind to their receptors Frizzled (FZD) and low-density lipoprotein receptor-related protein 5/6 (Lrp5/6) at the surface of on ISCs. In *Drosophila*, muscle[21] and enteroblasts[25] secrete wingless which binds Frizzled (Fz) and Frizzled 2 (Fz2) in ISCs. Wnt/wg activation leads to the stabilization and nuclear entry of the transcriptional co-activator β-catenin (mammals) or Armadillo (*Drosophila*) to drive target genes expression involved in ISC division or maintenance[21,35]. *Adenomatous polyposis coli (Apc*) is a part of a destruction complex that marks β-catenin (mammals) or Armadillo (*Drosophila*) for proteosomal degradation. Remarkably, *Apc* mutation is considered a cancer driver mutation, which leads to the activation of wnt/wg signaling, thereby, promoting the formation of small adenomas in both mammals[36] and *Drosophila*[37]. Subsequently, additional mutations in KRAS, BRAF, p53, MLH1, or TGF-β signaling promote the progression to colorectal carcinomas[38,39].

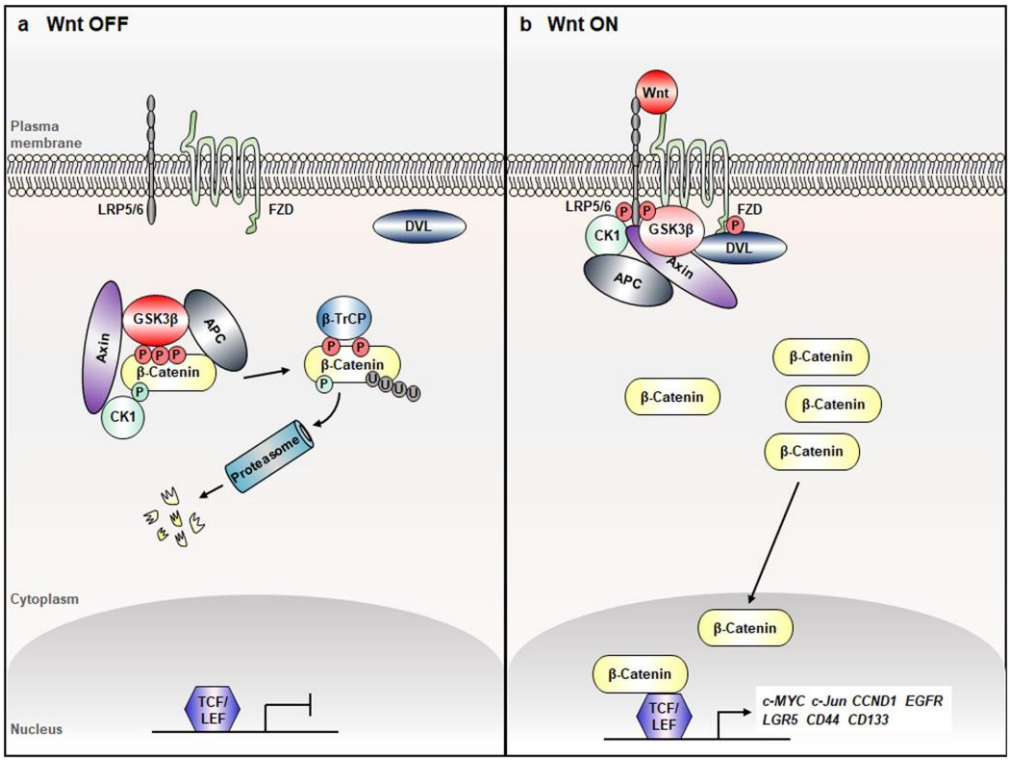


**Figure 1.2: An illustration of the canonical Wnt signaling in mammals.** (a) In the absence of Wnt ligands, APC (adenomatous polyposis coli) and Axin are recruited into the "β-catenin destruction complex". The phosphorylations by CK1α (casein kinase 1α) and GSK3β (glycogen synthase kinase 3β) recruit β-TrCP E3 linker (β-transducin repeat-containing protein, an E3 ubiquitin ligase), which signal β-catenin for its ubiquitination and degradation via the proteasome pathway. (b) The presence of Wnt ligands causes the association of Axin with phosphorylated LRP5/6 (lipoprotein receptor-related protein 5/6) and recruitment of phosphorylated DVL (dishevelled) to FZD (frizzled) lead to the dissociation of the destruction complex. This causes the accumulation and stabilization of β-Catenin, leading to its translocation into the nucleus, forms the complex with TCF/LEF (T-cell factor/lymphoid enhancer factor), and subsequently activates the target genes. CCND1, cyclin D1; EGFR, epidermal growth factor receptor; LGR5, Leucine-rich repeat-containing G protein coupled receptor 5, CD44 cell-surface glycoprotein involved in cell adhesion and CD133 transmembrane glycoprotein that is enriched in the stem cells. P, phosphorylation; U, ubiquitination. Adopted from: Jeong Jeong et al,2018.

**b. EGF signaling:**

EGF signaling is yet another highly conserved pathway that is required for intestinal stem

cell proliferation and maintenance in both mammals[40] and *Drosophila*[41]. EGF extracellular ligands stimulate cell growth, proliferation, and differentiation by binding to its cognate receptor the epidermal growth factor receptor (EGFR). Upon activation of EGFR, it dimerizes and its intrinsic intracellular protein-tyrosine kinase activity is activated leading to downstream signaling effectors including mitogen-activated protein kinase (MAPK), phosphatidyl- inositol 3-kinase (PI3K)/Akt, c-Jun N-terminal kinases (JNK), Jak/STAT and phospholipase C (PLC) pathways[42]. In mammals, similar to Wnt signaling, EGF ligands are produced in the ISC niche by the neighboring Paneth cells[33] and activate signaling in ISCs and transient amplifying cells[43]. In *Drosophila,* there are three EGF ligands, vein (vn), spitz (spi), and Keren (Krn) that are produced from visceral muscle, ISC, enteroblasts or enterocytes. Rhomboid (Rho) is an intramembrane protease that cleaves and activates EGF ligands, which act in a paracrine or autocrine manner on ISCs to stimulate ISC proliferation through the RAS/RAF/MAPK pathway[19,41]. Activation of EGFR signaling results in intestinal hyperplasia[19,44] and it is cell-autonomously required for homeostatic and regenerative ISC mitoses[44,45]. *Ras*-null mutant clones have differentiated ECs suggesting that EGFR signaling is not required for EC differentiation[26]. However, EGFR is required for EB to EC growth and endoreplication during stress- induced midgut regeneration[26].

**c. JAK/Stat pathway:**

The Janus kinase (JAK), signal transducer of activation (stat) pathway is another evolutionarily conserved signaling cascade from *Drosophila* to vertebrates that transduces cytokine signals and functions in ISC proliferation and maintenance. Mammals have a wide variety of extracellular ligands such as interferons and interleukins, which bind to the transmembrane receptors, causing the activation of the receptor-associated JAKs. Upon conformational activation and active phosphorylation, JA phosphorylates and activates STATs. Activated STATs translocate to the nucleus where they bind promoters of their target genes, activating their transcription[46]. In mammals there are four JAKs that activate seven downstream stats whereas in *Drosophila* only one transmembrane receptor called Domeless (dome) and one receptor-associated Janus Kinase Hopscotch (Hop) activate the downstream STAT3-like

transcription factor STAT92E[47,48]. Activation of the JAK/stat pathway cell autonomously and non-cell autonomously stimulates ISC mitoses. Indeed, EGFR and Jak/Stat pathways function synergistically to induce ISC proliferation[8,19,41]. Notably, Jak/Stat signaling is also required for ISC self-renewal and EB to EC differentiation. High Jak/Stat signaling and low Notch preferentially directs the fate of differentiating cells towards enteroendocrine (ee) cells[48]. STAT92E is normally expressed in both ISCs and EBs[48,49]. After stress-induced damage, dying enterocytes [41] and the surrounding muscle [45] presumably inactivate wingless signaling which in turn activate the expression of Upds[50]. Secreted Upd ligands non-cell autonomously act to drive ISC proliferation. Jak/Stat activation in ISCs is essential for the *P.e.*-induced ISC mitoses[8]. Similarly after intestinal injury in mammals, innate lymphoid cells (ILCs) produce interleukin-22 (IL-22) that activates Jak/Stat signaling in ISCs promoting their expansion [51]. Additionally, pervasive inflammation also activates JAK/STAT-1 signaling in reserve-ISCs to functionally contribute to epithelial restitution[52].

**d. Insulin signaling**

Insulin-like growth factors (IGFs) in *Drosophila* closely resemble insulin/IGF signaling and function in mammals functions[53]. Both pathways synchronize the nutritional homeostasis with systemic growth control. In mammals, three insulin ligands exist: insulin, insulin-like growth factor 1 (IGF1),and insulin-like growth factor 2 (IGF2), that bind and activate five distinct receptor isoforms: two insulin receptor isoforms, IRα and IRβ; the insulin-like growth factor receptor, IGF1R; and two hybrid dimer receptors[53]. Upon ligand binding to the receptor, tyrosine phosphorylation activates cellular substrates, include insulin receptor substrate (IRS)1, IRS2, IRS3 or IRS4, or other scaffold proteins—SHC, CBL, APS and SH2B, GAB1, GAB2, DOCK1 and DOCK2,and CEACAM1. These substrates activate downstream signaling cascades such as PI3K and AKT[53]. Similarly, the *Drosophila* genome encodes eight insulin-like peptides (Dilps). At least three of these (Dilp2, Dilp3 and Dilp5) are secreted from the insulin-producing cells (IPCs) in the brain, which are homologous to pancreatic beta cells in mammals[54]. Dilps regulate organ growth, triglyceride storage and glucose/trehalose levels in circulation[53]. Dilps interact with a single orthologous insulin-like receptor tyrosine kinase. Chico is the

*Drosophila* homolog of insulin receptor substrate that gets phosphorylated to activate phosphatidylinositol 3-kinase (PI3K) and AKT (Akt1). Among the downstream targets of AKT is the Forkhead box transcription factor *Drosophila* Foxo (dFOXO), which is negatively regulated by insulin and regulates many cell cycle, apoptosis, DNA repair, metabolic homeostasis, redox balance genes. FOXO phosphorylation promotes its accumulation in the cytosol and nuclear exclusion to regulate its target genes[53]. AKT also inhibits the tumor suppressor proteins TSC1 and TSC2, which inhibit a small GTPase called Rheb, an activator of *Drosophila* Tor (dTOR). dTOR also regulates the nutritional status through direct amino acid sensing independent of Dilp/InR. The mechanism how AKT regulates FOXO or mTOR is conserved from flies to humans [55,56].

Although not much is known about insulin signaling in the mammalian intestine, it is required for both homeostatic and regenerative aspects of the *Drosophila* midgut. Feeding behavior regulates adaptive gut growth, which requires visceral muscle secretion of Dilp3 as well as systemic Dilps to activate insulin receptor in ISCs leading to homeostatic ISC division[10]. Moreover, locally-secreted insulin from the niche is required to regulate intestinal cell density and organ growth[10]. Interestingly, scute mutant flies which are devoid of enteroendocrine cells have impaired Dilp3 expression from the visceral muscle and hence, the feeding-stimulated midgut growth is diminished and flies have a shorter lifespan[57].

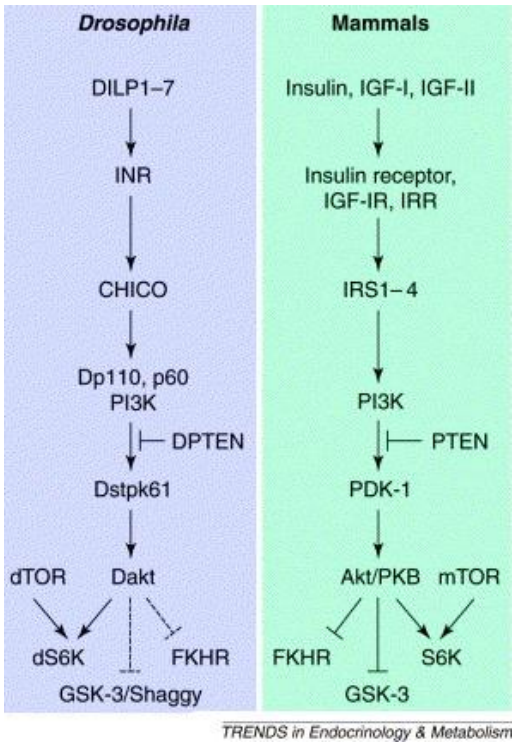


**Figure 1.3.: Insulin signaling pathway in Drosophila (left) or mammals (right).** Insulin-like peptides (dilp1-7 or Insulin, Insulin-like growth factors I,II) bind Insulin receptors (INR or IGF-IR,IRR) leading to its phosphorylation. Insulin Receptor Substrates (chico or IRS 1-4). Downstream of Insulin receptor activation, PI3K, Phosphatidylinositol-dependent kinase-1 (Dstpk61 or PDK-1) and serine/threonine-specific protein kinase B Akt (*Drosophila* akt or Akt/Protein Kinase B) homologs are activated. PI3K is negatively regulated at this step by homologs of the lipid phosphatase PTEN (*Drosophila* PTEN or PTEN). Akt/PKB inhibits the kinase Glycogen synthase kinase-3 (shaggy or

GSK-3), and Forkhead-related transcription factor (FKHR) in mammals though their homologs have been identifies in *Drosophila* but their relationship to the insulin signaling has not yet been demonstrated (broken line). In both species though, Target of rapamycin (dTOR, Drosophila TOR; mTOR, mammalian TOR) are upstream activators of p70 ribosomal S6 kinase (dS6k or S6K), most probably in response to nutrients, and act together with PI3K to upregulate translation and growth. Not included: Akt inactivation activates the downstream transcription factor: forkhead transcription factor (dFOXO or FOXO), which regulates the expression of target genes, which contribute to longevity. Adopted from: Garofalo,2002.

Collectively, these findings postulate a comprehensible model how different cell types communicate: enteroendocrine cells and visceral muscle to influence ISC mitoses and drive adaptive midgut growth through insulin signaling. Upon feeding with detergent or the DNA-damaging agent bleomycin, impaired systemic insulin signaling blocks the regenerative ISC mitoses[58]. Insulin signaling mutants are robustly long-lived[59-61], suggesting that the reduction of insulin signaling in intestinal dysplasia could extend longevity. Indeed, direct moderate depletion of insulin signaling or overexpression of FOXO targets in ISCs and EBs may significantly delay the onset of age-related dysplasia and extend lifespan[62]. The role of mammalian insulin in the gut remains far less understood. Nevertheless, insulin is reported to increase proliferation in the colorectal epithelium[63]. Analogous to the insulin-dependent midgut growth in *Drosophila*, diet-induced obesity increases insulin-like growth factor 1 (IGF1) levels and intestinal *Igf1* mRNA, increased crypt density and ISC numbers [64] Human studies also suggest that insulin receptor isoform A, which is expressed in highly proliferative ISCs in the crypts[65] is linked to development of adenoma cases in patients with high plasma insulin[66].

**e. JNK pathway:**

Jun-N-terminal Kinase (JNK) is a stress-activated protein MAPK-type kinase that is involved in compensatory injury-induced cell division in both *Drosophila* and mammals. Though its role in the mammalian gut is not well characterized, *Drosophila* JNK is upregulated upon UV irradiation, ROS or DNA damage, bacterial or fungal infection, and aging. *Drosophila* contains a single JNK, Basket (Bsk), and two JNK Kinases, Hemipterous (Hep) and dMKK4. After infection[8] or as the flies age[62], JNK is activated in ECs to stimulate compensatory ISC mitoses. While JNK activation in ECs is not required

for *P.e.*-induced ISC mitoses, its downregulation in either ISCs or ECs is sufficient to slow down aging-dependent elevation of ISC mitoses. Remarkably, dFOXO can also be phosphorylated and activated by JNK[67]. Indeed, ECs have a chronic age-dependent activation of JNK/dFOXO, which represses intestinal lipases leading to disruption of the systemic lipid homeostasis and of the ability the ECs to activate the innate immune responses[68]. In a more physiological context, long-lived insulin mutants similarly have lower levels of JNK signaling[62]. Moreover, Upd3 production is downstream of the activation of JNK signaling in weak/unfit cells, which is necessary for their elimination by fitter wild-type cells[11]. Similarly, activated JNK triggers apoptosis of enterocytes to stimulate compensatory ISC division[69]. JNK signaling also boosts $APC^{-/-}$ adenoma growth and drives cell competition[70]. In detergent-induced regenerative responses, JNK signaling in ISCs and EBs is necessary and sufficient to stimulate Hedgehog production and drive compensatory ISC division[71].

**f. Hippo/Wts pathway:**

The Hippo pathway is another highly conserved signaling pathway that regulates global growth and cell proliferation across *Drosophila* and mammals. Thus, it in interacts with several signaling cascades including TGFβ/BMP, Wnt, EGFR/MAPK, and others to regulate cell proliferation, tissue growth, apoptotic resistance, and tumor progression[72-74]. Hippo pathway deregulation is tightly associated with tumorigenesis, metastasis and chemo-resistance[75]. Hippo signaling regulates ISC division in *Drosophila* both cell autonomously and non-cell autonomously. Hippo pathway is comprised of genes that act as tumor suppressor genes such as *hippo* (*hpo*) and *warts* (*wts*), and oncogenes such as *yorkie* (*yki*). The mammalian homologs of yorkie are YAP and TAZ. In *Drosophila*, canonical Hippo signaling acts through a kinase cascade and involves activation of Hippo (Hpo) serine/threonine kinase, which forms a complex with Salvador (Sav) scaffold protein and Mob as a tumour suppressor (Mats) adaptor protein to phosphorylate and activate serine/threonine kinase Warts (Wts). Activated Wts phosphorylates Yki leading to its cytoplasmic sequestration, signaling it for proteasomal degradation and preventing its nuclear interaction with Scalloped (Sd) to regulate the target genes. Similarly, in mammals, mammalian sterile 20-like kinase 1/2 (MST1/2) kinases form a complex with Salvador family WW domain containing protein 1 (SAV1) and Mps one binder kinase

activator-like 1A and 1B (MOB1A/B or collectively, MOB1) to phosphorylate large tumour suppressor 1/2 (LATS1/2). LATS1/2 phosphorylation of Yes-associated protein (YAP) and its paralog, WW domain-containing transcription regulator 1 (TAZ) blocks the nuclear translocation of YAP/TAZ and their subsequent interaction with transcription factors (i.e., TEAD family members and others) to regulate downstream target gene transcription[76].

The precise roles of Hippo signaling in the mammalian intestine are gradually revealed. Endogenous YAP1 protein expression is restricted to the stem cell niche at the bottom of the intestinal crypts and its high activity promotes ISC division through positively regulating intestinal Notch[15,77]. *mst1/2* mutations or YAP1 overactivity are associated with expansion of the ISC pool and undifferentiated progenitors, that replace differentiated cells in the villi[78,79]. This leads to dysplastic epithelia enlarged crypt structures, increased polyps, adenoma formation and colorectal cancer progression[79-81].

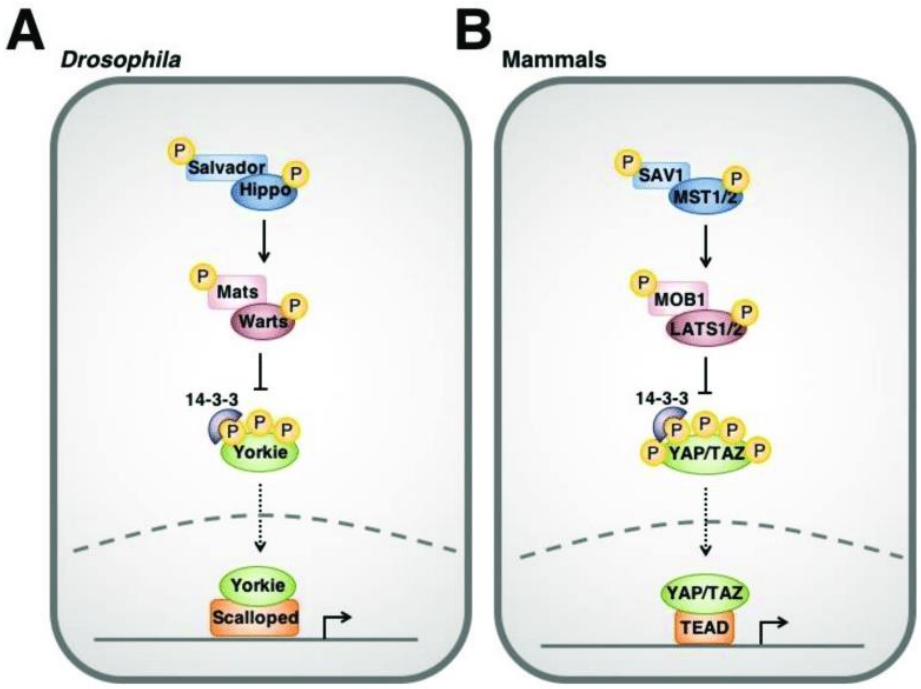


**Figure 1.4: Hippo signaling pathway in Drosophila (A) and mammals (B).** Hippo signaling is initiated by a variety of upstream stimuli such as cell-cell contact, mechanotransduction, cellular stress and oxygen availability. Activation of *Drosophila* Hippo or mammalian MST1/2 causes phosphorylation of Warts or mammalian LATS1/2. Downstream of the Hippo pathway is the effector *Drosophila* Yorkie or mammalian YAP/TAZ. Warts or LATS1/2 phosphorylation of Yorkie or YAP/TAZ leads to its cytoplasmic sequestration by 14-3-3 proteins and degradation. Unphosphorylated Yorkie

or YAP/TAZ translocates to the nucleus where it interacts with its *Drosophila* Scalloped or mammalian TEAD transcription factors to upregulate the transcription of a variety of genes involved in cell cycle progression and cell survival.

Nuclear YAP1/TAZ complex is also required for differentiation of progenitor cells towards the goblet cell secretory lineage[82]. After dextran sulfate sodium (DSS) or whole body irradiation-induced intestinal injury, YAP1 is essential for the crypt regenerative proliferation and survival[83]. Of note, over proliferation and liver enlargement is also associated with *sav1* and *mst1/2* mutations[84]. In *Drosophila*, Yki is required to control ISC division in cell-autonomously and non-cell autonomously from the niche components such as EBs and ECs. Under unstressed conditions, members of the Hippo complex function in the progenitors to restrict ISC division by limiting the nuclear activity of Yki/Sd complex. In contrast, Yki does not seem to function in regulating differentiation. Under stress conditions or Hippo pathway deregulation, Yki is cell-autonomously activated to regulate downstream genes such as *Cyclin E*, *Diap1* (apoptosis inhibitor) and *bantam* miRNA to stimulate ISC mitoses[85,86]. Yki is also activated in the ECs to induce a dramatic increase in the production of Jak/Stat and EGFR ligands to initiate non-cell autonomous compensatory ISC mitoses[87]. Additionally, Misshapen (Msn), a member of the germinal center protein kinase (GCK) family acts within the EBs to restrict the expression of Upd3, through interaction with Wts to inhibit Yki activity[28].

**g. Notch pathway:**

Both mammals and *Drosophila* ISCs require Notch signaling as a niche factor for ISC maintenance though they require it differently. Notch is a type I integral membrane cell surface receptor that forms a heterodimer after being cleaved. Notch signaling is initiated when Notch receptor (signal-receiving) binds one of several ligands (signal-sending) belonging to the Delta, Serrate, and Lag-2 (DSL) family of integral membrane proteins, which are expressed on the surface of neighboring cells. Ligand binding induces a conformational change in the Notch extracellular region that gets cleaved and releases Notch intracellular domain (NICD, a transcription factor) into the cytoplasm, which can then translocate to the nucleus, to recruit a transcriptional co-activator complex and regulate target gene expression. The level of Notch signaling is determined by receptor exposure to the ligand on the surface of the signal-sending cells i.e. Delta-positive cells[88].

In the mammalian gut, there are four Notch receptors (Notch 1–4) and five Notch ligands (Delta-like (DLL) 1, 3, 4 and Jagged (JAG) 1, 2), which are all transmembrane proteins[89]. Active Notch signaling defines the mammalian stem cells of the gut. The intestinal fast-cycling crypt base columnar stem cells express Notch1, 2 receptors while the neighbouring Paneth cells express Notch ligands Dll1 and Dll4[90] and Notch critically regulates the cell fate decision between absorptive and secretory cell types. Notch signaling induces expression of the transcription factor Hes1 (hairy and enhancer of split 1) that consequently represses cyclin-dependent kinase (CDK) inhibitors p27Kip1 and p57Kip2 and also suppresses the expression of Math1 (or Atoh1 (atonal homolog 1))-dependent differentiation towards secretory lineages[90,91].

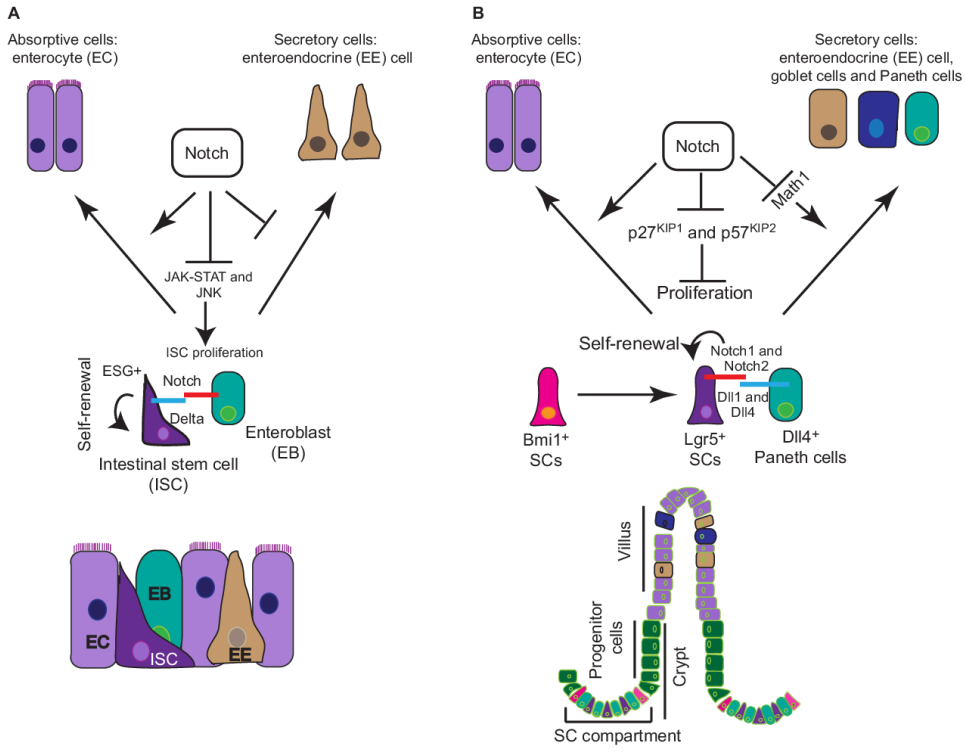


**Figure 1.5: An illustration of Notch regulation in *Drosophila* and mammalian intestine.** (A) In the *Drosophila* midgut, intestinal stem cells (ISCs) (escargot+) reside basally in an epithelial monolayer that consists of enteroblasts (EBs), enteroendocrine (EE) cells and enterocytes (ECs). ISCs express the Notch ligand Delta to bind to the Notch receptor expressing EBs. Strong Notch signaling in EBs favors the EC cell fate. Activated Notch signaling in EBs also blocks proliferation of ISCs by antagonizing the JAK-STAT and JNK pathways under physiological and stress conditions. (B) Role of Notch in mammalian ISCs: long-lived Bmi1+ SCs reside at the +4 position in the crypt compartment and when needed, divides to give rise to mitotically active Lgr5+ SCs. In the crypt compartment, Notch expressing Lgr5+ SCs are sandwiched between Delta-like 4+ Paneth cells. Activation of

Notch signaling in Lgr5+ cells maintains SC self-renewal and proliferation by negative regulation of the cyclin-dependent kinase inhibitors p27KIP1 and p57KIP2, and the transcription factor Math1, which is necessary for differentiation of the secretory cell lineages. Notch thus biases cell fate choice towards the absorptive lineage. Adopted from: Koch et al,2017.

Overexpression of Notch pathway components blocks the commitment of cells towards a secretory lineage fate and is highly associated with gastric and intestinal cancers[90]. Conversely, inhibition of Notch signaling leads to a loss of the proliferative ISCs and the crypt compartment and conversion of crypt progenitors into goblet secretory cells[90]. In contrast, in the *Drosophila* midgut, ISCs are always Delta-positive, and are located at the basal side of the epithelium. The daughter cells lack delta and express different levels of Notch that define fate specification of the ISC progeny. pre-ECs invariably express high levels of Delta in cytoplasmic vesicles, but EE precursor contained few or no cytoplasmic Delta vesicles[27]. Notch activates dTOR through the inhibition of TSC2 in the EB, leading to endoreplication and EC differentiation[26,92]. Ectopic activation of Notch signaling in ISCs causes a loss of ISCs through their differentiation[27] and Notch loss results in accumulation of ISC tumors with increased numbers of EEs and a loss of ECs[93].

Accordingly, Notch signaling acts in concert with Jak-Stat and EC-JNK or Yki/YAP signaling to determine the balance between ISCs and other cells of the midgut. For intestinal tumor outgrowth to develop in the *Drosophila* midgut, *Notch*-defective ISCs stimulate Spi production in an autocrine fashion, which is necessary for ISC divisions to initiate tumor growth. After a series of initial divisions, the adjacent ECs show elevated JNK and Yki/YAP activity, which promote their detachment, extrusion and apoptosis. Consequently, tumor-adjacent ECs express unpaired cytokines, while domeless and Stat92E are expressed in tumor cells and are necessary for tumor growth[94,95]. Interestingly, Stat92E is epistatic to Delta/Notch signaling in cell fate specification of the ISC daughters suggesting that Jak/Stat pathway functions downstream or in parallel during the differentiation of the ISC daughters such that low Notch signaling is associated with high Jak/Stat and results in EE differentiation[49].

Exogenous lipids strongly also influence Delta ligand and Notch extracellular domain stability and alter their trafficking and turnover in endosomal vesicles. This suggests an intriguing link between the dietary effects on the intestine relative to the levels of Delta

/Notch signaling that reflect the ISC number and differentiation towards EE secretory lineage[96]. In fact, intestinal tumor progression is slowed down on a low sterol diet[97]. Similarly, high fed diets in mammals also boost ISC numbers and their tumorigenicity[98] which suggest that the underlying concept of regulation is conserved.

**h. Dpp/BMP signaling:**

BMP signaling is conserved in both *Drosophila* and mammals. It functions to suppress ISC differentiation through secretion of Dpp/BMP ligands by the niche components in both GI tracts. Nevertheless, it is also cell-autonomously required in *Drosophila* ISCs to initiate stress-induced mitoses. BMP receptors are single transmembrane proteins that possess serine/threonine kinase activity in their intracellular domains. In *Drosophila*, Decapentaplegic (Dpp) and Glass bottom boat (Gbb) are the two major BMP ligands which synergistically act to bind two type-I receptors Thickvein (Tkv) and Saxophone (Sax), and a type-II receptor Punt (Put). Activated receptors causes phosphorylation of the *Drosophila* Smad Mothers-against-Dpp (Mad), which forms a complex with the co-Smad Medea and activate target gene expression in the nucleus. Dpp establishes an activity gradient that regulates expression of target genes in a concentration-dependent manner[99]. Both Dpp and Gbb are produced by ECs[100] and trachea[23]. Dpp is also expressed in the VM[22]. BMP signaling altogether plays complex and opposing roles in progenitors and ECs depending on the degree of activation of the signaling and in which cell type this occurs to regulate the balance between ISC self-renewal and proliferation of the adult *Drosophila* midgut. Below is a brief description of some observations. Firstly, clonal analyses of ISC with perturbed BMP signaling revealed that injury-induced BMP signaling acts autonomously in ISCs to inhibit over-proliferation. Thus, ectopic expression of BMP signaling components dampen the stress-induced ISC mitoses[22]. Secondly, BMP signaling seems to regulate differentiation and survival of ECs. EC-derived BMP stabilizes the EC fate and consequently dampens the production of JAK-STAT and EGFR pathway ligands also to limit unnecessary over-proliferation of ISCs[23]. As a result, Dpp inhibition in ECs leads to ectopic activation of EGF ligands that non-cell autonomously promote ISC over-proliferation[23,101]. Thirdly, BMP pathway is asymmetrically activated between ISC/EB pair such that ISCs, located basally, have

higher levels of BMP signaling activity than the apical EBs. BMP acts together with Notch to regulate the ISC/EB fate choice. Under homeostatic conditions, loss of Dpp in progenitors results in a significant loss of ISCs that differentiate into EBs and give rise to atypical EB/EB pairs. In contrast, BMP abundance within the ISCs favors symmetric ISC/ISC outcome of an ISC division and formation of large ISC-like cell clusters[100]. This evidence indicates that BMP signaling regulates ISC self-renewal. Fourthly, inhibition of Dpp receptors with a progenitor-specific driver suppress detergent- or bleomycin-induced ISC mitoses indicating that Dpp signaling is cell-autonomously required for ISC mitoses as well as lineage differentiation[100].

**Figure 1.6a: An illustration of the complex mammalian and Drosophila TGF-β signaling.** In mammals, TGFβ1 ligand activates TGFβ receptors (RI,RII) to activate the Smad2/3 that assembles with Smad4 to form a complex that, upon nuclear translocation, limits cell division. Loss of the inhibitory Smad4 in over-activated Kras$^{G12D}$- or BRAF$^{V600E}$-mutant cells alter the phosphorylated Smad2/3 activity to promote cell proliferation and survival. In *Drosophila,* Decapentaplegic (Dpp) ligand binds Punt (Put) and Thickveins (Tkv) receptors to activate the canonical nuclear complex that is comprised of Mothers against dpp (Mad) and Co-Smad Medea (Med), to regulate genes promoting cellular quiescence. Similarly, over-activated EGFR/Fos and Jak/Stat signaling re-directs Dpp to activate the alternate Put–Saxophone (Sax) receptor complex. This complex then activates dSmad2, which translocates into the nucleus independently of Med and induces tumor-like stem cell growth and dysplasia. Modified from: Ayyaz et al,2017.

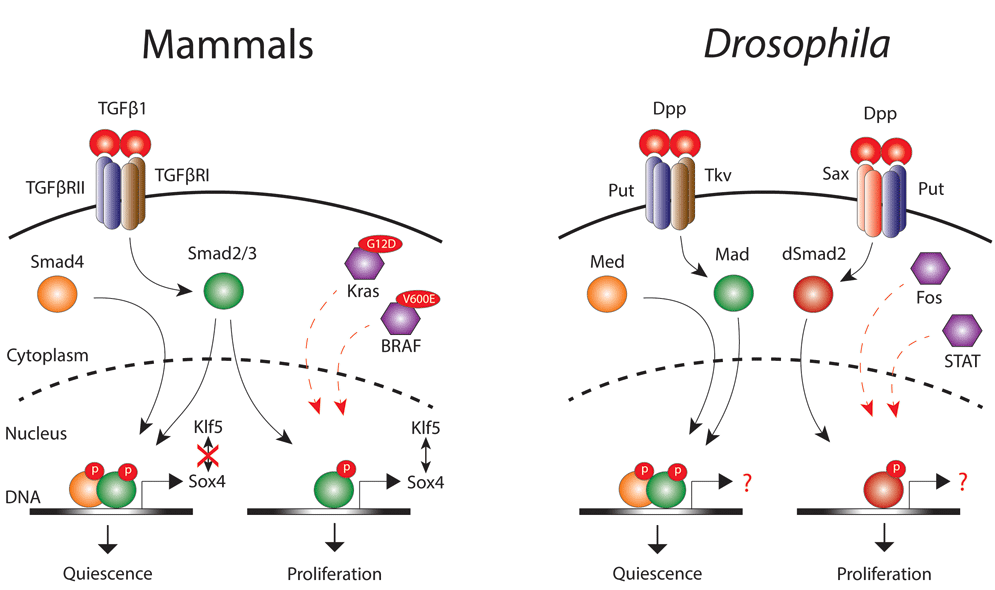


Remarkably, beside its complex roles in intestinal homeostasis, Dpp secreted from enterocytes at the regional boundaries between the posterior midgut and the middle

midgut sets up a morphogen gradient that determines the regional identity of the ISCs and defines the size of the gastric acidic copper cell region[102]. Similarly, in mammals, BMP ligands that belong to the transforming growth factor-β (TGF-β) superfamily of proteins bind BMP type I and type II receptors (Bmpr1–2) that form a hetero- tetrameric complex.

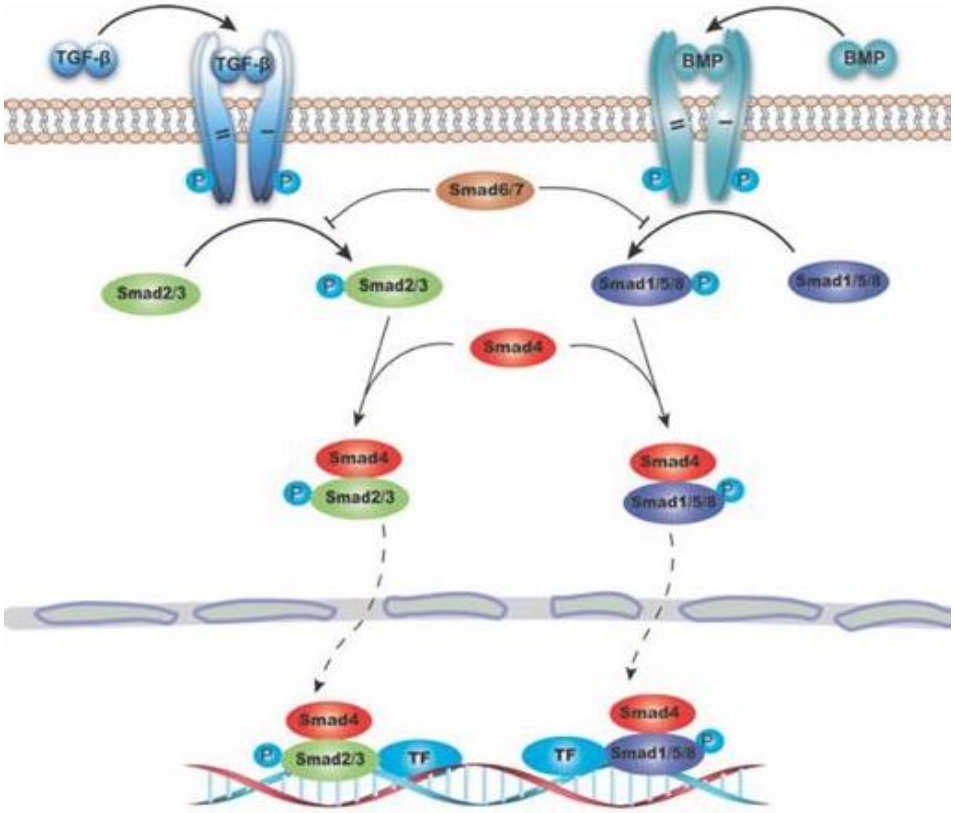


**Figure 1.6b: An illustration of mammalian TGF-β and BMP signaling in the intestine.** Ligands of the (TGF-β) superfamily includes TGF-βs and bone morphogenetic proteins (BMPs) which bind type II and I receptors (T-βR II and T-βR I) or (BMPR II and BMPR I) respectively. TGF-β R activation phosphorylates SMAD2/3 which forms a heterodimeric complex with SMAD4 and translocate to the nucleus to control target gene transcription. BMP R activation phosphorylates SMAD1/5/8 that also forms a complex with SMAD4 leading to its translocation to the nucleus to control target gene transcription. Adopted from: Zhao et al,2018

This causes phosphorylation of BMP-specific receptor-bound R-Smads1/5/8 (receptor-regulated Smads) which forms a complex with core mediator Smad4 to regulate target gene transcription. Several extracellular antagonists, such as Noggin, follistatin or gremlin sequester BMP ligands, thereby blocking their interaction with their receptors[103].

BMP pathway is activated to drive the differentiation of the mature epithelial cells and its inactivation is correlated with development of colorectal cancer. BMP ligands are expressed by the intravillus and intercrypt mesenchymal cells as well as differentiated epithelial cells to ensure that the epithelial villus cells are kept in their differentiated state[104]. BMP antagonists are tightly produced around the crypts to ensure ISCs remain functional and are capable of self-renewal. BMP represses the nuclear accumulation of β-catenin and is expressed in an opposing gradient along the crypt–villus axis, with highest BMP signaling in the differentiated cells at the luminal surface. Unlike *Drosophila* midgut, it is unclear whether BMP signaling plays a cell-autonomous role in the ISCs, though BMP receptor is present in ISCs.

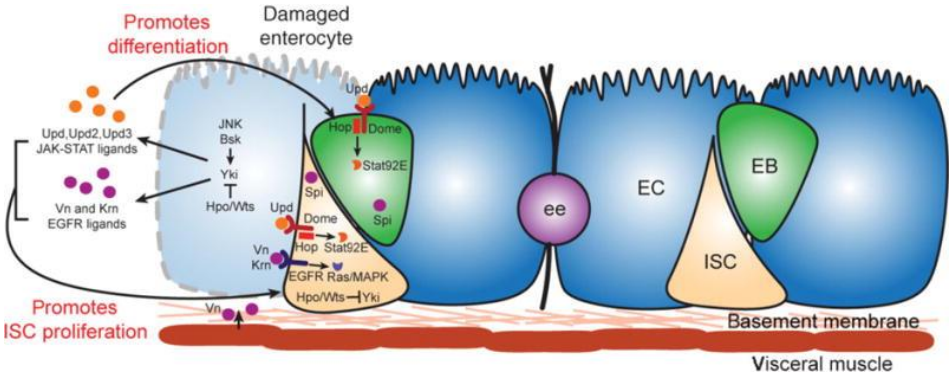


**Figure 1.7: Enterocyte (EC) damage causes compensatory ISC proliferation in the *Drosophila* midgut.** Damaged and dying ECs activate Jun N-terminal kinase (JNK) and inhibit Yorkie (Yki) signaling respectively to upregulate Janus Kinas-Signal Transducer and Activator of Transcription (Jak-Stat) ligands (unpaireds: upds) and EGF ligands production that activate EGFR and Jak-Stat signaling to stimulate regenerative ISC mitoses. Jak-Stat signaling activation in enteroblasts promotes their differentiation into enterocytes to compensate for the lost cells. EGFR signaling is required for the endoreplication of enterocytes. Adopted from Lucchetta and Ohlstein, 2012.

### 1.5. Epithelial aging and loss of integrity.

Continual bouts of ISCs division across the organismal lifespan bring about dysfunction in the homeostatic signaling mechanisms, which lead to chronic intestinal inflammation in both *Drosophila* and mammals. The ISCs are highly plastic, as they respond to stress and nutritional cues to sustain the epithelial integrity and to adjust epithelial size to changing dietary conditions[105]. Hence, maintaining the ISC function is critical for optimal

lifespan. In aging *Drosophila* animals however, deregulated elevated ISC divisions cause epithelial dysplasia and perturb epithelial function. This is accompanied by a prominent gut-wide increase in oxidative DNA damage, and increased ROS levels that is primarily sensed by ECs to promote accelerated ISC mitoses[105,106]. Consequently, this results in disruption of metabolic homeostasis[68], loss of barrier function, systemic infection[107], and ultimately mortality. Similarly, in aging mammalian intestines, the loss of regulatory mechanisms leads to intestinal barrier break down and increased microbiota loads (dysbiosis) accompanied by increasing cellular stress and DNA damage that disrupt the tissue homeostasis. Accordingly, individuals become more susceptible to infectious diseases, including inflammatory disorders[108], colorectal cancer[109], metabolic imbalances[110] and gastrointestinal infections[111]. The reports on the aging effects of crypt architecture are mixed. Some studies counter-intuitively reported a decline in crypt number but increased crypt length and width, decreased number of mitotic cells and attenuated regenerative capacity of aged crypts at the expense of increased ISC differentiation[112]. Others reported that aged mice or rat intestines have increased crypt numbers accompanied with hyperproliferation of active ISCs, activatable reserve ISC and enteroendocrine cells [113,114]. This disparity could be due to differences in the animal strains, housing conditions and whether or not they were cultured in a germ-free environment[112].

Besides the cell-autonomous deregulation of the pathways controlling ISC divisions or ISC maintenance, several signaling pathways non-cell autonomously lead to excessive activation of ISC divisions and eventually, intestinal dysplasia. In *Drosophila*, these include hyper-activation of innate immunity components[115], JNK signaling and insulin signaling[62] in ECs. Notably despite the limited knowledge of pathways involved in mammalian intestinal aging, mechanisms driving age-related dysplasia of the stem cell function are conserved from *Drosophila*[62,116] to mammals[117] such as expression of stress-protective FOXO target genes, that is sufficient to limit ISC over-division and maintain metabolic homeostasis[62].

### 1.6. Differences in male and female *Drosophila* ISC division and its consequences:

There were reported longstanding differences between the rate of the ISC epithelial homeostatic[8] or regenerative turnover in males and females in *Drosophila* [8,118] that are only recently beginning to be understood. Female fly intestines turn over at faster rates relative to males, which result in females being more susceptible to develop progressive age-mediated intestinal hyperplasia then dysplasia. These gut epithelial deregulation together with dysbiosis drive a loss of intestinal integrity and gut immune barrier[119], which may lead to compromised life span[62,120-122]. Further studies revealed that sex differences are owed to a combination of factors including: differences in food uptake[123], cell autonomous differences in stem cell behavior[118], differences in epithelial structure and loss of gut barrier function[124] possibly due to differential activation and hyper activity of pathways such as JNK or insulin signaling in females relative to males[62,120]. It remains much less carefully examined in mammals if the sexual identity also affects the intestinal turnover and response to regeneration. Indeed, studies usually report results of mixed intestines of males and females or prefer males to females to exclude the effects of the reproductive status on the intestinal function.

### 1.7. Nuclear Receptors

Cholesterol, fatty acids, fat-soluble vitamins, and other lipids are an essential component of the diet of both *Drosophila* and mammals. They do not only function in providing metabolic building blocks for macromolecules but, they also serve as precursors for ligands that bind to a class of transcription factors in the nucleus called nuclear receptors (NRs). NRs are integrators of hormonal and nutritional signals, mediating changes to metabolic pathways within the body. For lipids to become biologically active, they first get absorbed by the intestine then are enzymatically converted to metabolically active signaling molecules. Ultimately, a tight balance is achieved between the lipid absorption and elimination to maintain a normal physiological state. Hence, the need to study the detailed functions of NRs in the organ where nutrient absorption and excrement discharge occurs becomes crucial to our understanding of how the intestinal physiology is regulated and how impaired functions of NRs result in disease states[125].

NRs are best described as ligand regulated DNA-binding transcription factors that exert activating or repressive effects on target genes, thereby directly modulating target gene expression[126]. The human genome has 48 members of this highly conserved transcription factor family and the Drosophila genome has 18 members[127]. This superfamily includes: classic endocrine receptors that mediate the steroid hormones actions such as estrogen receptor (ER), androgen receptor (AR) glucocorticoid receptor (GR) or *Drosophila* ecdysone receptor (EcR), *Drosophila* Hormone Receptor 96 (Hr96). Receptors that bind non-steroid hormones include thyroid hormone receptor (TR) and retinoic acid receptor (RAR). Receptors that bind products of lipid metabolism i.e. fatty acids and their derivatives such as prostaglandins include peroxisome proliferator activated receptors (PPAR), liver X receptors (LXR), farnesoid X receptors (FXR) and the highly conserved *Drosophila* and mammalian Hepatocyte Nuclear Factor 4α[128]. Finally, the rest are grouped into orphan receptor subfamily for which the regulatory ligands were/are unknown[127].

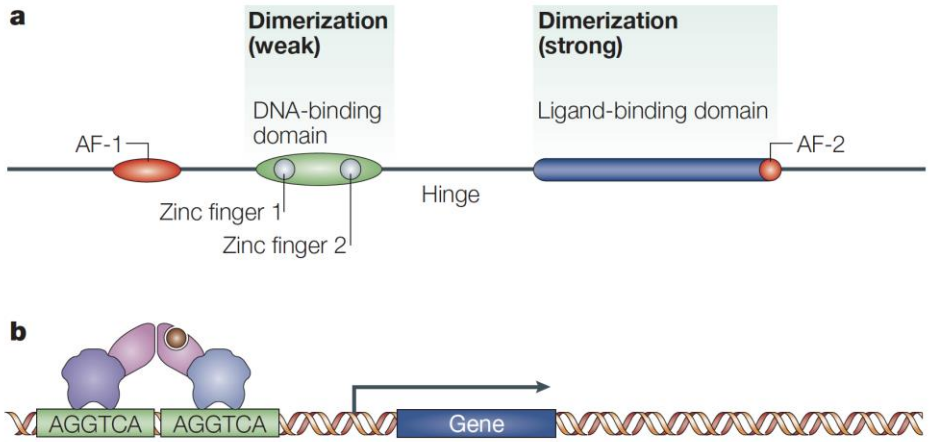


**Figure 1.8: Schematic illustrating the basic structural components of a Nuclear receptor and how it mediates its function.** a) Nuclear receptors are comprised of three domains, a highly conserved DNA-binding domain (DBD), a ligand-binding domain (LBD) that are joined by a flexible hinge region and a N-terminal domain that contains AF-1 transactivation domain. The DBD consists of two C4 zinc fingers that mediate specificity of target DNA binding. The less conserved LBD is located C-terminal to the DBD and has a strong dimerization surface to bind different receptors. The LBD comprises 11–13 α helices that form a hydrophobic pocket for the binding of small lipophilic molecules. Recruitment of coactivators takes place through ligand dependent

AF-2 and ligand independent AF-1 transactivation domains. b) Each nuclear receptor binds to a half site that is derived from, or identical to, the standard AGGTCA sequence through a stretch of five amino acids known as the P-box located in the DBD. Adopted from: Sara Ahmed's master thesis,2015[464] and originally from Krist-Jones & Thummel, 2005.

NRs consist of an amino terminus with a trans-activation domain (AF-1), highly conserved DNA- binding domain (DBD) and a less conserved C-terminal ligand-binding and dimerization domain (LBD). The AF-1 acts in a ligand-independent fashion and facilitates the recognition of NR by transcriptional co-regulators such as co-activators or co-repressors. The DBD comprises zinc-finger domains that provide DNA-binding specificity and a dimerization interface through which the interaction with a target DNA takes place[129]. The LBD consists of a hydrophobic binding pocket where the ligand docks and a transactivation domain AF-2, that recruits co-activators, often through a ligand-dependent fashion. NR bind target genes through receptor-specific conserved DNA sequences termed nuclear response elements[127].

Most ligand-bound activated NRs translocate to the nucleus to modulate transcriptional regulation of target genes themselves. However, reports also describe the existence of extranuclear receptor pools that coordinate the classic nuclear pools[130,131]. The actions of NRs can be non-genomic, genomic or epi-genetic[132]. Non-genomic functions include interaction with membrane-localized cell-signaling effectors such as estrogen-induced generation of cyclic AMP[133] or progesterone-induced interference with G-protein signaling to activate Erk[134], among many others[135]. Genomic functions include direct modification of the activity of transcription factors[136] such as estrogen-mediated down-regulation of transcriptional repressors such as Mad4 and JunB and up-regulation of cell cycle progression genes such as cyclin D[137]. The action of NR even extends to regulating epigenome[132,138] through regulating histone deacetylases (HDACs)[139,140], histone methyltransferase[141] or altering chromatin compaction[142,143]. Owing to their wide functions, dysfunction of nuclear receptor signaling is associated with proliferative, neuronal reproductive and metabolic diseases such as cancer, infertility, obesity and diabetes[144-147].

### 1.8. *Drosophila* ecdysone in development and adulthood:

*Drosophila* has two main physiologically active lipophilic hormones, the steroid hormone ecdysone and a sesquiterpinoid, juvenile hormone. Ecdysone signaling works in concert with juvenile hormone to regulate major developmental transitions in the *Drosophila* life cycle, including the larval molts and metamorphosis, as well as sexual maturation[148]. Most of the ecdysone signaling effects reported in the literature are investigating the actions of a 20-hydroxylated derivative of ecdysone (referred to as 20HE). Though it is becoming more evident that only studying the actions of 20HE is an all-too-simple view. Though it was recently described that *Drosophila* can produce different classes of ecdysteroids, which are derived from four types of dietary sterol precursors: cholesterol, C27 sterol, C28 and C29 plant sterols and C28 fungal sterols (e.g. ergosterol) with an epi-C-24methyl group, which has the opposite chirality to plant sterols[149]. In total, ecdysteroidome of *Drosophila* comprises seven major ecdysteroids: α-Ecdysone, 20HE, 20-hydroxylated derivative makisteroneA (MaA), 24-methylecdysone (24-methylE), 24-epi-methylE, 24-epi-MaA, 24(28)-dehydromakisterone (dhMaA), and two catabolites – 20-hydroxyecdysonoic acid (20Eoic) and MaAoic acids[149]. It remains very interesting to figure out how those different classes differ in their actions during development and in adulthood, whether they all bind EcR•Usp, and how they would dynamically regulate target gene expression. To date, 8 CYP450 enzymes (Halloween genes) are implicated in ecdysone synthesis from dietary cholesterol[150]. During larval development prothoracic glands are the principal source of ecdysone synthesis[151]. However, the main site of ecdysone synthesis during adulthood is the female ovaries and the male accessory glands are reported to express 20HE-synthesizing enzymes[152]. Higher levels of circulating ecdysone exist in females than males[153,154]. Accordingly, α-Ecdysone is released into the hemolymph after which it gets converted by the sexually dimorphic enzyme shade into 20HE at the target tissues[118,155]. After mating, there is a boost of ecdysone production in the female ovarian follicles and its levels double as early as 24 hours after mating[156-158].

Classically, the ecdysone receptor dimer consists of the ligand-binding *EcR* subunit and the DNA-binding subunit *Ultraspiracle (Usp)*, which are orthologous to human farnesoid X and liver X receptors (FXR, LXR), and the retinoid X receptor (RXR) respectively[127].

*Drosophila* ecdysone receptor gene (EcR) encodes up to six protein isoforms (Flybase Apr 14, 2020 release) including the functionally distinct, well characterized EcR-A, EcR-B1, and EcR-B2[159,160]. The difference in the isoforms lies in their N-terminal, A/B region but they share a common DBD and LBD. During *Drosophila* larval development, ecdysone-liganded EcR•Usp heterodimers activate transcription of "early" genes including the *Broad Complex (BR-C)* and the *ecdysone-inducible puff 75B (Eip75B)*, which in turn induce transcription of a set of ''late'' genes that orchestrate major developmental events in the life cycle[161-163]. In adults, ecdysone functions to regulate sleep [164], courtship memory formation[165], lifespan and stress resistance[166], and establishes a female metabolic state conducive to reproduction[123]. Ecdysone signaling has also been shown to be involved in terminal differentiation of neural stem cells in the adult *Drosophila* brain [167] and to maintain germline stem cells in the ovaries [168] and cyst stem cells in testes[169]. To date, a role of ecdysone EcR signaling in the adult gut has not yet been described, and it is this subject of this thesis, though its mammalian orthologs LXR and FXR regulate a multitude of metabolic pathways in the GI tract including bile acid, lipid and carbohydrate metabolism[170,171].

Downstream of the ecdysone cascade, there are many ecdysone-inducible targets that relay the ecdysone effects[172]. Below is a short summary of the ecdysone targets whose functions were examined during the course of this project.

### 1.9. Eip75B, Hr3 and Hr51 as hormone nuclear receptors in *Drosophila*:

Ecdysteroid-inducible protein 75B (Eip75B) is encoded by the early gene *E75* that maps to the 75B early puff. Puffs are enlargements of specific loci on the giant salivary gland polytene chromosomes after ecdysone binds them, which correlate with increased local transcriptional activity at these sites. The closest vertebrate homologues of Eip75B are members of the NR1D/Rev-Erb family. These mammalian nuclear receptors include Rev-Erb*α* (Rev-ErbA-*α*, THRAL, EAR-1; NR1D1) and Rev-erb*β* (Rev-ErbB-*β*, RVR, EAR-1R, BD-73; NR1D2) respectively[173]. The percentage amino acid identity in DBD/LBD of Eip75B to REV-ERB is 80/25 which ranks both NRs amongst the most highly conserved proteins during evolution[127]. Similar to REV-ERB, Eip75B tightly binds heme in its LBD. However unlike REV-ERB, heme is essential for Eip75B protein folding and accumulation. Both proteins undergo redox-dependent ligand switching and CO- and

NO-induced ligand displacement raising the possibility of their functions as redox sensors[174]. Indeed, cellular levels of Eip75B are proportional to heme amounts available in the cell suggesting that Eip75B acts as a heme sensor[175]. Generally, REV-ERBs and Eip75B function as repressors of transcription[173,176-178]. Accordingly, Eip75B and REV-ERB have overlapping functions in regulating circadian rhythm and metabolism in both *Drosophila*[179,180] and mammals[181,182]. Eip75B has at least seven protein isoform Eip75B-RC (E75A), RA (E75B), RF, RD, RG, RB and RE (Flybase Apr 14, 2020 release), 3 of which are characterized in the literature[183]. Alternative splicing gives rise to protein isoforms that differ in their N-terminal sequences but share a common LBD in the C-terminus. During development, Eip75B functions in development to regulate molting, pupal development, metamorphosis and adult viability[183]. Interestingly, Eip75B also acts as upstream of ecdysone as a regulator of ecdysone production in the prothoracic gland[184].

Drosophila Hormone Receptor 3 (Hr3) is orthologous to the vertebrate retinoid-related orphan receptor (ROR) and together they share a percentage amino acid identity in DBD/LBD of 76/35 [127]. Consistent with its similarity to ROR, Hr3 binds as a monomer to its response element on its target genes acting as a transcriptional activator. All Eip75B isoforms are reported to be able to bind Hr3 both in vivo and in vitro [175,177,184]. Classically, Eip75B binds Hr3 blocking its transcriptional activities on target genes. This Eip75B•Hr3 interaction is regulated by NO binding, which disrupts the interaction of Eip75B with Hr3. The function of this nuclear receptor cascade has been validated across development in various contexts. Eip75B•Hr3 regulates behavior, fat deposition and developmental timing[177,185-187].

Drosophila Hormone Receptor 51 or unfulfilled (unf/Hr51) is orthologous to the vertebrate PNR (photoreceptor-specific nuclear receptor) and together they share a percentage amino acid identity in DBD/LBD of 70/47[127]. Although not much is known about Hr51, it is reported to function together with Eip75B to regulate circadian rhythm in the pacemaker neurons [188] and direct developmental axon regrowth [189]in a-NO dependent fashion. However, it is unclear whether Hr51 is an ecdysone-inducible target.

### 1.10. Broad as an ecdysone target:

The *Broad-Complex* (*BR-C*) or *broad* is a complex gene that encodes a family of zinc finger transcription factors mapping to the 2B5 early puff. The *broad* complex contains up to four classical complementation groups (*broad*, *reduced bristles on palpus (rbp)*, *l(1)2Bc* and *l(1)2Bd*), as well as a group of non-pupariating (*npr1*) alleles. Through alternative splicing, at least 14 transcript isoforms form from a single pre-messenger RNA transcript. The broad family consists of a common core N-terminal region with a protein–protein interaction domain BTB/POZ that they use to interact with other transcription factors or with chromatin and a pair of cysteine (C2) and histidine (H2) zinc fingers that bind to DNA of its target genes. [190]. BR-C functions as an early ecdysone target to coordinate the stage-specificity of the ecdysone response during growth of imaginal discs, neuronal development, metamorphosis[191]. In adults, BR-C functions in regulating oogenesis[192] and modulating innate immune responses[193].

### 1.11. Sex determination in mammals and *Drosophila*:

As shortly presented in the introduction and discussed further, the steroid NRs bind steroid hormones and the active hormone receptor complex binds its hormone response elements to control target gene expression. The gonadal sex steroids are a subclass of the steroid NRs that are mainly synthesized from the gonads to act on many target tissues. Accordingly, sex hormones act as chemical mediators of gonadal sex that are involved in sex differentiation too. Sex hormones interact with the intrinsic genetic sex at different levels and, synchronously work to regulate the organismal homeostatic needs. Under certain conditions: predisposition to genetic diseases or exposure to external environmental cues result in disturbance of this interaction, posing a significant risk on the organism's general and reproductive health or survival. Studies on how the two sex components: genetic and gonadal sex interact to control mechanisms that lead to sex differences would expand the knowledge of the fundamental biology of sex differences in physiology and disease processes, facilitating therapeutic outcomes of sporadic and genetic diseases. The interplay between gonadal sex, psychological sex and the intrinsic sex chromosome constitution of individual cells is likely to determine several behavioral aspects of organ physiology and disease as shown in examples ([194-196]). Hence, it remains interesting to study how the non-cell autonomous sex-determining mechanisms and the

sex hormones cross talk with the cell-autonomous cellular composition of the sex chromosomes to regulate tissue homeostasis.

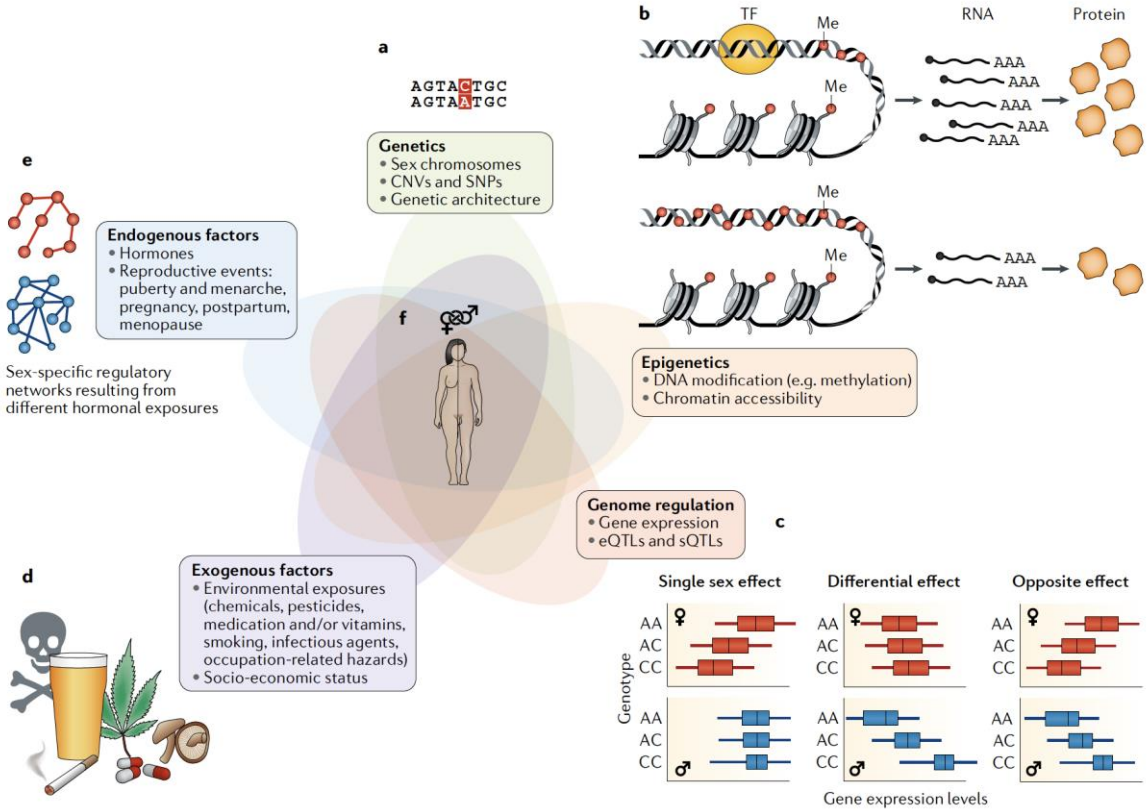


**Figure 1.9: Factors contributing to phenotypic sex differences in physiology and disease.** A multitude of factors contribute to the disease and non- disease human traits including the intrinsic genetic makeup of the cells (genetic components that lead to genetic variation in an individual's genome represented in (a) single- nucleotide polymorphisms (SNPs) and copy number variants (CNVs)) and de novo mutations, (b) epigenetic differences in DNA accessibility and methylation status such that hypomethylation associates with accessibility of transcription factor (TF) binding to promote transcription and hypermethylation associates with compact chromatin. (c) the genotype imparted differences in gene expression vary between males and females. Genetic variants that affect RNA splicing are termed sQTLs, splicing quantitative trait loci. Genetic variants that differ in their regulatory mechanisms i.e. they can act in one sex and not the other, or with different effect sizes or even allelic direction in males and females are termed eQTLs, expression quantitative trait loci. (d) exogenous factors such as environmental exposures, lifestyle choices and occupation- related hazards (e) endogenous factors such as sex hormones and reproductive status all function together to regulate sex-biased gene expression and formation of sex- specific regulatory networks. Adopted from: Khramtsova et al,2019.

In mammals, our current understanding is that there are distinct levels of sex determination and identity. There is the environmental sex determination (ESD) whereby external factors such as temperature, toxicants, population density, nutrients and hormones regulate the sex of the organism. There is also the genetic sex determination (GSD), which is driven by mechanisms regulating gonadal sex determination as well as the chromosomal differences between the sexes.

Gonadal sex determination is dominant over most sexually dimorphic characteristics. There is also the much-less understood psychological sex determination, which acts in the brain to determine gender identity and partner preference[197]. Sex chromosomes (XY) have evolved as morphologically distinct from autosomes. The Y chromosome carries the sex determining region Y (*Sry*) gene, which translates into a transcription factor that initiates testicular development in a gonad with the potential to be of male or female fates equally[198-200]. Expression of SRY in the somatic supporting cell lineage (i.e Sertoli cells in testis) causes the activation of its downstream target *Sox9*, which acts in a feed-forward loop with fibroblast growth factor 9 (FGF9), to suppress Wnt 4 and the female signature and instead, amplify the male biased signature of desert hedgehog (*Dhh*)[201], prostaglandin D2 synthase (*Ptgds*) [202]and platelet-derived growth factor (PDGF)[203]. In many egg-laying species including birds and turtles, despite the presence of a strong genetic sex determination system, they can be sex-reversed to female by the application of estrogen during the critical period of gonad formation and commitment to testis or ovarian fate, thereby reverting a testis into an ovarian fate[204]. In a similar context, in mammals that develop within a uterus (eutherian mammals), XX individuals can be fully sex-reversed to phenotypic males if *Sry* initiates testicular development, suggesting that gonadal sex determination non-cell autonomously exert control over the sex chromosome constitution of individual cells[200]. In *Drosophila* however, cells know their sex by their sex chromosome constitution, independent of their neighbors. An elegant demonstration of this concept is the existence of Gynandromorphs, which are animals that possess male regions and female regions in their body. This can happen when an X chromosome is lost from one embryonic nucleus. As a result, the cells that descend from this particular cell, instead of being XX (female), are XO (male)[205,206].

Fly sex determination is achieved through a combination of dosage compensation and sex

chromosome sensing mechanisms[207], where X/X is female and X/Y is male. The bigger ratio of X chromosomes to autosomes (In females, the X:A ratio is 1) leads to activation of the expression of the master X-linked regulatory gene cascade starting with sex-lethal (sxl) that becomes activated in a positive-feedback loop to maintain its own alternative splicing, and also the splicing of transformer (tra) and female-specific isoforms of the transcription factor genes doublesex (dsx) and fruitless (fru) resulting in expression of a "female" transcriptional regulatory complex and a female sexual development genetic landscape i.e. female "ON" state[207]. At the same time, Sxl expression regulates dosage compensation through inhibiting male specific lethal-2 (msl-2) expression. Conversely, when msl-2 protein is expressed, it causes the formation of the male-specific MSL complex which is targeted to the single male X chromosome to activate 2-fold upregulation of the male chromosome (dosage compensation)[208]. In parallel, msl-2 promotes the expression of male-specific doublesex (dsx) and fruitless (fru) isoforms, all of which work in synchrony to instruct male specific traits. So far, the majority of the sexual differentiation in *Drosophila* sex traits are reported to largely depend on the on/off state of Sxl[209]. Although, recent studies reveal the existence in *Drosophila* of sex-biased expression of tissue specific miRNAs that contribute in maintaining the sex identity of various tissues, through rather complex mechanisms that are still not fully understood. 30 miRNAs are enriched at least fivefold in the male body suggesting distinct somatic functions. Whereas in females, 45 miRNAs are enriched in female somatic tissues, 28 of which are almost exclusively detected in the somatic tissues rather than the ovaries. As an example, miRNA let-7 expression is sexually dimorphic and regulated by the sex-biased hormone ecdysone. Ecdysone-regulated let-7 modulates the sex-determination hierarchy. During the late-larval to late pupal developmental stages, Let-7 levels are important to specify male and female sexual identity. While, during adulthood, let-7 helps establish and sustain gonadal differentiation and sexual identity in males and females[210]. This growing evidence demonstrates that sex-hormonal control of cellular sexual identity exists in *Drosophila*, similar to vertebrates[211].

Mammalian sexual differentiation is related to *Drosophila* sexual differentiation in a number of ways. First, females are X/X and males are X/Y. Second, in mammals females have two copies of a large, gene-rich X chromosome, whereas males have one X and a small, gene-poor Y chromosome. Hence, to avoid imbalance of genes and proteins and

drastic phenotypic effects, dosage compensation mechanisms have evolved that equilibrate the level of X-linked gene products between the sexes. Accordingly, twofold up-regulation in the expression of X-linked gene in males[212] exists as well as the almost complete (but not all) inactivation of the genes on one of the two X chromosomes in females[213]. Third, *Drosophila* dsx, which is expressed in a male-specific pattern and is required for male differentiation, shares a high degree of homology to Mab3[214], which is present in *C.elegans,* and Doublesex and Mab3 Related Transcription factor 1 (DMRT1) in reptiles, zebrafish[215] and mammals[216]. It remains striking that the sex determination mechanisms is highly conserved across species from *C.elegans* to *Drosophila* and mammals and argues that future studies will reveal even more similarities in the global regulation of sex traits.

Environmental cues also influence sex determination. One example is the regulation of sex identity by estrogen through the differential expression of an epigenetic histone modifier in reptiles. It has been shown that temperature or estrogen levels affect the sex determination pathway in reptiles by modulating the expression of the histone demethylase KDM6B in a sexually dimorphic manner. Expression of the chromatin modifier: KDM6B is high at male- producing temperatures (26°C) and low at warmer, female producing temperatures (32°C). KDM6B demethylates the trimethylated histone H3 lysine 27 (H3K27me3) which activates gene expression at the highly conserved key sex-determining gene locus, *Dmrt1*[217]. This leads to the expression of the testicular Sertoli cell markers *Sox9* and *Amh* and the inhibition of ovarian markers *Cyp19a1* and *Foxl2.* In contrast, high temperature or the presence of estrogen at low temperatures is sufficient to down-regulate relative expression levels of KDM6B, which gives rise to females[*217*].

Hence there is a strong interaction across species[218] between the cell-autonomous sex determination whereby cells know their sex by their sex chromosome constitution, and non-cell autonomous gonadal sex whereby the gonadal sex elements primarily creates a system that is responsive to the sex-specific endocrine milieu characteristic of the stage of development, as well as the specific male and female environments, controling at least in part some aspects of the cellular sex as well as secondary sex characteristics[211,219] .

### 1.12. Effect of sex hormones on sex and non-sex organs:

Sex hormones are the chief systemic mediators of the sex differences imparted by the gonadal sex. They are responsible for many aspects of the sexual maturation and appearance of secondary sex characteristics. Nevertheless, there is accumulating evidence linking sex hormones to the physiology of non-sex organs as well. Sex steroids are steroid hormones that are cholesterol-derived[220], and synthesized by Cytochrome P450 enzymes mainly in the gonads of the animal but also to much lesser extents in the kidney, adipose tissue, skin, and brain[220]. In mammals, sex steroids include: estrogen, progesterone and testosterone. Sex hormones are involved in many processes including stem cell division[221,222], renewal of reproductive[223,224] and non-reproductive organs[225,226], central regulation of systemic metabolism[227] and stimulating appetite and food intake[228].Similarly, sex steroids are known for their pro-[229,230]or anti-inflammatory[231,232], immune-modulatory[233,234], angiogenic[235,236] roles as well as for the recruitment of stromal cells in the tumour microenvironment during cancer development[237,238]. Even development of severe body-wasting syndrome called cachexia shows a strong sex preference with higher prevalence in males than females possibly due to the protective effects of estrogen on the muscle mass[239,240]. Since the 20HE hormone I studied is of high resemblance to estrogen in both its structure and function[123], I focus on the roles of estrogen and to a lesser extent progesterone (collectively termed female sex steroids) in the next paragraph. There are four naturally occurring steroid estrogens: estrone (E1), 17β-estradiol (E2), estriol (E3) and the pregnancy-specific estetrol (E4). All estrogens are derived from cholesterol. E2 is the major product during the premenopausal period in a woman's life, whereas E1 is synthesized from the adipose tissue[241] and plays a larger role after menopause. E3 is the least potent estrogen and together with E4 they are secreted by the placenta and remodel the organs during pregnancy. Estrogens are interconverted to each other through CYP450 enzymes in a process named metabolism. Metabolism is the enzymatic modification of exogenous or endogenous compounds, which either alters their metabolic stability or detoxifies them for clearance outside the body[242]. Similarly, endogenous hormones are metabolized into less active forms such as estrogen inactivation of E2 involves its conversion to a lesser active form E1 or E3 or addition of sulfation adducts by estrogen sulfotransferases which inactivate the estrogens[243,244]. Estrogens bind to at least three different estrogen receptors (ERs), ESR1 (ERalpha, or

ER$\alpha$), ESR2 (ERbeta or ER$\beta$) and a membrane G-protein coupled receptor, GPR30 (or GPER1). ER$\alpha$ and ER$\beta$ are well-identified nuclear receptors and are products of distinct genes located on different chromosomes. The actions of ER$\beta$ seem to be opposing to ER$\alpha$-mediated transcriptional responses[245,246]. 17β-estradiol binds equally to ER$\alpha$ and ER$\beta$, hence the genomic response in the target tissue depends on the ratio between ER$\alpha$ and ER$\beta$[247]. Stimulation of target gene expression in response to estrogen-bound ERs occurs through (i) 'direct binding' to estrogen response elements (EREs) in the target genes and interacting directly with coactivator proteins and components of the RNA polymerase II transcription initiation complex resulting in enhanced transcription or (ii) 'tethering' of liganded ER to another DNA-bound transcription factor such as RARα, Sp1, AP-1, and NFκB in a way that stabilizes the DNA binding of that transcription factor and/or recruits coactivators to the complex[246]. The latter mode of ER transactivation extends the ER influence to genes that do not contain ERE sequences in their promoter regions adding yet more complexity to the transcriptional regulation. Similarly, both ERα and ERβ interact with receptor tyrosine kinases, scaffolding proteins, guanine nucleotide exchange (G)-proteins, as well as other intracellular signaling proteins, to activate a wide array of cytoplasmic signaling pathways, independent of their transcriptional effects[248]. Alternatively, the transmembrane or endoplasmic reticulum-bound GPR30 was shown to bind endogenous E2 as a ligand and to activate Erk and PI3K–Akt signaling in breast cancer cell lines[249,250].

Generally, female sex steroids regulate the growth, development and physiology of the reproductive organs during puberty, the estrus cycle and pregnancy [224,251-254] as well as their carcinogenesis[255,256]. Moreover, the female sex steroids are required in a paracrine or intracrine fashion to regulate the physiology and tissue-specific functions of the brain[257,258], bone[259] or adipose tissue[260] with or without dependency on circulating levels of ovary-derived sex hormones. Surprisingly, estrogen-synthesizing aromatase and estrogen receptors are also expressed in diverse sites of the male gonads. E2 is required for spermiogenesis, sperm maturation and sperm motility [261,262]. Additionally, estrogen is required for neuronal functions and aromatase-knockout mice, which are unable to synthesize estrogen, are impaired in many behaviors including sexual, aggressive, and locomotive behaviors[263]. Hence, there's a tight balance between estrogen synthesis and deactivation to regulate organ-wide homeostasis and its deregulation leads to many

pathologies[264].

### 1.13. Impact of exogenous sex hormones on health.

In the more recent years, exogenous exposure to sex steroid hormones has proven to have harmful effects on the reproductive health of many organisms in the ecosystem, including humans. As an example, estrogen will be discussed below as nearly all body tissues develop a response to estrogens[265]. Exogenous sources of estrogen may include exposure from environmental sources, dietary sources or through use of oral contraceptives and hormone replacement therapies. Estrogen can leak into the environment through the wastewater or manure of livestock as well as urine of women on oral contraceptives or hormone replacement therapy[266,267]. Of note, all food of animal origin contains detectable estrogen and its metabolites at variable concentrations. 17β-estradiol is the most potent estrogen, but even the least potent naturally occurring or synthetic estrogens have drastic effects that warrant for concern[267]. The relative potency of 17β-estradiol is $10^4$ to $10^6$ times compared to some xenoestrogens in-vitro[268]. Elevated levels of 17β-estradiol in the environment[266,269-271] are responsible for a plethora of endocrine disturbances including predisposition to obesity[272], increased occurrence of genital abnormalities among new born boys and precocious puberty in girls[273,274], disturbances in male spermatogenesis and fertility [262]as well as sex reversal in fish[275,276]. As dietary or environmental exposure to steroid hormones and their metabolites is inevitable, it is therefore of prime importance to investigate if there is an impact of environment loading[267] or dietary exposure of steroid hormones on the physiology of mammalian organs and health. Indeed, as an example dietary exposure to milk products supplies about 60-80% of ingested female sex steroids, that come from the animal's endogenous stores even without the animals being raised on estradiol[277,278]. As early as 1-2 hours after cow milk consumption, both serum and urine concentrations of estrogen and progesterone metabolites were significantly increased in all men, women and children[277,279]. Milk consumption from pregnant cows also caused suppression of gonadotropin hormone secretion concurrent with the absorption of exogenous estrogens[279]. Elevated sex hormones are known to result in a negative feedback loop on the hypothalamic-pituitary-gonadal axis, which suppress gonadotropin hormone secretion. Gonadotropin hormone secretion is essential for the

regulation of the menstrual cycle and its disturbances is associated with some reproductive endocrine disorders including anovulatory amenorrhea and hypoestrogenemia[280]. In congruence with the hypothesis that dietary intake of estrogen-rich foods interferes with the normal reproductive functions, dairy food intake is associated with twice higher risk of sporadic anovulation[281], reproductive senescence and diminished ovarian reserve (accelerated ovarian aging)[282]. Similarly, suggestive evidence shows that exogenous dietary hormone intake, through milk consumption is associated with significantly higher risk of endometrial cancer progression, especially in post-menopausal women[283]. Collectively, the current evidence associating sex hormone intake with reproductive health suggests that indeed the hormones in the food get absorbed to the blood, which are associated with detrimental long-term consequences on the reproductive health. Accordingly, the effect of dietary intake of naturally occurring sources of high sex steroids on the organismal health deserves more detailed study.

**1.14. Fly genetics.**

Most of the experiments done in this thesis were based on the GAL4-UAS$^{ts}$ binary expression system, a P element based system –that allows patterns of an enhancer-driven expression to reflect the expression of any gene of interest. P elements are transposable DNA elements that hop and insert themselves into the genomic DNA, preferentially into sequences that regulate gene expression (i.e. enhancers). A GAL4-UAS is designed by replacing an "enhancer trap" P construct with the yeast transcription factor, Gal4 followed by the introduction of the gene of interest in a second P element.

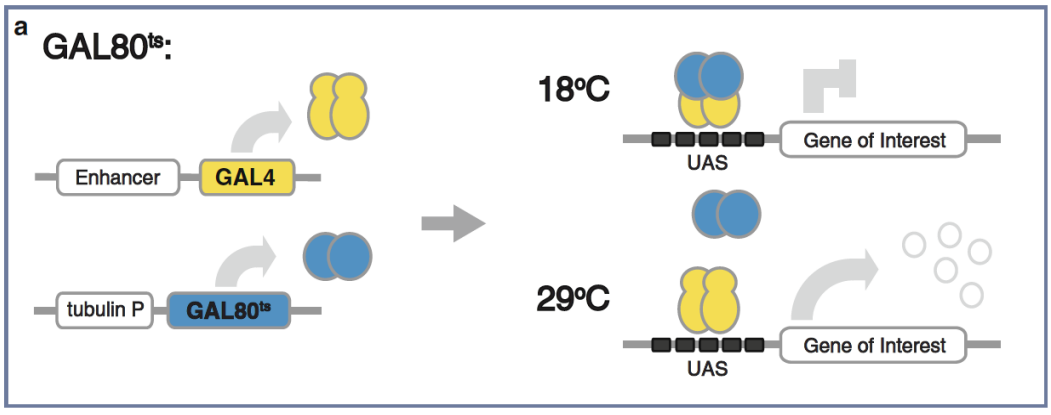

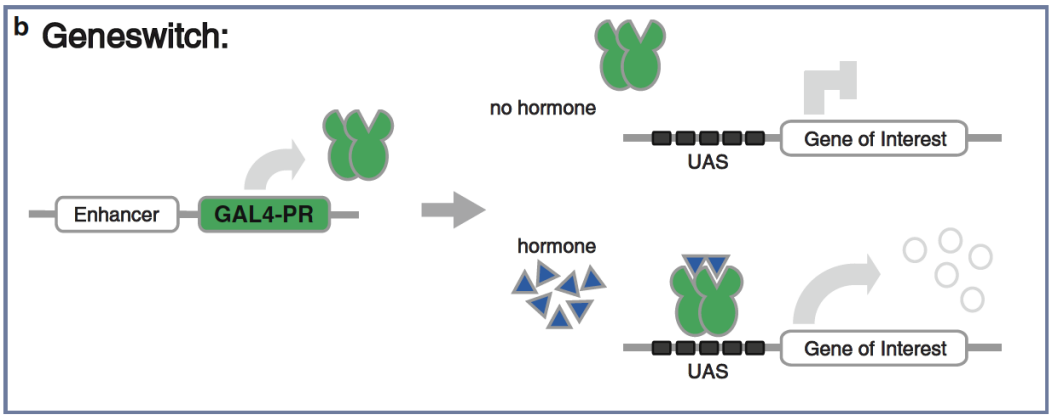


**Figure 1.10 Genetic modifications of the GAL4 system to obtain spatiotemporal control of gene expression.** (a) Ubiquitously expression of temperature- sensitive allele of GAL80 (tubGAL80$^{ts}$ ) will inhibit GAL4 activity at the permissive temperature of 18 °C. At the restrictive temperature of 29 °C GAL80$^{ts}$ cannot bind GAL4 to inhibit it, therefore allowing GAL4-dependent transgene expression. (b) The GeneSwitch system is an example of ligand- inducible GAL4. Fusion of the GAL4 DNA binding domain to the ligand-binding domain of the progesterone receptor results in GAL4 activity only in the presence of the drug RU486/Mifprestone. Illustrations adopted from: Caygill and Brand, 2016. DOI 10.1007/978-1-4939-6371-3_2

Hence, the promoter will be activated by Gal4 binding and the candidate gene of interest will be expressed wherever Gal4 is expressed. Then, the GAL4-UAS system has another modification which is the introduction of a temperature sensitive version of the Gal4 repressor a Gal80 protein that represses Gal4 at permissive temperature (18ºC) but allows Gal4 expression upon shift to a higher temperature (25-29ºC). This method allows for spatiotemporal control of gene expression such that other tissues where the gene of interest is expressed are not affected and the phenotype results from the specific manipulation of gene expression where the Gal4 is expressed. This system can be extended for clonal analysis by the introduction of *UAS-flp Act>CD2>Gal4*). This introduction of a sequence encoding for flippase enzyme flips a stop codon cassette spaced between the Act and Gal4 sequence, allowing the ubiquitous expression of actin-driven genes thereafter[8]. Enhancers used for the Gal4 conditional systems include *esg* expressed in progenitor cells, *esg$^{ts}$ Su(H)Gal80* expressed in ISCs, *Su(H)* expressed in enreroblasts, *Myo1A* expressed in enterocytes, *pros* expressed in enteroendocrine cells and *how* expressed in visceral muscle. A different modification of the Gal4 system includes GeneSwitch GAL4 system which replaces the traditional Gal4 with chimeric

Gal4 protein, that it is activated only in response to feeding with the hormone analog mifepristone/RU486[284].

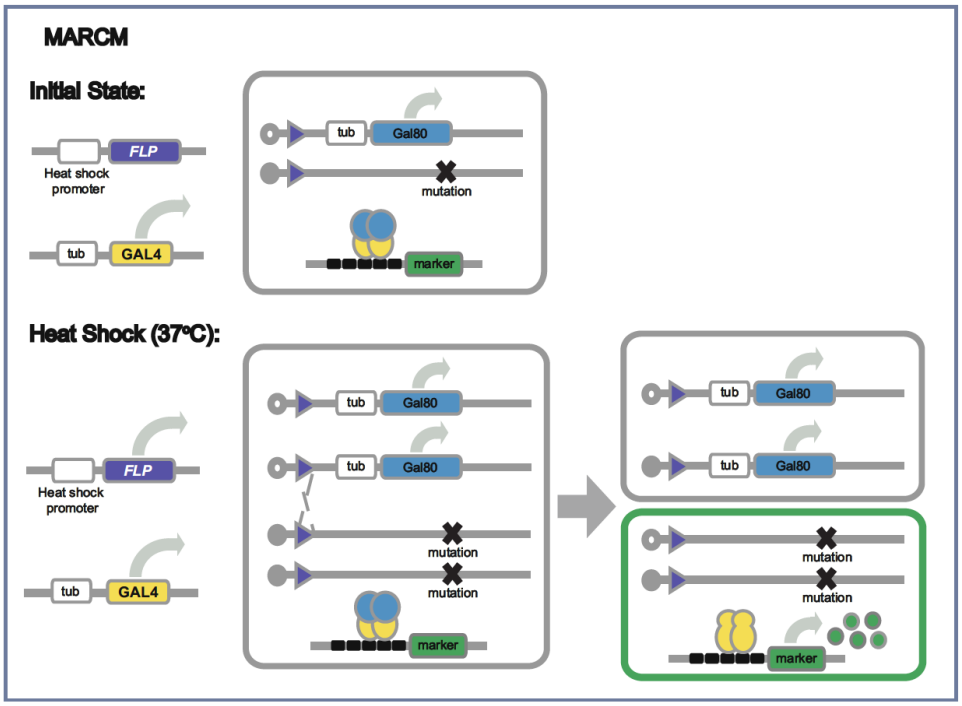


**Figure 1.11 Mosaic Analysis with a Repressible Cell Marker (MARCM) uses FLP/FRT system to generate loss-of- function clones.** Both GAL4 and GAL80 are ubiquitously expressed from the tubulin promoter, which causes the repression of the GAL4-inducible marker. Heat shock at 37°C induces expression of FLP recombinase that catalyzes recombination between FRTs on homologous chromosomes carrying either the mutation of interest or a tubGAL80 construct. GAL80 segregates from the mutation into different daughter cells, one that inherits two copies of the tubGAL80 and remains wildtype and the other that carries the mutation on the two chromosome arms i.e. homozygous mutant cell. GAL4 labels these mutant clones. Illustrations adopted from: Caygill and Brand, 2016. DOI 10.1007/978-1-4939-6371-3_2

Alternatively, to analyze the function of impaired a small subset of cells in otherwise phenotypically wild-type organism, A MARCM (mosaic analysis with a repressible cell marker) system can be used to label homozygous mutant cells uniquely in mosaic tissues, In MARCM, initially, all cells are heterozygous for transgene encoding Gal80, which keeps the Gal4 activity inhibited. Then, FLP/FRT-mediated mitotic recombination takes place as the cells receive the stimulus to divide resulting in one daughter cell that expresses 2 copies of Gal80,and another cell that is devoid of Gal80, instead allowing the

expression of a Gal4-driven membrane-targeted green fluorescent protein (GFP) (mCD8-GFP). Usually, a mutation is located on the chromosome arm *in-trans* to the chromosome arm containing the Gal80 transgene, the uniquely labeled Gal80-negative (Gal80−) cells should be homozygous for this mutation. Hence, homozygous mutant cells become labeled in a mosaic tissue[285].

# Results

The text of the following section (**Results**) has been taken and strongly modified from (Ahmed et al., 2020) and has been originally written by myself:

### 2.1. 20HE induces ISC proliferation in male and female guts.

To study the effects of steroid hormones on the gut, I first hypothesized that exogenous exposure of flies to steroids will be absorbed by the fly gut, similar to the human studies[265,277]. Therefore, I added 20HE to high sucrose, low yeast food or standard fly food and I fed the flies overnight between 16hrs to 22hrs, then I assayed actively dividing ISCs/midgut by phospho-Ser10-histone 3 staining. I used enteric infection with *Pseudomonas entomophila* (*P.e.*) as a positive control that is known to cause strong ISC proliferation in mated females but not in males[118] (Fig 2.1.1a). In contrast, I discovered that exogenous overnight feeding of 20HE induces ISC division in midguts of males or mated females regardless of the nutrient composition (Fig 2.1.1a,c). Next, I used the intestinal lineage-tracing system *esg-FlipOut* (*esg$^{ts}$-FO*) that marks ISCs and their resulting progeny by GFP[41]. Feeding 5mM 20HE overnight resulted in ISC division accompanied by clonal expansion and growth in the midgut of both sexes, though the clonal expansion was more prominent in females (Fig 2.1.1b).

20HE is known to act through the EcR•Usp complex, whereby 20HE binds the EcR•Usp complex, activating it to modulate target gene expression. To test if 20HE acts through EcR•Usp complex in the midgut and whether this effect is strictly ISC-autonomous or not, I used temperature sensitive esgGal4 tub-Gal80ts (*esg$^{ts}$*) driver to deplete either EcR or Usp specifically in progenitors. The robust 20HE induced ISC divisions in control flies were efficiently blocked when EcR or Usp was knocked-down in either males or females indicating that 20HE acts cell-autonomously through midgut progenitors (Fig 2.1.1c,d). I

validated the results by an independent/isoform specific RNAi line (Fig 2.1.1e-f) or ectopic misexpression of dominant negative EcR isoform (Fig 2.1.1g-h).

In both cases, I have used *P.e.* as a positive control but I will explain and refer to these results in a later section. Additionally, I used the MARCM system to generate GFP-marked ISC clones homozygous for depleted EcR levels[285]. Consistent with the RNAi results, MARCM EcR depleted ISC clones failed to divide under basal conditions and after 20HE-feeding. In both cases, they mostly remained less than 10 small cells/clone (Fig 2.1.2c-d).

EcR has 3 prominent isoforms: EcR A, EcR B1 and EcR B2 that are reported to regulate target gene expression differently[159,286,287]. In an attempt to figure out which isoform is functional in ISCs of the gut, I used dominant negative (DN) isoforms to mis-express EcR A or B1. Ectopic expression of DN EcR A in progenitors competes with endogenous EcR A and blocks 20HE induced mitoses (Fig 2.1.1g-h). Additionally, I used isoform specific UAS-RNAi constructs to deplete EcR A or EcR B in progenitors and fed the flies overnight with 5mM 20HE then I scored ISC-mitoses. I found that EcR A depletion blocks the 20HE-induced mitoses while EcR B depleted progenitors show a minor defect in their division rates relative to control ISCs (Fig 2.1.1f).

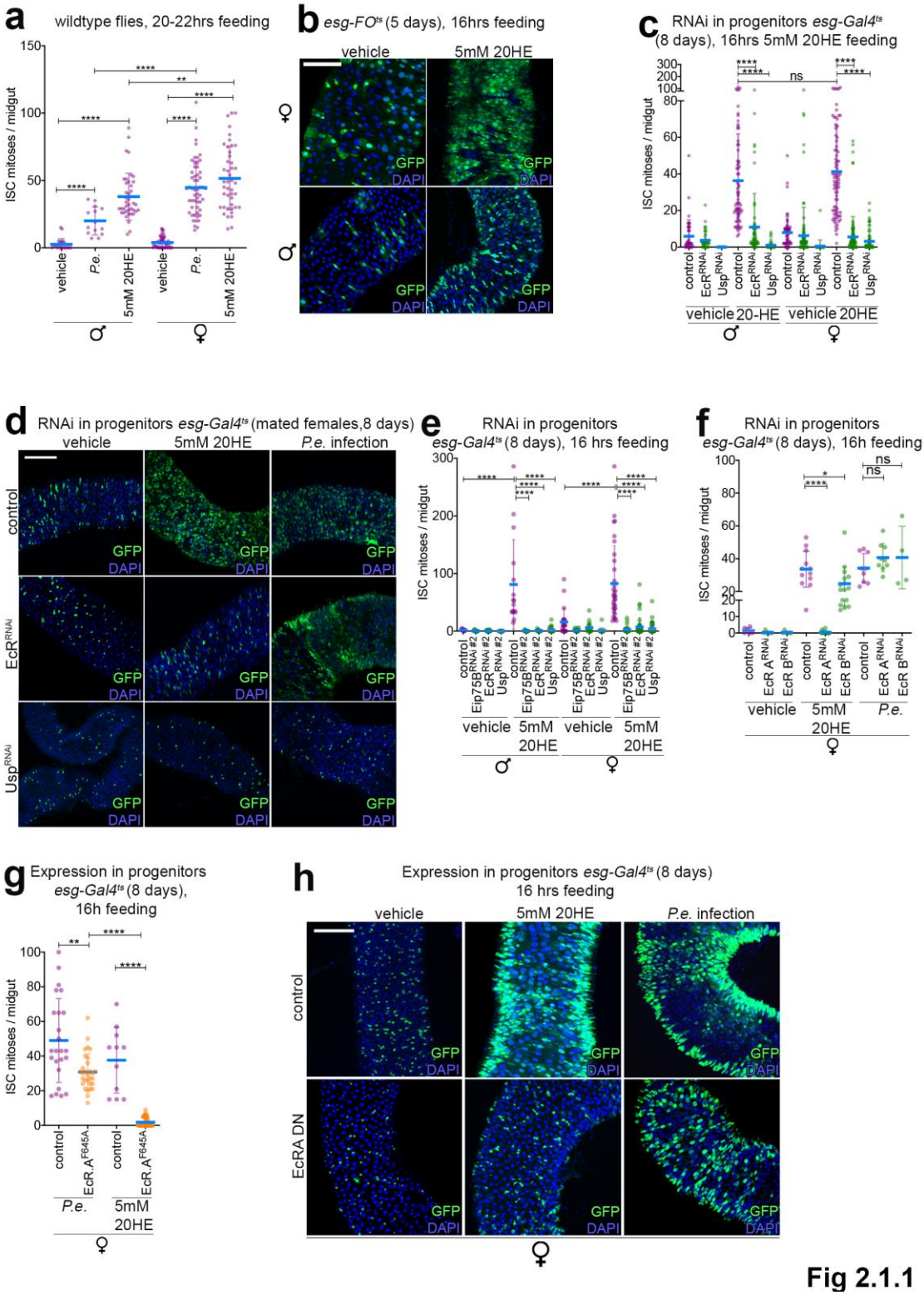
a
wildtype flies, 20-22hrs feeding
ISC mitoses / midgut
vehicle
P.e.
5mM 20HE
♂
♀
b
esg-FO^ts (5 days), 16hrs feeding
vehicle
5mM 20HE
GFP
DAPI
c
RNAi in progenitors esg-Gal4^ts (8 days), 16hrs 5mM 20HE feeding
ns
control
EcR^RNAi
Usp^RNAi
vehicle 20-HE
d
RNAi in progenitors esg-Gal4^ts (mated females,8 days)
vehicle
5mM 20HE
P.e. infection
control
EcR^RNAi
Usp^RNAi
e
RNAi in progenitors esg-Gal4^ts (8 days), 16 hrs feeding
Eip75B^RNAi #2
EcR^RNAi #2
Usp^RNAi #2
f
RNAi in progenitors esg-Gal4^ts (8 days), 16h feeding
EcR A^RNAi
EcR B^RNAi
g
Expression in progenitors esg-Gal4^ts (8 days), 16h feeding
control
EcR.A^F645A
h
Expression in progenitors esg-Gal4^ts (8 days) 16 hrs feeding
EcRA DN

**Fig 2.1.1**

**Figure 2.1.1: 20HE promotes ISC division through EcR A/Usp cell autonomously in male and female progenitors.** Text and images have been taken and modified from (Ahmed et al., 2020) and have been originally written and made by myself: (a) Midguts from adult wildtype animals were treated for 20 hrs with enteric infection with *Pseudomonas entomophila* (*P.e.*) bacteria or 5mM 20HE exogenous feeding on low yeast diet overnight. Midguts were scored for phospho-histone3+ mitotic ISCs per time point. Males ISCs modestly divide while female ISCs divide strongly in response to *P.e.* infection. Both males and females had strong mitotic counts upon exogenous 5mM 20HE feeding. I have produced the female data of this panel during my master's study and I used it in my master's thesis as well, Sara Ahmed,2015[464].
(b) Using ISC lineage tracing tool, *esgFO$^{ts}$*. clonal growth was assessed such that GFP labels ISCs as well as their progeny. Upon 18-20 hrs 20HE feeding, females had a vast turnover in their epithelium whereas males had a slightly moderate turnover in their epithelium reflected by the mild increase in the GFP$^{+}$ cells. This result shows that exogenous 20-HE boosts ISC mitoses and ISC clonal growth.
(c-d) EcR and Usp are cell-autonomously required in progenitors for 20HE-induced mitoses c) Mitotic counts of *EcR$^{RNAi}$* and *Usp$^{RNAi}$* male and females progenitors fed with 20HE overnight. d) EcR is not required for *P.e.*-induced ISC mitoses unlike Usp. Representative confocal images of the R4 region in the posterior midgut of mated females. Mated females were fed with exogenous 20HE, infected with *P.e.* for 20-22 hrs. I have produced the female data of this panel during my master's study and I used it in my master's thesis as well Sara Ahmed,2015[464].
(e) Mitotic counts of 20HE-fed *EcR$^{RNAi}$*, *Usp$^{RNAi}$*, *Eip75B$^{RNAi}$* (EcR-downstream target) male and females progenitors. Results are shown for an alternative independent RNAi line.
(f) 20HE through isoform EcR-A but not EcR-B mediates ISC division. Progenitor specific depletion of *EcR-A$^{RNAi}$* and *EcR-B$^{RNAi}$* shows that EcR-A mainly, and to a much lesser extent EcR-B is required in progenitors for their 20HE-induced ISC response 18 hrs after feeding. Depletion of EcR-A or EcR-B did not affect the strength of *P.e.*-induced ISC mitoses relative to age-matched controls.
(g-h) (g) Expression of EcR A dominant negative isoform inhibits the ISC proliferative response to 20HE but not to enteric infection 18-20 hrs after feeding. (h) Representative images of progenitors expansion following 20HE feeding indicative of ISC proliferation in control mated females, which is restricted by expression of EcR A DN in progenitors. Progenitors of control mated females or with EcR A DN misexpression expand across the epithelium to replace lost cells after infection.

To check the requirement of EcR-specific isoform in basal ISC mitoses, I induced ISC clones with EcR A or B DN expression and I let the clones form under non-stressed basal conditions. ISC clones with EcR A DN expression have impeded growth. While, ISC

clones with EcR B DN induces a full epithelial turnover accompanied with mild hyperplasia of the gut at 3 days after clonal formation (Fig 2.1.2a-b). Hence, my results indicate that EcR isoform A is the main functioning receptor partner that forms a complex with Usp in the ISCs of the midgut to regulate target gene transcription.

To further validate my findings, I checked the pattern of 20HE activation. I used EcR.LBD >GFP ligand trap reporter flies [186,288] that express GFP in cells with active 20HE signaling. The ‘‘ligand/sensor trap’’ system consists of the DNA-binding domain of yeast GAL4 (hs-Gal4>) fused to the nuclear receptor ligand-binding domain (LBD) under control of a heat-shock inducible promoter.

The expression of the fusion protein binds a UAS-controlled GFP reporter gene. Heat shock in these transgenic flies will drive ubiquitous expression of the transgenic fusion proteins only when the ligand is present, it will bind to the Gal4 fusion protein and activate the UAS-GFP reporter expression. As the active protein binds a UAS-linked GFP, nuclear GFP expression is induced[186]. Additionally, I labeled delta (ISC marker) positive cells or Su(H) (EB marker) positive cells. After 20HE feeding, I detected active 20HE signaling in many ISC singlets, ISC doublets and in fewer enteroblasts of both males and females (Fig 2.2e-h). Remarkably, 20HE feeding activated EcR signaling in delta$^{+}$ ISC pairs in the midguts of both males and females, suggestive of symmetric ISC division[12]. This finding is particularly intriguing because most instances of reported ISC mitoses in the *Drosophila* midgut occur in the asymmetric mode of division[5,93].

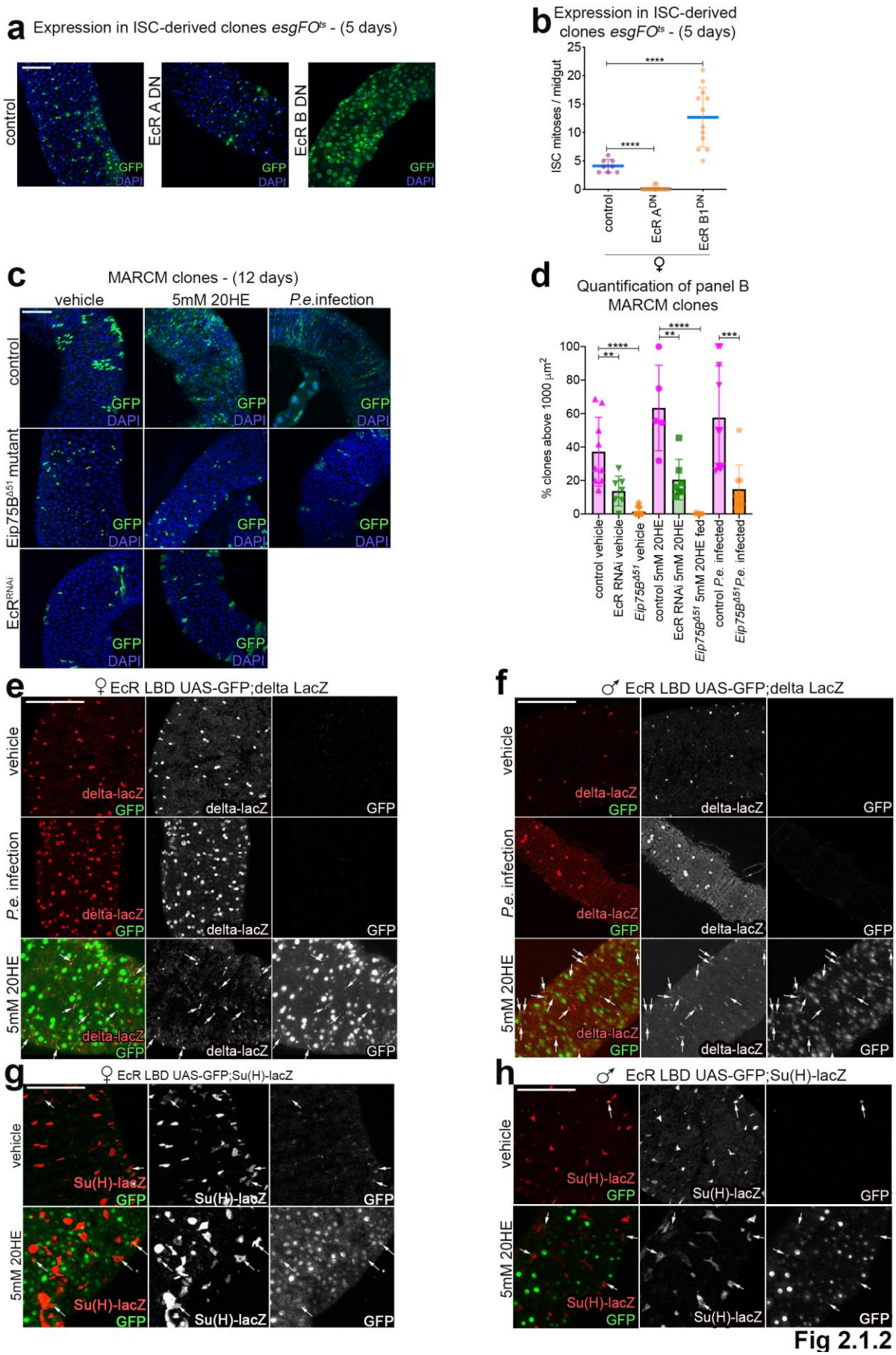


Fig 2.1.2

**Fig 2.1.2 20HE feeding to male and female flies require EcR and Eip75B to activate**

**EcR LBD reporters in symmetrically and asymmetrically dividing ISCs.**

Text and images have been taken and modified from (Ahmed et al., 2020) and have been originally written and made by myself: (a) EcR isoform A but not B is required for driving intestinal hyperplasia in mated females as shown by representative images of the posterior midgut of mated females expressing EcR A DN or EcR B DN. EcR isoform A but not isoform B is required for ISC-derived epithelial turnover.
(b) ISC-derived clones with low levels of EcR A have impaired basal ISC mitoses. ISC mitotic counts were quantified after expressing different EcR dominant negative isoforms in mated female midguts.
(c-d) (c) EcR depleted and the ecdysone-inducible target Eip75B mutant clones fail to divide after 20HE feeding. Eip75B mutant clones fail to regenerate the epithelium after enteric infection. Representative images of MARCM ISC clones that were generated through heat shock induction and the R4 region of the posterior midgut was examined 12 days after clonal induction. Vehicle-fed control clones were multicellular and spread throughout the epithelium but, EcR depleted clones were considerably small, mostly between 2-4 cells and rarely up to 10 small cells/clone and Eip75B mutant ISC clones mostly remained single-celled clones. After 16hrs of 20-HE feeding, the epithelium is populated with newly formed cells within the control clones however, Eip75B mutant and EcR depleted ISC clones failed to promote ISC division. Upon enteric infection, Eip75B mutant clones minimally divide to give rise to clones with ≤10 cells in contrast to control clones. (d) Quantification of panel k by a macro designed to assess clonal sizes/maximum Z projection. (see methods).
(e-h) 5mM 20-HE feeding caused a strong increase in the activity of EcR reporter indicated by increased GFP expression in the posterior midgut Males or mated females of the genotypes Gal4.DBD-EcR.LBD>GFP (Gal4-EcR>GFP) were heat shocked for 30 min, infected with *P.e.*, fed with 5mM 20HE or vehicle and dissected 18-20hrs later. These GFP ligand traps express GFP under the control of heat-inducible promoter and mark cells with active 20HE signaling. When fed with vehicle, Gal4-EcR>GFP is expressed in few cells in the R4 region posterior midgut (image shown) and in a lot more in the anterior midgut (image not shown). White arrows indicate cells that are double positive for delta or Su(H) lacZ markers. GFP was expressed in many $delta^{+}$ cells (panels m,n) and much fewer $Su(H)^{+}$ (panels o,p) of both males and females upon 5mM 20-HE feeding. The majority of the remaining positive cells are enterocytes. Upon 20 hrs of *P.e.* infection, GFP signal disappears from males and females guts indicating that EcR does not play a role in infection-induced stress response (panels m,n).

**2.2. 20HE acts independent of the sex-determination pathway.**

In *Drosophila*, the cell-intrinsic sex determination pathway controls growth and metabolism through differential sex-biased expression of splicing factors[118]. Accordingly, females express sex lethal (sxl) and transformer (tra), the master regulators of both sexual development and dosage compensation. Presence of sxl and tra activates a "feminized" epi-/genetic landscape in the ISC that cell-autonomously controls ISC division[118]. When virgin females are challenged with SDS or enteric infection with *P.e.*. ISC proliferation increases in control virgin females, and this is blunted when ISCs are masculinized through sxl or tra depletion (Fig 2.2a)[118], partly explaining the difference in the ISC behavior between males and females. I then hypothesized that the hormonal differences in 20HE titers between males and females would act as an additional non-cell autonomous signal that influences ISC proliferation, independent of the sex identity. To test the former, I fed tra-depleted virgin female flies with 5mM 20HE overnight and found that it strongly induced ISC divisions at similar rates to control virgins (Fig 2.2a) accompanied by a fast epithelial turnover represented by the numerous GFP+ progenitors populating the posterior midgut (Fig 2.2b). These results indicate that masculinized female progenitors remain competent to respond to the 20HE mitotic stimulus, partly simulating the competence of male ISCs to divide in response to 20HE. In turn, this evidence suggests that 20HE functions independently of the sex identity of the ISCs. Thus, a combination of ISC-autonomous and non-autonomous hormonal factors affect ISC proliferation.

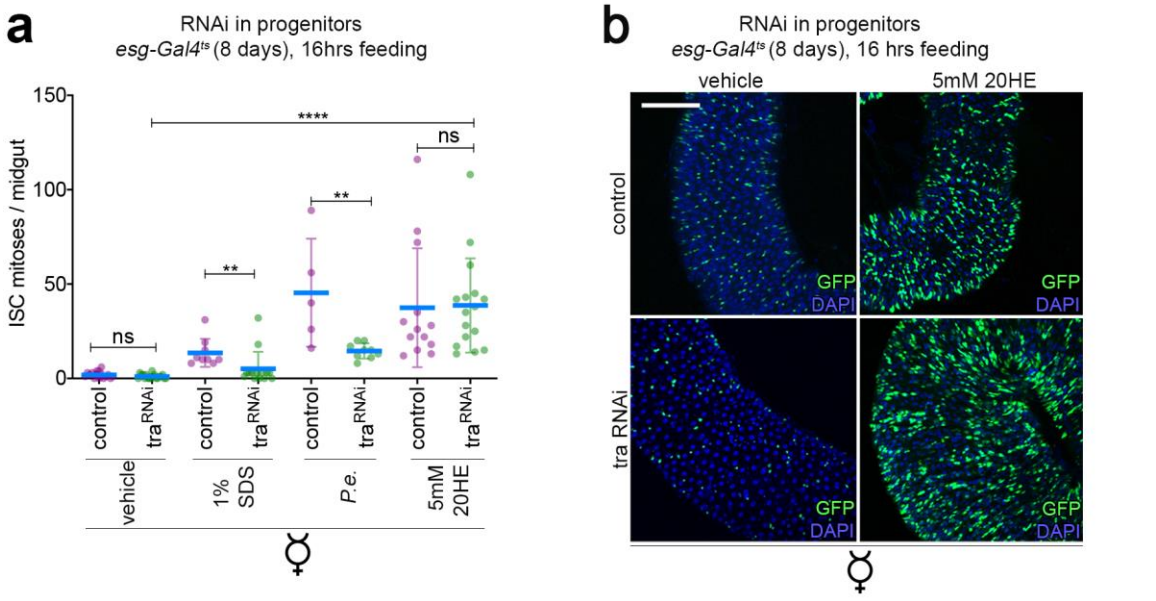


**Fig 2.2.**

**Fig 2.2 20HE induces ISC mitoses independent of the ISC-intrinsic sex determination pathway.** Text and images have been taken and modified from (Ahmed et al., 2020) and have been originally written and made by myself: (a-b) Masculinized progenitors (ISC+EB) exhibit impaired mitoses in response to *P.e.* or SDS, but not to exogenous 20HE. (a) Mitotic counts of $tra^{RNAi}$ treated virgin progenitors after 16-18 hrs *P.e.* infection, 5mM 20HE or SDS feeding. (b) Representative images of expanding GFP-marked $tra^{RNAi}$-treated progenitors upon feeding with exogenous 5mM 20HE.

## 2.3. EBs provide pro-mitotic factors that non-cell autonomously regulate 20HE-induced mitoses.

In an attempt to figure out whether other midgut cell types besides the ISCs require EcR to signal for the ISCs to divide after 20HE feeding, I targeted the different midgut cell types using conditional, cell type-specific Gal4 drivers and multiple independent UAS-RNAi lines or dominant negative expression to check which cells require EcR for the 20HE-induced ISC mitoses. Mitotic counts revealed that ISCs cell autonomously require EcR and Usp for the 20HE-induced ISC mitoses (Fig 2.3a). Surprisingly, EcR depletion in enteroblasts also completely blunted the 20HE-induced ISC mitoses (Fig 2.3b). In contrast, the ISC divisions were only mildly compromised when EcR was depleted in enterocytes with RNAi or dominant negative expression (Fig 2.3c). Similarly, requirement of EcR in enteroendocrine cells for the 20HE-induced ISC mitoses was rather marginal (Fig 2.3d). As some cells of the nervous system also express esg[289], I validated if EcR is required in those cells for the intestinal 20HE-induced mitoses. Expression of a pan-neuronal driver $elav^{ts}$ [290] did not alter the mitotic counts of dividing ISCs to 20HE feeding in EcR depleted neurons relative to control neurons (Fig 2.3e). Hence, cell-specific analysis of EcR function in the different cells revealed that EcR is unexpectedly important in enteroblasts as well as ISCs for 20HE's proliferative actions in the midgut, suggestive of cell-autonomous and non-autonomous roles of EcR.

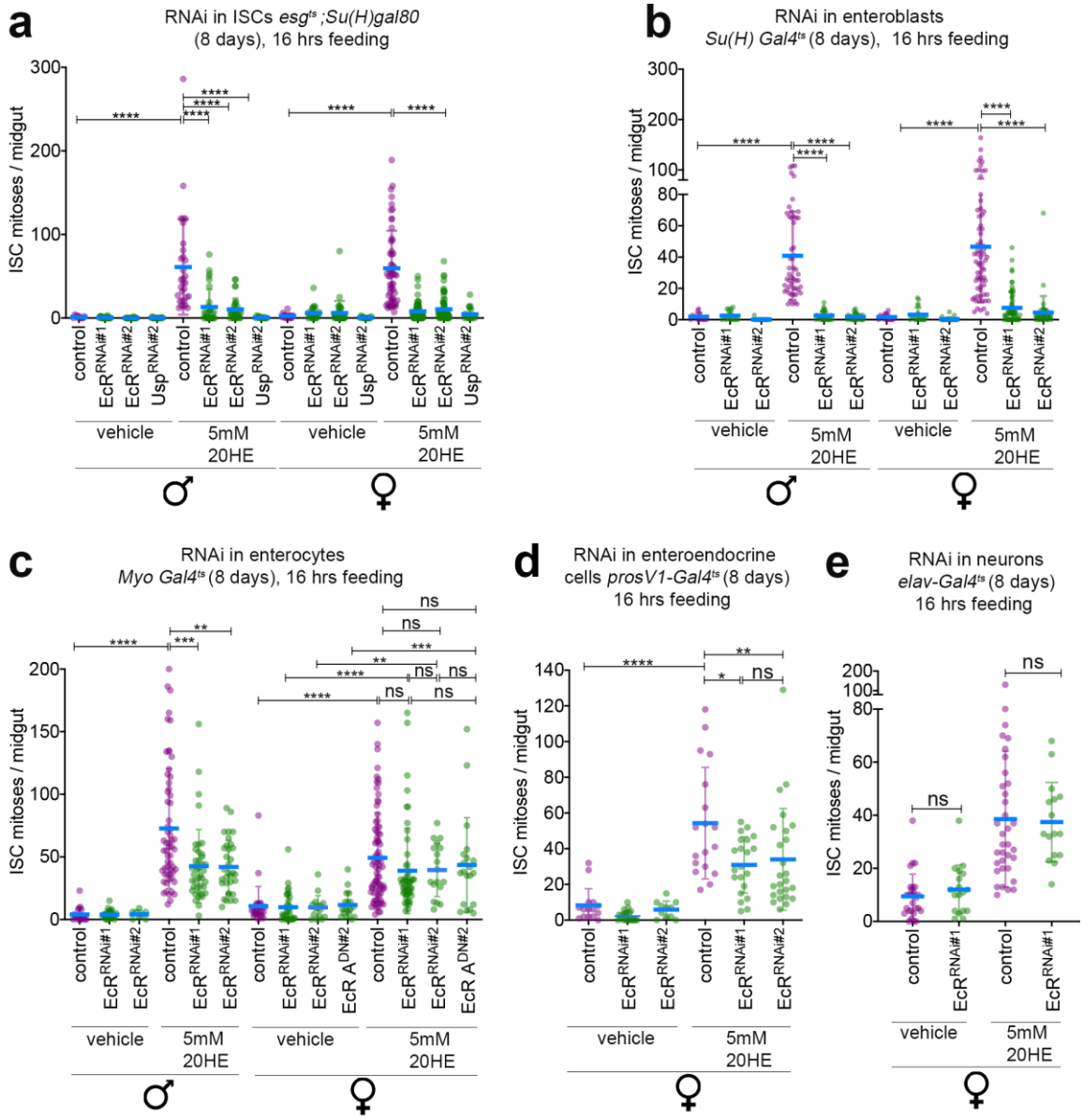


**Fig 2.3.**

**Fig 2.3 The mitotic wave of 20HE feeding at 16-18 hrs requires EcR and Usp in enteroblasts.** Text and images have been taken and modified from (Ahmed et al., 2020) and have been originally written and made by myself: (a) Both EcR and Usp are required by the ISCs for the 20HE induced-mitoses. Scored mitotic counts after 16-18hrs of 20HE feeding show diminished ISC mitoses upon 5mM 20-HE feeding in males and mated females midguts with ISC-specific $EcR^{RNAi}$ or $Usp^{RNAi}$. Results shown are for 2 different RNAi lines.

(b) EcR is required by the enteroblasts for promoting the mitoses induced by 16hrs of 20HE feeding. ISCs cannot divide after 20HE feeding when enteroblasts lack EcR in males and mated females. Results shown are for 2 different RNAi lines. This experiment

indicates that EcR is required non-cell autonomously in EBs for 20HE induced ISC divisions.
(c) EcR is marginally required in enterocytes for peak induction of ISC mitoses 16 hrs after 20HE feeding. ISC mitoses to 20HE are slightly compromised relative to controls when EcR levels are reduced in enterocytes. Results shown are for 2 different RNAi lines for both males and females, and dominant negative isoform of EcR in females. This indicates a non-cell autonomous requirement of EcR in ECs to induce optimal ISC mitoses in response to 20-HE.
(d) EcR in enteroendocrine cells plays a minimal role in 20HE-induced ISC mitoses of the male and female midguts. Enteroendocrine cells-specific $EcR^{RNAi}$ slightly compromises 20HE-induced ISC mitoses indicating that EcR in enteroendocrine cells is rather dispensable to 20HE-induced ISC mitoses. Results are shown for 2 different RNAi lines.
(e) EcR in the central nervous system neurons is not required for 20HE-induced ISC mitoses of the midgut. $Elav^{ts}$; that is a pan-neuronal driver for the adult central nervous system was used to induce $EcR^{RNAi}$. Mitotic counts show that EcR depletion in the CNS did not alter the ISC division rates relative to control females. The period of RNAi induction is indicated above every panel. Results are from 3 or more pooled independent experiments. N≥10, for each genotype in the scatter plot. Error bars represent ± SD. Statistical analysis was performed using unpaired non-parametric two-tailed Mann-Whitney test (*p≤ 0.05,**p≤0.01,***p≤0.001, ****p<0.0001). The overnight standard period of feeding the flies was 16-20 hours. ♂ refers to males and ♀ refers to mated females.

## 2.4. 20HE induces ISC mitoses in 2 distinct waves, ISC autonomous then ISC non-cell autonomous wave.

The intriguing observation that EcR in EBs contributes to the 20HE-induced mitoses had led us to question the cell-autonomous role of ISCs after 20HE feeding and I attempted to examine if there is a period of the proliferative response where EcR is exclusively and initially required only in ISCs. If EcR is always required in the EBs to signal to the ISCs to divide then it means that the only ISCs with intact EcR would never divide to the mitotic stimulus of 20HE feeding. It also would suggest that the 20HE-induced mitoses are not a direct consequence of 20HE feeding but rather a secondary effect of the EBs sensing increased levels of 20HE in the midgut. So, I tried a time course feeding of 20HE to mated female flies and I scored the mitoses/midgut at 5 different time points. Strikingly, I discovered an early peak of 20HE-induced ISC mitoses that starts at 6hrs and

it blunts already by 9hrs then ISC division peaks again by 16hrs until 22hrs after feeding (Fig 2.4a), (compare to Fig 2.1a). Strikingly, when males were fed with 20HE for 6hrs their ISCs barely divided, whereas female ISCs had been dividing already albeit at slightly lower levels relative to 16hrs (Fig 2.4b). This could be due to biological variability in the potency of 20HE to induce ISC mitoses or that those flies particularly did not eat so much 20HE by 6hrs relative to ones in Fig2.4a. This is quite spectacular because the male ISCs seem to either have delayed or skipped initial ISC mitoses at 6hrs but then they become equally competent to female ISCs in their divisions after 20HE feeding. This finding goes in line with the evidence suggesting sex specific differences in the proportions of ISCs in the different cell cycle phases[118].

After revealing the earlier peak of 20HE-induced ISCs mitoses in females, I tried to figure out if EcR in enteroblasts contribute to that phase as well. Hence, I depleted EcR specifically in the progenitors (ISCs+EBs) or enteroblasts and then fed mated females with 20HE for 6 hrs (first mitotic peak) or 16 hrs (second mitotic peak). Progenitor-specific reduction of endogenous EcR suppressed ISC mitoses at both time points, because the ISCs have reduced EcR levels. In contrast, depletion of EcR in enteroblasts had no effect on the ISC mitoses during the 1$^{st}$ mitotic peak but it blocked ISCs from dividing again at 16 hrs (Fig 2.4c). Hence, I was able to conclude that in females 20HE through EcR induces an ISC autonomous mitotic phase early after exposure, and then induces an ISC-non-cell autonomous mitotic phase that requires signals from enteroblasts.

Next, I wanted to check whether the kinetics of ISC response is similar to other pro-mitotic stimuli in the intestine (supplementary fig 1c in [291]), (supplementary fig 4[292]). Thus, I did a time course of SDS feeding and I scored the mitoses at 3 different time points (compare to Fig 2.2c). Mitotic count analyses revealed that SDS-induced mitoses are detected by 6hrs of feeding however, unlike 20HE, the mitoses are extended over the assayed different time points (Fig 2.4d) (compare to Fig 2.2c). Upon provoking the midgut with different mitotic stimuli i.e. *P.e.* infection, detergent-induced stress that cause ISC divisions, the dynamics of the ISC mitoses are relatively extended over a time period ranging from 6 hrs to 48 hrs. Unlike, 20HE feeding, which causes at least a biphasic response of ISC mitoses, a unique behavior of 20HE-fed ISCs.

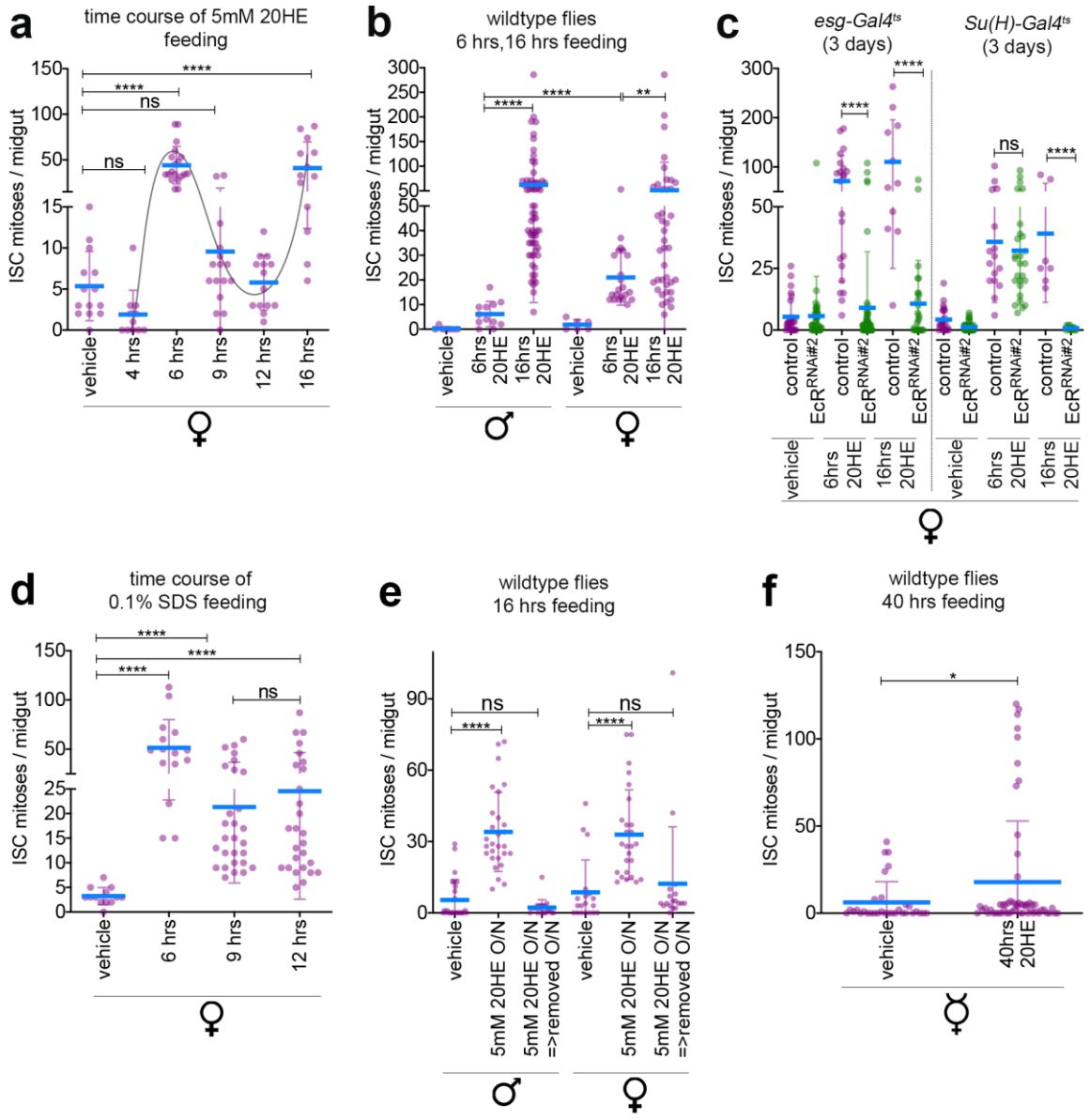


**Fig 2.4.**

**Fig 2.4 20HE induces ISC mitoses in a bi-phasic manner.** Text and images have been taken and modified from (Ahmed et al., 2020) and have been originally written and made by myself: (a) 20HE induces 2 successive waves of ISC division, the first at 6hrs and the second at 16hrs. ISC mitotic counts of control mated females fed with 5mM 20HE for different durations.

(b) At 6hrs, male ISCs unlike female ISCs fail to divide upon 20HE feeding, however, at 16hrs, both male and female ISCs are equally competent to divide in response to 20HE feeding. ISC mitotic counts of control males or mated females fed with 5mM 20HE for 6hrs or 16hrs.

(c) EcR is required in ISCs but not EBs during the 1$^{st}$ mitotic wave at 6hrs. However, EcR is required in both ISCs and EBs for the 2$^{nd}$ mitotic wave. ISC mitoses in midguts

expressing $EcR^{RNAi}$ in progenitors (left) or enteroblasts (right) after 6 or 16hrs of exogenous 20HE feeding. RNAi was induced for 3 days before 20HE feeding. ISCs of control and EcR depleted enteroblasts divide at equal rates at 6 hrs. Midguts with EcR depleted enteroblasts have diminished ISC mitoses by 16hrs.
(d) ISCs start dividing by 6 hrs and the ISC mitoses extend over a period of at least 12hrs. ISC mitotic counts of control mated females fed with 0.1% SDS feeding.
(e) 20HE induces ISC mitoses briefly then mitoses return to basal levels, quantified by mitotic indices of male and female wildtype flies subjected to 2-day treatment regimes. ISC proliferation was restored to basal levels after 5mM 20HE was withdrawn, suggesting that 20HE's actions are not detrimental. Male and female flies were fed vehicle or 20HE in different successions such that flies were exposed for 20hrs to the first treatment, then for another 24hrs to the second treatment. ISC mitoses returned to basal levels after 16-20hrs treatments with 20HE then vehicle.
(f) 20HE-induced mitoses returns back to basal levels within 40hrs of feeding. Virgin females were fed with 5mM 20HE and ISC mitoses were scored after 40hrs. ISC mitoses stimulated at 16hrs of feeding (refer to Fig 2.14) subside to basal mitoses by 40hrs.
Statistical tests performed by unpaired non-parametric two-tailed Mann-Whitney test (ns $p>0.05$, **$p\leq0.01$,***$p<0.001$, ****$p<0.0001$). ♂: males. ♀: mated females.

Stress stimuli such as bleomycin feeding or *P.e.* enteric infection are known to cause massive ISC divisions for at least 48hrs[8,293]. Injury stimulated expansion of ISCs such as combined bleomycin and heatshock treatments can recover back to basal levels, although not entirely after 72 hrs of recovery[292]. Hence, I asked whether 20HE similarly ISC mitoses. So, I fed the flies overnight with 20HE then removed it for another 16-18hrs after which I scored mitotic counts. The 20HE induced ISC mitoses quickly subsided and returned to basal levels similar to mock-fed males and females (Fig 2.4e). In a separate set of experiments, I subjected female virgins to 20HE for 40hrs (Fig 2.4f) during which the flies were constantly feeding on 20HE, yet the 20HE-induced ISC mitoses were very low and almost comparable to basal ISC mitoses. The former finding indicates that the 20HE-mitotic effect is readily reversible while the latter finding supports the biphasic manner of 20HE-induced mitoses observed in Fig 2.4a.

**2.5.1-3 20HE induces ISC mitoses cell autonomously through EGF signaling and unpaired cytokines in the first peak then unpaired cytokines are required in EBs or ECs non-cell autonomously to induce ISCs mitoses in the second peak.**

To find out how 20HE causes ISCs to divide, I first asked which targets are being transcriptionally upregulated after 20HE, then I tested several reporters of some critical pathways involved in stress-inducible ISC mitoses[8,41]. Finally, I continued to functionally deplete the targets via RNAi or whole body mutants when available. According to previous reports, stress-induced damage to the epithelium causes EGF ligands and unpaireds 2,3 (Jak-Stat) ligands production mainly from the ECs and to a lesser extent from the EBs that in a positive feedback loop stimulate compensatory ISC division[294]. In contrast, what I found is that the 20HE-induced ISC mitoses in the 1$^{st}$ wave at 6hrs initially require EGFR signaling and maybe upd2 from the ISCs. Then, 20HE feeding requires and regulates both upd2 in EBs and ECs and to a lesser extent upd3 in the progenitors for the 2$^{nd}$ wave of mitoses at 16-18hrs to occur (Fig 2.5.3c). When the cell cycle and the initial mitoses are halted, upd2 and upd3-transcriptional upregulation does not occur in response to 20HE feeding. The novelty of these described results is in that they support a model[295] in which 20HE-induced ISC divisions is a primary not a secondary consequence of 20HE feeding.

To obtain the findings described above, I started by measuring endogenous induction of some of the well-studied signaling pathway components of Egfr and Jak-Stat signaling at an early time point after 20HE feeding (coincides with the first mitotic phase) and I used enteric infection as a positive control. I found that while *P.e.* infection caused mild upregulation of vein, keren Egf ligands, rho the protease cleaving them, it caused a drastic upregulation of upd2, upd3 and Socs36E in infected whole midguts (Fig 2.5.1a)[8]. In contrast, 20HE caused a mild increase of keren, spi, rho, very slightly upd2 but, unchanged upd3 and Socs36E mRNA levels (Fig 2.5.1a). Thus, I deduced that 20HE at its first mitotic phase of 6 hrs-post feeding regulates Egf signaling. Next, I noticed a very mild induction of upd2 at 6hrs and I wondered how is Jak-Stat signaling regulated by EcR in response to 20HE feeding.

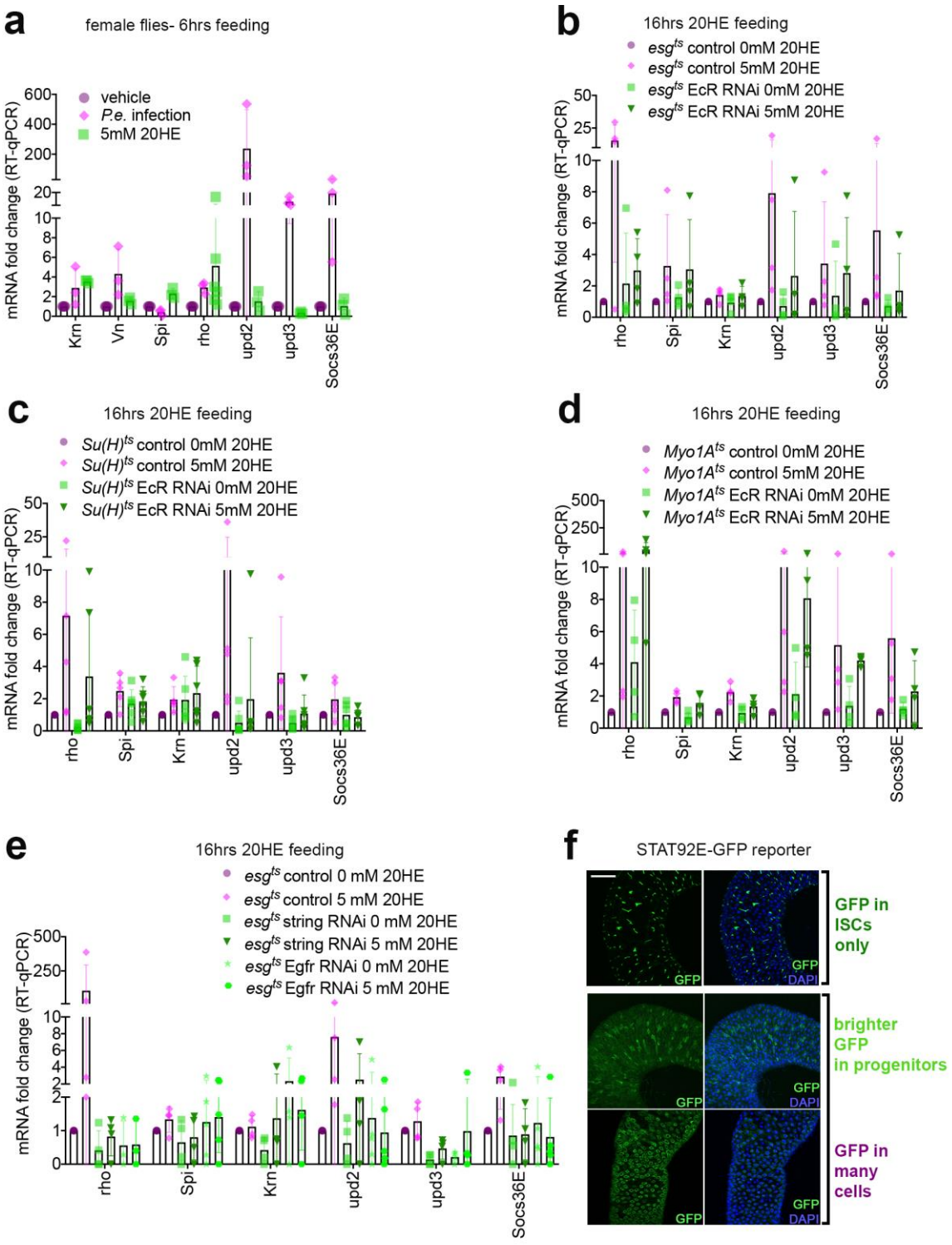
a
female flies- 6hrs feeding
vehicle
P.e. infection
5mM 20HE
mRNA fold change (RT-qPCR)
Krn
Vn
Spi
rho
upd2
upd3
Socs36E
b
16hrs 20HE feeding
esgts control 0mM 20HE
esgts control 5mM 20HE
esgts EcR RNAi 0mM 20HE
esgts EcR RNAi 5mM 20HE
c
16hrs 20HE feeding
Su(H)ts control 0mM 20HE
Su(H)ts control 5mM 20HE
Su(H)ts EcR RNAi 0mM 20HE
Su(H)ts EcR RNAi 5mM 20HE
d
16hrs 20HE feeding
Myo1Ats control 0mM 20HE
Myo1Ats control 5mM 20HE
Myo1Ats EcR RNAi 0mM 20HE
Myo1Ats EcR RNAi 5mM 20HE
e
16hrs 20HE feeding
esgts control 0 mM 20HE
esgts control 5 mM 20HE
esgts string RNAi 0 mM 20HE
esgts string RNAi 5 mM 20HE
esgts Egfr RNAi 0 mM 20HE
esgts Egfr RNAi 5 mM 20HE
f
STAT92E-GFP reporter
GFP
DAPI
GFP in ISCs only
brighter GFP in progenitors
GFP in many cells

**Fig 2.5.1**

**Fig 2.5.1 2nd mitotic wave of 20HE feeding regulates EGF and JAK-STAT signaling.** Text and images have been taken and modified from (Ahmed et al., 2020) and have been originally written and made by myself: (a) 20HE transcriptionally induces rho and spi or krn EGF ligands, but very mildly induces unpaired ligands relative to infected controls. Mated females were fed with 20HE or *P.e.* bacteria for 6 hrs. Midguts were extracted and the mRNA levels were analyzed by qRT-PCR, normalized to β-tubulin. Expression is indicated as mean fold change relative to vehicle-treated midguts ± SD (n≥3).
(b) Expression of rho, upd2 and STAT target Socs36E is transcriptionally upregulated through EcR in progenitors 16-18 hrs after 20HE feeding. Midguts were extracted and mRNA levels were analyzed by qRT-PCR, normalized to β-tubulin. Expression is indicated as mean fold change relative to vehicle-treated midguts ± SD (n≥3).
(c) Expression of rho, upd2 and STAT target Socs36E is transcriptionally upregulated through EcR in enteroblasts 16-18 hrs after 20HE feeding. Midguts were extracted and mRNA levels were analyzed by qRT-PCR, normalized to β-tubulin. Expression is indicated as mean fold change relative to vehicle-treated midguts ± SD (n≥3).
(d) $EcR^{RNAi}$ in enterocytes does not control the 20HE-induced transcriptional upregulation of rho, upd2 and Socs36E. Midguts were extracted and mRNA levels were analyzed by qRT-PCR, normalized to β-tubulin. Expression is indicated as mean fold change relative to vehicle-treated midguts ± SD (n≥3).
(e) Reduced EGF signaling through $Egfr^{RNAi}$ in progenitors or cell cycle arrest via $string^{RNAi}$ in progenitors blocks the 20HE-induced transcriptional upregulation of rho, upd2 and Socs36E. EFG signaling and cell cycle cell-autonomously control the subsequent induction of JAK-STAT signaling. Expression is indicated as mean fold change relative to vehicle-treated midguts ± SD (n≥3).
(f) Representative images of the STAT92E-GFP reporter phenotypes on chromosome II or III. Reporter activation is grouped into 3 different categories. Category: GFP in ISCs only has GFP expression in single ISCs and is labeled dark green. Category: brighter GFP in progenitors has GFP expression in doublets and is labeled bright green. Category: GFP in many cells has GFP expression diffuse throughout most cells. GFP, in green; DAPI, in blue. Scale bar, 100 μm.

The following experiments were all done at the time point that coincides with the 2nd mitotic phase of ISCs to 20HE feeding and it is the time point where I observed the most transcriptional induction of upd2. To investigate how EcR regulates Egf and Jak-Stat signaling components, I proceeded with cell-specific depletion of EcR (in progenitors, enteroblasts or enterocytes) and I measured transcriptional induction of the same targets I used earlier. 16 hours post feeding, 20HE caused rho, upd2, modest upd3 and Socs36E induction, which is dependent on EcR in progenitors (Fig 2.5.1b). Although, there was a mild increase in spi and keren ligands, it did not seem to be regulated through EcR in

progenitors. Enteroblast-specific *EcR*$^{RNAi}$ blocked the 20HE-induction of rho, upd2, upd3 and Socs36E (Fig 2.5.1c). In contrast, enterocyte-specific *EcR*$^{RNAi}$ did not affect the 20HE-induction of rho, upd3 at all, though there was a marginal decrease in upd2 and Socs36E. Moreover, it slightly impaired the modest increase of spi and keren transcripts (Fig 2.5.1d). In summary, EcR seems to regulate rho, upd2 upd3 and Socs36E in progenitors, partly through enteroblasts while EcR in enterocytes seems to regulate Egf ligands after 16-18 hrs of 20HE feeding. Next to investigate whether EC- or EB-dependent upregulation of upd2 was a secondary consequence of ISC division. To test this hypothesis, I first blocked ISC mitoses using an RNAi against String (stg), a Cdc25 homolog required for all somatic cell mitoses in *Drosophila*[296]. Alternatively, I blocked ISC reception of EGF ligand by *Egfr*$^{RNAi}$ in progenitors. Progenitor-specific *Egfr*$^{RNAi}$ or *string*$^{RNAi}$ almost completely blocks the inductive peaks of rho, upd2, upd3 and Socs36E caused by EBs and ECs. This result argues that the ISC autonomous division is what consequently drives the non-cell autonomous inductive peaks of rho and upd2 (Fig 2.5.1e). Afterwards, I proceeded to validate the qPCR results by examining the expression of Jak-Stat pathway activation reporter after 20HE feeding in the different cell types of the posterior midgut. 10×Stat92E-GFP is a GFP reporter with 10 copies of STAT-binding sites at the promoter, which serves as a reliable marker for STAT92E activation *in vivo*[297]. Fig 2.5.1f shows example images of the categories of Jak-Stat activity, with GFP signal localized in mostly single cells (basal), in many pairs (moderate) or in all cells (strong). Under basal conditions, I found the Stat92E reporter to be active in mostly single cells and to a lesser extent in doublets. After 6 hrs of 20HE feeding, activity of the reporter was more diffuse, in doublets or small clusters (Fig 2.5.2a). In contrast, 18 hrs after 20HE feeding, Stat92E activity varied from moderate to strong depending on the reporter's genetic background. However, the 20HE-induced reporter's activity was much weaker in comparison to the strong reporter activity induced by *P.e.*, observed in all infected guts (Fig 2.5.2b).

I also tested the upd3-lacZ reporter, a lacZ enhancer trap of upd3, which shows expression of β-galactosidase in the epithelial cells producing upd3[298]. I found the upd3-lacZ reporter to be unchanged after 20HE feeding relative to its strong activity in cell

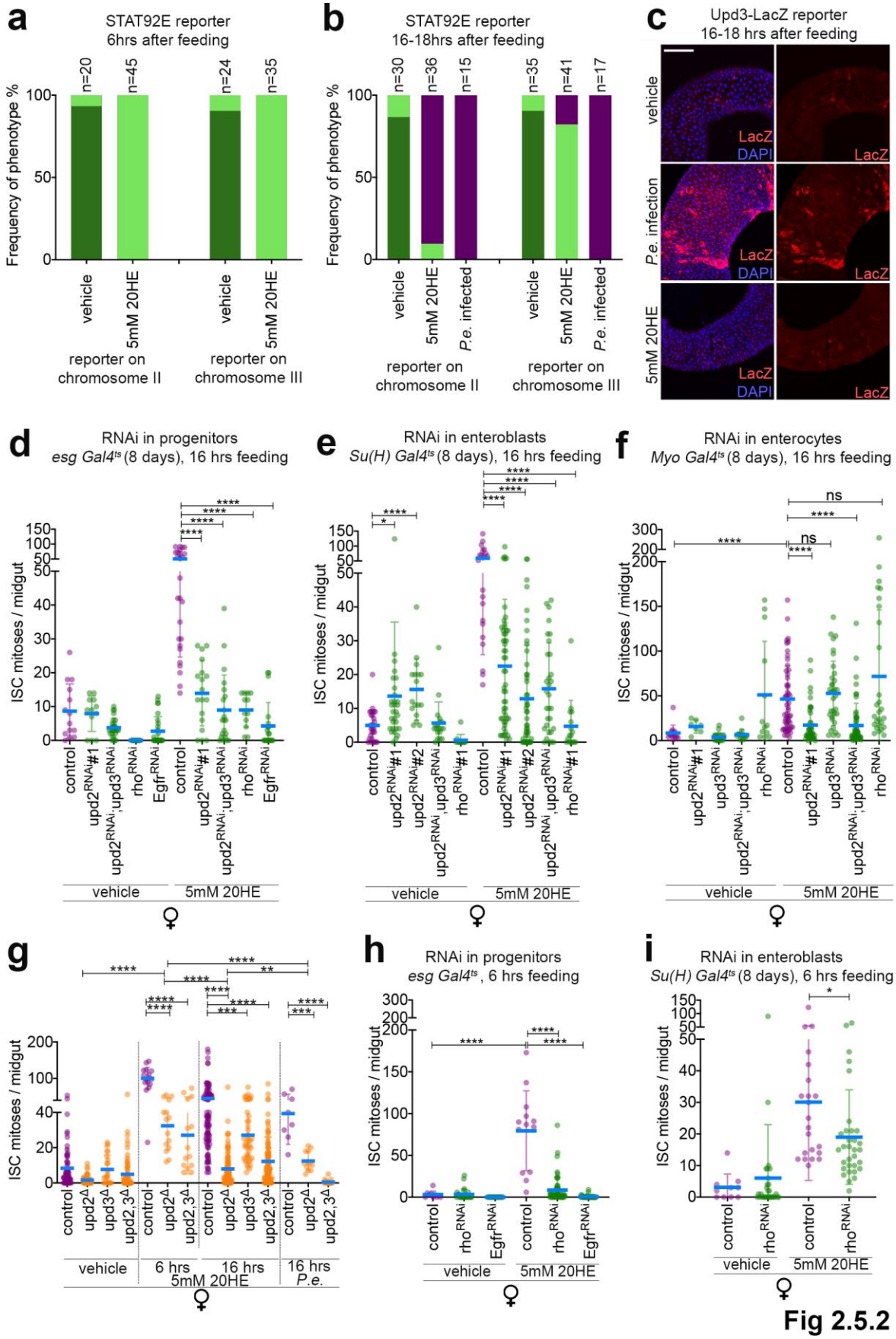
a
STAT92E reporter
6hrs after feeding
Frequency of phenotype %
n=20
n=45
n=24
n=35
vehicle
5mM 20HE
vehicle
5mM 20HE
reporter on chromosome II
reporter on chromosome III
b
STAT92E reporter
16-18hrs after feeding
n=30
n=36
n=15
n=35
n=41
n=17
P.e. infected
c
Upd3-LacZ reporter
16-18 hrs after feeding
vehicle
P.e. infection
5mM 20HE
LacZ
DAPI
d
RNAi in progenitors
esg Gal4ts (8 days), 16 hrs feeding
ISC mitoses / midgut
control
upd2RNAi#1
upd2RNAi;upd3RNAi
rhoRNAi
EgfrRNAi
vehicle
5mM 20HE
e
RNAi in enteroblasts
Su(H) Gal4ts (8 days), 16 hrs feeding
upd2RNAi#2
upd2RNAi;upd3RNAi
f
RNAi in enterocytes
Myo Gal4ts (8 days), 16 hrs feeding
upd3RNAi
ns
g
upd2Δ
upd3Δ
upd2,3Δ
6 hrs
16 hrs
P.e.
h
RNAi in progenitors
esg Gal4ts, 6 hrs feeding
i
RNAi in enteroblasts
Su(H) Gal4ts (8 days), 6 hrs feeding

**Fig 2.5.2**

**Fig 2.5.2 Upd2, rho and Egfr are required in progenitors for 20HE-induced mitoses.** Text and images have been taken and modified from (Ahmed et al., 2020) and have been originally written and made by myself: (a) Under homeostatic conditions, the reporter expresses GFP mostly in ISCs alone (dark green bar). By 6 hrs of 20HE feeding, GFP is localized in midgut progenitors all over the gut (bright green bar). 18% of the guts that express the reporter on chromosome II show a slight accumulation of GFP in other cells upon 20HE feeding, but the GFP signal was not as strong as in the category "GFP in many cells". Phenotypes were scored in the R4 region. Bright green bars denote a milder activation pattern while dark green bars denote no activation of the reporter. 5-7 days old mated females were used for the experiment.
(b) 20HE feeding induces STAT92E-GFP reporter activity much slighter than does *P.e.* infection. Frequency of phenotype occurrence is analyzed based on the categories of activity in panel f. Under homeostatic conditions, the reporter expresses GFP only in ISCs (dark green bar). 16 hrs after 20HE feeding, most midguts of the reporter on chromosome II have GFP localized in many midgut cells including polyploid enterocytes (purple bar). However, most midguts of the reporter on chromosome III have GFP localized in the midgut progenitors (bright green bar). In contrast, *P.e.* infected midguts of the reporters on either chromosome exhibited a strong uniform activation pattern in all midgut cells of the R4 region. % Frequency of phenotype was plotted in reference to phenotypes observed in the R4 region. Purple bars denote the strongest activation pattern; bright green bars denote a milder activation pattern while dark green bars denote no activation of the reporter. 5-7 days old mated females were used for the experiment.
(c) Upd3-lacZ reporter is not activated by 20HE feeding. Images of the R4 region of the midgut showing basal expression of the upd3 reporter in vehicle fed flies relative to strong activation of the reporter upon *P.e.* infection. In contrast, 16hrs of 20HE feeding did not appreciably activate the upd3 reporter. This data indicates that 20HE does not primarily activate upd3 to promote ISC mitoses in the midgut. 5-7 days old mated females were used for the experiment. All images were acquired at the same settings and the intensities of activation are accurately represented.
(d) Number of mitoses in control and progenitor-specific downregulation of *upd2, upd2, upd3, Egfr* or *rho* for 8 days. Flies were exposed to exogenous 20HE feeding for 16 hrs. *upd2, upd3, Egfr* and *rho* from progenitors are required for the 20HE-induced ISC mitoses.
(e) Number of mitoses in control and enteroblast-specific downregulation of *upd2, upd2, upd3* or *rho* for 8 days. Flies were exposed to exogenous 20HE feeding for 16 hrs. *upd2, upd3* and *rho* from enteroblasts are required for the 20HE-induced ISC mitoses.
(f) Number of mitoses in control and enterocyte-specific downregulation of *upd2, upd2, upd3* or *rho* for 8 days. Flies were exposed to exogenous 20HE feeding for 16 hrs. *upd2* but not *upd3, rho* from enterocytes are required for the 20HE-induced ISC mitoses.
(g) Midgut mitotic counts of *upd2Δ, upd3Δ, upd2,3Δ* whole body mutants and control flies after 6 or 16hrs of 20HE feeding and 16hrs of *P.e.* infection. ISCs of *upd2Δ* and

*upd2,3Δ* mutants can divide yet, to a weaker extent relative to controls in response to the 1st wave of ISC mitoses at 6 hrs. ISCs of *upd3Δ* mutants show a minimal defect in ISC division at the 2nd wave of 20HE induced mitoses however ISCs of *upd2Δ* and *upd2,3Δ* are unable to divide at the 2nd mitotic wave of 20HE feeding. *upd2Δ* and *upd2,3Δ* cannot divide after *P.e.* infection. Thus, chiefly upd2 and marginally upd3 are required for ISC activation the 2nd mitotic wave of 20HE-mitoses while both are additively required for *P.e.* infection.
(h) Number of mitoses in control and progenitor-specific downregulation of *Egfr* or *rho* for 8 days. Flies were exposed to exogenous 20HE feeding for 6 hrs. *Egfr* and *rho* from progenitors are required for the 20HE-induced ISC mitoses.
(i) Number of mitoses in control and enteroblast-specific downregulation of *rho* for 8 days. Flies were exposed to exogenous 20HE feeding for 6 hrs. *rho* from enteroblasts is required to a lesser extent for the 20HE-induced ISC mitoses. Error bars represent ± SD. Statistical analysis was performed using unpaired non-parametric two-tailed Mann-Whitney test (ns $p>0.05$, $^{**}p\leq0.01$,$^{****}p<0.0001$). LacZ, in red; DAPI, in blue. Scale bar, 100 μm.

clusters after *P.e*. infection (Fig 2.5.2c). These reporter data are consistent with the qPCR data, which suggest the mild activation of upd3-Jak-Stat signaling induced by 20HE feeding.

To validate the functional involvement of the pathway components I tested above, I proceeded with depleting them with the cell-specific drivers and scored 20HE-induced mitoses. Consistent with the qPCR results, RNAi-mediated progenitor specific depletion of upd2 alone, upd2 upd3, rho or EGFR suppresses the 20HE-mediated mitotic response (Fig 2.5.2d).

As I observed earlier that EcR in progenitors and to a lesser extent in ECs regulate Jak-Stat and EGF signaling components, I sought to deplete upd2, upd3 and rho in progenitors to examine if they are required for 20HE-induced ISC mitoses. EB-specific depletion of upd2 alone, upd2 upd3 or rho severely compromised the mitotic response to 20HE feeding (Fig 2.5.2e). Consistent with the qPCR data, upd3 and rho were not required in ECs for 20HE-mediated ISC divisions. However, EC-specific depletion of upd2 or upd2,upd3 prevented the ISCs from dividing after 20HE feeding (Fig 2.5.2f). This effect could be due to the RNAi perduring to the young newly born ECs as a result of the rapid 20HE-mediated divisions.

By now, I had identified that mainly upd2 is required in progenitors including EBs as well as ECs for the 20HE-induced ISC mitoses. To further corroborate the role of 20HE-induced upd2-Jak-Stat signaling in the midgut, I used single whole body mutants for upd2, upd3 or the double mutant upd2,3 which I fed with 20HE for 6hrs (1$^{st}$ peak), 16hrs (2$^{nd}$ peak) and I used enteric *P.e*. infection as a positive control that absolutely requires upd2 and upd3 in an additive manner for the regenerative *P.e*.–induced ISC mitoses[299]. At the 1$^{st}$ mitotic peak after 20HE feeding, ISCs of the mutant backgrounds upd2$^{\Delta}$ or upd2,3$^{\Delta}$ were competently dividing in response to 20HE feeding, albeit at lower levels relative to control midguts. However, at the 2$^{nd}$ mitotic wave, ISCs of upd2$^{\Delta}$ or upd2,3$^{\Delta}$ flies barely divided (Fig 2.5.2g). upd3$^{\Delta}$ ISCs showed some defect in their response to 20HE feeding, indicating the marginal significance of upd3 in 20HE-induced mitoses. Relative to 20HE mitotic stimulus, ISCs of upd2$^{\Delta}$ are moderately impaired in their *P.e*.-induced mitoses (Fig 2.5.2g), which shows the specificity of the differential requirement of upd2 for 20HE divisions.

Then owing to the transcriptional peak of EGF ligands I observed 6 hrs after 20HE feeding, I hypothesized that active EGF signaling in progenitors would contribute to the latter effect. To examine this, I depleted EGF signaling in progenitors through *Egfr-RNAi* or *rho-RNAi*, which caused a complete suppression of ISC mitoses after 20HE feeding (Fig 2.5.2h). Nevertheless, active EGF signaling was marginally required from EBs specifically to provide active EGF ligands, suggesting that majorly ISC cell-autonomous EGF is sufficient to sustain 20HE-induced mitoses at 6 hrs (Fig 2.5.2i). The EGFR activity readout, diphospho-ERK (dpERK), was also mildly activated by 20HE after 16hrs, mostly in progenitors but occasionally in ECs[19]. Consistent with this result, EGF signaling through EGFR or rho from progenitors and mainly ISCs, but not ECs is indispensible to the 20HE-induced mitoses. Furthermore, Erk activation in response to the 20HE-induced mitoses requires upd2 in the midgut cells (Fig 2.5.3a,b). Collectively, mostly upd2 and to a lesser extent upd3 are required for 20HE-induced mitoses possibly relaying signals for EGFR activation.

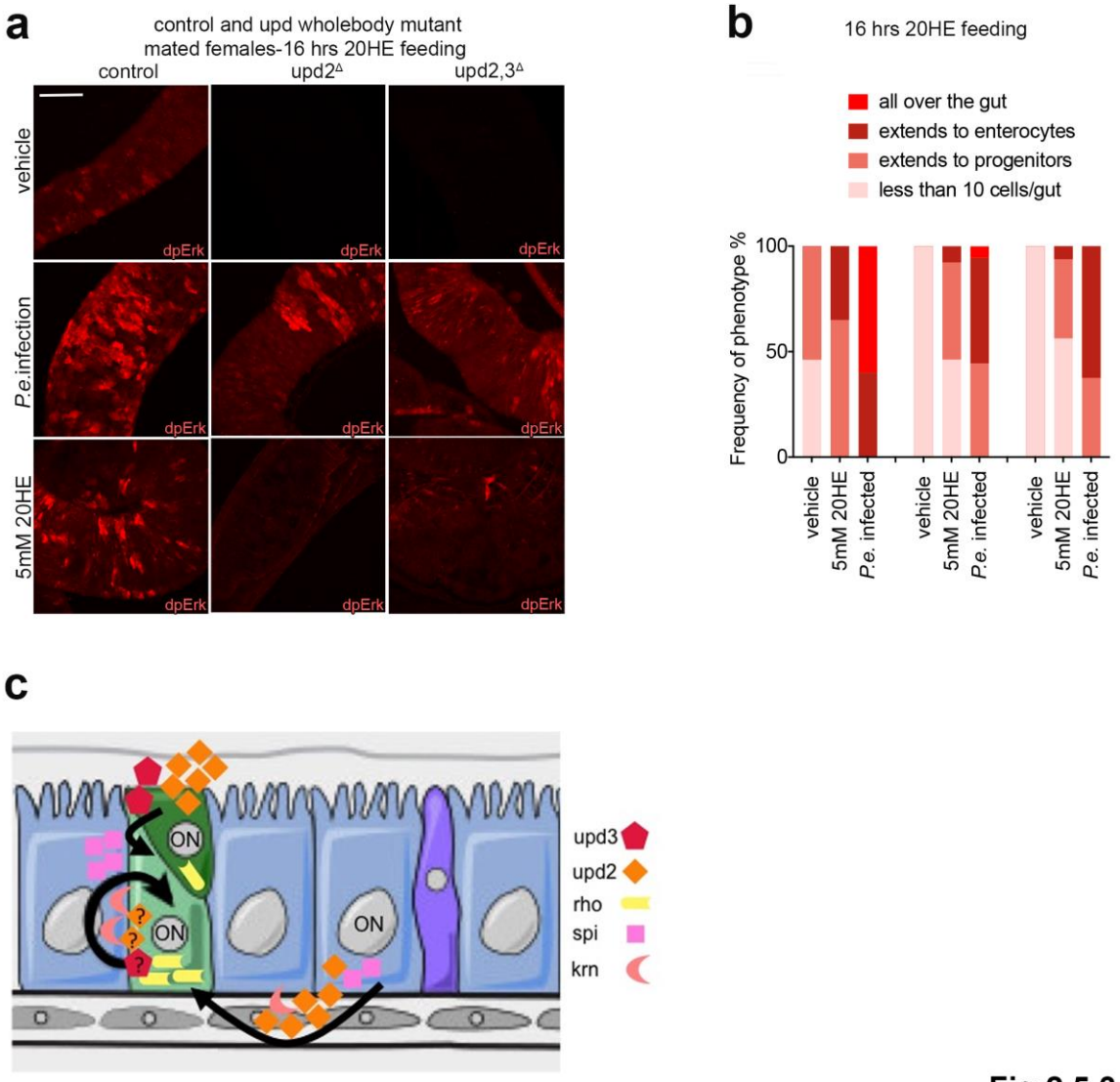


Fig 2.5.3

**Fig 2.5.3 20HE feeding activates dpErk in an-upd2 dependent fashion.** Text and images have been taken and modified from (Ahmed et al., 2020) and have been originally written and made by myself: (a-b) 20HE feeding increases dpErk activity in progenitors. (a) Representative images of Erk activity showing the most prevalent phenotype for each condition, assayed as (diphospho-Erk) dpErk after 20HE feeding or enteric infection. (b) Quantifications of dpErk staining. Under non-stressed conditions, dpErk is present either in very few ECs per gut, or in progenitor cells and very few ECs. Upon enteric infection, dpErk is substantially increased mainly in ECs. Although 20HE feeding also induces dpErk in midguts, the pattern is distinct from the one caused by enteric infection. Upon 20HE feeding, dpErk in mainly visible in progenitors and young ECs, and the signal is often localized to small patches of cells. In contrast, *P.e.* infection induces strong dpErk broadly throughout the gut. dpErk is absent in non-stressed upd2 or upd2,3 mutants. Enteric infection induces dpErk also in upd2 or upd2,3 mutants, albeit to a lower level than wildtype flies. In contrast, upd2 or upd2,3 mutants show very little or no dpErk upon

20HE feeding. 5-8 days old mated females were used for the experiment. Representative images are shown. dpErk, in red. Scale bar, 100 μm.
(c) A model summarizing the cell-type specific supply of Jak-Stat and EGF ligands after 20HE feeding. ON denotes cells with active 20HE EcR signaling. ISCs and to a lesser extent EBs have active rho signaling. ISCs produce their EGF ligands to stimulate cell-autonomous divisions. EBs and ECs produce mainly upd2, and EBs only produce much less upd3 ligands that are required for 20HE induced mitoses. ECs do not seem to require active rho signaling though some EGF ligand induction is regulated by the ECs. Whether ISCs cell-autonomously produce upd2 and upd3 or not remains an open question, although the data presented in Fig 2.7.1e supports this possibility.

## 2.6. Sexually dimorphic 20HE levels lead to increased ISC divisions and midgut growth in males or virgins.

Male ISCs divide less strongly than female ISCs in response to any mitotic stimulus[118]. This coincides with the females having more abundant expression of transcripts related to cell cycle processes in the midgut and more female ISCs in G2/S-phase, suggestive of sex-biased differences in ISC mitoses, that are partly dependent on the intrinsic ISC identity[118]. Consistent with this idea, feminizing the male ISCs by expressing a feminizing variant of transformer, traF, in male progenitors increased stress-induced ISC mitoses[118]. However, under non-stressed conditions, feminized male ISCs did not divide any more than control male ISCs[118]. In parallel, mated females produce more ecdysone than virgin females or males[300-302]. Thus, I was intrigued to examine whether the dimorphic circulating ecdysone levels between males and mated females regulates sex-specific differences in the intestinal stem cell divisions. Congruous with this notion, raising males on 1mM 20HE-laced food for 2 weeks increased male ISC mitoses, accelerated epithelial turnover, and increased midgut size (Fig 2.6a-b, c-d). 20HE also promoted male ISC proliferation on a low protein diet (Fig 2.6e), implying that it enhances ISC proliferation independently of protein or nutrient availability. Of note, no other stimulus is reported to similarly affect male ISC mitoses or illicit gut growth[8,118,303]. In order to figure out if the 20HE-dependent gut growth acts in part via the sex determination pathway, I overexpressed a feminizing variant of transformer, traF, in male progenitors (Fig 2.6d), which failed to drive midgut growth.

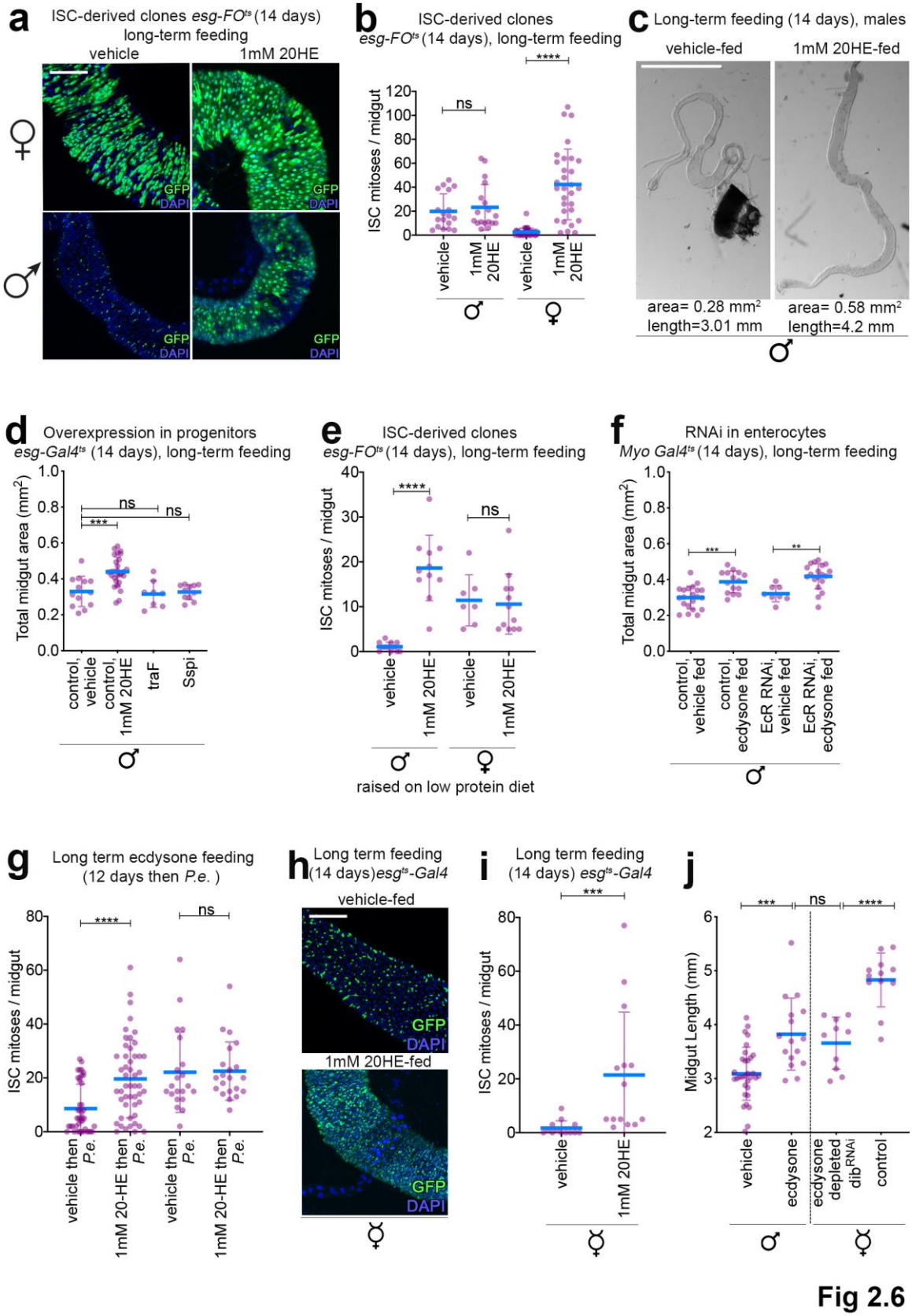


**Fig 2.6**

**Fig 2.6: Prolonged 20HE feeding abrogates the sex differences in ISC division.** Text and images have been taken and modified from (Ahmed et al., 2020) and have been originally written and made by myself: (a-b) (a) Representative images of the ISC lineage tracing: *esgF/O*$^{ts}$ in both sexes after 14 days of feeding with low 20HE doses. 20HE

feeding promotes ISC clonal growth and gut epithelial renewal. 1mM 20HE feeding stimulates epithelial turnover more rapidly in males than females.
(b) 20HE induces an atypical boost in male ISC mitoses. Mitotic counts of control flies fed on 20HE-laced food relative to age-matched controls. At homeostatic conditions, vehicle-fed females divide at much-elevated rates than vehicle-fed males. However, dietary supplementation of 1mM 20HE in fly food caused male ISCs to divide dramatically, matching basal ISC mitoses in females.
(c-d) Male midguts with *traF*-feminized progenitors are unable to grow. Similarly, male midguts overexpressing secreted spitz (Sspi) in progenitors are unable to grow. (c) Representative brightfield images of vehicle-fed or 20HE-fed males, 14 days after feeding showing that 20HE-fed males grow in length and area. (d) Long term 20HE feeding causes male-specific midgut growth, a unique phenotype to males. Midgut areas of vehicle-fed or 20HE-fed males relative to genetically manipulated males.
(e) 20HE causes a strong increase in male ISC divisions on a nutrient-deprived diet. Mitoses of control flies fed on 20HE-laced low yeast high sugar diet relative to age-matched controls. At homeostatic conditions, more vehicle-fed female ISCs divide than ISCs of vehicle-fed males. However, 20HE-fed males had a strong increase in their mitotic index compared to vehicle-fed males.
(f) 20HE triggers midgut growth independent of EcR in ECs. Raising males on prolonged 20HE-laced diet causes 20HE-dependent midgut growth in midguts with EcR depleted ECs. This suggests that EcR in ECs is not required for the 20HE-induced midgut growth and implies that EcR in progenitors is sufficient to elicit 20HE-dependent midgut growth.
(g) 20HE promotes ISC mitoses in *P.e.* infected males, altering their behavior to resemble *P.e.*-induced ISC division in females, as assayed by mitotic counts of males and females. Flies were raised on 20HE or vehicle-supplemented food for 12 days then the treatment was withdrawn overnight followed by *P.e.* infection for 20hrs. Male ISCs that were 20HE-fed were able to respond to *P.e.* infection at similar rates to the age-controlled females fed on 20HE or vehicle.
(h-i) Long-term 20HE-supplemented virgins have an accelerated midgut turnover in comparison to age-controlled virgins. Age-controlled virgins have infrequently dividing ISCs. (h) Representative images of control progenitors in virgins raised on vehicle or 20HE-laced food for 14 days. 20HE-fed virgins have accumulated GFP+ progenitors across the intestinal epithelium. (i) ISC mitotic counts show increased ISC mitoses of 20HE fed virgins relative to vehicle-fed virgins. 20HE fed virgins resemble the basal mitotic behavior of aged mated females.
(j) Midgut lengths of control males, vehicle and 20HE-fed or virgins with ecdysone-depleted ovaries via $dib^{RNAi}$ or control virgins showing the plasticity of male and female midgut growth to circulating 20HE levels. Virgins with $dib^{RNAi}$ have much shorter gut length than control virgins. 20HE-fed males have a longer gut length than vehicle-fed males. Error bars represent ± SD. Statistical analysis was performed using one-way ANOVA, followed by Bonferroni's multiple comparisons test and unpaired non-

parametric two-tailed Mann-Whitney test (ns $p>0.05$, *** $p\leq 0.001$, ****$p<0.0001$). ♀ refers to mated females. ☿ refers to virgins. ♂: males. Representative images are shown.

Similarly, if a boost in pro-mitotic factors are sufficient to induce midgut growth, then expression of sSpi, a potent ISC mitogen[19] would be sufficient to enlarge the male midgut. However, sSpi-overexpressing progenitors had no difference in their gut sizes similar to control males (Fig 2.6d). This result implied that 20HE does more than simply triggering ISC mitoses.

Finally, since the gut's densest populations (numbers/total cells) are enterocytes followed by progenitors (ISCs+enteroblasts)[291], I asked whether enterocytes contribute to the 20HE-induced male midgut growth. Hence, I induced enterocyte-specific depletion of EcR in males and fed the males with 1mM 20HE for 14 days only to find that the 20HE-fed midguts were still able to grow. This result indicates that progenitors are sufficient to elicit 20HE-induced midgut growth (Fig 2.6f). Another sex difference between males and females is that female ISCs proliferate more strongly upon enteric infection than male ISCs[41,118] (Fig 2.1.1a). Hence, I sought to test whether 20HE feeding would sensitize more male ISCs to divide in response to stress. Indeed, pre-feeding males with 20HE potentiated their ISC proliferative response to levels similar to those in females (Fig 2.6g). Likewise, long-term 20HE feeding caused virgin female ISCs to proliferate under basal conditions similar to basal counts of ISCs mitoses in mated females (Fig 2.6h,i). In contrast, reduced ovarian-ecdysteroids (Fig 2.6j) or intestinal EcR signaling in midgut progenitors led to reduced midgut sizes (Fig 2.6j). In summary, my results show that sexually dimorphic aspects of ISC proliferative behavior as well as gut sizing are determined in part by 20HE levels.

### 2.7 1-6 Prolonged 20HE feeding in males causes a change in the ISC metabolic signature.

Since there are no preceding reports of sex steroid feeding causing non-sex organ growth, I was intrigued to figure out how in this case ecdysone elicits the male-specific intestinal growth. To answer this question, I focused on the genetic changes that could be attributed to the gain-of-function phenotype, caused by exogenous 20HE feeding in males. Hence, I

fed both control males and females with 20HE or vehicle for 14 days in the background of mira-GFP (which marks only the ISCs) then I FACS-sorted the ISCs and sequenced the transcriptome of the sorted ISCs and aligned the single reads with STAR aligner (Fig 2.7.1a-d). I have aligned the reads using the *Drosophila* transcriptome as a reference and with built-in gene model with splice junction information, to detect isoform abundance. Firstly, the abundance of normalized transcript reads/sample shows that Oatp74D: the ecdysone transporter was indeed expressed in the ISCs[304] and it is slightly higher expressed in males than females. Moreover, EcR variant A and the Eip75B variant C (used for overexpression in later sections of this thesis) are indeed the major variants expressed in the ISCs of the midgut (Fig 2.7.1a-b). It is interesting to note that there are several Eip75B isoforms expressed in the ISCs, all of which are ecdysone-inducible in males (Fig 2.7.1b). Br isoforms are much less abundant than Eip75B (Fig 2.7.1c). One predominant isoform variant B is normally expressed at higher levels in males and is induced after 20HE feeding. Components of Egf signaling such as rho, the ligands-cleaving protease, Spitz, Keren and Vein are also present in sorted ISCs of both males and females though do not appear to be significantly changed after 20HE feeding consistent with the result in (Fig 2.6d) which showed that enforced spi expression is insufficient to elicit the 20HE-induced midgut growth (Fig 2.7.1d). Similarly, my results confirmed that upd2 and upd3 are expressed in the sorted ISCs, though at lower levels in males (Fig 2.7.1e) and Stat92E, the transcriptional activator of the Jak/Stat pathway was expressed at slightly higher levels in males relative to females consistent with the higher reporter activity also observed in males[305]. 20HE caused upd2 and upd3 transcriptional upregulation in ISCs, better seen in the male samples. Alternatively, a negative regulator of Jak/Stat signaling Heix, a tumor suppressor gene[306], with unexplored functions in the midgut is transcriptionally inhibited by 20HE feeding in both males and females (Fig 2.7.1e).

As previously reported, genes with sex differences in expression are enriched for distinct biological processes; genes assigned to cell cycle-related processes, lipid and fatty acid metabolism were upregulated in females (Table 2.1b,c,d), whereas genes coding for proteins that function in MAPK, Wnt pathways, carbohydrate metabolism and glutathione oxidoreductive processes are preferentially expressed in males ISCs (Table 2.2a,e,f), (Fig 2.7.2a-b)[118].

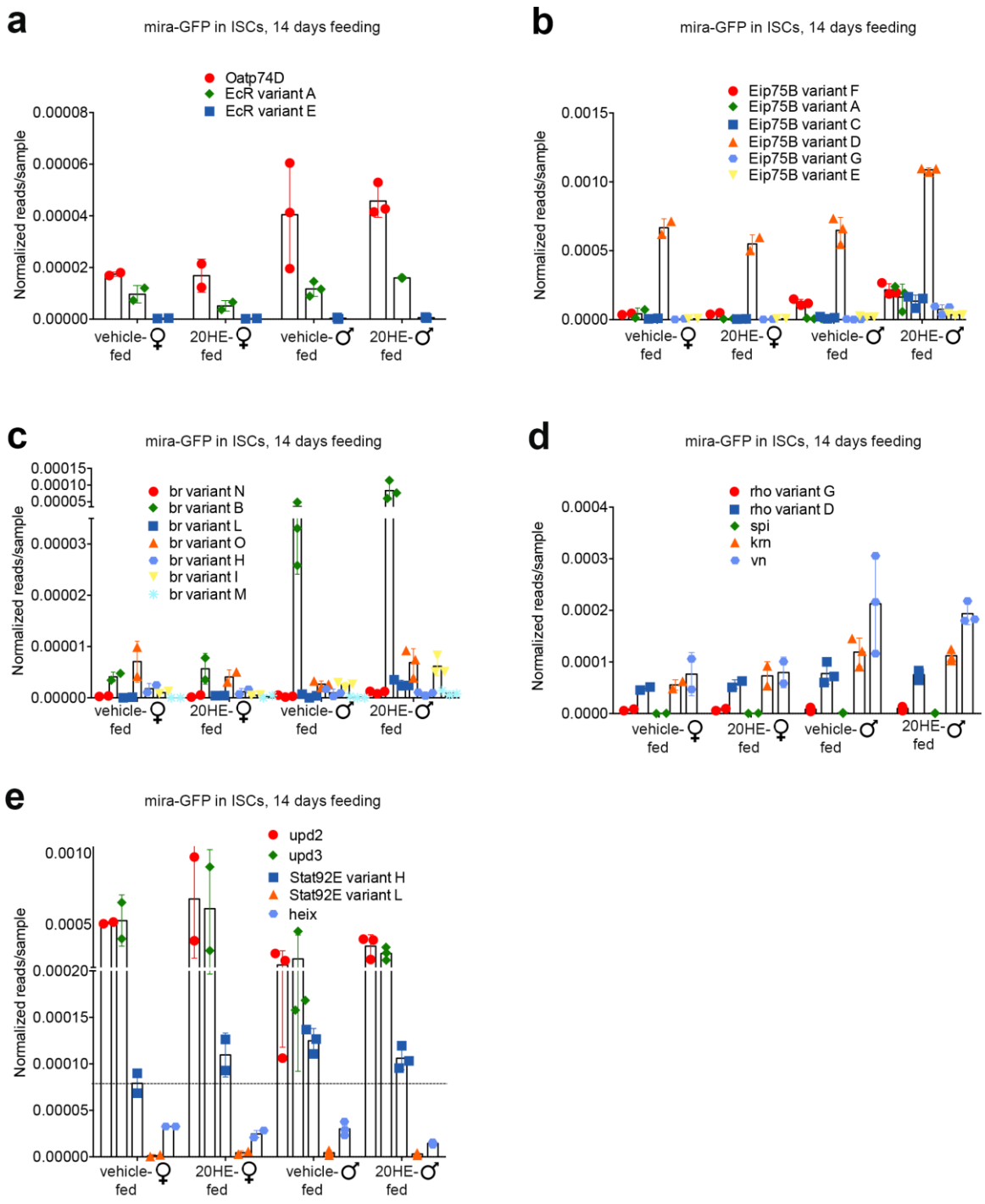


Fig 2.7.1

**Fig 2.7.1: 20HE feeding transcriptionally upregulates ecdysone-inducible genes, Jak/Stat and EGF ligands.** (a) EcR A and Oatp74D are expressed in *Drosophila* ISCs. Normalized transcript reads of the ecdysone transporter Oatp74D and EcR variants outputted after STAR alignment to reflect transcript abundance in GFP sorted ISCs of both females and males +/- exogenous 20HE feeding.

(b) Eip75B variant D is predominantly expressed in *Drosophila* ISCs yet, all Eip75B variants are induced in 20HE-fed males. Normalized transcript reads of the ecdysone-

inducible Eip75B outputted after STAR alignment to reflect transcript abundance in GFP sorted ISCs of both females and males +/- exogenous 20HE feeding.

(c) Br variant B is predominantly expressed in male *Drosophila* ISCs yet, br variants B,L,O,I are mildly induced in 20HE-fed males. Normalized transcript reads of the ecdysone-inducible br outputted after STAR alignment to reflect transcript abundance in GFP sorted ISCs of both females and males +/- exogenous 20HE feeding.

(d) Egf signaling pathway components are relatively unchanged by long term 20HE feeding. Normalized transcript reads of rho variants, spi, krn and vn (latter are 3 EFG ligands) outputted after STAR alignment to reflect transcript abundance in GFP sorted ISCs of both females and males +/- exogenous 20HE feeding.

(e) Upd2 and upd3 are expressed at higher levels in females relative to males. Downstream target Stat92E is expressed at slightly higher levels in males relative to females. Normalized transcript reads of Jak/Stat signaling pathway components outputted after STAR alignment to reflect transcript abundance in GFP sorted ISCs of both females and males +/- exogenous 20HE feeding.

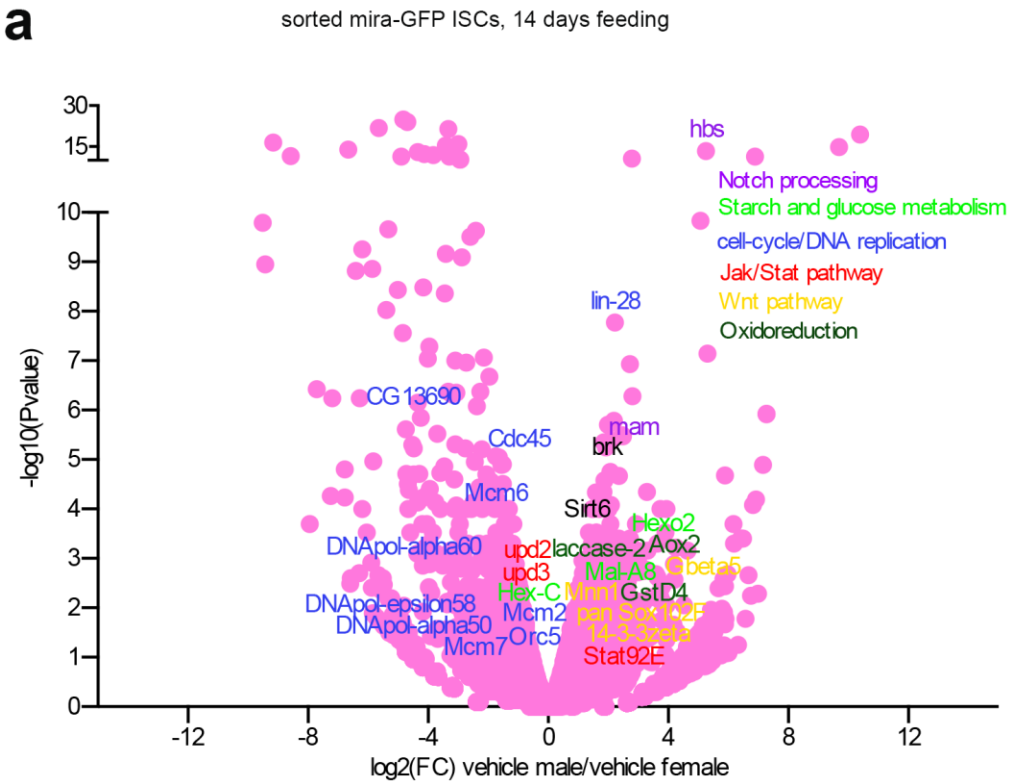


**Fig 2.7.2**

**b** sorted mira-GFP ISCs, 14 days feeding
Genes differentially upregulated
in vehicle-fed females/vehicle-fed males

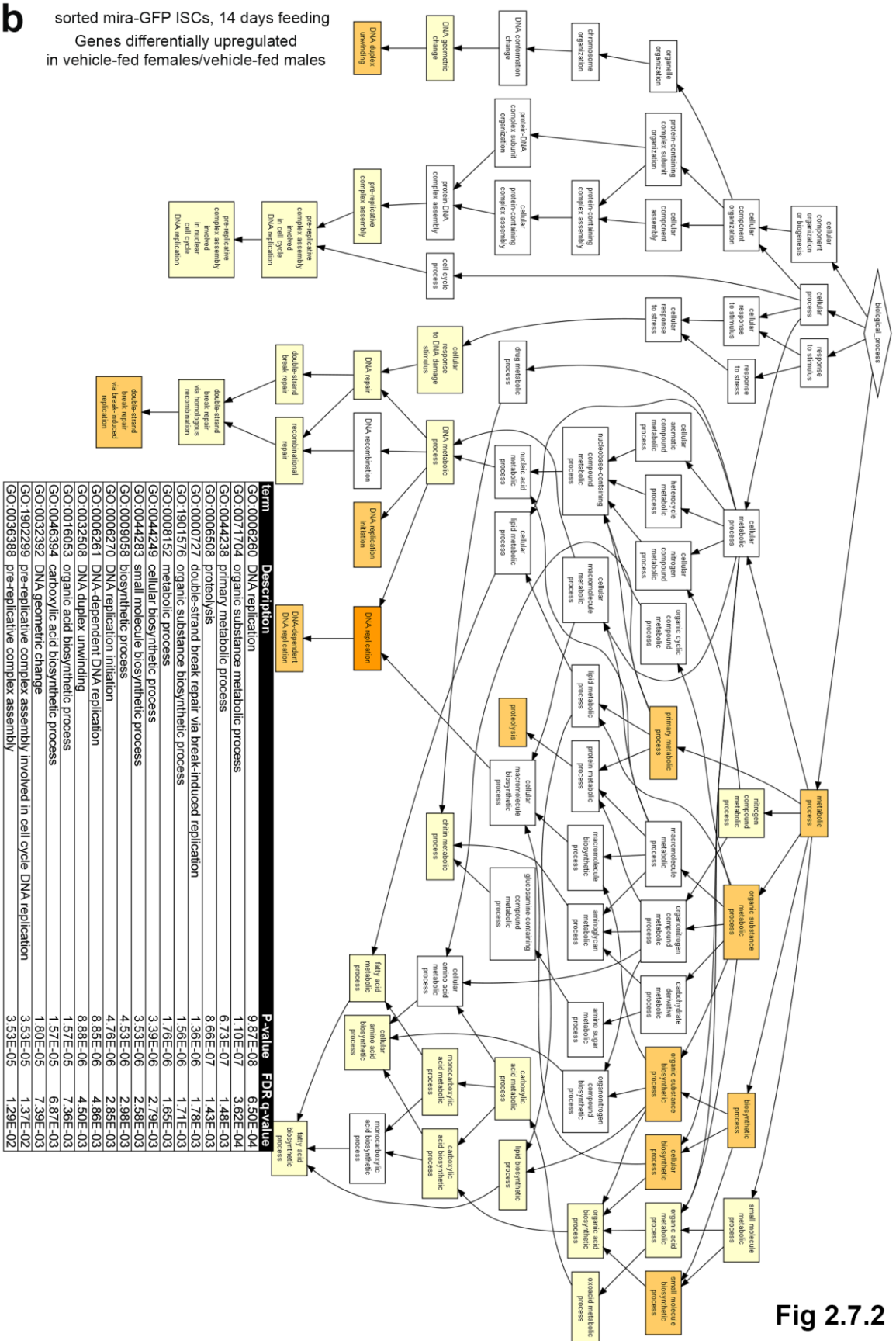


| term | Description | P-value | FDR q-value |
|---|---|---|---|
| GO:0006260 | DNA replication | 9.87E-08 | 6.50E-04 |
| GO:0071704 | organic substance metabolic process | 1.10E-07 | 3.62E-04 |
| GO:0044238 | primary metabolic process | 6.73E-07 | 1.48E-03 |
| GO:0006508 | proteolysis | 8.66E-07 | 1.43E-03 |
| GO:0000727 | double-strand break repair via break-induced replication | 1.36E-06 | 1.78E-03 |
| GO:1901576 | organic substance biosynthetic process | 1.56E-06 | 1.71E-03 |
| GO:0008152 | metabolic process | 1.76E-06 | 1.65E-03 |
| GO:0044249 | cellular biosynthetic process | 3.39E-06 | 2.79E-03 |
| GO:0044283 | small molecule biosynthetic process | 3.53E-06 | 2.58E-03 |
| GO:0009058 | biosynthetic process | 4.53E-06 | 2.98E-03 |
| GO:0006270 | DNA replication initiation | 4.76E-06 | 2.85E-03 |
| GO:0006261 | DNA-dependent DNA replication | 8.85E-06 | 4.86E-03 |
| GO:0032508 | DNA duplex unwinding | 8.88E-06 | 4.50E-03 |
| GO:0016053 | organic acid biosynthetic process | 1.57E-05 | 7.36E-03 |
| GO:0046394 | carboxylic acid biosynthetic process | 1.57E-05 | 6.87E-03 |
| GO:0032392 | DNA geometric change | 1.80E-05 | 7.39E-03 |
| GO:1902299 | pre-replicative complex assembly involved in cell cycle DNA replication | 3.53E-05 | 1.37E-02 |
| GO:0036388 | pre-replicative complex assembly | 3.53E-05 | 1.29E-02 |

**Fig 2.7.2**

**Fig 2.7.2 Sex-biased differential gene expression between vehicle fed males and females.** (a) Volcano plot of differentially expressed genes between vehicle-fed female to vehicle-fed male sorted ISCs with some annotated hits to complement Table 2.1
(b) An interactive map outputted by Gorilla tool of GO terms that are enriched between vehicle-fed females/vehicle-fed males at p-value threshold of $10^{-3}$. Yellow-colored terms are presented by p-value $10^{-3}$ to $10^{-5}$ and orange-colored terms are presented by p value: $10^{-5}$ to $10^{-7}$. A short table is presented below with the 'FDR q-value' , which is the correction of the above p-value for multiple testing using the Benjamini and Hochberg method.

Males exposed to 20HE for a longtime have elevated string and png (positive regulators of the mitotic cell cycle) levels as well as a highly abundant metabolic signature associated with starch, aminoacid derivatives and lipid metabolism in their ISCs (Fig 2.7.3a,d). This enrichment in metabolic hits reflects an upgrade in the metabolic capacity of the 20HE-fed males, possibly to satisfy increasing tissue homeostatic needs (Fig 2.7.3a,d), (Table 2.2ab,d-g). Positively enriched metabolic signature of lipid and carbohydrate processing in 20HE-fed males is also consistent with the sexually dimorphic role of 20HE in promoting triglyceride and glycogen uptake in fertilized females[123].
Next, a previous report determined the presence of sex-biased expression of different genes in the *Drosophila* midgut[118]. Those genes were inherently different in their expression levels between males and females such that it is highly expressed in one sex and is inversely expressed in the other sex. Interestingly, differential analysis of the sorted 20HE-fed male ISCs showed an enhanced expression of a subset of those sexually dimorphic genes (75 hits in the ISCs from 826 hits detected in the ISC transcriptome or 1305 hits from all cell types in whole midguts) (Fig 2.7.3b,c), (Table 2.2c). Those genes showed a striking upregulation in their expression relative to control males. The colored genes in the volcano plot were hits with identified metabolic function, yet the functions of the rest remain uncharacterized (Fig 2.7.3b,c).
Next, as a control for the male effects, I examined how 20HE affects females. Despite not having obvious differences on ISC proliferation in females (refer to Fig 2.6a-b), 20HE feeding still affected several aspects of the transcriptome of the sorted female ISCs. 20HE caused a strong positive enrichment for regulation of immune response modulators, antimicrobial peptide production consistent with previous reports of how ecdysone-

inducible transcriptional networks controls the IMD immune response in Drosophila[307,308] (Fig 2.7.4a).

20HE feeding also correlated with positive histone acetylation of H2 and H4 but a strongly downregulated enrichment in carbohydrate metabolizing genes (Fig 2.7.4a) (Table 2.3,a,b,d-g).

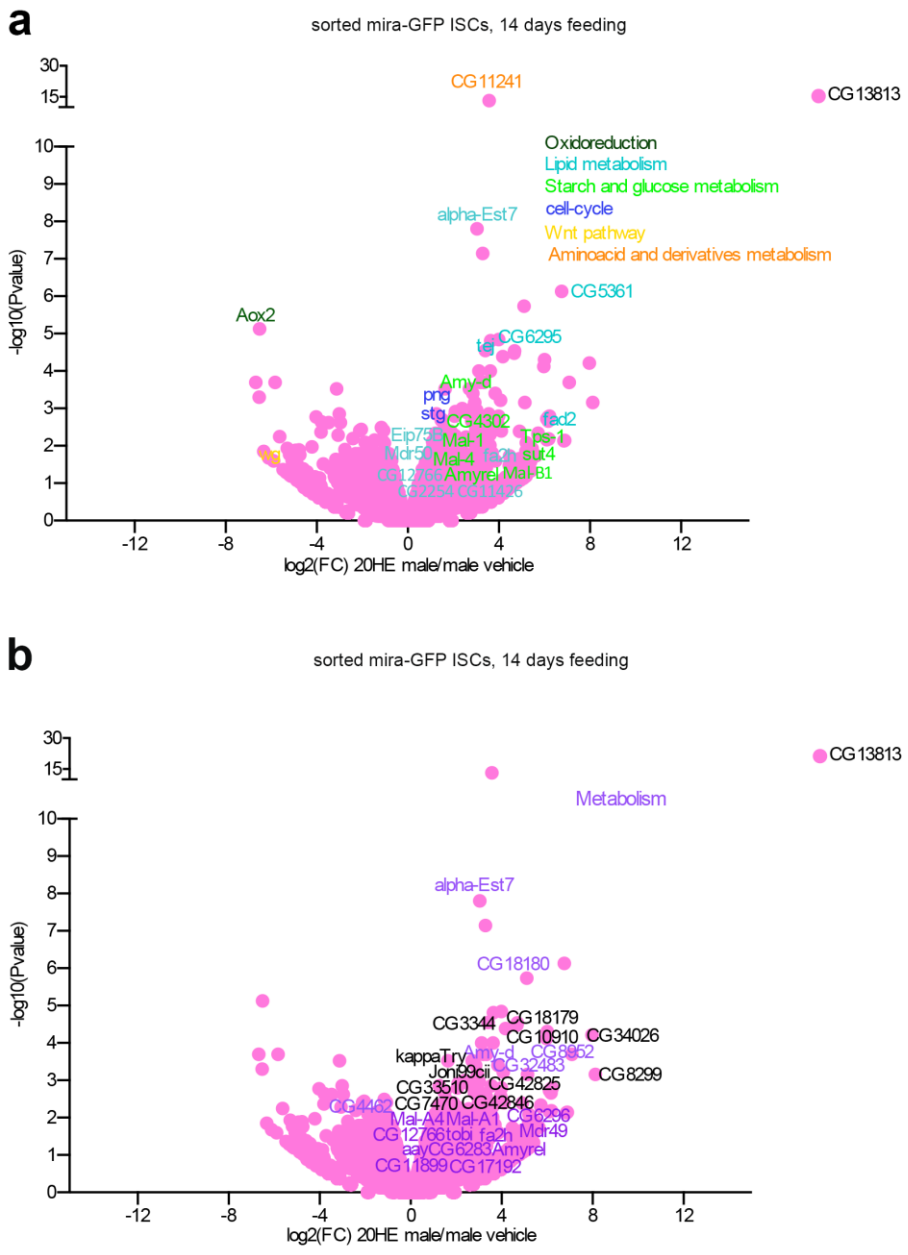


**Fig 2.7.3**

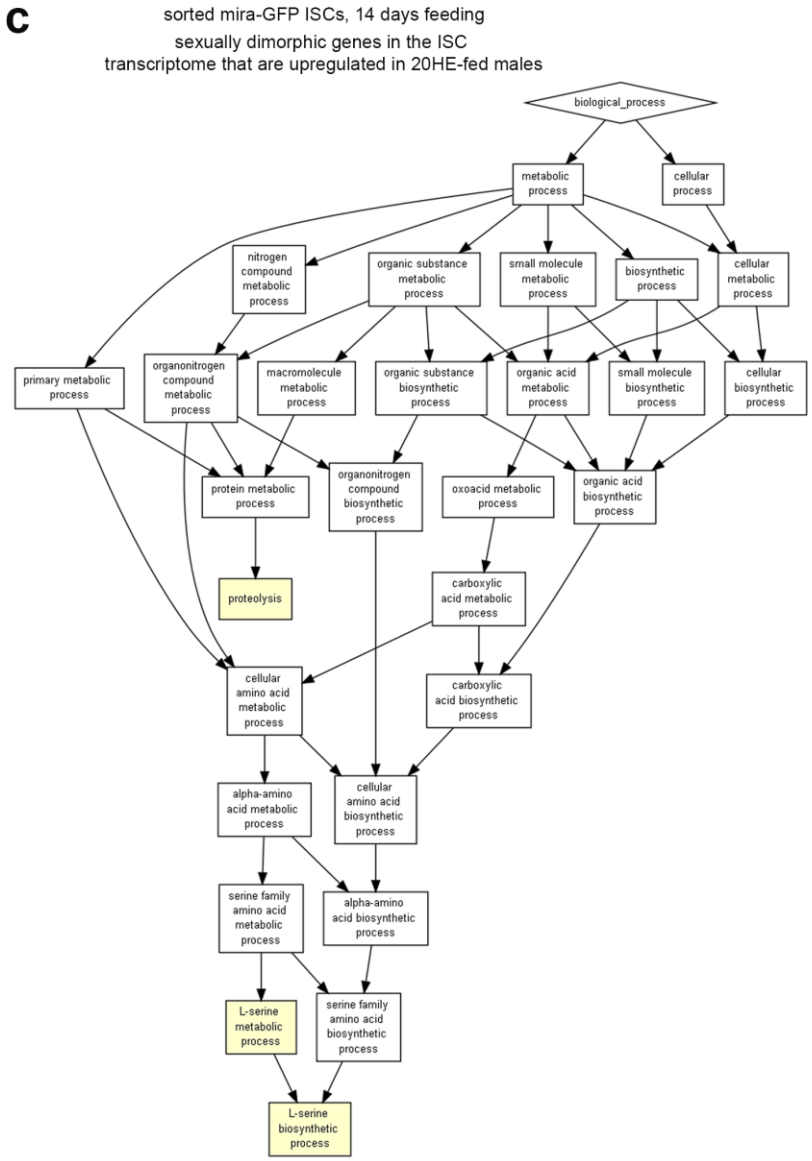


| GO term | Description | P-value | FDR q-value |
|---|---|---|---|
| GO:0006508 | proteolysis | 2.34E-05 | 1.54E-01 |
| GO:0006564 | L-serine biosynthetic process | 3.92E-04 | 1.00E+00 |
| GO:0006563 | L-serine metabolic process | 3.92E-04 | 8.60E-01 |

**Fig 2.7.3**

**Fig 2.7.3 20HE feeding alters the metabolic transcriptome of males.**
(a) Volcano plot of differentially expressed genes between 20HE-fed males to vehicle-fed male sorted ISCs with some annotated hits to complement Table 2.2.
(b) Volcano plot of genes that are the sexually dimorphic between males and females but are revealed to be regulated by 20HE feeding in males. The annotated hits in purple are hits of known metabolic function. These hits complement Table 2.2c.

(c) An interactive map outputted by Gorilla tool of GO terms that sexually dimorphic between males and females yet, are upregulated between ecdysone-fed males/vehicle-fed males at p-value threshold of $10^{-3}$. Yellow-colored terms are presented by p-value $10^{-3}$ to

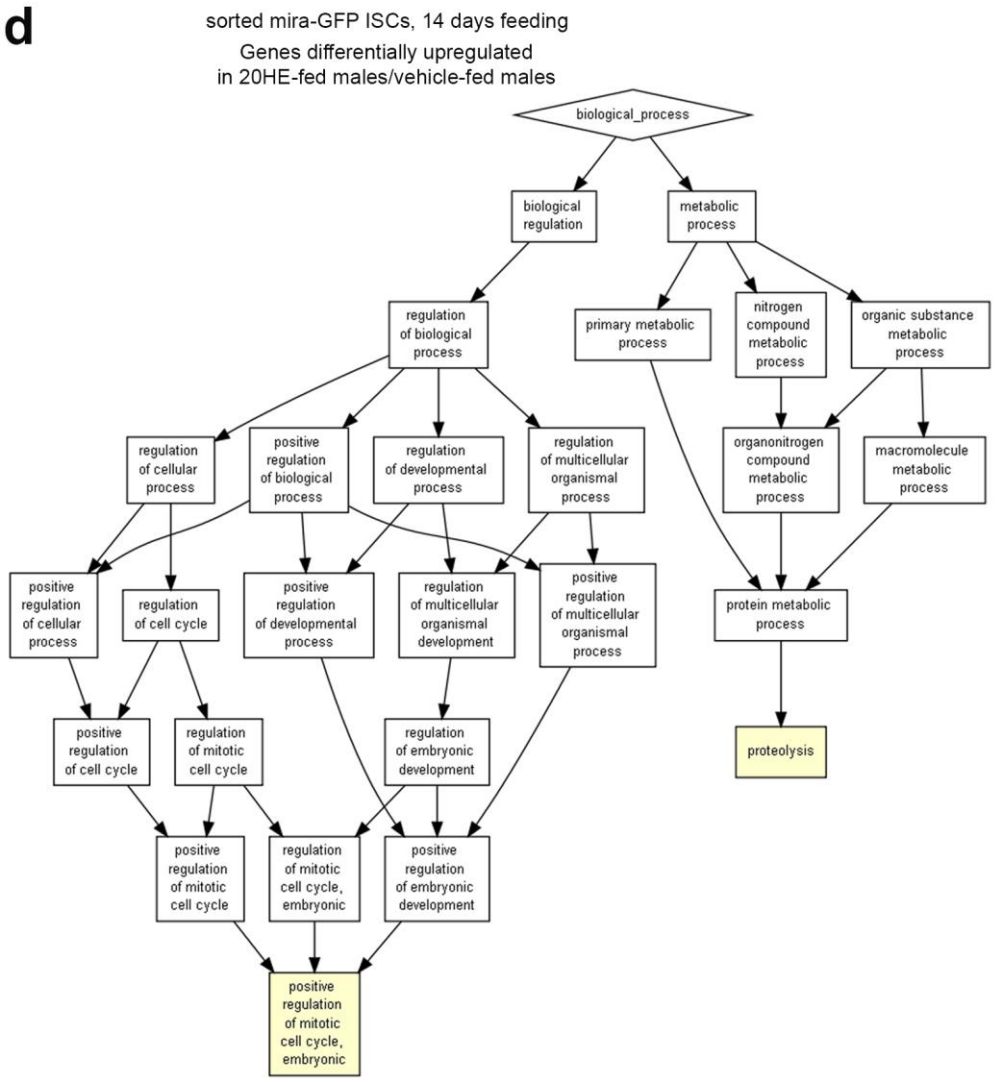


| GO term | Description | P-value | FDR q-value |
|---|---|---|---|
| GO:0006508 | proteolysis | 3.42E-05 | 2.25E-01 |
| GO:0045977 | positive regulation of mitotic cell cycle, embryonic | 7.67E-04 | 1.00E+00 |

**Fig 2.7.3**

$10^{-5}$ A short table is presented below with the 'FDR q-value' , which is the correction of the above p-value for multiple testing using the Benjamini and Hochberg method.

(d) An interactive map outputted by Gorilla tool of GO terms that are upregulated between ecdysone-fed males/vehicle-fed males at p-value threshold of $10^{-3}$. Yellow-colored terms are presented by p-value $10^{-3}$ to $10^{-5}$ A short table is presented below with the 'FDR q-value' , which is the correction of the above p-value for multiple testing using the Benjamini and Hochberg method.

Strikingly, another subset of the aforementioned sexually dimorphic genes[118] were downregulated (n=62) and upregulated (n=9) in vehicle-fed females relative to 20HE-fed females (Table 2.3c), suggesting the high plasticity of the ISCs to adapt to increased levels of 20HE, though the number of replicates (n=2 vs 3 for females vs male samples) was quite low and the statistical significance was not as robust as in the male samples. This data suggests the presence of a subset of sexually dimorphic genes within ISCs that are regulated by 20HE feeding, implying that in part the circulating levels of the sex hormones could function to maintain the identity of the intrinsic sex of the cells, partly through metabolic changes.

RNA seq analyses showed an increased abundance of fatty acid metabolic, carboxylic acid genes and DNA replication/cell cycle related processes in vehicle fed females relative to 20HE-fed males (Table 2.4a,f-g,i). 20HE-fed males have upregulated hits associated with improved carbohydrate metabolism, increased receptor tyrosine kinase, insulin receptor signaling, formation of piwi RNAs and notch processing (Fig 2.7.5a-c) (Table 2.4b,d,e). Intriguingly, among the gene candidates that is highly expressed in 20HE-fed males relative to vehicle-fed females is lin-28. Lin-28 is highly enriched in the ISCs and it positively regulates insulin signaling, promotes symmetric ISC divisions and mediates gut growth in response to nutrients[309]. This candidate provides an interesting link between ISC symmetric divisions and insulin signaling that could explain the underlying boost of metabolic functions and subsequent gut growth.

Since it is known that the levels of 20HE are sexually dimorphic, I asked if this would also affect the underlying gene regulation between males and females. Fig 2.7.6a shows a correlation plot of normalized reads to ecdysone feeding between males and females that shows an inverse correlation between the presence of ecdysone and the abundance of the transcript. Transcripts skewed to the right bottom are enriched in females and diminished in males and are dependent on 20HE. While transcripts skewed to the upper left quadrant are highly abundant in males but lack in females and are 20HE dependent. Similarly, Fig 2.7.6b (left) shows a correlation plot of normalized reads to ecdysone feeding in males relative to normalized reads between vehicle-fed males and females. Transcripts skewed to the upper left are of higher levels in 20HE-fed males relative to vehicle-fed males and are also higher in vehicle-fed females relative to vehicle-fed males.

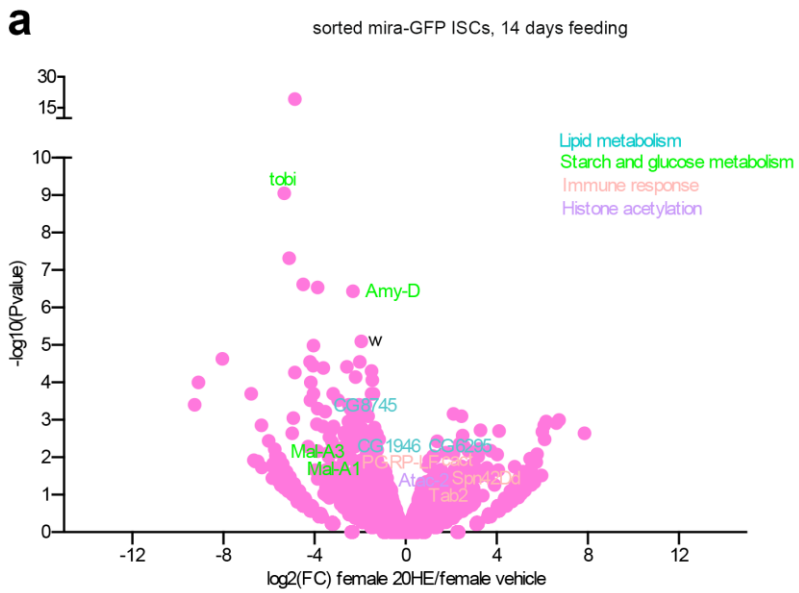


Fig 2.7.4

**Fig 2.7.4 20HE feeding alters the metabolic transcriptome of females.**
(a) Volcano plot of differentially expressed genes between 20HE-fed females to vehicle-fed female sorted ISCs with some annotated hits to complement Table 2.3.

While transcripts skewed to right bottom of the plot are more abundant in vehicle-fed males relative to vehicle-fed females but, downregulated by 20HE feeding in males. This distribution is strongly dependent on 20HE, hence revealing a sexually dimorphic pattern in the gene expression between males and females.

Then, I explored if and which subsets of genes would be similar between females with physiological levels of 20HE and males with supra-physiological levels of exogenous 20HE. I reasoned that the subset of genes that would be equalized by exogenous 20HE feeding in males would be one of the underlying reasons for the unique sexually dimorphic 20HE-induced ISC mitoses and subsequent midgut growth. Accordingly, I searched for the list of hits that satisfy the criteria of being sex-biased differentially expressed between control males and females yet at the same time were equalized to or surpassed female levels by 20HE feeding (Fig 2.6.b (right)).

Table 2.4ci-ii,h shows the list of these hits and their GO or pathway enrichment terms. 20HE availability seems to correlate with many metabolic aspects as well as regulation of the cell cycle (Fig 2.7.6c-d).

**a**

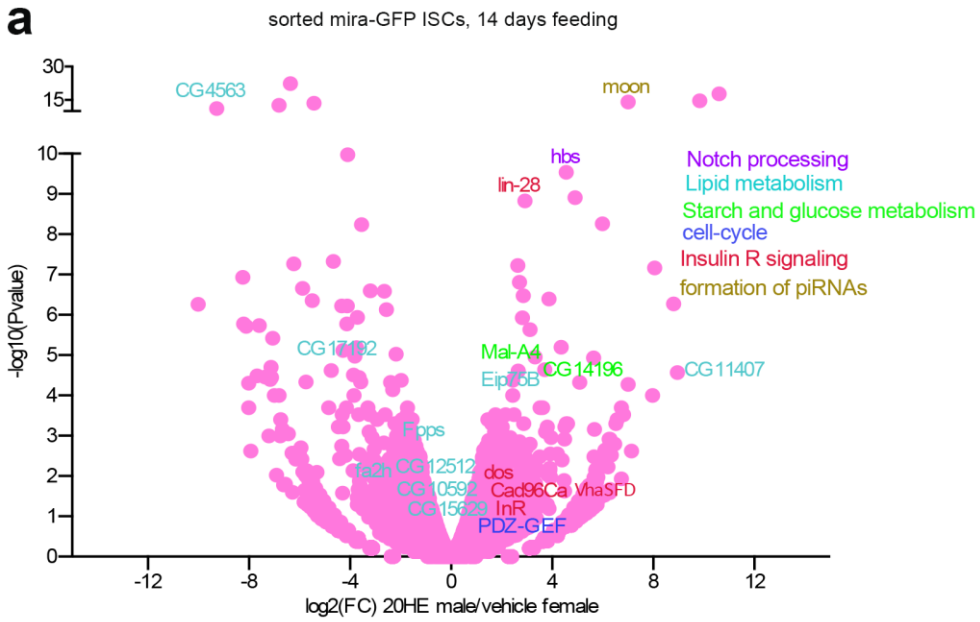


**b**

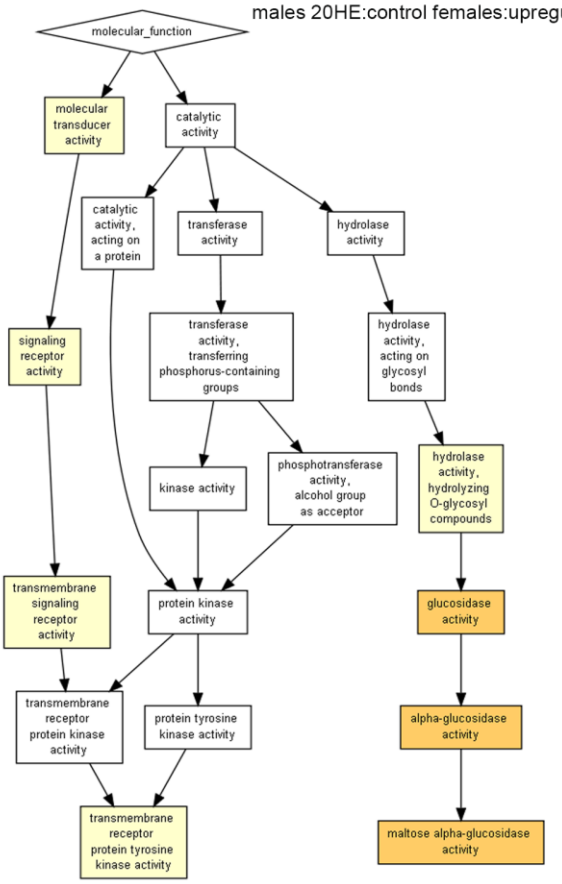


| GO term | Description | P-value | FDR q-val |
|---|---|---|---|
| GO:0032450 | maltose alpha-glucosidase activity | 2E-06 | 0.00555 |
| GO:0090599 | alpha-glucosidase activity | 2E-06 | 0.00278 |
| GO:0015926 | glucosidase activity | 6E-06 | 0.00477 |
| GO:0038023 | signaling receptor activity | 8E-05 | 0.0449 |
| GO:0004888 | transmembrane signaling receptor activ | 0.0002 | 0.0706 |
| GO:0004553 | hydrolase activity, hydrolyzing O-glycos | 0.0004 | 0.133 |
| GO:0060089 | molecular transducer activity | 0.0005 | 0.147 |
| GO:0004714 | transmembrane receptor protein tyrosir | 0.0005 | 0.147 |

**Fig 2.7.5**

**c**

sorted mira-GFP ISCs, 14 days feeding
control females: males 20HE upregulated

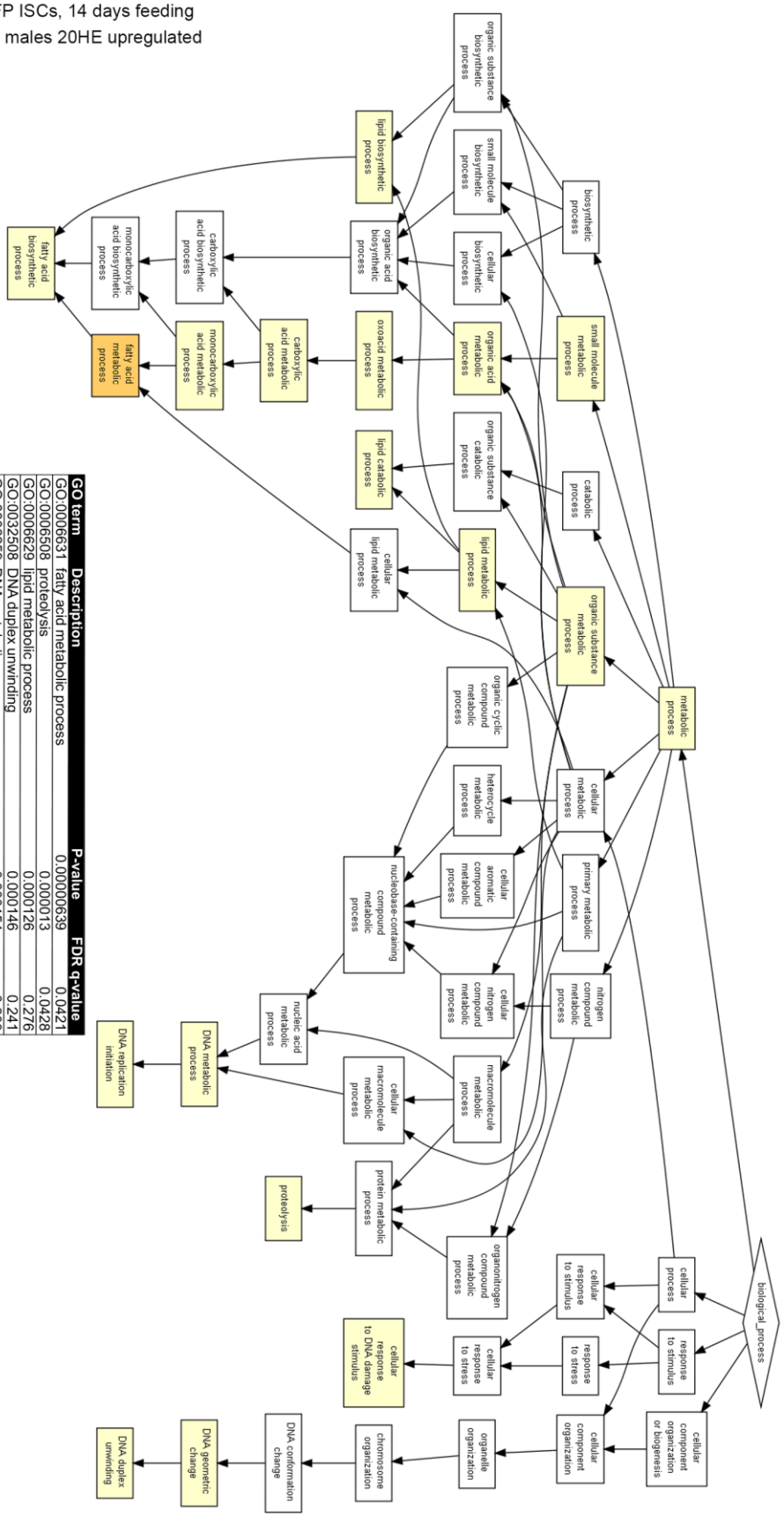


| GO term | Description | P-value | FDR q-value |
|---|---|---|---|
| GO:0006631 | fatty acid metabolic process | 0.0000639 | 0.0421 |
| GO:0006508 | proteolysis | 0.000013 | 0.0428 |
| GO:0006629 | lipid metabolic process | 0.000126 | 0.276 |
| GO:0032508 | DNA duplex unwinding | 0.000146 | 0.241 |
| GO:0006259 | DNA metabolic process | 0.000154 | 0.203 |
| GO:0008610 | lipid biosynthetic process | 0.000211 | 0.232 |
| GO:0032392 | DNA geometric change | 0.000229 | 0.215 |
| GO:0032787 | monocarboxylic acid metabolic process | 0.000314 | 0.258 |
| GO:0044281 | small molecule metabolic process | 0.000345 | 0.252 |
| GO:0043436 | oxoacid metabolic process | 0.00043 | 0.283 |
| GO:0006082 | organic acid metabolic process | 0.00043 | 0.257 |
| GO:0006270 | DNA replication initiation | 0.000493 | 0.27 |
| GO:0006633 | fatty acid biosynthetic process | 0.000524 | 0.266 |
| GO:0016042 | lipid catabolic process | 0.000637 | 0.3 |
| GO:0071704 | organic substance metabolic process | 0.000724 | 0.318 |
| GO:0019752 | carboxylic acid metabolic process | 0.000741 | 0.305 |
| GO:0008152 | metabolic process | 0.000815 | 0.316 |
| GO:0006974 | cellular response to DNA damage stimulus | 0.000843 | 0.308 |

**Fig 2.7.5**

**Fig 2.7.5: 20HE feeding upregulates metabolic hits in the ISC transcriptome of 20HE-fed males relative to control females.** (a) Volcano plot of differentially expressed genes between vehicle-fed female to 20HE-fed male sorted ISCs with some annotated hits to complement Table 2.4.
(b) An interactive map outputted by Gorilla tool of GO terms that are enriched between 20HE-fed males/vehicle-fed females at p-value threshold of $10^{-3}$. Yellow-colored terms are presented by p-value $10^{-3}$ to $10^{-5}$ and orange-colored terms are presented by p value: $10^{-5}$ to $10^{-7}$. A short table is presented below with the 'FDR q-value', which is the correction of the above p-value for multiple testing using the Benjamini and Hochberg method.
(c) An interactive map outputted by Gorilla tool of GO terms that are enriched between vehicle-fed females /20HE-fed males at p-value threshold of $10^{-3}$. Yellow-colored terms are presented by p-value $10^{-3}$ to $10^{-5}$ and orange-colored terms are presented by p value: $10^{-5}$ to $10^{-7}$. A short table is presented below with the 'FDR q-value', which is the correction of the above p-value for multiple testing using the Benjamini and Hochberg method.

Collectively, this experiment reveals the novelty of a sex steroid maybe partly adjusting the metabolism and cell cycle independent of the intrinsic genetic landscape of cells within non-sex organs, a hypothesis that remains highly unexplored and should prove interesting for future studies. As shortly presented in the introduction and discussed further, understanding how sex steroids act as signaling relays from sex organs to other non-sex organs would help us understand the physiological effects of sex hormones and evaluate their outcome on disease risk, prognosis and treatment efficacy[310].

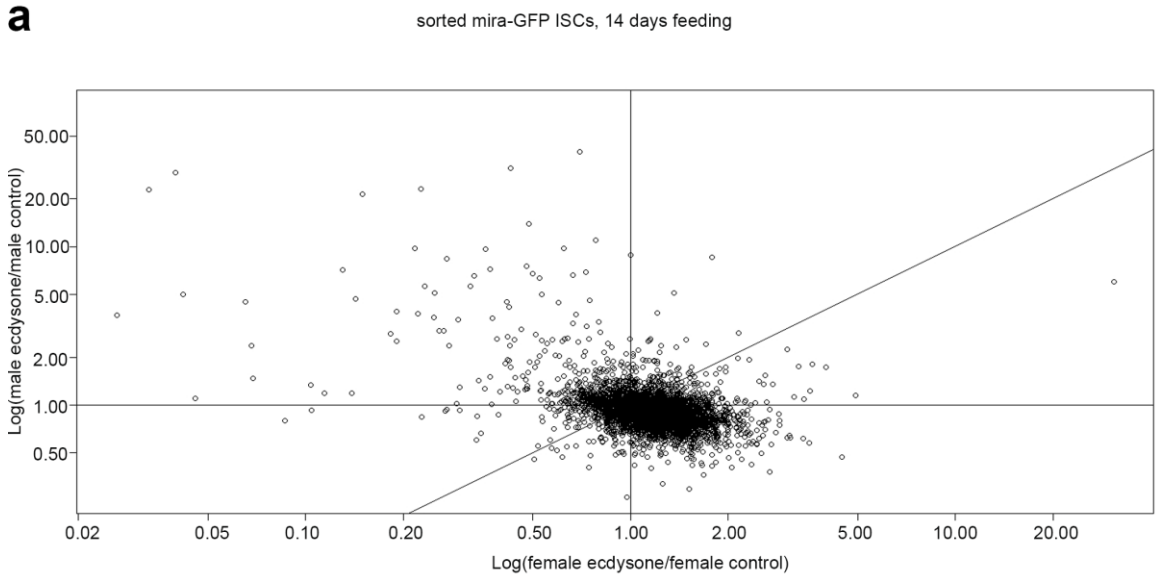

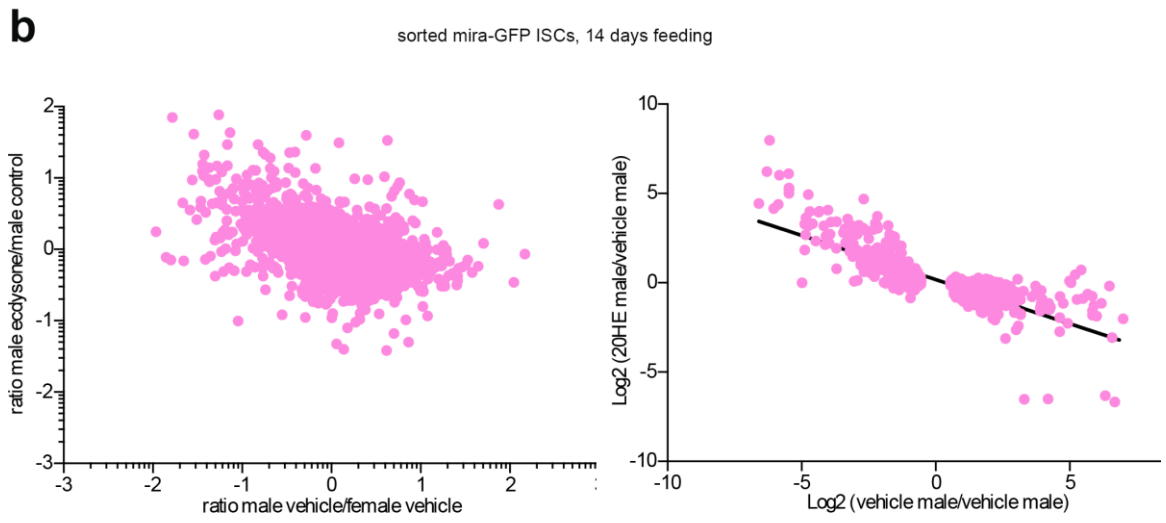


**Fig 2.7.6**

**Fig 2.7.6: 20HE feeding normalizes metabolic and cell cycle hits in the ISC transcriptome of 20HE-fed males.** (a) LC scatter plot showing the correlation between 2 variables: ecdysone and the fly sex. Females or males were normalized as follows: log values of 20HE-fed samples/ vehicle-fed samples for each gender. Ratio higher than 1 are genes that are transcriptionally induced by 20HE feeding. The left upper quadrant shows the proportion of genes that are inversely correlated between "being male" and 20HE feeding. Highly abundant transcripts in this quadrant are specific to 20HE-fed males and are extremely low in 20HE-fed females. The lower right quadrant shows that the majority of the genes cluster together which suggests that the exogenous 20HE feeding does not correlate with "being female". This negative correlation between the "male" sex and 20HE presence suggests that a decrease of 20HE was correlated with an increase in the abundance of male-specific genes.

(b) (left) LC scatter plot showing the correlation between 2 variables: ecdysone feeding in males and genes that are different between the females and males. Females or males were normalized as follows: ratio of normalized reads of 20HE-fed samples/ vehicle-fed samples relative to ratio of normalized reads of vehicle-fed male/ vehicle-fed female. Axes are in log scale. The left upper quadrant shows the proportion of genes that are regulated by 20HE feeding in males and are low expressed in females. The lower right quadrant shows genes that are highly abundant in males but downregulated by 20HE feeding. (right) The log2 values from EdgeR are shown for the subset of genes from Table 2.4cii. $R^2$ is 0.6402.

(c) An interactive map outputted by Gorilla tool of GO terms that are differentially expressed between males and females but are rather unchanged between vehicle-fed females and 20HE-fed males at p-value threshold of $10^{-3}$. Yellow-colored terms are presented by p-value $10^{-3}$ to $10^{-5}$, orange-colored terms are presented by p value: $10^{-5}$ to $10^{-7}$ and red-colored terms are presented by p value:$10^{-7}$ to $10^{-9}$. A short table is presented

below with the 'FDR q-value', which is the correction of the above p-value for multiple testing using the Benjamini and Hochberg method.

(d) An interactive map outputted by Gorilla tool of GO terms that are differentially expressed between males and females but are rather unchanged between vehicle-fed females and 20HE-fed males at p-value threshold of $10^{-3}$. Yellow-colored terms are presented by p-value $10^{-3}$ to $10^{-5}$ and orange-colored terms are presented by p value: $10^{-5}$ to $10^{-7}$. A short table is presented below with the 'FDR q-value', which is the correction of the above p-value for multiple testing using the Benjamini and Hochberg method.

**C** sorted mira-GFP ISCs, 14 days feeding

Genes that are not changing between control females and 20HE-fed males, but are differentially expressed between vehicle-fed males and females

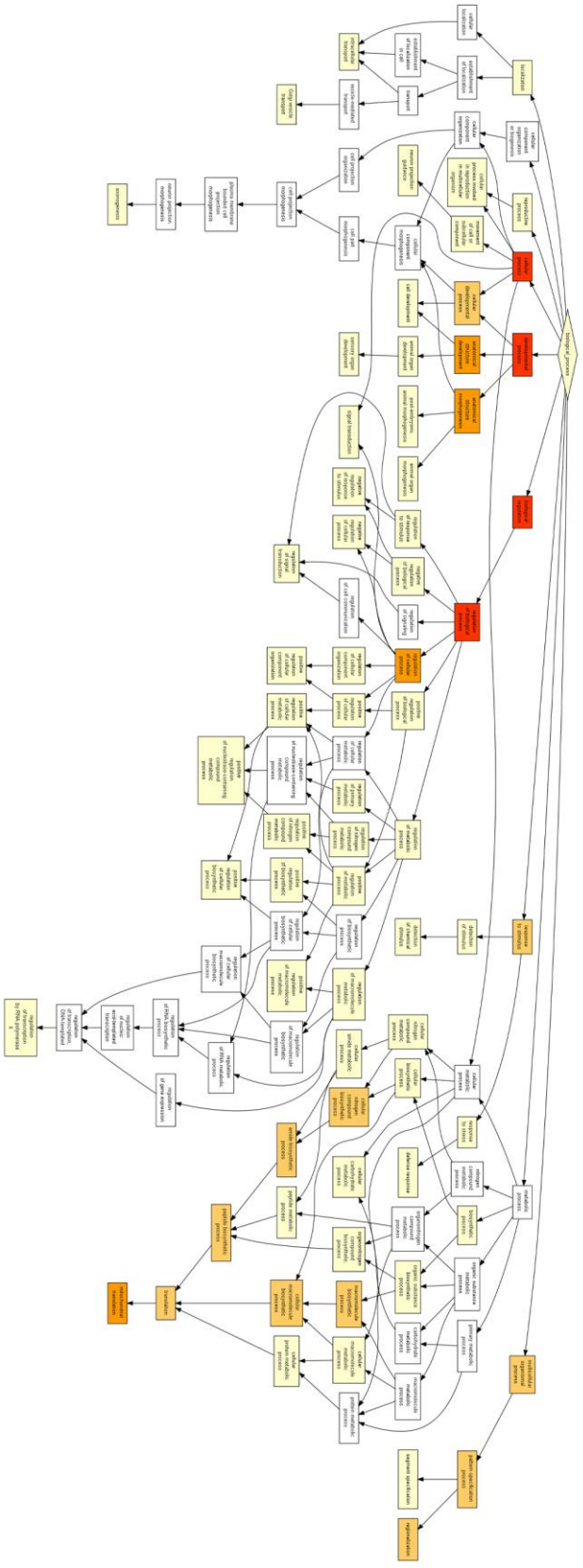

**Fig 2.7.6**

**d** sorted mira-GFP ISCs, 14 days feeding

Genes that are not changing between control females and 20HE-fed males, but are downregulated between vehicle-fed males and females

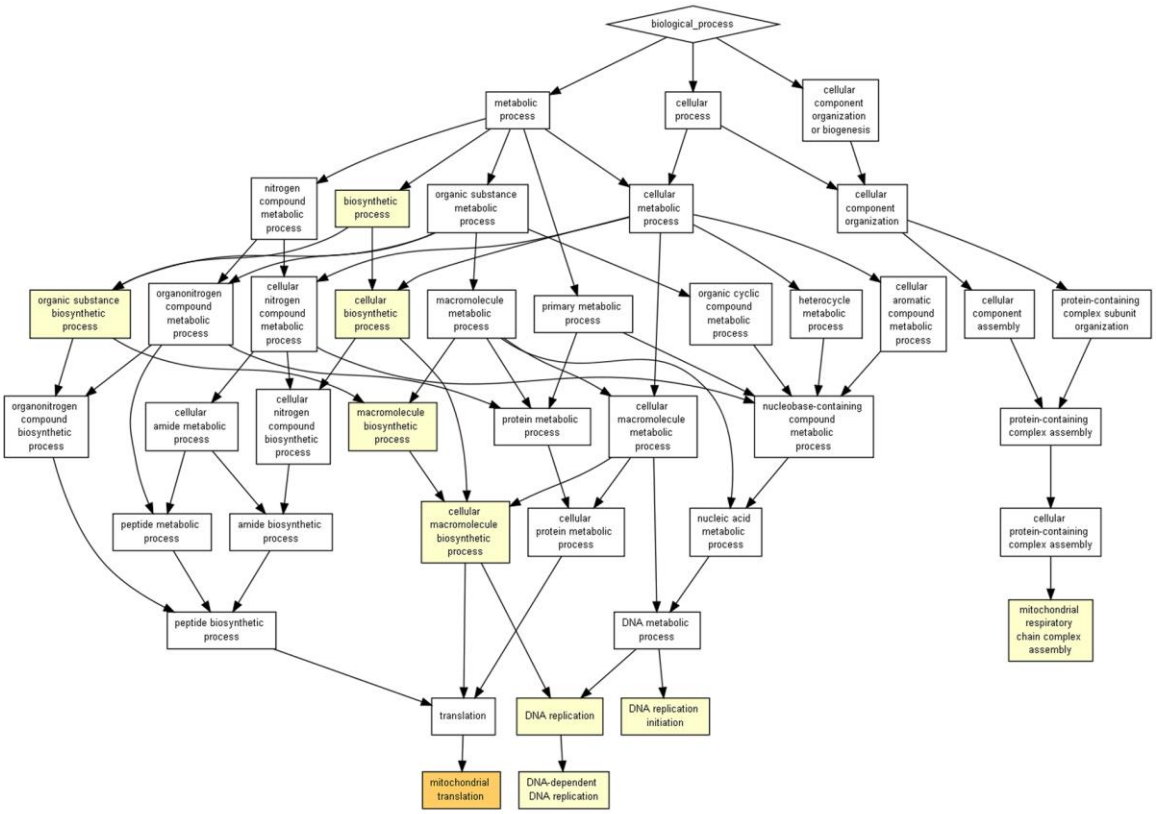


| GO term | Description | P-value | FDR q-value |
|---|---|---|---|
| GO:0032543 | mitochondrial translation | 3.86E-06 | 2.54E-02 |
| GO:0006261 | DNA-dependent DNA replication | 1.50E-05 | 4.93E-02 |
| GO:0006270 | DNA replication initiation | 2.44E-05 | 5.36E-02 |
| GO:0006260 | DNA replication | 2.85E-05 | 4.69E-02 |
| GO:0033108 | mitochondrial respiratory chain complex assembly | 1.14E-04 | 1.50E-01 |
| GO:0034645 | cellular macromolecule biosynthetic process | 1.94E-04 | 2.13E-01 |
| GO:0044249 | cellular biosynthetic process | 3.20E-04 | 3.01E-01 |
| GO:1901576 | organic substance biosynthetic process | 4.30E-04 | 3.54E-01 |
| GO:0009059 | macromolecule biosynthetic process | 6.14E-04 | 4.49E-01 |
| GO:0009058 | biosynthetic process | 8.80E-04 | 5.79E-01 |

**Fig 2.7.6**

**2.8.1-2 Intestinal EcR signaling regulates post-mating ISC mitoses in the female midguts.**

The consequence of 20HE feeding on ISC divisions and gut growth begged the question of whether those exogenous feeding effects could have any physiological relevance? Mated females have much higher ecdysteroid levels than virgin females or males[301] and the endogenous ecdysone is mainly produced by the ovaries[153]. Total ecdysteroid levels almost doubles only 24 hours after mating[302]. Thus, I sought to mate the flies for different durations and assay the actively dividing ISC divisions as a consequence of mating. It has been reported that 3 days post mating, flies experience an increase in the number and diameter of their enterocytes accompanied with a very modest increase in ISC divisions[311]. Hence, I mated female virgins and checked the ISC mitoses 2 and 3 days post-mating. Indeed, mating induced a transient, yet, massive increase in ISC proliferation (Fig 2.8.1a), expansion of gut progenitors and consequently an enlarged gut size across the whole midgut (Fig 2.8.2a-c), and not only growth restricted to the most posterior gut region as reported earlier[311]. This GFP progenitor expansion was also transient and 5 days after mating, the GFP signal was restricted to many doublets unlike the initial post-mating expansion (Fig 2.8.1b,c). Next, I asked if intestinal ecdysone signaling in progenitors was responsible for these ISC divisions and resulting midgut growth. EcR depletion in progenitors or ISCs impaired both the expansion of GFP-expressing progenitors (Fig 2.8.1d) or ISC clones (Fig 2.8.1e) as well as ISC mitoses (Fig 2.8.1f,g) and in both cases the resulting gut growth was repressed (Fig 2.8.2a-e). Similarly, Usp, EcR's receptor partner was required for mating-induced ISC mitoses (Fig 2.8.1f) and mating-dependent gut sizing (Fig 2.8.2d).

In further tests, I examined the role of non-cell autonomous role of EcR signaling in EBs or ECs on the mating-induced ISC mitoses and the mating-dependent gut sizing. Similar to 20HE feeding, mating-induced ISC mitoses absolutely necessitated EcR in EBs at later time points by 72 hrs but, EcR was dispensable to the initial ISC mitoses by 48 hrs (Fig 2.8.1h). Interestingly, in addition to the cell-autonomous roles of EcR in ISCs to drive mitoses and midgut sizing, ecdysone/EcR-dependent midgut resizing marginally required EcR in enteroblasts for the optimal gut resizing after mating (Fig 2. 8.2h). In contrast, EcR in ECs was not required for the mating induced ISC mitoses (Fig 28.1i).

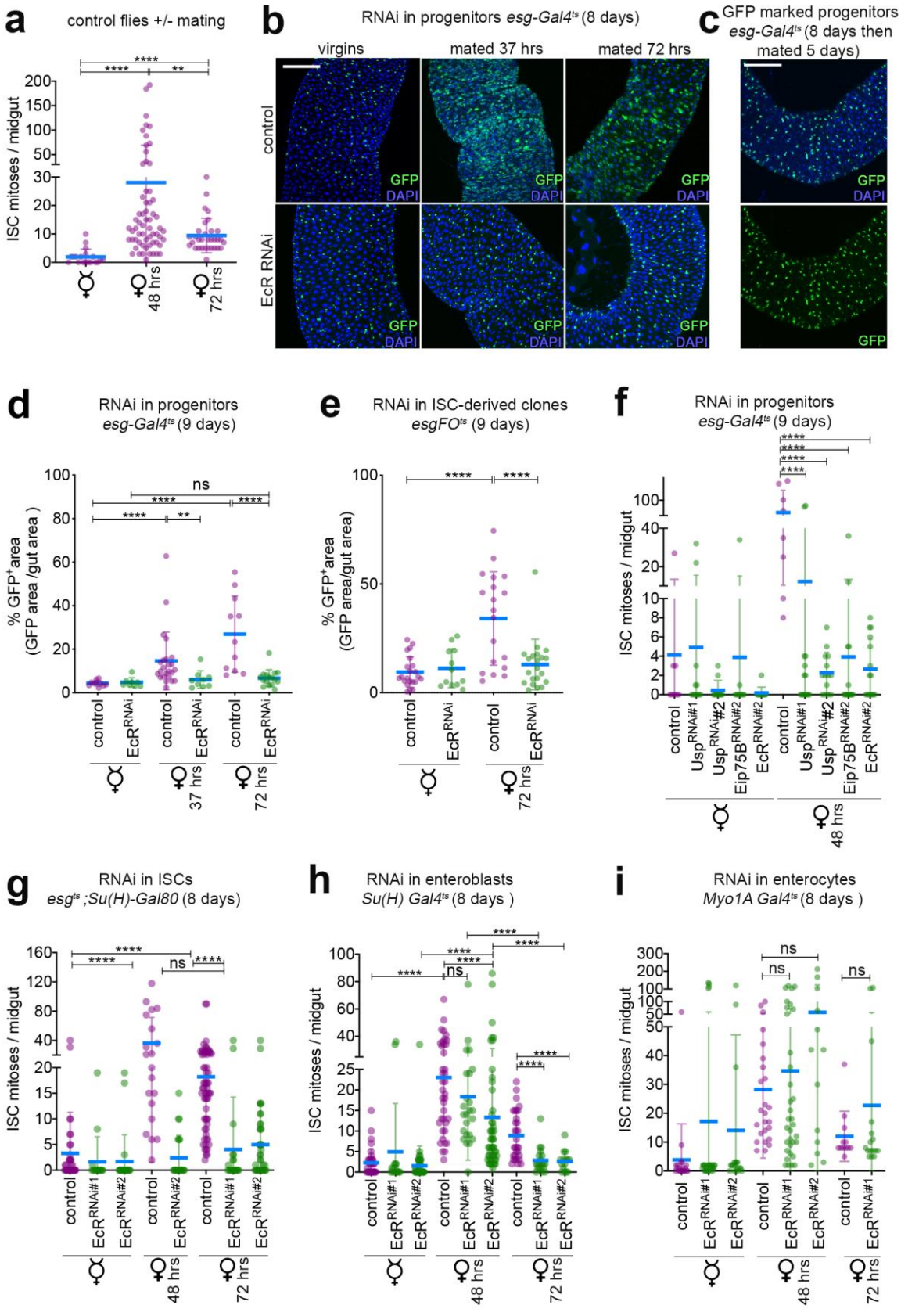
a
control flies +/- mating
ISC mitoses / midgut
48 hrs
72 hrs
b
RNAi in progenitors esg-Gal4ts (8 days)
virgins
mated 37 hrs
mated 72 hrs
control
EcR RNAi
GFP
DAPI
c
GFP marked progenitors
esg-Gal4ts (8 days then mated 5 days)
d
RNAi in progenitors
esg-Gal4ts (9 days)
% GFP+area (GFP area /gut area )
control
EcRRNAi
37 hrs
72 hrs
e
RNAi in ISC-derived clones
esgFOts (9 days)
% GFP+area (GFP area/gut area)
f
RNAi in progenitors
esg-Gal4ts (9 days)
UspRNAi#1
UspRNAi#2
Eip75BRNAi#2
EcRRNAi#2
48 hrs
g
RNAi in ISCs
esgts ;Su(H)-Gal80 (8 days)
EcRRNAi#1
EcRRNAi#2
h
RNAi in enteroblasts
Su(H) Gal4ts (8 days )
i
RNAi in enterocytes
Myo1A Gal4ts (8 days )
ns

**Fig 2.8.1**

**Fig 2.8.1: Mating induces a burst of EcR-dependent ISC mitoses.** Text and images have been taken and modified from (Ahmed et al., 2020) and have been originally written and made by myself: (a) Mating leads to an increase in the number of ISC mitoses/gut. Mitotic counts of control virgin females 48hrs and 72hrs post mating.

(b) Representative confocal images of transient progenitor expansion seen in control females after mating and upon progenitors-specific downregulation of EcR in the R4 region of the posterior midgut of females (below). Females were mated to males with no genetic manipulations. Equal number of males and females were allowed to mate (a ratio of 1:1) and females were allowed to mate for the indicated times above the panels. GFP, in green; DAPI, in blue. Scale bar, 100 μm.

(c) Representative images of the progenitor distribution in females that were mated for 5 days. This shows how the GFP expression is restricted in progenitor doublets after their transient dense coverage at earlier time points (compare to panel b) suggesting that the mating effects are transient. GFP, in green; DAPI, in blue. Scale bar, 100 μm.

(d) Progenitors expand shortly after mating and EcR regulates this progenitor expansion as shown in (b). Percentage of cells positive for the intestinal progenitor marker (esg+ GFP+/gut area) in controls and females with progenitor-restricted downregulation of *EcR*. Quantifications are done through a macro that calculates the area of GFP+ cells relative to the gut area (see methods)

(e) ISC clones require EcR to expand after mating. Percentage of ISC clones covering the posterior midguts with *EcR*-depleted ISC clones relative to control midguts. Quantifications are done through a macro that calculates the area of GFP+ cells relative to the gut area (see methods)

(f) *Usp, Eip75B, EcR* in progenitors are required for the mating-induced ISC mitoses. Number of mitoses in control and progenitor-specific depletion of *Usp, Eip75B, EcR* for 8 days. Virgins were allowed to mate for 48 hrs. Results are shown for 2 independent RNAi lines for Usp .

(g) *EcR* in ISCs are required for the mating-induced ISC mitoses. Number of mitoses in control and ISC-specific downregulation of *EcR* for 8 days. Virgins were allowed to mate for 48 hrs and 72 hrs. Results are shown for 2 independent RNAi lines.

(h) *EcR* in enteroblasts is not required at an earlier time point but, is rather required at the later 72 hour time point for the mating-induced ISC mitoses. Number of mitoses in control and enteroblast-specific downregulation of *EcR* for 8 days. Virgins were allowed to mate for 48 hrs and 72 hrs. Results are shown for 2 independent RNAi lines.

(i) *EcR* in enterocytes is not required at either time points for the mating-induced ISC mitoses. Number of mitoses in control and enterocyte-specific downregulation of *EcR* for 8 days. Virgins were allowed to mate for 48 hrs and 72 hrs. All panels: Error bars represent ± SD. Statistical analysis was performed using unpaired non-parametric two-tailed Mann-Whitney test (ns $p>0.05$, $^{**}p\leq0.01$, $^{****}p<0.0001$). ♀ refers to mated females. ☿ refers to virgins. Representative images are shown.

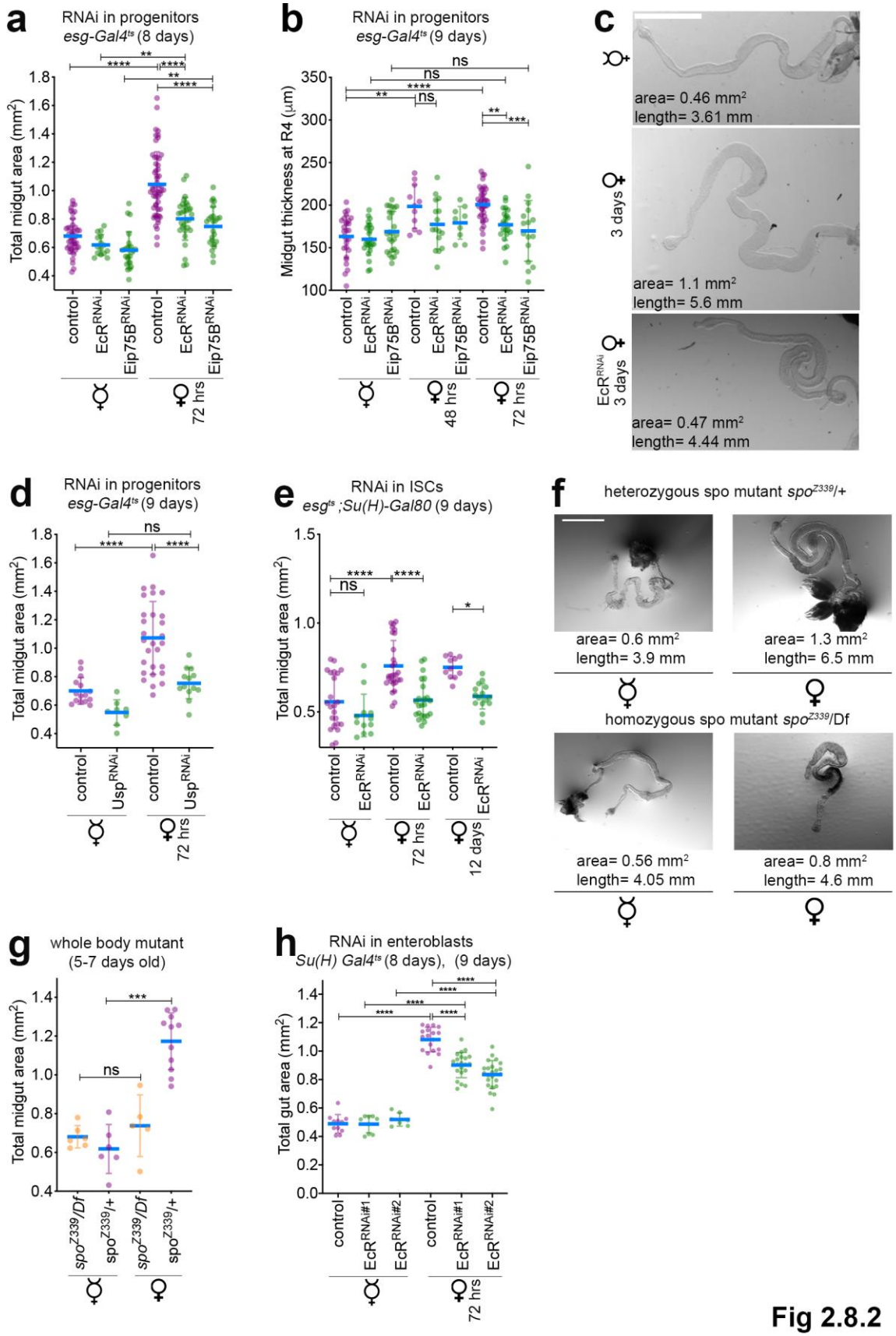
a
RNAi in progenitors
esg-Gal4ts (8 days)
Total midgut area (mm2)
control
EcRRNAi
Eip75BRNAi
72 hrs
b
RNAi in progenitors
esg-Gal4ts (9 days)
Midgut thickness at R4 (μm)
48 hrs
c
area= 0.46 mm2
length= 3.61 mm
3 days
area= 1.1 mm2
length= 5.6 mm
EcRRNAi 3 days
area= 0.47 mm2
length= 4.44 mm
d
RNAi in progenitors
esg-Gal4ts (9 days)
UspRNAi
e
RNAi in ISCs
esgts ;Su(H)-Gal80 (9 days)
12 days
f
heterozygous spo mutant spoZ339/+
area= 0.6 mm2
length= 3.9 mm
area= 1.3 mm2
length= 6.5 mm
homozygous spo mutant spoZ339/Df
area= 0.56 mm2
length= 4.05 mm
area= 0.8 mm2
length= 4.6 mm
g
whole body mutant
(5-7 days old)
spoZ339/Df
spoZ339/+
h
RNAi in enteroblasts
Su(H) Gal4ts (8 days), (9 days)
Total gut area (mm2)
EcRRNAi#1
EcRRNAi#2

**Fig 2.8.2**

**Fig 2.8.2: Mating induces EcR-dependent gut growth.** Text and images have been taken and modified from (Ahmed et al., 2020) and have been originally written and made by myself: (a) Midguts with *EcR*- or *Eip75B*-depleted progenitors do not grow post mating. Midgut size measurements of virgin and mated females, with and without $EcR^{RNAi}$ or $Eip75B^{RNAi}$ expressed in progenitors. Quantifications are done through a macro that calculates aspects of midgut morphology (see methods). Midgut areas are outputted and plotted in prism.
(b) Midguts with EcR- or Eip75B-depleted progenitors fail to increase the midgut width after mating. Midgut width at R4 of virgin and mated females, with and without $EcR^{RNAi}$ or $Eip75B^{RNAi}$ expressed in progenitors. Quantifications are done through a macro that calculates aspects of midgut morphology (see methods).
(c) Mating causes EcR-dependent gut growth. Representative bright-field images of a virgin, control or *EcR*-depleted mated female.
(d) Midguts with Usp-depleted progenitors do not grow post-mating Midgut areas of virgin and mated females, with and without $Usp^{RNAi}$ expressed in progenitors..
(e) Control females reveal a mating-dependent increase in gut size that is regulated by EcR in ISCs. Midgut size measurements of virgin and mated females, with and without $EcR^{RNAi}$ expressed in ISCs. Females were allowed to mate for 72 hrs only or raised mated.
(f) Ovary production of ecdysone is essential for mating-dependent midgut growth. Representative bright field images of whole body spo mutants that are heterozygous and hence, viable with no growth or egg laying defects (1st upper panels) and survivor sterile homozygous spo mutants that are rescued to adulthood by a pulse of 20HE given to dechorionated embryos (2nd lower panels), quantified in (g). Scale bar 1mm.
(g) *spo* mutants fail to undergo mating-dependent gut growth. Midgut areas from whole-body homozygous *spo* mutants ($spo^{Z339}/Df$) rescued to adulthood by an exogenous 20HE pulse given to embryos, and heterozygous controls ($spo^{Z339}/+$).
(h) EcR is needed in enteroblasts for an optimal full-grown gut post-mating. Midgut areas of virgin and mated females, with and without $EcR^{RNAi}$ expressed in enteroblasts.
Error bars represent ± SD. Statistical analysis was performed using one-way ANOVA, followed by Bonferroni's multiple comparisons test (ns $p>0.05$, *$p\leq 0.05$, **$p\leq 0.01$, *** $p\leq 0.001$, ****$p<0.0001$). ♀ refers to mated females. ☿ refers to virgins. Representative images are shown.

Whether EcR in ECs is required for the mating-dependent midgut resizing remains unexplored. Additionally, to validate the RNAi results, I used whole body spo mutant animals, that are ecdysone-deficient and embryonic lethal, but can be rescued to adulthood by exogenous 20HE given during embryogenesis[312]. Remarkably, surviving adult mated *spo* mutant females were sterile and failed to resize their midguts (Fig 2. 8.2g-h), suggesting that ovary-to-gut signaling is essential for mating-adaptive gut

resizing.

**2.9. Ovary-derived ecdysone signaling regulates post-mating gut growth in the female midguts.**

The main source of 20HE production is the ovaries[153,301]. So, in a next step I investigated if they are the source of 20HE that affects the midgut. Hence, I depleted 2 different ecdysone biosynthetic cytochrome P450 enzymes *disembodied* (*dib*) or *spook* (*spo*) with ovary-specific drivers (*C587-Gal4*$^{ts}$, *tj-Gal4*)[123,302,313,314], then I examined the effects on the gut post-mating.

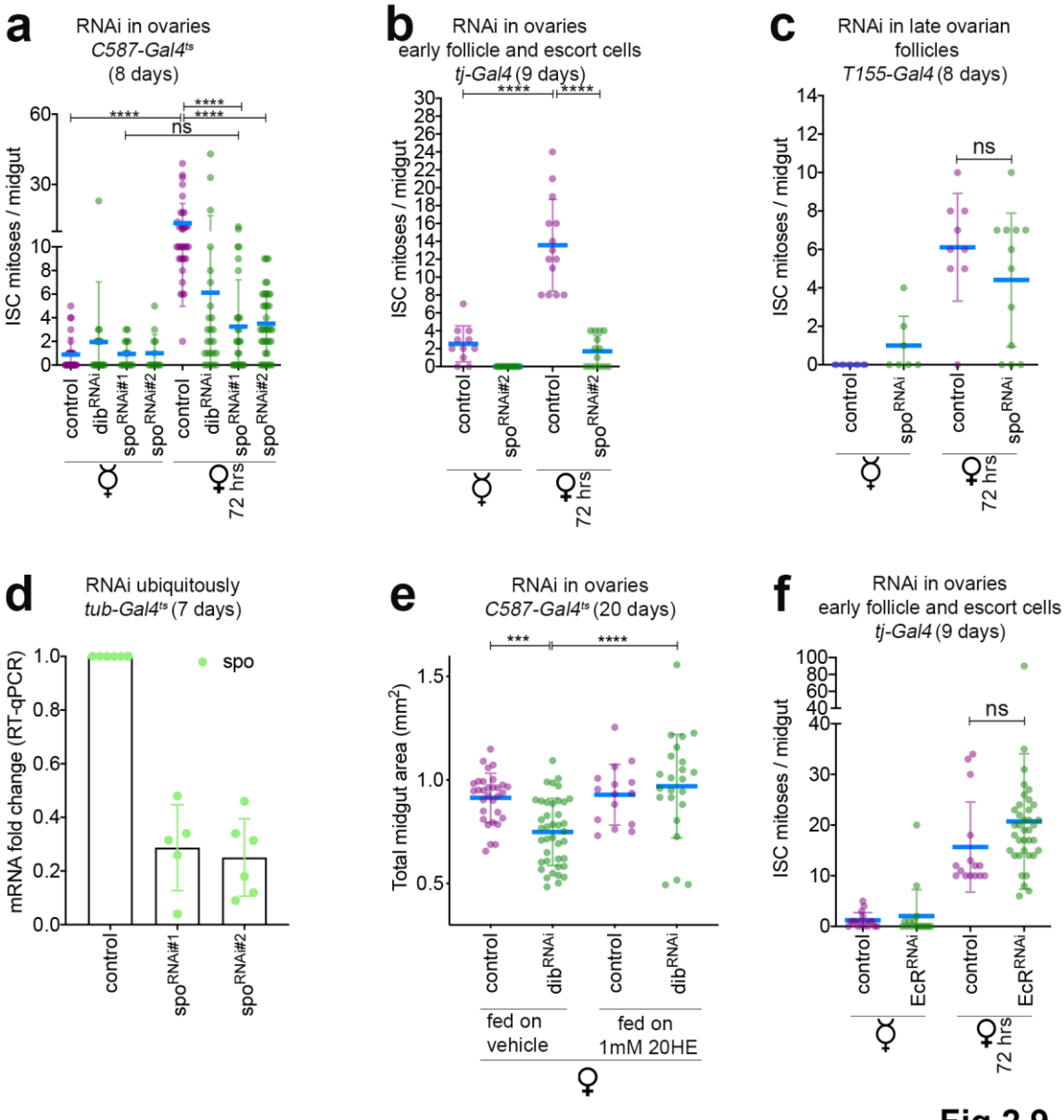


**Fig 2.9**

**Fig 2.9: Ovary-derived 20HE production regulates mating-induced ISC mitoses.** Text and images have been taken and modified from (Ahmed et al., 2020) and have been originally written and made by myself: (a) Ovarian ecdysone controls mating-induced ISC mitoses. Ecdysone production was suppressed in adult females by expressing *spo*$^{RNAi}$ or *dib*$^{RNAi}$ under the control of the ovarian somatic cell-specific Gal4 driver *c587*$^{ts}$. Midguts were scored for mitotic cells 3 days after mating. Mated females with reduced ecdysteroidogenic enzymes in the ovaries have impairment in their mating-induced ISC mitoses. Results are shown for 2 independent RNAi lines for *spo*.
(b) Ovarian ecdysone controls mating-induced ISC mitoses. Ecdysone production was suppressed in adult females by expressing *spo*$^{RNAi}$ under the control of the ovarian somatic cell-specific Gal4 driver traffic jam (*tj*). Midguts were scored for mitotic cells 3 days after mating. Mated females with reduced spo in the ovaries have impairment in their mating-induced ISC mitoses.
(c) Ovarian ecdysone from early stage follicles contributes to most of the mating-induced ISC mitoses. Ecdysone production was suppressed in adult females by expressing *spo*$^{RNAi}$ under the control of the ovarian late follicle cell-specific Gal4 driver (*T155*). Midguts were scored for mitotic cells 3 days after mating. Mated females with reduced spo in their late follicle have a slight non-significant impairment in their mating-induced ISC mitoses.
(d) Knock down efficiency of *spo* was confirmed by qPCR on adult ovaries constitutively expressing the RNAi construct under the control of *tub*$^{ts}$.
(e) Ecdysone production was suppressed in adult females by expressing *dib*$^{RNAi}$ under the control *c587*$^{ts}$. Midgut sizes of mated females defective in ecdysteroidogenic enzymes are significantly smaller than age-matched controls. This gut size defect was rescued by raising the females on 20HE-supplemented food.
(f) Maintenance of ovarian somatic cells does not affect mating ISC-induced mitoses of the gut. *EcR*$^{RNAi}$ was expressed under the control of the ovarian somatic cell-specific Gal4 driver *c587*$^{ts}$. Midguts were scored for mitotic cells 3 days after mating. Mated females with reduced EcR signaling in the ovaries do not impact mating-induced intestinal EcR signaling in the gut. All panels: Error bars represent ± SD. Statistical analysis in e was performed by one-way ANOVA, followed by Bonferroni's multiple comparisons test otherwise unpaired non-parametric two-tailed Mann-Whitney test was used (ns $p>0.05$, *** $p\leq 0.001$, **** $p<0.0001$). ♀ refers to mated females. ☿ refers to virgins.

Ecdysone production is reported to occur in the early follicles and escort cells of the ovaries and the drivers I used *C587-Gal4*$^{ts}$, *tj-Gal4* are also reported to act in those cells[313,314]. As predicted, reduced ecdysone levels abolished the mating-induced ISC proliferation (Fig 2.9a-b) and midgut re-sizing, which could be restored by raising the flies on exogenous 20HE in their diet (Fig 2.9e). The suppressed gut effects were specific to the depletion of the ecdysone-synthesizing enzymes because *EcR*$^{RNAi}$ in the early

ovarian follicles, which is vital for the follicle formation[315], was uncoupled from its actions on the mating-induced ISC mitoses of the midgut (Fig 2.9f). In contrast, depleting *spo* with a late ovarian-follicle specific driver (*T155-Gal4)* did not completely diminish the mating-induced ISC mitoses indicating that the late ovarian follicles are not the predominant source of endogenous ecdysone (Fig 2.9c). These results complement the whole body mutant results and prove that ovary-derived ecdysone regulate intestinal stem cell division and gut size.

**2.10 Masculinized female progenitors are able to resize their midguts after mating.**

My results so far have suggested that there are 2 non-overlapping pathways controlling ISC mitoses: 1st is the cell-autonomous sex determination pathway and 2nd is the non-cell autonomous ovary to gut 20HE signaling. Thus, I asked whether the consequences of ovary-derived 20HE after mating diverge from the effects of the sex determination pathway on ISC behavior. So, I induced progenitor-specific *tra*$^{RNAi}$ in virgin females, then I mated them for 3 days, and found that virgins with *tra*$^{RNAi}$ progenitors remain competent to expand their gut size post-mating (Fig 2.10a). Consequently, control virgin midguts or masculinized virgin midguts with *tra*$^{RNAi}$ progenitors grow similarly after mating. When control females or females with masculinized progenitors were raised mated, the sizes of their midguts were comparable (Fig 2.10a).

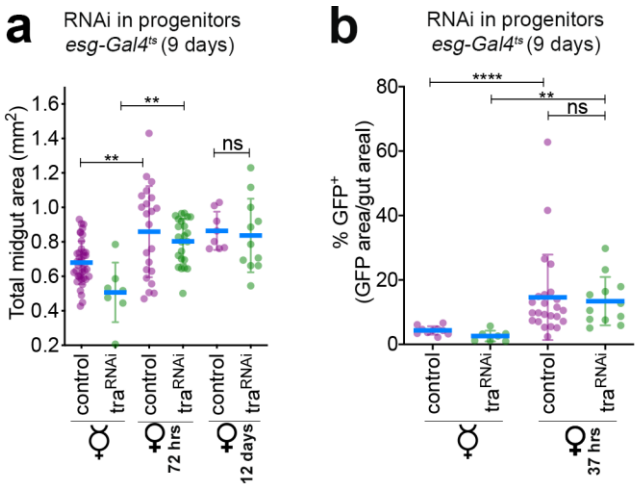


Fig 2.10

**Fig 2.10: Females with progenitors masculinized by *tra*$^{RNAi}$ are able to resize their midguts after mating**. Text and images have been taken and modified from (Ahmed et al., 2020) and have been originally written and made by myself: (a) Both control and *tra*$^{RNAi}$ progenitors female midguts exhibit a mating-dependent increase in gut size. Gut

growth is unaffected by masculinizing the identity of the progenitors. Midgut size measurements of virgin and mated females, with masculinized progenitors by *tra*-depletion. Females were only allowed to mate for 72 hrs or raised mated.
(b) Progenitors expand shortly after mating and this expansion is independent of *tra*. Percentage of progenitors positive for the GFP+/gut area in controls and females with progenitor-restricted downregulation of *tra.* Error bars represent ± SD. Statistical analysis in a was performed by one-way ANOVA, followed by Bonferroni's multiple comparisons test otherwise unpaired non-parametric two-tailed Mann-Whitney test was used (ns $p>0.05$, ** $p\leq 0.01$, ****$p<0.0001$). ♀ refers to mated females. ☿ refers to virgins.

Similarly, quantification of the GFP signal, reflective of progenitor expansion in masculinized progenitors reveals that the progenitors are competent to expand after mating similar to control progenitors (Fig 2.10b). The absence of an intestinal resizing defect in masculinized progenitors after mating is consistent with the hypothesis that the intestinal growth is non-cell autonomously controlled by the ovaries of mated females, independent of the cell-intrinsic mechanisms regulating ISC behavior.

**2.11. Mating leads to an additive advantage on female ISC proliferation.**

Next, I asked whether endogenous hormonal differences between virgin females (physiological low 20HE levels) relative to mated ones (physiological high 20HE level)[301] would impart any differences on the ISC proliferation under stress or during homeostasis. To test this hypothesis, I induced masculinization of virgin or mated ISCs by repressing the sex-determination genes sex lethal or transformer in ISC clones. I raised some flies are virgins and others were left to mate with males until dissection then I let the flies feed on SDS detergent,16-18hrs before dissection[118]. ISC mitotic counts show that indeed ISCs of wildtype mated females are more efficient in dividing after detergent-induced stress relative to wildtype virgin females. Furthermore, as previously shown ISC mitoses in virgin sxl-/tra- depleted ISC clones were completely suppressed (Fig 2.11a)[118]. In contrast, ISCs of mated females with $sxl^{RNAi}$ or $tra^{RNAi}$ in their ISC clones are somewhat proficient in their regenerative mitoses. Alternately, I sought to suppress intestinal EcR signaling via EcR or its downstream target Eip75B-depletion in ISCs and assayed their mitotic responses to detergent-induced stress (Fig 2.11b). ISCs in $EcR^{RNAi}$ or $Eip75B^{RNAi}$ ISC clones shown significant defects in replenishing the midguts upon detergent-induced stress. This suggests that the mating status relays a stimulatory signal

via intestinal EcR signaling to improve the response of the midguts to stress-induced midgut mitoses. Additionally, mating also regulates basal ISC mitoses under non-stressed conditions. Aging ISCs of virgin $tra^{RNAi}$ or $sxl^{RNAi}$ ISC clones barely divide, nonetheless ISCs of mated $tra^{RNAi}$ or $sxl^{RNAi}$ ISC clones divide 11-76 times more frequent than virgin clones (Fig 2.11c).

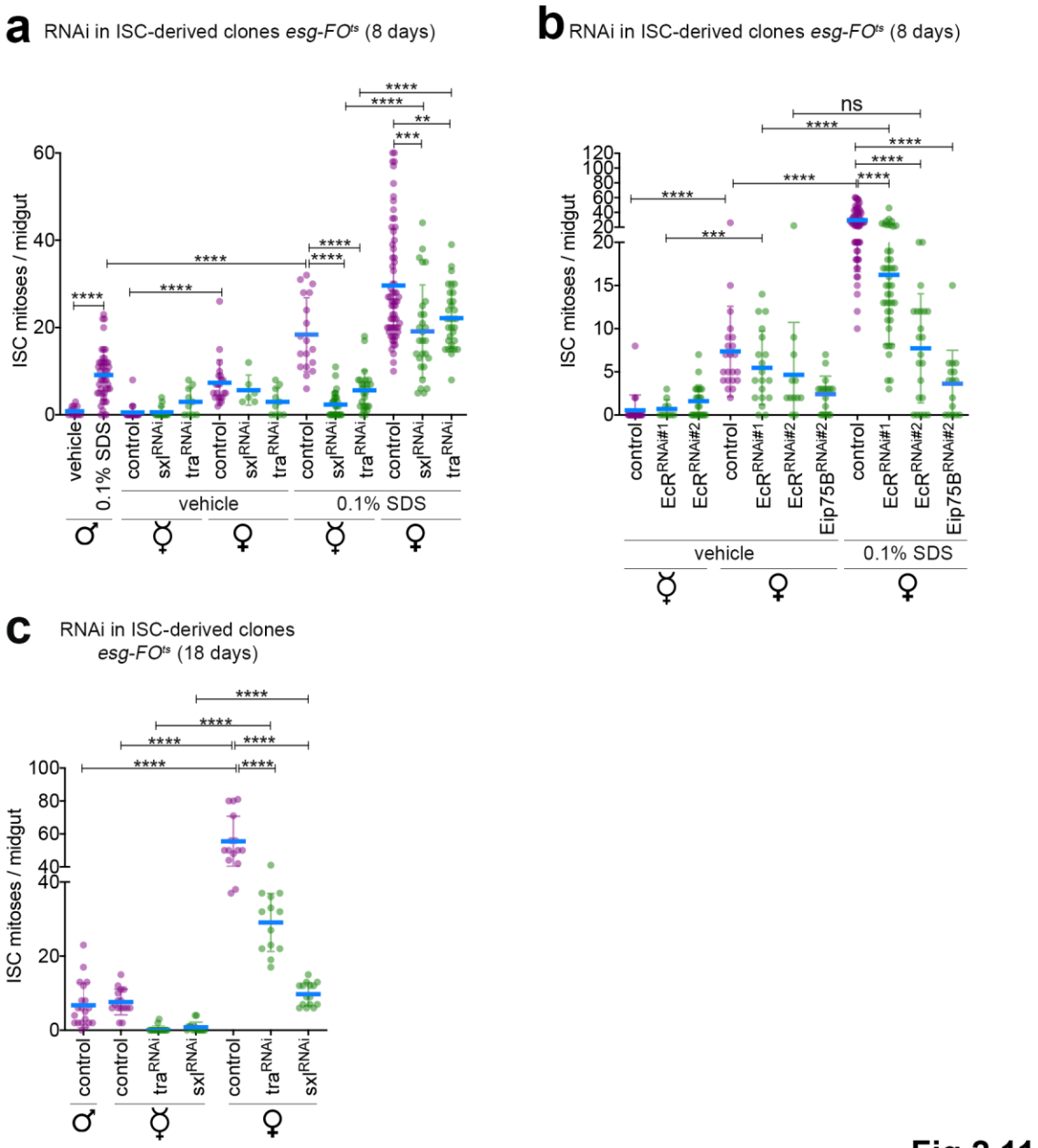


**Fig 2.11**

**Fig 2.11: Mating cross talks with the cell-autonomous sex determination pathway to regulate ISC mitoses basally and under stress.** Text and images have been taken and modified from (Ahmed et al., 2020) and have been originally written and made by myself: (a) Mating boosts the mitotic divisions of ISCs. Feeding 0.1% SDS for 16 hrs to

virgin females induces ISCs mitoses while male ISCs divide minimally to the stress. Mitoses are suppressed by masculinizing ISC clones using $sxl^{RNAi}$ or $tra^{RNAi}$. Mating increases the ISC mitotic responses to SDS feeding and somewhat restores the ability to masculinized ISCs to divide to detergent-stress.
(b) Ecdysone signaling via EcR and Eip75B is required in ISC clones of mated females for optimal regenerative SDS-induced ISC mitoses. ISC mitotic counts of virgin females are minimal under basal conditions. Basal mitoses are increased in mated females. Upon SDS feeding, control mated ISC clones divide to regenerate the epithelium but EcR or Eip75B depleted ISC clones are significantly impaired in their ability to divide. RNAi was induced in ISC clones for 8 days before 16-18 hrs of 0.1%SDS feeding.
(c) Mating causes an additive increase in homeostatic divisions independent of the sex identity. ISC counts of masculinized ISC clones using $sxl^{RNAi}$ or $tra^{RNAi}$ show that masculinized midguts can still adapt to the increased basal ISC mitoses in mated relative to virgin females. Error bars represent ± SD. Statistical analysis was performed using unpaired non-parametric two-tailed Mann-Whitney test. (ns $p>0.05$,**$p\leq0.01$,***$p\leq0.001$,****$p<0.0001$). ♂ refers to males, ☿ refers to virgins and ♀ refers to mated females.

These results indicate that the mating status per se transduces additional hormonal non-cell autonomous signals to the gut that promote the ISC mitoses upon detergent-induced ISC response and during aging. Highly competent ISCs have the advantage and the benefit of meeting the homeostatic tissue needs and high reproductive demand of the females, however, if this comes at the expense of faster deterioration of the gut or not is something I will explore in later sections. Hence, both ISC-autonomous and non-autonomous hormonal factors alter ISC proliferation.

### 2.12. *rho* and *upd2* induction are a physiological consequence of mating

As I discovered that 20HE exogenous feeding up-regulates rho and upd2, I wondered if mating induces the midgut expression of *upd2* and *rho* to a similar degree as 20HE feeding (Fig 2.12a) (Compare to Fig 2.5b). Indeed, whole gut qPCRs show that *upd2* and *rho* induction also occur in response to mating suggesting that they are a part of the normal physiological mating response. This is particularly intriguing because these

targets were only previously described as a part of the gut epithelial damage or stress responses in *Drosophila*[8,41,291].

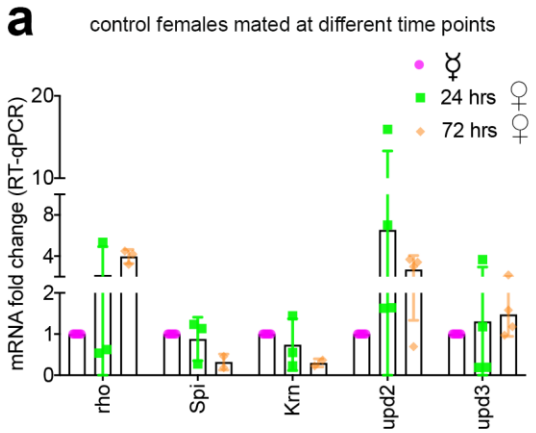


Fig 2.12

**Fig 2.12: Mating prompts *rho* and *upd2* upregulation.** Text and images have been taken and modified from (Ahmed et al., 2020) and have been originally written and made by myself: (a) Mating-induced *rho* and *upd2* induction is physiological and not stress-related. mRNA expression was measured by qPCR of control midguts that are virgins or mated for 24 hrs or 72 hrs. Relative to virgins, a moderate increase in mRNA expression levels of *rho* and *upd2* is detected as a consequence of mating.

## 2.13. 20HE feeding is not supra physiological and induces target genes similar to mated females.

Since in earlier sections I described mitotic effects and midgut growth that occurs in male and virgin *Drosophila* in response to different 20HE feedings, which hasn't been unparalleled in previous reports, I wondered if this 20HE I was giving the flies was within the physiological range or not.

Thus, I fed virgin females with various doses of 20HE and I compared the strength of the 20HE-target gene induction to virgin flies that I mated for 24hrs or 48hrs (Fig 2.13a). I picked 2 of the well-known early 20HE-inducible targets the nuclear receptor *Eip75B* and the transcription factor *Broad* that I will refer to again in later chapters of this thesis. In parallel, I fed the flies with the same doses of 20HE and assayed the ISC mitoses 16-18 hrs after feeding and compared it to basal mitoses in young mated female guts (Fig 2.13b). Firstly, mating induced target genes 2-2.5 fold higher than virgin females,

consistent with the increased ecdysone levels produced by the ovaries. Similarly, ranges of 20HE doses between 0.5-5mM 20HE induced target genes 2-2.5 fold higher than that of mated females, while 10mM 20HE induced target genes almost 3 fold higher than that of mated females. Secondly, mitotic counts of 0.25-1mM 20HE-fed virgin flies were not significantly changed compared to mitotic counts of mated non-stressed females. Only 2mM 20HE modestly increased ISC mitoses, but consistent with previous data, 5mM 20HE boosted mitotic counts. These experiments indicate that the 20HE-dependent target gene induction did not reach its highest levels with the doses of 20HE that I have used in my studies. Also, a mild induction of 20HE target genes caused by exogenous feeding was not sufficient to induce a transient boost of ISC mitoses unlike mating where target genes were induced ≈2 fold accompanied by many transient ISC mitoses (compare to Fig 2.8.1a). Probably, mating results in different kinetics of 20HE-target gene induction, in parallel with an organism-wide activation of metabolic processes that work in synchrony to direct ISC mitoses and gut growth[311]. These experiments also implied that 1mM 20HE that I have used for my long-term feeding experiments was well tolerated by the flies.

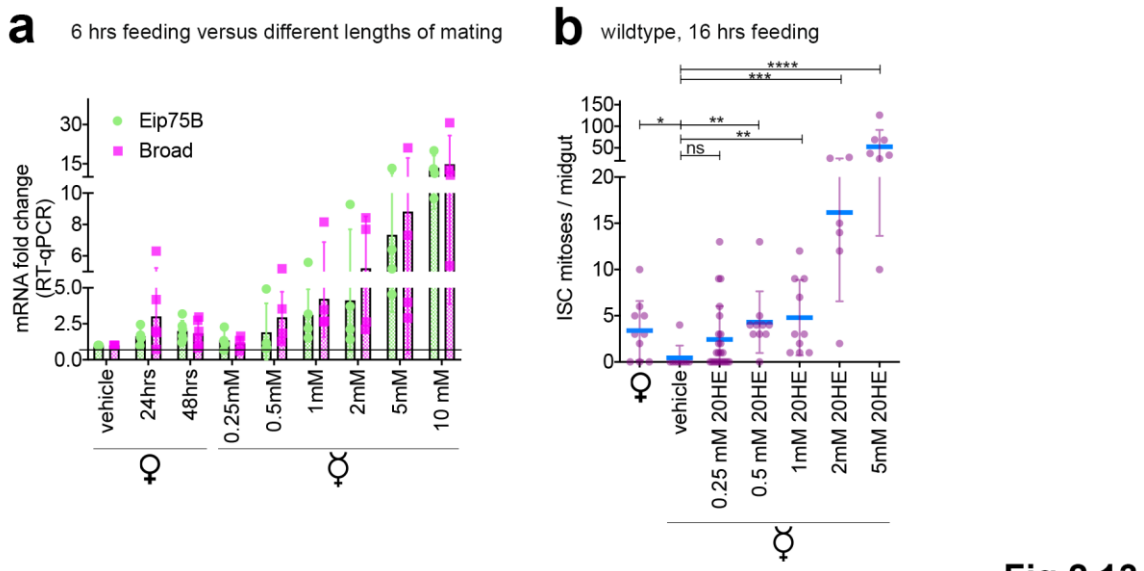


Fig 2.13

**Fig 2.13: 20HE causes a dose-dependent induction in target genes and subsequent ISC mitoses.**

(a) Midguts of 24-48 hrs post-mated flies have upregulated levels of their ecdysone targets, similar to exogenous 20HE feeding. qRT-PCR measurements from whole midguts show that expression levels of *Eip75B* and *broad* mRNA are induced in a dose-dependent manner after 20HE feeding relative to vehicle-fed virgins.

(b) 20HE feeding causes 20HE causes ISC divisions in a dose-dependent manner in ISCs of virgin females. Virgins were fed different concentrations of 20HE and their mitotic indexes were assessed after 16- 18hrs of feeding. At 0.25-1mM 20HE, ISCs divide similar to basal levels in mated females. At 2mM 20HE feeding, ISCs mildly divide (3-4x higher than divisions induced by 1mM 20HE). At 5mM 20HE, ISCs divide at 10-11x higher that divisions induced by 1mM 20HE. Error bars represent ± SD. Statistical analysis was performed by unpaired non-parametric two-tailed Mann-Whitney test (ns $p>0.05$,*$p\leq 0.05$,**$p\leq0.01$,***$p\leq0.001$, ****$p<0.0001$). ♀ refers to mated females. ☿ refers to virgins.

**2.14. Mating induces symmetric ISC divisions and ISC expansion.**

As the gut size is enlarged post-mating, it could be a consequence of increased cell number, size or both. As, I have discovered that there is a massive transient increase in ISC divisions, I wondered if the mode of most of those divisions was asymmetric or symmetric as previously described during regeneration[316] or homeostatic adaptive gut growth[12]. If ISCs divide symmetrically, they give rise to two competent ISCs. Asymmetric ISC division however, gives rise to one ISC and a short-lived enteroblast[316]. To figure this out, I have used virgin female midguts with GFP-marked enteroblasts and LacZ-marked delta$^+$ ISCs. Then, I mated them for 24, 40 hrs and 7 days. 24hrs-post mating, LacZ$^+$ ISCs remained singlets, similar to virgins (Fig 2.14a-b). However, 40 hrs-post mating, LacZ$^+$ ISCs had mostly become doublets or triplets, indicating that those young ISCs are partly a result of symmetric ISC divisions. 7 days post mating, regardless of whether the flies have mated once/night or co-housed with males for the whole duration, there was an irreversible increase in the number of LacZ$^+$ ISCs across the epithelial layer, with occasional doublets or triplets as a result of mating. However, the number of enteroblasts remained relatively low. This observation supports the view of an asymmetric division signature (Fig 2.14a-b). All in all, mating causes an ovarian ecdysone-dependent-(Fig 2.1.2m, Fig 2.14d) and EcR-dependent (Fig 2.8a,b,f, Fig 2.14c) increase in ISC numbers after mating. The claim that the increase in the progenitor population drives mating-dependent gut growth was supported by the quantification of EC size between EcR-depleted ECs of mated females versus ECs of control mated females (Fig 2.14e,f), and the quantification of EC numbers between flies that were raised as virgins or mated respectively (Fig 2.14g,h).

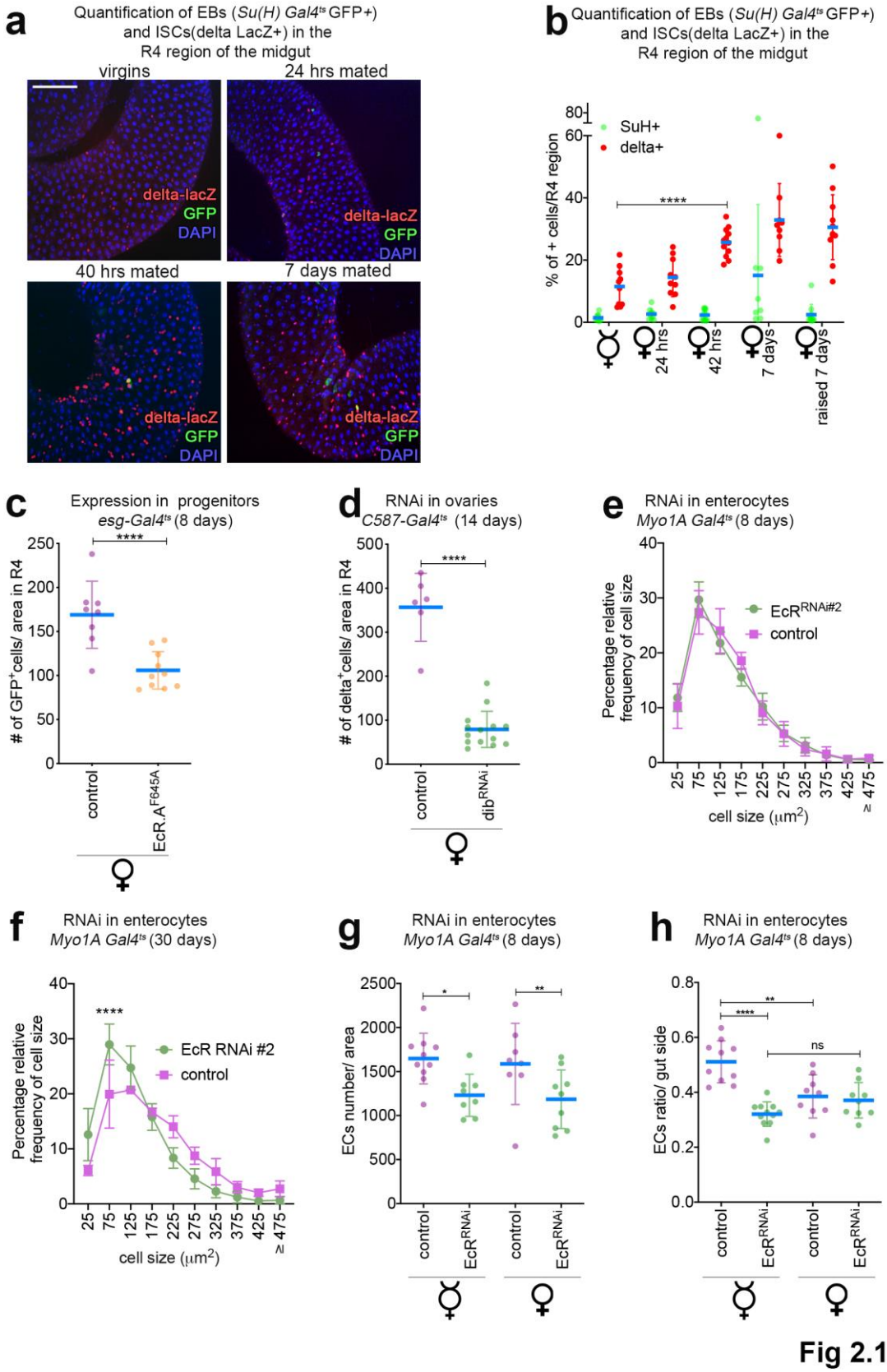


Fig 2.14

**Fig 2.14: Mating induced 20HE regulates symmetric ISC divisions, ISC cell number, EC size and numbers.** Text and images have been taken and modified from (Ahmed et al., 2020) and have been originally written and made by myself: (a-b) (a) Mating induces a symmetric increase in delta+ cells shortly after mating. Representative images of the R4

region of the midgut in virgin females shortly after mating or 7 days after mating. ISCs are marked with delta+ (red) and EBs are marked with GFP (green) Su(H)+ cells. At 24 hrs post mating, most delta+ cells remain singlets, similar to virgins. At 40 hrs post mating, most delta+ cells expand to become doublets or triplets. At 7 days after the 1$^{st}$ mating, most delta positive cells are again singlets, however their numbers are irreversibly increased relative to virgins. Females were mated to males with no genetic manipulations. Equal number of males and females were allowed to mate (a ratio of 1:1) and females were allowed to mate for 18-20 hrs after which males were removed, except for the condition "raised mated for 7 days" whereby males were always in the vial with the females. Images are acquired in the R4 region. delta, in red; GFP, in green; DAPI, in blue. Scale bar, 100 μm. (b) Quantification of (a). Each dot represents a gut, and % of delta+ or Su(H)+ cells are derived from absolute number of positive cells relative to total DAPI+ cells (see Methods).

(c) Intestinal EcR signaling regulates progenitor cell number in the R4 region. Quantification of GFP+ progenitors/area of the midgut stack shows that *EcRA*$^{DN}$ progenitors are reduced relative to control progenitors of mated females.

(d) Ovarian ecdysone signaling regulates delta+ cell numbers in the R4 region. Quantification of delta+ cells/area of the midgut stack shows that *dib*$^{RNAi}$ ovaries have intestines with drastically reduced numbers of delta+ cells relative to delta+ cells of control mated females.

(e) R4 midgut enterocytes expressing *EcR*$^{RNAi}$ in young mated flies causes a non-significant accumulation of smaller-sized cell populations relative to age controlled mated females. Shown is a frequency distribution of the different cell sizes. EcR depleted enterocytes have a very slight bigger proportion of cells sized 75-175 μm$^2$ than control midguts (also observed in other contexts). However, the differences in distribution of the cell sizes are statistically non-significant.

(f) Depletion of EcR in midgut enterocytes of old mated flies causes an accumulation of smaller-sized cell populations relative to age controlled mated females. Cells of the midgut were stained with a cytoplasmic stain and a macro was designed to segment the cells according to their sizes (see Methods). Shown is a frequency distribution of the different cell sizes. Control flies have a bigger proportion of cells sized 200-825 μm$^2$ than midguts with *EcR*$^{RNAi}$ enterocytes. Images are taken in the R4 region.

Collectively, data in panels e and f indicate that EcR regulates cell size of enterocytes that may consequently alter nutrient absorption from the gut. Data are from n≤5 stacks of midguts taken at the R4 region.

(g) EcR is required for optimal increase of ECs number irrespective of mating. Midguts with EcR depleted ECs have a defect in the number of their ECs of the R4 region. Each dot represents the number of ECs/midgut quantified from R4 stitches (see Methods). While mating does not cause an increase in the number of ECs per se, EcR depleted ECs have a defect in their numbers that is not compensated by the "mating" process.

(h) Mating causes an increase in the ratio of other midgut cell types/ECs. Virgins have a higher number of ECs/total DAPI+ cells as quantified from R4 stitches. Mating causes a drop in this ratio indicative of a relative increase in the number of total EC$^-$DAPI+ cells. Conversely, virgins with EcR depleted ECs have a defect in sustaining a high ratio of ECs/total DAPI+ cells suggesting that these midguts have a higher ratio of EC$^-$DAPI+ cell types. This ratio is not altered after mating. Statistical analysis was performed using one-way ANOVA, followed by Bonferroni's multiple comparisons test panels: g,h or unpaired non-parametric two-tailed Mann-Whitney test (ns $p>0.05$,*$p\leq 0.05$,**$p\leq 0.01$, ****$p<0.0001$). ♀ refers to mated females. ☿ refers to virgins.

To figure out the size distribution of cells in the R4 region, I stained the gut with a plasma membrane stain, then I imaged cells in the R4 region and counted them and generated a frequency distribution histogram of the percentage of cells versus cell size. EcR depletion in ECs of young guts did not show a measurable or significant difference in their distribution relative to control guts (Fig 2.14e). However, EcR depletion in ECs of old mated females caused a significant reduction in EC size (fractions higher than 176μm$^2$) relative to control guts indicating that intestinal EcR signaling affects EC size (Fig 2.14f). Secondly, mated females did not show a striking increase in EC numbers in R4 region as a consequence of mating per se (Fig 2.13g,h) but there were specific effects of EcR on ECs on aspects of cell number, which I re-allude to in later sections of this thesis. This comes slightly in contrast to what a previous report finds[311] though the differences could be attributed to two factors: Reiff et al focuses on R5 region which is the most posterior region of the midgut and it is a much smaller and functionally distinct than R4[2,3]. Moreover, the differences they observe are slight, and they quantify the enterocytes across the whole gut, while I only took stitches focusing on the R4 region. Thus, I conclude that gut growth is highly dependent on the action of ovary-derived ecdysone on the midgut progenitors.

### 2.15. 20HE is involved in the regulation of enteroblast differentiation into enterocytes as well as maintaining proper EC number.

Several results I had from my experiments pointed towards a possible role of ecdysone signaling in differentiation, .in this section I will gather all the evidence I obtained during

the course of my thesis to support the role of intestinal EcR signaling in differentiating EBs or differentiated ECs.

Enteroblasts are the cell type that differentiates to give rise to either absorptive enterocytes (ECs) or secretory entero-endocrine cells (ees)[5,93,317]. This fate specification step depends on the level of Notch signalling in the enteroblasts: High level of notch activates a transcriptional program in the enteroblasts that leads to its differentiation into an EC [317-319]. ECs can be marked by nubbin (Pdm1) expression, a POU-domain transcription factor specifically expressed in mature ECs[320]. Firstly, EcR depleted ISC clones of mated females leads to formation of clones with smaller cell sizes, which mostly fail to give rise to the large polyploid enterocytes (Fig 2.1.2k,l and Fig 2.23d,e). Then, as I investigated earlier which cell types are required for the 20HE-induced mitoses, I noticed that EcR depleted enteroblasts by $SuH^{ts}$ leads to accumulation of many enteroblasts (Fig 2.15.1a). Conversely, overexpression of the ecdysone-inducible target Eip75B I characterize in later sections of the thesis (Fig 2.17-19) led to the accumulation of $Pdm1^{+}$, $GFP^{+}$ polyploid big-sized cells (Fig 2.15.1b), or large enteroblasts (Fig 2.17f) suggestive of Eip75B pushing cells through differentiation. As a matter of fact, every time the ISCs expressed high levels of Eip75B but were not triggered to divide, the ISCs start developing abnormal morphology and misdifferentiate. This adverse effect was rescued by sensitizing the ISCs to proliferate with a brief heatshock prior to ectopically increasing the Eip75B levels by shifting to 29ºC (Fig 2.17e). So primary evidence suggests that intestinal EcR signaling, through Eip75B regulates EB differentiation.

To determine whether EcR plays a role in establishing the cell number/size of both enteroblasts or ECs, I conducted a series of experiments to measure the number of EBs or ECs from microscope stitches taken in the R4 region of the midgut of males and females. This allowed me to count the number of cells from the respective driver background to examine the effects of EcR depletion in EBs or ECs upon exogenous 20HE feeding or mating. For this experiment, I fed males and females with vehicle or 20HE for 14 days that was replaced every 1-2 days. Fig 2.15.1c shows the total number of cells of male or female guts from different genetic backgrounds $SuH^{ts}$ *or* $Myo1A^{ts}$ to reflect the robustness of the quantification. Indeed, the technique I used for getting the automated stitches and counting them is quite robust, reflected by the narrow standard deviation. Remarkably, 20HE supplementation for 14 days causes a significant increase in the cellularity of the

midguts relative to vehicle-fed flies (Fig 2.15.1d). Nevertheless, 20HE feeding to control flies for 15 days does not increase the number of EBs relative to vehicle-fed control flies. This is not the case with transient overnight 20HE feeding, whereby there is an increase in the number of enteroblasts (data not shown), probably consistent with the state of increased transient ISC mitoses.

Then, I examined the effect of reduced EcR levels in the EB population of the male and female midguts. When EcR was depleted in EBs of either male or female flies, there was a substantial accumulation of the enteroblast population in the posterior midgut suggesting that differentiation to ECs is blocked (Fig 2.15.1e,f). Strikingly, 20HE supplementation in the food releases this block and the number of EBs return to similar levels relative to control animals (Fig 2.15.1e,f). It remains unclear how 20HE would function to rescue this prominent EB defect of EcR depleted EBs in both sexes. It could be that the remaining EcR would be enough to transduce 20HE signalling to the EBs though highly unlikely as EcR depleted EBs suppress 20HE- or mating-induced ISC mitoses (Fig 2.3b and Fig 2.8.1h). Alternatively, EcR depletion with the co-increase of 20HE availability could cause a compensatory changes such as upregulation of EcR expression or slowed trafficking or recycling of EcR in response to its hypofunction similar to a paradigm described for dopaminergic or seretonergic receptors[321,322].

Since there is hyperplasia of the midguts of 20HE-fed flies, I attributed it to increased number of the remaining midgut populations: ECs, ISCs or EECs (Fig 2.15.1d). Consistent with this idea, midguts with EcR depleted EBs that are raised on exogenous 20HE have bigger midguts, though the effect is more pronounced in females (Fig 2.15.1g). Thus, 20HE feeding causes hyperplasia which results in some gut growth and it is required also required for EB differentiation.

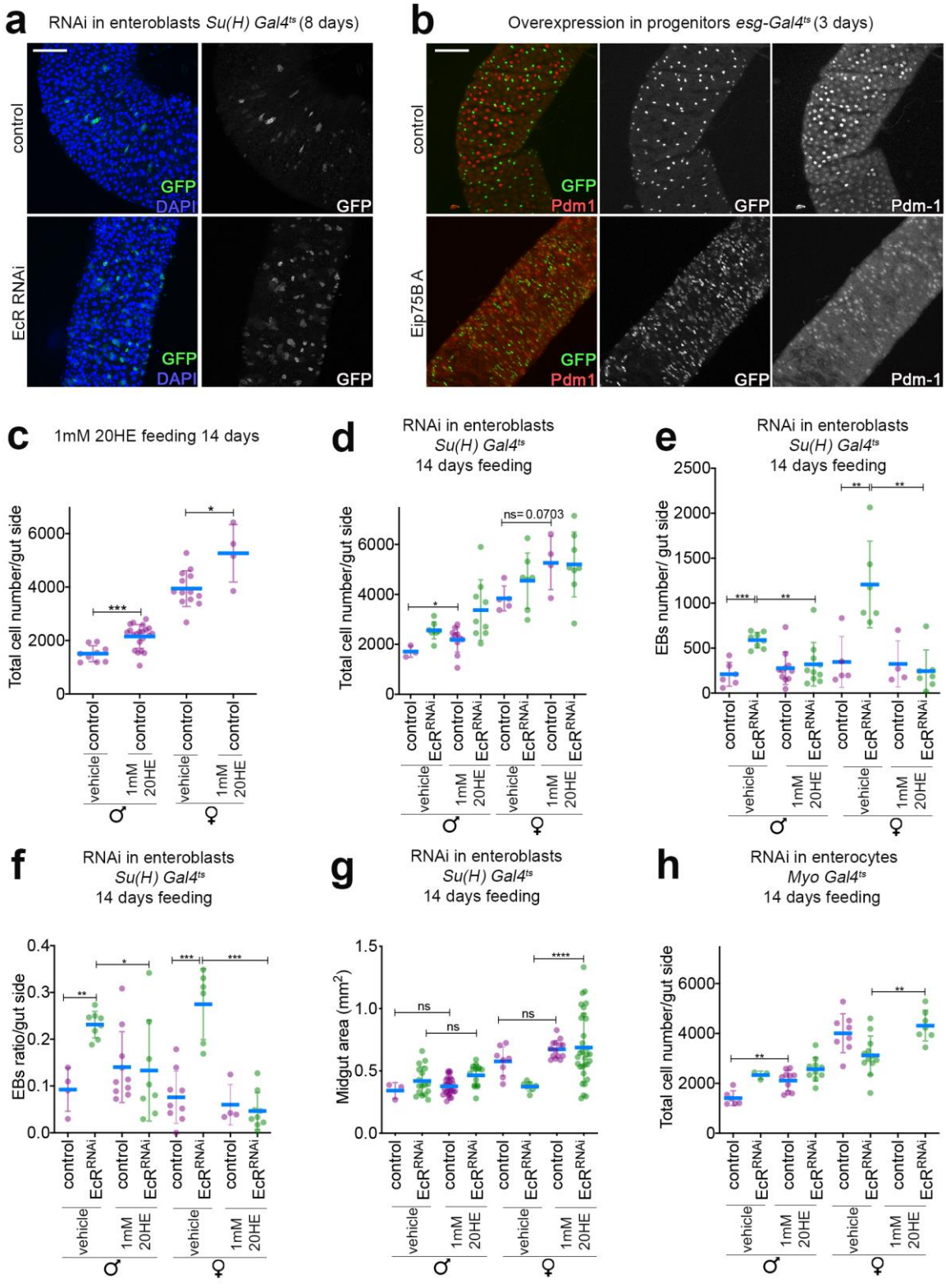


Fig 2.15.1

**Fig 2.15.1: Intestinal EcR signaling functions in fine-tuning the balance between proliferation and differentiation.**

(a) Mated female midguts with *EcR*$^{RNAi}$ expressing EBs accumulate numerous EBs relative to age-matched mated control females. Representative confocal images of midgut with EcR depleted EBs.
(b) Eip75B overexpression leads to the appearance of GFP+ /Pdm1+ cells, suggestive of aberrant cell growth or precocious differentiation. Representative confocal images of midguts overexpressing Eip75B in the progenitors co-stained with the EC differentiation marker Pdm1+.
(c) Total cell number of DAPI$^{+}$ cells/gut side/midgut stitch in the R4 region from the different driver backgrounds: *Su(H)$^{ts}$* Gal4 or *MyoIA$^{ts}$* Gal4 of male and female midguts +/- prolonged 20HE feeding. Females have more than double the number of cells relative to males. 20HE feeding in both males and females causes a significant increase in the total number of cells/midgut R4 region as quantified from automated stitches/R4 gut region (refer to methods section). Each dot represents a midgut. The same stitches are used for analyses in panels d-f.
(d) 20HE feeding causes an increase in the total number of DAPI$^{+}$ cells/gut side/midgut stitch in the R4 region of *Su(H)$^{ts}$* Gal4 male and female midguts.
(e) EcR depletion in EBs causes a significant sturdy accumulation in EBs that is relieved by 20HE feeding in both males and females. Quantification of the EB number from midgut stitches from the genetic background *Su(H)$^{ts}$* Gal4 +/- EcR depletion shows that the loss of EcR in EBs leads to tripling the amounts of the EBs in male midguts and 4 times increase in the number of EBs in females. Such massive increase in EBs is stabilized back to basal levels when the flies are raised on 20HE for 14 days, suggesting that 20HE promotes the differentiation of the depleted EcR EBs.
(f) Ratios of EB numbers/total DAPI$^{+}$ cells in midgut stitches of males and females in the background of *Su(H)$^{ts}$* Gal4 shows the relative increase in EB number upon EcR depletion and its drop back to basal levels relative to vehicle-fed animals after raising the animals on exogenous 20HE.
(g) A rescue in the area of midguts with EcR depleted EBs, particularly that of females after 20HE feeding suggest that 20HE feeding is capable of rescuing the EcR depleted EB defects directly or indirectly. Midgut areas of animals raised on exogenous 20HE for 14 days in the background of *Su(H)$^{ts}$* Gal4.
(f) 20HE feeding causes an increase in the total number of DAPI$^{+}$ cells/gut side/midgut stitch in the R4 region of *MyoIA$^{ts}$* Gal4 male and female midguts. Cells/midgut R4 region are quantified from automated stitches/R4 gut region (refer to methods section). Each dot represents a midgut. The same stitches are used for analyses in panels 1f and 2a-b.All panels: Error bars represent ± SD. Statistical analysis was performed using one-way ANOVA, followed by Bonferroni's multiple comparisons test for panel g or unpaired parametric t-test with Welch's correction. Unless specified, p values are (ns $p>0.05$,*$p\leq 0.05$,**$p\leq0.01$,***$p\leq0.001$, ****$p<0.0001$). ♂ refers to males, ♀ refers to mated females.

Initially, I aimed to investigate the effects of EcR RNAi depletion on the transcriptome of progenitor cells that are virgins or mated. For that reason, I raised female flies as virgins then I mated them for 37hrs prior to the dissection of their midguts and FACS-sorting their progenitors to extract RNA from and sequence afterwards. I never managed to sequence the RNA from this experiment yet, I observed an interesting phenotype that complements the data I show in Fig 2.15a to support the requirement of EcR for differentiating EBs. FACS-sorted female $GFP^{+}$ progenitors have 3 different $GFP^{+}$ expressing populations ($GFP^{low}$ P6, $GFP^{medium}$ P7, $GFP^{high}$ P8). They are seemingly different in the intensities of their $GFP^{+}$ expression. Mated control flies have predominantly a uniform population of $GFP^{medium}$ expressing progenitors, with not so obvious changes in distribution of the GFP population between the virgins and the mated flies (Fig 2.15.2a,b). However, EcR depleted progenitors of female virgins show an accumulation of the $GFP^{low}$ P6 and $GFP^{medium}$ P7 (compare Fig 2.15.2a,b). This accumulation is quickly relieved when the females were mated, as early as 37hrs after mating (Fig 2.15.2b,d). This phenotype was replicated thrice with similar distribution of the GFP population, indicating an accumulation of cells that gets relieved after mating. Thus, both the FACS data and the microscope stitches suggest that non-cell autonomous mating that release endogenous 20HE or feeding exogenous 20HE affects the process of differentiating enteroblasts.

Afterwards, I examined the effects of intestinal EcR signaling on EC numbers. 20HE feeding to control flies causes a slight increase in the number of ECs though I couldn't conclude that with a lot of confidence due to the small (n) numbers and the missing control female guts.

When EcR was depleted from ECs of females; there was a significant reduction in the number of ECs (Fig 2.15.2e). 20HE-feeding to female guts with EcR depleted ECs increases the number of ECs albeit non-significantly, possibly due to the high variability between the midguts and the small (n) numbers. 20HE seems to rescue the EC numbers in guts with EcR depleted ECs to similar numbers in the control flies (Fig 2.15.2e-f).

.

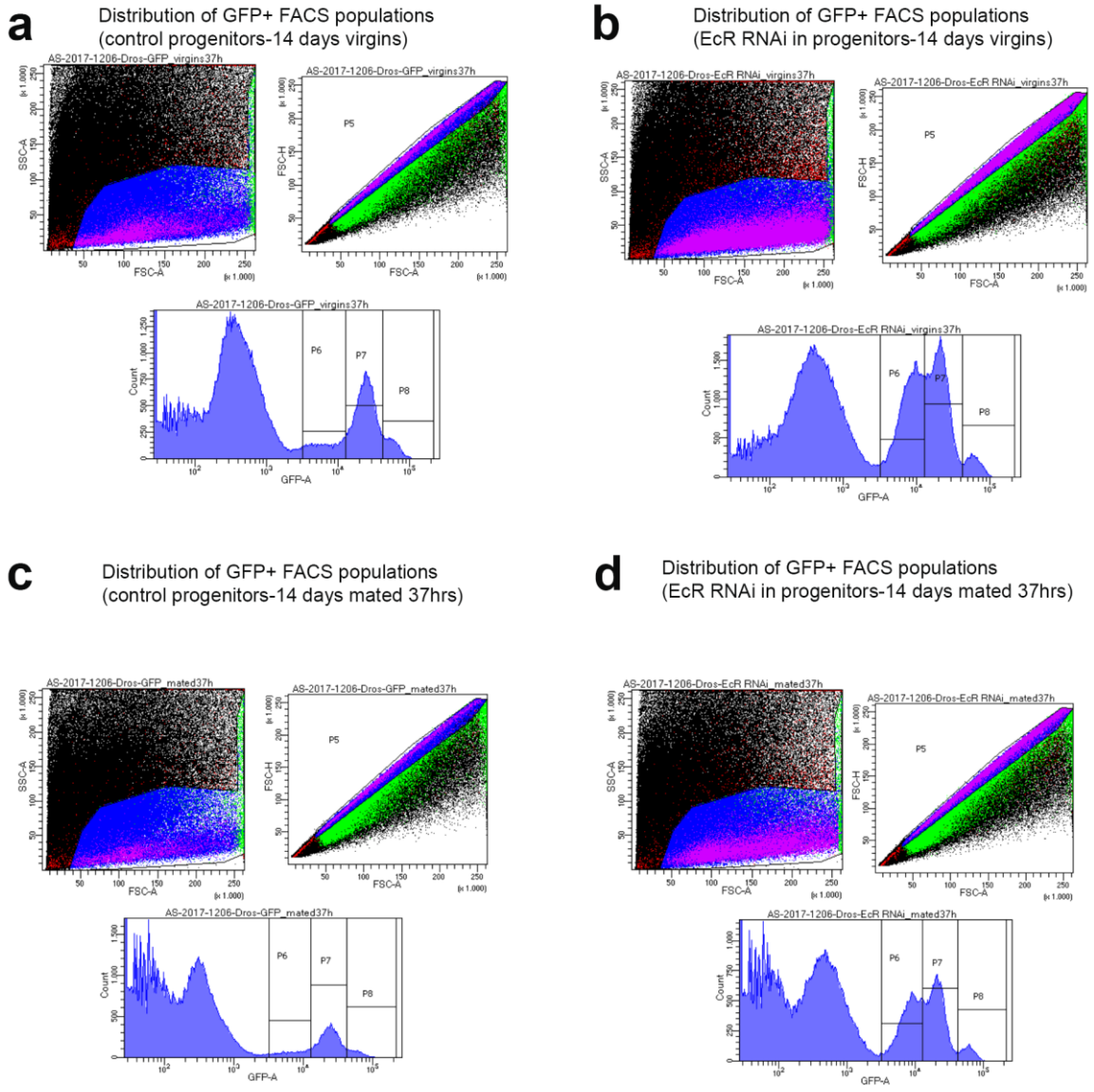
a
Distribution of GFP+ FACS populations
(control progenitors-14 days virgins)
b
Distribution of GFP+ FACS populations
(EcR RNAi in progenitors-14 days virgins)
c
Distribution of GFP+ FACS populations
(control progenitors-14 days mated 37hrs)
d
Distribution of GFP+ FACS populations
(EcR RNAi in progenitors-14 days mated 37hrs)
e
RNAi in enterocytes
Myo Gal4ts
14 days feeding
ECs number/ gut side
f
RNAi in enterocytes
Myo Gal4ts
14 days feeding
ECs ratio/ gut side
n=0.0526
n=0.1734
g
RNAi in enterocytes
Myo Gal4ts
14 days feeding
Midgut area (mm2)
control
EcRRNAi
vehicle
1mM 20HE
♂
♀

**Fig 2.15.2**

**Fig 2.15.2: Intestinal EcR signaling regulates EB differentiation to ECs.**
(a) Histogram distribution of FACS sorted GFP+ cells isolated from progenitors of 14 days old control virgins. 3 different GFP+ populations exist and the same gating strategy is applied for panels l-o ($GFP^{low}$ P6, $GFP^{medium}$ P7, $GFP^{high}$ P8). $GFP^{low}$ and $GFP^{high}$ are less than 250 counts, $GFP^{medium}$ are around 750 counts.
(b) Histogram distribution of FACS sorted GFP+ cells isolated from EcR-depleted progenitors of 14 days old virgins. $GFP^{low}$ are 1500 counts, $GFP^{medium}$ are 1800 counts and $GFP^{high}$ are less than 250 counts.
(c) Histogram distribution of FACS sorted GFP+ cells isolated from progenitors of 14 days old mated controls. Mating commenced 37 hours prior to dissection. . $GFP^{low}$ and $GFP^{high}$ are less than 100 counts, $GFP^{medium}$ are around 300 counts.
(d) Histogram distribution of FACS sorted GFP+ cells isolated from EcR-depleted progenitors of 14 days old mated females. Mating commenced 37 hours prior to dissection. $GFP^{low}$ are around 500 counts, $GFP^{medium}$ are around 700 counts and $GFP^{high}$ are around 100 counts. Accumulation of GFP+ progenitors is more observed when EcR is depleted and mating relieves this effect. All panels: Error bars represent ± SD. Statistical analysis was performed using one-way ANOVA, followed by Bonferroni's multiple comparisons test for panel k or unpaired parametric t-test with Welch's correction. Unless specified, p values are (ns $p>0.05$,*$p\leq 0.05$,**$p\leq 0.01$). ♂ refers to males, ♀ refers to mated females.
(e) EcR depletion in ECs causes a pronounced drop in the number of ECs/R4 midgut region in females that is fully rescued by exogenous 20HE feeding for 14 days. A similar increase of EC number in male midguts is also detected after 20HE feeding though a reduction of EC number is not observed in males possibly because of the low n number.
(f) Ratios of EC numbers/total $DAPI^{+}$ cells in midgut stitches of males and females in the background of *Myo1A$^{ts}$* Gal4 shows the relative drop of EC ratio in control males after 20HE feeding. This complements the result in Fig 2.6f and suggests that there is an increase in other $EC^{-}$ cell types upon prolonged 20HE feeding. Conversely, EcR depleted ECs have an inherent defect in their numbers that is fully rescued by exogenous 20HE feeding. EcR depleted female ECs do not seem to be rescued by exogenous 20HE.
(g) Midgut areas of females raised on exogenous 20HE for 14 days in the background of *Myo1A$^{ts}$* Gal4. There seems to be an initial increase in the midgut areas with EcR-depleted ECs but no additional increase in the midgut area occurs after exogenous 20HE feeding.

20HE feeding recovers the deficit in the number of ECs so that their numbers/R4 region matches vehicle-fed control midguts. Yet, the experiment's results were not so robust due to the small n numbers. However, preliminary results suggest that EcR depletion in ECs causes a reduction in their number that is rescued by raising the flies on 20HE (Fig 2.15.2e-f). Nevertheless, the 20HE-mediated increase in the number of ECs is not so

pronounced to explain the hyper-cellularity phenotype observed in 20HE-fed guts (Fig 2.15.2a). Although there are differences in the number of EcR depleted ECs with 20HE feeding, it does not seem to exert much difference on midgut areas (Fig 2.15.2g). Midguts with $EcR^{RNAi}$-enterocytes are initially slightly bigger than vehicle-fed control females. 20HE-fed midguts with $EcR^{RNAi}$-enterocytes have slightly higher but insignificant increase in their overall midgut area relative to vehicle fed midguts with $EcR^{RNAi}$-enterocytes. Hence, there seems to be an effect of intestinal 20HE signaling on EC size and number in the posterior region of the midgut. Altogether, my data suggest that intestinal EcR is involved in the epithelial differentiation of EB to ECs, possibly also regulate EC number to supply the gut with optimal number of nutrient-absorbing enterocytes. This preliminary evidence suggests that investigating the role of EcR in differentiating EBs or differentiated ECs should prove relevant and interesting in the future.

**2.16.1-2 Intestinal EcR is required for optimal reproductive capacity.**

Reproduction is a costly process and it is crucial for the females that conduct most of the reproductive burden to devise mechanisms that maximize their reproductive fitness[323]. Accordingly, ovary-induced steroid signaling causes both behavioral and metabolic changes that lead to maximal reproductive output [158,252,253,301,302,123,324,325].

A female fly at its reproductive peak lays up to 5 times its weight per day in its fertilized eggs [326,327], which is limited by nutrient availability to the ovaries[328,329]. Thus, I wondered if intestinal EcR is involved in remodeling the gut size to maximize the reproductive output.

This would be in line with the hypothesis that mating-induced gut growth increases the nutrients absorbed by the intestine and, thereby, nutrient availability to the fly's other organs such as the ovary. For that, I expressed $EcR^{RNAi}$ in midgut progenitors or ISCs under the control of the $esg^{ts}$-Gal4 driver, or the $esg^{ts}$ -Gal4 *Su(H)*-Gal80 driver respectively. Then, I monitored the amount of eggs deposited by females over a long period of time. Both approaches to reduce intestinal EcR signaling diminished egg production by up to ~40% (Fig. 2.16.1a-b).

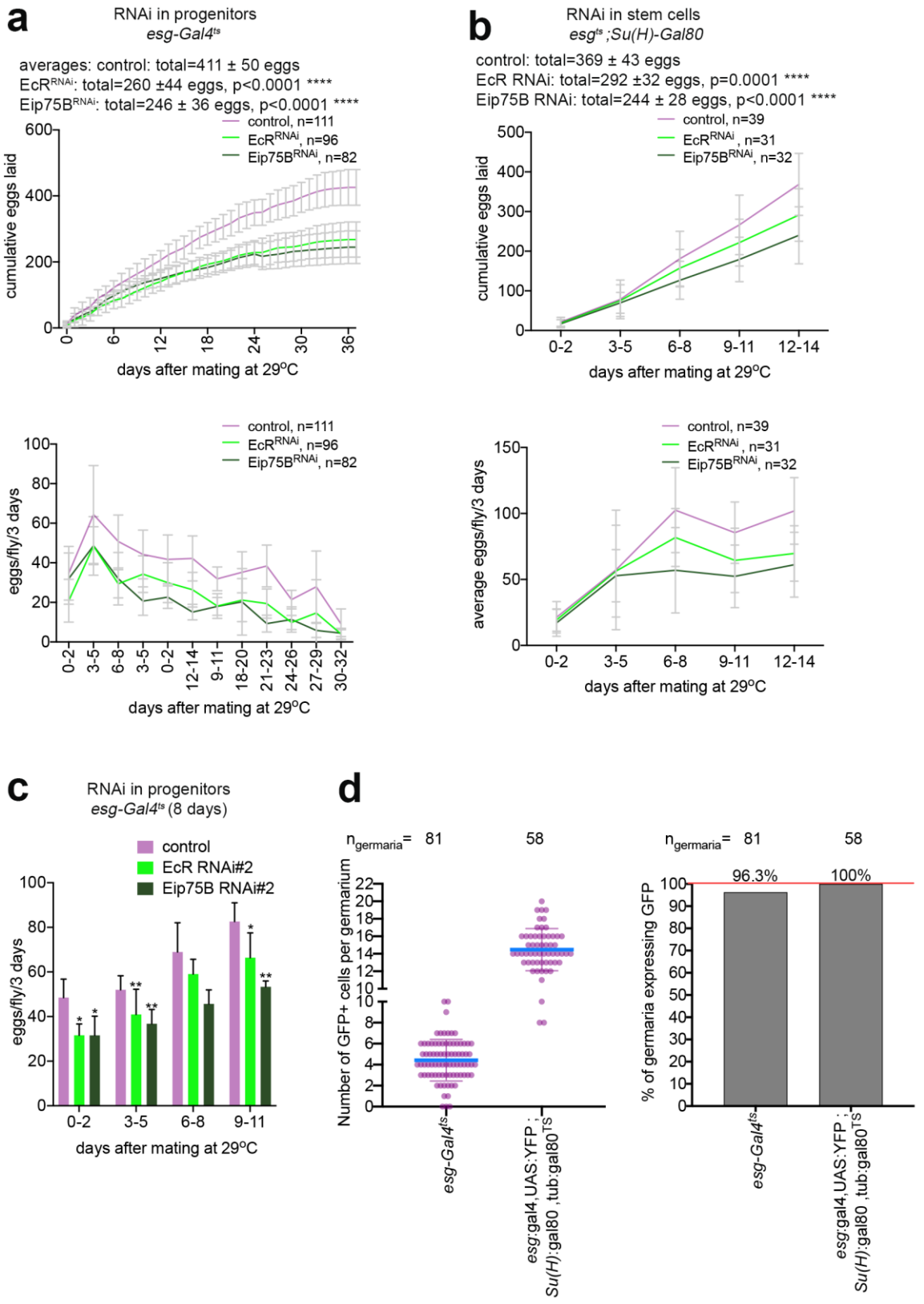
a
RNAi in progenitors
esg-Gal4ts
averages: control: total=411 ± 50 eggs
EcRRNAi: total=260 ±44 eggs, p<0.0001 ****
Eip75BRNAi: total=246 ± 36 eggs, p<0.0001 ****
control, n=111
EcRRNAi, n=96
Eip75BRNAi, n=82
cumulative eggs laid
days after mating at 29°C
eggs/fly/3 days
b
RNAi in stem cells
esgts ;Su(H)-Gal80
control: total=369 ± 43 eggs
EcR RNAi: total=292 ±32 eggs, p=0.0001 ****
Eip75B RNAi: total=244 ± 28 eggs, p<0.0001 ****
control, n=39
EcRRNAi, n=31
Eip75BRNAi, n=32
average eggs/fly/3 days
c
RNAi in progenitors
esg-Gal4ts (8 days)
control
EcR RNAi#2
Eip75B RNAi#2
d
ngermaria= 81 58
Number of GFP+ cells per germarium
% of germaria expressing GFP
96.3%
100%
esg-Gal4ts
esg:gal4,UAS:YFP ; Su(H):gal80 ,tub:gal80TS

**Fig 2.16.1**

**Fig 2.16.1: Intestinal EcR signaling is required to maintain reproductive demand of females.** Text and images have been taken and modified from (Ahmed et al., 2020) and have been originally written and made by myself: (a) Mated females expressing *EcR*$^{RNAi}$ or *Eip75B*$^{RNAi}$ in their midgut progenitors have reduced reproductive output. Flies with control, EcR- or Eip75B-depleted midgut progenitors were raised as virgins for 1-2 days then were shifted to the permissive temperature and mated to males with no genetic manipulations at a ratio of 1:1 in populations of 5-7 females/cage. Eggs were collected from the fly vials every day for up to 40 days and the cumulative sums (upper graph) or average total eggs/fly every 3 days (lower graph) are plotted. Control females lay more eggs than midguts expressing *EcR*$^{RNAi}$ or *Eip75B*$^{RNAi}$ in progenitors. Replicates from 3 independent experiments are shown. Error bars represent S.D. and p-values are calculated by general linear mixed model (GLM).

(b) Mated females expressing *EcR*$^{RNAi}$ or *Eip75B*$^{RNAi}$ in their midgut ISCs have reduced reproductive output. Flies with control, EcR- or Eip75B-depleted midgut ISCs were raised at 18$^{o}$C for 2 days maximum then were shifted to 29$^{o}$C and allowed to mate to males with no genetic manipulations at a ratio of 1:1. Flies were pooled together the first night of mating to ensure mating then on the next day, a single female was housed with a control male in a single vial. Eggs were collected from the fly vials every 48hrs for up to 14 days and the first graph on top shows the cumulative eggs laid across 14 days while the graph below shows the same data as a function of the average total eggs/fly every 3 days plotted across 14 days. Control females lay more eggs than midguts with *EcR*$^{RNAi}$ or *Eip75B*$^{RNAi}$ in ISCs. Error bars represent S.D. and p-values are calculated by GLM.

(c) Egg laying assay with an independent alternative 2$^{nd}$ RNAi against EcR and Eip75B is shown to complement results in a-b. Females were raised as virgins from 8 days at 29$^{o}$C then they were allowed to mate to males with no genetic manipulations at a ratio of 1:1 and their eggs were scored for up to 11 days post mating. 3 days averages are plotted, error bars represent S.D. and p-values are calculated by two-tailed t-test with Welch's correction.

(d left) The number of GFP+ cells per germarium for both midgut drivers: *esg*$^{ts}$ or *esg*$^{ts}$ *Su(H)gal80* which is expressed in midgut progenitors and ISCs respectively. Examination of *esg*$^{ts}$ driver shows that it is expressed in around 4 escort cells while *esg*$^{ts}$ *Su(H)gal80* driver shows expression in around 14 escort cells. n of germaria analyzed is indicated above each driver. Control germaria typically have 45-70 escort cells[330]. This quantification was done by Dr. Clothilde Pénalva in the Edgar Lab. (d right) Most midgut drivers express GFP in their germaria. The frequency of germaria expressing GFP is displayed in a bar graph. Ovaries of the *esg*$^{ts}$ driver have some escapers that have no GFP in their germarium while almost all ovaries of the *esg*$^{ts}$ *Su(H)gal80* driver have no escapers and all ovaries express GFP. This quantification was done by Dr. Clothilde Pénalva in the Edgar Lab.

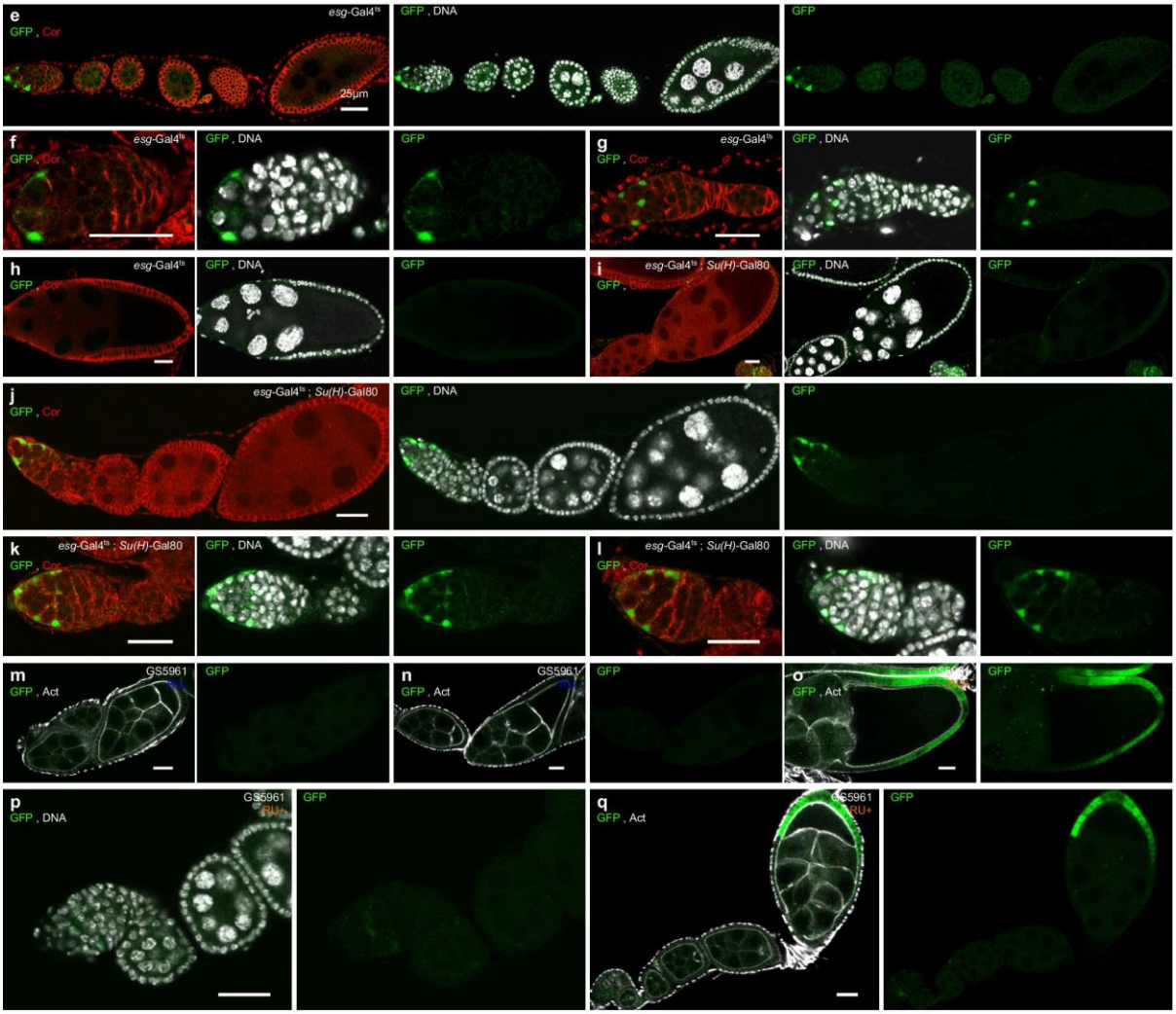


Fig 2.16.2

**Fig 2.16.2: *Drosophila* midgut drivers express GFP at different stages of the developing egg chambers.** Text and images have been taken and modified from (Ahmed et al., 2020) and have been originally written and made by Dr. Pénalva. e-q) Drosophila ovaries are composed of 16 ovarioles. At the anterior tip of every ovariole the germarium contains the germline stem cells and the somatic stem cells that constantly produce follicles or egg chambers. As the follicles progress to the posterior end of the ovariole they develop to lead to the formation of a mature egg. Follicle development is divided into 14 stages. In the most anterior part of the germarium (Region I) the cap cells and the escort cells constitute the niche required for the maintenance of the GSCs and the proper differentiation of the early germline cyst. expression of the esg-Gal4ts and the esgts Su(H)-Gal80 drivers was detected within the germarium in a subset of escort cells. e-h) Confocal sections of follicles from stage 2-7 (e), stage 9 (h) and germaria (f,g) isolated from esg-Gal4ts flies and stained for GFP (green), Coracle (red) and DNA (DAPI, gray). No GFP signal was detected in follicles from stage 2 to 9 (e,h)or in later stages (not

shown). However, 96% of germaria showed GFP in a subset of cells in the anterior region I (f,g). The GFP expressing cells were located in between the germline cysts and exhibited a triangular shape indicating that they were the escort cells. i-l) Similarly, all germaria from esgtsSu(H)-Gal80 flies presented GFP expression in escort cells (a,j,k,l) and no GFP expression was detected from stage 2 to 9 (i,j) or in later stages (not shown). m-q) The expression of the Switch GS5961-Gal4 driver was detected within the posterior follicular cells of the ovaries from stage 8 of oogenesis. Confocal section of follicles isolated from GS5961/UAS-GFP flies kept 4 days on yeast paste only (RU-) or yeast paste supplemented with RU486 (RU+) for 4 days and stained for GFP (green), actin (phalloidin, gray) or DNA (DAPI, gray). In absence of RU induction no GFP was detected in the ovary (m,n). After RU feeding no expression was detected in germaria or follicles prior to stage 7 (p,q). At stage 7 a subset of the most posterior follicular cells started to express weakly the GFP, this expression was then stronger and spreading to more follicular cells in a posterior to anterior gradient during stage 8 of oogenesis (q - most posterior follicle)and maintained later on in most of the posterior follicular cells that cover the oocyte (o -stage10).
*All pictures are presented with the anterior on the left and the posterior on the right.

I have validated the fecundity result by using an independent alternative RNAi (Fig. 2.16.1c). Thus, I concluded that midgut resizing affects the female fecundity to optimize their reproductive output.

However, these drivers were reported to express in some cells of the ovary[311]. I have asked an expert in *Drosophila* ovary stainings in the Edgar lab of Utah to stain the ovaries of both drivers and check which ovarian cells express GFP. Dr. Pénalva (Edgar lab) found that GFP is expressed in a subset of escort cells in the germarium of the ovary. *esg$^{ts}$*-Gal4 has an average of 4 GFP$^{+}$ cells, while *esg$^{ts}$* -Gal4 *Su(H)*-Gal80 has an average of 14 GFP$^{+}$ cells (Fig. 2.16d-l)[330]. It remains unexplored if EcR might be required in these ovarian escort cells and would in turn contribute to the optimal fecundity. Notably, control germaria typically have 45-70 escort cells[330]. Thus only 8.3%-24% would be affected by genetic manipulations with both midgut drivers *esg$^{ts}$*-Gal4 and *esg$^{ts}$* -Gal4 *Su(H)*-Gal80 respectively. Collectively, my results reveal a post-mating organ cross-talk between the gut to deliver nutrients to the ovaries to maximize nutrient deposition in their fertilized eggs.

## 2.17 Functional bifurcation of the canonical heterodimeric EcR•Usp during regenerative ISC mitoses.

As EcR was required for detergent-induced ISC mitoses, I next wondered if intestinal ecdysone signaling is required for regenerative compensatory ISC proliferation following infection with pathogenic bacteria. To answer that, I induced progenitor-specific depletion of EcR, then infected the flies overnight, and scored their mitotic indexes (Fig 2.1d,f 2.17.1a). Reduced EcR levels did not affect the *P.e.*-induced ISC mitoses relative to control flies. Strikingly, Usp depletion abolished the regenerative response (Fig 2.17.1a). The result was confirmed using an independent alternative RNAi line to Usp and EcR (Fig 2.17.1a). This result is surprising because most of ecdysone's functions described during development and throughout this thesis too (20HE feeding or mating), act through the EcR/Usp heterodimer[331].

Yet, a number of results support that reduced levels of EcR is not necessary for *P.e.*-induced ISC mitoses. The efficacy of the EcR RNAi was validated by its ability to suppress 20HE- or mating-induced mitoses (Fig 2.1.1c). Likewise, the expression of isoform specific RNAi against EcR A or B as well as EcR A DN did not compromise the ISC mitoses to *P.e.* infection (Fig 2.1.1f-h). Next, I sought to identify which cell type specifically require EcR or Usp. I used ISC- or EB-specific drivers to deplete EcR or Usp and then I scored mitoses after *P.e.* infection. $EcR^{RNAi}$ in either ISCs or EBs did not cause any significant change in the mitotic response to *P.e.* infection (Fig 2.17.1b,c). However, $Usp^{RNAi}$ in ISCs but not in EBs strongly compromised the ISCs to divide after infection (Fig 2.17.1b-c). This indicates a cell autonomous requirement of Usp only by ISCs to control their proliferation in a context where EcR is dispensable to ISCs. To check whether EcR in ECs would also contribute to the non-cell autonomous *P.e.*-induced ISC mitoses, I depleted EcR from ECs (Fig 2.17.1d). EcR-depleted enterocytes cause the ISCs to remain competent to the *P.e. regenerative* responses, even at slightly higher rates relative to controls. Consistently, when constitutive $tub^{ts}$ driver was used to deplete EcR or Usp, the same phenotypes described above were recapitulated (Fig 2.17.1e). To confirm Usp activity *in vivo* during *P.e.* infection or 20HE feeding, I used the Usp Gal4-LBD 'ligand trap'[186,288]. 20hrs after heat shock induction, at basal conditions, Usp is mildly active in a few small cells in the posterior midgut of control flies. 20HE feeding

activates ecdysone signaling in midgut cell clusters containing singlets, neighboring cell pairs and big polyploid cells (Fig 2.17.1f). After *P.e.* infection though, the Usp reporter was still detected in most cells (Fig 2.17.1f), though contrastingly, EcR reporter activity was absent from all cells (Fig 2.1.2 m-p). Altogether, my results show that unlike detergent-induced ISC mitoses, EcR in all epithelial cells is dispensable to the *P.e.*-induced ISC mitoses. More importantly, this is the first report of a functional bifurcation between EcR and Usp in the adult *Drosophila*[332].

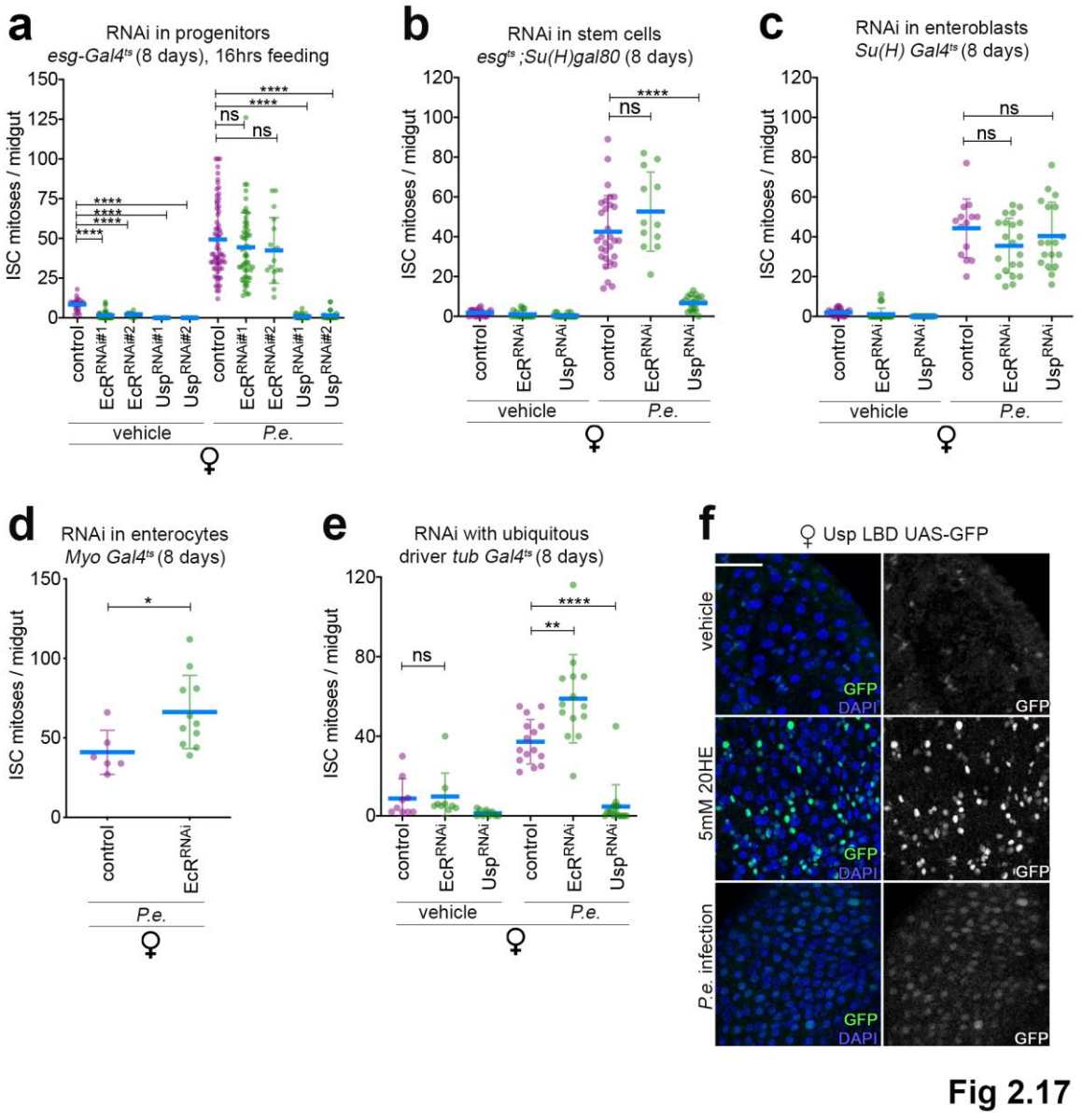


Fig 2.17

**Fig 2.17: Only Usp but not EcR is required in ISCs during *P.e.* infection.** Text and images have been taken and modified from (Ahmed et al., 2020) and have been originally

written and made by myself: (a) Usp is essential while EcR is dispensable to the regenerative response after infection. Progenitor-specific expression of *Usp*$^{RNAi}$ after enteric infection strongly ablates *P.e.*-induced ISC mitoses however; progenitor-specific expression of *EcR*$^{RNAi}$ did not deplete *P.e.*-induced ISC mitoses. Hence, Usp but not EcR is indispensable regenerative infection-induced ISC mitoses. Results are shown for 2 independent RNAi lines. I have produced half of this panel during my master's study and I used it in my master's thesis as well, Sara Ahmed,2015[464].
(b) Usp is essential while EcR is dispensable to the regenerative response after infection. ISC-specific expression of *Usp*$^{RNAi}$ after enteric infection strongly ablates *P.e.*-induced ISC mitoses however; ISC-specific expression of *EcR*$^{RNAi}$ did not deplete *P.e.*-induced ISC mitoses. Hence, Usp but not EcR is indispensable regenerative infection-induced ISC mitoses.
(c) EcR and Usp are dispensable to the enteroblasts during the regenerative response after infection. Enteroblast-specific expression of *EcR*$^{RNAi}$ and *Usp*$^{RNAi}$ after enteric infection does not inhibit *P.e.*-induced ISC mitoses. Hence, depletion of EcR and Usp from the enteroblasts is not important to regenerative infection-induced ISC mitoses.
(d) EcR is dispensable to the enterocytes during the regenerative response after infection. Enterocyte-specific expression of *EcR*$^{RNAi}$ after enteric infection does not inhibit *P.e.*-induced ISC mitoses. Hence, depletion of EcR from the enterocytes is not important to regenerative infection-induced ISC mitoses.
(e) Usp is essential while EcR is dispensable to the regenerative response after infection. Ubiquitous expression of *Usp*$^{RNAi}$ with tub$^{ts}$ driver after enteric infection causes a strong suppression of *P.e.*-induced ISC mitoses however; expression of *EcR*$^{RNAi}$ did not deplete *P.e.*-induced ISC mitoses. Hence, constitutive depletion of EcR from the different cell types is not important to regenerative infection-induced ISC mitoses.
(f) Usp activity is present after *P.e.* infection and 20HE feeding. Representative images of the heat-shock inducible *Gal4.DBD-Usp.LBD>GFP* reporter. Mated female flies were heat shocked for 30 mins then exposed to vehicle, *P.e.* infection or 5mM 20HE for 20 hrs. Gal4-*Usp* activity was detected in few cells under basal conditions. However, following *P.e.* infection, low levels of the Usp reporter were detected in most cells of the midgut. 20HE feeding induces the Gal4-*Usp* activity restricted in distinct doublets or large polyploid cells. GFP, in green; DAPI, in blue. Scale bar, 100 μm.
Statistical analysis was performed using unpaired non-parametric two-tailed Mann-Whitney test (*p≤0.05,**p≤0.01, ****p<0.0001).

**2.18 Usp may function with Hr38 to regulate ISC mitoses.**

My interesting observations about Usp functions raised the possibility that a nuclear receptor other than EcR might interact with Usp in ISCs, modulating the *P.e.*-induced regenerative ISC mitoses. Hence, I tested a panel of hormone receptors (*e.g.* Hr38, Hr96,

Hr83 and Hr51) known to heterodimerize with the Usp mammalian homologue RXR[333,334].

Progenitor-specific depletion of receptor partners (Hr96, Hr51) (data not shown for Hr83 RNAi +*P.e.*) was not required for *P.e.* infection. Nevertheless, Hr51 and Hr83 were required for 20HE-induced mitoses. In contrast, Progenitor-specific depletion of Hr38 strongly suppressed the ISC divisions in response to *P.e.* infection or 20HE feeding (Fig 2.18a). Moreover, Hr38 reduction also causes a drastic loss in the number of $GFP^{+}$ progenitors, which suggests that Hr38 functions in progenitors survival (Fig 2.18b). I validated these results using an alternative independent RNAi line against Hr38 (Fig 2.18a). Conversely, *P.e.*-induced ISC mitoses do not require Hr51 or Hr96 and Hr83 (data not shown for Hr83 RNAi +*P.e.*). Next, I examined the function of the same receptor partners during homeostatic epithelial renewal. ISC with reduced levels of Hr96 either did not form clones or completely renewed the midgut epithelia (prevalence of the phenotype was assessed and a representative picture is shown) (Fig 2.18d). Similarly, ISC clones with depleted Hr51; Hr83 did not exhibit a recognizable perturbation in their basal ISC clonal formation (data not shown). However, only Hr38-depleted ISC clones exhibited a striking defect in their renewal functions (Fig 2.18d). Considerably, a significant number of ISCs were absent or remained a single cell. Nevertheless when the ISCs divided they gave rise to multicellular clones as depicted in the representative picture (Fig 2.18d) (compare to Fig 2.23e for Usp). Hence, my results strongly suggest that loss of Hr38 phenocopies the loss of Usp function. Consequently, I hypothesized that Usp and Hr38 interact together *in vivo* to regulate ISC mitoses. To determine the validity of this hypothesis, I used heterozygous whole body mutants for Usp or Hr38 then, I combined both mutations in trans to generate Usp Hr38 double mutant animals. Either heterozygous mutant displayed a defect in their *P.e.* or 20HE-induced ISC mitoses (Fig 2.18e). Trans-heterozygotes Usp $^{\Delta/x}$Hr38$^{\Delta/2}$ showed a synergistic defect in their ISC response to *P.e.* infection or 20HE feeding suggesting that they both interact together to modulate ISC division (Fig 2.18e). Jointly, these results all solidify the hypothesis that indeed Hr38 and Usp interact in a heterodimeric complex to regulate aspects of ISC division, maintenance or both. Notably, Hr38 is the only other *Drosophila* nuclear receptor known to heterodimerize with Usp to regulate cuticle formation[335-337]

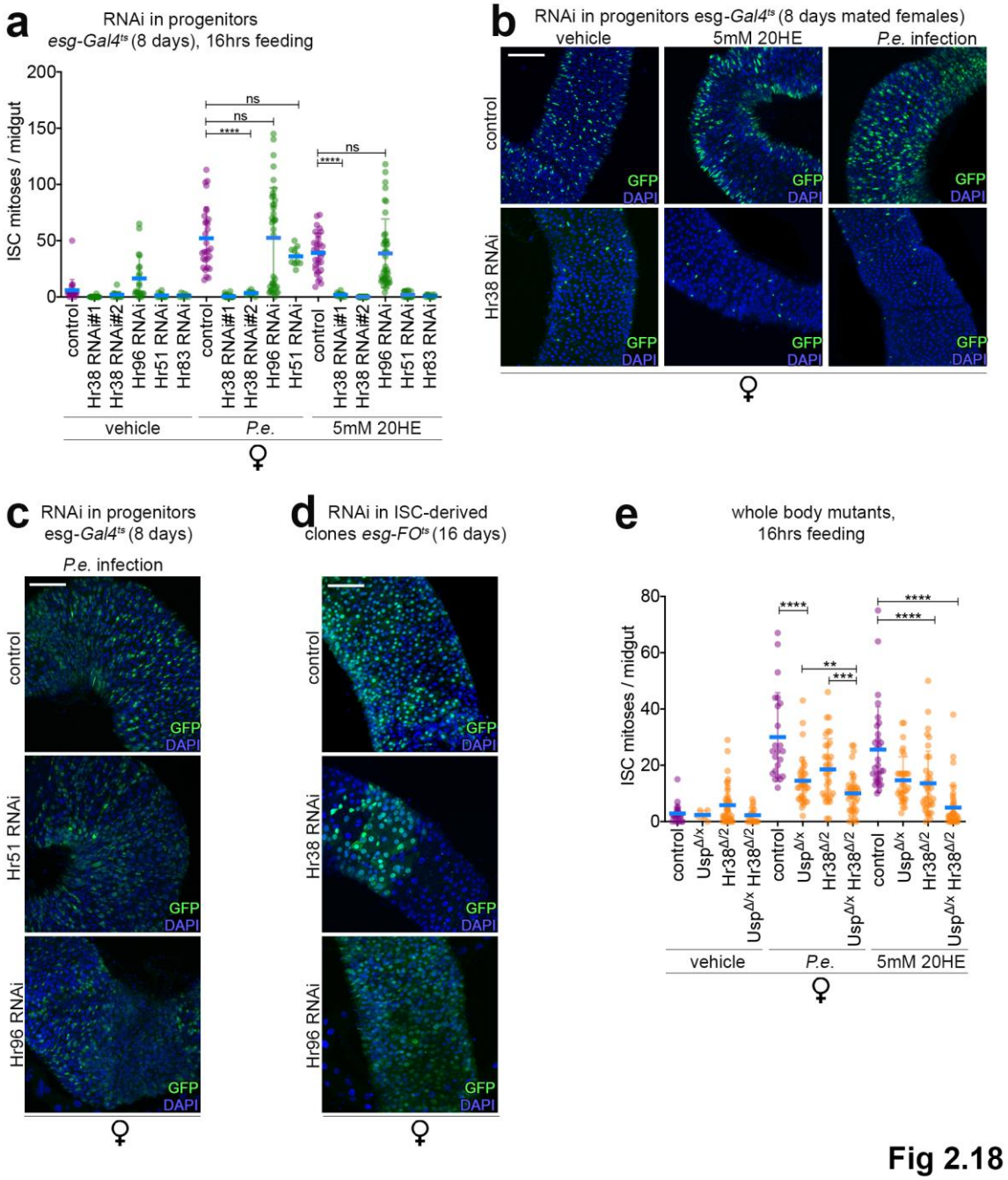


Fig 2.18

**Fig 2.18: Hr38 loss of function phenocopies Usp depletion in ISCs.** (a-b) (a) Depletion of Hr38 ablates *P.e.*- or 20HE- induced mitoses. Progenitors-specific depletion of some hormone receptor candidates: Hr38, Hr96 and Hr51 thought to partner with Usp after enteric infection or 20HE feeding. Progenitor-specific depletion of Hr83 was also tested and was not found to phenocopy Usp depletion (data not shown for *P.e.* infection). ISCs of *Hr96*$^{RNAi}$ progenitors divide at similar extents relative to control midguts after *P.e.*- or 20HE-feeding. ISCs of *Hr51*$^{RNAi}$ progenitors divide at similar extents relative to control midguts after *P.e.*-feeding. Conversely, 20HE-induced mitoses are strongly impaired in ISCs of midguts with *Hr51*$^{RNAi}$ progenitors while Hr96 is dispensable to 20HE-induced

mitoses. ISCs of *Hr38*$^{RNAi}$ progenitors are unable to divide to neither pro-mitotic stimuli. Hence, Hr38 depletion resembles Usp depletion in midgut progenitors.
(b) Representative images of Hr38-depleted progenitors after 20HE feeding or enteric infection. A strong reduction in the number of GFP+ progeniitors was noticed after Hr38 is depleted, implicating Hr38 in the viability as well as proliferation of the progenitors.
(c) Representative images of *Hr51*$^{RNAi}$ or *Hr96*$^{RNAi}$ progenitors after *P.e.*-feeding shows that GFP progenitors expand after infection at similar extents to control midguts.
(d) *Hr38*$^{RNAi}$ or *Hr96*$^{RNAi}$ and control ISC clones in the midgut 16 days after clonal induction under homeostatic conditions. Epithelia in control midguts are almost completely turned over. In midguts with Hr38 depleted ISC clones, ISCs are occasionally lost, however when the ISCs divided, they gave rise to big well-differentiated multicellular clones. Hr96 depleted ISC clones divide at normal rates relative to control midguts, marked by the complete epithelial renewal observed in most guts.
(e) Hr38 and Usp may partner together in ISCs of the midgut. Genetic interaction between heterozygous whole body Hr38, Usp mutants or Hr38 Usp whole body double mutants in trans-heterozygosis. After 20HE- or *P.e.*-infection, there is an additive defect in ISC mitoses of trans-heterozygote double mutants. Representative images are shown. GFP, in green; DAPI, in blue. Scale bars, 100 μm. Statistical analysis was performed using unpaired non-parametric two-tailed Mann-Whitney test (*p≤0.05, **p≤0.01, ***p≤0.001, ****p<0.0001).

**Fig 2.19 *Eip75B* and *Broad* are downstream effectors of midgut ecdysone signaling.**

The nuclear receptor Eip75B and the zinc finger transcription factor Broad are well-characterized as early ecdysone effector genes during embryogenesis [338], [339]metamorphosis[177,191]and oogenesis[340,341]. I have demonstrated earlier that Broad and Eip75B are transcriptionally regulated by 20HE feeding (Fig 2.13a). Then, I sought to examine if either or both relays the ecdysone signals to ISCs of the midgut and how does the more relevant effector then act to regulate ISC functions, with a deeper focus on ISC mitoses. Firstly, I asked whether Broad and Eip75B are more generally regulated by other pro-mitotic stimuli or not. I checked their mRNA regulation after *P.e.* infection. Indeed, they were transcriptionally induced after *P.e.* infection suggesting that they function independently of the ecdysone hierarchy and not only explicitly ecdysone targets (Fig 2.19a). Next, to determine if Broad and Eip75B are required for 20HE or *P.e.*-induced mitoses, I specifically depleted Broad or Eip75B from progenitors (Fig 2.19b). Consistent with the PCR data, both Broad and Eip75B were essential to the 20HE or *P.e.*-induced

mitoses (Fig 2.19b). To examine the role of Broad and Eip75B in the homeostatic epithelial renewal, I induced ISC clones with reduced levels of Eip75B and broad over time. Clonal analyses revealed that Broad was dispensable for the basal ISC divisions that sustain the midgut during homeostasis. However, Eip75B was essential for the ISC clonal growth (Fig 2.19d). Conversely, overexpression of Eip75B causes massive clonal over-growth and increased mitotic indexes supporting the hypothesis that Eip75B is sufficient to cause ISC division (Fig 2.19c). When I tried validating this result in the background of the progenitor-specific *esg*$^{ts}$, I found that increased levels of Eip75B in progenitors only did not increase the PH3 counts per-se (Fig 2.19g). Nevertheless, the GFP signal that should only be restricted to progenitor doublets was widely spread to include many polyploid cells (Fig 2.19g). The same results were obtained with the ISC-specific driver that supposedly only mark single or doublet cells. Similarly, overexpression of Eip75B with the EB-specific driver gives rise to increased numbers of enteroblasts with aberrant morphology (Fig 2.19f-g). This has led me to propose several ideas about the discrepancy in the phenotype observed in *UAS-Eip75B*-expressing ISC clones relative to *UAS-Eip75B*-expressing progenitors or ISCs. Firstly, despite not detecting ISC mitoses, ISCs appear to have divided, evident by the strong GFP signal that extends to the polyploid enterocytes and the formation of what appears to be a clone of ISC progeny. Secondly, there were definitively always changes in the cellular morphology of cells overexpressing Eip75B. *UAS-Eip75B*-expressing cells look bigger relative to control cells (Fig 2.19g).
Lastly, despite repeating each experiment many times, the *esg*$^{ts}$*FO* driver was the only background in which Eip75B overexpression resulted in increased ISC mitoses. Interestingly. This effect was not likely due to damage to ECs, since driving *Eip75B* with the EC-specific *MyoIA*$^{ts}$ driver did not trigger ISC mitoses (data not shown). This ambiguous result has led me to think that either the highly expressing Eip75B ISCs divide too fast or they mis-differentiate and ISC pool is somewhat severely depleted[316,342]. Consistent with the latter hypothesis, overexpression of Eip75B for 9 days caused a prominent loss in regionalization of the midgut (Fig 2.21f).

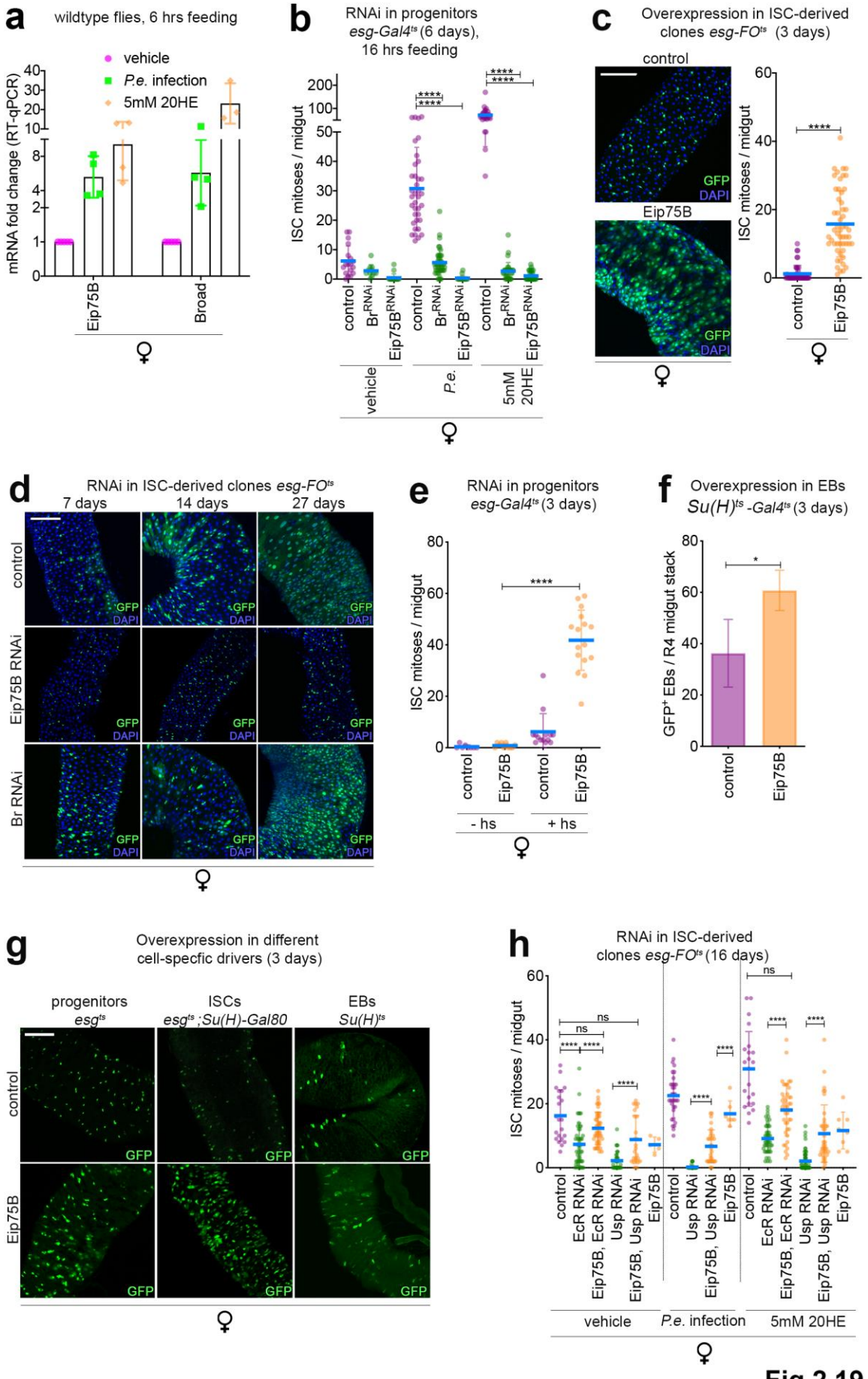
a
wildtype flies, 6 hrs feeding
vehicle
P.e. infection
5mM 20HE
mRNA fold change (RT-qPCR)
Eip75B
Broad
b
RNAi in progenitors
esg-Gal4ts (6 days),
16 hrs feeding
ISC mitoses / midgut
control
BrRNAi
Eip75BRNAi
vehicle
P.e.
5mM 20HE
c
Overexpression in ISC-derived
clones esg-FOts (3 days)
control
Eip75B
GFP
DAPI
ISC mitoses / midgut
d
RNAi in ISC-derived clones esg-FOts
7 days
14 days
27 days
control
Eip75B RNAi
Br RNAi
e
RNAi in progenitors
esg-Gal4ts (3 days)
ISC mitoses / midgut
- hs
+ hs
f
Overexpression in EBs
Su(H)ts-Gal4ts (3 days)
GFP+ EBs / R4 midgut stack
g
Overexpression in different
cell-specfic drivers (3 days)
progenitors
esgts
ISCs
esgts;Su(H)-Gal80
EBs
Su(H)ts
h
RNAi in ISC-derived
clones esg-FOts (16 days)
ISC mitoses / midgut
control
EcR RNAi
Eip75B, EcR RNAi
Usp RNAi
Eip75B, Usp RNAi
Eip75B
vehicle
P.e. infection
5mM 20HE

**Fig 2.19**

**Fig 2.19: Eip75B and broad are downstream 20HE-inducible targets in the *Drosophila* midgut.** Text and images have been taken and modified from (Ahmed et al., 2020) and have been originally written and made by myself: (a) 20HE feeding or *P.e.* infection transcriptionally upregulate the ecdysone-inducible targets Eip75B and broad. qRT-PCR measurements from whole midguts show that expression levels of *Eip75B* and *broad* mRNA are induced by *P.e.* infection or 20HE feeding 6 hrs after treatment. Expression is indicated as mean fold change relative to vehicle-treated midguts ± SD (n≥3).

(b) 20HE and *P.e.*-induced ISC mitoses require *Eip75B* and *broad.* Midguts with RNAi-mediated depletion of *Eip75B* or *broad* in progenitors had suppressed ISC mitoses relative to control midguts18 hrs after 20HE feeding or enteric infection.

(c) Overexpression of Eip75B in ISC clones is sufficient to promote ISC mitoses. ISC clones ectopically expressing Eip75B show that Eip75B is pro-proliferative and sufficient to induce clonal growth (left). Mitotic counts show that clonal Eip75B overexpression activates ISC proliferation (right). I have produced this data during my master's study and I used it in my master's thesis as well, Sara Ahmed,2015[464].

(d) Eip75B but not broad is required for epithelial renewal. ISC-GFP marked clones are generated by the *esgF/O* system showing that control mated females have constantly renewed epithelium, with full replacement taking 1-2 weeks. The size of ISC clones with $Eip75B^{RNAi}$ was dramatically reduced but, the size of $Broad^{RNAi}$ ISC clones was seemingly unaffected.

(e) Heatshock-sensitized midguts with progenitor-specific *Eip75B* overexpression vigorously triggers ISCs mitoses. Midgut mitotic figures were quantified after overexpressing *Eip75B* under the control of the progenitor-specific driver $esg^{ts}$ for 3 days. Prior to inducing *Eip75B* overexpression via temperature shift, flies were subjected to heat-shock for 30 mins or left untreated. Heat-shock alone causes a mild increase in ISC mitoses. Eip75B overexpression in progenitors was insufficient to increase ISC divisions. Heat-shock of Eip75B overexpressing progenitors resulted in a synergistic effect on ISC mitoses.

(f) Overexpression of E75A in enteroblasts induces a slight expansion in their number as shown by the counts of enteroblasts/midgut stack at the R4 region. I have produced this data during my master's study and I used it in my master's thesis as well, Sara Ahmed,2015[464].

(g) Eip75B overexpression results in aberrant enlargement of the cell size and precocious differentiation. Eip75B was induced by different cell-specific drivers in progenitors ($esg^{ts}$), ISCs ($esg^{ts}$ *Su(H)gal80*) or enteroblasts ($Su(H)^{ts}$) respectively. In all cases, the numbers of $GFP^+$ cells were much higher than in age-controlled midguts without genetic manipulation. When misexpressed in progenitors or only in ISCs, many cells with large nuclei, typically enterocytes also accumulated. Eip75B misexpression in EBs resulted in more cells with abnormal morphology. Hence, Eip75B is maybe involved in both proliferation and differentiation.

(i) Eip75B is downstream of EcR and Usp receptors. Mitotic indexes of ISCs reflecting the epistatic relationship between EcR/Usp depletion and Eip75B misexpression under homeostatic conditions or after 20HE feeding. Under both conditions, Eip75B partially rescues the proliferative defect of clonal EcR or Usp depletion which suggest that Eip75B relays at least part of the intestinal EcR•Usp in the ISCs. Representative images are shown. GFP, in green; DAPI, in blue. Scale bars, 100 μm. Statistical analysis was performed using unpaired non-parametric two-tailed Mann-Whitney test (ns $p>0.05$, *$p\leq0.05$, ****$p<0.0001$).

Given this massive disturbance in the dynamic of dividing ISCs, I sought to prompt immediate activation of ISC divisions from the moment I induced Eip75B expression. Hence, I sensitized the flies with a brief heat shock (15 min, 37 degrees) prior to shifting them to 29°C to activate *UAS-Eip75B* in progenitors. 3 days later, Eip75B over expressing ISCs were markedly pro-mitotic (Fig 2.19e). Similar results were obtained with Hr3 depletion in ISC clones, as will be shown in a later section (Fig 2.20j). Next to determine whether Eip75B acts as a downstream effector of the intestinal ecdysone signaling pathway, I examined the effect of Eip75B depletion on the mating-induced midgut mitoses (Fig 2.8.1i) and subsequent midgut growth (Fig 2.8.2a-b). In both contexts, Eip75B was required to transduce the ovary-derived ecdysone signaling in ISCs of the midgut post-mating. Similarly, reduced Eip75B levels in progenitors suppressed the reproductive output of mated females (Fig 2.16.1a-c). Next, I performed epistatic tests between the loss of function of EcR/Usp together with the overexpression of Eip75B (Fig 2.19h). Usp-depleted ISC clones had dramatically impaired ISC divisions. However, when Eip75B was co-overexpressed with $Usp^{RNAi}$, ISC mitoses were partially rescued. Importantly, this mitotic rescue was not observed only under basal homeostatic conditions but also after 20HE feeding yet, much less after *P.e.*-infection. Similarly, loss of function of EcR after 20HE feeding was rescued by Eip75B co-overexpression (Fig 2.19h). These results indicate that Eip75B functions downstream of the EcR•Usp receptor complex.

**Fig 2.20 Eip75B interacts with Hr3 to modulate ISC divisions.**

I have figured out that Eip75B is the more relevant 20HE target in the general context of basal and regenerative ISC mitoses. I next aimed to investigate how Eip75B functions to

regulate ISCs. Traditionally, Eip75B binds Hr3 and block its ability to regulate target genes during development[175,185,189]. In a less traditional model, Hr51 was also shown to interact with Eip75B in the *Drosophila* circadian pacemaker neurons and axon regeneration[189,343].

To control the proper balance between stem cell division, self-renewal and differentiated progeny, the ISCs must be maintained that they are not lost from the tissue over time. So, first, I determined whether Eip75B is involved in maintenance of the ISCs within the ISC pool, prolonged loss of Eip75B in progenitors was induced and 23 days later, the cell numbers were counted by Dr. Gabi de Silva in the Edgar lab. There was only a 30% decrease of intestinal stem cell number, suggesting that Eip75B is non-essential for ISC maintenance (Fig 2.20a). To investigate the role of Eip75B in proliferation, I suppressed Eip75B in ISC clones and fed the flies with various stresses that are known to cause compensatory ISC proliferation and midgut epithelial regeneration[30]. When Eip75B signaling was suppressed in ISC clones by Eip75B RNAi, midgut regeneration was completely inhibited in response to ROS-induced stress or *P.e.* infection as well as 20HE feeding (Fig 2.20b,c). The mild mitotic response of heme feeding also requires the presence of Eip75B in the ISCs (Fig 2.20b,c) consistent with the fact that heme is the obligate ligand for Eip75B and is required for the Eip75B stability and accumulation[175]. Hence, Eip75B plays an essential role in ISC proliferation. To further explore whether Eip75B is required for ISC mitoses in a ISC-autonomous or non-autonomous manner, I depleted Eip75B from ISCs or EBs with the cell-type specific drivers, then I fed the flies with *P.e.* or 20HE to stimulate ISC mitoses. Eip75B was not required in EBs for either the *P.e.* or 20HE-induced ISC mitoses (Fig 2.20e), but the ISCs failed to divide when they had suppressed levels of Eip75B (Fig 2.20d) revealing the ISC-autonomous requirement of Eip75B for ISC mitoses.

To validate the phenotype of Eip75B in ISCs, I generated mosaic ISC clones homozygous for *Eip75B*$^{\Delta 51}$, a null allele for all Eip75B isoforms [184] via the MARCMs system[285] (Fig 2.20f, Fig 2.1.2k). I used two different recombinants and for one I quantified the size of generated ISC clones after clone induction then overnight 20HE feeding or *P.e.* infection.

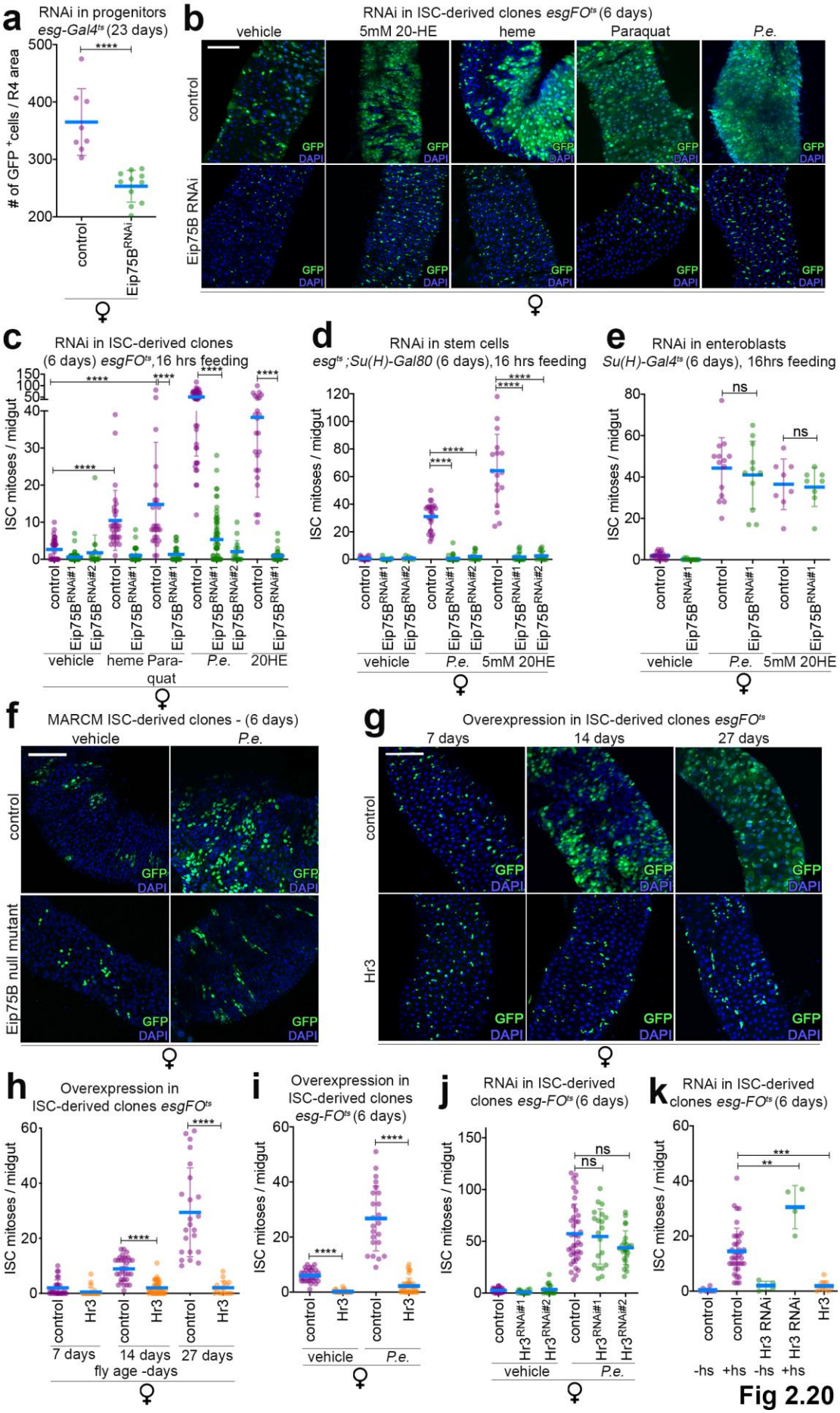
a
RNAi in progenitors
esg-Gal4ts (23 days)
# of GFP +cells / R4 area
control
Eip75BRNAi
b
RNAi in ISC-derived clones esgFOts (6 days)
vehicle
5mM 20-HE
heme
Paraquat
P.e.
control
Eip75B RNAi
GFP
DAPI
c
RNAi in ISC-derived clones
(6 days) esgFOts,16 hrs feeding
ISC mitoses / midgut
vehicle
heme
Para-quat
P.e.
20HE
d
RNAi in stem cells
esgts;Su(H)-Gal80 (6 days),16 hrs feeding
e
RNAi in enteroblasts
Su(H)-Gal4ts (6 days), 16hrs feeding
ns
f
MARCM ISC-derived clones - (6 days)
Eip75B null mutant
g
Overexpression in ISC-derived clones esgFOts
7 days
14 days
27 days
Hr3
h
Overexpression in
ISC-derived clones esgFOts
fly age -days
i
Overexpression in
ISC-derived clones
esg-FOts (6 days)
j
RNAi in ISC-derived
clones esg-FOts (6 days)
k
RNAi in ISC-derived
clones esg-FOts (6 days)
Hr3 RNAi
-hs
+hs

**Fig 2.20**

**Fig 2.20: Eip75B stimulates ISC proliferation through inhibiting Hr3.** Text and images have been taken and modified from (Ahmed et al., 2020) and have been originally written and made by myself: (a) Basal levels of Eip75B are required for ISC maintenance. Quantification of the number of GFP+ progenitor cells 23 days after RNAi-mediated depletion showed a small reduction (~25%) in the GFP+ progenitor pool size implying that Eip75B does not critically function in ISC survival. This quantification was done by Dr. Gabriela Da Silva from the Edgar Lab. I have used it in my master's thesis as well, Sara Ahmed,2015[464].

(b-c) Eip75B depletion in ISC clones completely represses any stress-induced or stimulatory ISC proliferative responses. (b) Representative images of ISC clones in mated females after 20HE, heme, paraquat and *P.e*. infection. While control mated females were able to replace almost the entire epithelium 18 hrs after feeding. (c) Mitotic counts of *Eip75B*-depleted clones were strongly suppressed after being subjected to different promitotic stimuli. Results for *P.e.*-induced mitoses are shown for 2 independent Eip75B RNAi lines.

(d) Eip75B is cell-autonomously required by ISCs for proliferation caused by *P.e*.-or 20HE feeding. Mitotic indexes of midguts with ISC-specific depletion of Eip75B ablated both the *P.e*.-or 20HE induced ISC mitoses

(e) Eip75B in EBs is dispensable to ISC mitoses as shown by mitotic indexes of midguts with EB-specific depletion of Eip75B. Eip75B-depleted EBs did not affect the *P.e*.-or 20HE induced ISC mitoses.

(f) *Eip75B* mutant clones fail to divide and grow after *P.e.* infection. MARCM ISC Eip75B null mutant or control clones were induced in female adult midgut epithelia. Vehicle-fed control clones were multicellular but, Eip75B null mutant clones remained as single ISC clones. After *P.e.* infection, progeny expanded in control clones yet, Eip75B null mutant clones were incapable of replenishing the lost epithelial cells. I have produced this data during my master's study and I used it in my master's thesis as well, Sara Ahmed,2015[464].

(g-h) ISC clones overexpressing *Hr3* are unable to divide and maintain the homeostatic tissue demands of the epithelium. (g) Representative images of the gut epithelial turnover upon *Hr3* misexpression using the *esgF/O* system. ISC clones in control female guts give rise to newborn progeny and self-replenish the whole epithelium in contrast to *Hr3* overexpressing clones, (h) Mitotic counts of accumulating ISC divisions in control epithelia as the flies age, however increased levels of *Hr3* prevent basal ISC divisions. I have produced this data during my master's study and I used it in my master's thesis as well, Sara Ahmed,2015[464].

(i) Hr3 inhibits ISC proliferation. Mitotic counts of midguts misexpressing Hr3 in ISC clones strongly inhibited *P.e*.-induced ISC mitoses relative to control infected females.

(j) Hr3 depletion is insufficient to induce ISC proliferation. Mitotic indexes of midguts with ISC clonal induction of $Hr3^{RNAi}$ after 18-20 hrs of enteric infection. No significant difference was observed relative to control infected flies. Results are shown for 2

independent RNAi lines. Dr.Gabriela Da Silva from the Edgar Lab did this experiment. I have used this data in my master's thesis as well, Sara Ahmed,2015[464].
(k) After being sensitized with heatshock, midguts with *Hr3*$^{RNAi}$ ISC clones have elevated ISCs mitoses. Midgut mitotic figures were quantified after heatshock in *Hr3*$^{RNAi}$ ISC clones relative to control or Hr3-overexpressing flies. Prior to inducing Hr3 depletion via temperature shift, flies were subjected to heat-shock for 30 mins or left untreated. Heat-shock alone caused a mild increase in ISC mitoses. When Hr3 was depleted in ISC clones without heatshock, basal ISC mitoses were minimal similar to guts with Hr3 overexpressing ISC clones. Representative images are shown. GFP, in green; DAPI, in blue. Scale bars, 100 μm. Statistical analysis was performed using unpaired non-parametric two-tailed Mann-Whitney test (ns $p>0.05$, *$p\leq0.05$, ****$p<0.0001$).

The clonal size of Eip75B mutant clones was severely compromised and most cells remained singlets or each clone consisted of very few cells (Fig 2.1.2k). Then, based on both models of Eip75B's action described above, I sought to investigate which binding partner does Eip75B have in the gut. Hr51 depletion in progenitors was insufficient to block the *P.e.*-induced ISC mitoses despite being required for the 20HE-induced ISC mitoses excluding the possibility that Eip75B binds Hr51 (Fig 2.18a,c). Afterwards, I was prompted to test if Hr3 is the binding partner of Eip75B. Therefore, I hypothesized that overexpressing UAS-Hr3 would mimic the loss of Eip75. To validate that, I induced ISC clones with increased levels of Hr3, and then I traced the clonal sizes at intervals after clone induction under homeostatic conditions as well as the mitotic activity of ISCs. By 26 days, the whole epithelium was renewed in mated control females accordant with the elevated ISC mitoses; however, Hr3-overexpressing ISC clones had barely divided. (Fig 2.20g,h). Consistently, ISC clones ectopically expressing Hr3 had ablated ISC mitoses after being subjected to *P.e.* infection (Fig 2.20i).
Hence, I concluded that the loss of Eip75B phenocopies overexpression of Hr3. As Hr3 overexpression modulated the ISC mitoses, I expected that Hr3 depletion could potentiate the ISC mitoses, so ISC clones with suppressed Hr3 levels were generated and upon infection, ISC mitoses were scored. Nevertheless, control and Hr3-depleted ISC clones divided at similar rates implying that the increased Eip75B availability in the cell per se is not sufficient to promote ISC mitoses or that additional 20HE-dependent targets may be required downstream of Eip75B (Fig 2.20j). In an alternative approach to sensitize those ISCs to a promitotic stimulus prior to the RNAi-mediated depletion of Hr3, flies were

heatshocked prior to shifting to 29$^{o}$C. 6 days later, the quantification of the basal mitotic indexes of the sensitized Hr3 depleted flies revealed that they were mitotically even more active than "heat-shock" sensitized control flies (Fig 2.20k).

**Fig 2.21 NO regulates Eip75B to Hr3 to modulate ISC divisions.**

To validate the interaction between Eip75B and Hr3, I used a Gal4-LBD 'ligand sensor' system to monitor the transcriptional activity of Eip75B and Hr3[186]. Due to the transcriptional repressive function of Eip75B, I could not use the GFP reporter to monitor the interaction in the reversible manner[186]. No GFP signal was detected in guts expressing the Gal4-Eip75B fusion protein (data not shown). After heatshock, the Gal4-Hr3 sensor showed a strong GFP signal in most midgut cells (progenitors and enterocytes, but not pros$^{+}$ enteroendocrine cells; Fig 2.21a), reflective of Hr3 activity in those cells. Gal4-Hr3 activity was significantly repressed by co-expression of Eip75B or by stimuli that are shown to induce Eip75B activity or transcriptional levels i.e.: heme feeding, *P.e.* infection or 20HE feeding (Fig 2.21a). Furthermore, NO interacts with the heme moiety of Eip75B, thereby restraining its ability to interact with Hr3[176,185]. Accordingly, I proposed that increased NO levels would stabilize Hr3 reporter activity. To prove that, I fed the reporter flies with NO donor (±)- S-Nitroso-N-acetylpenicillamine (SNAP) in combination with enteric infection, which effectively reversed the *P.e.*-suppressed Hr3 reporter activity (Fig 2.21a). Interestingly, heat-shocked reporter flies were more sensitized to heme feeding (Fig 2.21b) relative to flies that are not subjected to this treatment (compared to Fig 2.20c), in agreement with the idea that heatshock would stress the midgut and induce upregulation of Eip75B in ISCs which is further stabilized by heme addition, resulting in a more pronounced mitotic effect (Fig 2.21b). Consistently, *P.e.*-induced ISC division was also significantly repressed by SNAP feeding (Fig 2.21b). Conversely, feeding the flies with NO inhibitor, Nω-Nitro-L-arginine methyl ester (L-NAME) rescued the GFP expansion and mitotic defects shown in ISCs ectopically expressing Hr3 (Fig 2.21c,d). Finally, my findings were corroborated by epistasis experiments showing that the Eip75-mediation repression of ISC mitoses was

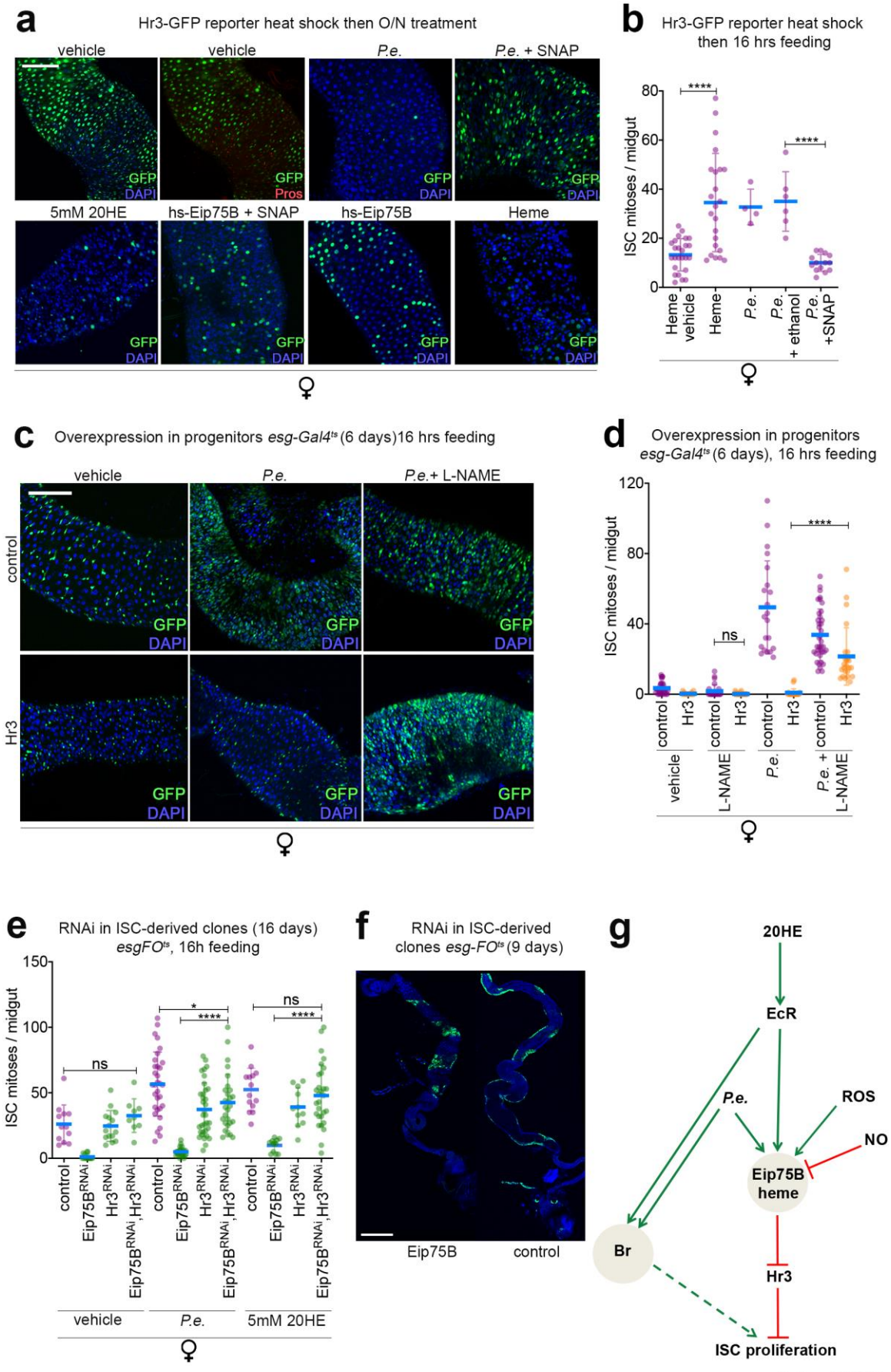
a
Hr3-GFP reporter heat shock then O/N treatment
vehicle
vehicle
P.e.
P.e. + SNAP
5mM 20HE
hs-Eip75B + SNAP
hs-Eip75B
Heme
GFP
DAPI
Pros
♀
b
Hr3-GFP reporter heat shock then 16 hrs feeding
ISC mitoses / midgut
****
Heme
vehicle
Heme
P.e.
P.e. + ethanol
P.e. +SNAP
c
Overexpression in progenitors esg-Gal4ts (6 days)16 hrs feeding
vehicle
P.e.
P.e.+ L-NAME
control
Hr3
d
Overexpression in progenitors esg-Gal4ts (6 days), 16 hrs feeding
ISC mitoses / midgut
ns
control
Hr3
vehicle
L-NAME
P.e.
P.e. + L-NAME
e
RNAi in ISC-derived clones (16 days) esgFOts, 16h feeding
ISC mitoses / midgut
ns
*
control
Eip75BRNAi
Hr3RNAi
Eip75BRNAi,Hr3RNAi
vehicle
P.e.
5mM 20HE
f
RNAi in ISC-derived clones esg-FOts (9 days)
Eip75B
control
g
20HE
EcR
P.e.
ROS
NO
Eip75B heme
Br
Hr3
ISC proliferation

**Fig 2.21**

**Fig 2.21: NO regulates *Eip75B/Hr3* to adjust ISC mitoses.** Text and images have been taken and modified from (Ahmed et al., 2020) and have been originally written and made by myself: (a-b) (a) Eip75B activity is regulated by heme. Representative images of heatshock inducible Hr3 reporter (hs-Gal4.DBD-Hr3.LBD>GFP) activity in the posterior midgut of mated flies after different treatments. *Eip75B* interacts with the heat-shock inducible GAL4-*Hr3* fusion protein, blocking its ability to activate GFP expression. Upon heat shock for 30 mins, flies were exposed for 20 hrs to vehicle, hs-*Eip75B*, hs-*Eip75B* +10mM SNAP feeding (NO donor compound), 0.5mM Heme, *P.e.*, *P.e.* +10mM SNAP or 5mM 20HE. Upon vehicle feeding, *Gal4-Hr3* fusion protein was active and induced strong GFP expression in most cells. The *Hr3*-mediated GFP expression was repressed by the co-expression of *Eip75B*, 20HE or heme feeding, *P.e.* infection. Increasing NO levels by SNAP feeding in hs-*Eip75B* transgenic flies or during *P.e.* infection relieved the repressive action on GFP expression. I have produced half of the panel (a) during my master's study and I used it in my master's thesis as well, Sara Ahmed,2015[464].
(b) SNAP feeding acts as Nitric Oxide (NO) donor and increased NO binding prevents Eip75B interaction with Hr3. The *Gal4-Hr3* reporter repression upon exposure to heme and *P.e* caused a significant increase in ISC proliferation. SNAP feeding inhibited *P.e*-induced ISC division. Mitotic counts of the Hr3 reporter after different pro-mitotic treatments. Heme or *P.e* feeding stimulates ISC division.
(c-d) NO inhibition rescues the repressive effects of Hr3 misexpression on ISC mitoses. (c) Representative images (d) mitotic counts of progenitors with ectopic Hr3 expression after treatment with L-NAME (NO inhibitor) +/- enteric infection. Increased Hr3 levels in progenitors suppress *P.e.*-induced ISC mitoses. NO interferes with the ability of the Eip75B protein to interact with Hr3 protein thereby, allowing Hr3's transcriptional regulation of its targets. Treatment with L-NAME rescued the Hr3-repressed ISC mitoses and progenitor expansion after enteric infection. I have produced this data during my master's study and I used it in my master's thesis as well, Sara Ahmed,2015[464].
(e) Hr3 is epistatic to Eip75B. Mitotic counts of midguts examining the epistatic relationship between Hr3 and Eip75B during homeostasis, after 20HE feeding or *P.e.* infection. *Eip75B*$^{RNAi}$, *Hr3*$^{RNAi}$ was induced in ISC clones of the epithelial midgut. *Eip75B*$^{RNAi}$ in ISC clones prevents ISC mitoses basally or to any of the treatments. *Hr3*$^{RNAi}$ in ISC clones does not have an obvious phenotype. However, repressed ISC mitoses in Eip75B depleted ISC clones are entirely rescued by Hr3 depletion under all conditions.
(f) Overexpression of Eip75B causes a significant loss of gut regionalization. Representative confocal stitches of guts with Eip75B-overexpressing ISCs relative to aged-matched controls.
(g) A model summarizing my findings. Representative images are shown. GFP, in green; DAPI, in blue. Scale bars, 100 μm. Error bars represent ± SD. Statistical analysis was performed using two-tailed Mann-Whitney test (ns $p>0.05$, *$p\leq0.05$, ****$p<0.0001$).
reversed by co-depletion of Hr3 under homeostatic conditions, 20HE feeding or *P.e.*

infection (Fig 2.21e). Altogether these results suggest a model in which 20HE-activated EcR regulates the expression of Eip75B and broad. Nevertheless, both genes seem to be regulated also independently from EcR during *P.e*. regenerative responses. In all cases, Eip75B binds its ligand heme and negatively regulates Hr3's action on its target genes. Hr3 presumably promotes expression of anti-mitotic genes in ISCs, and Eip75B interfere with this function, thereby promoting ISC division (Fig 2.21g).

**Fig 2.22 Endogenous JH is required for infection-induced ISC mitoses while exogenous JH feeding has suppressive effects on ISC mitoses.**

Since I figured out in a very detailed manner how 20HE and its downstream pathway affect ISC mitoses, I further inquired how 20HE interacts with the other sesquiterpenoid hormone named JH. In the midgut, JH was reported to promote mating-dependent gut growth[311] and its feeding to virgins had a slight pro-mitotic effect on ISC mitoses[311]. Hence, I started with feeding virgins with several hormone treatments alone or in combination for different durations of time (Fig2.22a). Feeding the virgins with 1mM JH overnight caused no effect on dividing ISCs and feeding the flies constantly for 3 days actually seemed to inhibit ISC mitoses, yet it definitively did not exert a promitotic effect on ISCs (Fig2.22a).

On the other hand, feeding virgins with the JH agonist, methoprene overnight or continually for 3 days caused a slight but significant promitotic effect on dividing ISCs (Fig2.22a). Alternatively, overnight feeding of 2mM like 5mM 20HE stimulates ISC mitoses albeit at lower levels (Fig2.22a). As shown earlier however, 3-day feeding of 5mM 20HE causes most ISC mitoses to return to almost basal levels. Surprisingly, synergistic effect of 20HE and methoprene feeding causes the ISC mitoses to significant drop to close to basal levels (compare the magnitude of the drop vehicle vs 20HE vs 20HE+M or JH). This antagonistic effect of combined hormone feeding on ISC mitoses is observed after overnight or 3 days feeding (Fig2.22a). Hence, the relationship between the 20HE and JH signaling seems antagonistic rather than synergistic. Next, I asked how 20HE-induced ISC mitoses interact with the endogenous JH receptors. Thus, I depleted the JH receptors Methoprene-tolerant (met) or germ cell-expressed bHLH-PAS (gce)

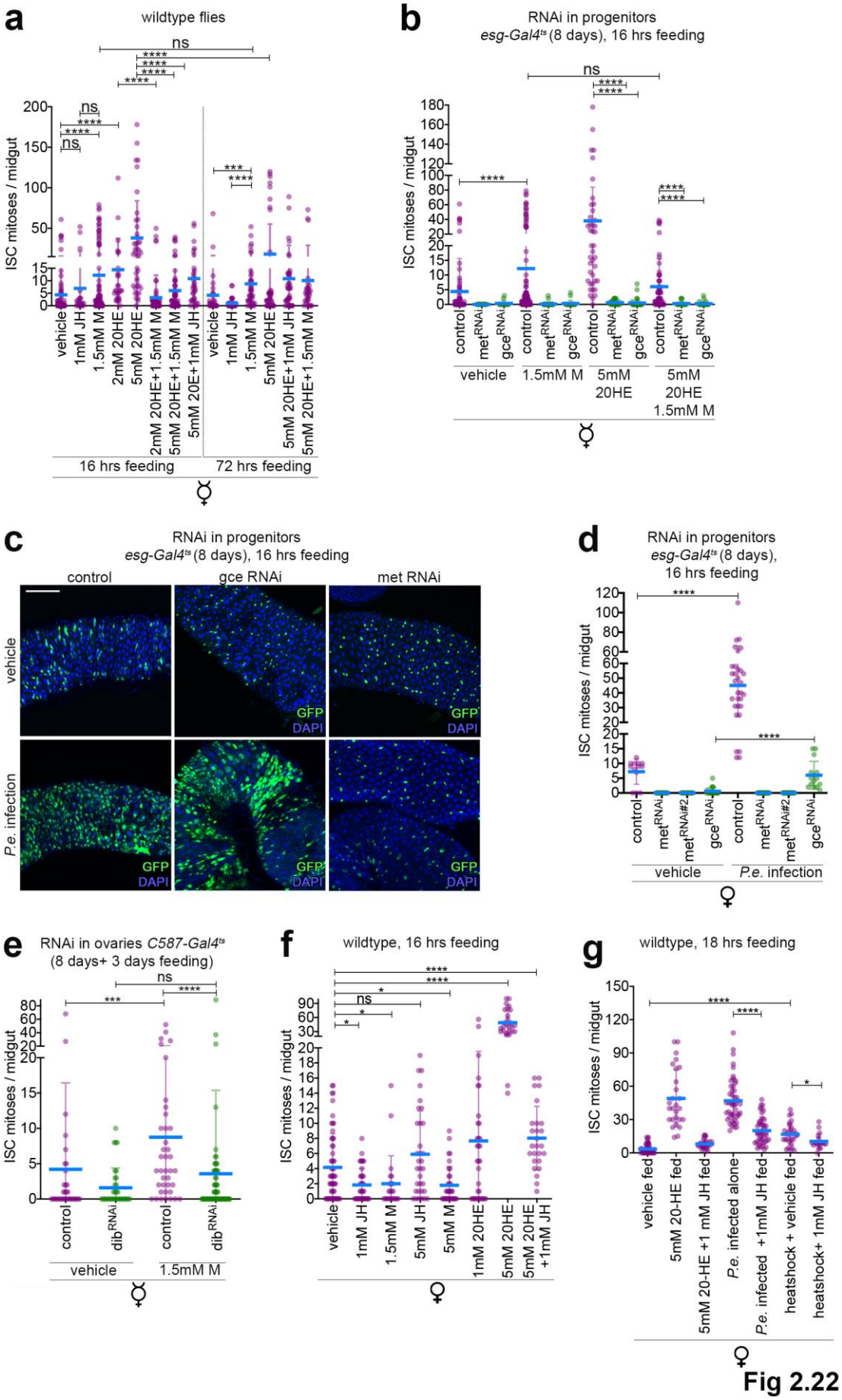
a
wildtype flies
ISC mitoses / midgut
vehicle
1mM JH
1.5mM M
2mM 20HE
5mM 20HE
2mM 20HE+1.5mM M
5mM 20HE+1.5mM M
5mM 20E+1mM JH
5mM 20HE+1mM JH
5mM 20HE+1.5mM M
16 hrs feeding
72 hrs feeding
b
RNAi in progenitors
esg-Gal4ts (8 days), 16 hrs feeding
ISC mitoses / midgut
control
metRNAi
gceRNAi
vehicle
1.5mM M
5mM 20HE
5mM 20HE 1.5mM M
c
RNAi in progenitors
esg-Gal4ts (8 days), 16 hrs feeding
control
gce RNAi
met RNAi
vehicle
P.e. infection
GFP
DAPI
d
RNAi in progenitors
esg-Gal4ts (8 days),
16 hrs feeding
ISC mitoses / midgut
control
metRNAi
metRNAi#2
gceRNAi
vehicle
P.e. infection
e
RNAi in ovaries C587-Gal4ts
(8 days+ 3 days feeding)
ISC mitoses / midgut
control
dibRNAi
vehicle
1.5mM M
f
wildtype, 16 hrs feeding
ISC mitoses / midgut
vehicle
1mM JH
1.5mM M
5mM JH
5mM M
1mM 20HE
5mM 20HE
5mM 20HE +1mM JH
g
wildtype, 18 hrs feeding
ISC mitoses / midgut
vehicle fed
5mM 20-HE fed
5mM 20-HE +1 mM JH fed
P.e. infected alone
P.e. infected +1mM JH fed
heatshock + vehicle fed
heatshock+ 1mM JH fed

**Fig 2.22**

**Fig 2.22: JH and methoprene act as mild pro-mitotic stimuli.** Text and images have been taken and modified from (Ahmed et al., 2020) and have been originally written and made by myself: (a) 20HE acts as a strong promitotic stimulus that peaks transiently at 16-18 hrs then ISC mitoses revert to basal levels by 3 days. JH or methoprene is a mild ISC-inducing agent that causes few but enduring ISC mitoses, which lasts after 3 days of feeding. Combination feeding of 20HE and methoprene or JH has an inhibitory effect on 20HE-induced ISC mitoses. Different feeding regimes single or in a combination (JH, methoprene and 20HE) were given to virgin females overnight or for 3 days then mitotic counts were assayed.
(b) JH receptors met or gce are required for 20HE-induced ISC mitoses. Progenitor-specific depletion of gce or met suppresses the ISC mitoses induced by 20HE or methoprene feeding to virgin females, as shown by ISC counts.
(c-d) Progenitor-specific depletion of met completely ablates *P.e.*-induced ISC mitoses while reduced levels of gce strongly inhibited *P.e.*-induced ISC mitoses but, ISCs still slightly divided following infection. (c) Representative images of gce or met depleted progenitors after *P.e.*-infection relative to the control female midguts. Gce-depleted progenitors show mild expansion after enteric infection. (d) Met and gce in progenitors are required for *P.e.*-induced ISC mitoses.
(e) Methoprene requires ovarian ecdysone for its mild proliferative effect on ISCs. Virgin guts with depleted ovaries have impaired ISC mitotic response to methoprene feeding, as shown by ISC counts.
(f) 1mM or 5mM methoprene feeding insignificantly affect ISC mitoses after 16hrs feeding to mated females. Similar to feedings of virgin females, JH or methoprene alone did not induce ISC mitoses. 20HE feeding induced strong ISC mitoses but combined JH and 20HE feeding inhibit the 20HE induced ISC mitoses, as shown by ISC counts.
(g) Exogenous JH feeding inhibits the mitotic response to any ISC stimulus. Combined feeding of JH and enteric bacteria strongly inhibit *P.e.*-induced ISC mitoses. Similarly, heat shock causes mild ISC mitoses that are suppressed by exogenous feeding of JH after the heat shock, as shown by ISC counts. Duration of treatment or feeding is 16 to 18hrs. Representative images are shown. GFP, in green; DAPI, in blue. Scale bars, 100 μm. Statistical analysis was performed using unpaired non-parametric two-tailed Mann-Whitney test (ns $p>0.05$, *$p\leq0.05$, ***$p<0.001$, ****$p<0.0001$).

then, I fed the flies with methoprene, 20HE or both (Fig2.22b). As previously reported, met or gce depleted progenitors could not divide in response to the methoprene-induced mitoses consistent with the hypothesis that met or gce are redundant JH receptors[311]. Surprisingly, feeding 20HE to midguts with met or gce depleted progenitors completely represses the 20HE-induced mitoses (Fig2.22b). Additionally, reduction of met or gce in the progenitors of mated females completely ablated the *P.e.*-induced ISC mitoses

(Fig2.22c,d). Both latter data indicate that endogenous JH signaling is required for the ecdysone- or *P.e.*-stimulated ISC mitoses. Additionally, this also suggests that the effect of endogenous JH signaling pathway components is permissive to ISC divisions yet, the exogenous JH feeding has an inhibitory effect on ISC mitoses. Next I examined the epistatic relationship between methoprene and ecdysone. Feeding ecdysone-depleted ovary-mediated $dib^{RNAi}$ virgin flies with methoprene impaired their mild stimulatory effect on ISC division indicating that intact ecdysone signaling is also required for the methoprene-induced ISC mitoses to occur (Fig2.22e). The various magnitudes of effects the different treatments had on stimulating ISC mitoses had intrigued me to examine whether the same effects apply to mated females (Fig2.22f). Intriguingly, feeding mated flies with JH or methorprene at the same or much higher concentrations did not cause ISC mitoses in mated females, indicating that the methoprene-promitotic effects are context specific to virgin females. Similar to virgins, combined ecdysone and JH hormone treatments blocked the ecdysone-induced ISC mitoses (Fig2.22f). I then asked, if this inhibitory effect of exogenous JH is specific to 20HE or general to other stimuli. Hence, I stressed mated flies with different mitotic stimuli such as *P.e.* infection or heat shock (Fig2.22g). All in all, my results reveal an interplay between 20HE and JH, yet further work is required to elucidate the discrepancy in the effect between endogenous and exogenous JH feeding on dividing ISCs, and their physiological relevance.

**Fig 2.23 Intestinal EcR signaling drives dysplasia and epithelial aging.**

As females age, they experience progressive gut dysplasia, wherein ISCs over-proliferate and fail to differentiate properly, leading to intestinal barrier breakdown, and a decrease in lifespan [8,62,68,118,120,124,311,344]. I thereby asked how the ecdysone/EcR signaling axis affects the gut as the flies age. Consistent with previous reports[62,120], I observed that aged fly guts accumulate many actively dividing ISCs as well as $GFP^{+ve}$ progenitors that are positive for enterocyte differentiation marker Pdm-1. Occasionally, these cells are also double positive for Ph3 (Fig 2.23.1a-c). Remarkably, progenitor-specific reduction of EcR signaling components at the receptor complex level or downstream target Eip75B in the gut significantly inhibited the hallmarks of gut aging, whether it is accumulation of progenitors or mis-differentiated progenitors or elevated ISC mitoses (Fig 2.23.1a-c).

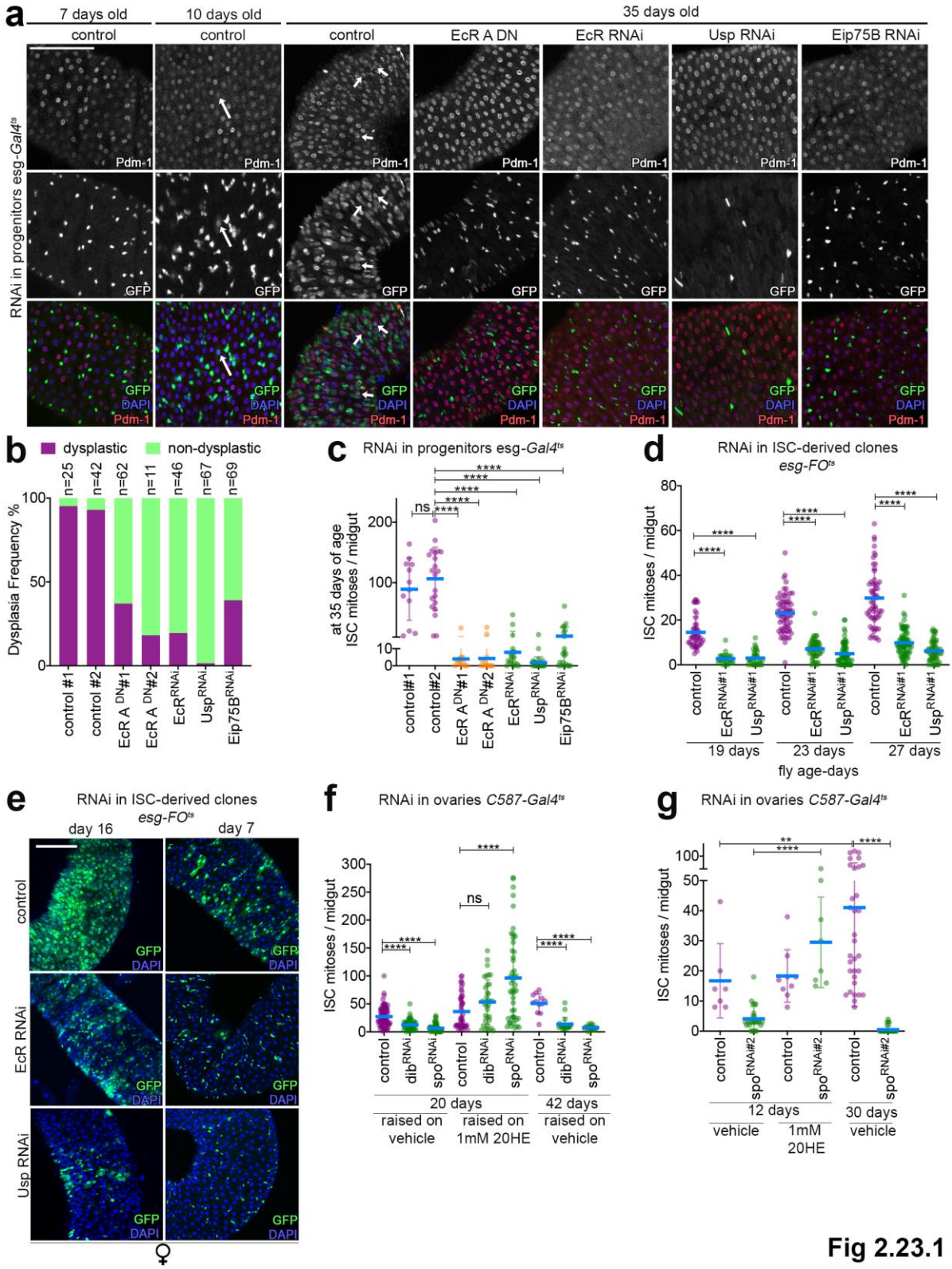


**Fig 2.23.1: Ovary derived ecdysone to intestinal EcR signaling regulates age-dependent gut dysplasia.** Text and images have been taken and modified from (Ahmed

et al., 2020) and have been originally written and made by myself: (a-c) (a) Aging progenitors of the control mated female midguts start accumulating aberrantly misdifferentiated dividing GFP+ progenitors. (Shown by representative images: compare 7 days, 10 days and 35 days old control flies. Thick white arrows point to Pdm-1$^{+}$, GFP$^{+}$ progenitors. The small arrow points to a dividing Pdm-1$^{+}$, GFP+ progenitor cell. The occurrence of this process across the midgut I refer to hereafter as dysplasia. Gut dysplasia is strongly dependent on intestinal EcR signaling through Eip75B. Progenitor-specific reduction of EcR, Usp Eip75B levels strongly hinders the gut from becoming dysplastic. Quantification of dysplastic guts is shown in (b). If at least 10 cells accumulate pdm-1+ GFP+ signal in the R4 region, it is classified as dysplastic, otherwise the gut is termed non-dysplastic. (c) Mitotic counts of midguts with progenitor-specific depletion of EcR, Usp, Eip75B or EcR A dominant negative expression.
(d-e) (d) Mitotic counts of the ISC clones using the *esgF/O* system with EcR or Usp depletion at different ages. (e) Representative images of EcR or Usp depleted ISC clones relative to age-matched controls at 2 different time points. Female gut turnover is slowed down upon reduced 20HE intestinal signaling. I have produced this data during my master's study and I used it in my master's thesis as well, Sara Ahmed,2015[464].
(f) Ecdysone-depleted ovaries have midguts with impaired ISC mitoses. Ecdysone production was suppressed in mated female flies by expressing *spo*$^{RNAi}$ or *dib*$^{\text{RNAi}}$ under the control of the ovarian somatic cell-specific *C587*$^{ts}$-Gal4 driver. Mitotic counts show diminished ISC mitoses of ovary-depleted guts as the flies age (20 and 42 days old) and their mitotic indexes remain low relative to aged control midguts. The mitotic defect of *spo*$^{RNAi}$ or *dib*$^{\text{RNAi}}$ midguts was fully rescued when the adult flies were raised on 20HE-supplemented food.
(g) Ovarian-specific depletion of spo inhibits ISC mitoses and is fully rescued by 20HE feeding. A second alternative RNAi was used against *spo*$^{RNAi}$ to complement results in panel f. Representative images are shown. GFP, in green; DAPI, in blue. Scale bars, 100 μm. Error bars represent ± SD. Statistical analysis was performed using two-tailed Mann-Whitney test (ns $p>0.05$, **$p\leq0.01$, ****$p<0.0001$).

The phenotype was also replicated with *esg*$^{ts}$*-FO* driver to assess the clonal growth and ISC divisions. As expected, the whole midgut epithelium was renewed by day 16 and this clonal growth was severely suppressed by EcR or Usp depletion in aging flies (Fig 2.23.1d-e). Similarly, I found that depleting ecdysteroigenic-synthesizing enzymes (*dib, spo*) from the ovary follicles (Fig 2.23.1f,g) or ubiquitously by a *tub*$^{ts}$ driver (Fig 2.23.2h), also significantly inhibited the age-dependent elevation of mitotic counts. This impaired ISC function was completely rescued when the females were reared on exogenous 20HE implicating the ovaries as a main organ to drive and potentiate gut dysplasia (Fig 2.23.1f-g). Intestinal dysplasia is accompanied by a decrease in the midgut

size and a subsequent loss of regionalization (Fig 2.23.2i) (compare to Fig 2.8.2a). Nevertheless, midguts of EcR and Eip75B-depleted progenitors were detectably more shrunken than aged control midguts, reflective of the idea that they cannot sustain the homeostatic tissue needs (Fig 2.23.2i)

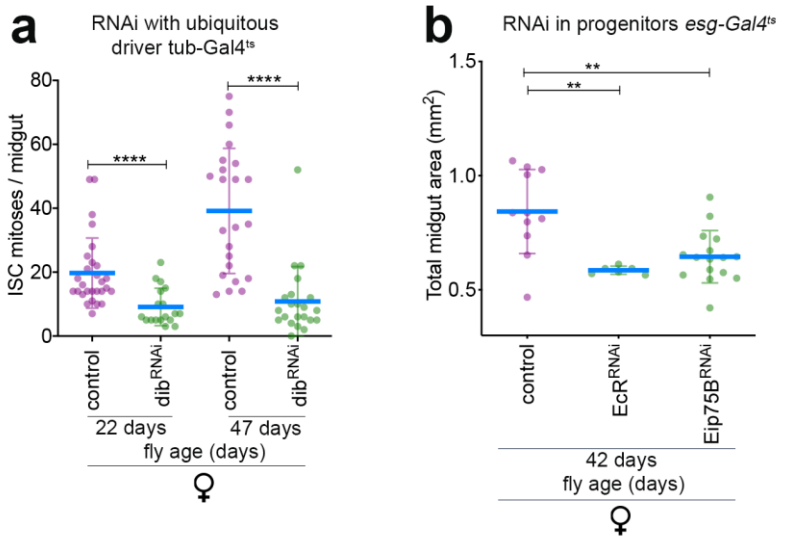


Fig 2.23.2

**Fig 2.23.2: Ovary ecdysone to EcR in the intestine signaling regulates the hallmarks of aging.** Text and images have been taken and modified from (Ahmed et al., 2020) and have been originally written and made by myself: (a) Ubiquitous expression of *dib*$^{RNAi}$ under the control of the *tub*$^{ts}$ driver in mated females significantly impaired ISC mitosis at 22 and 47 days old.
(b) Reduced intestinal EcR signaling in progenitors accelerates the loss of midgut size. Midgut sizes of EcR/Eip75B depleted progenitors show that Eip75 and EcR are required to maintain midgut cellularity and morphology, without which it deteriorates somewhat faster than control epithelia. Error bars represent ± SD. Statistical analysis was performed using two-tailed Mann-Whitney test (**p≤0.01, ****p<0.0001).

**Fig 2.24 Intestinal EcR signaling possibly shortens the female lifespan.**

The gastrointestinal tract, due to its role as a digestive organ and function as a barrier between the exterior and interior milieu, is critically impacted by dietary, environmental, and inflammatory conditions that influence the organismal health and lifespan[105]. Indeed, both gut dysplasia and tumorigenesis shorten lifespan [62,95,107,345,346].

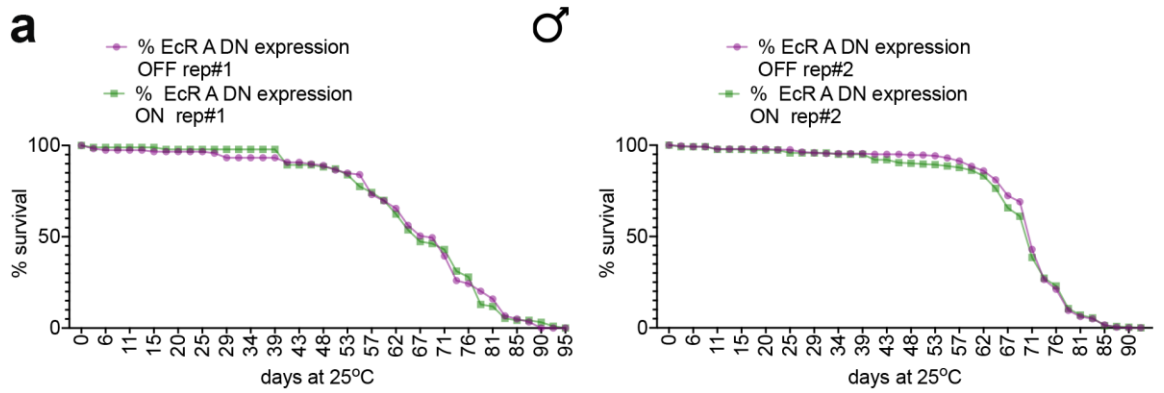


| Condition | $X^2$ | P-value |
|---|---|---|
| EcR A DN expression OFF rep#1 v.s. EcR A DN expression ON rep#1 | 0.01 | 0.9301 |
| Condition | $X^2$ | P-value |
| EcR A DN expression OFF rep#2 v.s. EcR A DN expression ON rep#2 | 0.240 | 0.625 |

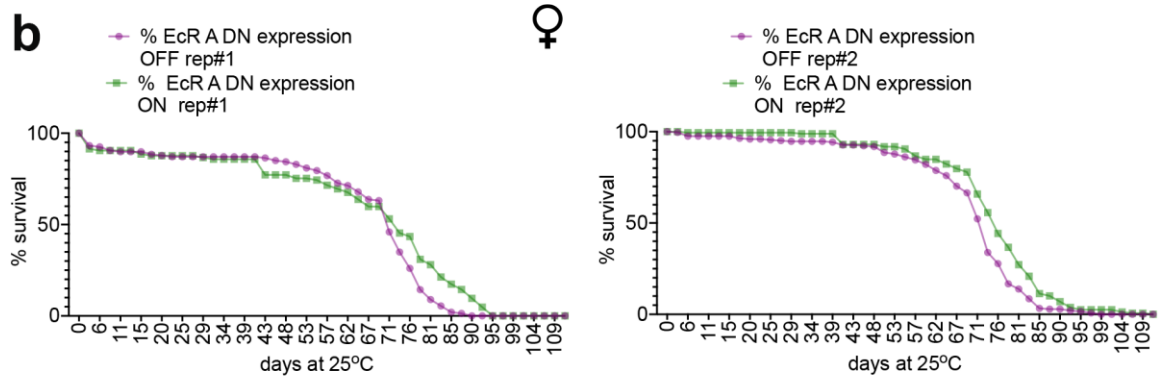


| Condition | $X^2$ | P-value |
|---|---|---|
| EcR A DN expression OFF rep#1 v.s. EcR A DN expression ON rep#1 | 11.330 | 0.001 |
| Condition | $X^2$ | P-value |
| EcR A DN expression OFF rep#2 v.s. EcR A DN expression ON rep#2 | 17.730 | 0.000026 |

**c** Collective life span analyses (% mortality)

| ♂ | | | | | Age in days at % mortality | | | | |
|---|---|---|---|---|---|---|---|---|---|
| Name | No. of subjects | Days | S.E. | 95% C.I. | 25% | 50% | 75% | 90% | 100% |
| EcR A DN expression OFF rep#1 | 119 | 65.60 | 1.58 | 62.51 ~ 68.69 | 57.00 | 69.00 | 76.00 | 83.00 | 90.00 |
| EcR A DN expression ON rep#1 | 94 | 66.12 | 1.58 | 63.03 ~ 69.20 | 57.00 | 67.00 | 78.00 | 83.00 | 95.00 |
| EcR A DN expression OFF rep#2 | 243 | 69.42 | 0.84 | 67.77 ~ 71.08 | 67 | 71 | 76 | 78 | 90 |
| EcR A DN expression ON rep#2 | 263 | 67.98 | 0.9 | 66.21 ~ 69.75 | 67 | 71 | 76 | 81 | 92 |
| ♀ | | | | | Age in days at % mortality | | | | |
| Name | No. of subjects | Days | S.E. | 95% C.I. | 25% | 50% | 75% | 90% | 100% |
| EcR A DN expression OFF rep#1 | 161 | 63.39 | 1.86 | 59.75 ~ 67.04 | 60 | 71 | 78 | 81 | 90 |
| EcR A DN expression ON rep#1 | 117 | 64.62 | 2.5 | 59.72 ~ 69.51 | 55 | 74 | 83 | 90 | 95 |
| EcR A DN expression OFF rep#2 | 247 | 68.90 | 1.05 | 66.84 ~ 70.96 | 67.00 | 74.00 | 78.00 | 83.00 | 99.00 |
| EcR A DN expression ON rep#2 | 173 | 74.26 | 1.12 | 72.07 ~ 76.46 | 71.00 | 76.00 | 83.00 | 90.00 | 111.00 |

**Fig 2.24**

**Fig 2.24: Reduction of intestinal EcR signaling may extend the lifespan of *Drosophila* females.** Text and images have been taken and modified from (Ahmed et al., 2020) and have been originally written and made by myself: Progeny of the genotype GS5961-Gal4 UAS-EcRF645A were mated for 48 hrs. The populations followed up were segregated based on their sex and separated into groups of 25 flies/vial. Approximately half of the flies were fed with 0.2 mg/ml RU486 to induce RNAi depletion in progenitors

and the other half were fed with vehicle. RU486 or vehicle (ethanol) were deposited on the food vials 4-6 hrs before flipping the flies into the vials at 48 hr intervals. Dead flies were visually identified and recorded. Life span assays were performed in two replicates and for each replicate days elapsed after the start of the assay were plotted as a function of percentage survival. (a) shows the 2 independent replicates performed on male subjects whereas (b) shows the 2 independent replicates performed on female subjects. Statistical analysis was performed using log rank test. x2 represents chi-squared value and is present below the plots. (c) displays the analyses of the experimental male or female replicates.

As I have confirmed that mating-induced ecdysone is pro-mitotic and accordingly pro-dysplastic, my findings suggested that ecdysone might also have an adverse effect on lifespan.

Consistent with this idea, whole-body suppression of ecdysone signaling is reported to extend *Drosophila* lifespan[166]. To figure out whether this life span extension is in part due to suppression of age-dependent gut dysplasia, I conducted a lifespan assay with EcR dominant negative misexpression via the RU-inducible gut driver *GS5961*[62] in both males and females, in 2 independent replicates. EcR misexpression in male intestines had no apparent advantage on the lifespan (Fig 2.24a,c). In contrast, EcR misexpression in female intestines ameliorated their survival fitness relative to controls (Fig 2.24b,c). Despite being a highly significant effect, the magnitude of the lifespan extension effect was not so drastic (Fig 2.24c). Unfortunately, in figuring out in whether the *GS5961* is highly specific to the gut, Dr. Pénalva in the Edgar lab detected GFP expression in the posterior follicular cells from stage 8 of oogenesis (Fig 2.16.2m-q). This result confounds with the lifespan extension effect I observed during my experiments, as reduced fecundity was also reported to extend lifespan in *Drosophila* [347]. Thus, the effect of the driver on the gut could be explained as a result of slower gut aging or lesser eggs laid due to a smaller gut. And the effect of the driver on the ovary could be through an off-target indirect effect from the damaged ovarian follicles since EcR functions in migration, differentiation, and production of the egg shell [348]. Nevertheless, misexpression of the same EcR allele I used in my assay was found to cause female sterility when expressed in late stage follicle cells [348], (the stages where Dr. Pénalva detected the driver expression in the ovary) but, the flies I used for the assay were perfectly fertile across their lifespan. This indicates and suggests that the magnitude of the *GS5961* driver effect in the ovary is relatively minor. Crucially, the careful examination of all the midgut drivers by Dr.

Pénalva indicated that the same caveat applies to all the commonly used midgut drivers (*esg-Gal4, MyoIA-Gal4, Mex-Gal4, Su(H)-Gal4*), each of which had some expression in the ovary (Fig 2.16 and data not shown). Hence, it remains currently imprecise whether the lifespan advantage in all lifespan reports come from gene effects on the gut, in the ovary or both and it remains of prime importance to find highly tissue specific gut or ovary drivers for future studies.

**Fig 2.25 Elevated ecdysone levels pre-disposes flies to intestinal tumorigenesis.**

It is well known that females are more susceptible to forming ISC-derived tumors than males [95,345,346]. There are several models to induce intestinal tumorigenesis in *Drosophila* [346,349,350] among which is depletion of *Notch* receptor required for EB differentiation which leads to accumulation of constantly dividing undifferentiated tumor masses along the midgut (Fig 2.25a-h). $Notch^{RNAi}$ in mated females resulted in tumor induction in 100% of the flies (Fig 2.25a,b). Notably, $Notch^{RNAi}$ in virgin females was far less tumorigenic. Similarly, males display lower tumor burden despite being more prone to develop spontaneous neoplasias[303] (Fig 2.25c,g,h). I thereby proposed that the tumorigenic potential was dependent on 20HE-EcR signaling. To test that, I blocked EcR signaling in mated females in the $Notch^{RNAi}$ expressing progenitors with dominant negative expression of EcR A, which drastically repressed the tumor growth and progression (Fig 2.25a-c). Conversely, I used $Notch^{RNAi}$ virgin females, which were unable to form tumors, and I fed them with 20HE prior to $Notch^{RNAi}$ induction. This treatment augmented the tumor initiation frequencies (Fig 2.25 b,d,e).

Moreover, to test the tumorigenicity of ecdysone in males, I reared them on 20HE-laced food, which led to increased tumor burden (Fig 2.25c,g,h).

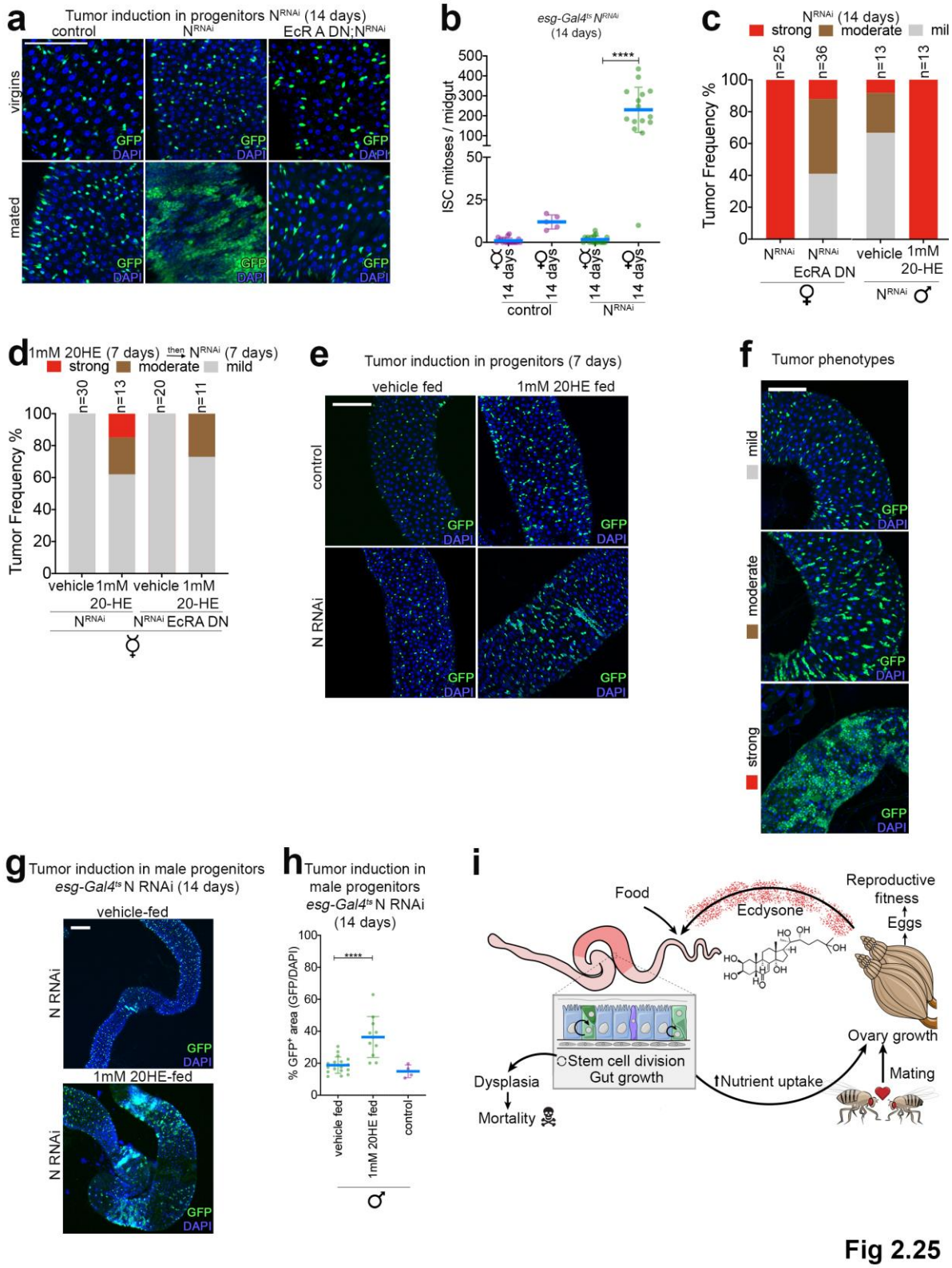


Fig 2.25

**Fig 2.25: 20HE signaling predisposes intestinal tumorigenesis.** Text and images have been taken and modified from (Ahmed et al., 2020) and have been originally written and made by myself: (a-b) Intestinal tumor progression is dependent on intestinal EcR signaling in progenitors and Notch depleted tumors fail to initiate in virgin females. (a)

Representative images of midguts with tumor induction in virgins, mated females or EcR A DN misexpressing progenitors. (b) Mitotic counts of Notch depleted adult virgin or mated females.
(c) Quantification of the phenotypes of the intestinal tumors in mated females +/- reduced 20HE signaling scored as categorized in (f) (first half of the panel). 2$^{nd}$ half of the panel is the phenotypes scored in male intestines raised on 1mM 20HE supplemented food as categorized in (g).
(d) Tumors initiate in virgins fed on 20HE for 1 week prior to induction of Notch depletion. Quantification of the phenotypes of the intestinal tumors scored as categorized in (e).
(e) Representative images of virgins fed on 20HE-laced food with initiated tumors relative to vehicle-fed virgins without tumor clusters.
(f) Representative images of the 3 categories scored in female tumors: strong tumors are denoted in red, moderate are depicted in brown while non-tumorous are depicted in grey.
(g-h) Representative images of 20-HE-fed notch depleted males that develop and progress tumors faster than in intestines that are vehicle-fed. (h) Quantifications are shown by deriving ratios between GFP+/DAPI+ areas of 20-HE or vehicle-fed *Notch*$^{RNAi}$ males. Tumor induction commenced few days prior to 20-HE feeding. GFP, in green; DAPI, in blue. Scale bars, 100 μm. Statistical analysis was performed using unpaired non-parametric two-tailed Mann-Whitney test (****$p<0.0001$).
(i) Model summarizing my conclusions. Ovary-derived ecdysone is released after mating, whereby it resizes the midgut expanding its area through partly symmetric ISC mitoses. Subsequently, this gut resizing allows better nutrient uptake to satisfy the high reproductive demands of the mated female. This progressive midgut growth comes at the expense of increased predisposition to dysplasia and tumors, hence shortening the lifespan.

To sum up, my experiments showed that steroid hormone signaling robustly stimulated ISC division in the midgut of both sexes independently of the sex identity of the ISCs, possibly through exerting metabolic effects. Moreover, I also revealed a cross-talk between the ovary and the gut whereby, mating-induced release of ovary-derived ecdysone stimulates phasic ISC mitoses, conceivably EB differentiation and increased gut cellularity, that leads to gut growth. Gut growth occurs to expand the gut's capacity to absorb nutrients thereby, meeting the female's reproductive demand. However, this gut re-sizing process comes at the cost of promoting age-dependent gut dysplasia, increased tumor burden and shortened lifespan (Fig 2.25i).

# Discussion

I reveal an organ-organ communication signal through which the release of an ovary-derived sex specific signal directs intestinal stem cells of the gut to divide and initiate intiestinal growth. This depends on the actions of the highly conserved EcR signaling and its downstream target Eip75B. Below I provide a brief overview of the resemblances between *Drosophila* and mammals in the context of their female sex hormones ecdysone and estrogen: their actions on the gut and their similarities in the sexual maintenance mechanisms as well as similarities in the phenotypes they regulate. This goes along a number of implications and connections to existing data, which are worth discussing further and could present possible avenues for future research.

**3.1 Parallels between the mechanisms of action of ecdysone and estrogen:**

Both estrogen and ecdysone are cholesterol-derived sex-specific steroid hormones that are known to control aspects of sexual behavior and reproductive function in mammals[264] and *Drosophila*[300]. They are both being produced by the ovaries[302,351]. Estrogen release is directed by luteinizing hormone (LH), follicle-stimulating hormone (FSH) and gonadotropin-releasing hormone (GNRH) in mammals while ecdysone release is modulated by PTTH (prothoracicotropic hormone) in *Drosophila* during development but a similar brain axis is not described yet in adult *Drosophila*[352]. The similarity in their structure, site of synthesis, regulated secretion and actions on the reproductive system implies that they could have resemblances in their actions in other organs too.

Although there is still a lot more to be discovered, there are interesting parallels in our current knowledge on how estrogen and ecdysone works.

Liganded ERα, which is most highest expressed in intestinal crypts has been implicated in several cell cycle regulatory events. First, estrogen-activated ERα shortens the cell cycle significantly by altering the cell cycle duration in the S and $G_2$/M phases. Notably, cyclins A and B and well as ERα protein levels display a synchronous behavior in their kinetics as the cells progress through the cell cycle after release from $G_1$ arrest. These cell-cycle dependent changes in ERα protein expression are likely not mediated via transcriptional changes in gene expression, rather via a post-transcriptional

mechanism[353,354]. Secondly, ERα also interacts with cyclins A, B, D1 and E and it too directly interferes with the nuclear accumulation of CDK inhibitors including p27, CCNG2, $p21^{CIP1}$ (CDKN1A), GADD45 to promote cell cycle progression[355,356] both in-vitro and in-vivo. Thirdly, distinct patterns of gene regulation are identified after estrogen administration most prominently between 4-8 hrs and 24-48 hrs, most of which are genes involved in cell cycle and nucleotide processing[357].

Short term pulses of 20HE or estrogen lead to upregulation of EGF and Jak/Stat signaling components. I have not had the chance to study the ecdysone-induced genetic profiles with such detail. However, remarkably, I find interesting similarities in the pathways they activate such as transcriptional induction of Egfr/MAPK and Jak/Stat pathways after overnight 20HE feeding consistent with their requirement for cell division to occur[357,358]. This suggests that 20HE and estrogen impinge to some extent on similar pathways, sharing at least a degree of conservation in their actions to direct cellular proliferation.

All these mechanistic details that underlie the rhythmicity of the response to female sex hormones are very relevant to study and understand because they probably direct most growth in a female's lifetime (in the sex organs to satisfy the reproductive demand but, also now I show that the effects extend to non-sex organs too). Indeed, the biphasic response of ISC mitotic stimulation was unique to 20HE feeding in females. Notably, as I have observed rhythmicity in the pattern of ISC divisions after mating or 20HE feeding in the intestine, the female reproductive tissues similarly undergo cyclical changes of growth and degeneration in-vivo directed by gonadal sex hormones. For example: the rodent uterine tissues are highly responsive to estrogen, and it causes cell division in a biphasic manner similar to what I have observed with 20HE feeding on ISCs of the midgut. A single dose of estradiol (most bioactive estrogen) causes early and late tissue responses to estrogen. The strength of the response is dependent on the bioavailability of the estrogen and the duration of interaction with its receptor. The early response usually occurs during the first 6 hrs after estrogen administration and it corresponds to increases in RNA and protein synthesis, stimulation of proliferative genes such as MYC and fos as well as water retention. This is followed by late estrogen responses include cycles of DNA synthesis and epithelial cell mitosis, which begin 10–16 hrs after estrogen administration. Two waves of mitoses occur: one wave after ~16 hrs and the other after ~24 hrs[356].

Accordingly, it would be interesting to profile ecdysone's response on ISC divisions of the gut in-vivo in further detail. I propose repeating the ecdysone feeding and the mating experiments in an extended time course from 0-72 hrs (feeding), 0-5 days (mating) to define whether: 1. The phasic response observed in 20HE-fed flies extends over time or there are only 2 distinct proliferative peaks as I have described. 2. Using RNA seq, identifying different patterns of gene regulation to identify early only, late only and early and late 20HE regulated genes that correspond to 20HE-induced ISC mitoses. 3.Similar rhythmicity of ISC mitoses occurs in response to mating and if they correlate with changes in the female uterus to maximize nutrient deposition in fertilized eggs.

### 3.2. Physiological functions of estrogen and ecdysone signaling in the intestine

Estrogens and ecdysone contribute to the physiological function of the intestine. Not only do ecdysone and female mammalian sex hormones share a strong resemblance in reproductive actions in *Drosophila* [123,158,359] and mammals [323,360], evidence emerged suggesting that they have similar actions in other organs. Prior to this report, functions of sex-specific steroids on the intestine remain uncharacterized in flies and controversial in humans. ERα and ERβ are present in the stomach and intestine of both males and females[247,361-363]. ERα is mainly expressed at the base of the intestinal and colonic crypts of males and females, where the ISCs lie and can stimulate c-fos in an estrogen-dependent manner[361,364]. ERβ expression is predominantly restricted to the differentiated epithelial cells of the intestine[365]. To date, ER functions in the maintenance of the epithelial integrity through the sexually dimorphic estrogen levels, that regulates mucosal bicarbonate secretion in the duodenum in mice and humans[366,367]. Estrogen signaling deregulation correlates with prevalence of duodenal ulcers[366]. Moreover, female sex hormones also function to regulate of smooth muscle contractility and motility of the GI tract, inhibit pro-inflammatory cytokine production, stimulate wound healing, and increase barrier function of the intestinal epithelial cells[362,368]. The data I gathered during my work suggests that EcR functions in the ISCs to regulate mitotic responses during epithelial renewal and detergent-induced regeneration. Moreover, my RNA sequencing data suggests that ecdysone is associated with increased abundance of digestive enzymes, lipid and starch metabolic enzymes. EcR also functions in the enteroblasts to regulate

their differentiation in enterocytes. EcR seems to also be required for maintenance of the epithelial cells in the midgut raising the possibility that it could function in maintaining the epithelial integrity or barrier function, similar to ER functions in the mammalian GI tract. To date, the function of the sex hormones regulating digestive functions or metabolic enzymes in the gut is not well-characterized which should not be peculiar given the conserved roles of sex steroids as central regulators of systemic metabolism in mammals acting at CNS, adipose tissue and skeletal muscle[369] and in *Drosophila* acting at CNS[167], ovaries[123] and fat body[370]. However, the novel notion revealed by my experiments here is that at least some aspects of metabolism in a non-sex organ are controlled in a sexually dimorphic manner through the sex-specific hormone, 20HE.

### 3.3. Pathophysiological implications of sex steroids in GI tumors

Increased levels of estrogen correlate with tumorigenesis in the GI tract of males and females. Similarly, I show that tumor initiation and progression in the *Drosophila* males and females depend on ecdysone levels and the extent of active EcR signaling. Ecdysone feeding promotes tumor initiation in virgin females and increases tumor aggressiveness presented in the males. Reduced EcR levels in progenitors drastically slow tumor progression. In line with these results, accumulating biological evidence from mammalian studies strongly suggest a link between gastrointestinal adenomas and malignant tumors arising from different GI tissues and higher estrogen levels in both males and females[371-382]. Moreover, the rather conflicting long-held view that higher estrogens lower the risk of CRC has been debunked by recent studies[383]. In fact, increased circulating endogenous female hormones are linked to promoting CRC tumor progression in postmenopausal women[384-386].

Precisely, metabolism and inactivation of endogenous estrogens is suppressed in the vicinity of the GI tumors. Hence, the bioavailability of estrogen is higher in the tumor microenvironment relative to the surrounding tissues[380,387,388]. Moreover, in-vivo and in-vitro studies show that estrogen acts a pro-mitotic stimulus to colorectal cells and it drives its tumorigenic effects through induction of c-fos. C-src and activation of the mitogen-activated protein kinase (MAPK) cascades[389,390]. Interestingly, estrogen also increases DNA replication activity and mediates alkalinization of colonic crypts isolated

from human distal colon and colorectal cancer cell lines through activation of calcium-dependent protein kinase C (PKC) that alters pH in human colonic cells[391]. Similarly, increased expression of ERα is shown after DSS-induced intestinal inflammation[122] and GI tumors such as, duodenal familial adenomatous polyposis[392]. In ERα and ERβ negative cell lines, GPER is also alternatively upregulated to transduce estrogen's proliferative and pro-angiogenic actions. In CRC, GPER expression is significantly associated with poor survival[393]. Collectively, tumor progression is potentiated by estrogen actions on its receptors. The fact that estrogen increases DNA replication is interesting and it coincides with several observations from my RNA seq experiments. Males and females are intrinsically different in the expression of DNA-replication and cell cycle related genes such that females express higher levels of DNA polymerases and other helicases involved in DNA replication initiation. There are also more ISCs in the S/G2-phase in females than males in the adult midgut[118]. These differences could be in part explained by the differences in 20HE levels, as 20HE-fed males become more similar to females in genes associated with DNA replication.

### 3.4. Exogenous exposure to steroids has detrimental consequences:

As briefly introduced in the first chapter, many estrogens from oral contraceptives or hormone replacement therapy, dietary sources, livestock production and manure persist in the environment posing serious risks on the individuals health and ecosystem. Indeed, recent studies show that ethinyl estradiol ($EE_2$, the active component of many birth control formulations) initiate rapid non-genomic (i.e. without modulation of target gene expression) activation of MAPK, ERK, and JNK pathways in pituitary tumor cells[394]. Moreover, environmental estrogen modulates hepatic insulin sensitivity, energy expenditure and distribution of body fat and adipose tissue[369]. This suggests that exogenous exposure to bioactive steroids or endocrine disruptors can mimic endogenous estrogens, exacerbating cell proliferation, altering their metabolic profile and increasing tumor predisposition. In light of the above and my findings on the actions of exogenous 20HE feeding promoting ISC mitoses at the expense of faster aging of the gut, I suggest that exogenous steroids exposure may represent a real risk factor in the development of the metabolic syndrome and their actions should be studied in more detail.

### 3.5. JH signaling is dually required for stimulation or inhibition of ISC proliferation:

My epistasis and feeding experiments led me to a series of conclusions regarding the regulation of the cross-talk between the highly complex JH and 20HE signaling networks. Exogenous feeding of JH agonist methoprene, but not JH stimulates ISC proliferation in virgin females[311]. Endogenous JH receptors Gce and met are required for the mating-induced ISC division[311], as well as homeostatic maintenance of progenitors. Additionally, they are also required for tumor growth [395], 20HE-induced ISC mitoses and stress-induced mitoses (i.e. in response to paraquat [311] or *P.e.* infection) in both virgins and mated females. Collectively, these findings rather argue that met and partly gce are generally required for basal ISC divisions. JH production from at least two different sources influences the midgut ISC mitoses. After mating, ovary-derived ecdysone causes JH production from the corpora allata, to trigger ISC mitoses[324]. Additionally, midgut progenitors also locally synthesize JH, which is required for their maintainence[395]. The required level of JH signaling in mated females but not virgin females seems sufficient because exogenous JH or methoprene cause ISC division in virgin females, not in fertilized females.

Interestingly, the epistasis experiments between 20HE and JH signaling propose a model whereby JH signaling components act downstream of 20HE and it is accordingly also differentially expressed between males and females. First, in adult flies, reproductive success in both males and females is achieved through ecdysone-mediated release of JH[324]. Accordingly, JH is also produced in the corpora allata of males and its release is a consequential effect of ecdysone[324]. Congruent to this model[324], my results also suggest that JH signaling require ovary-derived ecdysone to trigger methoprene-induced ISC mitoses. Hence, I propose that at least partly, ecdysone and JH follow a similar hierarchy through which the 20HE regulates JH, partly through converging on similar targets such as: Eip75B [396,397] and Krh-1[311,398]. Consistent with the sexual dimorphism in 20HE, there is a sex-biased expression of both met and gce between female and male midguts[118]. This argues that 20HE levels may regulate the extent of activation of JH signaling.

Additionally, JH signaling needs to be tightly controlled for ISCs to divide. Exogenous JH or methoprene feeding suppressed any stimulus-induced ISC mitoses in either virgin or mated females. The stimuli tested included: heatshock, *P.e.* infection 20HE-feeding.

### 3.6. Mating causes symmetric ISC mitoses:

In response to feeding, ISCs remodel the gut by expanding the ISC pool via symmetric divisions, and by increasing their proliferation rate[10]. This causes a feeding-induced gut growth that is highly adaptable to nutritional cues. Subsequent rounds of feeding, fasting, and re-feeding cause an adjustable change in gut sizes leading to growth, shrinkage then growth[10]. My experiments suggest that mating-dependent 20HE release from the ovary causes an increase in the number of ISCs, possibly via symmetric stem cell divisions as shown by EcR reporter activation in delta $LacZ^{+}$ doublets. In contrast to nutrient-dependent gut resizing, overnight mating during which females presumably copulate with males once appears to cause an irreversible increase in the ISC numbers, which fail to regress back to a "virgin-state". Hence, Mating in flies irreversibly alter the physiology, and perhaps the life history, of female flies. I propose these changes to be analogous to morphological changes in different organs accompanied with the state of parity in mammals (termed as: the number of pregnancies in mammals)[399,400]. In an analogous manner, one could argue that a primigravida state (that is referring to a female pregnant once) may be sufficient to similarly alter the mammalian gut physiology. This is likely to be an important distinction that is mostly unaccounted for in mammalian studies.

### 3.7. Functional bifurcation of EcR and Usp

EcR and Usp function together to modulate gene expression in response to 20HE feeding or mating. However, I discovered the first evidence of functional bifurcation between EcR and Usp upon *P.e.* infection in adult *Drosophila*. EcR was dispensable to the ISCs or other midgut cell types for the *P.e.*-induced ISC mitoses, while Usp depletion completely suppressed *P.e.*-induced ISC mitoses. This is one of the non-overlapping functions described for Usp that fit with literature reports suggesting that Usp interacts with other nuclear receptor partners across the developmental stages of *Drosophila* [332]. During embryogenesis, mutation in DBD/LBD of EcR results in embryonic lethality but,

mutation in the DBD of Usp causes lethality only in larval stages: during the first to second larval molt[159,401]. Ecdysone-dependent induction of larval glue genes, a behavioral event prior to pupal commitment is also mediated by EcR but, not through Usp[402]. Additionally, Usp forms a complex with Hr38 that is indirectly activated by ecdysteroids to function in cuticle formation [336,337], carbohydrate metabolism[403], or regulating 20-HE-dependent transcription[335,337]. Intriguingly, this interaction is also mediated by the mammalian counterparts and is conserved across the vertebrate species[333]. In the *Drosophila* midgut ISCs, loss of Hr38 phenocopies depleted Usp functions suggesting that they function in ISC maintenance. While depletion of other possible Usp partners such as Hr96, Hr51, and Hr83 did not suppress *P.e.*-induced mitoses. Moreover, genetic interaction tests validated the interaction between Usp and Hr38 mutants to mediate *P.e.*- or 20HE-induced ISC mitoses. Hence, Usp seems to interact with Hr38 in midgut ISCs, similar to other contexts[335-337,404,405].

### 3.8. Role of Eip75B in ISC proliferation

Downstream of 20HE feeding, I identified Eip75B as a critical regulator of ISC mitoses. Eip75B is highly homologous to the mammalian REV-ERB[127]. They are both heme-bound[182], structurally conserved and function in regulating proliferative and metabolic genes[181,185,406,407]. Eip75B functions as a transcriptional repressor, functioning directly at promoters of target genes[176,184] or through repressing the activatory functions of Hr3[175,177] or Hr51[189,408]. Genetic epistasis data imply that Eip75B does not function with Hr51 in the Drosophila midgut ISCs. Rather, Eip75B represses the transcriptional functions of Hr3 not Hr51 to regulate ISC proliferation. Expression of many Eip75B isoforms were detected in the transcriptome of the sorted ISCs, not ruling out the likelihood that Eip75B can regulate transcriptional targets through direct binding to DNA. Furthermore, I showed that Eip75B actions in ISCs are modulated *in-vivo* through nitric oxide (NO) availability in the midgut. NO binds the heme moiety of Eip75B interfering with its ability to inhibit Hr3's activity or recruit co-repressors[176,185,189]. This implicates Eip75B as a redox sensor in the ISCs of the midgut[175,182]. Indeed, Eip75B was required for Paraquat-induced (ROS-producing agent that leads to oxidative stress) and age-dependent elevation of ISC mitoses that also occurs as a result of increased oxidative stress[106].

Accordingly, it becomes particularly interesting to address the role of Eip75B in redox homeostasis to control regenerative and self-renewal ISC mitoses, or age-related changes in redox state which result in the age-related stem cell dysfunction of ISCs and intestinal dysplasia.

Similarly, heme is required for Eip75B stability and heme availability determines Eip75B levels[175]. Indeed, exogenous heme feeding induces ISC mitoses in an Eip75B dependent manner suggesting that Eip75B might act as a heme sensor in the gut. Heme is essentially required by metabolic, free radical detoxifying enzymes, hormone synthesizing CYP450 and energy utilizing enzymes[175,409]. If indeed Eip75B is sensing heme, it would function to regulate a balance between heme availability and enzyme biogenesis[175,409-413]. This notion is supported by the evidence that steroidogenesis in *Drosophila* require both ferredoxins for Fe-S cluster biosynthesis and Eip75B isoform A (now called variant D) [184,414-416]. Notably, the requirement of ferredoxins for steroidogenesis is conserved across mammals[416]. How Eip75B would similarly function in tightly regulating redox or metabolic enzymes in the midgut remains an open question.

In summary, my findings are consistent with the previous reports that established the function and validated the interaction of this Eip75B•Hr3 complex in other contexts during *Drosophila* development[175,185,189]. As Eip75B is highly expressed basally in all midgut cell types (Flygutseq database) but also in ISCs of 20HE-fed animals (my sequencing data), it should be interesting to identify which genes it actually regulates. Given that Eip75B and REV-ERB have overlapping functions in regulating circadian rhythm and metabolism in both *Drosophila* [179,180] and mammals [181,182] and the fact that REV-ERB is highly expressed across the GI tract (human Protein Atlas database), further studies on the impact of REV-ERB in the context of intestinal stem cell biology should prove interesting.

### 3.9.The influence of hormones on sex traits: parallels from fly to humans

Sex is a fundamental biological characteristic that influences nearly all-organismal traits from health to disease to mortality. According to the classical textbook definition traits can refer to an observable phenotype (termed phenotypic trait) or the underlying genetic loci that cause the phenotype (termed genotypic trait). Often traits are termed complex because they are multi-factorial. There is increasing evidence from model organisms to

genome-wide association studies (GWAS) in humans that suggest that sexually differentiated traits are the result of a coalescence of genetic, epigenetic, gonadal hormone and external environmental cues. As an example I discuss evidence I obtained which supports the contribution of hormonal signaling: 20HE regulation and its parallel in humans to the phenotypic and underlying genotypic sex differences in ISC mitoses, determined by 20HE levels.

The central dogma is that sex maintenance arises from the primary sex-determining genes i.e. sex chromosomes in and outside of the gonads and gonadal sex-biased downstream products, such as gonadal hormones, which interact together to impart female and male specific sex traits, thereby defining and maintaining the sex of the individual, as discussed further.

**a) Sexually dimorphic ecdysone levels regulate ISC mitoses in males versus females**

My results identify circulating ecdysone levels as a sex-specific non-cell autonomous systemic signal that acts in concert with the intrinsic sex determination pathway to strongly regulate the mitotic ISC behavior in both males and females. Exposure to increased levels of exogenous 20HE for varying durations caused striking different phenotypes in both sexes. Firstly I begin with the phenotypes observed after short exposure to 20HE. 20HE feeding for 6 hrs stimulated 20HE only in females but not in males. Then, by 18 hrs, 20HE feeding promoted ISC mitoses rather equally in both sexes. Several open questions remain. How can the male ISCs miss the 1$^{st}$ mitotic wave but, remain competent to divide at the 2$^{nd}$ wave? Considering that the male gut area is only one third that of a young mated female, does this mean that males have less ISCs/gut? It could generally be implied that they have less ISCs/midgut because males do not to have a significantly higher density of ISCs than male ISCs/area[118,316], hence it remains quite possible that the total number of available ISCs to divide/time point across the gut is different between a male and a female. Males and females do not have differences in the ratio of symmetric versus asymmetric divisions but, females have higher proportion of their ISCs at the G2/S transition indicating that they have shorter cell cycles[118]. Interestingly, the ratio of ISCs in the G2/S phase relative to the G1 phase is an aspect regulated by the intrinsic sex determination pathway[118]. It is interesting to note that the

EcR reporter was active in many delta $LacZ^+$ doublets in the posterior midgut, linking 20HE activity to symmetric ISC mitoses. So does 20HE exposure boost symmetric ISC division in male midguts that suddenly the guts are filled with unusual numbers of dividing ISCs? Does 20HE synchronously push the male ISCs through shorter cell cycles thereby, bypassing the male-specific trait of the "slower cell cycle" dictated by the intrinsic sex of the ISCs? However 20HE is acting, it surely acts differently between males and females, which begs further investigation of the sex-specific underlying mechanisms that stimulate ISC mitoses.

Remarkably, short-term 20HE effects on the ISC mitoses remain transient because overnight withdrawal of 20HE was sufficient to regress ISC mitoses to basal levels in either sex. That is not typical of other pro-mitotic stimuli in the midgut that cause persistent ISC mitoses. Interestingly also, 20HE-induced mitoses plummet by 16-20 hrs after 20HE feeding but by 40 hrs of continuous exogenous feeding on 20HE, the ISC mitoses fall back to basal levels. Does that mean that females have developed the capacity to adapt to increased 20HE levels, thus protecting the ISCs from exhausting their ecdysone-responsive proliferative transcriptional network to limit over-proliferation?

Indeed, suggestive of the previous idea, long term exogenous 20HE feeding in mated females does not give an obvious advantage to dividing ISCs, and they divide at similar rates relative to age-matched controls. Consistent with this, ecdysone targets are known to autoregulate their expression, hence limiting the activation of their target genes[151]. Suggestive evidence to support this idea is the fact that 14 days 20HE-fed females do not have a transcriptional upregulation of their ecdysone-inducible targets in contrast to the transcriptional upregulation of the same targets observed as early as 6 hrs of 20HE feeding. In other earlier experiments I did, I observed that the transcriptional induction of the ecdysone-inducible targets was not as strong by 20 hrs of 20HE feeding (data not shown). Hence, 20HE appear to transiently upregulate its targets to cause ISC divisions in mated females.

Do males possess the same machinery to adapt and downsize the effects of prolonged 20HE exposure on ISC mitoses? Augmented ISC divisions accompanied by a strong induction of the ecdysone-inducible targets after 14 days of feeding males on exogenous 20HE dispute that males deploy the identical "20HE-female specific" mechanisms to limit over division of the ISCs. It is possible that such discrepancy occurs because male

ISCs do not have an evolutionary benefit in experiencing such high ecdysone levels. Indeed, this notion coincides with the male ISCs being quite resistant to stress responses[8,118,303].

Collectively, my findings identify the relevance of non-cell autonomous sex steroid signaling as a critical determinant of the mitotic ISC behavior, possibly acting through different effectors.

**b) Factors influencing sex genotypic traits and how could sex hormones possibly regulate them:**

There are several mechanisms with which the sexually different traits could be explained including the gonadal or sex-biased hormones. Hence, below, I concisely mention each mechanism and discuss the sex hormones factor more in depth since it is most relevant to my work. There are generally 4 mechanisms recently proposed to best explain the sex differences in the transcriptome and epigenome[417]. First is the sex biased gene expression between males and females in different tissues and across different developmental or environmental changes. This difference can be attributed to the difference in the sex chromosomes (X in males versus XX in females). Indeed, the X chromosome is enriched for sexually dimorphic genes. Of note, the relative change between female and male expression levels in sexually dimorphic genes is rather small[310]. The sex bias in differential gene expression often results in a higher predisposition to a certain disease, depending on the affected tissue. For example females have higher predisposition to autoimmune diseases, consistent with gene ontology enrichment for female-biased genes regulated by estrogen or linked to inflammation in gene expression data from the blood[418,419]. The study of 2,500 samples from 15 different human tissues and 9 different organs revealed differential expression between males and females in several tissues, including anterior cortex in the brain (1,818 genes), heart (375 genes), kidney (224 genes), colon (163 genes) and thyroid (163 genes). Most sexually dimorphic genes had a magnitude fold change <1 between males and females[420]. In *Drosophila*, sex differences in intestinal physiology and predisposition to tumors exist between males and females. Accordingly, sex biased gene expression between males and females exist too. 8.3% of all genes in the midgut display significant sexual dimorphism in gene expression[118]. Not

surprisingly, the genes cluster into distinct biological processes[118]. I also observed similar sex biased gene expression in ISCs of the midgut. In total (around 800 in ISCs from the 1305 genes detected from the whole midgut) genes are also differentially expressed between male and female ISCs.

Additionally, sex- biased splicing also contributes to sex differences in gene expression levels[421,422]. This adds a powerful layer of transcriptional complexity because nearly all genes in the genome undergo alternative splicing. 95% of the sex-biased spliced genes in the human genome reside on the autosomes and 50% of sex- biased spliced genes are associated with genetic diseases[423]. Importantly, even though hormones are known to regulate differential gene expression for example in the context of immunity[424], only 32% of the sexually dimorphic autosomal genes contain androgen or estrogen hormone response elements, suggesting that around two- thirds of the rest of the sexually dimorphic genes are not directly regulated by sex hormones[420]. Additionally, sex hormone receptors do not show sex-biased expression in most tissues, suggesting that the downstream sex-biased gene regulation is not solely explained by differences in mRNA levels of these receptors. Indeed, network analyses of gene regulation revealed extensive regulation by the sex hormone receptors and other non-steroid transcription factors, that drive the underlying sex differences in the gene regulatory networks[425]. Similarly, in the *Drosophila* ISC transcriptome, I do not find differences in the abundance of EcR mRNA between males and females, instead the differences are in some ecdysone pathway components that determine the amounts of 20HE within the cells[118] such as controlled transport by Oatp74D transporter[304] and activation by Shade enzyme[155]. This suggests that 20HE is tightly regulated systemically via its controlled production from the sex organs[300] and also locally within the midgut.

It remains an open question if the difference in 20HE levels between males and females contribute to the sex-biased differences in gene splicing. Of note, approximately 5.6% of the whole midgut transcriptome shows sex-biased isoform gene expression among which is Shade enzyme, that transforms ecdysone to its more active form 20HE[118,155].

The second mechanism, which could explain sex-biased gene expression, is the presence of genetically inherited variants that either influence RNA splicing and are termed splicing quantitative trait loci (sQTLs), or genetic variants that exert their effects through gene regulatory mechanisms and are termed expression quantitative trait loci

(eQTLs)[426,427]. Sexually-biased eQTLs may act in one sex but not the other or could be shared by both sexes but with larger effect in one sex over the other. Sex-biased eQTLs and sQTLs have not received so much attention in *Drosophila* or mammals yet, however, it is hypothesized that predisposition to sex-biased genetic disease could be due to accumulation of small effects across a broad range of variants[417]. The third mechanism is the underlying sex differences in the epigenome which include differentially methylated autosomal CpG sites[428,429]. Sex differences in chromatin accessibility result in sex-biased expression of genes. Sites with sex- specific chromatin accessibility are enriched for genes with sex- biased expression and eQTL genetic variants[427]. 20HE feeding may affect positive regulation of histone acetylation through the upregulation of the evolutionarily conserved histone acetyltransferase Atac2[430], which is involved in nucleosome remodeling[431]. Notably, the pattern of Atac2 expression displays a sex antagonistic relationship in males and females, that is, 20HE-feeding results in higher levels of Atac2 transcript in females but appears to show an opposite effect in males. Another histone acetylase Hcf is not detected in vehicle-fed control males yet it is increased in males after 20HE feeding[432]. This could suggest that 20HE exerts some of its actions indirectly through the modulation of chromatin accessibility of its target genes. It is known that Atac2 activity regulates ISC identity; its high levels cause the ISCs to directly differentiate without interfering with lineage specification and its low levels cause expansion of ISCs clusters[430]. Atac2 is also involved in coordinating cellular responses to stress through interactions with several kinases such as MAPKs, Msn, JNK[433,434]. What are Atac2 targets in the ISCs? Whether 20HE indeed regulates their functions or not is interesting to figure out. It would support the growing body of evidence that steroid hormones affect the epigenome through regulating histone deacetylases (HDACs)[139] and histone methyltransferases[141].

The fourth mechanism is the underlying sex differences in the gonadal sex hormones and its direct interaction with gene regulation. Growing evidence suggests that sexually dimorphic gene expression could be explained in part due to the interaction of hormone-regulated transcription factors such as FOXA and STAT5 with sex-biased histone modifications that lead to differential responsiveness to ligand-activated nuclear receptor signaling and distinct enrichments for functional gene categories between males and females[435,436]. This is in part caused by differences in hormone receptor binding, for

example: the effect of growth hormone (GH) signaling on the liver. GH is secreted by the pituitary gland in a highly pulsatile manner in males, while in females GH secretion is continual and it is considered as a major hormonal determinant of liver sex differences[436,438]. Accordingly, continuous growth hormone infusion causes feminization of the male-specific patterns of gene expression and inhibition of a vast majority of male-specific transcript patterns in the liver[437]. This is very interesting because it identifies the role of growth hormone, an extra-gonadal hormone that exhibits a sex-biased secretory pattern from the pituitary gland. Such example for hormonal regulation suggests that sexual dimorphism is not only limited to gonadal hormones but may also be determined by extra-gonadal hormones.

As intestinal ecdysone/EcR signaling is causing both male and female ISCs to divide and EcR is a nuclear receptor, which exerts its effects mainly through transcriptional regulation of target genes. I reasoned that the different circulating 20HE levels would lead to differential gene expression between males and females, partly through 20HE. Indeed, my primary analyses of the RNA seq dataset revealed the presence of sexually dimorphic genes in the transcriptome of the ISCs of the *Drosophila* midgut, a subset of which are regulated by 20HE feeding (75 genes/826 genes at p-value cut off of 0.05 and 103 genes at a p-value cut off of 0.1) (discussed more below). Notably, this is the first report of sexually dimorphic subset of genes in a specific cell type within a tissue in *Drosophila* (ISCs of the midgut) and also reporting changes upon 20HE feeding. The elegance of *Drosophila* genetics is that it gives us the ability to investigate particular subtypes of cells within a tissue in a way that is not yet possible in humans. Functional in-depth validation of the gene signatures I define as possibly regulated by 20HE will provide a mechanistic insight on the hormonal control of the genotypic sex trait that would, in part explain the underlying differences in ISC mitoses.

**Steroid-mediated regulation of metabolic function**

Differential gene expression between 20HE –fed and vehicle-fed males revealed that at least 20 of the 75 sexually dimorphic ISC transcripts regulated by 20HE are associated with metabolic functions[118]. Yet, the functions of many remain uncharacterized. Additionally, 20HE feeding in males resulted in upregulation of lipid and carbohydrate transcriptional signatures including digestive enzymes, transporters and metabolizing

enzymes in ISCs, all correlating with the amplified ISC divisions, possibly enhanced nutrient absorption that would result in the midgut growth. It is worth noting that increased 20HE levels in females are similarly reported to regulate glycogen and triglyceride levels through EcR signaling in the ovaries of mated flies, to maximize nutrient deposition in their fertilized eggs[123]. 20HE-fed males also have transcriptional upregulation of the insulin pathway components. Along this line of evidence, mammalian estrogen also increases the expression of insulin receptors in adipocytes and skeletal muscle via regulating the expression and translocation of glucose transporters. This increases glucose utilization, decreases lipid deposition preventing the development of obesity or insulin resistance[439,440]. Interestingly, from my RNA seq data, Lin-28, a highly expressed candidate of this insulin signature is involved in positively regulating symmetric ISC mitoses and nutrient-driven adaptive gut growth[309]. Similarly, the highly conserved mammalian Lin-28 is required for symmetric divisions in many stem cell and progenitor populations[441-443]. It does so partly through promoting sensitization to insulin, stimulating glucose uptake and metabolism, and oxidative phosphorylation[444,445]. Thus, it is defined as a central regulator of mammalian glucose metabolism. This implies that ecdysone might regulate insulin signaling, in part to satisfy the increased intestinal metabolic demands of the 20HE-fed males. Additionally, my results suggested that upd2 is preferentially regulated by 20HE in EBs, ECs and possibly in ISCs. Intriguingly, upd2 is known be a growth promoting factor and to have metabolic functions in the adult fly. Upd2 is secreted from the fat body to regulate insulin-like peptide secretion from the insulin-producing cells in the brain, to promote systemic growth and fat storage[446]. Upd2 is homologous to mammalian Leptin hormone, which is also secreted by adipose tissue, to act on its receptors in the brain to regulate energy homeostasis[447]. The differential regulation of upd2 by 20HE in the midgut signals could signal for a preferential nutrient uptake of more carbohydrate and lipids Does that also indirectly contribute to the "fed-state" of a fly?

Future studies on how 20HE affects metabolism in the midgut should prove very insightful.

### 3.10. Fecundity versus lifespan

Often fecundity and longevity appear to anti-correlate in females, and a common belief is

that this is due to limited resources, that need to be allocated either towards egg laying or towards repairing one's own tissues. However, it has been shown that fecundity and longevity can be uncoupled[166,448]. Furthermore, it has been shown that this balance in resource allocation does not fit with tracer experiments using stable isotope-labeled food[449]. This work argued that reproductive costs are not caused by resource allocation, but rather by indirect damage to the soma when reproduction is activated. Indeed, there is a growing body of evidence that suggests that gonadal steroid signaling activates lipid metabolism in the gut to regulate aging. Adult *Drosophila* flies lacking germline stem cells (GSCs) live 50 % longer than the controls[450]. The underlying mechanism suggesting that gonadal inputs could regulate aging and determine longevity may well be conserved. Also in mice, ovary transplantation from young females increases the life expectancy of the older female recipients[451]. Additionally, arrested germ cell proliferation also promotes longevity in *C.elegans*[452]. The underlying longevity effects require gonadal steroids from the somatic gonad that signal to the intestine and the nervous system of *C.elegans*[453,454]. In *C.elegans,* ecdysone equivalents, dafachronic acids (DA), are synthesized in the somatic gland via DAF-9/cytochrome P450 and other hydroxysteroid dehydrogenase enzymes, similar to the steroid-synthesizing enzymatic cascade in the *Drosophila* ovary. In the intestine, the DA receptor DAF-12, EcR paralog in *C.elegans* increases longevity in germline-ablated animals via regulating downstream target lipolytic genes expression[455], activating nuclear receptors to regulate the expression of stearoyl-CoA-Δ 9-desaturases and via promoting FOXO/DAF-16 nuclear localization in the intestine[456]. Notably, DA supplementation can restore longevity of the whole gonad-deficient worms lacking both germline and somatic gonad, which requires the presence of intestinal receptor DAF- 12[457]. In parallel, my results show that the activation of reproduction comes at the cost of increased dysplasia and tumor risk so also, strengthening this gonadal-gut axis regulation that determines the organism's lifespan. Intriguingly, human FOXO3 variants are also associated with longevity again suggesting that the regulatory mechanism is evolutionarily conserved [458,459].

My findings within this work thus contribute to the growing insight of the hormonal regulation on the intestine. I propose that active gonadal sex hormones render the gut more responsive to increased reproductive demands thereby, creating a trade-off between

satisfying reproductive demands and longevity in flies. This may be reminiscent of a conserved strategy in mammals where estrogens might have an initial advantage to the female gut functions, but over time accumulation of more estrogen metabolites contributes to inflammation and tumorigenesis of the GI tract. Given the evidence, I propose that the possible contribution of sex hormones to intestinal physiology deserves further investigation.

# Materials and Methods:

The text of the following section (**Materials and Methods**) has been taken from (Ahmed et al., 2020) and has been originally written by myself:

Fly stocks and cultures

*Drosophila melanogaster* were raised on standard media and maintained in incubators with controlled temperature and humidity on a 12 h light/dark cycle. Flies were transferred to fresh vials every 2 days. Male and female *Drosophila* were raised mated for all experiments, unless indicated otherwise. $w^{1118}$ (VDRC #60000) flies were typically used as wild-type controls and y w[1118];P{attP,y[+],w[3`] (VDRC #60100) were used as wild-type controls for KK RNAi lines.

Gal4 driver lines:

$esg^{ts}$: y,w; esg-Gal4/Cyo; tub-Gal80ts UAS-GFP/TM6B [5]

$esg^{ts}$ F/O: w; esg-Gal4 tub-Gal80ts UAS-GFP/Cyo; UAS-flp, act>CD2>Gal4/TM6B [41]

$esg^{ts}$ Su(H)-Gal80: esg-Gal4, UAS-2XEYFP; Su(H)GBE-Gal80 tub-$Gal80^{ts}$ (Gift from Steven Hou)

Su(H)-$GBE^{ts}$: Su(H)GBE-Gal4,UAS-CD8-GFP/CyO; tub-$Gal80^{ts}$/TM6B

$MyoIA^{ts}$: w; Myo1A-Gal4NP0001/CyO; tub-$Gal80^{ts}$, UAS-GFP/TM6B

$pros^{ts}$: w;tub-Gal80ts,UAS-GFP/CyO,wglacZ;Prosv1-Gal4

$tub^{ts}$: tub-Gal4; tub$Gal80^{ts}$/TM3, ser (Gift from Valeria Cavaliere's lab)

$how^{ts}$: how-Gal4; tub$Gal80^{ts}$

$elav^{ts}$: Elav-Gal4, UAS-GFP/FM7C;+; Tub-Gal80TS/TM2Ubx

$C587^{ts}$: c587-Gal4; tubGAL$80^{ts}$

UAS transgenes:

UAS-Eip75B on II (kindly provided by Henry Krause, University of Toronto, Canada)

UAS-Hr3 on III (kindly provided by Henry Krause, University of Toronto, Canada)

UAS-EcR.A.F645A (BDSC 9452)

UAS-EcR.A.W650A (BDSC 9451)

UAS-EcR.B1-ΔC655.W650A (BDSC 6872)

UAS-TraF (kindly provided by Irene Miguel-Aliaga)

RNAi stocks:

UAS-EcR $^{RNAi}$ (VDRC GD 37059, BDSC 29374 TRiP JF02538)

UAS-Usp$^{RNAi}$ (VDRC GD 16893 and BDSC 27258)

UAS-tra$^{RNAi}$ (BL:2851 kindly provided by Irene Miguel-Aliaga)

UAS-Eip75B$^{RNAi}$ (VDRC GD 44851 and BDSC 35780, TRiP.HMS01530)

UAS-Hr3$^{RNAi}$ (VDRC GD 12044, BDSC 27253, TRiP.JF02542, and NIG 12208R-2)

UAS-Spo$^{RNAi}$ (BDSC 51496, spok RNAi 2A2;2A3 kindly provided by Michael O'Connor)

UAS-Dib$^{RNAi}$ (v101117 kindly provided by Michael O'Connor)

UAS-Br$^{RNAi}$ (KK 104648)

UAS-Notch$^{RNAi}$ (VDRC GD 27228)

UAS-Upd2$^{RNAi}$ (TRIP 33988, HMS00948)

UAS-Upd3$^{RNAi\ 460}$

UAS-Rho$^{RNAi}$ (TRIP 41699)

UAS-string$^{RNAi}$ (NIG 1395R-1)

UAS-Egfr$^{RNAi}$ (TRIP 31183)

UAS-met$^{RNAi}$ (KK100638, TRIP 26205)

UAS-gce$^{RNAi}$ (TRIP 26323)

MARCM stocks:

MARCM 80B yw hs-flp1.22 tub-Gal4 UAS-GFP(NLS); +; tub-Gal80 FRT80B/TM6B

FRT 80B: W; [neoFRT]80B/TM6B,sb1

Eip75B$^{\Delta 51}$ FRT 80B: Eip75B$^{\Delta 51}$P[neoFRT]80B ry506 (recombinant #1)/TM3.sb in Fig ED 3b,c (kindly provided by, Elizabeth T.Ables East Carolina University School of Biology, North Carolina, USA).

Eip75B$^{\Delta 51}$ FRT 80B: Eip75B$^{\Delta 51}$P[neoFRT]80B/TM3.sb in ED Fig 16c (kindly provided by Yijie Li, Johns Hopkins University School of Medicine, Baltimore, USA)

Reporter lines:

w$^{1118}$; hs-GAL4-DHR3.LBD.HA; UAS-Stinger (BDSC 28868)

w$^{1118}$; UAS-Stinger; hs-GAL4-EcR.LBD (BDSC 28863)

w$^{1118}$; UAS-Stinger; hs-GAL4-Usp.LBD (BDSC 28864)

w$^{1118}$; P{10XStat92E-GFP}1 (BDSC 26197)

w$^{1118}$; P{10XStat92E-GFP}1 (BDSC 26198)

IF/CyO; Upd3.1 LacZ/TM6B

Gbet Su(H)-lacZ/x

Delta05151/tm3.sb

Mutant stocks:

w* upd2Δ (BDSC 55727)

w* upd2Δ upd3Δ (BDSC 55729)

w* upd3Δ (BDSC 55728)

Dmspo$^{Z339}$ (Kindly provided by Michael O'Connor)

spo$^{1}$ st$^{1}$ e$^{1}$/TM3, Sb1 (BDSC 3276)

Deficiency stocks:

w[1118]; Df(3L)Exel6105, P{w[+mC]=XP-U}yorkExel6105/TM6B, Tb[1] Bloomington #7584

w[1118]; Df(3L)BSC387/TM6C, Sb[1] cu[1] ] Bloomington #24411

Drosophila husbandry

For transgene expression using the Gal4/Gal80$^{ts}$ system, experimental crosses were maintained at 18°C (permissive temperature for GAL80$^{ts}$) in standard medium. Animals of the desired sex and genotype were collected within 48h of eclosion and aged for an average of 5 days before shifting to 29°C (restrictive temperature for GAL80$^{ts}$) to induce UAS transgene expression. Adult midguts were dissected after different periods of time as indicated in on top of each figure panel. The esg-Flip-Out system (esgF/O$^{ts}$)[41] and the MARCM system[285] were used to generate ISC-derived clones. Flies were aged for 3-6 days after eclosion before clonal induction by temperature shift to 29°C for esg-FO clones or heat-shock for MARCM clones. Additional details on transgene expression times are indicated in the corresponding figure legends. MARCM 80B flies were heat shocked for 45-60 min in a 37°C water bath, and then aged for 12 days at 29°C before overnight treatment with vehicle, 5mM 20HE or *Psuedomonas entomophila (P.e.).*

Mating experiments

At least 10-15 virgin females for each genotype were collected at 18$^{o}$C as they emerged. They were aged for ~5 days and then shifted to 29$^{o}$C until the time points indicated in each figure panel. At the start of mating, females were transferred to fresh vials and allowed to mate with equal numbers of adult 3-7 days old wild type $w^{1118}$ males, devoid of any transgenes, at 25$^{o}$C, for optimal fecundity. Time when males were introduced to females in the same vial is denoted as t0. If indicated as mated once, then after 18-20 hours, the males were removed and the females were flipped into fresh vials every 48 hours until the indicated time in the respective figure panels. Otherwise, males were left together with the females for the following time points: 24 hours, 37-40 hours, 46-48 hours or 72-74 hours.

GAL4-LBD 'ligand sensor' system

Adult flies with bipartite detection system consisting of the LBD of the Drosophila nuclear receptor (NR) fused to the DNA-binding domain of yeast GAL4, along with a GAL4 UAS-controlled GFP reporter gene were used as previously described[186,288]. Flies were raised and maintained at 25°C. For visualization of ligand sensor patterns, 5-7 day-old mated females were starved for 2-4h, heat-treated for 30 min in a 37°C water bath only once for EcR, Usp and Hr3 reporters, and allowed to recover at room temperature for 15 minutes. Then, flies were transferred to vials containing a fresh feeding vial (see Feeding Experiments) and kept at 25 °C for 16-18 hrs until dissection.

In vivo 10XSTAT92E-GFP reporter system:

Adult mated female flies of the genetic background 10XSTAT92E-GFP that have 10 Stat92E binding sites driving GFP expression were aged for 5-7 days and treated for 6hrs with 5mM 20HE and for 16-18 hrs with 5mM 20HE or *P.e.* infection.

In vivo Upd3 lacZ reporter:

Adult mated female flies of the genetic background Upd3.1 LacZ/TM6B were aged for 5-7 days and treated for 16-18 hrs with 5mM 20HE or *P.e.* infection.

Overnight Feeding Experiments

For all experiments except 20HE/SDS feeding (as indicated in the fig panel), flies were fed for 16-20 hrs, then dissected to remove the intestines, which were analyzed using immunofluorescence and confocal imaging. For 20HE feeding, flies were fed as early as 4 hrs , then 6, 9, 12, 16 hrs and as late as 22 hrs. We observed a window of strong mitotic response at 6 hrs and again at 16-18 hrs that persisted to 22 hrs after exposing the flies to the 20HE feeding solution.

For 20HE removal experiments, flies were fed overnight (O/N) for 16-18hrs with 5mM 20HE, and then transferred to a fresh vial for another O/N treatment after which the midguts were dissected and stained.

20-hydroxy-ecdysone (20HE) feeding: 10-15 adult male, mated female, or virgin female flies were used for the ecdysone feeding experiments, as indicated. 20HE was weighed out of the supplier's vial and was first dissolved in 100% ethanol. Water was then added to make up a 25mM stock solution in 10% ethanol. 25mM 20HE stocks were stored at -20$^{o}$C. A final concentration of 0.25-10 mM ecdysone or 2% ethanol (as control) was used for the feeding experiments as indicated. 200µL of 5% sucrose solution, 5 mg/ 1mL dry yeast + 5mM 20HE (Sigma-Aldrich H5142) mix was deposited on top of a standard food vial to which flies were transferred. If the experiment required *P.e.* infection, then 400 µL of the same yeast/sucrose mix (described above) was deposited on filter-paper discs (Whatmann) to which flies were being transferred. The sucrose yeast mix with 2% ethanol was used as vehicle treatment.

Detergent treatment: flies were left to feed on yeast sucrose solution (described above) with 0.1% or 1% SDS for 18-20h or at the times indicated.

Enteric *P.e.* infection: A 25 mL pre-culture was started the first day by inoculating *Pseudomonas entomophila* (*P.e.*) bacteria from glycerol stocks (stored at -80°C) in Rifampicin-supplemented Luria Broth (LB; final antibiotic concentration: 100 µg /mL). The pre-culture was grown overnight at 29°C, shaking at 130 rpm. Next day, the pre-culture was diluted in 175 mL Rifampicin supplemented LB and the culture was again grown overnight at 29°C, shaking at 130 rpm. After the growth of the bacterial culture reached optical density (O.D) ≈ 0.5, the culture was spun down at 2500 g for 25 min at 4°C and the pellet was re-suspended in 3 mL of 5% sucrose + 150 µL yeast. Prior to infection, flies were starved for 2 hrs (optional step), and then placed in vials with 500 µL of this *P.e.* solution or 5% sucrose with yeast as the control vehicle.

Other treatments include feeding with 2.5mM Paraquat , Nω-Nitro-L-arginine methyl ester hydrochloride (Sigma-Aldrich, N5751) (200 mM L-NAME stock solution in distilled water; final 10mM concentration was used), (±)-S-Nitroso-N-acetylpenicillamine (Sigma-Aldrich, N3398) (500 mM SNAP stock solution in 10% ethanol and 10mM SNAP final solution was used), Hemin (Frontier Scientific, H651-9) (2 mM stock solution dissolved in 0.1M NaOH, pH adjusted to 7 with sodium phosphate buffer and 0.5 mM final solution was immediately used) and their corresponding vehicle. Treatments were diluted in 400 µL total volume of 5% sucrose and 5 mg/1 mL yeast then added vials containing a fresh feeding paper.

Long term ecdysone feeding

At least 10-15 adult male and/or female flies were transferred to standard fresh food vials (2.5 cm diameter) containing circa 3 mL of food. To prepare ecdysone treated food, the food in the vial was scraped on the surface and 200 µL 1mM 20HE, 22 mg/mL yeast in 5% sucrose solution was added. After 15 minutes, this solution diffused into the food. Flies were added to these vials and flipped into fresh 20HE containing vials every 48 hrs for 14 days unless otherwise indicated. As vehicle, vials with fly media containing 200 µL 0.43% ethanol in sucrose/yeast solution were used. Flies were dissected to remove the intestines, which were analyzed using immunofluorescence and confocal imaging. For the flies raised on low nutrient food, flies were fed with 1mM 20HE, 5 mg/mL yeast in 5% sucrose solution that was deposited on filter-paper discs (Whatmann) and exchanged every 24-30 hrs. For *P.e.* infection after long-term 20HE feeding, I discontinued feeding the flies on ecdysone-containing food for one day before the flies were fed with the *P.e.* bacterial solution.

Fecundity assays

At max 10-15 virgin females for each genotype/replicate were collected at 18$^{o}$C as they eclosed, and pooled in one vial. For each genotype 3-4 replicates were performed. Virgins were aged one day and then shifted to 29$^{o}$C to activate Gal4. Females were then transferred to fresh cages and allowed to mate with equal numbers of $w^{1118}$ males. Females were housed in groups of 7-10 with equal number of males for this experiment.

Standard Drosophila media was poured in 5 cm plates and stored at 4$^{o}$C. Flies in each egg collection cage were flipped onto fresh food plates every 24-48 hours for the indicated number of days, the number of eggs/replicate were scored and averaged over the number of flies in each cage. 3-4 replicates were pooled for each genotype.

Virgins were aged 8 days at shifted 29$^{o}$C to activate Gal4 first before mating to equal number of males. Females were housed in groups of 7-10 with equal number of males for this experiment. Flies in each egg collection cage were flipped onto fresh food plates every 24-48 hours for the indicated number of days, the number of eggs/replicate were scored and averaged over the number of flies in each cage.

Virgins were aged one day and then shifted to 29$^{o}$C to activate Gal4. Females were then transferred to fresh vials and allowed to mate with equal numbers of $w^{1118}$ males. All subjects were housed overnight in the same vial to ensure mating success and numbers of eggs were counted and averaged for the number of females/vial. Next day, every female/male pair was separated and individual female/vial were followed up for 14 days. Vials were exchanged every 24-48 hours in this experiment and total number of eggs laid/2 days was counted for every female fly.

A 3 day sum was calculated from the average number of eggs/fly laid every day, then an average sum of eggs laid/fly/3 days across the replicates was plotted with error bars ± confidence intervals (c.i.). Alternatively, the average/individual cumulative numbers of eggs were summed up and mean values were plotted with error bars ± standard deviation (s.d.). To test statistical significance for each day (source data), Two-sample unequal variance t-test were performed, with a two-tailed distribution assuming unequal variance for test genotype relative to control at every time point. Alternatively, general linear models (GLMs) with binomial errors were used to examine the effect of the genotype on the average cumulative number of eggs.

*spo* mutant rescue experiment

Males of either deficiency backgrounds BM#7584 or BM#24411 were crossed to heterozygous *spo* mutant virgins and allowed to lay eggs on apple plates for several days prior to the experiment. 2 deficiency genotypes were used to increase the likelihood to getting rescued homozygous spo mutant flies. On the day of the experiment, the parents were left to lay eggs for 4 hours then, were removed. The eggs were allowed to age 4-6

hours at 25ºC then, were all pooled in a sieve and de-chorionated by bleach. After washing in PBS-T, the de-chorionated embryos were incubated in PBS-T supplemented with 100 µM 20E for 3 hours. The embryos were covered with Halocarbon 27 *Oil and incubated at 18ºC overnight. Over the next 2 days,* homozygous spo embryos were selected under a fluorescent stereoscope by the lack of GFP expression in the hatched larvae. The phenotypically correct larvae were collected in fresh food vials at the density of 40-60 larvae/vial and allowed to develop at 25ºC until eclosion and selection of virgin or mated homozygous spo mutant flies.

Lifespan assays

Males and females of the genotype 5961GS EcR A DN were allowed to mate for 48hrs then were isolated in groups of 25 flies of the same sex/vial. For RU486 food supplementation, 100 µl of a 5 mg/ml solution of RU486 or vehicle (ethanol 80%) were deposited on top of a food vial and dried for at least 4-6 hours, resulting in a 0.2 mg/ml concentration of RU486 in the food accessible to flies. Flies were flipped every 48hrs into a fresh vial. Dead flies were visually identified (flies not moving, not responding to mechanical stimulation and laying on their side or back were deemed dead), and the number of dead flies was recorded. Oasis software was used for data analysis[461]. Logrank non-parametric test was performed by the software and the p values were derived from pairwise comparison with Bonferroni correction as displayed in ED 10 g-h.

FACS sorting of ISCs:

C587$^{ts}$ mira-GFP on chromosome II progeny were collected and aged 7-9 days at 18 degrees then shifted at 29 degrees in groups of 60. (so, 30 males and 30 females/vial). 350 µL of 1mM ecdysone or 10% ethanol are supplied to the flies daily for 15 days till sequencing date.

FACS sorting protocol is adopted from Dutta et al, 2015.

Midguts were dissected in in nuclease/RNAse free 1xPBS (80-100 midguts per sample) then transferred to 1.5 ml eppis with 450 µl nuclease/RNAse free 1xPBS on ice. 100uL elastase (0.4% w/v stock solution kept at -20°C) was added. This was incubated for 1.5 hour at 27°C (300 rpm only the last 30 minutes) and the tube flicked every 10 mins.

Then,centrifuged at 2500 rpm for 12 mins. The supernatant was discarded without letting the pellet dry and fresh 500 µl nuclease/RNAse free 1xPBS was added. Propidium Iodide (PI) 1:1000 to stain dead cells. Then,cell suspension was pipetted onto blue cap of FACS tubes and gently tapped to help flow through. (RNAse free) 1.5 ml eppis with 250 µl Extraction Buffer was prepared for FACS sorting and RNA was extracted and sent for sequencing. The kit for RNA extraction used was Arcturus PicoPure RNA isolation kit (Applied Biosystems) according to the manufacturer's instructions.

Sequencing:

Library prep (done by DKFZ core facility) using SMARTer® Ultra® Low Input RNA Kit for Sequencing (Clontech Laboratories, Inc.) and Low Input Library Prep Kit (Clontech Laboratories, Inc. ) . Ultra Low RNA Seq was carried out using HiSeq V4 SR50 sequencer. Total RNA was sequenced.

Sequencing analysis: The FASTA files were aligned to the Drosophila transcriptome as follows: Adaptor-trimmed reads were mapped to a file containing coding sequences of combined *Dmel* transcripts and filtered for only uniquely mapping reads . Unique *Dmel* reads were re-mapped to the transcriptome *Dmel* release 6.02 genome using STAR (Spliced Transcripts Alignment to a Reference) Aligner on the galaxy.org server with the following settings: single-end reads. The mapped.bam alignment files were then assessed for their strandedness and counted with featurecounts on the Galaxy server. Single alignment was ensured and the percentage of reads mapped to multiple loci for every sample was 0%. The percentage of uniquely mapped reads for each sample was around 80%. All hits were filtered for >10 reads and normalized for the total number of reads aligned. Afterwards, differentially expressed genes were determined using edgeR on the count data files.

edgeR differential expression: count files were imported into the compaRNA function of the Husar Platform with the following parameters: P-Value Threshold for EdgeR 5.0e-2. The results were imported to excel, 0.05 p value was set as a cut-off for enriched hits in any sample, then -log10(p values) were calculated. The enriched hits were imported to Flymine v49 2020. Gene Ontology Enrichment or Pathway Enrichment widgets were used to compare hits against the background of my aligned reads filtered for reads>10,

max p-value was set to 0.05. Homologues were retrieved from Mouse or Human Mines and similarly Gene Ontology Enrichment or Pathway Enrichment widgets were used.
The sexually dimorphic hits were determined in reference to the supplementary table of Hudry et al,2016 list of sexually dimorphic genes.
The set of similar hits between 20HE fed males and vehicle fed females were determined by comparing the lists of genes that are differentially expressed between males and females and the list of genes that are differentially expressed between 20HE fed males and females (a p-value cut off of 0.05 or 0.1) and have more than 10 total reads. Through a series of vlookup functions, the list of genes that are different between males and females but are no longer different between 20HE fed males and females are the list of genes presented in 2.7.6 and table 2.4. Those hits reflect genes that are becoming "more similar to vehicle females" after 20HE feeding.

Immunohistochemistry and microscopy

*Drosophila* adult midguts were dissected in 1x phosphate-buffered saline (PBS) and fixed with 4% paraformaldehyde for 30 min at room temperature (RT). For all immune-stainings except anti-dpErk, samples were washed with 0.015% Triton-X in PBS thrice at RT, then permeabilized with 0.15% Triton-X in PBS for 15 min at RT with shaking. Then, samples were re-washed and blocked in PBS with 2.5% BSA, 10% normal goat serum and 0.1% Tween-20 (blocking solution) for at least 1hr at RT. Midguts were incubated with primary antibody at 4 °C overnight at the following dilutions: chicken anti-GFP (Life Technologies/Molecular probes, 1:500); rabbit anti-phospho-Histone 3 (Merck Millipore 1:1000); mouse anti-phospho-Histone 3 (Cell Signaling, 1:1000); guinea pig anti-GFP (Teleman Lab, 1:1000); chicken anti-□-galactosidase (Abcam, 1:1000).
For the dpErk detection, samples were fixed in 4% paraformaldehyde, dehydrated for 5 min in 50%, 75%, 87.5%, and 100% methanol, and rehydrated for 5 min in 50%, 25%, and 12.5% methanol in PBST (0.1% Triton X-100 in 1×PBS). After washing in 1×PBST, midguts were blocked in PBS with 2.5% BSA, 10% normal goat serum and 0.1% Tween-20 (Blocking solution) for at least 1hr at RT then incubated with rabbit phospho-p44/42 MAPK (Erk1/2) (Thr202/Tyr204) #9101 (Cell Signaling, 1:400) at 4 °C overnight.

After washing, all samples were incubated with secondary antibodies (Alexa 488, 568 or 633, Invitrogen) >2 hours at RT at a dilution of 1:1000. All antibody incubations were performed in blocking solution. DNA was stained with 0.5 µg/mL DAPI (Sigma).

For the plasma membrane cell stain: Freshly dissected midguts were stained with CellMask™ deep red plasma membrane stain, Thermofisher® in 1x PBS at a concentration of 1:1000 then fixed in 4% formaldehyde and stained with 1x PBS/DAPI according to the manufacturer's instructions.

Ovary staining: One day old mated females have been place on active yeast paste for 4-5 days at 29°c. Ovary have been dissected in dPBS, transfer in PBS, PFA8% and fixed for 10min at room temperature under mixing. After washes in PBS triton 0.15% the ovaries have been blocked for 1 hour in PBST0.15%, BSA 2,5%. The primary antibodies incubated at 4°c overnight in blocking buffer: chicken anti-GFP 1/500, mouse anti-coracle 1/500 (http://dshb.biology.uiowa.edu/C566-9_2). Then the ovaries have been washed 5 times 5 minutes in PBS T0.15% and incubated 1h30 with the secondary antibodies +dyes in blocking buffer at room temperature: Goat anti-chicken488 1/1000, Goat anti- Mouse568 1/1000, Hoechst 1/1000, phalloidine633 1/10000 . After two washes of 10min in PBST0.15%, the ovaries have been mounted between slide and coverslip in Vectashield. Images have been acquired using a Leica Sp8 confocal microscope and the figures made using Fiji with the ScientiFig plugin.

Imaging: Midguts were mounted on glass slides in VectaShield (Linaris®). All midgut images were acquired on a Leica TCS SP5II inverted confocal microscope, equipped with HCX Plan APO 20x/1.30 glycerol-immersion (for quantifications) or 40x/1.30 oil-immersion objectives (for representative images/ quantifications), using Leica Application Suite (LAS) AF software and processed with Fiji/ImageJ software[462]. Representative images are shown. GFP, in green (native GFP for all genotypes except for the reporter midguts and *Su(H)*+ cells marked with $Su(H)^{ts}$ driver that were additionally stained with GFP for better visualization of the signal); DNA: DAPI, in blue. For displaying images in the figure panels, a Z-stack of defined steps for control and test genotypes in a single field was acquired in the R4 region (a region which is bounded by the apex of the midgut tube's most distal 180° turn) as described in[463]. Images represent maximal intensity projections of the acquired Z-Stacks. Scale bars are 100 µm in all images, unless otherwise indicated.

Quantifications and statistics

ISC proliferation: Mitotic indices were determined by manually counting all PH3 positive cells in entire midguts using Leica DM5000B or Zeiss Axiophot fluorescence microscopes through a 40x objective. Statistical analysis of all the mitotic counts was performed using two-tailed Mann-Whitney test (ns $p > 0.05$,*$p \leq 0.05$,**$p \leq 0.01$,***$p \leq 0.001$,****$p \leq 0.0001$). All dot plot graphs indicating mitoses are showing mean values ± s.d. Exact p values are provided in a table in the supplemental material. Data were plotted from at least 3 independent experiments.

Quantification of the $GFP^+$/$delta^+$ cells: Z-stacks of both epithelial sides in R4a/b region were imaged at steps of 5.0 μm at 40x then the total number of $GFP^+$ or $delta^+$ cells were analyzed after limiting the particle size to 10-250 μm, circularity 0.00-1.00 and excluding holes after maximal Z-projects have been applied.

Quantification of the delta+ and Su(H)+ cells: Z-stacks of both epithelial sides in the R4a/b region were imaged by confocal Zeiss LSM 780 Spinning Disc. The total number of DAPI+, Su(H)+ and delta+ cells were automatically segmented and counted by a designed Image J/FIJI macro. Su(H)+ and delta+ cells were manually recounted and verified and the numbers of each cell type were recorded to derive %cell type to total cell number/stack.

Quantification of cell size: Midguts were mounted as previously described and Z-stacks of both epithelial sides in the R4a/b were imaged at steps 5.0 μm at 40x then an Image J/FIJI macro was created to segment the cytoplasm in reference to DAPI nuclear stain and internuclear distances. Area of the cells in $\mu m^2$ were outputted to Microsoft Excel and a mixed effects 2-way ANOVA statistical model was computed to calculate the significance between the different conditions.

Quantification of clonal size: Z-stacks of both epithelial sides in the R4a/b were imaged at steps 5.0 μm at 40x then an Image J/FIJI macro was designed to semi-automatically segment and determine the location and size of the GFP+ clones then the sizes in $\mu m^2$

were outputted to Microsoft Excel and a mixed effects 2-way ANOVA statistical model was computed to calculate the significance between the different conditions.

Quantification of the $GFP^+$ areas: For analysis of the mating effects, Z-stacks of both epithelial sides in R4a/b region were imaged at steps 5.0 µm either at 40x or at 20xs. For analysis, the quantification of the area occupied by $GFP^+$ cells was performed automatically using an ImageJ / FIJI macro. The macro created maximum Z-Projection of image stacks, median and gaussian filtering, automatic thresholding and measurement of $GFP^+$ and gut occupying area. The measurements were exported to Microsoft Excel and the $GFP^+$ / gut area ratio was derived from these values for at least 10 midguts for most experiments.

Quantification of the $GFP^+$ area/ $DAPI^+$ cells: For analysis of the tumor effects (ED 10e), a fixed median filter was created for each stack, a fixed gaussian blur value was applied then the midgut was thresholded for the $DAPI^+$ cells and $GFP^+$ cells then areas for both have been calculated and a ratio was derived. An Image J/FIJI macro was used.

Data are displayed in scatter plots with the mean values ± standard deviation (s.d.) for each series of experiments. Data shown are representative of at least 2-3 independent repeated experiments with similar results. Statistical significance was calculated either by two-tailed Mann-Whitney test without a multiple comparison test. Results were considered to be significantly different at $p<0.05$. All calculations were performed using the Prism 7.0 software (GraphPad Software, La Jolla, CA, USA).

Gut measurements: After immunofluorescence staining and prior to mounting, midguts were put on a glass slide and imaged using a Leica M205 FA Stereo Microscope or Stereo Discovery.V8, unmounted guts were imaged at a defined magnification and these images were exported to Fiji for further analysis. An Image J/FIJI macro was designed to threshold each image then measure the area of every midgut and with the distance mapping technique, the midgut length was derived. For the width measurements, a line was drawn. Before quantifying any midgut dimensions, the genotype of each sample was concealed. Samples were randomly analyzed then the genotype was revealed only after

completing analysis. For statistical analyses of gut sizes, normality test was performed with Shaprio-Wilk normality test and the gut sizes showed normal Gaussian distribution. Thus, statistical significance of gut size measurements was calculated by ordinary ANOVA test, followed by Bonferroni's multiple comparisons test. P values were calculated as follows: (ns $p > 0.05$,*$p \leq 0.05$,**$p \leq 0.01$,***$p \leq 0.001$,****$p \leq 0.0001$). Data are displayed in scatter plots with the mean values ± standard deviation (s.d.). Data were plotted from at least 3 independent repeated experiments with similar results.

All Image J/FIJI macros are available as supplementary online source material, or upon request from the authors.

Sample sizes, Randomization, and Blinding

No statistical method was used to predetermine sample sizes, but typically between 5 and 20 flies were used per replicate per genotype in each experiment. Exact n values for each experiment can be found in the online source data. When selecting animals for an experiment, the parental genotype was not concealed because it was required to select pertinent progeny. Animals were first selected by genotype and then randomly chosen for experimental analysis. For measurements of mitoses/gut, gut sizes and tumor frequencies, the genotype of each sample was concealed during analysis. Samples were then randomly scored and genotypes were revealed only after completing the analysis.

RT-qPCR

10–12 female intestines per genotype were dissected and RNA isolated using the RNAeasy kit (QIAGEN). 750 ng of total RNA was used for cDNA synthesis reactions using the QuantiTect reverse transcription kit (QIAGEN). RT-qPCR was performed on a Light Cycler 480 II (Roche) using SYBR Green I (Roche). Experiments were performed in at least biological triplicates. Relative fold differences in expression level of target genes were calculated as ratios to the mean of the reference genes rp49 and tubulin using the ΔΔCt method. A series of 10-fold dilutions of an external standard was used in each run to produce a standard curve. Primer sequences are listed in the online Supplementary Information.

ΔΔCt method: ΔΔCt (or log2 fold change) is the difference in threshold cycles for the test and control sample normalized to the threshold cycles for the reference gene.

$\Delta\Delta C_t = \Delta C_t$ (test)$- \Delta C_t$ (control)

$\Delta C_t$ (test) or $\Delta C_t$ (control) = $C_t$ target gene $- C_t$ reference gene

All data are presented as mean fold change ($\log_2$ ) with s.d.

RT-qPCR primers

Rp49 –Forward:TCGATATGCTAAGCTGTC

Rp49–Reverse:GGCATCAGATACTGTCCCTTG

β-tubulin-Forward: ACATCCCGCCCCGTGGTC

β-tubulin-Reverse: AGAAAGCCTTGCGCCTGAACATAG

Actin5C-Forward: CTCGCCACTTGCGTTTACAGT

Actin5C- Reverse: TCCATATCGTCCCAGTTGGTC

Rho-Forward: ATCGGCTTTCTGGTGCTAAA

Rho-Reverse: GTGCAACAGATGCTGGGTAA

Eip75-Forward: AACTGCACCACCACTTGACA

Eip75-Reverse: TTCTTCTCGTTGCCCGACTC

spi- Forward: CCTTCTATTTGCGCTTCGAG

spi- Reverse: CGCATGTGGTAGGGTAGCTT

krn- Forward: CGTGTTTGGCAACAACAAGT

krn- Reverse: TGTGGCAATGCAGTTTAAGG

Upd2- Forward: CACAAGTGCGGTGAAGCTAA

Upd2- Reverse: GGCTCTTCTGCTGATCCTTG

Upd3- Forward: CCACAGTGAGCACCAAGACT

Upd3- Reverse: GCGAAGGTTCAACTGTTTGCT

Socs36E- Forward: CAGTCAGCAATATGTTGTCG

Socs36E- Reverse: ACTTGCAGCATCGTCGCTTC

Spo-Forward: TCCGCGAGGTGCTCAATCAA

Spo-Reverse: CGCTCGCCACCAAATAGTTT

# References:


1 Pitsouli, C., Apidianakis, Y. & Perrimon, N. Homeostasis in Infected Epithelia: Stem Cells Take the Lead. *Cell Host & Microbe* **6**, 301-307, doi:https://doi.org/10.1016/j.chom.2009.10.001 (2009).

2 Marianes, A. & Spradling, A. C. Physiological and stem cell compartmentalization within the Drosophila midgut. *eLife* **2**, e00886, doi:10.7554/eLife.00886 (2013).

3 Buchon, N. *et al.* Morphological and Molecular Characterization of Adult Midgut Compartmentalization in Drosophila. *Cell Reports* **3**, 1725-1738, doi:https://doi.org/10.1016/j.celrep.2013.04.001 (2013).

4 Barker, N. *et al.* Identification of stem cells in small intestine and colon by marker gene Lgr5. *Nature* **449**, 1003-1007, doi:10.1038/nature06196 (2007).

5 Micchelli, C. A. & Perrimon, N. Evidence that stem cells reside in the adult Drosophila midgut epithelium. *Nature* **439**, 475-479, doi:10.1038/nature04371 (2006).

6 Spit, M., Koo, B.-K. & Maurice, M. M. Tales from the crypt: intestinal niche signals in tissue renewal, plasticity and cancer. *Open Biology* **8**, 180120, doi:doi:10.1098/rsob.180120 (2018).

7 Kux, K. & Pitsouli, C. Tissue communication in regenerative inflammatory signaling: lessons from the fly gut. *Frontiers in Cellular and Infection Microbiology* **4**, doi:10.3389/fcimb.2014.00049 (2014).

8 Jiang, H. *et al.* Cytokine/Jak/Stat signaling mediates regeneration and homeostasis in the Drosophila midgut. *Cell* **137**, 1343-1355, doi:10.1016/j.cell.2009.05.014 (2009).

9 Beumer, J. & Clevers, H. Regulation and plasticity of intestinal stem cells during homeostasis and regeneration. *Development (Cambridge, England)* **143**, 3639-3649, doi:10.1242/dev.133132 (2016).

10 O'Brien, L. E., Soliman, S. S., Li, X. & Bilder, D. Altered modes of stem cell division drive adaptive intestinal growth. *Cell* **147**, 603-614, doi:10.1016/j.cell.2011.08.048 (2011).

11 Kolahgar, G. *et al.* Cell Competition Modifies Adult Stem Cell and Tissue Population Dynamics in a JAK-STAT-Dependent Manner. *Developmental Cell* **34**, 297-309, doi:https://doi.org/10.1016/j.devcel.2015.06.010 (2015).

12 de Navascues, J. *et al.* Drosophila midgut homeostasis involves neutral competition between symmetrically dividing intestinal stem cells. *The EMBO journal* **31**, 2473-2485, doi:10.1038/emboj.2012.106 (2012).

13 Miguel-Aliaga, I., Jasper, H. & Lemaitre, B. Anatomy and Physiology of the Digestive Tract of Drosophila melanogaster. *Genetics* **210**, 357-396, doi:10.1534/genetics.118.300224 (2018).

14 Lucchetta, E. M. & Ohlstein, B. Amitosis of Polyploid Cells Regenerates Functional Stem Cells in the Drosophila Intestine. *Cell Stem Cell* **20**, 609-620.e606, doi:https://doi.org/10.1016/j.stem.2017.02.012 (2017).

15 Barker, N. Adult intestinal stem cells: critical drivers of epithelial homeostasis and regeneration. *Nature reviews. Molecular cell biology* **15**, 19-33, doi:10.1038/nrm3721 (2014).
16 Kaestner, K. H. The Intestinal Stem Cell Niche: A Central Role for Foxl1-Expressing Subepithelial Telocytes. *Cellular and Molecular Gastroenterology and Hepatology* **8**, 111-117, doi:https://doi.org/10.1016/j.jcmgh.2019.04.001 (2019).
17 Degirmenci, B., Valenta, T., Dimitrieva, S., Hausmann, G. & Basler, K. GLI1-expressing mesenchymal cells form the essential Wnt-secreting niche for colon stem cells. *Nature* **558**, 449-453, doi:10.1038/s41586-018-0190-3 (2018).
18 Sato, T. *et al.* Paneth cells constitute the niche for Lgr5 stem cells in intestinal crypts. *Nature* **469**, 415-418, doi:10.1038/nature09637 (2011).
19 Jiang, H., Grenley, M. O., Bravo, M. J., Blumhagen, R. Z. & Edgar, B. A. EGFR/Ras/MAPK signaling mediates adult midgut epithelial homeostasis and regeneration in Drosophila. *Cell Stem Cell* **8**, 84-95, doi:10.1016/j.stem.2010.11.026 (2011).
20 Lin, G., Xu, N. & Xi, R. Paracrine unpaired signaling through the JAK/STAT pathway controls self-renewal and lineage differentiation of drosophila intestinal stem cells. *Journal of molecular cell biology* **2**, 37-49, doi:10.1093/jmcb/mjp028 (2010).
21 Lin, G., Xu, N. & Xi, R. Paracrine Wingless signalling controls self-renewal of Drosophila intestinal stem cells. *Nature* **455**, 1119-1123, doi:10.1038/nature07329 (2008).
22 Guo, Z., Driver, I. & Ohlstein, B. Injury-induced BMP signaling negatively regulates Drosophila midgut homeostasis. *J Cell Biol* **201**, 945-961, doi:10.1083/jcb.201302049 (2013).
23 Li, Z., Zhang, Y., Han, L., Shi, L. & Lin, X. Trachea-Derived Dpp Controls Adult Midgut Homeostasis in Drosophila. *Developmental Cell* **24**, 133-143, doi:https://doi.org/10.1016/j.devcel.2012.12.010 (2013).
24 Lucchetta, E. M. & Ohlstein, B. The Drosophila midgut: a model for stem cell driven tissue regeneration. *Wiley interdisciplinary reviews. Developmental biology* **1**, 781-788, doi:10.1002/wdev.51 (2012).
25 Cordero, J. B., Stefanatos, R. K., Scopelliti, A., Vidal, M. & Sansom, O. J. Inducible progenitor-derived Wingless regulates adult midgut regeneration in Drosophila. *The EMBO journal* **31**, 3901-3917, doi:10.1038/emboj.2012.248 (2012).
26 Xiang, J. *et al.* EGFR-dependent TOR-independent endocycles support Drosophila gut epithelial regeneration. *Nature communications* **8**, 15125, doi:10.1038/ncomms15125 (2017).
27 Ohlstein, B. & Spradling, A. Multipotent Drosophila Intestinal Stem Cells Specify Daughter Cell Fates by Differential Notch Signaling. *Science (New York, N.Y.)* **315**, 988-992, doi:10.1126/science.1136606 (2007).
28 Li, Q. *et al.* The Conserved Misshapen-Warts-Yorkie Pathway Acts in Enteroblasts to Regulate Intestinal Stem Cells in Drosophila. *Developmental Cell* **31**, 291-304, doi:https://doi.org/10.1016/j.devcel.2014.09.012 (2014).

29 Tauc, H. M., Tasdogan, A., Meyer, P. & Pandur, P. Nipped-A regulates intestinal stem cell proliferation in <em>Drosophila</em&gt. *Development* **144**, 612, doi:10.1242/dev.142703 (2017).
30 Chatterjee, M. & Ip, Y. T. Pathogenic stimulation of intestinal stem cell response in Drosophila. *J Cell Physiol* **220**, 664-671, doi:10.1002/jcp.21808 (2009).
31 Chakrabarti, S., Liehl, P., Buchon, N. & Lemaitre, B. Infection-Induced Host Translational Blockage Inhibits Immune Responses and Epithelial Renewal in the Drosophila Gut. *Cell Host & Microbe* **12**, 60-70, doi:https://doi.org/10.1016/j.chom.2012.06.001 (2012).
32 Buchon, N., Broderick, N. A., Poidevin, M., Pradervand, S. & Lemaitre, B. Drosophila intestinal response to bacterial infection: activation of host defense and stem cell proliferation. *Cell Host Microbe* **5**, 200-211, doi:10.1016/j.chom.2009.01.003 (2009).
33 Sato, T. *et al.* Paneth cells constitute the niche for Lgr5 stem cells in intestinal crypts. *Nature* **469**, 415-418, doi:10.1038/nature09637 (2011).
34 Valenta, T. *et al.* Wnt Ligands Secreted by Subepithelial Mesenchymal Cells Are Essential for the Survival of Intestinal Stem Cells and Gut Homeostasis. *Cell Rep* **15**, 911-918, doi:10.1016/j.celrep.2016.03.088 (2016).
35 van de Wetering, M. *et al.* The beta-catenin/TCF-4 complex imposes a crypt progenitor phenotype on colorectal cancer cells. *Cell* **111**, 241-250, doi:10.1016/s0092-8674(02)01014-0 (2002).
36 Kinzler, K. W. & Vogelstein, B. Cancer-susceptibility genes. Gatekeepers and caretakers. *Nature* **386**, 761, 763, doi:10.1038/386761a0 (1997).
37 Lee, W.-C., Beebe, K., Sudmeier, L. & Micchelli, C. A. <em>Adenomatous polyposis coli</em> regulates <em>Drosophila</em> intestinal stem cell proliferation. *Development (Cambridge, England)* **136**, 2255, doi:10.1242/dev.035196 (2009).
38 Martorell, Ò. *et al.* Conserved mechanisms of tumorigenesis in the Drosophila adult midgut. *PloS one* **9**, e88413-e88413, doi:10.1371/journal.pone.0088413 (2014).
39 Vogelstein, B. *et al.* Genetic alterations during colorectal-tumor development. *The New England journal of medicine* **319**, 525-532, doi:10.1056/nejm198809013190901 (1988).
40 Suzuki, A., Sekiya, S., Gunshima, E., Fujii, S. & Taniguchi, H. EGF signaling activates proliferation and blocks apoptosis of mouse and human intestinal stem/progenitor cells in long-term monolayer cell culture. *Laboratory investigation; a journal of technical methods and pathology* **90**, 1425-1436, doi:10.1038/labinvest.2010.150 (2010).
41 Jiang, H. & Edgar, B. A. EGFR signaling regulates the proliferation of Drosophila adult midgut progenitors. *Development* **136**, 483-493, doi:10.1242/dev.026955 (2009).
42 Jorissen, R. N. *et al.* Epidermal growth factor receptor: mechanisms of activation and signalling. *Experimental cell research* **284**, 31-53, doi:10.1016/s0014-4827(02)00098-8 (2003).

43 Yang, Y.-P. *et al.* A Chimeric Egfr Protein Reporter Mouse Reveals Egfr Localization and Trafficking In Vivo. *Cell Reports* **19**, 1257-1267, doi:https://doi.org/10.1016/j.celrep.2017.04.048 (2017).
44 Xu, N. *et al.* EGFR, Wingless and JAK/STAT signaling cooperatively maintain Drosophila intestinal stem cells. *Developmental Biology* **354**, 31-43, doi:https://doi.org/10.1016/j.ydbio.2011.03.018 (2011).
45 Buchon, N., Broderick, N. A., Kuraishi, T. & Lemaitre, B. Drosophila EGFR pathway coordinates stem cell proliferation and gut remodeling following infection. *BMC Biol* **8**, 152, doi:10.1186/1741-7007-8-152 (2010).
46 O'Shea, J. J. *et al.* The JAK-STAT pathway: impact on human disease and therapeutic intervention. *Annu Rev Med* **66**, 311-328, doi:10.1146/annurev-med-051113-024537 (2015).
47 Arbouzova, N. I. JAK/STAT signalling in Drosophila: insights into conserved regulatory and cellular functions. *Development (Cambridge, England)* **133**, 2605-2616, doi:10.1242/dev.02411 (2006).
48 Lin, G., Xu, N. & Xi, R. Paracrine Unpaired Signaling through the JAK/STAT Pathway Controls Self-renewal and Lineage Differentiation of Drosophila Intestinal Stem Cells. *Journal of molecular cell biology* **2**, 37-49, doi:10.1093/jmcb/mjp028 (2009).
49 Beebe, K., Lee, W.-C. & Micchelli, C. A. JAK/STAT signaling coordinates stem cell proliferation and multilineage differentiation in the Drosophila intestinal stem cell lineage. *Developmental Biology* **338**, 28-37, doi:https://doi.org/10.1016/j.ydbio.2009.10.045 (2010).
50 Tian, A., Benchabane, H., Wang, Z. & Ahmed, Y. Regulation of Stem Cell Proliferation and Cell Fate Specification by Wingless/Wnt Signaling Gradients Enriched at Adult Intestinal Compartment Boundaries. *PLOS Genetics* **12**, e1005822, doi:10.1371/journal.pgen.1005822 (2016).
51 Lindemans, C. A. *et al.* Interleukin-22 promotes intestinal-stem-cell-mediated epithelial regeneration. *Nature* **528**, 560-564, doi:10.1038/nature16460 (2015).
52 Richmond, C. A. *et al.* JAK/STAT-1 Signaling Is Required for Reserve Intestinal Stem Cell Activation during Intestinal Regeneration Following Acute Inflammation. *Stem Cell Reports* **10**, 17-26, doi:10.1016/j.stemcr.2017.11.015 (2018).
53 Taguchi, A. & White, M. F. Insulin-Like Signaling, Nutrient Homeostasis, and Life Span. *Annual Review of Physiology* **70**, 191-212, doi:10.1146/annurev.physiol.70.113006.100533 (2008).
54 Rulifson, E. J., Kim, S. K. & Nusse, R. Ablation of Insulin-Producing Neurons in Flies: Growth and Diabetic Phenotypes. *Science (New York, N.Y.)* **296**, 1118, doi:10.1126/science.1070058 (2002).
55 Astrinidis, A. & Henske, E. P. Tuberous sclerosis complex: linking growth and energy signaling pathways with human disease. *Oncogene* **24**, 7475-7481, doi:10.1038/sj.onc.1209090 (2005).
56 Brown, A. K. & Webb, A. E. Regulation of FOXO Factors in Mammalian Cells. *Current topics in developmental biology* **127**, 165-192, doi:10.1016/bs.ctdb.2017.10.006 (2018).

57 Amcheslavsky, A. *et al.* Enteroendocrine cells support intestinal stem-cell-mediated homeostasis in Drosophila. *Cell Rep* **9**, 32-39, doi:10.1016/j.celrep.2014.08.052 (2014).
58 Amcheslavsky, A., Jiang, J. & Ip, Y. T. Tissue damage-induced intestinal stem cell division in Drosophila. *Cell Stem Cell* **4**, 49-61, doi:10.1016/j.stem.2008.10.016 (2009).
59 Tatar, M. *et al.* A mutant Drosophila insulin receptor homolog that extends life-span and impairs neuroendocrine function. *Science (New York, N.Y.)* **292**, 107-110, doi:10.1126/science.1057987 (2001).
60 Clancy, D. J. *et al.* Extension of life-span by loss of CHICO, a Drosophila insulin receptor substrate protein. *Science (New York, N.Y.)* **292**, 104-106, doi:10.1126/science.1057991 (2001).
61 Wessells, R. J., Fitzgerald, E., Cypser, J. R., Tatar, M. & Bodmer, R. Insulin regulation of heart function in aging fruit flies. *Nature genetics* **36**, 1275-1281, doi:10.1038/ng1476 (2004).
62 Biteau, B. *et al.* Lifespan extension by preserving proliferative homeostasis in Drosophila. *PLoS Genet* **6**, e1001159, doi:10.1371/journal.pgen.1001159 (2010).
63 Tran, T. *et al.* Hyperinsulinemia, But Not Other Factors Associated with Insulin Resistance, Acutely Enhances Colorectal Epithelial Proliferation in Vivo. *Endocrinology* **147**, 1830-1837, doi:10.1210/en.2005-1012 (2006).
64 Mah, A. T., Van Landeghem, L., Gavin, H. E., Magness, S. T. & Lund, P. K. Impact of diet-induced obesity on intestinal stem cells: hyperproliferation but impaired intrinsic function that requires insulin/IGF1. *Endocrinology* **155**, 3302-3314, doi:10.1210/en.2014-1112 (2014).
65 Andres, S. F. *et al.* Insulin receptor isoform switching in intestinal stem cells, progenitors, differentiated lineages and tumors: evidence that IR-B limits proliferation. *Journal of cell science* **126**, 5645-5656, doi:10.1242/jcs.132985 (2013).
66 Santoro, M. A. *et al.* Reduced insulin-like growth factor I receptor and altered insulin receptor isoform mRNAs in normal mucosa predict colorectal adenoma risk. *Cancer epidemiology, biomarkers & prevention : a publication of the American Association for Cancer Research, cosponsored by the American Society of Preventive Oncology* **23**, 2093-2100, doi:10.1158/1055-9965.EPI-14-0177 (2014).
67 Wang, M. C., Bohmann, D. & Jasper, H. JNK extends life span and limits growth by antagonizing cellular and organism-wide responses to insulin signaling. *Cell* **121**, 115-125, doi:10.1016/j.cell.2005.02.030 (2005).
68 Karpac, J., Biteau, B. & Jasper, H. Misregulation of an Adaptive Metabolic Response Contributes to the Age-Related Disruption of Lipid Homeostasis in Drosophila. *Cell Reports* **4**, 1250-1261, doi:https://doi.org/10.1016/j.celrep.2013.08.004 (2013).
69 Apidianakis, Y., Pitsouli, C., Perrimon, N. & Rahme, L. Synergy between bacterial infection and genetic predisposition in intestinal dysplasia. *Proceedings of the National Academy of Sciences* **106**, 20883-20888, doi:10.1073/pnas.0911797106 (2009).

70 Suijkerbuijk, S. J. E., Kolahgar, G., Kucinski, I. & Piddini, E. Cell Competition Drives the Growth of Intestinal Adenomas in Drosophila. *Current Biology* **26**, 428-438, doi:https://doi.org/10.1016/j.cub.2015.12.043 (2016).
71 Tian, A. *et al.* Injury-stimulated Hedgehog signaling promotes regenerative proliferation of Drosophila intestinal stem cells. *Journal of Cell Biology* **208**, 807-819, doi:10.1083/jcb.201409025 (2015).
72 Moroishi, T., Hansen, C. G. & Guan, K. L. The emerging roles of YAP and TAZ in cancer. *Nat Rev Cancer* **15**, 73-79, doi:10.1038/nrc3876 (2015).
73 Attisano, L. & Wrana, J. L. Signal integration in TGF-β, WNT, and Hippo pathways. *F1000Prime Rep* **5**, 17-17, doi:10.12703/P5-17 (2013).
74 Ayyaz, A., Attisano, L. & Wrana, J. Recent advances in understanding contextual TGF? signaling [version 1; peer review: 2 approved]. *F1000Research* **6**, doi:10.12688/f1000research.11295.1 (2017).
75 Kim, W. & Jho, E. H. The history and regulatory mechanism of the Hippo pathway. *BMB reports* **51**, 106-118, doi:10.5483/bmbrep.2018.51.3.022 (2018).
76 Taha, Z., Janse van Rensburg, H. J. & Yang, X. The Hippo Pathway: Immunity and Cancer. *Cancers* **10**, doi:10.3390/cancers10040094 (2018).
77 Camargo, F. D. *et al.* YAP1 increases organ size and expands undifferentiated progenitor cells. *Curr Biol* **17**, 2054-2060, doi:10.1016/j.cub.2007.10.039 (2007).
78 Camargo, F. D. *et al.* YAP1 Increases Organ Size and Expands Undifferentiated Progenitor Cells. *Current Biology* **17**, 2054-2060, doi:https://doi.org/10.1016/j.cub.2007.10.039 (2007).
79 Zhou, D. *et al.* Mst1 and Mst2 protein kinases restrain intestinal stem cell proliferation and colonic tumorigenesis by inhibition of Yes-associated protein (Yap) overabundance. *Proc Natl Acad Sci U S A* **108**, E1312-1320, doi:10.1073/pnas.1110428108 (2011).
80 Zhang, L. *et al.* NDR functions as a physiological YAP1 kinase in the intestinal epithelium. *Curr Biol* **25**, 296-305, doi:10.1016/j.cub.2014.11.054 (2015).
81 Cai, J. *et al.* The Hippo signaling pathway restricts the oncogenic potential of an intestinal regeneration program. *Genes & development* **24**, 2383-2388, doi:10.1101/gad.1978810 (2010).
82 Imajo, M., Ebisuya, M. & Nishida, E. Dual role of YAP and TAZ in renewal of the intestinal epithelium. *Nat Cell Biol* **17**, 7-19, doi:10.1038/ncb3084 (2015).
83 Hong, A. W., Meng, Z. & Guan, K.-L. The Hippo pathway in intestinal regeneration and disease. *Nature Reviews Gastroenterology & Hepatology* **13**, 324-337, doi:10.1038/nrgastro.2016.59 (2016).
84 Lu, L. *et al.* Hippo signaling is a potent in vivo growth and tumor suppressor pathway in the mammalian liver. *Proceedings of the National Academy of Sciences* **107**, 1437, doi:10.1073/pnas.0911427107 (2010).
85 Huang, H. *et al.* Bantam is essential for Drosophila intestinal stem cell proliferation in response to Hippo signaling. *Developmental Biology* **385**, 211-219, doi:https://doi.org/10.1016/j.ydbio.2013.11.008 (2014).

86 Karpowicz, P., Perez, J. & Perrimon, N. The Hippo tumor suppressor pathway regulates intestinal stem cell regeneration. *Development* **137**, 4135-4145, doi:10.1242/dev.060483 (2010).
87 Ren, F. *et al.* Hippo signaling regulates <em>Drosophila</em> intestine stem cell proliferation through multiple pathways. *Proceedings of the National Academy of Sciences* **107**, 21064, doi:10.1073/pnas.1012759107 (2010).
88 Conner, S. D. in *International Review of Cell and Molecular Biology* Vol. 323 (ed Kwang W. Jeon) 107-127 (Academic Press, 2016).
89 Demitrack, E. S. & Samuelson, L. C. Notch regulation of gastrointestinal stem cells. *J Physiol* **594**, 4791-4803, doi:10.1113/JP271667 (2016).
90 Pellegrinet, L. *et al.* Dll1- and Dll4-Mediated Notch Signaling Are Required for Homeostasis of Intestinal Stem Cells. *Gastroenterology* **140**, 1230-1240.e1237, doi:10.1053/j.gastro.2011.01.005 (2011).
91 Riccio, O. *et al.* Loss of intestinal crypt progenitor cells owing to inactivation of both Notch1 and Notch2 is accompanied by derepression of CDK inhibitors p27Kip1 and p57Kip2. *EMBO reports* **9**, 377-383, doi:10.1038/embor.2008.7 (2008).
92 Kapuria, S., Karpac, J., Biteau, B., Hwangbo, D. & Jasper, H. Notch-mediated suppression of TSC2 expression regulates cell differentiation in the Drosophila intestinal stem cell lineage. *PLoS genetics* **8**, e1003045-e1003045, doi:10.1371/journal.pgen.1003045 (2012).
93 Ohlstein, B. & Spradling, A. The adult Drosophila posterior midgut is maintained by pluripotent stem cells. *Nature* **439**, 470-474, doi:10.1038/nature04333 (2006).
94 Patel, P. H., Dutta, D. & Edgar, B. A. Niche appropriation by Drosophila intestinal stem cell tumours. *Nature Cell Biology* **17**, 1182-1192, doi:10.1038/ncb3214 (2015).
95 Cordero, J. B., Stefanatos, R. K., Myant, K., Vidal, M. & Sansom, O. J. Non-autonomous crosstalk between the Jak/Stat and Egfr pathways mediates Apc1-driven intestinal stem cell hyperplasia in the Drosophila adult midgut. *Development* **139**, 4524-4535, doi:10.1242/dev.078261 (2012).
96 Fre, S. *et al.* Notch signals control the fate of immature progenitor cells in the intestine. *Nature* **435**, 964-968, doi:10.1038/nature03589 (2005).
97 Obniski, R., Sieber, M. & Spradling, A. C. Dietary Lipids Modulate Notch Signaling and Influence Adult Intestinal Development and Metabolism in Drosophila. *Developmental cell* **47**, 98-111.e115, doi:10.1016/j.devcel.2018.08.013 (2018).
98 Beyaz, S. *et al.* High-fat diet enhances stemness and tumorigenicity of intestinal progenitors. *Nature* **531**, 53-58, doi:10.1038/nature17173 (2016).
99 Hamaratoglu, F., Affolter, M. & Pyrowolakis, G. Dpp/BMP signaling in flies: From molecules to biology. *Seminars in Cell & Developmental Biology* **32**, 128-136, doi:https://doi.org/10.1016/j.semcdb.2014.04.036 (2014).
100 Tian, A. & Jiang, J. Intestinal epithelium-derived BMP controls stem cell self-renewal in Drosophila adult midgut. *eLife* **3**, e01857, doi:10.7554/eLife.01857 (2014).

101 Tian, A. & Jiang, J. Intestinal epithelium-derived BMP controls stem cell self-renewal in Drosophila adult midgut. *eLife* **3**, e01857-e01857, doi:10.7554/eLife.01857 (2014).
102 Li, H., Qi, Y. & Jasper, H. Dpp signaling determines regional stem cell identity in the regenerating adult Drosophila gastrointestinal tract. *Cell reports* **4**, 10-18, doi:10.1016/j.celrep.2013.05.040 (2013).
103 Hardwick, J. C., Kodach, L. L., Offerhaus, G. J. & van den Brink, G. R. Bone morphogenetic protein signalling in colorectal cancer. *Nature reviews. Cancer* **8**, 806-812, doi:10.1038/nrc2467 (2008).
104 Hardwick, J. C., Kodach, L. L., Offerhaus, G. J. & Van Den Brink, G. R. Bone morphogenetic protein signalling in colorectal cancer. *Nature Reviews Cancer* **8**, 806-812, doi:10.1038/nrc2467 (2008).
105 Jasper, H. Exploring the physiology and pathology of aging in the intestine of Drosophila melanogaster. *Invertebr Reprod Dev* **59**, 51-58, doi:10.1080/07924259.2014.963713 (2015).
106 Hochmuth, C. E., Biteau, B., Bohmann, D. & Jasper, H. Redox regulation by Keap1 and Nrf2 controls intestinal stem cell proliferation in Drosophila. *Cell Stem Cell* **8**, 188-199, doi:10.1016/j.stem.2010.12.006 (2011).
107 Guo, L., Karpac, J., Tran, S. L. & Jasper, H. PGRP-SC2 promotes gut immune homeostasis to limit commensal dysbiosis and extend lifespan. *Cell* **156**, 109-122, doi:10.1016/j.cell.2013.12.018 (2014).
108 Clemente, J. C., Ursell, L. K., Parfrey, L. W. & Knight, R. The impact of the gut microbiota on human health: an integrative view. *Cell* **148**, 1258-1270, doi:10.1016/j.cell.2012.01.035 (2012).
109 Patel, B. B. *et al.* Age-related increase in colorectal cancer stem cells in macroscopically normal mucosa of patients with adenomas: a risk factor for colon cancer. *Biochem Biophys Res Commun* **378**, 344-347, doi:10.1016/j.bbrc.2008.10.179 (2009).
110 Roberts, S. B. & Rosenberg, I. Nutrition and aging: changes in the regulation of energy metabolism with aging. *Physiological reviews* **86**, 651-667, doi:10.1152/physrev.00019.2005 (2006).
111 Duncan, S. H. & Flint, H. J. Probiotics and prebiotics and health in ageing populations. *Maturitas* **75**, 44-50, doi:10.1016/j.maturitas.2013.02.004 (2013).
112 Nalapareddy, K. *et al.* Canonical Wnt Signaling Ameliorates Aging of Intestinal Stem Cells. *Cell reports* **18**, 2608-2621, doi:10.1016/j.celrep.2017.02.056 (2017).
113 Moorefield, E. C. *et al.* Aging effects on intestinal homeostasis associated with expansion and dysfunction of intestinal epithelial stem cells. *Aging* **9**, 1898-1915, doi:10.18632/aging.101279 (2017).
114 Holt, P. R. & Yeh, K. Y. Small intestinal crypt cell proliferation rates are increased in senescent rats. *Journal of gerontology* **44**, B9-14, doi:10.1093/geronj/44.1.b9 (1989).
115 Guo, L., Karpac, J., Tran, S. L. & Jasper, H. PGRP-SC2 promotes gut immune homeostasis to limit commensal dysbiosis and extend lifespan. *Cell* **156**, 109-122, doi:10.1016/j.cell.2013.12.018 (2014).

116 Biteau, B., Hochmuth, C. E. & Jasper, H. Maintaining tissue homeostasis: dynamic control of somatic stem cell activity. *Cell stem cell* **9**, 402-411, doi:10.1016/j.stem.2011.10.004 (2011).
117 Tothova, Z. *et al.* FoxOs are critical mediators of hematopoietic stem cell resistance to physiologic oxidative stress. *Cell* **128**, 325-339, doi:10.1016/j.cell.2007.01.003 (2007).
118 Hudry, B., Khadayate, S. & Miguel-Aliaga, I. The sexual identity of adult intestinal stem cells controls organ size and plasticity. *Nature* **530**, 344-348, doi:10.1038/nature16953 (2016).
119 Bonnay, F. *et al.* big bang gene modulates gut immune tolerance in Drosophila. *Proceedings of the National Academy of Sciences of the United States of America* **110**, 2957-2962, doi:10.1073/pnas.1221910110 (2013).
120 Biteau, B., Hochmuth, C. E. & Jasper, H. JNK activity in somatic stem cells causes loss of tissue homeostasis in the aging Drosophila gut. *Cell Stem Cell* **3**, 442-455, doi:10.1016/j.stem.2008.07.024 (2008).
121 Regan, J. C. *et al.* Sex difference in pathology of the ageing gut mediates the greater response of female lifespan to dietary restriction. *eLife* **5**, e10956-e10956, doi:10.7554/eLife.10956 (2016).
122 Buchon, N., Broderick, N. A., Chakrabarti, S. & Lemaitre, B. Invasive and indigenous microbiota impact intestinal stem cell activity through multiple pathways in Drosophila. *Genes & development* **23**, 2333-2344, doi:10.1101/gad.1827009 (2009).
123 Sieber, M. H. & Spradling, A. C. Steroid Signaling Establishes a Female Metabolic State and Regulates SREBP to Control Oocyte Lipid Accumulation. *Curr Biol* **25**, 993-1004, doi:10.1016/j.cub.2015.02.019 (2015).
124 Regan, J. C. *et al.* Sex difference in pathology of the ageing gut mediates the greater response of female lifespan to dietary restriction. *Elife* **5**, e10956, doi:10.7554/eLife.10956 (2016).
125 Chawla, A., Repa, J. J., Evans, R. M. & Mangelsdorf, D. J. Nuclear Receptors and Lipid Physiology: Opening the X-Files. *Science* **294**, 1866, doi:10.1126/science.294.5548.1866 (2001).
126 Perissi, V. & Rosenfeld, M. G. Controlling nuclear receptors: the circular logic of cofactor cycles. *Nature reviews. Molecular cell biology* **6**, 542-554, doi:10.1038/nrm1680 (2005).
127 King-Jones, K. & Thummel, C. S. Nuclear receptors--a perspective from Drosophila. *Nat Rev Genet* **6**, 311-323, doi:10.1038/nrg1581 (2005).
128 Storelli, G., Nam, H. J., Simcox, J., Villanueva, C. J. & Thummel, C. S. Drosophila HNF4 Directs a Switch in Lipid Metabolism that Supports the Transition to Adulthood. *Dev Cell* **48**, 200-214.e206, doi:10.1016/j.devcel.2018.11.030 (2019).
129 Renaud, J. P. & Moras, D. Structural studies on nuclear receptors. *Cellular and molecular life sciences : CMLS* **57**, 1748-1769, doi:10.1007/pl00000656 (2000).
130 Sen, A. *et al.* Paxillin mediates extranuclear and intranuclear signaling in prostate cancer proliferation. *J Clin Invest* **122**, 2469-2481, doi:10.1172/JCI62044 (2012).

131 Pedram, A., Razandi, M. & Levin, E. R. Nature of functional estrogen receptors at the plasma membrane. *Molecular endocrinology (Baltimore, Md.)* **20**, 1996-2009, doi:10.1210/me.2005-0525 (2006).
132 Levin, E. R. & Hammes, S. R. Nuclear receptors outside the nucleus: extranuclear signalling by steroid receptors. *Nature reviews. Molecular cell biology* **17**, 783-797, doi:10.1038/nrm.2016.122 (2016).
133 Spaziani, E. & Szego, C. M. Early effects of estradiol and cortisol on water and electrolyte shifts in the uterus of the immature rat. *The American journal of physiology* **197**, 355-359, doi:10.1152/ajplegacy.1959.197.2.355 (1959).
134 Lutz, L. B., Kim, B., Jahani, D. & Hammes, S. R. G protein beta gamma subunits inhibit nongenomic progesterone-induced signaling and maturation in Xenopus laevis oocytes. Evidence for a release of inhibition mechanism for cell cycle progression. *J Biol Chem* **275**, 41512-41520, doi:10.1074/jbc.M006757200 (2000).
135 Fuentes, N. & Silveyra, P. Estrogen receptor signaling mechanisms. *Adv Protein Chem Struct Biol* **116**, 135-170, doi:10.1016/bs.apcsb.2019.01.001 (2019).
136 Frasor, J. *et al.* Profiling of estrogen up- and down-regulated gene expression in human breast cancer cells: insights into gene networks and pathways underlying estrogenic control of proliferation and cell phenotype. *Endocrinology* **144**, 4562-4574, doi:10.1210/en.2003-0567 (2003).
137 Sabbah, M., Courilleau, D., Mester, J. & Redeuilh, G. Estrogen induction of the cyclin D1 promoter: involvement of a cAMP response-like element. *Proceedings of the National Academy of Sciences of the United States of America* **96**, 11217-11222, doi:10.1073/pnas.96.20.11217 (1999).
138 Glass, C. K. & Ogawa, S. Combinatorial roles of nuclear receptors in inflammation and immunity. *Nature reviews. Immunology* **6**, 44-55, doi:10.1038/nri1748 (2006).
139 Pedram, A. *et al.* Estrogen regulates histone deacetylases to prevent cardiac hypertrophy. *Mol Biol Cell* **24**, 3805-3818, doi:10.1091/mbc.E13-08-0444 (2013).
140 Shay, N. F. & Banz, W. J. Regulation of gene transcription by botanicals: novel regulatory mechanisms. *Annual review of nutrition* **25**, 297-315, doi:10.1146/annurev.nutr.25.050304.092639 (2005).
141 Bredfeldt, T. G. *et al.* Xenoestrogen-induced regulation of EZH2 and histone methylation via estrogen receptor signaling to PI3K/AKT. *Molecular endocrinology (Baltimore, Md.)* **24**, 993-1006, doi:10.1210/me.2009-0438 (2010).
142 Green, K. A. & Carroll, J. S. Oestrogen-receptor-mediated transcription and the influence of co-factors and chromatin state. *Nature Reviews Cancer* **7**, 713-722, doi:10.1038/nrc2211 (2007).
143 Aranda, A. & Pascual, A. Nuclear hormone receptors and gene expression. *Physiological reviews* **81**, 1269-1304, doi:10.1152/physrev.2001.81.3.1269 (2001).
144 Tobin, J. F. & Freedman, L. P. Nuclear receptors as drug targets in metabolic diseases: new approaches to therapy. *Trends Endocrinol Metab* **17**, 284-290, doi:10.1016/j.tem.2006.07.004 (2006).

145 Moutinho, M., Codocedo, J. F., Puntambekar, S. S. & Landreth, G. E. Nuclear Receptors as Therapeutic Targets for Neurodegenerative Diseases: Lost in Translation. *Annual Review of Pharmacology and Toxicology* **59**, 237-261, doi:10.1146/annurev-pharmtox-010818-021807 (2019).
146 Zollner, G. & Trauner, M. Nuclear receptors as therapeutic targets in cholestatic liver diseases. *British Journal of Pharmacology* **156**, 7-27, doi:10.1111/j.1476-5381.2008.00030.x (2009).
147 Garattini, E. *et al.* Lipid-sensors, enigmatic-orphan and orphan nuclear receptors as therapeutic targets in breast-cancer. *Oncotarget* **7** (2016).
148 Riddiford, L. M. Hormone receptors and the regulation of insect metamorphosis. *Receptor* **3**, 203-209 (1993).
149 Lavrynenko, O. *et al.* The ecdysteroidome of Drosophila: influence of diet and development. *Development* **142**, 3758-3768, doi:10.1242/dev.124982 (2015).
150 Gilbert, L. I. Halloween genes encode P450 enzymes that mediate steroid hormone biosynthesis in Drosophila melanogaster. *Mol Cell Endocrinol* **215**, 1-10, doi:10.1016/j.mce.2003.11.003 (2004).
151 Ou, Q. & King-Jones, K. What goes up must come down: transcription factors have their say in making ecdysone pulses. *Current topics in developmental biology* **103**, 35-71, doi:10.1016/b978-0-12-385979-2.00002-2 (2013).
152 Hentze, J. L. *et al.* Accessory Gland as a Site for Prothoracicotropic Hormone Controlled Ecdysone Synthesis in Adult Male Insects. *PLOS ONE* **8**, e55131, doi:10.1371/journal.pone.0055131 (2013).
153 Bownes, M., Dübendorfer, A. & Smith, T. Ecdysteroids in adult males and females of Drosophila melanogaster. *Journal of Insect Physiology* **30**, 823-830, doi:https://doi.org/10.1016/0022-1910(84)90019-2 (1984).
154 Handler, A. M. Ecdysteroid titers during pupal and adult development in Drosophila melanogaster. *Dev Biol* **93**, 73-82, doi:10.1016/0012-1606(82)90240-8 (1982).
155 Petryk, A. *et al.* Shade is the Drosophila P450 enzyme that mediates the hydroxylation of ecdysone to the steroid insect molting hormone 20-hydroxyecdysone. *Proc Natl Acad Sci U S A* **100**, 13773-13778, doi:10.1073/pnas.2336088100 (2003).
156 Harshman, L. G., Loeb, A. M. & Johnson, B. A. Ecdysteroid titers in mated and unmated Drosophila melanogaster females. *Journal of Insect Physiology* **45**, 571-577, doi:https://doi.org/10.1016/S0022-1910(99)00038-4 (1999).
157 Ameku, T. & Niwa, R. Mating-Induced Increase in Germline Stem Cells via the Neuroendocrine System in Female Drosophila. *PLoS genetics* **12**, e1006123-e1006123, doi:10.1371/journal.pgen.1006123 (2016).
158 Deady, L. D., Shen, W., Mosure, S. A., Spradling, A. C. & Sun, J. Matrix metalloproteinase 2 is required for ovulation and corpus luteum formation in Drosophila. *PLoS Genet* **11**, e1004989, doi:10.1371/journal.pgen.1004989 (2015).
159 Bender, M., Imam, F. B., Talbot, W. S., Ganetzky, B. & Hogness, D. S. Drosophila ecdysone receptor mutations reveal functional differences among receptor isoforms. *Cell* **91**, 777-788, doi:10.1016/s0092-8674(00)80466-3 (1997).

160 Davis, M. B., Carney, G. E., Robertson, A. E. & Bender, M. Phenotypic analysis of EcR-A mutants suggests that EcR isoforms have unique functions during Drosophila development. *Developmental biology* **282**, 385-396, doi:10.1016/j.ydbio.2005.03.019 (2005).
161 Buszczak, M. & Segraves, W. A. Insect metamorphosis: out with the old, in with the new. *Curr Biol* **10**, R830-833 (2000).
162 Thummel, C. S. From embryogenesis to metamorphosis: the regulation and function of Drosophila nuclear receptor superfamily members. *Cell* **83**, 871-877 (1995).
163 Thummel, C. S. Flies on steroids--Drosophila metamorphosis and the mechanisms of steroid hormone action. *Trends Genet* **12**, 306-310 (1996).
164 Ishimoto, H. & Kitamoto, T. The steroid molting hormone Ecdysone regulates sleep in adult Drosophila melanogaster. *Genetics* **185**, 269-281, doi:10.1534/genetics.110.114587 (2010).
165 Ishimoto, H., Sakai, T. & Kitamoto, T. Ecdysone signaling regulates the formation of long-term courtship memory in adult Drosophila melanogaster. *Proc Natl Acad Sci U S A* **106**, 6381-6386, doi:10.1073/pnas.0810213106 (2009).
166 Simon, A. F., Shih, C., Mack, A. & Benzer, S. Steroid control of longevity in Drosophila melanogaster. *Science* **299**, 1407-1410, doi:10.1126/science.1080539 (2003).
167 Homem, C. C. F. *et al.* Ecdysone and mediator change energy metabolism to terminate proliferation in Drosophila neural stem cells. *Cell* **158**, 874-888, doi:10.1016/j.cell.2014.06.024 (2014).
168 Morris, L. X. & Spradling, A. C. Steroid signaling within Drosophila ovarian epithelial cells sex-specifically modulates early germ cell development and meiotic entry. *PLoS One* **7**, e46109, doi:10.1371/journal.pone.0046109 (2012).
169 Li, Y., Ma, Q., Cherry, C. M. & Matunis, E. L. Steroid signaling promotes stem cell maintenance in the Drosophila testis. *Developmental Biology* **394**, 129-141, doi:https://doi.org/10.1016/j.ydbio.2014.07.016 (2014).
170 Calkin, A. & Tontonoz, P. Transcriptional integration of metabolism by the nuclear sterol-activated receptors LXR and FXR. *Nature reviews. Molecular cell biology* **13**, 213-224, doi:10.1038/nrm3312 (2012).
171 Hong, C. & Tontonoz, P. Liver X receptors in lipid metabolism: opportunities for drug discovery. *Nature Reviews Drug Discovery* **13**, 433-444, doi:10.1038/nrd4280 (2014).
172 Ashburner, M., Chihara, C., Meltzer, P. & Richards, G. Temporal control of puffing activity in polytene chromosomes. *Cold Spring Harbor symposia on quantitative biology* **38**, 655-662, doi:10.1101/sqb.1974.038.01.070 (1974).
173 Kojetin, D. J. & Burris, T. P. REV-ERB and ROR nuclear receptors as drug targets. *Nature Reviews Drug Discovery* **13**, 197-216, doi:10.1038/nrd4100 (2014).
174 Marvin, K. A. *et al.* Nuclear Receptors Homo sapiens Rev-erbβ and Drosophila melanogaster E75 Are Thiolate-Ligated Heme Proteins Which Undergo Redox-Mediated Ligand Switching and Bind CO and NO. *Biochemistry* **48**, 7056-7071, doi:10.1021/bi900697c (2009).

175 Reinking, J. *et al.* The Drosophila nuclear receptor e75 contains heme and is gas responsive. *Cell* **122**, 195-207, doi:10.1016/j.cell.2005.07.005 (2005).
176 Johnston, D. M. *et al.* Ecdysone- and NO-mediated gene regulation by competing EcR/Usp and E75A nuclear receptors during Drosophila development. *Mol Cell* **44**, 51-61, doi:10.1016/j.molcel.2011.07.033 (2011).
177 White, K. P., Hurban, P., Watanabe, T. & Hogness, D. S. Coordination of Drosophila metamorphosis by two ecdysone-induced nuclear receptors. *Science* **276**, 114-117 (1997).
178 Palanker, L. *et al.* Dynamic regulation of <em>Drosophila</em> nuclear receptor activity in vivo. *Development (Cambridge, England)* **133**, 3549, doi:10.1242/dev.02512 (2006).
179 Uryu, O., Ameku, T. & Niwa, R. Recent progress in understanding the role of ecdysteroids in adult insects: Germline development and circadian clock in the fruit fly Drosophila melanogaster. *Zoological Lett* **1**, 32, doi:10.1186/s40851-015-0031-2 (2015).
180 Kamoshida, Y. *et al.* Ecdysone receptor (EcR) suppresses lipid accumulation in the Drosophila fat body via transcription control. *Biochem Biophys Res Commun* **421**, 203-207, doi:10.1016/j.bbrc.2012.03.135 (2012).
181 Kojetin, D. J. & Burris, T. P. REV-ERB and ROR nuclear receptors as drug targets. *Nature reviews. Drug discovery* **13**, 197-216, doi:10.1038/nrd4100 (2014).
182 Marvin, K. A. *et al.* Nuclear receptors homo sapiens Rev-erbbeta and Drosophila melanogaster E75 are thiolate-ligated heme proteins which undergo redox-mediated ligand switching and bind CO and NO. *Biochemistry* **48**, 7056-7071, doi:10.1021/bi900697c (2009).
183 Bialecki, M., Shilton, A., Fichtenberg, C., Segraves, W. A. & Thummel, C. S. Loss of the Ecdysteroid-Inducible E75A Orphan Nuclear Receptor Uncouples Molting from Metamorphosis in Drosophila. *Developmental Cell* **3**, 209-220, doi:https://doi.org/10.1016/S1534-5807(02)00204-6 (2002).
184 Bialecki, M., Shilton, A., Fichtenberg, C., Segraves, W. A. & Thummel, C. S. Loss of the ecdysteroid-inducible E75A orphan nuclear receptor uncouples molting from metamorphosis in Drosophila. *Dev Cell* **3**, 209-220, doi:S1534580702002046 [pii] (2002).
185 Caceres, L. *et al.* Nitric oxide coordinates metabolism, growth, and development via the nuclear receptor E75. *Genes & development* **25**, 1476-1485, doi:10.1101/gad.2064111 (2011).
186 Palanker, L. *et al.* Dynamic regulation of Drosophila nuclear receptor activity in vivo. *Development* **133**, 3549-3562, doi:10.1242/dev.02512 (2006).
187 Ruaud, A.-F., Lam, G. & Thummel, C. S. The Drosophila nuclear receptors DHR3 and betaFTZ-F1 control overlapping developmental responses in late embryos. *Development (Cambridge, England)* **137**, 123-131, doi:10.1242/dev.042036 (2010).
188 Jaumouillé, E., Pedro, Stähli, P., Koch, R. & Nagoshi, E. Transcriptional Regulation via Nuclear Receptor Crosstalk Required for the Drosophila Circadian Clock. *Current Biology* **25**, 1502-1508, doi:10.1016/j.cub.2015.04.017 (2015).

189 Rabinovich, D., Yaniv, S. P., Alyagor, I. & Schuldiner, O. Nitric Oxide as a Switching Mechanism between Axon Degeneration and Regrowth during Developmental Remodeling. *Cell* **164**, 170-182, doi:10.1016/j.cell.2015.11.047 (2016).
190 DiBello, P. R., Withers, D. A., Bayer, C. A., Fristrom, J. W. & Guild, G. M. The Drosophila Broad-Complex encodes a family of related proteins containing zinc fingers. *Genetics* **129**, 385-397 (1991).
191 Karim, F. D., Guild, G. M. & Thummel, C. S. The Drosophila Broad-Complex plays a key role in controlling ecdysone-regulated gene expression at the onset of metamorphosis. *Development* **118**, 977-988 (1993).
192 Tzolovsky, G., Deng, W. M., Schlitt, T. & Bownes, M. The function of the broad-complex during Drosophila melanogaster oogenesis. *Genetics* **153**, 1371-1383 (1999).
193 Rus, F. *et al.* Ecdysone triggered PGRP-LC expression controls Drosophila innate immunity. *The EMBO journal* **32**, 1626-1638, doi:10.1038/emboj.2013.100 (2013).
194 Pol, H. *et al.* Changing your sex changes your brain: Influences of testosterone and estrogen on adult human brain structure. *European Journal of Endocrinology, Supplement* **155**, doi:10.1530/eje.1.02248 (2006).
195 Klein, K. O. *et al.* Estrogen Replacement in Turner Syndrome: Literature Review and Practical Considerations. *The Journal of Clinical Endocrinology & Metabolism* **103**, 1790-1803, doi:10.1210/jc.2017-02183 (2018).
196 Unger, C. A. Hormone therapy for transgender patients. *Transl Androl Urol* **5**, 877-884, doi:10.21037/tau.2016.09.04 (2016).
197 Capel, B. Vertebrate sex determination: evolutionary plasticity of a fundamental switch. *Nat Rev Genet* **18**, 675-689, doi:10.1038/nrg.2017.60 (2017).
198 Koopman, P., Gubbay, J., Vivian, N., Goodfellow, P. & Lovell-Badge, R. Male development of chromosomally female mice transgenic for Sry. *Nature* **351**, 117-121, doi:10.1038/351117a0 (1991).
199 Sinclair, A. H. *et al.* A gene from the human sex-determining region encodes a protein with homology to a conserved DNA-binding motif. *Nature* **346**, 240-244, doi:10.1038/346240a0 (1990).
200 McClelland, K., Bowles, J. & Koopman, P. Male sex determination: insights into molecular mechanisms. *Asian J Androl* **14**, 164-171, doi:10.1038/aja.2011.169 (2012).
201 Yao, H. H., Whoriskey, W. & Capel, B. Desert Hedgehog/Patched 1 signaling specifies fetal Leydig cell fate in testis organogenesis. *Genes & development* **16**, 1433-1440, doi:10.1101/gad.981202 (2002).
202 Wilhelm, D. *et al.* SOX9 regulates prostaglandin D synthase gene transcription in vivo to ensure testis development. *J Biol Chem* **282**, 10553-10560, doi:10.1074/jbc.M609578200 (2007).
203 Brennan, J., Tilmann, C. & Capel, B. Pdgfr-alpha mediates testis cord organization and fetal Leydig cell development in the XY gonad. *Genes & development* **17**, 800-810, doi:10.1101/gad.1052503 (2003).

204 Scheib, D. Effects and role of estrogens in avian gonadal differentiation. *Differentiation; research in biological diversity* **23 Suppl**, S87-92, doi:10.1007/978-3-642-69150-8_15 (1983).
205 Szabad, J. & Nöthiger, R. Gynandromorphs of Drosophila suggest one common primordium for the somatic cells of the female and male gonads in the region of abdominal segments 4 and 5. *Development* **115**, 527-533 (1992).
206 Janning, W. Gynandromorph fate maps in Drosophila. *Results and problems in cell differentiation* **9**, 1-28, doi:10.1007/978-3-540-35803-9_1 (1978).
207 Salz, H. & Erickson, J. W. Sex determination in Drosophila: The view from the top. *Fly* **4**, 60-70, doi:10.4161/fly.4.1.11277 (2010).
208 Lucchesi, J. C. & Kuroda, M. I. Dosage compensation in Drosophila. *Cold Spring Harbor perspectives in biology* **7**, doi:10.1101/cshperspect.a019398 (2015).
209 Pomatto, L. C. D., Tower, J. & Davies, K. J. A. Sexual Dimorphism and Aging Differentially Regulate Adaptive Homeostasis. *J Gerontol A Biol Sci Med Sci* **73**, 141-149, doi:10.1093/gerona/glx083 (2018).
210 Fagegaltier, D. *et al.* A genome-wide survey of sexually dimorphic expression of Drosophila miRNAs identifies the steroid hormone-induced miRNA let-7 as a regulator of sexual identity. *Genetics* **198**, 647-668, doi:10.1534/genetics.114.169268 (2014).
211 Kinsley, C., Bardi, M., Neigh, G. N. & Lambert, K. in *Sex Differences in Physiology* (eds Gretchen N. Neigh & Megan M. Mitzelfelt) 5-15 (Academic Press, 2016).
212 Deng, X. *et al.* Evidence for compensatory upregulation of expressed X-linked genes in mammals, Caenorhabditis elegans and Drosophila melanogaster. *Nature genetics* **43**, 1179-1185, doi:10.1038/ng.948 (2011).
213 Brockdorff, N. & Turner, B. M. Dosage compensation in mammals. *Cold Spring Harb Perspect Biol* **7**, a019406-a019406, doi:10.1101/cshperspect.a019406 (2015).
214 Yi, W., Ross, J. M. & Zarkower, D. Mab-3 is a direct tra-1 target gene regulating diverse aspects of C. elegans male sexual development and behavior. *Development* **127**, 4469 (2000).
215 Kossack, M. E. & Draper, B. W. Genetic regulation of sex determination and maintenance in zebrafish (Danio rerio). *Current topics in developmental biology* **134**, 119-149, doi:10.1016/bs.ctdb.2019.02.004 (2019).
216 Huang, S., Ye, L. & Chen, H. Sex determination and maintenance: the role of DMRT1 and FOXL2. *Asian journal of andrology* **19**, 619-624, doi:10.4103/1008-682x.194420 (2017).
217 Ge, C. *et al.* The histone demethylase KDM6B regulates temperature-dependent sex determination in a turtle species. *Science (New York, N.Y.)* **360**, 645, doi:10.1126/science.aap8328 (2018).
218 DeFalco, T. & Capel, B. Gonad morphogenesis in vertebrates: divergent means to a convergent end. *Annu Rev Cell Dev Biol* **25**, 457-482, doi:10.1146/annurev.cellbio.042308.13350 (2009).
219 Capel, B. Vertebrate sex determination: evolutionary plasticity of a fundamental switch. *Nature Reviews Genetics* **18**, 675-689, doi:10.1038/nrg.2017.60 (2017).

220 Hu, J., Zhang, Z., Shen, W.-J. & Azhar, S. Cellular cholesterol delivery, intracellular processing and utilization for biosynthesis of steroid hormones. *Nutr Metab (Lond)* **7**, 47-47, doi:10.1186/1743-7075-7-47 (2010).
221 Nakada, D. *et al.* Oestrogen increases haematopoietic stem-cell self-renewal in females and during pregnancy. *Nature* **505**, 555-558, doi:10.1038/nature12932 (2014).
222 Tiede, B. & Kang, Y. From milk to malignancy: the role of mammary stem cells in development, pregnancy and breast cancer. *Cell Res* **21**, 245-257, doi:10.1038/cr.2011.11 (2011).
223 Sasson, I. E. & Taylor, H. S. Stem cells and the pathogenesis of endometriosis. *Annals of the New York Academy of Sciences* **1127**, 106-115, doi:10.1196/annals.1434.014 (2008).
224 Cheng, G., Weihua, Z., Warner, M. & Gustafsson, J.-Å. Estrogen receptors ERα and ERβ in proliferation in the rodent mammary gland. *Proceedings of the National Academy of Sciences of the United States of America* **101**, 3739, doi:10.1073/pnas.0307864100 (2004).
225 Patrone, C. *et al.* Regulation of postnatal lung development and homeostasis by estrogen receptor beta. *Mol Cell Biol* **23**, 8542-8552, doi:10.1128/mcb.23.23.8542-8552.2003 (2003).
226 Wada-Hiraike, O. *et al.* Role of estrogen receptor beta in colonic epithelium. *Proc Natl Acad Sci U S A* **103**, 2959-2964, doi:10.1073/pnas.0511271103 (2006).
227 Barros, R. P. & Gustafsson, J. A. Estrogen receptors and the metabolic network. *Cell metabolism* **14**, 289-299, doi:10.1016/j.cmet.2011.08.005 (2011).
228 Faas, M. M., Melgert, B. N. & de Vos, P. A Brief Review on How Pregnancy and Sex Hormones Interfere with Taste and Food Intake. *Chemosens Percept* **3**, 51-56, doi:10.1007/s12078-009-9061-5 (2010).
229 Lai, J. J. *et al.* Monocyte/macrophage androgen receptor suppresses cutaneous wound healing in mice by enhancing local TNF-alpha expression. *J Clin Invest* **119**, 3739-3751, doi:10.1172/jci39335 (2009).
230 Fang, L. Y. *et al.* Infiltrating macrophages promote prostate tumorigenesis via modulating androgen receptor-mediated CCL4-STAT3 signaling. *Cancer Res* **73**, 5633-5646, doi:10.1158/0008-5472.Can-12-3228 (2013).
231 Straub, R. H. The complex role of estrogens in inflammation. *Endocr Rev* **28**, 521-574, doi:10.1210/er.2007-0001 (2007).
232 Monteiro, R., Teixeira, D. & Calhau, C. Estrogen signaling in metabolic inflammation. *Mediators Inflamm* **2014**, 615917-615917, doi:10.1155/2014/615917 (2014).
233 Fish, E. N. The X-files in immunity: sex-based differences predispose immune responses. *Nature reviews. Immunology* **8**, 737-744, doi:10.1038/nri2394 (2008).
234 Lai, J. J. *et al.* Androgen receptor influences on body defense system via modulation of innate and adaptive immune systems: lessons from conditional AR knockout mice. *The American journal of pathology* **181**, 1504-1512, doi:10.1016/j.ajpath.2012.07.008 (2012).

235 Pequeux, C. *et al.* Stromal estrogen receptor-alpha promotes tumor growth by normalizing an increased angiogenesis. *Cancer Res* **72**, 3010-3019, doi:10.1158/0008-5472.Can-11-3768 (2012).
236 Seo, K. H. *et al.* Estrogen enhances angiogenesis through a pathway involving platelet-activating factor-mediated nuclear factor-kappaB activation. *Cancer Res* **64**, 6482-6488, doi:10.1158/0008-5472.Can-03-2774 (2004).
237 Slavin, S. *et al.* Estrogen receptor alpha in cancer-associated fibroblasts suppresses prostate cancer invasion via modulation of thrombospondin 2 and matrix metalloproteinase 3. *Carcinogenesis* **35**, 1301-1309, doi:10.1093/carcin/bgt488 (2014).
238 Gupta, P. B. *et al.* Systemic stromal effects of estrogen promote the growth of estrogen receptor-negative cancers. *Cancer Res* **67**, 2062-2071, doi:10.1158/0008-5472.Can-06-3895 (2007).
239 Baracos, V. E., Reiman, T., Mourtzakis, M., Gioulbasanis, I. & Antoun, S. Body composition in patients with non-small cell lung cancer: a contemporary view of cancer cachexia with the use of computed tomography image analysis. *The American journal of clinical nutrition* **91**, 1133s-1137s, doi:10.3945/ajcn.2010.28608C (2010).
240 Cosper, P. F. & Leinwand, L. A. Cancer causes cardiac atrophy and autophagy in a sexually dimorphic manner. *Cancer research* **71**, 1710-1720, doi:10.1158/0008-5472.CAN-10-3145 (2011).
241 Misso, M. L. *et al.* Adipose aromatase gene expression is greater in older women and is unaffected by postmenopausal estrogen therapy. *Menopause (New York, N.Y.)* **12**, 210-215, doi:10.1097/00042192-200512020-00016 (2005).
242 Di, L. & Kerns, E. H. in *Drug-Like Properties (Second Edition)* (eds Li Di & Edward H. Kerns) 161-194 (Academic Press, 2016).
243 Kotov, A., Falany, J. L., Wang, J. & Falany, C. N. Regulation of estrogen activity by sulfation in human Ishikawa endometrial adenocarcinoma cells. *The Journal of steroid biochemistry and molecular biology* **68**, 137-144, doi:10.1016/s0960-0760(99)00022-9 (1999).
244 Xu, Y. *et al.* Effect of estrogen sulfation by SULT1E1 and PAPSS on the development of estrogen-dependent cancers. *Cancer Sci* **103**, 1000-1009, doi:10.1111/j.1349-7006.2012.02258.x (2012).
245 Matthews, J. & Gustafsson, J. A. Estrogen signaling: a subtle balance between ER alpha and ER beta. *Molecular interventions* **3**, 281-292, doi:10.1124/mi.3.5.281 (2003).
246 Paech, K. *et al.* Differential ligand activation of estrogen receptors ERalpha and ERbeta at AP1 sites. *Science* **277**, 1508-1510 (1997).
247 Foley, E. F., Jazaeri, A. A., Shupnik, M. A., Jazaeri, O. & Rice, L. W. Selective loss of estrogen receptor beta in malignant human colon. *Cancer Res* **60**, 245-248 (2000).
248 Caiazza, F., Ryan, E. J., Doherty, G., Winter, D. C. & Sheahan, K. Estrogen receptors and their implications in colorectal carcinogenesis. *Front Oncol* **5**, 19, doi:10.3389/fonc.2015.00019 (2015).

249 Revankar, C. M., Cimino, D. F., Sklar, L. A., Arterburn, J. B. & Prossnitz, E. R. A Transmembrane Intracellular Estrogen Receptor Mediates Rapid Cell Signaling. *Science* **307**, 1625, doi:10.1126/science.1106943 (2005).
250 Filardo, E. J. Epidermal growth factor receptor (EGFR) transactivation by estrogen via the G-protein-coupled receptor, GPR30: a novel signaling pathway with potential significance for breast cancer. *The Journal of steroid biochemistry and molecular biology* **80**, 231-238, doi:10.1016/s0960-0760(01)00190-x (2002).
251 Kumar, P. & Magon, N. Hormones in pregnancy. *Nigerian Medical Journal : Journal of the Nigeria Medical Association* **53**, 179-183, doi:10.4103/0300-1652.107549 (2012).
252 Reed, B. G. & Carr, B. R. in *Endotext* (eds L. J. De Groot *et al.*) (2000).
253 Tal, R., Taylor, H. S., Burney, R. O., Mooney, S. B. & Giudice, L. C. in *Endotext* (eds L. J. De Groot *et al.*) (2000).
254 Pedram, A., Razandi, M., Lewis, M., Hammes, S. & Levin, E. R. Membrane-localized estrogen receptor α is required for normal organ development and function. *Developmental cell* **29**, 482-490, doi:10.1016/j.devcel.2014.04.016 (2014).
255 Deroo, B. J. & Korach, K. S. Estrogen receptors and human disease. *J Clin Invest* **116**, 561-570, doi:10.1172/JCI27987 (2006).
256 Clocchiatti, A., Cora, E., Zhang, Y. & Dotto, G. P. Sexual dimorphism in cancer. *Nature Reviews Cancer* **16**, 330-339, doi:10.1038/nrc.2016.30 (2016).
257 Bakker, J. & Baum, M. J. Role for estradiol in female-typical brain and behavioral sexual differentiation. *Frontiers in neuroendocrinology* **29**, 1-16, doi:10.1016/j.yfrne.2007.06.001 (2008).
258 Do Rego, J. L. *et al.* Neurosteroid biosynthesis: enzymatic pathways and neuroendocrine regulation by neurotransmitters and neuropeptides. *Frontiers in neuroendocrinology* **30**, 259-301, doi:10.1016/j.yfrne.2009.05.006 (2009).
259 Frenkel, B. *et al.* Regulation of adult bone turnover by sex steroids. *J Cell Physiol* **224**, 305-310, doi:10.1002/jcp.22159 (2010).
260 Santen, R. J., Brodie, H., Simpson, E. R., Siiteri, P. K. & Brodie, A. History of aromatase: saga of an important biological mediator and therapeutic target. *Endocr Rev* **30**, 343-375, doi:10.1210/er.2008-0016 (2009).
261 Carreau, S., de Vienne, C. & Galeraud-Denis, I. Aromatase and estrogens in man reproduction: a review and latest advances. *Advances in medical sciences* **53**, 139-144, doi:10.2478/v10039-008-0022-z (2008).
262 O'Donnell, L., Robertson, K. M., Jones, M. E. & Simpson, E. R. Estrogen and spermatogenesis. *Endocr Rev* **22**, 289-318, doi:10.1210/edrv.22.3.0431 (2001).
263 Honda, S.-I., Wakatsuki, T. & Harada, N. Behavioral analysis of genetically modified mice indicates essential roles of neurosteroidal estrogen. *Front Endocrinol (Lausanne)* **2**, 40-40, doi:10.3389/fendo.2011.00040 (2011).
264 Cui, J., Shen, Y. & Li, R. Estrogen synthesis and signaling pathways during aging: from periphery to brain. *Trends Mol Med* **19**, 197-209, doi:10.1016/j.molmed.2012.12.007 (2013).

265 Malekinejad, H. & Rezabakhsh, A. Hormones in Dairy Foods and Their Impact on Public Health - A Narrative Review Article. *Iran J Public Health* **44**, 742-758 (2015).
266 Wise, A., O'Brien, K. & Woodruff, T. Are Oral Contraceptives a Significant Contributor to the Estrogenicity of Drinking Water? *Environmental Science & Technology* **45**, 51-60, doi:10.1021/es1014482 (2011).
267 Adeel, M., Song, X., Wang, Y., Francis, D. & Yang, Y. Environmental impact of estrogens on human, animal and plant life: A critical review. *Environment International* **99**, 107-119, doi:https://doi.org/10.1016/j.envint.2016.12.010 (2017).
268 Jobling, S. & Sumpter, J. P. Detergent components in sewage effluent are weakly oestrogenic to fish: An in vitro study using rainbow trout (Oncorhynchus mykiss) hepatocytes. *Aquatic Toxicology* **27**, 361-372, doi:https://doi.org/10.1016/0166-445X(93)90064-8 (1993).
269 Johnson, A. C., Williams, R. J. & Matthiessen, P. The potential steroid hormone contribution of farm animals to freshwaters, the United Kingdom as a case study. *The Science of the total environment* **362**, 166-178, doi:10.1016/j.scitotenv.2005.06.014 (2006).
270 Combalbert, S. & Hernandez-Raquet, G. Occurrence, fate, and biodegradation of estrogens in sewage and manure. *Applied microbiology and biotechnology* **86**, 1671-1692, doi:10.1007/s00253-010-2547-x (2010).
271 Lange, I. G. *et al.* Sex hormones originating from different livestock production systems: fate and potential disrupting activity in the environment. *Analytica Chimica Acta* **473**, 27-37, doi:https://doi.org/10.1016/S0003-2670(02)00748-1 (2002).
272 Remesar, X. *et al.* Estrone in food: a factor influencing the development of obesity? *European journal of nutrition* **38**, 247-253, doi:10.1007/s003940050068 (1999).
273 Aksglaede, L., Juul, A., Leffers, H., Skakkebaek, N. E. & Andersson, A. M. The sensitivity of the child to sex steroids: possible impact of exogenous estrogens. *Human reproduction update* **12**, 341-349, doi:10.1093/humupd/dml018 (2006).
274 Cutler, G. B., Jr. The role of estrogen in bone growth and maturation during childhood and adolescence. *The Journal of steroid biochemistry and molecular biology* **61**, 141-144 (1997).
275 Nichols, D. J., Daniel, T. C., Moore Jr., P. A., Edwards, D. R. & Pote, D. H. Runoff of Estrogen Hormone 17β-Estradiol from Poultry Litter Applied to Pasture. *Journal of Environmental Quality* **26**, 1002-1006, doi:10.2134/jeq1997.00472425002600040011x (1997).
276 Jobling, S. *et al.* Predicted exposures to steroid estrogens in U.K. rivers correlate with widespread sexual disruption in wild fish populations. *Environ Health Perspect* **114 Suppl 1**, 32-39, doi:10.1289/ehp.8050 (2006).
277 Hartmann, S., Lacorn, M. & Steinhart, H. Natural occurrence of steroid hormones in food. *Food Chemistry* **62**, 7-20, doi:https://doi.org/10.1016/S0308-8146(97)00150-7 (1998).
278 Maruyama, K., Oshima, T. & Ohyama, K. Exposure to exogenous estrogen through intake of commercial milk produced from pregnant cows. *Pediatrics*

*international : official journal of the Japan Pediatric Society* **52**, 33-38, doi:10.1111/j.1442-200X.2009.02890.x (2010).
279 Maruyama, K., Oshima, T. & Ohyama, K. Exposure to exogenous estrogen through intake of commercial milk produced from pregnant cows. *Pediatrics International* **52**, 33-38, doi:10.1111/j.1442-200x.2009.02890.x (2010).
280 Marques, P., Skorupskaite, K., George, J. T. & Anderson, R. A. in *Endotext* (eds K. R. Feingold *et al.*) (MDText.com, Inc., 2000).
281 Kim, K. *et al.* Dairy Food Intake Is Associated with Reproductive Hormones and Sporadic Anovulation among Healthy Premenopausal Women. *The Journal of nutrition* **147**, 218-226, doi:10.3945/jn.116.241521 (2017).
282 Souter, I. *et al.* The association of protein intake (amount and type) with ovarian antral follicle counts among infertile women: results from the EARTH prospective study cohort. *BJOG : an international journal of obstetrics and gynaecology* **124**, 1547-1555, doi:10.1111/1471-0528.14630 (2017).
283 Ganmaa, D., Cui, X., Feskanich, D., Hankinson, S. E. & Willett, W. C. Milk, dairy intake and risk of endometrial cancer: a 26-year follow-up. *International journal of cancer* **130**, 2664-2671, doi:10.1002/ijc.26265 (2012).
284 Nicholson, L. *et al.* Spatial and temporal control of gene expression in Drosophila using the inducible GeneSwitch GAL4 system. I. Screen for larval nervous system drivers. *Genetics* **178**, 215-234, doi:10.1534/genetics.107.081968 (2008).
285 Lee, T. & Luo, L. Mosaic analysis with a repressible cell marker for studies of gene function in neuronal morphogenesis. *Neuron* **22**, 451-461 (1999).
286 Cherbas, L., Hu, X., Zhimulev, I., Belyaeva, E. & Cherbas, P. EcR isoforms in Drosophila: testing tissue-specific requirements by targeted blockade and rescue. *Development* **130**, 271-284 (2003).
287 Mouillet, J. F., Henrich, V. C., Lezzi, M. & Vogtli, M. Differential control of gene activity by isoforms A, B1 and B2 of the Drosophila ecdysone receptor. *European journal of biochemistry* **268**, 1811-1819 (2001).
288 Kozlova, T. & Thummel, C. S. Spatial patterns of ecdysteroid receptor activation during the onset of Drosophila metamorphosis. *Development* **129**, 1739-1750 (2002).
289 Loza-Coll, M. A., Southall, T. D., Sandall, S. L., Brand, A. H. & Jones, D. L. Regulation of Drosophila intestinal stem cell maintenance and differentiation by the transcription factor Escargot. *The EMBO journal* **33**, 2983-2996, doi:10.15252/embj.201489050 (2014).
290 Koushika, S. P., Lisbin, M. J. & White, K. ELAV, a Drosophila neuron-specific protein, mediates the generation of an alternatively spliced neural protein isoform. *Curr Biol* **6**, 1634-1641, doi:10.1016/s0960-9822(02)70787-2 (1996).
291 Buchon, N., Broderick, N. A., Kuraishi, T. & Lemaitre, B. DrosophilaEGFR pathway coordinates stem cell proliferation and gut remodeling following infection. *BMC Biology* **8**, 152, doi:10.1186/1741-7007-8-152 (2010).
292 Tian, A., Wang, B. & Jiang, J. Injury-stimulated and self-restrained BMP signaling dynamically regulates stem cell pool size during <em>Drosophila</em> midgut regeneration. *Proceedings of the*

*National Academy of Sciences* **114**, E2699, doi:10.1073/pnas.1617790114 (2017).
293 Dutta, D. *et al.* Regional Cell-Specific Transcriptome Mapping Reveals Regulatory Complexity in the Adult Drosophila Midgut. *Cell Reports* **12**, 346-358, doi:https://doi.org/10.1016/j.celrep.2015.06.009 (2015).
294 Lucchetta, E. M. & Ohlstein, B. The Drosophila midgut: a model for stem cell driven tissue regeneration. *Wiley Interdiscip Rev Dev Biol* **1**, 781-788, doi:10.1002/wdev.51 (2012).
295 Zhang, P. *et al.* An SH3PX1-Dependent Endocytosis-Autophagy Network Restrains Intestinal Stem Cell Proliferation by Counteracting EGFR-ERK Signaling. *Dev Cell* **49**, 574-589.e575, doi:10.1016/j.devcel.2019.03.029 (2019).
296 Edgar, B. A. & O'Farrell, P. H. Genetic control of cell division patterns in the Drosophila embryo. *Cell* **57**, 177-187, doi:https://doi.org/10.1016/0092-8674(89)90183-9 (1989).
297 Bach, E. A. *et al.* GFP reporters detect the activation of the Drosophila JAK/STAT pathway in vivo. *Gene Expr Patterns* **7**, 323-331, doi:10.1016/j.modgep.2006.08.003 (2007).
298 Zhou, F., Rasmussen, A., Lee, S. & Agaisse, H. The UPD3 cytokine couples environmental challenge and intestinal stem cell division through modulation of JAK/STAT signaling in the stem cell microenvironment. *Developmental biology* **373**, 383-393, doi:10.1016/j.ydbio.2012.10.023 (2013).
299 Osman, D. *et al.* Autocrine and paracrine unpaired signaling regulate intestinal stem cell maintenance and division. *Journal of Cell Science* **125**, 5944, doi:10.1242/jcs.113100 (2012).
300 Schwedes, C. C. & Carney, G. E. Ecdysone signaling in adult Drosophila melanogaster. *J Insect Physiol* **58**, 293-302, doi:10.1016/j.jinsphys.2012.01.013 (2012).
301 Harshman, L. G., Loeb, A. M. & Johnson, B. A. Ecdysteroid titers in mated and unmated Drosophila melanogaster females. *J Insect Physiol* **45**, 571-577 (1999).
302 Ameku, T. & Niwa, R. Mating-Induced Increase in Germline Stem Cells via the Neuroendocrine System in Female Drosophila. *PLoS Genet* **12**, e1006123, doi:10.1371/journal.pgen.1006123 (2016).
303 Siudeja, K. *et al.* Frequent Somatic Mutation in Adult Intestinal Stem Cells Drives Neoplasia and Genetic Mosaicism during Aging. *Cell Stem Cell* **17**, 663-674, doi:10.1016/j.stem.2015.09.016 (2015).
304 Okamoto, N. *et al.* A Membrane Transporter Is Required for Steroid Hormone Uptake in Drosophila. *Dev Cell* **47**, 294-305 e297, doi:10.1016/j.devcel.2018.09.012 (2018).
305 Hudry, B. *et al.* Sex Differences in Intestinal Carbohydrate Metabolism Promote Food Intake and Sperm Maturation. *Cell* **178**, 901-918.e916, doi:10.1016/j.cell.2019.07.029 (2019).
306 Xia, Y., Midoun, S. Z., Xu, Z. & Hong, L. Heixuedian (heix), a potential melanotic tumor suppressor gene, exhibits specific spatial and temporal expression

pattern during Drosophila hematopoiesis. *Dev Biol* **398**, 218-230, doi:10.1016/j.ydbio.2014.12.001 (2015).
307 Rus, F. *et al.* Ecdysone triggered PGRP-LC expression controls Drosophila innate immunity. *The EMBO journal* **32**, 1626-1638, doi:10.1038/emboj.2013.100 (2013).
308 Flatt, T. *et al.* Hormonal regulation of the humoral innate immune response in Drosophila melanogaster. *The Journal of experimental biology* **211**, 2712-2724, doi:10.1242/jeb.014878 (2008).
309 Chen, C. H., Luhur, A. & Sokol, N. Lin-28 promotes symmetric stem cell division and drives adaptive growth in the adult Drosophila intestine. *Development* **142**, 3478-3487, doi:10.1242/dev.127951 (2015).
310 Khramtsova, E. A., Davis, L. K. & Stranger, B. E. The role of sex in the genomics of human complex traits. *Nat Rev Genet* **20**, 173-190, doi:10.1038/s41576-018-0083-1 (2019).
311 Reiff, T. *et al.* Endocrine remodelling of the adult intestine sustains reproduction in Drosophila. *Elife* **4**, e06930, doi:10.7554/eLife.06930 (2015).
312 Ono, H. *et al.* Spook and Spookier code for stage-specific components of the ecdysone biosynthetic pathway in Diptera. *Dev Biol* **298**, 555-570, doi:10.1016/j.ydbio.2006.07.023 (2006).
313 Kai, T. & Spradling, A. An empty Drosophila stem cell niche reactivates the proliferation of ectopic cells. *Proc Natl Acad Sci U S A* **100**, 4633-4638, doi:10.1073/pnas.0830856100 (2003).
314 Li, M. *et al.* Traffic jam regulates the function of the ovarian germline stem cell progeny differentiation niche during pre-adult stage in Drosophila. *Scientific Reports* **9**, 10124, doi:10.1038/s41598-019-45317-6 (2019).
315 Morris, L. X. & Spradling, A. C. Steroid signaling within Drosophila ovarian epithelial cells sex-specifically modulates early germ cell development and meiotic entry. *PloS one* **7**, e46109-e46109, doi:10.1371/journal.pone.0046109 (2012).
316 Jin, Y. *et al.* Intestinal Stem Cell Pool Regulation in Drosophila. *Stem Cell Reports* **8**, 1479-1487, doi:10.1016/j.stemcr.2017.04.002 (2017).
317 Pasco, M., Loudhaief, R. & Gallet, A. The cellular homeostasis of the gut: What the Drosophila model points out. *Histology and histopathology* **30**, doi:10.14670/HH-30.277 (2014).
318 Ohlstein, B. & Spradling, A. Multipotent Drosophila intestinal stem cells specify daughter cell fates by differential notch signaling. *Science (New York, N.Y.)* **315**, 988-992, doi:10.1126/science.1136606 (2007).
319 Bardin, A. J., Perdigoto, C. N., Southall, T. D., Brand, A. H. & Schweisguth, F. Transcriptional control of stem cell maintenance in the Drosophila intestine. *Development (Cambridge, England)* **137**, 705-714, doi:10.1242/dev.039404 (2010).
320 Lee, W. C., Beebe, K., Sudmeier, L. & Micchelli, C. A. Adenomatous polyposis coli regulates Drosophila intestinal stem cell proliferation. *Development (Cambridge, England)* **136**, 2255-2264, doi:10.1242/dev.035196 (2009).
321 Reinholz, J. *et al.* Compensatory weight gain due to dopaminergic hypofunction: new evidence and own incidental observations. *Nutr Metab (Lond)* **5**, 35-35, doi:10.1186/1743-7075-5-35 (2008).

322 Arango, V. *et al.* Serotonin 1A receptors, serotonin transporter binding and serotonin transporter mRNA expression in the brainstem of depressed suicide victims. *Neuropsychopharmacology : official publication of the American College of Neuropsychopharmacology* **25**, 892-903, doi:10.1016/s0893-133x(01)00310-4 (2001).
323 Speakman, J. R. The physiological costs of reproduction in small mammals. *Philos Trans R Soc Lond B Biol Sci* **363**, 375-398, doi:10.1098/rstb.2007.2145 (2008).
324 Meiselman, M. *et al.* Endocrine network essential for reproductive success in Drosophila melanogaster. *Proc Natl Acad Sci U S A* **114**, E3849-E3858, doi:10.1073/pnas.1620760114 (2017).
325 Meiselman, M. R., Kingan, T. G. & Adams, M. E. Stress-induced reproductive arrest in Drosophila occurs through ETH deficiency-mediated suppression of oogenesis and ovulation. *BMC Biol* **16**, 18, doi:10.1186/s12915-018-0484-9 (2018).
326 Church, R. B. & Robertson, F. W. A biochemical study of the growth of Drosophila melanogaster. *Journal of Experimental Zoology* **162**, 337-351, doi:10.1002/jez.1401620309 (1966).
327 Barnes, A. I., Wigby, S., Boone, J. M., Partridge, L. & Chapman, T. Feeding, fecundity and lifespan in female Drosophila melanogaster. *Proceedings of the Royal Society B: Biological Sciences* **275**, 1675-1683, doi:doi:10.1098/rspb.2008.0139 (2008).
328 Ikeya, T., Galic, M., Belawat, P., Nairz, K. & Hafen, E. Nutrient-Dependent Expression of Insulin-like Peptides from Neuroendocrine Cells in the CNS Contributes to Growth Regulation in Drosophila. *Current Biology* **12**, 1293-1300, doi:https://doi.org/10.1016/S0960-9822(02)01043-6 (2002).
329 Drummond-Barbosa, D. & Spradling, A. C. Stem Cells and Their Progeny Respond to Nutritional Changes during Drosophila Oogenesis. *Developmental Biology* **231**, 265-278, doi:https://doi.org/10.1006/dbio.2000.0135 (2001).
330 Su, Y.-H. *et al.* Diet regulates membrane extension and survival of niche escort cells for germline homeostasis via insulin signaling. *Development (Cambridge, England)* **145**, dev159186, doi:10.1242/dev.159186 (2018).
331 Hall, B. L. & Thummel, C. S. The RXR homolog ultraspiracle is an essential component of the Drosophila ecdysone receptor. *Development* **125**, 4709 (1998).
332 Buszczak, M. & Segraves, W. A. Drosophila metamorphosis: the only way is USP? *Curr Biol* **8**, R879-882 (1998).
333 Evans, R. M. & Mangelsdorf, D. J. Nuclear Receptors, RXR, and the Big Bang. *Cell* **157**, 255-266, doi:10.1016/j.cell.2014.03.012 (2014).
334 Safe, S. *et al.* Nuclear receptor 4A (NR4A) family - orphans no more. *J Steroid Biochem Mol Biol* **157**, 48-60, doi:10.1016/j.jsbmb.2015.04.016 (2016).
335 Baker, K. D. *et al.* The Drosophila orphan nuclear receptor DHR38 mediates an atypical ecdysteroid signaling pathway. *Cell* **113**, 731-742 (2003).
336 Kozlova, T. *et al.* Drosophila hormone receptor 38 functions in metamorphosis: a role in adult cuticle formation. *Genetics* **149**, 1465-1475 (1998).

337 Sutherland, J. D., Kozlova, T., Tzertzinis, G. & Kafatos, F. C. Drosophila hormone receptor 38: a second partner for Drosophila USP suggests an unexpected role for nuclear receptors of the nerve growth factor-induced protein B type. *Proc Natl Acad Sci U S A* **92**, 7966-7970 (1995).
338 Bilder, D. & Scott, M. P. Genomic regions required for morphogenesis of the Drosophila embryonic midgut. *Genetics* **141**, 1087-1100 (1995).
339 Ruaud, A. F., Lam, G. & Thummel, C. S. The Drosophila nuclear receptors DHR3 and betaFTZ-F1 control overlapping developmental responses in late embryos. *Development* **137**, 123-131, doi:10.1242/dev.042036 (2010).
340 Buszczak, M. *et al.* Ecdysone response genes govern egg chamber development during mid-oogenesis in Drosophila. *Development* **126**, 4581-4589 (1999).
341 Tzolovsky, G., Deng, W. M., Schlitt, T. & Bownes, M. The function of the broad-complex during Drosophila melanogaster oogenesis. *Genetics* **153**, 1371-1383 (1999).
342 Zipper, L., Jassmann, D., Görlich, B. & Reiff, T. Ecdysone steroid hormone remote controls intestinal stem cell fate decisions via the <em>PPARγ</em>-homologue <em>E75B</em> in <em>Drosophila</em&gt. *bioRxiv*, 2020.2002.2024.962829, doi:10.1101/2020.02.24.962829 (2020).
343 Jaumouillé, E., Machado Almeida, P., Stähli, P., Koch, R. & Nagoshi, E. Transcriptional Regulation via Nuclear Receptor Crosstalk Required for the Drosophila Circadian Clock. *Current Biology* **25**, 1502-1508, doi:https://doi.org/10.1016/j.cub.2015.04.017 (2015).
344 Biteau, B., Karpac, J., Hwangbo, D. & Jasper, H. Regulation of Drosophila lifespan by JNK signaling. *Exp Gerontol* **46**, 349-354, doi:10.1016/j.exger.2010.11.003 (2011).
345 Martorell, O. *et al.* Conserved mechanisms of tumorigenesis in the Drosophila adult midgut. *PLoS One* **9**, e88413, doi:10.1371/journal.pone.0088413 (2014).
346 Patel, P. H., Dutta, D. & Edgar, B. A. Niche appropriation by Drosophila intestinal stem cell tumours. *Nat Cell Biol* **17**, 1182-1192, doi:10.1038/ncb3214 (2015).
347 Yamamoto, R., Bai, H., Dolezal, A. G., Amdam, G. & Tatar, M. Juvenile hormone regulation of Drosophila aging. *BMC Biol* **11**, 85, doi:10.1186/1741-7007-11-85 (2013).
348 Hackney, J. F., Pucci, C., Naes, E. & Dobens, L. Ras signaling modulates activity of the ecdysone receptor EcR during cell migration in the Drosophila ovary. *Dev Dyn* **236**, 1213-1226, doi:10.1002/dvdy.21140 (2007).
349 Zhai, Z. *et al.* Accumulation of differentiating intestinal stem cell progenies drives tumorigenesis. *Nature communications* **6**, 10219, doi:10.1038/ncomms10219 (2015).
350 Brumby, A. M. *et al.* Identification of novel Ras-cooperating oncogenes in Drosophila melanogaster: a RhoGEF/Rho-family/JNK pathway is a central driver of tumorigenesis. *Genetics* **188**, 105-125, doi:10.1534/genetics.111.127910 (2011).

351 Fowler, P. A., Sorsa-Leslie, T., Harris, W. & Mason, H. D. Ovarian gonadotrophin surge-attenuating factor (GnSAF): where are we after 20 years of research? *Reproduction* **126**, 689-699 (2003).
352 McBrayer, Z. *et al.* Prothoracicotropic hormone regulates developmental timing and body size in Drosophila. *Dev Cell* **13**, 857-871, doi:10.1016/j.devcel.2007.11.003 (2007).
353 JavanMoghadam, S., Weihua, Z., Hunt, K. K. & Keyomarsi, K. Estrogen receptor alpha is cell cycle-regulated and regulates the cell cycle in a ligand-dependent fashion. *Cell Cycle* **15**, 1579-1590, doi:10.1080/15384101.2016.1166327 (2016).
354 Dalvai, M. & Bystricky, K. Cell Cycle and Anti-Estrogen Effects Synergize to Regulate Cell Proliferation and ER Target Gene Expression. *PLOS ONE* **5**, e11011, doi:10.1371/journal.pone.0011011 (2010).
355 Moghadam, S. J., Hanks, A. M. & Keyomarsi, K. Breaking the cycle: An insight into the role of ERα in eukaryotic cell cycles. *Journal of carcinogenesis* **10**, 25, doi:10.4103/1477-3163.90440 (2011).
356 Groothuis, P. G., Dassen, H. H. N. M., Romano, A. & Punyadeera, C. Estrogen and the endometrium: lessons learned from gene expression profiling in rodents and human. *Human Reproduction Update* **13**, 405-417, doi:10.1093/humupd/dmm009 (2007).
357 Frasor, J. *et al.* Profiling of Estrogen Up- and Down-Regulated Gene Expression in Human Breast Cancer Cells: Insights into Gene Networks and Pathways Underlying Estrogenic Control of Proliferation and Cell Phenotype. *Endocrinology* **144**, 4562-4574, doi:10.1210/en.2003-0567 (2003).
358 Improta-Brears, T. *et al.* Estrogen-induced activation of mitogen-activated protein kinase requires mobilization of intracellular calcium. *Proceedings of the National Academy of Sciences of the United States of America* **96**, 4686-4691, doi:10.1073/pnas.96.8.4686 (1999).
359 Sun, J. & Spradling, A. C. Ovulation in Drosophila is controlled by secretory cells of the female reproductive tract. *Elife* **2**, e00415, doi:10.7554/eLife.00415 (2013).
360 Hammond, K. A. Adaptation of the maternal intestine during lactation. *J Mammary Gland Biol Neoplasia* **2**, 243-252 (1997).
361 Thomas, M. L., Xu, X., Norfleet, A. M. & Watson, C. S. The presence of functional estrogen receptors in intestinal epithelial cells. *Endocrinology* **132**, 426-430, doi:10.1210/endo.132.1.8419141 (1993).
362 van der Giessen, J., van der Woude, C. J., Peppelenbosch, M. P. & Fuhler, G. M. A Direct Effect of Sex Hormones on Epithelial Barrier Function in Inflammatory Bowel Disease Models. *Cells* **8**, 261, doi:10.3390/cells8030261 (2019).
363 Gan, L. *et al.* Expression profile and prognostic role of sex hormone receptors in gastric cancer. *BMC Cancer* **12**, 566, doi:10.1186/1471-2407-12-566 (2012).
364 Cho, N. L., Javid, S. H., Carothers, A. M., Redston, M. & Bertagnolli, M. M. Estrogen receptors alpha and beta are inhibitory modifiers of Apc-dependent tumorigenesis in the proximal colon of Min/+ mice. *Cancer Res* **67**, 2366-2372, doi:10.1158/0008-5472.CAN-06-3026 (2007).

365 Wada-Hiraike, O. *et al.* Role of estrogen receptor β in colonic epithelium. *Proceedings of the National Academy of Sciences of the United States of America* **103**, 2959-2964, doi:10.1073/pnas.0511271103 (2006).
366 Tuo, B. *et al.* Estrogen regulation of duodenal bicarbonate secretion and sex-specific protection of human duodenum. *Gastroenterology* **141**, 854-863, doi:10.1053/j.gastro.2011.05.044 (2011).
367 Smith, A. *et al.* Gender-specific protection of estrogen against gastric acid-induced duodenal injury: stimulation of duodenal mucosal bicarbonate secretion. *Endocrinology* **149**, 4554-4566, doi:10.1210/en.2007-1597 (2008).
368 Zielińska, M. *et al.* G protein-coupled estrogen receptor and estrogen receptor ligands regulate colonic motility and visceral pain. *Neurogastroenterology & Motility* **29**, e13025, doi:10.1111/nmo.13025 (2017).
369 Ropero, A. B., Alonso-Magdalena, P., Quesada, I. & Nadal, A. The role of estrogen receptors in the control of energy and glucose homeostasis. *Steroids* **73**, 874-879, doi:10.1016/j.steroids.2007.12.018 (2008).
370 Delanoue, R., Slaidina, M. & Léopold, P. The steroid hormone ecdysone controls systemic growth by repressing dMyc function in Drosophila fat cells. *Dev Cell* **18**, 1012-1021, doi:10.1016/j.devcel.2010.05.007 (2010).
371 Heijmans, J. *et al.* Oestrogens promote tumorigenesis in a mouse model for colitis-associated cancer. *Gut* **63**, 310-316, doi:10.1136/gutjnl-2012-304216 (2014).
372 Basu, A., Seth, S., Arora, K. & Verma, M. Evaluating Estradiol Levels in Male Patients with Colorectal Carcinoma. *Journal of Clinical and Diagnostic Research : JCDR* **9**, BC08-BC10, doi:10.7860/JCDR/2015/10508.5397 (2015).
373 Wu, H. *et al.* Association of estrogen receptor betavariants and serum levels of estradiol with risk of colorectal cancer: a case control study. *BMC Cancer* **12**, 276, doi:10.1186/1471-2407-12-276 (2012).
374 Gunter, M. J. *et al.* Insulin, insulin-like growth factor-I, endogenous estradiol, and risk of colorectal cancer in postmenopausal women. *Cancer Res* **68**, 329-337, doi:10.1158/0008-5472.Can-07-2946 (2008).
375 Glinkova, V., Shevah, O., Boaz, M., Levine, A. & Shirin, H. Hepatic haemangiomas: possible association with female sex hormones. *Gut* **53**, 1352-1355, doi:10.1136/gut.2003.038646 (2004).
376 Giannitrapani, L. *et al.* Sex hormones and risk of liver tumor. *Annals of the New York Academy of Sciences* **1089**, 228-236, doi:10.1196/annals.1386.044 (2006).
377 Howard, J. H. & Pollock, R. E. Intra-Abdominal and Abdominal Wall Desmoid Fibromatosis. *Oncology and Therapy* **4**, 57-72, doi:10.1007/s40487-016-0017-z (2016).
378 Di Leo, A. *et al.* Epithelial turnover in duodenal familial adenomatous polyposis: A possible role for estrogen receptors? *World Journal of Gastroenterology* **22**, 3202-3211, doi:10.3748/wjg.v22.i11.3202 (2016).
379 Mignemi, N. A. *et al.* Signal transduction pathway analysis in desmoid‐type fibromatosis: Transforming growth factor–β, COX2 and sex steroid receptors. *Cancer Science* **103**, 2173-2180, doi:10.1111/cas.12037 (2012).

380 English, M. A. *et al.* Loss of estrogen inactivation in colonic cancer. *J Clin Endocrinol Metab* **84**, 2080-2085, doi:10.1210/jcem.84.6.5772 (1999).
381 Sato, R. *et al.* Aromatase in colon carcinoma. *Anticancer research* **32**, 3069-3075 (2012).
382 Gilligan, L. C. *et al.* Estrogen Activation by Steroid Sulfatase Increases Colorectal Cancer Proliferation via GPER. *The Journal of Clinical Endocrinology & Metabolism* **102**, 4435-4447, doi:10.1210/jc.2016-3716 (2017).
383 Charlton, B. M. *et al.* Oral Contraceptive Use and Colorectal Cancer in the Nurses' Health Study I and II. *Cancer epidemiology, biomarkers & prevention : a publication of the American Association for Cancer Research, cosponsored by the American Society of Preventive Oncology* **24**, 1214-1221, doi:10.1158/1055-9965.EPI-15-0172 (2015).
384 Chlebowski, R. T. *et al.* Estrogen plus progestin and colorectal cancer in postmenopausal women. *The New England journal of medicine* **350**, 991-1004, doi:10.1056/NEJMoa032071 (2004).
385 Foster, P. A. Oestrogen and colorectal cancer: mechanisms and controversies. *International journal of colorectal disease* **28**, 737-749, doi:10.1007/s00384-012-1628-y (2013).
386 Gunter, M. J. *et al.* Insulin, insulin-like growth factor-I, endogenous estradiol, and risk of colorectal cancer in postmenopausal women. *Cancer research* **68**, 329-337, doi:10.1158/0008-5472.CAN-07-2946 (2008).
387 Oduwole, O. O., Isomaa, V. V., Nokelainen, P. A., Stenbäck, F. & Vihko, P. T. Downregulation of estrogen-metabolizing 17 beta-hydroxysteroid dehydrogenase type 2 expression correlates inversely with Ki67 proliferation marker in colon-cancer development. *International journal of cancer* **97**, 1-6, doi:10.1002/ijc.1567 (2002).
388 Rawłuszko, A. A., Horbacka, K., Krokowicz, P. & Jagodziński, P. P. Decreased expression of 17β-hydroxysteroid dehydrogenase type 1 is associated with DNA hypermethylation in colorectal cancer located in the proximal colon. *BMC cancer* **11**, 522-522, doi:10.1186/1471-2407-11-522 (2011).
389 Hennessy, B. A., Harvey, B. J. & Healy, V. 17beta-Estradiol rapidly stimulates c-fos expression via the MAPK pathway in T84 cells. *Mol Cell Endocrinol* **229**, 39-47, doi:10.1016/j.mce.2004.10.001 (2005).
390 Di Domenico, M., Castoria, G., Bilancio, A., Migliaccio, A. & Auricchio, F. Estradiol activation of human colon carcinoma-derived Caco-2 cell growth. *Cancer Res* **56**, 4516-4521 (1996).
391 Winter, D. C., Taylor, C., G, C. O. S. & Harvey, B. J. Mitogenic effects of oestrogen mediated by a non-genomic receptor in human colon. *The British journal of surgery* **87**, 1684-1689, doi:10.1046/j.1365-2168.2000.01584.x (2000).
392 Di Leo, A. *et al.* Epithelial turnover in duodenal familial adenomatous polyposis: A possible role for estrogen receptors? *World J Gastroenterol* **22**, 3202-3211, doi:10.3748/wjg.v22.i11.3202 (2016).
393 Bustos, V. *et al.* GPER mediates differential effects of estrogen on colon cancer cell proliferation and migration under normoxic and hypoxic conditions. *Oncotarget* **8**, 84258-84275, doi:10.18632/oncotarget.20653 (2017).

394 Saraf, M. K., Jeng, Y. J. & Watson, C. S. Nongenomic effects of estradiol vs. the birth control estrogen ethinyl estradiol on signaling and cell proliferation in pituitary tumor cells, and differences in the ability of R-equol to neutralize or enhance these effects. *Steroids*, 108411, doi:10.1016/j.steroids.2019.01.008 (2019).
395 Rahman, M. M., Franch-Marro, X., Maestro, J. L., Martin, D. & Casali, A. Local Juvenile Hormone activity regulates gut homeostasis and tumor growth in adult Drosophila. *Sci Rep* **7**, 11677, doi:10.1038/s41598-017-11199-9 (2017).
396 Dubrovsky, E. B. *et al.* The Drosophila FTZ-F1 nuclear receptor mediates juvenile hormone activation of E75A gene expression through an intracellular pathway. *J Biol Chem* **286**, 33689-33700, doi:10.1074/jbc.M111.273458 (2011).
397 Dubrovskaya, V. A., Berger, E. M. & Dubrovsky, E. B. Juvenile hormone regulation of the E75 nuclear receptor is conserved in Diptera and Lepidoptera. *Gene* **340**, 171-177, doi:10.1016/j.gene.2004.07.022 (2004).
398 Pecasse, F., Beck, Y., Ruiz, C. & Richards, G. Krüppel-homolog, a Stage-Specific Modulator of the Prepupal Ecdysone Response, Is Essential for Drosophila Metamorphosis. *Developmental Biology* **221**, 53-67, doi:https://doi.org/10.1006/dbio.2000.9687 (2000).
399 D'Cruz, C. *et al.* Persistent parity-induced changes in growth factors, TGF-beta 3, and differentiation in the rodent mammary gland. *Molecular endocrinology (Baltimore, Md.)* **16**, 2034-2051, doi:10.1210/me.2002-0073 (2002).
400 Ginger, M. R. & Rosen, J. M. Pregnancy-induced changes in cell-fate in the mammary gland. *Breast Cancer Res* **5**, 192-197, doi:10.1186/bcr603 (2003).
401 Oro, A. E., McKeown, M. & Evans, R. M. The Drosophila retinoid X receptor homolog ultraspiracle functions in both female reproduction and eye morphogenesis. *Development (Cambridge, England)* **115**, 449-462 (1992).
402 Costantino, B. F. *et al.* A novel ecdysone receptor mediates steroid-regulated developmental events during the mid-third instar of Drosophila. *PLoS Genet* **4**, e1000102, doi:10.1371/journal.pgen.1000102 (2008).
403 Ruaud, A. F., Lam, G. & Thummel, C. S. The Drosophila NR4A nuclear receptor DHR38 regulates carbohydrate metabolism and glycogen storage. *Mol Endocrinol* **25**, 83-91, doi:10.1210/me.2010-0337 (2011).
404 Kozlova, T., Lam, G. & Thummel, C. S. Drosophila DHR38 nuclear receptor is required for adult cuticle integrity at eclosion. *Developmental dynamics : an official publication of the American Association of Anatomists* **238**, 701-707, doi:10.1002/dvdy.21860 (2009).
405 Hall, B. L. & Thummel, C. S. The RXR homolog ultraspiracle is an essential component of the Drosophila ecdysone receptor. *Development* **125**, 4709-4717 (1998).
406 De Mei, C. *et al.* Dual inhibition of REV-ERBβ and autophagy as a novel pharmacological approach to induce cytotoxicity in cancer cells. *Oncogene* **34**, 2597, doi:10.1038/onc.2014.203
https://www.nature.com/articles/onc2014203#supplementary-information (2014).

407 Cho, H. *et al.* Regulation of circadian behaviour and metabolism by REV-ERB-alpha and REV-ERB-beta. *Nature* **485**, 123-127, doi:10.1038/nature11048 (2012).
408 Jaumouillé, E., Machado Almeida, P., Stähli, P., Koch, R. & Nagoshi, E. Transcriptional regulation via nuclear receptor crosstalk required for the Drosophila circadian clock. *Curr Biol* **25**, 1502-1508, doi:10.1016/j.cub.2015.04.017 (2015).
409 Pardee, K., Reinking, J. & Krause, H. Nuclear hormone receptors, metabolism, and aging: what goes around comes around. Transcription factors link lipid metabolism and aging-related processes. *Sci Aging Knowledge Environ* **2004**, re8, doi:10.1126/sageke.2004.47.re8 (2004).
410 Schulman, I. G. Nuclear Receptors as Drug Targets for Metabolic Disease. *Advanced drug delivery reviews* **62**, 1307-1315, doi:10.1016/j.addr.2010.07.002 (2010).
411 Calkin, A. C. & Tontonoz, P. Transcriptional integration of metabolism by the nuclear sterol-activated receptors LXR and FXR. *Nature Reviews Molecular Cell Biology* **13**, 213, doi:10.1038/nrm3312 (2012).
412 Kojetin, D. J. & Burris, T. P. REV-ERB and ROR nuclear receptors as drug targets. *Nature Reviews Drug Discovery* **13**, 197, doi:10.1038/nrd4100 (2014).
413 Lonard, D. M. & O'Malley, B. W. Nuclear receptor coregulators: modulators of pathology and therapeutic targets. *Nature Reviews Endocrinology* **8**, 598, doi:10.1038/nrendo.2012.100 (2012).
414 Ou, Q. *et al.* The Insect Prothoracic Gland as a Model for Steroid Hormone Biosynthesis and Regulation. *Cell Rep* **16**, 247-262, doi:10.1016/j.celrep.2016.05.053 (2016).
415 Llorens, J. V., Metzendorf, C., Missirlis, F. & Lind, M. I. Mitochondrial iron supply is required for the developmental pulse of ecdysone biosynthesis that initiates metamorphosis in Drosophila melanogaster. *J Biol Inorg Chem* **20**, 1229-1238, doi:10.1007/s00775-015-1302-2 (2015).
416 Palandri, A., L'Hote, D., Cohen-Tannoudji, J., Tricoire, H. & Monnier, V. Frataxin inactivation leads to steroid deficiency in flies and human ovarian cells. *Hum Mol Genet* **24**, 2615-2626, doi:10.1093/hmg/ddv024 (2015).
417 Khramtsova, E. A., Davis, L. K. & Stranger, B. E. The role of sex in the genomics of human complex traits. *Nature Reviews Genetics* **20**, 173-190, doi:10.1038/s41576-018-0083-1 (2019).
418 Jansen, R. *et al.* Sex differences in the human peripheral blood transcriptome. *BMC genomics* **15**, 33, doi:10.1186/1471-2164-15-33 (2014).
419 Ngo, S. T., Steyn, F. J. & McCombe, P. A. Gender differences in autoimmune disease. *Frontiers in neuroendocrinology* **35**, 347-369, doi:10.1016/j.yfrne.2014.04.004 (2014).
420 Mayne, B. T. *et al.* Large Scale Gene Expression Meta-Analysis Reveals Tissue-Specific, Sex-Biased Gene Expression in Humans. *Frontiers in genetics* **7**, 183, doi:10.3389/fgene.2016.00183 (2016).
421 Manning, K. S. & Cooper, T. A. The roles of RNA processing in translating genotype to phenotype. *Nature reviews. Molecular cell biology* **18**, 102-114, doi:10.1038/nrm.2016.139 (2017).

422 Li, Y. I. *et al.* RNA splicing is a primary link between genetic variation and disease. *Science* **352**, 600-604, doi:10.1126/science.aad9417 (2016).
423 Hamosh, A., Scott, A. F., Amberger, J., Valle, D. & McKusick, V. A. Online Mendelian Inheritance in Man (OMIM). *Human mutation* **15**, 57-61, doi:10.1002/(sici)1098-1004(200001)15:1<57::Aid-humu12>3.0.Co;2-g (2000).
424 Vasanthakumar, A. *et al.* Sex-specific adipose tissue imprinting of regulatory T cells. *Nature* **579**, 581-585, doi:10.1038/s41586-020-2040-3 (2020).
425 Chen, C.-Y. *et al.* Sexual dimorphism in gene expression and regulatory networks across human tissues. *bioRxiv*, 082289, doi:10.1101/082289 (2016).
426 Stranger, B. E. & Raj, T. Genetics of human gene expression. *Current opinion in genetics & development* **23**, 627-634, doi:10.1016/j.gde.2013.10.004 (2013).
427 Kukurba, K. R. *et al.* Impact of the X Chromosome and sex on regulatory variation. *Genome research* **26**, 768-777, doi:10.1101/gr.197897.115 (2016).
428 Singmann, P. *et al.* Characterization of whole-genome autosomal differences of DNA methylation between men and women. *Epigenetics & chromatin* **8**, 43, doi:10.1186/s13072-015-0035-3 (2015).
429 van Dongen, J. *et al.* Genetic and environmental influences interact with age and sex in shaping the human methylome. *Nature communications* **7**, 11115, doi:10.1038/ncomms11115 (2016).
430 Ma, Y., Chen, Z., Jin, Y. & Liu, W. Identification of a histone acetyltransferase as a novel regulator of Drosophila intestinal stem cells. *FEBS Lett* **587**, 1489-1495, doi:10.1016/j.febslet.2013.03.013 (2013).
431 Suganuma, T. *et al.* ATAC is a double histone acetyltransferase complex that stimulates nucleosome sliding. *Nature structural & molecular biology* **15**, 364-372, doi:10.1038/nsmb.1397 (2008).
432 Guelman, S. *et al.* Host cell factor and an uncharacterized SANT domain protein are stable components of ATAC, a novel dAda2A/dGcn5-containing histone acetyltransferase complex in Drosophila. *Molecular and cellular biology* **26**, 871-882, doi:10.1128/mcb.26.3.871-882.2006 (2006).
433 Feller, C., Forné, I., Imhof, A. & Becker, P. B. Global and specific responses of the histone acetylome to systematic perturbation. *Mol Cell* **57**, 559-571, doi:10.1016/j.molcel.2014.12.008 (2015).
434 Suganuma, T. *et al.* The ATAC acetyltransferase complex coordinates MAP kinases to regulate JNK target genes. *Cell* **142**, 726-736, doi:10.1016/j.cell.2010.07.045 (2010).
435 Sugathan, A. & Waxman, D. J. Genome-wide analysis of chromatin states reveals distinct mechanisms of sex-dependent gene regulation in male and female mouse liver. *Molecular and cellular biology* **33**, 3594-3610, doi:10.1128/mcb.00280-13 (2013).
436 Zhang, Y., Laz, E. V. & Waxman, D. J. Dynamic, Sex-Differential STAT5 and BCL6 Binding to Sex-Biased, Growth Hormone-Regulated Genes in Adult Mouse Liver. *Molecular and cellular biology* **32**, 880-896, doi:10.1128/mcb.06312-11 (2012).
437 Ling, G., Sugathan, A., Mazor, T., Fraenkel, E. & Waxman, D. J. Unbiased, genome-wide in vivo mapping of transcriptional regulatory elements reveals

sex differences in chromatin structure associated with sex-specific liver gene expression. *Molecular and cellular biology* **30**, 5531-5544, doi:10.1128/MCB.00601-10 (2010).

438 Ling, G., Sugathan, A., Mazor, T., Fraenkel, E. & Waxman, D. J. Unbiased, genome-wide in vivo mapping of transcriptional regulatory elements reveals sex differences in chromatin structure associated with sex-specific liver gene expression. *Molecular and cellular biology* **30**, 5531-5544, doi:10.1128/mcb.00601-10 (2010).

439 Clegg, D. J., Brown, L. M., Woods, S. C. & Benoit, S. C. Gonadal hormones determine sensitivity to central leptin and insulin. *Diabetes* **55**, 978-987, doi:10.2337/diabetes.55.04.06.db05-1339 (2006).

440 Björnholm, M. & Zierath, J. R. Insulin signal transduction in human skeletal muscle: identifying the defects in Type II diabetes. *Biochemical Society transactions* **33**, 354-357, doi:10.1042/bst0330354 (2005).

441 Yang, M. *et al.* Lin28 promotes the proliferative capacity of neural progenitor cells in brain development. *Development* **142**, 1616, doi:10.1242/dev.120543 (2015).

442 Cimadamore, F., Amador-Arjona, A., Chen, C., Huang, C.-T. & Terskikh, A. V. SOX2–LIN28/let-7 pathway regulates proliferation and neurogenesis in neural precursors. *Proceedings of the National Academy of Sciences* **110**, E3017, doi:10.1073/pnas.1220176110 (2013).

443 Zheng, K., Wu, X., Kaestner, K. H. & Wang, P. J. The pluripotency factor LIN28 marks undifferentiated spermatogonia in mouse. *BMC Developmental Biology* **9**, 38, doi:10.1186/1471-213X-9-38 (2009).

444 Zhu, H. *et al.* The Lin28/let-7 axis regulates glucose metabolism. *Cell* **147**, 81-94, doi:10.1016/j.cell.2011.08.033 (2011).

445 Shyh-Chang, N. *et al.* Lin28 enhances tissue repair by reprogramming cellular metabolism. *Cell* **155**, 778-792, doi:10.1016/j.cell.2013.09.059 (2013).

446 Rajan, A. & Perrimon, N. Drosophila cytokine unpaired 2 regulates physiological homeostasis by remotely controlling insulin secretion. *Cell* **151**, 123-137, doi:10.1016/j.cell.2012.08.019 (2012).

447 Kelesidis, T., Kelesidis, I., Chou, S. & Mantzoros, C. S. Narrative review: the role of leptin in human physiology: emerging clinical applications. *Ann Intern Med* **152**, 93-100, doi:10.7326/0003-4819-152-2-201001190-00008 (2010).

448 Piper, M. D., Partridge, L., Raubenheimer, D. & Simpson, S. J. Dietary restriction and aging: a unifying perspective. *Cell metabolism* **14**, 154-160, doi:10.1016/j.cmet.2011.06.013 (2011).

449 O'Brien, D. M., Min, K.-J., Larsen, T. & Tatar, M. Use of stable isotopes to examine how dietary restriction extends Drosophila lifespan. *Current biology : CB* **18**, R155-156, doi:10.1016/j.cub.2008.01.021 (2008).

450 Flatt, T. *et al.* Drosophila germ-line modulation of insulin signaling and lifespan. *Proceedings of the National Academy of Sciences of the United States of America* **105**, 6368-6373, doi:10.1073/pnas.0709128105 (2008).

451 Cargill, S. L., Carey, J. R., Müller, H. G. & Anderson, G. Age of ovary determines remaining life expectancy in old ovariectomized mice. *Aging cell* **2**, 185-190, doi:10.1046/j.1474-9728.2003.00049.x (2003).

452 Arantes-Oliveira, N., Apfeld, J., Dillin, A. & Kenyon, C. Regulation of life-span by germ-line stem cells in Caenorhabditis elegans. *Science* **295**, 502-505, doi:10.1126/science.1065768 (2002).
453 Beckstead, R. B. & Thummel, C. S. Indicted: Worms Caught using Steroids. **124**, 1137-1140, doi:10.1016/j.cell.2006.03.001 (2006).
454 Wollam, J. *et al.* A novel 3-hydroxysteroid dehydrogenase that regulates reproductive development and longevity. *PLoS biology* **10**, e1001305, doi:10.1371/journal.pbio.1001305 (2012).
455 Wang, M. C., O'Rourke, E. J. & Ruvkun, G. Fat metabolism links germline stem cells and longevity in C. elegans. *Science* **322**, 957-960, doi:10.1126/science.1162011 (2008).
456 Libina, N., Berman, J. R. & Kenyon, C. Tissue-specific activities of C. elegans DAF-16 in the regulation of lifespan. *Cell* **115**, 489-502, doi:10.1016/s0092-8674(03)00889-4 (2003).
457 Lin, C.-c. J. & Wang, M. C. in *Stem Cell Aging: Mechanisms, Consequences, Rejuvenation* (eds Hartmut Geiger, Heinrich Jasper, & Maria Carolina Florian) 51-70 (Springer Vienna, 2015).
458 Willcox, B. J. *et al.* FOXO3A genotype is strongly associated with human longevity. *Proc Natl Acad Sci U S A* **105**, 13987-13992, doi:10.1073/pnas.0801030105 (2008).
459 Flachsbart, F. *et al.* Association of FOXO3A variation with human longevity confirmed in German centenarians. *Proc Natl Acad Sci U S A* **106**, 2700-2705, doi:10.1073/pnas.0809594106 (2009).
460 Agaisse, H., Petersen, U.-M., Boutros, M., Mathey-Prevot, B. & Perrimon, N. Signaling Role of Hemocytes in Drosophila JAK/STAT-Dependent Response to Septic Injury. *Developmental Cell* **5**, 441-450, doi:https://doi.org/10.1016/S1534-5807(03)00244-2 (2003).
461 Han, S. K. *et al.* OASIS 2: online application for survival analysis 2 with features for the analysis of maximal lifespan and healthspan in aging research. *Oncotarget* **7**, 56147-56152, doi:10.18632/oncotarget.11269 (2016).
462 Schindelin, J. *et al.* Fiji: an open-source platform for biological-image analysis. *Nature methods* **9**, 676-682, doi:10.1038/nmeth.2019 (2012).
463 Liang, J., Balachandra, S., Ngo, S. & O'Brien, L. E. Feedback regulation of steady-state epithelial turnover and organ size. *Nature* **548**, 588-591, doi:10.1038/nature23678 (2017).

464 Where it is indicated, parts of this work were done during my thesis study titled: A novel perspective of regenerative stem cell biology: the role of Ecdysone-induced protein 75B (Eip75B) and its upstream regulators in directing the decisions of intestinal stem cells in homeostasis and regeneration of Drosophila midgut and presented to: Faculty of Biosciences at the Ruprecht-Karls-Universität Heidelberg in 2015.

# Tables

**Table 2.1a: list of genes differentially upregulated in control males relative to control females**

| list of hits>10 raw reads | log2FC edgeR | p-value edgeR | -log10(pvalue) |
|---|---|---|---|
| roX2 | 10.3968 | 3.43E-20 | 19.46470588 |
| CR43961 | 9.6857 | 1.36E-15 | 14.86646109 |
| hbs | 5.2622 | 4.35E-14 | 13.36151074 |
| CG12721 | 6.8849 | 3.43E-12 | 11.46470588 |
| CG3703 | 2.7943 | 2.13E-11 | 10.6716204 |
| CG43101 | 5.0713 | 1.47E-10 | 9.832682665 |
| lin-28 | 2.2286 | 1.67E-08 | 7.777283529 |
| CG42854 | 5.3013 | 7.13E-08 | 7.14691047 |
| CG31436 | 2.7205 | 1.17E-07 | 6.931814138 |
| CR44748 | 2.8154 | 5.16E-07 | 6.287350298 |
| CG34323 | 7.2681 | 1.17E-06 | 5.931814138 |
| rha | 7.2782 | 1.21E-06 | 5.91721463 |
| Dcp-1 | 2.1891 | 1.63E-06 | 5.787812396 |
| RNaseMRP:RNA | 1.9841 | 1.99E-06 | 5.701146924 |
| mam | 2.4681 | 3.22E-06 | 5.492144128 |
| CG3568 | 2.4859 | 3.38E-06 | 5.4710833 |
| Sik2 | 2.0738 | 4.07E-06 | 5.390405591 |
| brk | 1.8637 | 4.50E-06 | 5.346787486 |
| CG32638 | 1.9232 | 5.64E-06 | 5.248720896 |
| vilya | 7.1651 | 1.29E-05 | 4.88941029 |
| CG44006 | 2.0812 | 1.78E-05 | 4.749579998 |
| CG15263 | 5.8997 | 2.07E-05 | 4.684029655 |
| Cyp6a20 | 2.3502 | 2.15E-05 | 4.66756154 |
| CG10337 | 1.8802 | 2.66E-05 | 4.575118363 |
| olf413 | 3.2921 | 4.47E-05 | 4.349692477 |
| CG13917 | 1.8386 | 4.51E-05 | 4.345823458 |
| CG12643 | 1.5994 | 4.57E-05 | 4.3400838 |
| CG44329 | 6.9175 | 6.44E-05 | 4.191114133 |
| CR43257 | 2.0949 | 8.21E-05 | 4.085656843 |
| CR45522 | 6.833 | 8.31E-05 | 4.080398976 |
| Sirt6 | 1.8338 | 9.85E-05 | 4.00656377 |
| CG6040 | 1.4772 | 0.0001 | 4 |
| CR43973 | 1.7045 | 0.0001 | 4 |
| Faa | 2.0159 | 0.0001 | 4 |
| pirk | 1.9361 | 0.0001 | 4 |
| CG32599 | 3.9445 | 0.0001 | 4 |
| CG11656 | 3.7341 | 0.0001 | 4 |

| | | | |
|---|---|---|---|
| HP1D3csd | 2.9281 | 0.0002 | 3.698970004 |
| CG8468 | 2.0774 | 0.0002 | 3.698970004 |
| CG13894 | 6.1784 | 0.0002 | 3.698970004 |
| cv-2 | 1.3604 | 0.0003 | 3.522878745 |
| Vti1a | 1.605 | 0.0003 | 3.522878745 |
| CG14626 | 1.6102 | 0.0003 | 3.522878745 |
| CG34401 | 1.9702 | 0.0003 | 3.522878745 |
| CG14367 | 3.9078 | 0.0003 | 3.522878745 |
| CG44405 | 6.4872 | 0.0004 | 3.397940009 |
| SIFa | 6.4242 | 0.0004 | 3.397940009 |
| CG3739 | 2.7317 | 0.0004 | 3.397940009 |
| CG11374 | 1.9882 | 0.0004 | 3.397940009 |
| CG30356 | 2.1258 | 0.0004 | 3.397940009 |
| CG13659 | 2.3504 | 0.0004 | 3.397940009 |
| CG18599 | 6.1882 | 0.0005 | 3.301029996 |
| Hexo2 | 2.096 | 0.0005 | 3.301029996 |
| Arc1 | 1.4615 | 0.0005 | 3.301029996 |
| laccase2 | 1.7841 | 0.0005 | 3.301029996 |
| Ir41a | 3.6464 | 0.0005 | 3.301029996 |
| CR44547 | 1.5763 | 0.0006 | 3.22184875 |
| Rcd2 | 1.9022 | 0.0006 | 3.22184875 |
| Arc2 | 1.4441 | 0.0006 | 3.22184875 |
| CG13658 | 2.5539 | 0.0006 | 3.22184875 |
| snoRNA:Psi18S-1275 | 4.2518 | 0.0006 | 3.22184875 |
| CR44608 | 1.4873 | 0.0007 | 3.15490196 |
| daw | 3.3024 | 0.0007 | 3.15490196 |
| CG9422 | 2.9673 | 0.0007 | 3.15490196 |
| geko | 4.6444 | 0.0007 | 3.15490196 |
| CR46095 | 1.7289 | 0.0008 | 3.096910013 |
| CG12868 | 2.2823 | 0.0008 | 3.096910013 |
| CR44984 | 2.4553 | 0.0009 | 3.045757491 |
| Tie | 1.3156 | 0.001 | 3 |
| CG13893 | 2.1632 | 0.001 | 3 |
| CG31510 | 1.144 | 0.0011 | 2.958607315 |
| CG11275 | 1.3763 | 0.0011 | 2.958607315 |
| Mal-A8 | 2.9946 | 0.0011 | 2.958607315 |
| laza | 1.5465 | 0.0012 | 2.920818754 |
| CG18467 | 2.8655 | 0.0012 | 2.920818754 |
| AOX2 | 4.1932 | 0.0013 | 2.886056648 |
| Tab2 | 2.6302 | 0.0013 | 2.886056648 |

| | | | |
|---|---|---|---|
| bou | 1.6098 | 0.0015 | 2.823908741 |
| CR45820 | 1.5134 | 0.0016 | 2.795880017 |
| CG5644 | 2.3154 | 0.0016 | 2.795880017 |
| Paip2 | 1.2104 | 0.0017 | 2.769551079 |
| CG42393 | 2.0341 | 0.0017 | 2.769551079 |
| Gbeta5 | 3.2562 | 0.0017 | 2.769551079 |
| CG6405 | 2.6438 | 0.0018 | 2.744727495 |
| CG8072 | 3.1698 | 0.0018 | 2.744727495 |
| ed | 1.3308 | 0.0019 | 2.721246399 |
| CG42364 | 3.0074 | 0.0019 | 2.721246399 |
| CG17265 | 1.1532 | 0.002 | 2.698970004 |
| comm2 | 2.207 | 0.002 | 2.698970004 |
| fs(1)Yb | 5.9694 | 0.0021 | 2.677780705 |
| CG31627 | 3.5992 | 0.0021 | 2.677780705 |
| CG8343 | 2.6626 | 0.0021 | 2.677780705 |
| CG17111 | 2.2656 | 0.0022 | 2.657577319 |
| CG43968 | 6.6815 | 0.0022 | 2.657577319 |
| sinu | 1.3859 | 0.0024 | 2.619788758 |
| CR44566 | 1.5582 | 0.0024 | 2.619788758 |
| CR46093 | 1.6771 | 0.0024 | 2.619788758 |
| CR45922 | 3.6394 | 0.0024 | 2.619788758 |
| CG4404 | 1.2706 | 0.0025 | 2.602059991 |
| tut | 2.3639 | 0.0025 | 2.602059991 |
| swa | 5.8367 | 0.0026 | 2.585026652 |
| CG6628 | 4.2165 | 0.0027 | 2.568636236 |
| Mnn1 | 1.2723 | 0.0028 | 2.552841969 |
| CR41257 | 2.6619 | 0.0028 | 2.552841969 |
| CG10376 | 1.1156 | 0.0029 | 2.537602002 |
| CR44445 | 2.1109 | 0.0029 | 2.537602002 |
| GstD4 | 1.4306 | 0.0031 | 2.508638306 |
| CG15515 | 3.8202 | 0.0034 | 2.468521083 |
| PGRP-SD | 1.4328 | 0.0034 | 2.468521083 |
| pan | 2.0604 | 0.0035 | 2.455931956 |
| CR41620 | 5.893 | 0.0036 | 2.443697499 |
| GstD5 | 1.7283 | 0.0036 | 2.443697499 |
| kirre | 3.789 | 0.0037 | 2.431798276 |
| grim | 2.2474 | 0.0037 | 2.431798276 |
| CG31808 | 2.0769 | 0.0038 | 2.420216403 |
| ppk27 | 2.2913 | 0.0038 | 2.420216403 |
| CR41583 | 2.6348 | 0.0038 | 2.420216403 |

| | | | |
|---|---|---|---|
| CHKov2 | 1.1893 | 0.0039 | 2.408935393 |
| Pzl | 5.6772 | 0.004 | 2.397940009 |
| E(spl)malpha-BFM | 0.9859 | 0.0041 | 2.387216143 |
| CG15084 | 1.3227 | 0.0042 | 2.37675071 |
| Lac | 1.7848 | 0.0044 | 2.356547324 |
| CG18745 | 0.9955 | 0.0045 | 2.346787486 |
| CG4297 | 1.2786 | 0.0045 | 2.346787486 |
| CR46249 | 2.6149 | 0.0045 | 2.346787486 |
| Ugt86Dd | 2.012 | 0.0046 | 2.337242168 |
| CG42365 | 1.6352 | 0.0047 | 2.327902142 |
| sima | 1.3636 | 0.0048 | 2.318758763 |
| Tsp42Ej | 1.2016 | 0.005 | 2.301029996 |
| CR44538 | 2.5992 | 0.005 | 2.301029996 |
| NC2alpha | 1.0801 | 0.0051 | 2.292429824 |
| CG32040 | 1.5381 | 0.0051 | 2.292429824 |
| Ir85a | 6.991 | 0.0052 | 2.283996656 |
| Lcch3 | 1.6661 | 0.0054 | 2.26760624 |
| CG13436 | 1.9279 | 0.0055 | 2.259637311 |
| CG7966 | 1.1856 | 0.0056 | 2.251811973 |
| CG3556 | 3.7323 | 0.0057 | 2.244125144 |
| CR43242 | 1.2398 | 0.0057 | 2.244125144 |
| Eip75B | 1.4818 | 0.0057 | 2.244125144 |
| CR45625 | 1.8807 | 0.0057 | 2.244125144 |
| CR44862 | 6.7535 | 0.0057 | 2.244125144 |
| CG42553 | 1.5631 | 0.0059 | 2.229147988 |
| PDZ-GEF | 1.2065 | 0.006 | 2.22184875 |
| CG31370 | 1.4272 | 0.0061 | 2.214670165 |
| CG18368 | 3.4388 | 0.0061 | 2.214670165 |
| CR45028 | 2.0076 | 0.0061 | 2.214670165 |
| Or45a | 1.8044 | 0.0062 | 2.207608311 |
| CG3262 | 1.1419 | 0.0065 | 2.187086643 |
| CG30047 | 1.5275 | 0.0065 | 2.187086643 |
| ssx | 1.7262 | 0.0065 | 2.187086643 |
| CG3982 | 2.1697 | 0.0065 | 2.187086643 |
| CG6683 | 1.2906 | 0.0066 | 2.180456064 |
| sprt | 1.7393 | 0.0067 | 2.173925197 |
| E(spl)m7-HLH | 1.2983 | 0.0068 | 2.167491087 |
| Gld | 3.7078 | 0.0069 | 2.161150909 |
| CG14196 | 2.3556 | 0.0069 | 2.161150909 |
| CR45824 | 3.7784 | 0.007 | 2.15490196 |

| | | | |
|---|---|---|---|
| sing | 1.7179 | 0.0072 | 2.142667504 |
| CR44138 | 2.9391 | 0.0074 | 2.13076828 |
| CG14837 | 3.0839 | 0.0075 | 2.124938737 |
| ebd1 | 1.1263 | 0.0075 | 2.124938737 |
| CG4462 | 1.534 | 0.0075 | 2.124938737 |
| CR43974 | 1.5003 | 0.0077 | 2.113509275 |
| CG30440 | 3.1719 | 0.0078 | 2.107905397 |
| CR45745 | 2.6296 | 0.008 | 2.096910013 |
| CR45171 | 1.6826 | 0.0081 | 2.091514981 |
| CG8319 | 1.1084 | 0.0082 | 2.086186148 |
| a | 1.4025 | 0.0082 | 2.086186148 |
| CG3008 | 1.0991 | 0.0084 | 2.075720714 |
| CG34040 | 1.843 | 0.0084 | 2.075720714 |
| CG2064 | 1.0013 | 0.0085 | 2.070581074 |
| CG9328 | 1.3172 | 0.0087 | 2.060480747 |
| bnl | 3.9421 | 0.0089 | 2.050609993 |
| TTLL3B | 4.5217 | 0.0089 | 2.050609993 |
| shams | 1.2587 | 0.009 | 2.045757491 |
| CR45166 | 3.8602 | 0.0091 | 2.040958608 |
| mir-4968 | 1.903 | 0.0093 | 2.031517051 |
| CG11000 | 2.0193 | 0.0095 | 2.022276395 |
| sstn | 1.1359 | 0.01 | 2 |
| Hsromega | 0.9131 | 0.0103 | 1.987162775 |
| Spn85F | 5.7881 | 0.0105 | 1.978810701 |
| PlexA | 1.6684 | 0.0106 | 1.974694135 |
| CG4723 | 5.4225 | 0.0108 | 1.966576245 |
| CG32845 | 1.1811 | 0.011 | 1.958607315 |
| Tsp42El | 0.8762 | 0.0112 | 1.950781977 |
| CG14443 | 1.1166 | 0.0118 | 1.928117993 |
| Pig1 | 2.6019 | 0.0118 | 1.928117993 |
| Ptip | 0.9546 | 0.0119 | 1.924453039 |
| ect | 1.9081 | 0.012 | 1.920818754 |
| snoRNA:Me18S-U1356b | 2.9272 | 0.012 | 1.920818754 |
| Hsc70-3 | 1.6867 | 0.0122 | 1.913640169 |
| CG6602 | 1.5814 | 0.0122 | 1.913640169 |
| CG33928 | 5.854 | 0.0123 | 1.910094889 |
| CG6330 | 1.4688 | 0.0124 | 1.906578315 |
| CG34348 | 0.9579 | 0.0126 | 1.899629455 |
| CG10559 | 1.9955 | 0.0127 | 1.896196279 |
| MYPT-75D | 1.284 | 0.0128 | 1.89279003 |

| | | | |
|---|---|---|---|
| CG6465 | 1.085 | 0.0131 | 1.882728704 |
| CG32486 | 0.8503 | 0.0132 | 1.879426069 |
| Sox102F | 2.5682 | 0.0133 | 1.876148359 |
| ITP | 1.0552 | 0.0137 | 1.863279433 |
| NFAT | 1.0928 | 0.0138 | 1.860120914 |
| dpr1 | 2.6599 | 0.0139 | 1.8569852 |
| CG33267 | 1.7543 | 0.014 | 1.853871964 |
| CG12398 | 1.4175 | 0.0141 | 1.850780887 |
| Smurf | 1.4153 | 0.0144 | 1.841637508 |
| Muc14A | 2.6604 | 0.0146 | 1.835647144 |
| CG10730 | 2.0963 | 0.0146 | 1.835647144 |
| CG13088 | 1.7539 | 0.0147 | 1.832682665 |
| Gk2 | 1.9101 | 0.0147 | 1.832682665 |
| CR44276 | 1.7043 | 0.015 | 1.823908741 |
| Xpac | 1.1253 | 0.0152 | 1.818156412 |
| CG32795 | 1.1811 | 0.0153 | 1.815308569 |
| Cyp6d5 | 1.2239 | 0.0153 | 1.815308569 |
| Ugt86Dc | 2.1373 | 0.0154 | 1.812479279 |
| vn | 1.3266 | 0.0154 | 1.812479279 |
| Atac1 | 1.0038 | 0.0161 | 1.793174124 |
| bigmax | 0.8526 | 0.0162 | 1.790484985 |
| CR46015 | 1.6168 | 0.0165 | 1.782516056 |
| hog | 2.7888 | 0.0166 | 1.779891912 |
| CG8492 | 6.582 | 0.0167 | 1.777283529 |
| CG32450 | 5.904 | 0.0167 | 1.777283529 |
| InR | 1.0259 | 0.0167 | 1.777283529 |
| St3 | 5.4924 | 0.0168 | 1.774690718 |
| Csk | 0.975 | 0.0169 | 1.772113295 |
| Fhos | 2.1468 | 0.017 | 1.769551079 |
| Cad96Ca | 2.1732 | 0.0171 | 1.76700389 |
| Cad87A | 1.0345 | 0.0176 | 1.754487332 |
| Cpr64Ad | 3.7841 | 0.0177 | 1.752026734 |
| CG8281 | 0.9718 | 0.0179 | 1.747146969 |
| Dat | 0.9879 | 0.0179 | 1.747146969 |
| CG6791 | 1.1082 | 0.018 | 1.744727495 |
| Atf6 | 1.7831 | 0.0181 | 1.742321425 |
| CG17687 | 2.9685 | 0.0182 | 1.739928612 |
| Ppt2 | 1.0215 | 0.0185 | 1.732828272 |
| CG5059 | 0.9555 | 0.019 | 1.721246399 |
| CG30484 | 1.9182 | 0.019 | 1.721246399 |

| | | | |
|---|---|---|---|
| CG8369 | 5.3843 | 0.0192 | 1.716698771 |
| CG30441 | 2.0064 | 0.0192 | 1.716698771 |
| CG5114 | 2.7561 | 0.0196 | 1.707743929 |
| CG14074 | 1.0616 | 0.0198 | 1.70333481 |
| l(1)G0193 | 1.1074 | 0.0199 | 1.701146924 |
| mst | 1.2879 | 0.02 | 1.698970004 |
| Ir40a | 5.3376 | 0.0205 | 1.688246139 |
| CG4586 | 1.0314 | 0.0205 | 1.688246139 |
| Naam | 1.1167 | 0.0212 | 1.673664139 |
| Ac3 | 1.4742 | 0.0214 | 1.669586227 |
| CG30324 | 5.8996 | 0.0216 | 1.665546249 |
| snoRNA:Psi18S-1086 | 1.3938 | 0.0217 | 1.663540266 |
| CG14838 | 4.1728 | 0.0219 | 1.659555885 |
| lt | 1.8493 | 0.0219 | 1.659555885 |
| CR45939 | 1.3041 | 0.0222 | 1.653647026 |
| CG3838 | 2.0134 | 0.0226 | 1.645891561 |
| mdy | 1.37 | 0.0228 | 1.642065153 |
| CG9676 | 1.7505 | 0.0229 | 1.640164518 |
| snoRNA:Me28S-C437 | 2.023 | 0.023 | 1.638272164 |
| ric8a | 1.1698 | 0.0236 | 1.627087997 |
| Pih1D1 | 0.8711 | 0.0237 | 1.625251654 |
| stas | 1.5531 | 0.024 | 1.619788758 |
| Mal-A4 | 1.9423 | 0.0243 | 1.614393726 |
| CG8273 | 3.2718 | 0.0244 | 1.612610174 |
| GstD3 | 0.8419 | 0.0244 | 1.612610174 |
| CG3709 | 1.0353 | 0.0246 | 1.609064893 |
| row | 1.1986 | 0.0246 | 1.609064893 |
| CG6013 | 0.9282 | 0.0247 | 1.607303047 |
| CG11486 | 0.9139 | 0.025 | 1.602059991 |
| CR32636 | 2.1814 | 0.0252 | 1.598599459 |
| TSG101 | 0.7575 | 0.0253 | 1.596879479 |
| CG3995 | 0.9071 | 0.0253 | 1.596879479 |
| Obp18a | 1.0706 | 0.0258 | 1.588380294 |
| ttm2 | 1.0203 | 0.0258 | 1.588380294 |
| CR45549 | 1.7662 | 0.0258 | 1.588380294 |
| lbm | 0.9544 | 0.0259 | 1.586700236 |
| GstE8 | 1.8313 | 0.0259 | 1.586700236 |
| CG43925 | 5.2682 | 0.026 | 1.585026652 |
| CG11655 | 1.1625 | 0.026 | 1.585026652 |
| CR44440 | 3.0132 | 0.0262 | 1.581698709 |

| | | | |
|---|---|---|---|
| CG33640 | 1.3798 | 0.0265 | 1.576754126 |
| CG31111 | 0.9597 | 0.0267 | 1.573488739 |
| rost | 1.4463 | 0.0273 | 1.563837353 |
| sty | 0.7423 | 0.0276 | 1.559090918 |
| CG15760 | 3.1645 | 0.0278 | 1.555955204 |
| CG9945 | 2.1893 | 0.0278 | 1.555955204 |
| CG33463 | 2.5122 | 0.0279 | 1.554395797 |
| CG31347 | 1.1841 | 0.028 | 1.552841969 |
| CG32855 | 3.9694 | 0.0281 | 1.55129368 |
| CG11893 | 2.7618 | 0.0283 | 1.548213564 |
| CG17786 | 1.1182 | 0.0286 | 1.543633967 |
| CG17929 | 2.3807 | 0.0287 | 1.542118103 |
| CG34160 | 1.3319 | 0.0288 | 1.540607512 |
| Krn | 0.9228 | 0.0289 | 1.539102157 |
| CG10638 | 1.1155 | 0.029 | 1.537602002 |
| MFS3 | 1.2377 | 0.0294 | 1.53165267 |
| Elp1 | 1.2653 | 0.0295 | 1.530177984 |
| CR45082 | 1.2995 | 0.0295 | 1.530177984 |
| CkIIalpha-i1 | 1.019 | 0.0296 | 1.528708289 |
| CG32371 | 2.9078 | 0.0301 | 1.521433504 |
| mir-967 | 1.2742 | 0.0302 | 1.519993057 |
| CG4676 | 4.2871 | 0.0303 | 1.518557371 |
| AhcyL2 | 2.0109 | 0.0303 | 1.518557371 |
| ntc | 1.2166 | 0.0304 | 1.517126416 |
| CG31431 | 2.3541 | 0.0305 | 1.515700161 |
| Rbcn-3B | 0.9687 | 0.0306 | 1.514278574 |
| fs(1)Ya | 5.5434 | 0.0307 | 1.512861625 |
| CG11226 | 2.2606 | 0.0308 | 1.511449283 |
| CG3876 | 0.9948 | 0.0309 | 1.510041521 |
| MFS14 | 2.365 | 0.0312 | 1.505845406 |
| CG33710 | 1.6746 | 0.0315 | 1.501689446 |
| Rab2 | 0.839 | 0.0319 | 1.496209317 |
| CR45280 | 3.1041 | 0.032 | 1.494850022 |
| Drep4 | 1.0395 | 0.0322 | 1.492144128 |
| CG34231 | 1.2231 | 0.0322 | 1.492144128 |
| Snap24 | 0.903 | 0.0323 | 1.490797478 |
| ppk | 2.3817 | 0.0323 | 1.490797478 |
| Kif3C | 1.6404 | 0.0324 | 1.48945499 |
| Eaf6 | 0.8476 | 0.0326 | 1.4867824 |
| CR45128 | 2.8805 | 0.0327 | 1.485452247 |

| | | | |
|---|---|---|---|
| CG45782 | 1.7442 | 0.0327 | 1.485452247 |
| CG30022 | 0.9609 | 0.0329 | 1.482804102 |
| l(3)02640 | 1.2891 | 0.0329 | 1.482804102 |
| CG7194 | 1.1992 | 0.0332 | 1.478861916 |
| CG14252 | 1.007 | 0.0339 | 1.469800302 |
| PGRP-LF | 0.8559 | 0.0341 | 1.467245621 |
| CG18635 | 0.9945 | 0.0342 | 1.465973894 |
| CG7564 | 1.4161 | 0.0342 | 1.465973894 |
| Tsp42Ef | 0.8197 | 0.0346 | 1.460923901 |
| dsx-c73A | 1.6027 | 0.0348 | 1.458420756 |
| CG31817 | 1.1168 | 0.0349 | 1.457174573 |
| bun | 0.8356 | 0.035 | 1.455931956 |
| CG5282 | 5.0661 | 0.0353 | 1.452225295 |
| CR41544 | 0.9233 | 0.0354 | 1.450996738 |
| CG7706 | 0.9693 | 0.0354 | 1.450996738 |
| 14-3-3zeta | 2.6466 | 0.0355 | 1.449771647 |
| Cyp4p3 | 2.5236 | 0.0358 | 1.446116973 |
| CG30197 | 1.2278 | 0.0358 | 1.446116973 |
| CG14227 | 1.469 | 0.036 | 1.443697499 |
| Ugt37b1 | 1.4352 | 0.036 | 1.443697499 |
| CG32444 | 2.4488 | 0.0362 | 1.441291429 |
| cwo | 1.1985 | 0.0368 | 1.434152181 |
| SmydA-5 | 1.839 | 0.0369 | 1.432973634 |
| swi2 | 1.6533 | 0.0373 | 1.428291168 |
| CR44404 | 5.0069 | 0.0375 | 1.425968732 |
| CG14352 | 0.9396 | 0.0375 | 1.425968732 |
| CG16898 | 1.2699 | 0.0377 | 1.42365865 |
| baz | 0.8178 | 0.0379 | 1.42136079 |
| bip1 | 3.4011 | 0.0381 | 1.419075024 |
| CG30099 | 1.9384 | 0.0381 | 1.419075024 |
| Tbc1d15-17 | 2.6204 | 0.0382 | 1.417936637 |
| GstE1 | 0.7994 | 0.0382 | 1.417936637 |
| nmo | 1.5664 | 0.0382 | 1.417936637 |
| CG8223 | 5.0496 | 0.0384 | 1.415668776 |
| CrebA | 0.8864 | 0.0385 | 1.41453927 |
| CG9821 | 0.7877 | 0.0385 | 1.41453927 |
| bowl | 3.076 | 0.0387 | 1.412289035 |
| mthl14 | 0.7281 | 0.0387 | 1.412289035 |
| CG16833 | 1.646 | 0.0389 | 1.410050399 |
| GluRIIE | 1.2433 | 0.0391 | 1.407823243 |

| | | | |
|---|---|---|---|
| CG14965 | 1.2148 | 0.0393 | 1.40560745 |
| Rbp1 | 0.8507 | 0.0394 | 1.404503778 |
| CR46094 | 1.8881 | 0.0395 | 1.403402904 |
| lace | 0.8839 | 0.0399 | 1.399027104 |
| Mrp4 | 0.9631 | 0.0399 | 1.399027104 |
| fidipidine | 0.8277 | 0.04 | 1.397940009 |
| CG43672 | 3.1657 | 0.0401 | 1.396855627 |
| CG17684 | 2.164 | 0.0401 | 1.396855627 |
| CR32218 | 0.8255 | 0.0401 | 1.396855627 |
| CR43405 | 1.4843 | 0.0401 | 1.396855627 |
| CG45428 | 2.3132 | 0.0404 | 1.393618635 |
| Taf11 | 0.8644 | 0.0407 | 1.390405591 |
| JhI-26 | 1.2491 | 0.0409 | 1.388276692 |
| CR44817 | 0.9615 | 0.0413 | 1.384049948 |
| CG9684 | 0.7183 | 0.0414 | 1.382999659 |
| CR43653 | 1.5591 | 0.0416 | 1.380906669 |
| CR43849 | 1.8358 | 0.0417 | 1.379863945 |
| flfl | 0.7277 | 0.0419 | 1.377785977 |
| CR45915 | 1.0206 | 0.0421 | 1.375717904 |
| GstE7 | 1.4537 | 0.0421 | 1.375717904 |
| CG42818 | 3.3062 | 0.0422 | 1.374687549 |
| CR45054 | 0.8759 | 0.0431 | 1.36552273 |
| Cyp311a1 | 1.0462 | 0.0432 | 1.364516253 |
| CG14770 | 3.9382 | 0.0439 | 1.35753548 |
| CR46204 | 1.264 | 0.0443 | 1.353596274 |
| CR43909 | 2.1516 | 0.0445 | 1.351639989 |
| CG43646 | 1.4886 | 0.0447 | 1.349692477 |
| Axs | 0.9161 | 0.045 | 1.346787486 |
| CG14877 | 1.8853 | 0.0456 | 1.341035157 |
| pkaap | 0.9219 | 0.0457 | 1.3400838 |
| CR45148 | 1.3193 | 0.0458 | 1.339134522 |
| shg | 0.6812 | 0.046 | 1.337242168 |
| CG30456 | 3.1243 | 0.0468 | 1.329754147 |
| glec | 0.6871 | 0.0468 | 1.329754147 |
| CR45224 | 1.5462 | 0.0468 | 1.329754147 |
| mrt | 4.9315 | 0.0475 | 1.32330639 |
| CG17018 | 3.0817 | 0.0478 | 1.320572103 |
| foi | 3.0088 | 0.0479 | 1.319664487 |
| CG33160 | 4.9219 | 0.0479 | 1.319664487 |
| yuri | 2.7061 | 0.0482 | 1.316952962 |

| | | | |
|---|---|---|---|
| wts | 0.74 | 0.0489 | 1.310691141 |
| Tgi | 1.1551 | 0.0492 | 1.308034897 |
| Ir51b | 1.6574 | 0.0494 | 1.306273051 |
| CG9505 | 1.0175 | 0.0498 | 1.302770657 |
| CG33468 | 1.4953 | 0.0498 | 1.302770657 |
| Lap1 | 1.068 | 0.0499 | 1.301899454 |
| CG16716 | 2.2466 | 0.0501 | 1.300162274 |
| CG4660 | 2.3861 | 0.0504 | 1.297569464 |
| CR44145 | 1.1697 | 0.0505 | 1.296708622 |
| RhoGAP71E | 1.1517 | 0.0506 | 1.295849483 |
| dgt1 | 0.89 | 0.0508 | 1.294136288 |
| kune | 0.8278 | 0.0509 | 1.293282218 |
| CR45102 | 0.8436 | 0.051 | 1.292429824 |
| CG4455 | 0.7209 | 0.0512 | 1.290730039 |
| CR45256 | 2.5225 | 0.0514 | 1.289036881 |
| CG9425 | 1.4977 | 0.0514 | 1.289036881 |
| CG16711 | 0.9123 | 0.0515 | 1.288192771 |
| CG3163 | 0.8182 | 0.0518 | 1.28567024 |
| CR44348 | 2.2763 | 0.0521 | 1.283162277 |
| qkr58E-1 | 1.1166 | 0.0525 | 1.279840697 |
| Src42A | 0.9192 | 0.0528 | 1.277366077 |
| CR46064 | 0.6989 | 0.0531 | 1.274905479 |
| CG5642 | 0.6598 | 0.0531 | 1.274905479 |
| Atac2 | 1.024 | 0.0531 | 1.274905479 |
| mir-4964 | 1.4584 | 0.0532 | 1.274088368 |
| CR43399 | 0.8411 | 0.0533 | 1.273272791 |
| AttD | 1.3997 | 0.0533 | 1.273272791 |
| CG6843 | 0.8012 | 0.0534 | 1.272458743 |
| CG42816 | 5.3067 | 0.0535 | 1.271646218 |
| CG43192 | 1.3107 | 0.0538 | 1.269217724 |
| CG15563 | 2.6022 | 0.0541 | 1.266802735 |
| snoRNA:Psi18S-841b | 1.6456 | 0.0544 | 1.2644011 |

**Table 2.1b: list of genes differentially upregulated in control females relative to control males**

| list of hits>10 raw reads | log2FC edgeR | p-value edgeR | -log10(pvalue) |
|---|---|---|---|
| Pebp1 | -4.8196 | 9.78E-26 | 25.00966115 |
| CG6295 | -4.6944 | 8.94E-25 | 24.04866248 |
| pre-rRNA:CR45845 | -5.6419 | 1.58E-22 | 21.80134291 |
| yip7 | -3.3174 | 3.17E-22 | 21.49894074 |
| CG6296 | -9.1509 | 3.41E-17 | 16.46724562 |
| Jon65Aiii | -2.9835 | 9.12E-17 | 16.04000516 |

| | | | |
|---|---|---|---|
| Jon65Aiv | -3.4131 | 3.28E-16 | 15.48412616 |
| CG4563 | -6.6562 | 9.45E-15 | 14.02456819 |
| Jon25Biii | -4.3475 | 8.47E-14 | 13.07211659 |
| PGRP-SC2 | -4.1219 | 5.33E-13 | 12.27327279 |
| thetaTry | -3.8188 | 1.34E-12 | 11.8728952 |
| CG10182 | -8.576 | 2.52E-12 | 11.59859946 |
| CG11241 | -3.2885 | 4.75E-12 | 11.32330639 |
| CG5506 | -4.8881 | 4.93E-12 | 11.30715308 |
| CG42747 | -2.9459 | 4.37E-11 | 10.35951856 |
| CG18180 | -2.9197 | 6.50E-11 | 10.18708664 |
| CG13813 | -9.5056 | 1.63E-10 | 9.787812396 |
| CG12374 | -5.3231 | 2.19E-10 | 9.659555885 |
| CG30090 | -2.4048 | 2.37E-10 | 9.625251654 |
| RpS28b | -2.5891 | 3.10E-10 | 9.508638306 |
| Jon66Ci | -6.1965 | 5.52E-10 | 9.258060922 |
| CG8661 | -3.4006 | 6.89E-10 | 9.161780778 |
| CG8952 | -2.8699 | 8.09E-10 | 9.092051478 |
| CG8299 | -9.4315 | 1.13E-09 | 8.946921557 |
| CG17192 | -5.8606 | 1.37E-09 | 8.863279433 |
| CR42767 | -6.4065 | 1.52E-09 | 8.818156412 |
| CG6891 | -4.1601 | 3.26E-09 | 8.4867824 |
| CG8745 | -5.0092 | 3.71E-09 | 8.43062609 |
| Jon99Cii | -3.438 | 4.30E-09 | 8.366531544 |
| CR43264 | -5.3834 | 9.43E-09 | 8.025488307 |
| tej | -4.838 | 2.72E-08 | 7.565431096 |
| epsilonTry | -3.9521 | 5.15E-08 | 7.288192771 |
| pyd3 | -2.136 | 8.60E-08 | 7.065501549 |
| Muc68E | -4.0152 | 8.96E-08 | 7.04769199 |
| Cyp6d2 | -3.0961 | 1.00E-07 | 7 |
| alphaTry | -2.723 | 1.10E-07 | 6.958607315 |
| O-fut2 | -1.9538 | 2.12E-07 | 6.673664139 |
| CG9686 | -7.7017 | 3.80E-07 | 6.420216403 |
| CG12170 | -2.2561 | 4.19E-07 | 6.377785977 |
| CG4830 | -3.326 | 4.20E-07 | 6.37675071 |
| CG5804 | -3.0577 | 4.42E-07 | 6.354577731 |
| CG13690 | -3.2136 | 4.80E-07 | 6.318758763 |
| CR45714 | -7.1849 | 5.66E-07 | 6.247183569 |
| CG16775 | -6.2695 | 5.72E-07 | 6.242603971 |
| CG15605 | -4.3396 | 7.14E-07 | 6.146301788 |
| dgt3 | -2.3691 | 8.38E-07 | 6.076755981 |

| | | | |
|---|---|---|---|
| Jon25Bi | -4.2436 | 1.43E-06 | 5.844663963 |
| gt | -4.7392 | 2.43E-06 | 5.614393726 |
| CG3344 | -3.6964 | 3.00E-06 | 5.522878745 |
| CG14526 | -3.0884 | 4.91E-06 | 5.308918508 |
| Jon99Fii | -4.5286 | 5.05E-06 | 5.296708622 |
| RfC3 | -2.7579 | 5.88E-06 | 5.230622674 |
| Jon65Aii | -4.4725 | 5.97E-06 | 5.224025669 |
| CG33127 | -2.2061 | 6.15E-06 | 5.211124884 |
| CDC45L | -1.7469 | 8.65E-06 | 5.062983893 |
| Lrpprc2 | -1.6397 | 9.02E-06 | 5.044793462 |
| CG30411 | -5.8252 | 1.09E-05 | 4.962573502 |
| Pen | -2.4468 | 1.12E-05 | 4.950781977 |
| Npc2a | -1.5065 | 1.25E-05 | 4.903089987 |
| CG8460 | -1.5604 | 1.27E-05 | 4.896196279 |
| nrv3 | -3.465 | 1.38E-05 | 4.860120914 |
| CG15630 | -6.7702 | 1.58E-05 | 4.801342913 |
| bora | -3.5976 | 1.86E-05 | 4.730487056 |
| CG9825 | -4.7276 | 1.93E-05 | 4.714442691 |
| CG31041 | -4.2934 | 1.94E-05 | 4.71219827 |
| CG17633 | -4.4683 | 1.97E-05 | 4.705533774 |
| CG7280 | -2.0548 | 2.01E-05 | 4.696803943 |
| CG14205 | -3.132 | 2.54E-05 | 4.595166283 |
| CG34010 | -1.9096 | 2.76E-05 | 4.559090918 |
| Fmo-2 | -1.5026 | 3.08E-05 | 4.511449283 |
| Jon99Fi | -4.6745 | 3.09E-05 | 4.510041521 |
| alphaTub84D | -1.523 | 3.20E-05 | 4.494850022 |
| Meltrin | -2.2999 | 3.67E-05 | 4.435333936 |
| Cht9 | -3.9465 | 3.95E-05 | 4.403402904 |
| fa2h | -4.6489 | 4.07E-05 | 4.390405591 |
| mms4 | -2.0956 | 4.24E-05 | 4.372634143 |
| Mcm6 | -1.9351 | 4.64E-05 | 4.333482019 |
| CG6733 | -4.0288 | 5.09E-05 | 4.293282218 |
| Jon66Cii | -7.2419 | 5.45E-05 | 4.263603498 |
| CG31266 | -6.7755 | 5.83E-05 | 4.234331445 |
| LysX | -4.1949 | 5.99E-05 | 4.222573178 |
| RnrL | -1.7067 | 6.37E-05 | 4.195860568 |
| CG11700 | -1.7091 | 6.74E-05 | 4.171340103 |
| Zwilch | -2.0546 | 6.79E-05 | 4.168130226 |
| CG7298 | -4.3337 | 7.30E-05 | 4.13667714 |
| stv | -2.4853 | 7.42E-05 | 4.129596095 |

| | | | |
|---|---|---|---|
| Ag5r2 | -3.7558 | 7.42E-05 | 4.129596095 |
| CG7458 | -1.9279 | 7.61E-05 | 4.118615343 |
| Ntf-2 | -1.9192 | 7.64E-05 | 4.116906641 |
| Est-Q | -3.064 | 8.45E-05 | 4.073143291 |
| Amy-d | -1.716 | 9.15E-05 | 4.038578906 |
| Snm1 | -1.7708 | 9.87E-05 | 4.005682847 |
| Jon99Ciii | -3.1431 | 9.99E-05 | 4.000434512 |
| CG34026 | -6.1937 | 0.0001 | 4 |
| CG5590 | -1.3111 | 0.0001 | 4 |
| CG8834 | -1.5794 | 0.0001 | 4 |
| Arc42 | -1.5688 | 0.0001 | 4 |
| CG44475 | -2.5543 | 0.0001 | 4 |
| Fit2 | -2.1947 | 0.0001 | 4 |
| GILT3 | -4.6563 | 0.0001 | 4 |
| CG15044 | -3.599 | 0.0001 | 4 |
| CG5107 | -2.6941 | 0.0001 | 4 |
| CR44830 | -4.0446 | 0.0002 | 3.698970004 |
| amn | -1.2833 | 0.0002 | 3.698970004 |
| blw | -1.1524 | 0.0002 | 3.698970004 |
| CG6028 | -1.4401 | 0.0002 | 3.698970004 |
| CG33966 | -2.9453 | 0.0002 | 3.698970004 |
| Cht4 | -4.1867 | 0.0002 | 3.698970004 |
| MFS1 | -7.9437 | 0.0002 | 3.698970004 |
| CG8642 | -4.5985 | 0.0003 | 3.522878745 |
| LysE | -6.0438 | 0.0003 | 3.522878745 |
| CG3663 | -1.468 | 0.0003 | 3.522878745 |
| CG7246 | -1.4757 | 0.0003 | 3.522878745 |
| RnrS | -1.4527 | 0.0003 | 3.522878745 |
| CG5254 | -1.5475 | 0.0003 | 3.522878745 |
| GILT2 | -1.7271 | 0.0003 | 3.522878745 |
| CG5770 | -3.8369 | 0.0003 | 3.522878745 |
| CG10505 | -2.9852 | 0.0003 | 3.522878745 |
| CG11068 | -1.4338 | 0.0004 | 3.397940009 |
| Lim1 | -3.954 | 0.0005 | 3.301029996 |
| Fdh | -1.1835 | 0.0005 | 3.301029996 |
| psidin | -1.2624 | 0.0005 | 3.301029996 |
| CG14798 | -1.6379 | 0.0005 | 3.301029996 |
| CG18179 | -2.6814 | 0.0005 | 3.301029996 |
| CG14820 | -2.7741 | 0.0005 | 3.301029996 |
| CG6067 | -2.306 | 0.0005 | 3.301029996 |

| | | | |
|---|---|---|---|
| DNApol-alpha60 | -2.0268 | 0.0005 | 3.301029996 |
| ppk3 | -4.0899 | 0.0006 | 3.22184875 |
| CG32212 | -1.3523 | 0.0006 | 3.22184875 |
| CG33514 | -1.7575 | 0.0006 | 3.22184875 |
| Acox57D-d | -1.751 | 0.0006 | 3.22184875 |
| spd-2 | -1.9026 | 0.0006 | 3.22184875 |
| CG32698 | -1.8154 | 0.0007 | 3.15490196 |
| CG5767 | -3.2492 | 0.0007 | 3.15490196 |
| Sirt2 | -3.7083 | 0.0008 | 3.096910013 |
| CG31345 | -4.3575 | 0.0008 | 3.096910013 |
| CG30049 | -1.2043 | 0.0008 | 3.096910013 |
| CG6126 | -1.4303 | 0.0008 | 3.096910013 |
| CR42491 | -1.2842 | 0.0008 | 3.096910013 |
| Fpps | -1.2116 | 0.0009 | 3.045757491 |
| Debcl | -1.3602 | 0.0009 | 3.045757491 |
| CG13151 | -1.5259 | 0.0009 | 3.045757491 |
| CG3011 | -1.5287 | 0.0009 | 3.045757491 |
| CG33109 | -4.2282 | 0.0009 | 3.045757491 |
| CG43207 | -2.8238 | 0.0009 | 3.045757491 |
| Jheh3 | -1.5069 | 0.001 | 3 |
| Peritrophin-15a | -2.2241 | 0.001 | 3 |
| CG18404 | -3.0291 | 0.001 | 3 |
| Art7 | -1.2619 | 0.0011 | 2.958607315 |
| l(3)mbt | -1.4972 | 0.0011 | 2.958607315 |
| upd2 | -1.4017 | 0.0011 | 2.958607315 |
| CR43989 | -5.8887 | 0.0012 | 2.920818754 |
| CG11752 | -1.1346 | 0.0012 | 2.920818754 |
| CG31076 | -1.7577 | 0.0012 | 2.920818754 |
| Jon99Ci | -1.6693 | 0.0012 | 2.920818754 |
| CG45080 | -4.0419 | 0.0012 | 2.920818754 |
| dome | -1.0767 | 0.0013 | 2.886056648 |
| pav | -1.6301 | 0.0013 | 2.886056648 |
| Mesh1 | -1.4387 | 0.0013 | 2.886056648 |
| CG45061 | -1.4532 | 0.0013 | 2.886056648 |
| Rbf2 | -1.7261 | 0.0013 | 2.886056648 |
| alpha-Est7 | -2.1577 | 0.0013 | 2.886056648 |
| CG5724 | -3.9339 | 0.0013 | 2.886056648 |
| CG31198 | -2.3491 | 0.0013 | 2.886056648 |
| LysD | -4.1733 | 0.0014 | 2.853871964 |
| CG1827 | -1.1237 | 0.0014 | 2.853871964 |

| | | | |
|---|---|---|---|
| CG16734 | -1.4096 | 0.0014 | 2.853871964 |
| CG15127 | -2.2699 | 0.0014 | 2.853871964 |
| CG32750 | -3.5019 | 0.0014 | 2.853871964 |
| CG32641 | -1.2955 | 0.0015 | 2.823908741 |
| CG42327 | -2.9296 | 0.0015 | 2.823908741 |
| CG10869 | -3.1761 | 0.0015 | 2.823908741 |
| CG6180 | -1.1227 | 0.0016 | 2.795880017 |
| Irp-1B | -1.3168 | 0.0016 | 2.795880017 |
| w | -1.1467 | 0.0016 | 2.795880017 |
| Tina-1 | -1.6139 | 0.0016 | 2.795880017 |
| CG15414 | -1.5644 | 0.0016 | 2.795880017 |
| CG42397 | -2.9139 | 0.0016 | 2.795880017 |
| CG9577 | -1.2377 | 0.0017 | 2.769551079 |
| CG42825 | -2.6209 | 0.0017 | 2.769551079 |
| Syx4 | -1.9948 | 0.0017 | 2.769551079 |
| CG34288 | -1.8548 | 0.0018 | 2.744727495 |
| DNaseII | -2.5348 | 0.0018 | 2.744727495 |
| CG10000 | -6.2936 | 0.002 | 2.698970004 |
| CG9581 | -1.2346 | 0.002 | 2.698970004 |
| RecQ4 | -1.8007 | 0.002 | 2.698970004 |
| msd1 | -1.7031 | 0.002 | 2.698970004 |
| CG3625 | -5.6614 | 0.0022 | 2.657577319 |
| CG34132 | -1.0549 | 0.0022 | 2.657577319 |
| Gfat2 | -1.1256 | 0.0023 | 2.638272164 |
| ATPsyndelta | -1.462 | 0.0023 | 2.638272164 |
| CG4053 | -6.5793 | 0.0025 | 2.602059991 |
| bsf | -1.0145 | 0.0025 | 2.602059991 |
| CG42826 | -3.237 | 0.003 | 2.522878745 |
| CG10912 | -1.8515 | 0.003 | 2.522878745 |
| CG5892 | -6.5945 | 0.0032 | 2.494850022 |
| Vha36-1 | -0.9724 | 0.0032 | 2.494850022 |
| CG10911 | -1.731 | 0.0032 | 2.494850022 |
| CG2681 | -1.47 | 0.0033 | 2.48148606 |
| Tps1 | -5.4786 | 0.0034 | 2.468521083 |
| Rif1 | -1.3765 | 0.0034 | 2.468521083 |
| Osbp | -1.1662 | 0.0035 | 2.455931956 |
| dgt6 | -1.3624 | 0.0035 | 2.455931956 |
| upd3 | -1.2787 | 0.0035 | 2.455931956 |
| CG15617 | -2.6728 | 0.0035 | 2.455931956 |
| E(spl)m8-HLH | -1.4124 | 0.0036 | 2.443697499 |

| | | | |
|---|---|---|---|
| mag | -2.6766 | 0.0037 | 2.431798276 |
| CCHa2 | -3.9725 | 0.0038 | 2.420216403 |
| CR44692 | -1.5844 | 0.0038 | 2.420216403 |
| CG42714 | -2.3019 | 0.0038 | 2.420216403 |
| CG16700 | -5.8742 | 0.0039 | 2.408935393 |
| CG16749 | -2.0923 | 0.0039 | 2.408935393 |
| CG7630 | -0.947 | 0.004 | 2.397940009 |
| Muc68Ca | -2.1575 | 0.004 | 2.397940009 |
| CG6310 | -1.1733 | 0.0042 | 2.37675071 |
| CG7593 | -1.3492 | 0.0042 | 2.37675071 |
| CG13300 | -2.1127 | 0.0042 | 2.37675071 |
| asp | -1.5967 | 0.0042 | 2.37675071 |
| CG1946 | -2.8083 | 0.0043 | 2.366531544 |
| CG14629 | -1.1207 | 0.0044 | 2.356547324 |
| Hex-C | -1.6447 | 0.0044 | 2.356547324 |
| l(2)10685 | -1.4056 | 0.0045 | 2.346787486 |
| CG8562 | -2.4317 | 0.0046 | 2.337242168 |
| E(spl)m2-BFM | -1.508 | 0.0046 | 2.337242168 |
| CG31915 | -1.1234 | 0.0048 | 2.318758763 |
| CG33116 | -1.1036 | 0.0049 | 2.30980392 |
| CG31918 | -1.1841 | 0.0049 | 2.30980392 |
| Orc1 | -1.9861 | 0.0051 | 2.292429824 |
| SPH93 | -2.6705 | 0.0052 | 2.283996656 |
| CG13082 | -2.9375 | 0.0052 | 2.283996656 |
| DNApol-alpha180 | -1.5868 | 0.0053 | 2.27572413 |
| CG12512 | -1.842 | 0.0053 | 2.27572413 |
| CG12237 | -0.9133 | 0.0054 | 2.26760624 |
| Ctf4 | -1.7625 | 0.0054 | 2.26760624 |
| phyl | -3.076 | 0.0054 | 2.26760624 |
| lectin-46Ca | -2.2805 | 0.0054 | 2.26760624 |
| Oatp33Eb | -2.7066 | 0.0055 | 2.259637311 |
| AP-1-2beta | -0.9117 | 0.0056 | 2.251811973 |
| CG3906 | -2.1752 | 0.0056 | 2.251811973 |
| Pmm45A | -0.9843 | 0.0058 | 2.236572006 |
| CG12171 | -1.084 | 0.0059 | 2.229147988 |
| CG1287 | -1.2043 | 0.0059 | 2.229147988 |
| dmGlut | -2.2373 | 0.0059 | 2.229147988 |
| CG11899 | -1.8165 | 0.006 | 2.22184875 |
| CG32091 | -1.075 | 0.0061 | 2.214670165 |
| CG3430 | -1.143 | 0.0063 | 2.200659451 |

| | | | |
|---|---|---|---|
| Nup107 | -0.9609 | 0.0064 | 2.193820026 |
| CG7470 | -1.573 | 0.0065 | 2.187086643 |
| ecd | -1.2147 | 0.0066 | 2.180456064 |
| CG9663 | -1.1279 | 0.0069 | 2.161150909 |
| AIMP1 | -0.9664 | 0.007 | 2.15490196 |
| CG8773 | -1.1429 | 0.007 | 2.15490196 |
| CG4194 | -2.9168 | 0.0071 | 2.148741651 |
| CG6745 | -1.2721 | 0.0072 | 2.142667504 |
| Glo1 | -0.9258 | 0.0074 | 2.13076828 |
| CG4839 | -3.365 | 0.0075 | 2.124938737 |
| Gip | -0.9008 | 0.0076 | 2.119186408 |
| Ssb-c31a | -0.975 | 0.0077 | 2.113509275 |
| caix | -2.0302 | 0.0079 | 2.102372909 |
| rev7 | -1.159 | 0.0081 | 2.091514981 |
| CG10592 | -1.448 | 0.0081 | 2.091514981 |
| CG12926 | -1.5003 | 0.0081 | 2.091514981 |
| CR44478 | -1.5281 | 0.0081 | 2.091514981 |
| SLC22A | -1.4758 | 0.0082 | 2.086186148 |
| CG17855 | -1.021 | 0.0083 | 2.080921908 |
| CG7277 | -1.0007 | 0.0084 | 2.075720714 |
| CR43253 | -3.3622 | 0.0085 | 2.070581074 |
| CG17660 | -0.9807 | 0.0085 | 2.070581074 |
| CG10584 | -1.1102 | 0.0085 | 2.070581074 |
| CG43295 | -1.4949 | 0.0086 | 2.065501549 |
| ox | -0.9341 | 0.0087 | 2.060480747 |
| CG6178 | -0.9505 | 0.0087 | 2.060480747 |
| CR44724 | -1.5208 | 0.0087 | 2.060480747 |
| CG11911 | -2.3515 | 0.0087 | 2.060480747 |
| CG1942 | -3.0977 | 0.0088 | 2.055517328 |
| CR15061 | -1.1414 | 0.0089 | 2.050609993 |
| Npc2f | -1.511 | 0.0089 | 2.050609993 |
| CG10939 | -1.4819 | 0.0089 | 2.050609993 |
| LysP | -4.802 | 0.009 | 2.045757491 |
| Ndc1 | -1.073 | 0.009 | 2.045757491 |
| spdo | -1.4527 | 0.0091 | 2.040958608 |
| CG30339 | -1.1875 | 0.0092 | 2.036212173 |
| CG7379 | -0.9279 | 0.0093 | 2.031517051 |
| Tsr1 | -0.9652 | 0.0093 | 2.031517051 |
| Cbs | -2.6174 | 0.0094 | 2.026872146 |
| PRAS40 | -0.8926 | 0.0095 | 2.022276395 |

| | | | |
|---|---|---|---|
| CG9344 | -0.9773 | 0.0096 | 2.017728767 |
| CG10470 | -0.9783 | 0.0099 | 2.004364805 |
| ATPsynO | -0.8388 | 0.01 | 2 |
| CG31344 | -1.3962 | 0.01 | 2 |
| Vha14-1 | -0.8828 | 0.0101 | 1.995678626 |
| CG11403 | -1.0944 | 0.0104 | 1.982966661 |
| kappaTry | -1.5835 | 0.0105 | 1.978810701 |
| DNApol-epsilon58 | -1.5802 | 0.0108 | 1.966576245 |
| CG14120 | -1.9513 | 0.0111 | 1.954677021 |
| CR44704 | -1.6696 | 0.0111 | 1.954677021 |
| CG13364 | -0.9317 | 0.0112 | 1.950781977 |
| CG3021 | -0.9642 | 0.0115 | 1.93930216 |
| alpha-Est1 | -1.352 | 0.0115 | 1.93930216 |
| CG12288 | -1.6251 | 0.0117 | 1.931814138 |
| Mcm2 | -1.2083 | 0.0118 | 1.928117993 |
| CG14104 | -1.1868 | 0.0118 | 1.928117993 |
| Zw10 | -0.9916 | 0.0119 | 1.924453039 |
| msd5 | -1.3071 | 0.0121 | 1.91721463 |
| CG17278 | -1.3087 | 0.0123 | 1.910094889 |
| Mdr50 | -1.9491 | 0.0123 | 1.910094889 |
| CG1907 | -1.0513 | 0.0126 | 1.899629455 |
| CG6454 | -2.3263 | 0.0126 | 1.899629455 |
| Spindly | -1.059 | 0.0127 | 1.896196279 |
| Mur29B | -2.8587 | 0.0127 | 1.896196279 |
| CG8419 | -2.694 | 0.0128 | 1.89279003 |
| pont | -0.9701 | 0.0128 | 1.89279003 |
| Pex13 | -0.9569 | 0.0134 | 1.872895202 |
| schuy | -1.3296 | 0.0135 | 1.869666232 |
| CR44868 | -1.1198 | 0.0136 | 1.866461092 |
| cN-IIIB | -0.9915 | 0.0138 | 1.860120914 |
| CG12129 | -0.8985 | 0.0139 | 1.8569852 |
| CG32483 | -2.1871 | 0.0139 | 1.8569852 |
| CG1236 | -0.9315 | 0.014 | 1.853871964 |
| snoRNA:Psi18S-531 | -0.9388 | 0.014 | 1.853871964 |
| CG5958 | -2.2533 | 0.0142 | 1.847711656 |
| mRpS11 | -0.9011 | 0.0143 | 1.844663963 |
| ATPsynE | -2.7804 | 0.0147 | 1.832682665 |
| CG2781 | -1.7457 | 0.0149 | 1.826813732 |
| aurB | -1.1795 | 0.015 | 1.823908741 |
| CG14543 | -0.9749 | 0.0152 | 1.818156412 |

| | | | |
|---|---|---|---|
| CG7889 | -0.9004 | 0.0156 | 1.806875402 |
| CG5214 | -0.8173 | 0.016 | 1.795880017 |
| CG18765 | -1.6818 | 0.016 | 1.795880017 |
| Hsp70Bbb | -1.374 | 0.0162 | 1.790484985 |
| cry | -0.8161 | 0.0163 | 1.787812396 |
| Klp61F | -1.1187 | 0.0163 | 1.787812396 |
| Mcm5 | -1.1862 | 0.0164 | 1.785156152 |
| CG30283 | -1.0092 | 0.0165 | 1.782516056 |
| Sdhaf3 | -1.4575 | 0.0169 | 1.772113295 |
| Thiolase | -0.7639 | 0.0172 | 1.764471553 |
| CG15210 | -1.7408 | 0.0172 | 1.764471553 |
| ND-B15 | -0.8083 | 0.0174 | 1.759450752 |
| Ote | -1.0235 | 0.0174 | 1.759450752 |
| Gr94a | -1.4248 | 0.0174 | 1.759450752 |
| xit | -0.9028 | 0.0177 | 1.752026734 |
| CR45037 | -2.0532 | 0.0179 | 1.747146969 |
| CG12825 | -0.9348 | 0.0179 | 1.747146969 |
| CG31469 | -1.3156 | 0.0179 | 1.747146969 |
| beta'COP | -0.8089 | 0.0181 | 1.742321425 |
| sqa | -2.2568 | 0.0182 | 1.739928612 |
| CG13324 | -1.9554 | 0.0183 | 1.73754891 |
| Eip63F-1 | -4.8873 | 0.0184 | 1.735182177 |
| Hydr1 | -4.8873 | 0.0184 | 1.735182177 |
| msb1l | -1.06 | 0.0187 | 1.728158393 |
| Taldo | -0.7726 | 0.0189 | 1.723538196 |
| CG31126 | -0.9685 | 0.019 | 1.721246399 |
| CG5010 | -1.3646 | 0.019 | 1.721246399 |
| CG10184 | -0.8636 | 0.0192 | 1.716698771 |
| SdhB | -0.8379 | 0.0192 | 1.716698771 |
| CG14270 | -0.8766 | 0.0194 | 1.71219827 |
| CG34200 | -1.0483 | 0.0195 | 1.709965389 |
| CG30345 | -0.8749 | 0.0195 | 1.709965389 |
| Bap60 | -0.7654 | 0.0198 | 1.70333481 |
| CycE | -4.8498 | 0.02 | 1.698970004 |
| CG13008 | -2.2695 | 0.02 | 1.698970004 |
| ico | -1.0794 | 0.02 | 1.698970004 |
| Orc5 | -1.2574 | 0.0202 | 1.694648631 |
| CG32669 | -1.7431 | 0.0203 | 1.692503962 |
| Cpr73D | -1.2152 | 0.0204 | 1.690369833 |
| CG10472 | -1.8595 | 0.0204 | 1.690369833 |

| | | | |
|---|---|---|---|
| Ssrp | -0.8088 | 0.0206 | 1.68613278 |
| Mdh2 | -0.7414 | 0.0208 | 1.681936665 |
| rasp | -0.9329 | 0.0208 | 1.681936665 |
| CG5569 | -0.855 | 0.0213 | 1.671620397 |
| CG31550 | -1.6585 | 0.0213 | 1.671620397 |
| CG14079 | -2.1857 | 0.0214 | 1.669586227 |
| Cyp1 | -0.7485 | 0.0215 | 1.66756154 |
| CG34198 | -1.0695 | 0.0218 | 1.661543506 |
| Irp-1A | -0.7889 | 0.0219 | 1.659555885 |
| DNApol-alpha50 | -1.1517 | 0.0219 | 1.659555885 |
| CG8818 | -0.8412 | 0.0224 | 1.649751982 |
| CCHa1-R | -5.4678 | 0.0227 | 1.643974143 |
| Gr8a | -5.4678 | 0.0227 | 1.643974143 |
| Mms19 | -1.2029 | 0.0227 | 1.643974143 |
| Gycalpha99B | -5.4678 | 0.0228 | 1.642065153 |
| CG13704 | -1.6407 | 0.0235 | 1.628932138 |
| toy | -1.2875 | 0.0237 | 1.625251654 |
| CG8607 | -1.1266 | 0.0241 | 1.617982957 |
| CG32201 | -2.2022 | 0.0241 | 1.617982957 |
| CG7567 | -2.4586 | 0.0244 | 1.612610174 |
| CG11912 | -3.0418 | 0.0244 | 1.612610174 |
| IntS4 | -0.8836 | 0.0247 | 1.607303047 |
| Sc2 | -0.7491 | 0.0247 | 1.607303047 |
| Egm | -0.8233 | 0.0248 | 1.605548319 |
| CG4743 | -0.9078 | 0.0249 | 1.603800653 |
| Tgt | -0.7701 | 0.025 | 1.602059991 |
| RtcB | -0.884 | 0.025 | 1.602059991 |
| CG7837 | -1.0392 | 0.0252 | 1.598599459 |
| dnd | -2.1773 | 0.0257 | 1.590066877 |
| CG33080 | -2.8231 | 0.0258 | 1.588380294 |
| ida | -1.0191 | 0.0258 | 1.588380294 |
| CG2254 | -1.7202 | 0.0258 | 1.588380294 |
| Takl1 | -2.3563 | 0.0258 | 1.588380294 |
| CG5167 | -0.8917 | 0.0259 | 1.586700236 |
| beta4GalT7 | -0.9063 | 0.026 | 1.585026652 |
| Pcl | -1.2837 | 0.026 | 1.585026652 |
| Cisd2 | -0.8436 | 0.0262 | 1.581698709 |
| CG8258 | -0.8155 | 0.0262 | 1.581698709 |
| CG11878 | -1.5233 | 0.0262 | 1.581698709 |
| hdm | -3.6925 | 0.0263 | 1.580044252 |

| | | | |
|---|---|---|---|
| CG34404 | -1.6497 | 0.0263 | 1.580044252 |
| CG4627 | -0.9998 | 0.0267 | 1.573488739 |
| CG8728 | -0.8683 | 0.0267 | 1.573488739 |
| CG8891 | -0.815 | 0.0268 | 1.571865206 |
| CG12321 | -0.9057 | 0.0269 | 1.57024772 |
| mRpL36 | -0.8362 | 0.0271 | 1.567030709 |
| CG14499 | -3.3853 | 0.0274 | 1.562249437 |
| CG4557 | -0.8553 | 0.0279 | 1.554395797 |
| CG11777 | -1.035 | 0.0281 | 1.55129368 |
| Lgr3 | -1.6167 | 0.0281 | 1.55129368 |
| CG10910 | -1.4877 | 0.0284 | 1.54668166 |
| Gs1l | -0.9892 | 0.0287 | 1.542118103 |
| CG2144 | -1.0058 | 0.0291 | 1.536107011 |
| CG32284 | -2.498 | 0.0295 | 1.530177984 |
| mRpL12 | -0.7659 | 0.0296 | 1.528708289 |
| TBC1D5 | -0.9011 | 0.0297 | 1.527243551 |
| mRpL47 | -0.7491 | 0.0298 | 1.525783736 |
| CR45474 | -2.142 | 0.0301 | 1.521433504 |
| Vha100-4 | -2.4277 | 0.0302 | 1.519993057 |
| CG17841 | -0.7886 | 0.0304 | 1.517126416 |
| Pi3K59F | -0.8379 | 0.0305 | 1.515700161 |
| CG9568 | -1.335 | 0.0306 | 1.514278574 |
| Nsun2 | -0.8112 | 0.0313 | 1.504455662 |
| r-l | -0.8568 | 0.0314 | 1.503070352 |
| CG3868 | -1.14 | 0.0314 | 1.503070352 |
| mRpL20 | -0.9376 | 0.0315 | 1.501689446 |
| arx | -1.1859 | 0.0315 | 1.501689446 |
| CG11562 | -0.8511 | 0.0317 | 1.498940738 |
| mRpL34 | -0.867 | 0.0318 | 1.49757288 |
| CG30493 | -0.8443 | 0.0319 | 1.496209317 |
| GlcT-1 | -0.7685 | 0.0319 | 1.496209317 |
| CG31251 | -1.2222 | 0.0319 | 1.496209317 |
| CR45973 | -2.675 | 0.032 | 1.494850022 |
| CG15362 | -1.0852 | 0.0323 | 1.490797478 |
| CG18577 | -1.87 | 0.0324 | 1.48945499 |
| AsnRS-m | -0.9829 | 0.0332 | 1.478861916 |
| mRpL10 | -0.7908 | 0.0333 | 1.477555766 |
| CG7542 | -1.9263 | 0.0333 | 1.477555766 |
| CG9752 | -1.3752 | 0.0334 | 1.476253533 |
| Sld5 | -1.1048 | 0.0335 | 1.474955193 |

| | | | |
|---|---|---|---|
| CG1671 | -0.8347 | 0.0339 | 1.469800302 |
| Caf1-180 | -0.8242 | 0.034 | 1.468521083 |
| Rrp42 | -0.8999 | 0.034 | 1.468521083 |
| tam | -0.9897 | 0.0342 | 1.465973894 |
| CPT2 | -0.8034 | 0.0343 | 1.46470588 |
| CG17570 | -1.8716 | 0.0346 | 1.460923901 |
| Spp | -0.7317 | 0.0349 | 1.457174573 |
| p47 | -0.7331 | 0.0351 | 1.454692884 |
| CG12173 | -0.8793 | 0.0351 | 1.454692884 |
| CG12279 | -0.8807 | 0.0351 | 1.454692884 |
| CG13492 | -1.3371 | 0.0357 | 1.447331784 |
| vanin-like | -2.3264 | 0.0357 | 1.447331784 |
| CG9360 | -1.1292 | 0.0359 | 1.444905551 |
| lectin-46Cb | -1.3304 | 0.036 | 1.443697499 |
| Nrk | -0.9285 | 0.0367 | 1.435333936 |
| beg | -0.8028 | 0.0368 | 1.434152181 |
| Rrp46 | -0.9698 | 0.037 | 1.431798276 |
| CG16979 | -0.8644 | 0.0371 | 1.43062609 |
| mRpS35 | -0.8175 | 0.0372 | 1.42945706 |
| Adgf-C | -3.9081 | 0.0375 | 1.425968732 |
| mRpL18 | -0.7157 | 0.0376 | 1.424812155 |
| CstF-50 | -0.9761 | 0.0376 | 1.424812155 |
| TyrRS-m | -0.8269 | 0.0377 | 1.42365865 |
| AdSL | -0.7638 | 0.0378 | 1.4225082 |
| CG3909 | -0.878 | 0.0378 | 1.4225082 |
| CG4278 | -0.7921 | 0.0379 | 1.42136079 |
| Xpd | -0.8764 | 0.0387 | 1.412289035 |
| CG17145 | -1.3064 | 0.0391 | 1.407823243 |
| CG11964 | -0.7555 | 0.0393 | 1.40560745 |
| CG3706 | -2.3299 | 0.0394 | 1.404503778 |
| RpS14a | -0.9624 | 0.0395 | 1.403402904 |
| mRpL44 | -0.7429 | 0.0397 | 1.401209493 |
| CG17068 | -0.8435 | 0.0397 | 1.401209493 |
| CG12204 | -0.7785 | 0.0398 | 1.400116928 |
| Ing3 | -0.8467 | 0.0398 | 1.400116928 |
| CG11590 | -0.8507 | 0.0402 | 1.395773947 |
| Pdxk | -0.779 | 0.0405 | 1.392544977 |
| vls | -0.7659 | 0.0405 | 1.392544977 |
| CG7560 | -4.9788 | 0.0417 | 1.379863945 |
| Mgstl | -0.8917 | 0.042 | 1.37675071 |

| | | | |
|---|---|---|---|
| CG30371 | -3.6713 | 0.0424 | 1.372634143 |
| CG11164 | -2.283 | 0.043 | 1.366531544 |
| Gk1 | -1.0721 | 0.043 | 1.366531544 |
| Pgm | -0.7341 | 0.0434 | 1.36251027 |
| Surf4 | -0.7551 | 0.0436 | 1.360513511 |
| Fadd | -0.8332 | 0.0439 | 1.35753548 |
| tex | -0.7888 | 0.0442 | 1.354577731 |
| Acp53Ea | -1.2018 | 0.0442 | 1.354577731 |
| beta-PheRS | -0.7443 | 0.0445 | 1.351639989 |
| ATPsynB | -0.6863 | 0.0453 | 1.343901798 |
| mRpL54 | -0.7493 | 0.0456 | 1.341035157 |
| nht | -1.9533 | 0.0458 | 1.339134522 |
| Ibf2 | -1.198 | 0.0459 | 1.338187314 |
| NK7.1 | -0.8137 | 0.046 | 1.337242168 |
| Ptp52F | -0.9791 | 0.0461 | 1.336299075 |
| CG11858 | -0.8994 | 0.0464 | 1.333482019 |
| CG8323 | -0.8838 | 0.0466 | 1.331614083 |
| glu | -0.9794 | 0.0468 | 1.329754147 |
| IP3K2 | -1.0778 | 0.0468 | 1.329754147 |
| CG30287 | -0.8938 | 0.0469 | 1.328827157 |
| Sym | -0.7792 | 0.0471 | 1.326979093 |
| stg | -1.288 | 0.0472 | 1.326058001 |
| CG5255 | -1.9321 | 0.0482 | 1.316952962 |
| Mcm7 | -1.5807 | 0.049 | 1.30980392 |
| CG33178 | -1.6823 | 0.0494 | 1.306273051 |
| l(2)dtl | -0.8239 | 0.0496 | 1.304518324 |
| RpS15Ab | -0.7814 | 0.0497 | 1.303643611 |
| CG14424 | -2.1247 | 0.0499 | 1.301899454 |
| CG8311 | -0.7509 | 0.0499 | 1.301899454 |
| CG30001 | -0.9443 | 0.0499 | 1.301899454 |
| mRpL30 | -0.7406 | 0.0502 | 1.299296283 |
| Sas-4 | -0.962 | 0.0502 | 1.299296283 |
| GckIII | -0.7637 | 0.0503 | 1.298432015 |
| COX7A | -0.8646 | 0.0505 | 1.296708622 |
| CG34220 | -1.0087 | 0.0508 | 1.294136288 |
| CR32194 | -1.1546 | 0.051 | 1.292429824 |
| SelG | -0.8175 | 0.0515 | 1.288192771 |
| l(1)G0045 | -0.8147 | 0.0525 | 1.279840697 |
| CCHa1 | -1.822 | 0.0526 | 1.279014256 |
| SPE | -1.9281 | 0.0527 | 1.278189385 |

| | | | |
|---|---|---|---|
| CG15247 | -3.1939 | 0.053 | 1.27572413 |
| AGBE | -0.7303 | 0.053 | 1.27572413 |
| CG43120 | -1.1863 | 0.053 | 1.27572413 |
| Ddx1 | -0.8651 | 0.0531 | 1.274905479 |
| Gr66a | -2.2459 | 0.0533 | 1.273272791 |
| Tfb4 | -0.7257 | 0.0535 | 1.271646218 |
| cue | -0.7187 | 0.0546 | 1.262807357 |
| Oga | -0.7987 | 0.0549 | 1.260427656 |
| | | | |

**Table 2.1c: GO enrichment for hits differentially upregulated in control females relative to control males**

| GO enrichment | p-value | Hits | Genes matches | GO ID |
|---|---|---|---|---|
| organic substance metabolic process | 0.0020691 | FBgn0000078,FBgn0000477,FBgn0000543,FBgn0000591,FBgn0001150,FBgn0001187,FBgn0002441,FBgn0003044,FBgn0003076,FBgn0003257,FBgn0003356,FBgn0003357,FBgn0003358,FBgn0003525,FBgn0003863,FBgn0003996,FBgn0004403,FBgn0004406,FBgn0004432,FBgn0010278,FBgn0010382,FBgn0010425,FBgn0011211,FBgn0011555,FBgn0011703,FBgn0011704,FBgn0011762,FBgn0011768,FBgn0011770,FBgn0011787,FBgn0013725,FBgn0013972,FBgn0014023,FBgn0014427,FBgn0014861,FBgn0015075,FBgn0015271,FBgn0015277,FBgn0015299,FBgn0016691,FBgn0017577,FBgn0019644,FBgn0019650,FBgn0020391,FBgn0020633,FBgn0020906,FBgn0022700,FBgn0023477,FBgn0024194,FBgn0024227,FBgn0024321,FBgn0024957,FBgn0024958,FBgn0024997,FBgn0025352,FBgn0025373,FBgn0025463,FBgn0025592,FBgn0025680,FBgn0025814,FBgn0025815,FBgn0026079,FBgn0026143,FBgn0026411,FBgn0026679,FBgn0026702,FBgn0026741,FBgn0026876,FBgn0026879,FBgn0027560,FBgn0027578,FBgn0027791,FBgn0027794,FBgn0027868,FBgn0028342,FBgn0029718,FBgn0029823,FBgn0029828,FBgn0029856,FBgn0029906,FBgn0029977,FBgn0030054,FBgn0030081,FBgn0030136,FBgn0030507,FBgn0030688,FBgn0030945,FBgn0030966,FBgn0031003,FBgn0031092,FBgn0031145,FBgn0031231,FBgn0031248,FBgn0031249,FBgn0031252,FBgn0031260,FBgn0031309,FBgn0031321,FBgn0031381,FBgn0031653,FBgn0031663,FBgn0031678,FBgn0031703,FBgn0031713,FBgn0031875,FBgn0031996,FBgn0031999,FBgn0032144,FBgn0032187,FBgn0032244,FBgn0032638,FBgn0032781,FBgn0033179,FBgn0033187,FBgn0033235,FBgn0033377,FBgn0033382,FBgn0033431,FBgn0033454,FBgn0033527,FBgn0033549,FBgn0033555,FBgn0033733,FBgn0033774,FBgn0033890,FBgn0033921,FBgn0034052,FBgn0034065,FBgn0034085,FBgn0034141,FBgn0034177,FBgn0034564,FBgn0034579,FBgn0034582,FBgn0034614 | 160 | GO:0071704 |

| | | | | |
|---|---|---|---|---|
| | | ,FBgn0034629,FBgn0034817,FBgn0034988,FBgn0035006,FBgn0035064,FBgn0035154,FBgn0035374,FBgn0035383,FBgn0035471,FBgn0035644,FBgn0035665,FBgn0035666,FBgn0035670,FBgn0035718,FBgn0035779,FBgn0035886,FBgn0035887,FBgn0035901,FBgn0036023,FBgn0036024,FBgn0036157,FBgn0036321,FBgn0036335,FBgn0036512,FBgn0036691,FBgn0036738,FBgn0036826,FBgn0036948,FBgn0036953,FBgn0036996,FBgn0037045,FBgn0037073,FBgn0037146,FBgn0037301,FBgn0037305,FBgn0037330,FBgn0037338,FBgn0037345,FBgn0037356,FBgn0037371,FBgn0037513,FBgn0037534,FBgn0037569,FBgn0037669,FBgn0037678,FBgn0037815,FBgn0037996,FBgn0038038,FBgn0038135,FBgn0038173,FBgn0038224,FBgn0038390,FBgn0038437,FBgn0038467,FBgn0038474,FBgn0038482,FBgn0038485,FBgn0038546,FBgn0038742,FBgn0038788,FBgn0038928,FBgn0039052,FBgn0039094,FBgn0039102,FBgn0039156,FBgn0039175,FBgn0039258,FBgn0039403,FBgn0039404,FBgn0039470,FBgn0039471,FBgn0039472,FBgn0039580,FBgn0039596,FBgn0039650,FBgn0039687,FBgn0039777,FBgn0039778,FBgn0040060,FBgn0040078,FBgn0040290,FBgn0040337,FBgn0040959,FBgn0041103,FBgn0041147,FBgn0042112,FBgn0043471,FBgn0043575,FBgn0046689,FBgn0050049,FBgn0050085,FBgn0050090,FBgn0050287,FBgn0050371,FBgn0050493,FBgn0050502,FBgn0051126,FBgn0051198,FBgn0051266,FBgn0051469,FBgn0051550,FBgn0052201,FBgn0052284,FBgn0052483,FBgn0053080,FBgn0053116,FBgn0053127,FBgn0053138,FBgn0053178,FBgn0053265,FBgn0067102,FBgn0083983,FBgn0085249,FBgn0085484,FBgn0086708,FBgn0086712,FBgn0243511,FBgn0250815,FBgn0259113,FBgn0259227,FBgn0259676,FBgn0259678,FBgn0259748,FBgn0259791,FBgn0260477,FBgn0261850,FBgn0262559,FBgn0263133,FBgn0265140,FBgn0266420,FBgn0266465,FBgn0267824,FBgn0283525,FBgn0283680,FBgn0284256,FBgn0286788 | | |
| primary metabolic process | 0.0050247 | FBgn0000078,FBgn0000477,FBgn0000543,FBgn0000591,FBgn0001150,FBgn0001187,FBgn0002441,FBgn0003044,FBgn0003076,FBgn0003257,FBgn0003356,FBgn0003357,FBgn0003358,FBgn0003525,FBgn0003863,FBgn0004403,FBgn0004406,FBgn0004432,FBgn0010278,FBgn0010382,FBgn0010425,FBgn0011211,FBgn0011555,FBgn0011703,FBgn0011704,FBgn0011762,FBgn0011768,FBgn0011787,FBgn0013725,FBgn0013972,FBgn0014023,FBgn0014028,FBgn0014427,FBgn0014861,FBgn0015075,FBgn0015271,FBgn0015277,FBgn0015299,FBgn0016691,FBgn0017577,FBgn0019644,FBgn0019650,FBgn0020391,FBgn0020633,FBgn0020906,FBgn0022700,FBgn0023477,FBgn0024194,FBgn0024227,FBgn0024321,FBgn0024957,FBgn0024958,FBgn0024997,FBgn0025352,FBgn0025373,FBgn0025463,FBgn0025592,FBgn0025680,FBgn0025814,FBgn0025815,FBgn0026079,FBgn0026143,FBgn0026411,FBgn0026679,FBgn0026702,FBgn0026741,FBgn0026876,FBgn0026879,FBgn0027560,FBgn0027578,FBgn0027791,FBgn0027794,FBgn0027868,FBgn0028342,FBgn0029718 | 160 | GO:0044238 |

| | | | | |
|---|---|---|---|---|
| | | ,FBgn0029823,FBgn0029828,FBgn0029856,FBgn0029906,FBgn0029977,FBgn0030054,FBgn0030081,FBgn0030136,FBgn0030507,FBgn0030688,FBgn0030945,FBgn0031003,FBgn0031092,FBgn0031231,FBgn0031248,FBgn0031249,FBgn0031252,FBgn0031260,FBgn0031309,FBgn0031321,FBgn0031381,FBgn0031653,FBgn0031663,FBgn0031678,FBgn0031703,FBgn0031996,FBgn0031999,FBgn0032144,FBgn0032187,FBgn0032244,FBgn0032638,FBgn0032781,FBgn0033179,FBgn0033187,FBgn0033235,FBgn0033377,FBgn0033382,FBgn0033431,FBgn0033454,FBgn0033527,FBgn0033549,FBgn0033555,FBgn0033733,FBgn0033774,FBgn0033890,FBgn0033921,FBgn0034052,FBgn0034065,FBgn0034085,FBgn0034141,FBgn0034177,FBgn0034564,FBgn0034579,FBgn0034582,FBgn0034614,FBgn0034629,FBgn0034817,FBgn0034988,FBgn0035006,FBgn0035064,FBgn0035154,FBgn0035374,FBgn0035383,FBgn0035471,FBgn0035644,FBgn0035665,FBgn0035666,FBgn0035670,FBgn0035718,FBgn0035779,FBgn0035886,FBgn0035887,FBgn0035901,FBgn0036023,FBgn0036024,FBgn0036157,FBgn0036321,FBgn0036335,FBgn0036512,FBgn0036691,FBgn0036738,FBgn0036826,FBgn0036996,FBgn0037045,FBgn0037073,FBgn0037146,FBgn0037301,FBgn0037305,FBgn0037330,FBgn0037338,FBgn0037345,FBgn0037356,FBgn0037371,FBgn0037513,FBgn0037534,FBgn0037669,FBgn0037678,FBgn0037815,FBgn0037891,FBgn0037996,FBgn0038038,FBgn0038135,FBgn0038173,FBgn0038224,FBgn0038390,FBgn0038467,FBgn0038474,FBgn0038482,FBgn0038485,FBgn0038546,FBgn0038742,FBgn0038788,FBgn0038928,FBgn0039052,FBgn0039094,FBgn0039102,FBgn0039156,FBgn0039175,FBgn0039258,FBgn0039403,FBgn0039404,FBgn0039470,FBgn0039471,FBgn0039472,FBgn0039580,FBgn0039596,FBgn0039650,FBgn0039687,FBgn0039777,FBgn0039778,FBgn0040060,FBgn0040078,FBgn0040290,FBgn0040337,FBgn0041103,FBgn0041147,FBgn0042112,FBgn0043471,FBgn0046689,FBgn0050049,FBgn0050085,FBgn0050090,FBgn0050287,FBgn0050371,FBgn0050502,FBgn0051126,FBgn0051198,FBgn0051266,FBgn0051469,FBgn0051550,FBgn0052201,FBgn0052483,FBgn0053080,FBgn0053116,FBgn0053127,FBgn0053138,FBgn0053178,FBgn0067102,FBgn0083983,FBgn0086708,FBgn0086712,FBgn0243511,FBgn0250815,FBgn0259113,FBgn0259227,FBgn0259676,FBgn0259678,FBgn0259791,FBgn0260477,FBgn0261850,FBgn0262559,FBgn0263133,FBgn0265140,FBgn0266420,FBgn0266465,FBgn0267824,FBgn0283525,FBgn0284256,FBgn0286788 | | |
| metabolic process | 0.0058731 | FBgn0000078,FBgn0000477,FBgn0000543,FBgn0000591,FBgn0001150,FBgn0001187,FBgn0002441,FBgn0003044,FBgn0003076,FBgn0003257,FBgn0003356,FBgn0003357,FBgn0003358,FBgn0003525,FBgn0003863,FBgn0003996,FBgn0004403,FBgn0004406,FBgn0004432,FBgn0010278,FBgn0010380,FBgn0010382,FBgn0010425,FBgn0011211,FBgn0011227,FBgn0011555,FBgn0011703,FBgn0011704,FBgn0011762,FBgn0011768,FBgn0011770,FBgn0011787,FBgn0013725,FBgn0013 | 160 | GO:0008152 |

| | | | | |
|---|---|---|---|---|
| | | 972,FBgn0014023,FBgn0014028,FBgn0014427,FBgn0014861,FBgn0015075,FBgn0015271,FBgn0015277,FBgn0015299,FBgn0016691,FBgn0017577,FBgn0019644,FBgn0019650,FBgn0020391,FBgn0020633,FBgn0020906,FBgn0022700,FBgn0023477,FBgn0024194,FBgn0024227,FBgn0024321,FBgn0024957,FBgn0024958,FBgn0024997,FBgn0025352,FBgn0025373,FBgn0025463,FBgn0025592,FBgn0025680,FBgn0025814,FBgn0025815,FBgn0026079,FBgn0026143,FBgn0026411,FBgn0026679,FBgn0026702,FBgn0026741,FBgn0026876,FBgn0026879,FBgn0027560,FBgn0027578,FBgn0027791,FBgn0027794,FBgn0027868,FBgn0028342,FBgn0029131,FBgn0029718,FBgn0029823,FBgn0029828,FBgn0029856,FBgn0029906,FBgn0029977,FBgn0030054,FBgn0030081,FBgn0030136,FBgn0030507,FBgn0030688,FBgn0030945,FBgn0030966,FBgn0031003,FBgn0031092,FBgn0031145,FBgn0031231,FBgn0031248,FBgn0031249,FBgn0031252,FBgn0031260,FBgn0031309,FBgn0031321,FBgn0031381,FBgn0031653,FBgn0031663,FBgn0031678,FBgn0031703,FBgn0031713,FBgn0031875,FBgn0031996,FBgn0031999,FBgn0032144,FBgn0032187,FBgn0032244,FBgn0032638,FBgn0032781,FBgn0033079,FBgn0033179,FBgn0033187,FBgn0033235,FBgn0033377,FBgn0033382,FBgn0033431,FBgn0033454,FBgn0033527,FBgn0033549,FBgn0033555,FBgn0033733,FBgn0033774,FBgn0033890,FBgn0033921,FBgn0033961,FBgn0034052,FBgn0034065,FBgn0034085,FBgn0034141,FBgn0034177,FBgn0034564,FBgn0034579,FBgn0034582,FBgn0034614,FBgn0034629,FBgn0034756,FBgn0034817,FBgn0034988,FBgn0035006,FBgn0035064,FBgn0035154,FBgn0035374,FBgn0035383,FBgn0035471,FBgn0035619,FBgn0035644,FBgn0035665,FBgn0035666,FBgn0035670,FBgn0035718,FBgn0035779,FBgn0035886,FBgn0035887,FBgn0035901,FBgn0036023,FBgn0036024,FBgn0036157,FBgn0036321,FBgn0036335,FBgn0036512,FBgn0036691,FBgn0036738,FBgn0036826,FBgn0036948,FBgn0036953,FBgn0036996,FBgn0037045,FBgn0037073,FBgn0037146,FBgn0037301,FBgn0037305,FBgn0037330,FBgn0037338,FBgn0037345,FBgn0037356,FBgn0037370,FBgn0037371,FBgn0037513,FBgn0037534,FBgn0037569,FBgn0037669,FBgn0037678,FBgn0037815,FBgn0037891,FBgn0037996,FBgn0038038,FBgn0038135,FBgn0038173,FBgn0038224,FBgn0038390,FBgn0038437,FBgn0038467,FBgn0038474,FBgn0038482,FBgn0038485,FBgn0038546,FBgn0038742,FBgn0038788,FBgn0038928,FBgn0039052,FBgn0039094,FBgn0039099,FBgn0039102,FBgn0039156,FBgn0039175,FBgn0039258,FBgn0039403,FBgn0039404,FBgn0039470,FBgn0039471,FBgn0039472,FBgn0039580,FBgn0039596,FBgn0039650,FBgn0039687,FBgn0039777,FBgn0039778,FBgn0040060,FBgn0040069,FBgn0040078,FBgn0040290,FBgn0040337,FBgn0040529,FBgn0040959,FBgn0041103,FBgn0041147,FBgn0042112,FBgn0043471,FBgn0043575,FBgn0046689,FBgn0050049,FBgn0050085,FBgn0050090,FBgn0050287,FBgn0050371,FBgn0050493,FBgn0050502,FBgn0051126,FBgn0051198,FBgn0051266,FBgn0 | | |

| | | | | |
|---|---|---|---|---|
| | | 051469,FBgn0051550,FBgn0052201,FBgn0052284,FBgn0052483,FBgn0052750,FBgn0053080,FBgn0053116,FBgn0053127,FBgn0053138,FBgn0053178,FBgn0053265,FBgn0067102,FBgn0083983,FBgn0085249,FBgn0085484,FBgn0086708,FBgn0086712,FBgn0243511,FBgn0250815,FBgn0259113,FBgn0259227,FBgn0259676,FBgn0259678,FBgn0259748,FBgn0259791,FBgn0260477,FBgn0261850,FBgn0262559,FBgn0263133,FBgn0265140,FBgn0266420,FBgn0266465,FBgn0267824,FBgn0283525,FBgn0283680,FBgn0284256,FBgn0286788 | | |
| organonitrogen compound metabolic process | 0.0167065 | FBgn0001187,FBgn0003257,FBgn0003356,FBgn0003357,FBgn0003358,FBgn0003525,FBgn0003863,FBgn0003996,FBgn0004403,FBgn0004432,FBgn0010278,FBgn0010382,FBgn0010425,FBgn0011211,FBgn0011555,FBgn0011703,FBgn0011704,FBgn0011768,FBgn0011787,FBgn0013725,FBgn0013972,FBgn0014023,FBgn0014427,FBgn0016691,FBgn0019644,FBgn0020391,FBgn0020906,FBgn0022700,FBgn0024194,FBgn0024227,FBgn0024997,FBgn0026741,FBgn0026879,FBgn0027578,FBgn0027791,FBgn0027794,FBgn0028342,FBgn0029718,FBgn0029823,FBgn0029828,FBgn0029856,FBgn0029906,FBgn0030136,FBgn0030688,FBgn0030945,FBgn0031003,FBgn0031145,FBgn0031231,FBgn0031248,FBgn0031249,FBgn0031260,FBgn0031309,FBgn0031653,FBgn0031678,FBgn0031999,FBgn0032144,FBgn0032187,FBgn0032638,FBgn0033179,FBgn0033187,FBgn0033235,FBgn0033431,FBgn0033527,FBgn0033555,FBgn0033774,FBgn0034052,FBgn0034085,FBgn0034177,FBgn0034579,FBgn0034582,FBgn0034817,FBgn0034988,FBgn0035064,FBgn0035154,FBgn0035374,FBgn0035665,FBgn0035666,FBgn0035670,FBgn0035718,FBgn0035779,FBgn0035886,FBgn0035887,FBgn0036023,FBgn0036024,FBgn0036157,FBgn0036335,FBgn0036512,FBgn0036738,FBgn0036948,FBgn0036953,FBgn0037045,FBgn0037146,FBgn0037301,FBgn0037305,FBgn0037330,FBgn0037513,FBgn0037534,FBgn0037678,FBgn0038135,FBgn0038173,FBgn0038224,FBgn0038467,FBgn0038474,FBgn0038482,FBgn0038485,FBgn0038788,FBgn0038928,FBgn0039052,FBgn0039094,FBgn0039102,FBgn0039156,FBgn0039175,FBgn0039258,FBgn0039580,FBgn0039650,FBgn0039687,FBgn0039777,FBgn0039778,FBgn0040060,FBgn0040078,FBgn0040959,FBgn0041147,FBgn0042112,FBgn0043471,FBgn0043575,FBgn0046689,FBgn0050049,FBgn0050090,FBgn0050287,FBgn0050371,FBgn0051198,FBgn0051266,FBgn0051469,FBgn0052201,FBgn0052284,FBgn0052483,FBgn0053127,FBgn0053178,FBgn0053265,FBgn0067102,FBgn0083983,FBgn0085249,FBgn0085484,FBgn0086708,FBgn0243511,FBgn0250815,FBgn0259227,FBgn0259678,FBgn0259748,FBgn0259791,FBgn0260477,FBgn0262559,FBgn0263133,FBgn0265140,FBgn0266465,FBgn0267824,FBgn0284256 | 157 | GO:1901564 |
| small molecule metabolic process | 4.43E-07 | FBgn0000543,FBgn0001187,FBgn0003076,FBgn0003257,FBgn0011211,FBgn0011703,FBgn0011704,FBgn0011768,FBgn0011770,FBgn0013972,FBgn0014427,FBgn0016691,FBgn0019644,FBgn0024957,FBgn0024958,FBgn0025352,FBgn0025592,FBgn0025814,FBgn0028 | 62 | GO:0044281 |

| | | | | |
|---|---|---|---|---|
| | | 342,FBgn0029823,FBgn0030507,FBgn0030966,FBgn0031092,FBgn0031381,FBgn0031663,FBgn0031703,FBgn0031713,FBgn0033733,FBgn0034177,FBgn0034629,FBgn0034988,FBgn0035006,FBgn0035064,FBgn0035383,FBgn0035471,FBgn0036157,FBgn0036691,FBgn0037146,FBgn0037305,FBgn0037356,FBgn0037513,FBgn0037534,FBgn0037996,FBgn0038173,FBgn0038224,FBgn0038437,FBgn0038467,FBgn0038742,FBgn0039052,FBgn0039094,FBgn0039156,FBgn0039175,FBgn0039258,FBgn0039580,FBgn0039650,FBgn0050493,FBgn0050502,FBgn0053178,FBgn0085484,FBgn0086712,FBgn0262559,FBgn0283680 | | |
| proteolysis | 9.114E-06 | FBgn0003356,FBgn0003357,FBgn0003358,FBgn0003863,FBgn0010425,FBgn0011555,FBgn0011703,FBgn0011704,FBgn0013725,FBgn0020906,FBgn0024997,FBgn0027578,FBgn0029828,FBgn0029856,FBgn0030688,FBgn0031248,FBgn0031249,FBgn0031260,FBgn0031653,FBgn0031678,FBgn0032144,FBgn0032638,FBgn0033179,FBgn0033235,FBgn0033774,FBgn0034052,FBgn0035154,FBgn0035665,FBgn0035666,FBgn0035670,FBgn0035718,FBgn0035779,FBgn0035886,FBgn0035887,FBgn0036023,FBgn0036024,FBgn0036512,FBgn0036738,FBgn0037678,FBgn0038135,FBgn0038482,FBgn0038485,FBgn0038928,FBgn0039102,FBgn0039777,FBgn0039778,FBgn0040060,FBgn0041147,FBgn0043471,FBgn0050049,FBgn0050090,FBgn0050287,FBgn0050371,FBgn0051198,FBgn0051266,FBgn0052483,FBgn0053127,FBgn0250815,FBgn0260477,FBgn0262559,FBgn0265140 | 61 | GO:0006508 |
| cell cycle process | 0.0318894 | FBgn0000140,FBgn0003525,FBgn0003885,FBgn0004378,FBgn0004643,FBgn0010382,FBgn0011020,FBgn0011692,FBgn0014861,FBgn0015271,FBgn0015391,FBgn0017577,FBgn0020633,FBgn0024227,FBgn0025815,FBgn0026143,FBgn0026876,FBgn0027500,FBgn0027868,FBgn0029977,FBgn0030054,FBgn0031549,FBgn0032244,FBgn0033549,FBgn0033890,FBgn0033921,FBgn0034569,FBgn0035644,FBgn0038390,FBgn0039403,FBgn0039638,FBgn0040078,FBgn0040290,FBgn0041147,FBgn0050085,FBgn0061476,FBgn0259113,FBgn0259791,FBgn0261850,FBgn0286788 | 40 | GO:0022402 |
| organic acid metabolic process | 4.282E-06 | FBgn0001187,FBgn0011770,FBgn0014427,FBgn0024957,FBgn0024958,FBgn0025352,FBgn0025814,FBgn0029823,FBgn0030966,FBgn0031092,FBgn0031703,FBgn0033733,FBgn0034177,FBgn0034629,FBgn0035006,FBgn0035064,FBgn0035383,FBgn0035471,FBgn0036157,FBgn0036691,FBgn0037146,FBgn0037305,FBgn0037356,FBgn0037513,FBgn0037534,FBgn0037996,FBgn0038437,FBgn0038742,FBgn0039052,FBgn0039094,FBgn0039156,FBgn0039175,FBgn0039258,FBgn0050502,FBgn0053178,FBgn0086712,FBgn0262559 | 37 | GO:0006082 |
| oxoacid metabolic process | 4.282E-06 | FBgn0001187,FBgn0011770,FBgn0014427,FBgn0024957,FBgn0024958,FBgn0025352,FBgn0025814,FBgn0029823,FBgn0030966,FBgn0031092,FBgn0031703,FBgn0033733,FBgn0034177,FBgn0034629,FBgn0035006,FBgn0035064,FBgn0035383,FBgn0035471,FBgn0036157,FBgn0036691,FBgn0037146,FBgn0037305,FBgn0037356,FBgn0037513,FBgn0037534,FBgn0037996,FB | 37 | GO:0043436 |

| | | | | |
|---|---|---|---|---|
| | | gn0038437,FBgn0038742,FBgn0039052,FBgn0039094,FBgn0039156,FBgn0039175,FBgn0039258,FBgn0050502,FBgn0053178,FBgn0086712,FBgn0262559 | | |
| carbohydrate derivative metabolic process | 0.0015541 | FBgn0001187,FBgn0003257,FBgn0011211,FBgn0011703,FBgn0011704,FBgn0013972,FBgn0016691,FBgn0019644,FBgn0022700,FBgn0023477,FBgn0025592,FBgn0027791,FBgn0028342,FBgn0029906,FBgn0030507,FBgn0033187,FBgn0033431,FBgn0034582,FBgn0034988,FBgn0036948,FBgn0036953,FBgn0038038,FBgn0038173,FBgn0038224,FBgn0038467,FBgn0039156,FBgn0039258,FBgn0039580,FBgn0039650,FBgn0040959,FBgn0043575,FBgn0052284,FBgn0053265,FBgn0067102,FBgn0085249,FBgn0259748 | 36 | GO:1901135 |
| carboxylic acid metabolic process | 9.758E-06 | FBgn0001187,FBgn0011770,FBgn0014427,FBgn0024957,FBgn0024958,FBgn0025352,FBgn0025814,FBgn0029823,FBgn0031092,FBgn0031703,FBgn0033733,FBgn0034177,FBgn0034629,FBgn0035006,FBgn0035064,FBgn0035383,FBgn0035471,FBgn0036157,FBgn0036691,FBgn0037146,FBgn0037305,FBgn0037356,FBgn0037513,FBgn0037534,FBgn0037996,FBgn0038437,FBgn0038742,FBgn0039052,FBgn0039094,FBgn0039156,FBgn0039175,FBgn0050502,FBgn0053178,FBgn0086712,FBgn0262559 | 35 | GO:0019752 |
| lipid metabolic process | 0.0031557 | FBgn0000543,FBgn0015277,FBgn0025352,FBgn0025373,FBgn0025592,FBgn0025814,FBgn0029906,FBgn0031092,FBgn0031381,FBgn0031703,FBgn0033187,FBgn0033382,FBgn0033733,FBgn0034141,FBgn0034629,FBgn0035006,FBgn0035383,FBgn0035471,FBgn0036691,FBgn0036996,FBgn0037356,FBgn0037534,FBgn0037996,FBgn0038038,FBgn0038742,FBgn0039156,FBgn0039470,FBgn0039471,FBgn0039472,FBgn0050502,FBgn0053116,FBgn0053178,FBgn0067102,FBgn0086712 | 34 | GO:0006629 |
| oxidation-reduction process | 0.0252941 | FBgn0003076,FBgn0011211,FBgn0011227,FBgn0011703,FBgn0011704,FBgn0011768,FBgn0014028,FBgn0023477,FBgn0024957,FBgn0024958,FBgn0025352,FBgn0025814,FBgn0030966,FBgn0031092,FBgn0031713,FBgn0033079,FBgn0033961,FBgn0034629,FBgn0034756,FBgn0035383,FBgn0036157,FBgn0037146,FBgn0037370,FBgn0037891,FBgn0038038,FBgn0038742,FBgn0039099,FBgn0040529,FBgn0050502,FBgn0052201,FBgn0053138,FBgn0053178,FBgn0086712,FBgn0262559 | 34 | GO:0055114 |
| DNA metabolic process | 0.0001931 | FBgn0000477,FBgn0004406,FBgn0010382,FBgn0011762,FBgn0014861,FBgn0015075,FBgn0015271,FBgn0017577,FBgn0020633,FBgn0025815,FBgn0026143,FBgn0027868,FBgn0029977,FBgn0030054,FBgn0031252,FBgn0031309,FBgn0032244,FBgn0033549,FBgn0033890,FBgn0035644,FBgn0036321,FBgn0037301,FBgn0037338,FBgn0037345,FBgn0039403,FBgn0040290,FBgn0050085,FBgn0259113,FBgn0259676,FBgn0261850,FBgn0286788 | 31 | GO:0006259 |
| small molecule biosynthetic process | 1.60E-07 | FBgn0000543,FBgn0014427,FBgn0025814,FBgn0029823,FBgn0031381,FBgn0031663,FBgn0031703,FBgn0031713,FBgn0033733,FBgn0034988,FBgn0035006,FBgn0035383,FBgn0035471,FBgn0036157,FBgn0036691,FBgn0037146,FBgn0037305,FBgn0037356,FBgn0037 | 29 | GO:0044283 |

| | | | | |
|---|---|---|---|---|
| | | 513,FBgn0037534,FBgn0037996,FBgn0038173,FBgn0039094,FBgn0039156,FBgn0039650,FBgn0050493,FBgn0053178,FBgn0085484,FBgn0283680 | | |
| cellular lipid metabolic process | 0.0055799 | FBgn0015277,FBgn0025352,FBgn0025373,FBgn0025592,FBgn0025814,FBgn0029906,FBgn0031092,FBgn0031703,FBgn0033187,FBgn0033382,FBgn0033733,FBgn0034141,FBgn0034629,FBgn0035006,FBgn0035383,FBgn0035471,FBgn0036691,FBgn0037356,FBgn0037534,FBgn0037996,FBgn0038038,FBgn0038742,FBgn0039156,FBgn0050502,FBgn0053116,FBgn0053178,FBgn0067102,FBgn0086712 | 28 | GO:0044255 |
| mitotic cell cycle process | 0.0134237 | FBgn0000140,FBgn0003525,FBgn0003885,FBgn0004378,FBgn0004643,FBgn0010382,FBgn0011692,FBgn0014861,FBgn0015271,FBgn0015391,FBgn0024227,FBgn0025815,FBgn0026143,FBgn0031549,FBgn0033549,FBgn0034569,FBgn0035644,FBgn0038390,FBgn0039403,FBgn0039638,FBgn0040078,FBgn0040290,FBgn0041147,FBgn0061476,FBgn0259113,FBgn0259791,FBgn0261850,FBgn0286788 | 28 | GO:1903047 |
| organophosphate metabolic process | 0.0133514 | FBgn0001187,FBgn0003257,FBgn0011211,FBgn0011703,FBgn0011704,FBgn0013972,FBgn0015277,FBgn0016691,FBgn0019644,FBgn0023477,FBgn0025373,FBgn0025592,FBgn0028342,FBgn0030507,FBgn0031663,FBgn0033187,FBgn0034141,FBgn0034988,FBgn0038224,FBgn0038467,FBgn0039156,FBgn0039580,FBgn0039650,FBgn0053116,FBgn0085484,FBgn0283680 | 26 | GO:0019637 |
| drug metabolic process | 3.89E-06 | FBgn0011211,FBgn0011768,FBgn0016691,FBgn0019644,FBgn0022700,FBgn0024957,FBgn0024958,FBgn0028342,FBgn0029823,FBgn0034582,FBgn0035383,FBgn0036948,FBgn0036953,FBgn0037305,FBgn0038173,FBgn0038224,FBgn0038437,FBgn0038467,FBgn0039094,FBgn0040959,FBgn0052284,FBgn0053265,FBgn0085249,FBgn0085484,FBgn0259748 | 25 | GO:0017144 |
| cellular response to DNA damage stimulus | 0.0044455 | FBgn0004406,FBgn0014861,FBgn0015075,FBgn0017577,FBgn0020633,FBgn0025815,FBgn0026143,FBgn0027868,FBgn0029131,FBgn0029588,FBgn0029977,FBgn0030054,FBgn0031252,FBgn0031309,FBgn0032244,FBgn0033549,FBgn0033890,FBgn0035644,FBgn0037301,FBgn0037338,FBgn0039403,FBgn0040290,FBgn0050085,FBgn0261850 | 24 | GO:0006974 |
| DNA replication | 8.10E-08 | FBgn0004406,FBgn0010382,FBgn0011703,FBgn0011762,FBgn0014861,FBgn0015271,FBgn0017577,FBgn0020633,FBgn0025815,FBgn0026143,FBgn0030054,FBgn0031875,FBgn0032244,FBgn0033549,FBgn0033890,FBgn0035644,FBgn0039403,FBgn0040290,FBgn0050085,FBgn0259113,FBgn0259676,FBgn0286788 | 22 | GO:0006260 |
| DNA repair | 0.0008795 | FBgn0004406,FBgn0014861,FBgn0015075,FBgn0017577,FBgn0020633,FBgn0025815,FBgn0026143,FBgn0027868,FBgn0029977,FBgn0030054,FBgn0031252,FBgn0031309,FBgn0032244,FBgn0033549,FBgn0033890,FBgn0035644,FBgn0037301,FBgn0037338,FBgn0039403,FBgn0040290,FBgn0261850 | 21 | GO:0006281 |
| lipid biosynthetic process | 0.0009743 | FBgn0000543,FBgn0015277,FBgn0025373,FBgn0025814,FBgn0031381,FBgn0031703,FBgn0033187,FBgn0033733,FBgn0034141,FBgn0035006,FBgn0035471,FBgn0036691,FBgn0037356,FBgn0037534,FBgn0037996,FBgn0038038,FBgn0039156,FBgn0050502,FBgn0053 | 21 | GO:0008610 |

| | | | | |
|---|---|---|---|---|
| | | 116,FBgn0053178,FBgn0067102 | | |
| DNA-dependent DNA replication | 2.67E-07 | FBgn0004406,FBgn0011762,FBgn0014861,FBgn0015271,FBgn0017577,FBgn0020633,FBgn0025815,FBgn0026143,FBgn0030054,FBgn0031875,FBgn0032244,FBgn0033549,FBgn0033890,FBgn0035644,FBgn0039403,FBgn0040290,FBgn0050085,FBgn0259113,FBgn0259676,FBgn0286788 | 20 | GO:0006261 |
| monocarboxylic acid metabolic process | 0.000107 | FBgn0001187,FBgn0011770,FBgn0025352,FBgn0025814,FBgn0031092,FBgn0031703,FBgn0033733,FBgn0034629,FBgn0035006,FBgn0035383,FBgn0035471,FBgn0036691,FBgn0037356,FBgn0037534,FBgn0037996,FBgn0038742,FBgn0039156,FBgn0050502,FBgn0053178,FBgn0086712 | 20 | GO:0032787 |
| nucleobase-containing small molecule metabolic process | 0.0076182 | FBgn0001187,FBgn0003257,FBgn0011211,FBgn0011703,FBgn0011704,FBgn0013972,FBgn0016691,FBgn0019644,FBgn0028342,FBgn0029823,FBgn0030507,FBgn0031663,FBgn0034988,FBgn0037513,FBgn0038173,FBgn0038224,FBgn0038467,FBgn0039156,FBgn0039580,FBgn0039650 | 20 | GO:0055086 |
| carbohydrate derivative biosynthetic process | 0.0339194 | FBgn0003257,FBgn0011211,FBgn0011703,FBgn0011704,FBgn0013972,FBgn0016691,FBgn0019644,FBgn0025592,FBgn0027791,FBgn0028342,FBgn0029906,FBgn0033187,FBgn0038038,FBgn0038173,FBgn0038224,FBgn0038467,FBgn0039156,FBgn0039258,FBgn0039580,FBgn0067102 | 20 | GO:1901137 |
| organophosphate biosynthetic process | 0.0049102 | FBgn0003257,FBgn0011211,FBgn0011703,FBgn0011704,FBgn0013972,FBgn0015277,FBgn0016691,FBgn0019644,FBgn0025373,FBgn0025592,FBgn0028342,FBgn0033187,FBgn0034141,FBgn0038224,FBgn0038467,FBgn0039156,FBgn0053116,FBgn0085484,FBgn0283680 | 19 | GO:0090407 |
| regulation of mitotic cell cycle | 0.0108642 | FBgn0002441,FBgn0003525,FBgn0004643,FBgn0010382,FBgn0024227,FBgn0026143,FBgn0031549,FBgn0033549,FBgn0034569,FBgn0038390,FBgn0039403,FBgn0039638,FBgn0040290,FBgn0041147,FBgn0061476,FBgn0259791,FBgn0261850,FBgn0266465,FBgn0286788 | 19 | GO:0007346 |
| organic acid biosynthetic process | 3.645E-06 | FBgn0014427,FBgn0025814,FBgn0029823,FBgn0031703,FBgn0033733,FBgn0035006,FBgn0035471,FBgn0036157,FBgn0036691,FBgn0037146,FBgn0037305,FBgn0037356,FBgn0037513,FBgn0037534,FBgn0037996,FBgn0039094,FBgn0039156,FBgn0053178 | 18 | GO:0016053 |
| carboxylic acid biosynthetic process | 3.645E-06 | FBgn0014427,FBgn0025814,FBgn0029823,FBgn0031703,FBgn0033733,FBgn0035006,FBgn0035471,FBgn0036157,FBgn0036691,FBgn0037146,FBgn0037305,FBgn0037356,FBgn0037513,FBgn0037534,FBgn0037996,FBgn0039094,FBgn0039156,FBgn0053178 | 18 | GO:0046394 |
| fatty acid metabolic process | 5.632E-06 | FBgn0025352,FBgn0025814,FBgn0031092,FBgn0031703,FBgn0033733,FBgn0034629,FBgn0035006,FBgn0035383,FBgn0035471,FBgn0036691,FBgn0037356,FBgn0037534,FBgn0037996,FBgn0038742,FBgn0039156,FBgn0050502,FBgn0053178,FBgn0086712 | 18 | GO:0006631 |
| generation of precursor metabolites and energy | 0.007137 | FBgn0001187,FBgn0003076,FBgn0011211,FBgn0011227,FBgn0011768,FBgn0014028,FBgn0016691,FBgn0023477,FBgn0024957,FBgn0024958,FBgn0027794,FBgn0033961,FBgn0035383,FBgn0037891,FBgn0040529 | 18 | GO:0006091 |

| | | | | |
|---|---|---|---|---|
| | | ,FBgn0053138,FBgn0262559,FBgn0284256 | | |
| regulation of cell cycle process | 0.0098543 | FBgn0003525,FBgn0004643,FBgn0010382,FBgn0024227,FBgn0026143,FBgn0031549,FBgn0034569,FBgn0035644,FBgn0038390,FBgn0039403,FBgn0039638,FBgn0040290,FBgn0041147,FBgn0050085,FBgn0061476,FBgn0259791,FBgn0261850,FBgn0286788 | 18 | GO:0010564 |
| mitochondrial translation | 0.0011225 | FBgn0011787,FBgn0014023,FBgn0026741,FBgn0027794,FBgn0029718,FBgn0031231,FBgn0034579,FBgn0035064,FBgn0035374,FBgn0036335,FBgn0037330,FBgn0038474,FBgn0042112,FBgn0083983,FBgn0263133,FBgn0284256 | 16 | GO:0032543 |
| mitochondrial gene expression | 0.0043101 | FBgn0011787,FBgn0014023,FBgn0026741,FBgn0027794,FBgn0029718,FBgn0031231,FBgn0034579,FBgn0035064,FBgn0035374,FBgn0036335,FBgn0037330,FBgn0038474,FBgn0042112,FBgn0083983,FBgn0263133,FBgn0284256 | 16 | GO:0140053 |
| nucleoside phosphate metabolic process | 0.0107824 | FBgn0001187,FBgn0003257,FBgn0011211,FBgn0011703,FBgn0011704,FBgn0013972,FBgn0016691,FBgn0019644,FBgn0028342,FBgn0030507,FBgn0031663,FBgn0034988,FBgn0038224,FBgn0038467,FBgn0039156,FBgn0039650 | 16 | GO:0006753 |
| mitotic nuclear division | 0.016961 | FBgn0004378,FBgn0004643,FBgn0010382,FBgn0011692,FBgn0015271,FBgn0015391,FBgn0024227,FBgn0031549,FBgn0034569,FBgn0039638,FBgn0040078,FBgn0041147,FBgn0061476,FBgn0259791,FBgn0261850 | 15 | GO:0140014 |
| double-strand break repair | 0.0004804 | FBgn0014861,FBgn0015075,FBgn0017577,FBgn0020633,FBgn0025815,FBgn0026143,FBgn0027868,FBgn0029977,FBgn0030054,FBgn0033549,FBgn0037301,FBgn0037338,FBgn0039403,FBgn0040290 | 14 | GO:0006302 |
| regulation of cell cycle phase transition | 0.0025978 | FBgn0003525,FBgn0004643,FBgn0010382,FBgn0024227,FBgn0026143,FBgn0031549,FBgn0038390,FBgn0039403,FBgn0040290,FBgn0041147,FBgn0050085,FBgn0061476,FBgn0261850,FBgn0286788 | 14 | GO:1901987 |
| cell cycle phase transition | 0.0177676 | FBgn0003525,FBgn0004643,FBgn0010382,FBgn0024227,FBgn0026143,FBgn0031549,FBgn0038390,FBgn0039403,FBgn0040290,FBgn0041147,FBgn0050085,FBgn0061476,FBgn0261850,FBgn0286788 | 14 | GO:0044770 |
| nucleotide metabolic process | 0.0377349 | FBgn0001187,FBgn0003257,FBgn0011211,FBgn0011703,FBgn0011704,FBgn0013972,FBgn0016691,FBgn0019644,FBgn0028342,FBgn0030507,FBgn0038224,FBgn0038467,FBgn0039156,FBgn0039650 | 14 | GO:0009117 |
| DNA recombination | 0.0023796 | FBgn0014861,FBgn0017577,FBgn0020633,FBgn0025815,FBgn0026143,FBgn0027868,FBgn0029977,FBgn0030054,FBgn0033549,FBgn0037301,FBgn0039403,FBgn0040290,FBgn0261850 | 13 | GO:0006310 |
| regulation of mitotic cell cycle phase transition | 0.0044564 | FBgn0003525,FBgn0004643,FBgn0010382,FBgn0024227,FBgn0026143,FBgn0031549,FBgn0038390,FBgn0039403,FBgn0040290,FBgn0041147,FBgn0061476,FBgn0261850,FBgn0286788 | 13 | GO:1901990 |
| DNA conformation change | 0.0086556 | FBgn0014861,FBgn0015075,FBgn0015271,FBgn0015391,FBgn0017577,FBgn0020633,FBgn0024227,FBgn0025815,FBgn0026143,FBgn0026876,FBgn0030054,FBgn0040290,FBgn0261850 | 13 | GO:0071103 |
| small molecule catabolic | 0.010596 | FBgn0003076,FBgn0011768,FBgn0025352,FBgn0029823,FBgn0031092,FBgn0034629,FBgn0034988,FBgn0035383,FBgn0038173,FBgn0038742,FBgn0039094,FB | 13 | GO:0044282 |

| | | | | |
|---|---|---|---|---|
| process | | gn0039650,FBgn0086712 | | |
| mitotic cell cycle phase transition | 0.0238005 | FBgn0003525,FBgn0004643,FBgn0010382,FBgn0024227,FBgn0026143,FBgn0031549,FBgn0038390,FBgn0039403,FBgn0040290,FBgn0041147,FBgn0061476,FBgn0261850,FBgn0286788 | 13 | GO:0044772 |
| purine-containing compound metabolic process | 0.0258011 | FBgn0001187,FBgn0011211,FBgn0013972,FBgn0016691,FBgn0019644,FBgn0028342,FBgn0029823,FBgn0034988,FBgn0038173,FBgn0038224,FBgn0038467,FBgn0039156,FBgn0039650 | 13 | GO:0072521 |
| ribonucleotide metabolic process | 0.0270761 | FBgn0001187,FBgn0003257,FBgn0011211,FBgn0013972,FBgn0016691,FBgn0019644,FBgn0028342,FBgn0030507,FBgn0038224,FBgn0038467,FBgn0039156,FBgn0039650 | 12 | GO:0009259 |
| ATP metabolic process | 0.0294131 | FBgn0001187,FBgn0011211,FBgn0011227,FBgn0014028,FBgn0016691,FBgn0019644,FBgn0027794,FBgn0028342,FBgn0033961,FBgn0038224,FBgn0040529,FBgn0284256 | 12 | GO:0046034 |
| ribose phosphate metabolic process | 0.0345188 | FBgn0001187,FBgn0003257,FBgn0011211,FBgn0013972,FBgn0016691,FBgn0019644,FBgn0028342,FBgn0030507,FBgn0038224,FBgn0038467,FBgn0039156,FBgn0039650 | 12 | GO:0019693 |
| fatty acid biosynthetic process | 7.03E-05 | FBgn0025814,FBgn0031703,FBgn0033733,FBgn0035006,FBgn0035471,FBgn0036691,FBgn0037356,FBgn0037534,FBgn0037996,FBgn0039156,FBgn0053178 | 11 | GO:0006633 |
| monocarboxylic acid biosynthetic process | 0.0002471 | FBgn0025814,FBgn0031703,FBgn0033733,FBgn0035006,FBgn0035471,FBgn0036691,FBgn0037356,FBgn0037534,FBgn0037996,FBgn0039156,FBgn0053178 | 11 | GO:0072330 |
| aminoglycan metabolic process | 0.0007067 | FBgn0022700,FBgn0034582,FBgn0036948,FBgn0036953,FBgn0039258,FBgn0040959,FBgn0043575,FBgn0052284,FBgn0053265,FBgn0085249,FBgn0259748 | 11 | GO:0006022 |
| nucleotide biosynthetic process | 0.0175982 | FBgn0003257,FBgn0011211,FBgn0011703,FBgn0011704,FBgn0013972,FBgn0016691,FBgn0019644,FBgn0028342,FBgn0038224,FBgn0038467,FBgn0039156 | 11 | GO:0009165 |
| nucleoside phosphate biosynthetic process | 0.0194314 | FBgn0003257,FBgn0011211,FBgn0011703,FBgn0011704,FBgn0013972,FBgn0016691,FBgn0019644,FBgn0028342,FBgn0038224,FBgn0038467,FBgn0039156 | 11 | GO:1901293 |
| cell cycle DNA replication | 0.0003947 | FBgn0014861,FBgn0017577,FBgn0020633,FBgn0025815,FBgn0026143,FBgn0030054,FBgn0033890,FBgn0035644,FBgn0259113,FBgn0286788 | 10 | GO:0044786 |
| double-strand break repair via homologous recombination | 0.0005684 | FBgn0014861,FBgn0017577,FBgn0020633,FBgn0025815,FBgn0026143,FBgn0027868,FBgn0030054,FBgn0037301,FBgn0039403,FBgn0040290 | 10 | GO:0000724 |
| recombinational repair | 0.0005684 | FBgn0014861,FBgn0017577,FBgn0020633,FBgn0025815,FBgn0026143,FBgn0027868,FBgn0030054,FBgn0037301,FBgn0039403,FBgn0040290 | 10 | GO:0000725 |
| amino sugar metabolic process | 0.0010665 | FBgn0022700,FBgn0034582,FBgn0036948,FBgn0036953,FBgn0039580,FBgn0040959,FBgn0052284,FBgn0053265,FBgn0085249,FBgn0259748 | 10 | GO:0006040 |
| regulation of mitotic nuclear | 0.0036566 | FBgn0004643,FBgn0010382,FBgn0024227,FBgn0031549,FBgn0034569,FBgn0039638,FBgn0041147,FBgn0061476,FBgn0259791,FBgn0261850 | 10 | GO:0007088 |

| | | | | |
|---|---|---|---|---|
| division | | | | |
| regulation of nuclear division | 0.0065731 | FBgn0004643,FBgn0010382,FBgn0024227,FBgn0031549,FBgn0034569,FBgn0039638,FBgn0041147,FBgn0061476,FBgn0259791,FBgn0261850 | 10 | GO:0051783 |
| purine-containing compound biosynthetic process | 0.0075273 | FBgn0011211,FBgn0013972,FBgn0016691,FBgn0019644,FBgn0028342,FBgn0029823,FBgn0038173,FBgn0038224,FBgn0038467,FBgn0039156 | 10 | GO:0072522 |
| DNA replication initiation | 7.091E-06 | FBgn0014861,FBgn0015271,FBgn0017577,FBgn0020633,FBgn0025815,FBgn0026143,FBgn0050085,FBgn0259113,FBgn0286788 | 9 | GO:0006270 |
| chitin metabolic process | 0.0005122 | FBgn0022700,FBgn0034582,FBgn0036948,FBgn0036953,FBgn0040959,FBgn0052284,FBgn0053265,FBgn0085249,FBgn0259748 | 9 | GO:0006030 |
| glucosamine-containing compound metabolic process | 0.0023822 | FBgn0022700,FBgn0034582,FBgn0036948,FBgn0036953,FBgn0040959,FBgn0052284,FBgn0053265,FBgn0085249,FBgn0259748 | 9 | GO:1901071 |
| mitotic spindle organization | 0.0034304 | FBgn0000140,FBgn0004378,FBgn0011692,FBgn0015271,FBgn0024227,FBgn0034569,FBgn0039638,FBgn0040078,FBgn0259791 | 9 | GO:0007052 |
| chromosome separation | 0.0034304 | FBgn0004643,FBgn0015391,FBgn0017577,FBgn0024227,FBgn0029977,FBgn0031549,FBgn0033549,FBgn0041147,FBgn0061476 | 9 | GO:0051304 |
| ribonucleotide biosynthetic process | 0.0213646 | FBgn0003257,FBgn0011211,FBgn0013972,FBgn0016691,FBgn0019644,FBgn0028342,FBgn0038224,FBgn0038467,FBgn0039156 | 9 | GO:0009260 |
| ribose phosphate biosynthetic process | 0.0265672 | FBgn0003257,FBgn0011211,FBgn0013972,FBgn0016691,FBgn0019644,FBgn0028342,FBgn0038224,FBgn0038467,FBgn0039156 | 9 | GO:0046390 |
| microtubule cytoskeleton organization involved in mitosis | 0.0265672 | FBgn0000140,FBgn0004378,FBgn0011692,FBgn0015271,FBgn0024227,FBgn0034569,FBgn0039638,FBgn0040078,FBgn0259791 | 9 | GO:1902850 |
| positive regulation of cell cycle process | 0.002971 | FBgn0003525,FBgn0010382,FBgn0024227,FBgn0026143,FBgn0035644,FBgn0039403,FBgn0040290,FBgn0041147 | 8 | GO:0090068 |
| maturation of SSU-rRNA | 0.007443 | FBgn0004403,FBgn0030081,FBgn0030136,FBgn0033454,FBgn0034564,FBgn0037073,FBgn0038474,FBgn0039404 | 8 | GO:0030490 |
| proton transmembrane transport | 0.008749 | FBgn0011211,FBgn0016691,FBgn0019644,FBgn0022097,FBgn0028342,FBgn0038224,FBgn0038613,FBgn0262512 | 8 | GO:1902600 |
| positive regulation of cell cycle | 0.0204304 | FBgn0003525,FBgn0010382,FBgn0024227,FBgn0026143,FBgn0035644,FBgn0039403,FBgn0040290,FBgn0041147 | 8 | GO:0045787 |
| purine ribonucleotide biosynthetic process | 0.026053 | FBgn0011211,FBgn0013972,FBgn0016691,FBgn0019644,FBgn0028342,FBgn0038224,FBgn0038467,FBgn0039156 | 8 | GO:0009152 |
| purine | 0.0363 | FBgn0011211,FBgn0013972,FBgn0016691,FBgn0019 | 8 | GO:0006 |

| | | | | |
|---|---|---|---|---|
| nucleotide biosynthetic process | 772 | 644,FBgn0028342,FBgn0038224,FBgn0038467,FBgn0039156 | | 164 |
| ribosomal small subunit biogenesis | 0.0403551 | FBgn0004403,FBgn0030081,FBgn0030136,FBgn0033454,FBgn0034564,FBgn0037073,FBgn0038474,FBgn0039404 | 8 | GO:0042274 |
| DNA duplex unwinding | 3.362E-05 | FBgn0014861,FBgn0015075,FBgn0020633,FBgn0025815,FBgn0026876,FBgn0040290,FBgn0261850 | 7 | GO:0032508 |
| DNA geometric change | 5.886E-05 | FBgn0014861,FBgn0015075,FBgn0020633,FBgn0025815,FBgn0026876,FBgn0040290,FBgn0261850 | 7 | GO:0032392 |
| nuclear DNA replication | 9.773E-05 | FBgn0014861,FBgn0017577,FBgn0020633,FBgn0025815,FBgn0026143,FBgn0035644,FBgn0259113 | 7 | GO:0033260 |
| cellular amino acid biosynthetic process | 0.0022279 | FBgn0014427,FBgn0029823,FBgn0036157,FBgn0037146,FBgn0037305,FBgn0037513,FBgn0039094 | 7 | GO:0008652 |
| aerobic respiration | 0.0279379 | FBgn0011227,FBgn0014028,FBgn0024957,FBgn0024958,FBgn0037891,FBgn0040529,FBgn0262559 | 7 | GO:0009060 |
| double-strand break repair via break-induced replication | 1.359E-06 | FBgn0014861,FBgn0017577,FBgn0020633,FBgn0025815,FBgn0026143,FBgn0039403 | 6 | GO:0000727 |
| positive regulation of mitotic cell cycle phase transition | 0.0012276 | FBgn0003525,FBgn0010382,FBgn0026143,FBgn0039403,FBgn0040290,FBgn0041147 | 6 | GO:1901992 |
| positive regulation of cell cycle phase transition | 0.0023561 | FBgn0003525,FBgn0010382,FBgn0026143,FBgn0039403,FBgn0040290,FBgn0041147 | 6 | GO:1901989 |
| alpha-amino acid biosynthetic process | 0.0067269 | FBgn0014427,FBgn0029823,FBgn0036157,FBgn0037146,FBgn0037305,FBgn0039094 | 6 | GO:1901607 |
| maturation of SSU-rRNA from tricistronic rRNA transcript (SSU-rRNA, 5.8S rRNA, LSU-rRNA) | 0.0103453 | FBgn0004403,FBgn0030081,FBgn0033454,FBgn0037073,FBgn0038474,FBgn0039404 | 6 | GO:0000462 |
| positive regulation of mitotic cell cycle | 0.0103453 | FBgn0003525,FBgn0010382,FBgn0026143,FBgn0039403,FBgn0040290,FBgn0041147 | 6 | GO:0045931 |
| fatty acid catabolic process | 0.0151647 | FBgn0025352,FBgn0031092,FBgn0034629,FBgn0035383,FBgn0038742,FBgn0086712 | 6 | GO:0009062 |
| nucleoside triphosphate metabolic | 0.0151647 | FBgn0011211,FBgn0016691,FBgn0019644,FBgn0028342,FBgn0031663,FBgn0038224 | 6 | GO:0009141 |

| | | | | |
|---|---|---|---|---|
| process | | | | |
| carbohydrate derivative catabolic process | 0.018078 | FBgn0022700,FBgn0034582,FBgn0034988,FBgn0038173,FBgn0039650,FBgn0043575 | 6 | GO:1901136 |
| monocarboxylic acid catabolic process | 0.029054 7 | FBgn0025352,FBgn0031092,FBgn0034629,FBgn0035383,FBgn0038742,FBgn0086712 | 6 | GO:0072329 |
| regulation of chromosome segregation | 0.049438 9 | FBgn0004643,FBgn0024227,FBgn0031549,FBgn0041147,FBgn0061476,FBgn0261850 | 6 | GO:0051983 |
| DNA biosynthetic process | 0.049438 9 | FBgn0010382,FBgn0025815,FBgn0026143,FBgn0035644,FBgn0040290,FBgn0286788 | 6 | GO:0071897 |
| mitotic DNA replication | 0.000263 1 | FBgn0014861,FBgn0025815,FBgn0026143,FBgn0035644,FBgn0259113 | 5 | GO:1902969 |
| DNA amplification | 0.005786 7 | FBgn0010382,FBgn0025815,FBgn0026143,FBgn0040290,FBgn0286788 | 5 | GO:0006277 |
| energy coupled proton transport, down electrochemical gradient | 0.005786 7 | FBgn0011211,FBgn0016691,FBgn0019644,FBgn0028342,FBgn0038224 | 5 | GO:0015985 |
| ATP synthesis coupled proton transport | 0.005786 7 | FBgn0011211,FBgn0016691,FBgn0019644,FBgn0028342,FBgn0038224 | 5 | GO:0015986 |
| ATP biosynthetic process | 0.009998 | FBgn0011211,FBgn0016691,FBgn0019644,FBgn0028342,FBgn0038224 | 5 | GO:0006754 |
| purine nucleoside triphosphate biosynthetic process | 0.019562 3 | FBgn0011211,FBgn0016691,FBgn0019644,FBgn0028342,FBgn0038224 | 5 | GO:0009145 |
| purine ribonucleoside triphosphate metabolic process | 0.019562 3 | FBgn0011211,FBgn0016691,FBgn0019644,FBgn0028342,FBgn0038224 | 5 | GO:0009205 |
| purine ribonucleoside triphosphate biosynthetic process | 0.019562 3 | FBgn0011211,FBgn0016691,FBgn0019644,FBgn0028342,FBgn0038224 | 5 | GO:0009206 |
| tricarboxylic acid cycle | 0.023753 8 | FBgn0014028,FBgn0024957,FBgn0024958,FBgn0037891,FBgn0262559 | 5 | GO:0006099 |
| fatty acid beta-oxidation | 0.023753 8 | FBgn0025352,FBgn0031092,FBgn0034629,FBgn0035383,FBgn0086712 | 5 | GO:0006635 |
| purine nucleoside triphosphate metabolic | 0.023753 8 | FBgn0011211,FBgn0016691,FBgn0019644,FBgn0028342,FBgn0038224 | 5 | GO:0009144 |

| | | | | |
|---|---|---|---|---|
| process | | | | |
| regulation of mitotic metaphase/anaphase transition | 0.0284835 | FBgn0004643,FBgn0024227,FBgn0031549,FBgn0041147,FBgn0061476 | 5 | GO:0030071 |
| ribonucleoside triphosphate metabolic process | 0.0337694 | FBgn0011211,FBgn0016691,FBgn0019644,FBgn0028342,FBgn0038224 | 5 | GO:0009199 |
| ribonucleoside triphosphate biosynthetic process | 0.0337694 | FBgn0011211,FBgn0016691,FBgn0019644,FBgn0028342,FBgn0038224 | 5 | GO:0009201 |
| fatty acid oxidation | 0.0337694 | FBgn0025352,FBgn0031092,FBgn0034629,FBgn0035383,FBgn0086712 | 5 | GO:0019395 |
| regulation of metaphase/anaphase transition of cell cycle | 0.0337694 | FBgn0004643,FBgn0024227,FBgn0031549,FBgn0041147,FBgn0061476 | 5 | GO:1902099 |
| nucleoside triphosphate biosynthetic process | 0.0396254 | FBgn0011211,FBgn0016691,FBgn0019644,FBgn0028342,FBgn0038224 | 5 | GO:0009142 |
| lipid oxidation | 0.0396254 | FBgn0025352,FBgn0031092,FBgn0034629,FBgn0035383,FBgn0086712 | 5 | GO:0034440 |
| DNA endoreduplication | 0.0453913 | FBgn0017577,FBgn0030054,FBgn0033890,FBgn0035644,FBgn0286788 | 5 | GO:0042023 |
| pre-replicative complex assembly involved in nuclear cell cycle DNA replication | 3.541E-05 | FBgn0014861,FBgn0017577,FBgn0020633,FBgn0025815 | 4 | GO:0006267 |
| pre-replicative complex assembly | 3.541E-05 | FBgn0014861,FBgn0017577,FBgn0020633,FBgn0025815 | 4 | GO:0036388 |
| pre-replicative complex assembly involved in cell cycle DNA replication | 3.541E-05 | FBgn0014861,FBgn0017577,FBgn0020633,FBgn0025815 | 4 | GO:1902299 |
| DNA unwinding involved in DNA replication | 0.0019261 | FBgn0014861,FBgn0020633,FBgn0025815,FBgn0040290 | 4 | GO:0006268 |
| activation of cysteine-type endopeptidase activity | 0.0032566 | FBgn0011703,FBgn0011704,FBgn0038928,FBgn0262559 | 4 | GO:0006919 |

| | | | | |
|---|---|---|---|---|
| involved in apoptotic process | | | | |
| neuropeptide signaling pathway | 0.0050992 | FBgn0038147,FBgn0038199,FBgn0050106,FBgn0086782 | 4 | GO:0007218 |
| fatty acid derivative biosynthetic process | 0.0050992 | FBgn0025814,FBgn0035383,FBgn0039156,FBgn0053178 | 4 | GO:1901570 |
| DNA-dependent DNA replication maintenance of fidelity | 0.0144114 | FBgn0004406,FBgn0033549,FBgn0035644,FBgn0050085 | 4 | GO:0045005 |
| fatty acid derivative metabolic process | 0.0189686 | FBgn0025814,FBgn0035383,FBgn0039156,FBgn0053178 | 4 | GO:1901568 |
| eggshell chorion gene amplification | 0.0243231 | FBgn0010382,FBgn0025815,FBgn0040290,FBgn0286788 | 4 | GO:0007307 |
| neurotransmitter metabolic process | 0.0243231 | FBgn0011768,FBgn0029823,FBgn0037513,FBgn0039094 | 4 | GO:0042133 |
| positive regulation of cysteine-type endopeptidase activity involved in apoptotic process | 0.0243231 | FBgn0011703,FBgn0011704,FBgn0038928,FBgn0262559 | 4 | GO:0043280 |
| positive regulation of cysteine-type endopeptidase activity | 0.0375221 | FBgn0011703,FBgn0011704,FBgn0038928,FBgn0262559 | 4 | GO:2001056 |
| nucleobase-containing small molecule biosynthetic process | 0.0453913 | FBgn0031663,FBgn0034988,FBgn0038173,FBgn0039650 | 4 | GO:0034404 |
| positive regulation of DNA metabolic process | 0.0040921 | FBgn0037301,FBgn0037345,FBgn0261850 | 3 | GO:0051054 |
| insemination | 0.0077161 | FBgn0015584,FBgn0040092,FBgn0040093 | 3 | GO:0007320 |
| serine family amino acid biosynthetic process | 0.0077161 | FBgn0014427,FBgn0029823,FBgn0039094 | 3 | GO:0009070 |

| | | | | |
|---|---|---|---|---|
| sperm competition | 0.0077161 | FBgn0015584,FBgn0040092,FBgn0040093 | 3 | GO:0046692 |
| resolution of meiotic recombination intermediates | 0.0127341 | FBgn0017577,FBgn0029977,FBgn0033549 | 3 | GO:0000712 |
| regulation of oxidative phosphorylation | 0.0127341 | FBgn0027794,FBgn0040529,FBgn0284256 | 3 | GO:0002082 |
| purine nucleoside catabolic process | 0.0127341 | FBgn0034988,FBgn0038173,FBgn0039650 | 3 | GO:0006152 |
| multi-multicellular organism process | 0.0127341 | FBgn0015584,FBgn0040092,FBgn0040093 | 3 | GO:0044706 |
| purine ribonucleoside catabolic process | 0.0127341 | FBgn0034988,FBgn0038173,FBgn0039650 | 3 | GO:0046130 |
| nucleoside catabolic process | 0.0192188 | FBgn0034988,FBgn0038173,FBgn0039650 | 3 | GO:0009164 |
| N-terminal protein amino acid modification | 0.0192188 | FBgn0024194,FBgn0039687,FBgn0243511 | 3 | GO:0031365 |
| nucleobase-containing small molecule catabolic process | 0.0192188 | FBgn0034988,FBgn0038173,FBgn0039650 | 3 | GO:0034656 |
| ribonucleoside catabolic process | 0.0192188 | FBgn0034988,FBgn0038173,FBgn0039650 | 3 | GO:0042454 |
| positive regulation of G1/S transition of mitotic cell cycle | 0.0192188 | FBgn0010382,FBgn0026143,FBgn0039403 | 3 | GO:1900087 |
| mitochondrial transcription | 0.0271999 | FBgn0011787,FBgn0027794,FBgn0284256 | 3 | GO:0006390 |
| serine family amino acid metabolic process | 0.0271999 | FBgn0014427,FBgn0029823,FBgn0039094 | 3 | GO:0009069 |
| regulation of mitotic cell cycle, embryonic | 0.0271999 | FBgn0002441,FBgn0003525,FBgn0261850 | 3 | GO:0009794 |
| neurotransmitter biosynthetic process | 0.0271999 | FBgn0029823,FBgn0037513,FBgn0039094 | 3 | GO:0042136 |

| | | | | |
|---|---|---|---|---|
| nucleobase biosynthetic process | 0.0271999 | FBgn0003257,FBgn0029823,FBgn0037513 | 3 | GO:0046112 |
| response to acid chemical | 0.0366716 | FBgn0029823,FBgn0030108,FBgn0035870 | 3 | GO:0001101 |
| aminoglycan catabolic process | 0.0366716 | FBgn0022700,FBgn0034582,FBgn0043575 | 3 | GO:0006026 |
| copulation | 0.0366716 | FBgn0015584,FBgn0040092,FBgn0040093 | 3 | GO:0007620 |
| meiotic chromosome separation | 0.0366716 | FBgn0017577,FBgn0029977,FBgn0033549 | 3 | GO:0051307 |
| nucleoside phosphate catabolic process | 0.0366716 | FBgn0031663,FBgn0034988,FBgn0039650 | 3 | GO:1901292 |
| positive regulation of cell cycle G1/S phase transition | 0.0366716 | FBgn0010382,FBgn0026143,FBgn0039403 | 3 | GO:1902808 |
| DNA strand elongation involved in DNA replication | 0.0476 | FBgn0020633,FBgn0032244,FBgn0259113 | 3 | GO:0006271 |
| DNA strand elongation | 0.0476 | FBgn0020633,FBgn0032244,FBgn0259113 | 3 | GO:0022616 |
| glycosyl compound catabolic process | 0.0476 | FBgn0034988,FBgn0038173,FBgn0039650 | 3 | GO:1901658 |
| regulation of ATP metabolic process | 0.0476 | FBgn0027794,FBgn0040529,FBgn0284256 | 3 | GO:1903578 |
| DNA replication, synthesis of RNA primer | 0.0059794 | FBgn0011762,FBgn0259676 | 2 | GO:0006269 |
| activation of adenylate cyclase activity | 0.0059794 | FBgn0039354,FBgn0086782 | 2 | GO:0007190 |
| response to iron(II) ion | 0.0059794 | FBgn0024957,FBgn0024958 | 2 | GO:0010040 |
| positive regulation of G2/M transition of mitotic cell cycle | 0.0059794 | FBgn0003525,FBgn0040290 | 2 | GO:0010971 |
| nuclear envelope reassembly | 0.0059794 | FBgn0033179,FBgn0266420 | 2 | GO:0031468 |

| | | | | |
|---|---|---|---|---|
| positive regulation of DNA recombination | 0.0059794 | FBgn0037301,FBgn0261850 | 2 | GO:0045911 |
| guanosine-containing compound catabolic process | 0.0059794 | FBgn0034988,FBgn0039650 | 2 | GO:1901069 |
| response to L-canavanine | 0.0059794 | FBgn0030108,FBgn0035870 | 2 | GO:1901354 |
| cell cycle DNA replication initiation | 0.0059794 | FBgn0014861,FBgn0259113 | 2 | GO:1902292 |
| nuclear cell cycle DNA replication initiation | 0.0059794 | FBgn0014861,FBgn0259113 | 2 | GO:1902315 |
| positive regulation of cell cycle G2/M phase transition | 0.0059794 | FBgn0003525,FBgn0040290 | 2 | GO:1902751 |
| mitotic DNA replication initiation | 0.0059794 | FBgn0014861,FBgn0259113 | 2 | GO:1902975 |
| prostaglandin biosynthetic process | 0.0170167 | FBgn0025814,FBgn0053178 | 2 | GO:0001516 |
| citrate metabolic process | 0.0170167 | FBgn0024957,FBgn0024958 | 2 | GO:0006101 |
| glycine biosynthetic process | 0.0170167 | FBgn0029823,FBgn0039094 | 2 | GO:0006545 |
| L-serine metabolic process | 0.0170167 | FBgn0014427,FBgn0029823 | 2 | GO:0006563 |
| L-serine biosynthetic process | 0.0170167 | FBgn0014427,FBgn0029823 | 2 | GO:0006564 |
| deoxyribonucleotide biosynthetic process | 0.0170167 | FBgn0011703,FBgn0011704 | 2 | GO:0009263 |
| astral microtubule organization | 0.0170167 | FBgn0000140,FBgn0027500 | 2 | GO:0030953 |
| endoplasmic reticulum calcium ion homeostasis | 0.0170167 | FBgn0030350,FBgn0032746 | 2 | GO:0032469 |
| preblastoderm mitotic cell cycle | 0.0170167 | FBgn0002441,FBgn0033890 | 2 | GO:0035185 |

| | | | | |
|---|---|---|---|---|
| regulation of mitochondrial mRNA stability | 0.0170167 | FBgn0027794,FBgn0284256 | 2 | GO:0044528 |
| icosanoid biosynthetic process | 0.0170167 | FBgn0025814,FBgn0053178 | 2 | GO:0046456 |
| prostanoid biosynthetic process | 0.0170167 | FBgn0025814,FBgn0053178 | 2 | GO:0046457 |
| tRNA-guanine transglycosylation | 0.0170167 | FBgn0031321,FBgn0034614 | 2 | GO:0101030 |
| regulation of mitochondrial transcription | 0.0170167 | FBgn0027794,FBgn0284256 | 2 | GO:1903108 |
| reactive nitrogen species metabolic process | 0.0170167 | FBgn0011768,FBgn0030966 | 2 | GO:2001057 |
| prostanoid metabolic process | 0.0322968 | FBgn0025814,FBgn0053178 | 2 | GO:0006692 |
| prostaglandin metabolic process | 0.0322968 | FBgn0025814,FBgn0053178 | 2 | GO:0006693 |
| nuclear envelope organization | 0.0322968 | FBgn0033179,FBgn0266420 | 2 | GO:0006998 |
| deoxyribonucleotide metabolic process | 0.0322968 | FBgn0011703,FBgn0011704 | 2 | GO:0009262 |
| maintenance of gastrointestinal epithelium | 0.0322968 | FBgn0030904,FBgn0053542 | 2 | GO:0030277 |
| intracellular sterol transport | 0.0322968 | FBgn0031381,FBgn0039154 | 2 | GO:0032366 |
| intracellular cholesterol transport | 0.0322968 | FBgn0031381,FBgn0039154 | 2 | GO:0032367 |
| nuclear-transcribed mRNA catabolic process, exonucleolytic, 3'-5' | 0.0322968 | FBgn0034065,FBgn0037815 | 2 | GO:0034427 |
| U4 snRNA 3'-end processing | 0.0322968 | FBgn0034065,FBgn0037815 | 2 | GO:0034475 |
| tetrahydrofolate interconversio | 0.0322968 | FBgn0029823,FBgn0036157 | 2 | GO:0035999 |

| | | | | |
|---|---|---|---|---|
| n | | | | |
| DNA replication proofreading | 0.0322968 | FBgn0004406,FBgn0035644 | 2 | GO:0045004 |
| brain morphogenesis | 0.0322968 | FBgn0000140,FBgn0019650 | 2 | GO:0048854 |
| intestinal epithelial structure maintenance | 0.0322968 | FBgn0030904,FBgn0053542 | 2 | GO:0060729 |
| extrinsic apoptotic signaling pathway | 0.0322968 | FBgn0029131,FBgn0038928 | 2 | GO:0097191 |

**Table 2.1d: Pathway enrichment for hits differentially upregulated in control females relative to control males**

| Pathway enrichment | p-value | Hits | Gene matches | Pathway ID |
|---|---|---|---|---|
| Metabolism | 7.92553E-05 | FBgn0001187,FBgn0003076,FBgn0003257,FBgn0010241,FBgn0011211,FBgn0011227,FBgn0011703,FBgn0011704,FBgn0011768,FBgn0014028,FBgn0014427,FBgn0015277,FBgn0016691,FBgn0019644,FBgn0019982,FBgn0020626,FBgn0023477,FBgn0025352,FBgn0025373,FBgn0025463,FBgn0025592,FBgn0025814,FBgn0028342,FBgn0029823,FBgn0029994,FBgn0030816,FBgn0030966,FBgn0031048,FBgn0031248,FBgn0031663,FBgn0031703,FBgn0033215,FBgn0033216,FBgn0033377,FBgn0033382,FBgn0033961,FBgn0034629,FBgn0034919,FBgn0034988,FBgn0035383,FBgn0035471,FBgn0035619,FBgn0036157,FBgn0036381,FBgn0036691,FBgn0037146,FBgn0037186,FBgn0037305,FBgn0037370,FBgn0037513,FBgn0037534,FBgn0037891,FBgn0038224,FBgn0038407,FBgn0038467,FBgn0038742,FBgn0039258,FBgn0039470,FBgn0039471,FBgn0039472,FBgn0039486,FBgn0039674,FBgn0040069,FBgn0040383,FBgn0050345,FBgn0050502,FBgn0052669,FBgn0052750,FBgn0053116,FBgn0053178,FBgn0067102,FBgn0085484,FBgn0262559,FBgn0283450,FBgn0283680 | 75 | R-DME-1430728 |
| Metabolic pathways | 1.38283E-06 | FBgn0000078,FBgn0001187,FBgn0003076,FBgn0003257,FBgn0004406,FBgn0011211,FBgn0011227,FBgn0011703,FBgn0011704,FBgn0011762,FBgn0011768,FBgn0011770,FBgn0014028,FBgn0014427,FBgn0015277,FBgn0015568,FBgn0015575,FBgn0016691,FBgn0019644,FBgn0022097,FBgn0023477,FBgn0024957,FBgn0024958,FBgn0025352,FBgn0025373,FBgn0025592,FBgn0028342,FBgn0029823,FBgn0029906,FBgn0031048,FBgn0031663,FBgn0031703,FBgn0031713,FBgn0033377,FBgn0033961,FBgn003414 | 66 | 1100 |

| | | | | |
|---|---|---|---|---|
| | | 1,FBgn0034629,FBgn0035619,FBgn0035644,FBgn0036157,FBgn0036691,FBgn0037146,FBgn0037186,FBgn0037356,FBgn0037513,FBgn0037891,FBgn0038080,FBgn0038224,FBgn0038467,FBgn0038613,FBgn0038742,FBgn0039094,FBgn0039258,FBgn0039580,FBgn0039596,FBgn0040069,FBgn0052201,FBgn0053116,FBgn0053138,FBgn0067102,FBgn0085484,FBgn0259113,FBgn0259676,FBgn0262512,FBgn0262559,FBgn0283680 | | |
| Metabolism of lipids | 0.002585092 | FBgn0010241,FBgn0015277,FBgn0020626,FBgn0025352,FBgn0025373,FBgn0025463,FBgn0025592,FBgn0025814,FBgn0029994,FBgn0031048,FBgn0031703,FBgn0033215,FBgn0033216,FBgn0033382,FBgn0034629,FBgn0035383,FBgn0035471,FBgn0035619,FBgn0036381,FBgn0036691,FBgn0037534,FBgn0038407,FBgn0038742,FBgn0039470,FBgn0039471,FBgn0039472,FBgn0050502,FBgn0053116,FBgn0053178,FBgn0067102 | 30 | R-DME-556833 |
| Cell Cycle | 0.001655286 | FBgn0003525,FBgn0010382,FBgn0011692,FBgn0011762,FBgn0014861,FBgn0015271,FBgn0015391,FBgn0017577,FBgn0020633,FBgn0024227,FBgn0025463,FBgn0025815,FBgn0026143,FBgn0027868,FBgn0029856,FBgn0032244,FBgn0035644,FBgn0038390,FBgn0039125,FBgn0039403,FBgn0041147,FBgn0259113,FBgn0259676,FBgn0259791,FBgn0286788 | 25 | R-DME-1640170 |
| Cell Cycle, Mitotic | 0.00092757 | FBgn0003525,FBgn0010382,FBgn0011692,FBgn0011762,FBgn0014861,FBgn0015271,FBgn0015391,FBgn0017577,FBgn0020633,FBgn0024227,FBgn0025815,FBgn0026143,FBgn0027868,FBgn0029856,FBgn0032244,FBgn0035644,FBgn0038390,FBgn0039125,FBgn0039403,FBgn0041147,FBgn0259113,FBgn0259676,FBgn0259791,FBgn0286788 | 24 | R-DME-69278 |
| DNA Replication | 0.00028 0248 | FBgn0010382,FBgn0011762,FBgn0014861,FBgn0015271,FBgn0017577,FBgn0020633,FBgn0025815,FBgn0026143,FBgn0029856,FBgn0032244,FBgn0035644,FBgn0039403,FBgn0041147,FBgn0259113,FBgn0259676,FBgn0286788 | 16 | R-DME-69306 |
| G1/S Transition | 0.00016 0573 | FBgn0003525,FBgn0010382,FBgn0011762,FBgn0014861,FBgn0015271,FBgn0017577,FBgn0020633,FBgn0025815,FBgn0026143,FBgn0029856,FBgn0035644,FBgn0038390,FBgn0259113,FBgn0259676,FBgn0286788 | 15 | R-DME-69206 |
| Mitotic G1 phase and G1/S transition | 0.00058 2619 | FBgn0003525,FBgn0010382,FBgn0011762,FBgn0014861,FBgn0015271,FBgn0017577,FBgn0020633,FBgn0025815,FBgn0026143,FBgn0029856,FBgn0035644,FBgn0038390,FBgn0259113,FBgn0259676,FBgn0286788 | 15 | R-DME-453279 |
| Synthesis of DNA | 0.00077 2417 | FBgn0010382,FBgn0011762,FBgn0014861,FBgn0017577,FBgn0020633,FBgn0025815,FBgn0029856,FBgn0032244,FBgn0035644,FBgn0039403,FBgn0041147,FBgn0259113,FBgn0259676,FBgn0286788 | 14 | R-DME-69239 |

| | | | | |
|---|---|---|---|---|
| S Phase | 0.002324736 | FBgn0010382,FBgn0011762,FBgn0014861,FBgn0017577,FBgn0020633,FBgn0025815,FBgn0029856,FBgn0032244,FBgn0035644,FBgn0039403,FBgn0041147,FBgn0259113,FBgn0259676,FBgn0286788 | 14 | R-DME-69242 |
| Fatty acid metabolism | 0.000872613 | FBgn0025352,FBgn0025814,FBgn0031703,FBgn0033215,FBgn0033216,FBgn0034629,FBgn0035383,FBgn0035471,FBgn0036691,FBgn0037534,FBgn0038407,FBgn0038742,FBgn0053178 | 13 | R-DME-8978868 |
| DNA Replication Pre-Initiation | 0.000570692 | FBgn0011762,FBgn0014861,FBgn0015271,FBgn0017577,FBgn0020633,FBgn0025815,FBgn0026143,FBgn0029856,FBgn0035644,FBgn0259113,FBgn0259676,FBgn0286788 | 12 | R-DME-69002 |
| Oxidative phosphorylation | 0.004804838 | FBgn0011211,FBgn0011227,FBgn0014028,FBgn0016691,FBgn0019644,FBgn0022097,FBgn0028342,FBgn0033961,FBgn0038224,FBgn0038613,FBgn0040529,FBgn0262512 | 12 | 190 |
| Mitochondrial translation elongation | 0.005440535 | FBgn0011787,FBgn0014023,FBgn0026741,FBgn0029718,FBgn0031231,FBgn0034579,FBgn0035374,FBgn0037330,FBgn0038474,FBgn0042112,FBgn0083983,FBgn0263133 | 12 | R-DME-5389840 |
| Mitochondrial translation | 0.006912208 | FBgn0011787,FBgn0014023,FBgn0026741,FBgn0029718,FBgn0031231,FBgn0034579,FBgn0035374,FBgn0037330,FBgn0038474,FBgn0042112,FBgn0083983,FBgn0263133 | 12 | R-DME-5368287 |
| Phospholipid metabolism | 0.009688982 | FBgn0015277,FBgn0025352,FBgn0031048,FBgn0033215,FBgn0033216,FBgn0033382,FBgn0035619,FBgn0036381,FBgn0039470,FBgn0039471,FBgn0039472,FBgn0053116 | 12 | R-DME-1483257 |
| Cell Cycle Checkpoints | 0.019513066 | FBgn0003525,FBgn0014861,FBgn0015271,FBgn0017577,FBgn0020633,FBgn0025463,FBgn0025815,FBgn0026143,FBgn0029856,FBgn0032244,FBgn0041147,FBgn0286788 | 12 | R-DME-69620 |
| The citric acid (TCA) cycle and respiratory electron transport | 0.038233499 | FBgn0011211,FBgn0011227,FBgn0014028,FBgn0016691,FBgn0019644,FBgn0028342,FBgn0033961,FBgn0034919,FBgn0037891,FBgn0038224,FBgn0262559,FBgn0283450 | 12 | R-DME-1428517 |
| Activation of the pre-replicative complex | 5.19E-07 | FBgn0011762,FBgn0014861,FBgn0015271,FBgn0017577,FBgn0020633,FBgn0025815,FBgn0026143,FBgn0035644,FBgn0259113,FBgn0259676,FBgn0286788 | 11 | R-DME-68962 |
| DNA replication | 1.39539E-06 | FBgn0011762,FBgn0014861,FBgn0017577,FBgn0020633,FBgn0025815,FBgn0030507,FBgn0031252,FBgn0032244,FBgn0035644,FBgn0259113,FBgn0259676 | 11 | 3030 |
| Glycerophospholipid biosynthesis | 0.002066775 | FBgn0025352,FBgn0031048,FBgn0033215,FBgn0033216,FBgn0033382,FBgn0035619,FBgn0036381,FBgn0039470,FBgn0039471,FBgn0039472,FBgn0053116 | 11 | R-DME-1483206 |
| Mitochondrial translation termination | 0.016270993 | FBgn0011787,FBgn0014023,FBgn0026741,FBgn0029718,FBgn0031231,FBgn0034579,FBgn0035374,FBgn0037330,FBgn0038474,FBgn0042112,FBgn0083983 | 11 | R-DME-5419276 |
| Activation of ATR in | 6.18517E-05 | FBgn0003525,FBgn0014861,FBgn0015271,FBgn0017577,FBgn0020633,FBgn0025815,FBgn00 | 9 | R-DME-176187 |

| | | | | |
|---|---|---|---|---|
| response to replication stress | | 26143,FBgn0032244,FBgn0286788 | | |
| G2/M Checkpoints | 0.001329919 | FBgn0003525,FBgn0014861,FBgn0015271,FBgn0017577,FBgn0020633,FBgn0025815,FBgn0026143,FBgn0032244,FBgn0286788 | 9 | R-DME-69481 |
| Pyrimidine metabolism | 0.027219846 | FBgn0003257,FBgn0011703,FBgn0011704,FBgn0011762,FBgn0031663,FBgn0035644,FBgn0037513,FBgn0259113,FBgn0259676 | 9 | 240 |
| Metabolism of nucleotides | 0.010461081 | FBgn0003257,FBgn0011703,FBgn0011704,FBgn0019982,FBgn0031663,FBgn0034988,FBgn0037513,FBgn0038467 | 8 | R-DME-15869 |
| Switching of origins to a post-replicative state | 0.041337481 | FBgn0010382,FBgn0014861,FBgn0017577,FBgn0020633,FBgn0025815,FBgn0029856,FBgn0041147,FBgn0286788 | 8 | R-DME-69052 |
| Metabolism of water-soluble vitamins and cofactors | 0.045699379 | FBgn0029823,FBgn0031248,FBgn0036157,FBgn0040069,FBgn0050345,FBgn0052669,FBgn0052750,FBgn0085484 | 8 | R-DME-196849 |
| Amino sugar and nucleotide sugar metabolism | 0.002915205 | FBgn0001187,FBgn0003076,FBgn0004427,FBgn0022700,FBgn0033377,FBgn0034582,FBgn0039580 | 7 | 520 |
| Iron uptake and transport | 0.009970999 | FBgn0022097,FBgn0024957,FBgn0024958,FBgn0029856,FBgn0038613,FBgn0050345,FBgn0262512 | 7 | R-DME-917937 |
| Assembly of the pre-replicative complex | 0.032444058 | FBgn0014861,FBgn0015271,FBgn0017577,FBgn0020633,FBgn0025815,FBgn0029856,FBgn0286788 | 7 | R-DME-68867 |
| Fatty acid metabolism | 0.008588522 | FBgn0011768,FBgn0025352,FBgn0031703,FBgn0034629,FBgn0035383,FBgn0038742 | 6 | 71 |
| Formation of ATP by chemiosmotic coupling | 0.001389367 | FBgn0011211,FBgn0016691,FBgn0019644,FBgn0028342,FBgn0038224 | 5 | R-DME-163210 |
| Cristae formation | 0.001389367 | FBgn0011211,FBgn0016691,FBgn0019644,FBgn0028342,FBgn0038224 | 5 | R-DME-8949613 |
| Mitochondrial biogenesis | 0.002115626 | FBgn0011211,FBgn0016691,FBgn0019644,FBgn0028342,FBgn0038224 | 5 | R-DME-1592230 |
| Telomere Maintenance | 0.0043363 | FBgn0011762,FBgn0032244,FBgn0035644,FBgn0259113,FBgn0259676 | 5 | R-DME-157579 |
| Telomere C-strand (Lagging Strand) | 0.0043363 | FBgn0011762,FBgn0032244,FBgn0035644,FBgn0259113,FBgn0259676 | 5 | R-DME-174417 |

| | | | | |
|---|---|---|---|---|
| Synthesis | | | | |
| Extension of Telomeres | 0.0043363 | FBgn0011762,FBgn0032244,FBgn0035644,FBgn0259113,FBgn0259676 | 5 | R-DME-180786 |
| Chromosome Maintenance | 0.0043363 | FBgn0011762,FBgn0032244,FBgn0035644,FBgn0259113,FBgn0259676 | 5 | R-DME-73886 |
| DNA strand elongation | 0.00591267 | FBgn0011762,FBgn0032244,FBgn0039403,FBgn0259113,FBgn0259676 | 5 | R-DME-69190 |
| Citrate cycle TCA cycle | 0.029087828 | FBgn0014028,FBgn0024957,FBgn0024958,FBgn0037891,FBgn0262559 | 5 | 20 |
| Dual Incision in GG-NER | 0.029087828 | FBgn0029856,FBgn0031309,FBgn0032244,FBgn0035644,FBgn0261850 | 5 | R-DME-5696400 |
| Polymerase switching on the C-strand of the telomere | 0.001046392 | FBgn0011762,FBgn0032244,FBgn0259113,FBgn0259676 | 4 | R-DME-174411 |
| Telomere C-strand synthesis initiation | 0.001046392 | FBgn0011762,FBgn0035644,FBgn0259113,FBgn0259676 | 4 | R-DME-174430 |
| DNA replication initiation | 0.001046392 | FBgn0011762,FBgn0035644,FBgn0259113,FBgn0259676 | 4 | R-DME-68952 |
| Polymerase switching | 0.001046392 | FBgn0011762,FBgn0032244,FBgn0259113,FBgn0259676 | 4 | R-DME-69091 |
| Leading Strand Synthesis | 0.001046392 | FBgn0011762,FBgn0032244,FBgn0259113,FBgn0259676 | 4 | R-DME-69109 |
| Inhibition of replication initiation of damaged DNA by RB1/E2F1 | 0.001965216 | FBgn0011762,FBgn0038390,FBgn0259113,FBgn0259676 | 4 | R-DME-113501 |
| E2F mediated regulation of DNA replication | 0.001965216 | FBgn0011762,FBgn0038390,FBgn0259113,FBgn0259676 | 4 | R-DME-113510 |
| Glyoxylate and dicarboxylate metabolism | 0.005201449 | FBgn0011770,FBgn0024957,FBgn0024958,FBgn0262559 | 4 | 630 |
| mRNA decay by 3' | 0.005201449 | FBgn0027524,FBgn0034065,FBgn0034988,FBgn0037815 | 4 | R-DME-429958 |

| | | | | |
|---|---|---|---|---|
| to 5' exoribonuclease | | | | |
| Mitochondrial Fatty Acid Beta-Oxidation | 0.005201449 | FBgn0025352,FBgn0031703,FBgn0036691,FBgn0038742 | 4 | R-DME-77289 |
| Arachidonic acid metabolism | 0.007679416 | FBgn0025814,FBgn0033215,FBgn0033216,FBgn0053178 | 4 | R-DME-2142753 |
| Neuroactive ligand-receptor interaction | 0.014695025 | FBgn0003863,FBgn0010425,FBgn0011555,FBgn0039354 | 4 | 4080 |
| Metabolism of Angiotensinogen to Angiotensins | 0.019339339 | FBgn0031678,FBgn0032144,FBgn0033774,FBgn0035718 | 4 | R-DME-2022377 |
| Lagging Strand Synthesis | 0.019339339 | FBgn0011762,FBgn0032244,FBgn0259113,FBgn0259676 | 4 | R-DME-69186 |
| Glycine, serine and threonine metabolism | 0.046250778 | FBgn0014427,FBgn0029823,FBgn0037186,FBgn0039094 | 4 | 260 |
| Formation of the activated receptor complex | 0.001767154 | FBgn0030904,FBgn0043903,FBgn0053542 | 3 | R-DME-209209 |
| Vitamin B6 metabolism | 0.004163478 | FBgn0014427,FBgn0031048,FBgn0085484 | 3 | 750 |
| Formation of the activated STAT92E dimer and transport to the nucleus | 0.004163478 | FBgn0030904,FBgn0043903,FBgn0053542 | 3 | R-DME-209228 |
| The retinoid cycle in cones (daylight vision) | 0.004163478 | FBgn0029994,FBgn0033215,FBgn0033216 | 3 | R-DME-2187335 |
| Dephosphorylation by PTP61F phosphatases | 0.007849313 | FBgn0030904,FBgn0043903,FBgn0053542 | 3 | R-DME-210688 |

| | | | | |
|---|---|---|---|---|
| Synthesis of PE | 0.012951503 | FBgn0031048,FBgn0036381,FBgn0053116 | 3 | R-DME-1483213 |
| JAK/STAT pathway | 0.019543275 | FBgn0030904,FBgn0043903,FBgn0053542 | 3 | R-DME-209405 |
| Lysine catabolism | 0.019543275 | FBgn0036381,FBgn0037891,FBgn0040383 | 3 | R-DME-71064 |
| Triglyceride biosynthesis | 0.019543275 | FBgn0025592,FBgn0033215,FBgn0033216 | 3 | R-DME-75109 |
| Synthesis of bile acids and bile salts | 0.027653751 | FBgn0010241,FBgn0020626,FBgn0034629 | 3 | R-DME-192105 |
| Vitamin B5 (pantothenate) metabolism | 0.027653751 | FBgn0040069,FBgn0052669,FBgn0052750 | 3 | R-DME-199220 |
| Removal of the Flap Intermediate | 0.037276166 | FBgn0011762,FBgn0259113,FBgn0259676 | 3 | R-DME-69166 |
| Processive synthesis on the lagging strand | 0.048374947 | FBgn0011762,FBgn0259113,FBgn0259676 | 3 | R-DME-69183 |
| Glycogen synthesis | 0.0060594 | FBgn0003076,FBgn0033377 | 2 | R-DME-3322077 |
| Beta oxidation of hexanoyl-CoA to butanoyl-CoA | 0.0060594 | FBgn0025352,FBgn0038742 | 2 | R-DME-77350 |
| Phosphorylation of proteins involved in G1/S transition by active Cyclin E:Cdk2 complexes | 0.017240412 | FBgn0010382,FBgn0038390 | 2 | R-DME-69200 |
| Digestion of dietary carbohydrate | 0.032713669 | FBgn0000078,FBgn0022700 | 2 | R-DME-189085 |
| AKT phosphorylates targets in the cytosol | 0.032713669 | FBgn0025463,FBgn0267824 | 2 | R-DME-198323 |

| | | | | |
|---|---|---|---|---|
| mitochondrial fatty acid beta-oxidation of saturated fatty acids | 0.032713669 | FBgn0025352,FBgn0038742 | 2 | R-DME-77286 |
| Wax biosynthesis | 0.032713669 | FBgn0033215,FBgn0033216 | 2 | R-DME-9640463 |

**Table 2.1e: GO enrichment for hits differentially upregulated in control males relative to control females**

| GO enrichment | p-value | Hits | Gene matches | GO ID |
|---|---|---|---|---|
| multicellular organismal process | 0.0489251 | FBgn0000008,FBgn0000152,FBgn0000163,FBgn0000395,FBgn0000451,FBgn0000547,FBgn0000568,FBgn0000928,FBgn0001112,FBgn0001218,FBgn0001234,FBgn0002524,FBgn0002566,FBgn0002633,FBgn0002643,FBgn0002732,FBgn0003391,FBgn0003655,FBgn0003984,FBgn0004396,FBgn0004797,FBgn0004893,FBgn0004907,FBgn0010238,FBgn0010240,FBgn0010501,FBgn0010651,FBgn0010894,FBgn0011739,FBgn0011817,FBgn0014073,FBgn0014135,FBgn0014388,FBgn0015229,FBgn0015946,FBgn0016032,FBgn0020258,FBgn0020300,FBgn0022800,FBgn0023510,FBgn0024236,FBgn0024250,FBgn0024555,FBgn0025741,FBgn0026263,FBgn0028292,FBgn0028369,FBgn0028424,FBgn0029006,FBgn0029082,FBgn0030596,FBgn0030985,FBgn0031461,FBgn0031853,FBgn0031885,FBgn0032843,FBgn0033032,FBgn0033127,FBgn0033404,FBgn0033926,FBgn0034136,FBgn0034262,FBgn0035461,FBgn0035513,FBgn0035626,FBgn0035977,FBgn0036072,FBgn0036518,FBgn0036666,FBgn0036801,FBgn0037802,FBgn0038592,FBgn0039509,FBgn0039938,FBgn0040532,FBgn0040726,FBgn0041160,FBgn0041629,FBgn0043900,FBgn0045842,FBgn0050456,FBgn0051216,FBgn0052133,FBgn0052179,FBgn0052364,FBgn0053527,FBgn0085430,FBgn0085432,FBgn0259176,FBgn0259683,FBgn0259938,FBgn0261284,FBgn0261799,FBgn0262081,FBgn0263316,FBgn0264959,FBgn0265778,FBgn0266084,FBgn0266411,FBgn0283499,FBgn0283545,FBgn0286203 | 102 | GO:0032501 |
| anatomical structure development | 0.0470289 | FBgn0000008,FBgn0000163,FBgn0000395,FBgn0000451,FBgn0000547,FBgn0000568,FBgn0000928,FBgn0001112,FBgn0001234,FBgn0002524,FBgn0002566,FBgn0002633,FBgn0002643,FBgn0002732,FBgn0003391,FBgn0003655,FBgn0003984,FBgn0004396,FBgn0004797,FBgn0004893,FBgn0004907,FBgn0010238,FBgn0010501,FBgn0010651,FBgn0010894,FBgn0011705,FBgn0011739,FBgn0011817,FBgn0014073,FBgn0014135,FBgn0014388,FBgn0015229,FBgn0015946,FBgn0016032,FBgn0022800,FBgn0023510,FBgn0024236,FBgn0024250,FBgn0024555,FBgn0025741,FBgn0026263,FBgn0028292,FBgn0028369,FBgn0029006,FBgn0029082,FBgn0030596,FBgn0031461,FBgn0031853,FBgn0031885,FBgn0033032,FBgn0033127,FBgn0034262,FBgn0034279,FBgn0 | 88 | GO:0048856 |

| | | | | |
|---|---|---|---|---|
| | | 035153,FBgn0035461,FBgn0035513,FBgn0035626,FBgn0035977,FBgn0036518,FBgn0036666,FBgn0036801,FBgn0037802,FBgn0038592,FBgn0039048,FBgn0040532,FBgn0041160,FBgn0043900,FBgn0045842,FBgn0050456,FBgn0051216,FBgn0052133,FBgn0052179,FBgn0052364,FBgn0085430,FBgn0085432,FBgn0259176,FBgn0259938,FBgn0261245,FBgn0261284,FBgn0261799,FBgn0262081,FBgn0263316,FBgn0264959,FBgn0265778,FBgn0266084,FBgn0266411,FBgn0283499,FBgn0286203 | | |
| cell communication | 0.0322915 | FBgn0000395,FBgn0000547,FBgn0000568,FBgn0001218,FBgn0001234,FBgn0002566,FBgn0002643,FBgn0002732,FBgn0003984,FBgn0004907,FBgn0010240,FBgn0010501,FBgn0011739,FBgn0011817,FBgn0014009,FBgn0014073,FBgn0014135,FBgn0014388,FBgn0015946,FBgn0022800,FBgn0023416,FBgn0024250,FBgn0025625,FBgn0025741,FBgn0028292,FBgn0029006,FBgn0029082,FBgn0030011,FBgn0030505,FBgn0030850,FBgn0031461,FBgn0031885,FBgn0033926,FBgn0034136,FBgn0034262,FBgn0034647,FBgn0035023,FBgn0035153,FBgn0035626,FBgn0035806,FBgn0035977,FBgn0036518,FBgn0037007,FBgn0037163,FBgn0039273,FBgn0043900,FBgn0050440,FBgn0050456,FBgn0051201,FBgn0052179,FBgn0052476,FBgn0052638,FBgn0053527,FBgn0085432,FBgn0086358,FBgn0262081,FBgn0264959,FBgn0265778,FBgn0266411,FBgn0266720,FBgn0283499 | 61 | GO:0007154 |
| signaling | 0.0272355 | FBgn0000395,FBgn0000547,FBgn0000568,FBgn0001218,FBgn0001234,FBgn0002643,FBgn0002732,FBgn0003984,FBgn0004907,FBgn0010240,FBgn0010501,FBgn0011739,FBgn0011817,FBgn0014009,FBgn0014073,FBgn0014135,FBgn0014388,FBgn0015946,FBgn0022800,FBgn0023416,FBgn0024250,FBgn0025625,FBgn0025741,FBgn0028292,FBgn0029006,FBgn0029082,FBgn0030011,FBgn0030505,FBgn0030850,FBgn0031461,FBgn0031885,FBgn0033926,FBgn0034136,FBgn0034262,FBgn0034647,FBgn0035023,FBgn0035153,FBgn0035626,FBgn0035806,FBgn0035977,FBgn0036518,FBgn0037007,FBgn0037163,FBgn0039273,FBgn0043900,FBgn0050440,FBgn0050456,FBgn0051201,FBgn0052179,FBgn0052476,FBgn0052638,FBgn0053527,FBgn0085432,FBgn0086358,FBgn0262081,FBgn0264959,FBgn0265778,FBgn0266411,FBgn0266720,FBgn0283499 | 60 | GO:0023052 |
| signal transduction | 0.0281688 | FBgn0000395,FBgn0000547,FBgn0000568,FBgn0001218,FBgn0001234,FBgn0002643,FBgn0002732,FBgn0003984,FBgn0004907,FBgn0010240,FBgn0011739,FBgn0011817,FBgn0014009,FBgn0014073,FBgn0014135,FBgn0014388,FBgn0015946,FBgn0022800,FBgn0023416,FBgn0024250,FBgn0025625,FBgn0025741,FBgn0028292,FBgn0029006,FBgn0029082,FBgn0030011,FBgn0031461,FBgn0031885,FBgn0034262,FBgn0034647,FBgn0035023,FBgn0035153,FBgn0035626,FBgn0035806,FBgn0035977,FBgn0036518,FBgn0037007,FBgn0037163,FBgn0039273,FBgn0043900,FBgn0050440,FBgn0050456,FBgn0052179,FBgn0052476,FBgn0052638,FBgn0053527,FBgn0085432,FBgn0086358,FBgn0262081,FBgn0264959,FBgn0265778,FBgn0266411,FBgn0283499 | 53 | GO:0007165 |
| tube | 0.0057 | FBgn0000163,FBgn0000395,FBgn0000451,FBgn00005 | 34 | GO:003529 |

| | | | | |
|---|---|---|---|---|
| developme nt | 055 | 47,FBgn0002524,FBgn0002643,FBgn0003391,FBgn000 3984,FBgn0004893,FBgn0010651,FBgn0011739,FBgn0 011817,FBgn0014135,FBgn0014388,FBgn0023510,FBg n0024236,FBgn0024250,FBgn0029006,FBgn0029082,F Bgn0031461,FBgn0031885,FBgn0036518,FBgn003666 6,FBgn0036801,FBgn0040532,FBgn0043900,FBgn0050 456,FBgn0052133,FBgn0085432,FBgn0263316,FBgn02 64959,FBgn0265778,FBgn0266084,FBgn0283499 | | 5 |
| morphogen esis of an epithelium | 0.0424 701 | FBgn0000163,FBgn0000395,FBgn0000547,FBgn00026 43,FBgn0003391,FBgn0003984,FBgn0004893,FBgn001 0238,FBgn0010894,FBgn0011817,FBgn0014135,FBgn0 014388,FBgn0024236,FBgn0024250,FBgn0029082,FBg n0031461,FBgn0031885,FBgn0036518,FBgn0036666,F Bgn0036801,FBgn0043900,FBgn0050456,FBgn005217 9,FBgn0085432,FBgn0264959,FBgn0265778,FBgn0266 084 | 27 | GO:000200 9 |
| imaginal disc developme nt | 0.0356 385 | FBgn0000395,FBgn0000547,FBgn0002524,FBgn00026 43,FBgn0003391,FBgn0003984,FBgn0004893,FBgn001 0651,FBgn0011739,FBgn0011817,FBgn0014135,FBgn0 024250,FBgn0031461,FBgn0031885,FBgn0036518,FBg n0036801,FBgn0040532,FBgn0043900,FBgn0050456,F Bgn0052133,FBgn0085432,FBgn0263316,FBgn026495 9,FBgn0265778,FBgn0266084,FBgn0283499 | 26 | GO:000744 4 |
| tube morphogen esis | 0.0176 962 | FBgn0000163,FBgn0000395,FBgn0000547,FBgn00026 43,FBgn0003391,FBgn0003984,FBgn0004893,FBgn001 1817,FBgn0014135,FBgn0014388,FBgn0023510,FBgn0 024236,FBgn0024250,FBgn0029006,FBgn0031461,FBg n0031885,FBgn0036518,FBgn0036666,FBgn0036801,F Bgn0043900,FBgn0050456,FBgn0085432,FBgn026495 9,FBgn0265778,FBgn0266084 | 25 | GO:003523 9 |
| epithelial tube morphogen esis | 0.0273 455 | FBgn0000163,FBgn0000395,FBgn0000547,FBgn00026 43,FBgn0003391,FBgn0003984,FBgn0004893,FBgn001 1817,FBgn0014135,FBgn0014388,FBgn0024236,FBgn0 024250,FBgn0031461,FBgn0031885,FBgn0036518,FBg n0036666,FBgn0036801,FBgn0043900,FBgn0050456,F Bgn0085432,FBgn0264959,FBgn0265778,FBgn026608 4 | 23 | GO:006056 2 |
| regulation of cell differentiat ion | 0.0258 182 | FBgn0000547,FBgn0002633,FBgn0003391,FBgn00036 55,FBgn0003984,FBgn0004797,FBgn0011739,FBgn001 4073,FBgn0014388,FBgn0025741,FBgn0028369,FBgn0 031461,FBgn0052179,FBgn0085430,FBgn0259176,FBg n0259938,FBgn0263353,FBgn0264959,FBgn0265778,F Bgn0266084,FBgn0283499 | 21 | GO:004559 5 |
| response to abiotic stimulus | 0.0204 374 | FBgn0004832,FBgn0004907,FBgn0010651,FBgn00117 39,FBgn0011817,FBgn0014073,FBgn0015946,FBgn002 0258,FBgn0030505,FBgn0031885,FBgn0033132,FBgn0 034335,FBgn0037163,FBgn0038530,FBgn0039464,FBg n0045842,FBgn0263316,FBgn0266411,FBgn0267430,F Bgn0283499 | 20 | GO:000962 8 |
| regulation of cell developme nt | 0.0210 157 | FBgn0000547,FBgn0002633,FBgn0003391,FBgn00036 55,FBgn0003984,FBgn0004797,FBgn0011739,FBgn001 4073,FBgn0014388,FBgn0025741,FBgn0031461,FBgn0 052179,FBgn0085430,FBgn0259176,FBgn0259938,FBg n0264959,FBgn0265778,FBgn0266084,FBgn0283499 | 19 | GO:006028 4 |
| respiratory system developme | 0.0002 383 | FBgn0000163,FBgn0000547,FBgn0003391,FBgn00102 38,FBgn0010894,FBgn0011739,FBgn0014135,FBgn001 4388,FBgn0023510,FBgn0024236,FBgn0033032,FBgn0 | 18 | GO:006054 1 |

| | | | | |
|---|---|---|---|---|
| nt | | 036666,FBgn0085432,FBgn0261284,FBgn0264959,FBgn0266084,FBgn0266411,FBgn0283499 | | |
| enzyme linked receptor protein signaling pathway | 0.009184 | FBgn0000395,FBgn0000547,FBgn0003984,FBgn0004907,FBgn0014073,FBgn0014135,FBgn0014388,FBgn0022800,FBgn0024250,FBgn0025625,FBgn0029006,FBgn0031461,FBgn0035626,FBgn0052179,FBgn0264959,FBgn0266411,FBgn0283499 | 17 | GO:0007167 |
| post-embryonic appendage morphogenesis | 0.0436033 | FBgn0000395,FBgn0000547,FBgn0002643,FBgn0003391,FBgn0003984,FBgn0004893,FBgn0011817,FBgn0024250,FBgn0031461,FBgn0036518,FBgn0036801,FBgn0043900,FBgn0050456,FBgn0085432,FBgn0264959,FBgn0265778,FBgn0266084 | 17 | GO:0035120 |
| imaginal disc-derived appendage morphogenesis | 0.048628 | FBgn0000395,FBgn0000547,FBgn0002643,FBgn0003391,FBgn0003984,FBgn0004893,FBgn0011817,FBgn0024250,FBgn0031461,FBgn0036518,FBgn0036801,FBgn0043900,FBgn0050456,FBgn0085432,FBgn0264959,FBgn0265778,FBgn0266084 | 17 | GO:0035114 |
| open tracheal system development | 0.0012062 | FBgn0000163,FBgn0000547,FBgn0003391,FBgn0010238,FBgn0010894,FBgn0011739,FBgn0014135,FBgn0014388,FBgn0023510,FBgn0024236,FBgn0033032,FBgn0036666,FBgn0085432,FBgn0261284,FBgn0264959,FBgn0283499 | 16 | GO:0007424 |
| cell adhesion | 0.0007773 | FBgn0000163,FBgn0000547,FBgn0003391,FBgn0010238,FBgn0010894,FBgn0015229,FBgn0022800,FBgn0025741,FBgn0028369,FBgn0029082,FBgn0037963,FBgn0043900,FBgn0264959,FBgn0266084 | 14 | GO:0007155 |
| biological adhesion | 0.0008548 | FBgn0000163,FBgn0000547,FBgn0003391,FBgn0010238,FBgn0010894,FBgn0015229,FBgn0022800,FBgn0025741,FBgn0028369,FBgn0029082,FBgn0037963,FBgn0043900,FBgn0264959,FBgn0266084 | 14 | GO:0022610 |
| embryonic morphogenesis | 0.0163682 | FBgn0000163,FBgn0000547,FBgn0002643,FBgn0003391,FBgn0004893,FBgn0010238,FBgn0010894,FBgn0028292,FBgn0029006,FBgn0036518,FBgn0085432,FBgn0264959,FBgn0265778,FBgn0283499 | 14 | GO:0048598 |
| transmembrane receptor protein tyrosine kinase signaling pathway | 0.018795 | FBgn0000547,FBgn0003984,FBgn0004907,FBgn0014073,FBgn0014135,FBgn0014388,FBgn0022800,FBgn0025625,FBgn0035626,FBgn0052179,FBgn0264959,FBgn0266411,FBgn0283499 | 13 | GO:0007169 |
| defense response to bacterium | 0.0160245 | FBgn0024987,FBgn0033980,FBgn0034647,FBgn0035806,FBgn0035813,FBgn0035977,FBgn0038530,FBgn0040384,FBgn0052133,FBgn0086358,FBgn0264959,FBgn0265052 | 12 | GO:0042742 |
| response to bacterium | 0.0315131 | FBgn0024987,FBgn0033980,FBgn0034647,FBgn0035806,FBgn0035813,FBgn0035977,FBgn0038530,FBgn0040384,FBgn0052133,FBgn0086358,FBgn0264959,FBgn0265052 | 12 | GO:0009617 |
| cell-cell adhesion | 0.000445 | FBgn0000163,FBgn0000547,FBgn0003391,FBgn0010238,FBgn0015229,FBgn0022800,FBgn0028369,FBgn0029082,FBgn0037963,FBgn0043900,FBgn0264959 | 11 | GO:0098609 |
| determination of adult | 0.0261507 | FBgn0002566,FBgn0015946,FBgn0031461,FBgn0031885,FBgn0033127,FBgn0035977,FBgn0037802,FBgn005 | 11 | GO:0008340 |

| | | | | |
|---|---|---|---|---|
| lifespan | | 1216,FBgn0259176,FBgn0263316,FBgn0283499 | | |
| multicellular organism aging | 0.0276998 | FBgn0002566,FBgn0015946,FBgn0031461,FBgn0031885,FBgn0033127,FBgn0035977,FBgn0037802,FBgn0051216,FBgn0259176,FBgn0263316,FBgn0283499 | 11 | GO:0010259 |
| positive regulation of intracellular signal transduction | 0.0293142 | FBgn0000547,FBgn0001234,FBgn0003984,FBgn0004907,FBgn0014135,FBgn0031885,FBgn0050440,FBgn0050456,FBgn0262081,FBgn0264959,FBgn0283499 | 11 | GO:1902533 |
| aging | 0.0327437 | FBgn0002566,FBgn0015946,FBgn0031461,FBgn0031885,FBgn0033127,FBgn0035977,FBgn0037802,FBgn0051216,FBgn0259176,FBgn0263316,FBgn0283499 | 11 | GO:0007568 |
| cell-cell junction organization | 0.0007144 | FBgn0000163,FBgn0003391,FBgn0010238,FBgn0010894,FBgn0028369,FBgn0033032,FBgn0261284,FBgn0262081,FBgn0264959,FBgn0265778 | 10 | GO:0045216 |
| cell junction organization | 0.0008173 | FBgn0000163,FBgn0003391,FBgn0010238,FBgn0010894,FBgn0028369,FBgn0033032,FBgn0261284,FBgn0262081,FBgn0264959,FBgn0265778 | 10 | GO:0034330 |
| sulfur compound metabolic process | 0.0204494 | FBgn0010039,FBgn0010040,FBgn0010041,FBgn0015011,FBgn0032986,FBgn0034335,FBgn0050022,FBgn0063492,FBgn0063493,FBgn0265052 | 10 | GO:0006790 |
| positive regulation of phosphorus metabolic process | 0.0204494 | FBgn0001234,FBgn0003984,FBgn0014073,FBgn0014135,FBgn0022800,FBgn0025741,FBgn0031461,FBgn0031885,FBgn0264959,FBgn0283499 | 10 | GO:0010562 |
| positive regulation of phosphate metabolic process | 0.0204494 | FBgn0001234,FBgn0003984,FBgn0014073,FBgn0014135,FBgn0022800,FBgn0025741,FBgn0031461,FBgn0031885,FBgn0264959,FBgn0283499 | 10 | GO:0045937 |
| cell-cell adhesion via plasma-membrane adhesion molecules | 1.38E-05 | FBgn0000163,FBgn0000547,FBgn0003391,FBgn0010238,FBgn0015229,FBgn0022800,FBgn0028369,FBgn0029082,FBgn0037963 | 9 | GO:0098742 |
| regulation of locomotion | 0.0170422 | FBgn0003391,FBgn0003984,FBgn0014073,FBgn0014135,FBgn0025741,FBgn0052179,FBgn0085430,FBgn0266084,FBgn0266411 | 9 | GO:0040012 |
| regulation of cellular component movement | 0.0170422 | FBgn0003391,FBgn0003984,FBgn0014073,FBgn0014135,FBgn0025741,FBgn0052179,FBgn0085430,FBgn0266084,FBgn0266411 | 9 | GO:0051270 |
| positive regulation of | 0.0386117 | FBgn0001234,FBgn0003984,FBgn0014073,FBgn0014135,FBgn0022800,FBgn0031461,FBgn0031885,FBgn0264959,FBgn0283499 | 9 | GO:0042327 |

| | | | | |
|---|---|---|---|---|
| phosphorylation | | | | |
| MAPK cascade | 0.0487412 | FBgn0001234,FBgn0003984,FBgn0014135,FBgn0014388,FBgn0031885,FBgn0035977,FBgn0264959,FBgn0265778,FBgn0283499 | 9 | GO:0000165 |
| cell-cell junction assembly | 0.0008342 | FBgn0000163,FBgn0003391,FBgn0010238,FBgn0010894,FBgn0028369,FBgn0033032,FBgn0261284,FBgn0265778 | 8 | GO:0007043 |
| cell junction assembly | 0.0009864 | FBgn0000163,FBgn0003391,FBgn0010238,FBgn0010894,FBgn0028369,FBgn0033032,FBgn0261284,FBgn0265778 | 8 | GO:0034329 |
| cuticle development | 0.0045878 | FBgn0000451,FBgn0001112,FBgn0004396,FBgn0035513,FBgn0043900,FBgn0085432,FBgn0261799,FBgn0286203 | 8 | GO:0042335 |
| regulation of cell migration | 0.0071917 | FBgn0003391,FBgn0003984,FBgn0014073,FBgn0014135,FBgn0025741,FBgn0052179,FBgn0266084,FBgn0266411 | 8 | GO:0030334 |
| regulation of cell motility | 0.0097811 | FBgn0003391,FBgn0003984,FBgn0014073,FBgn0014135,FBgn0025741,FBgn0052179,FBgn0266084,FBgn0266411 | 8 | GO:2000145 |
| detection of stimulus | 0.0130077 | FBgn0020258,FBgn0033404,FBgn0035806,FBgn0037163,FBgn0037630,FBgn0040849,FBgn0050081,FBgn0259683 | 8 | GO:0051606 |
| stem cell proliferation | 0.0216965 | FBgn0000163,FBgn0011739,FBgn0024555,FBgn0028292,FBgn0031461,FBgn0035626,FBgn0085432,FBgn0259176 | 8 | GO:0072089 |
| stem cell division | 0.0273108 | FBgn0000163,FBgn0000928,FBgn0003391,FBgn0024555,FBgn0028292,FBgn0035626,FBgn0052364,FBgn0283499 | 8 | GO:0017145 |
| homophilic cell adhesion via plasma membrane adhesion molecules | 6.751E-05 | FBgn0000547,FBgn0003391,FBgn0010238,FBgn0022800,FBgn0028369,FBgn0029082,FBgn0037963 | 7 | GO:0007156 |
| glutathione metabolic process | 0.0021294 | FBgn0010039,FBgn0010040,FBgn0010041,FBgn0034335,FBgn0050022,FBgn0063492,FBgn0063493 | 7 | GO:0006749 |
| chitin-based cuticle development | 0.0025003 | FBgn0001112,FBgn0004396,FBgn0035513,FBgn0043900,FBgn0085432,FBgn0261799,FBgn0286203 | 7 | GO:0040003 |
| morphogenesis of a branching structure | 0.0033893 | FBgn0000163,FBgn0000547,FBgn0003391,FBgn0014135,FBgn0014388,FBgn0024236,FBgn0036666 | 7 | GO:0001763 |
| branching morphogenesis of an epithelial tube | 0.0033893 | FBgn0000163,FBgn0000547,FBgn0003391,FBgn0014135,FBgn0014388,FBgn0024236,FBgn0036666 | 7 | GO:0048754 |
| branching involved in open tracheal | 0.0033893 | FBgn0000163,FBgn0000547,FBgn0003391,FBgn0014135,FBgn0014388,FBgn0024236,FBgn0036666 | 7 | GO:0060446 |

| | | | | |
|---|---|---|---|---|
| system development | | | | |
| morphogenesis of a branching epithelium | 0.0033893 | FBgn0000163,FBgn0000547,FBgn0003391,FBgn0014135,FBgn0014388,FBgn0024236,FBgn0036666 | 7 | GO:0061138 |
| cellular modified amino acid metabolic process | 0.0118394 | FBgn0010039,FBgn0010040,FBgn0010041,FBgn0034335,FBgn0050022,FBgn0063492,FBgn0063493 | 7 | GO:0006575 |
| posttranscriptional gene silencing | 0.0145638 | FBgn0001218,FBgn0011291,FBgn0024987,FBgn0031488,FBgn0035626,FBgn0036451,FBgn0039972 | 7 | GO:0016441 |
| modulation of chemical synaptic transmission | 0.0324448 | FBgn0010501,FBgn0030505,FBgn0030850,FBgn0033926,FBgn0051201,FBgn0262081,FBgn0264959 | 7 | GO:0050804 |
| regulation of trans-synaptic signaling | 0.0324448 | FBgn0010501,FBgn0030505,FBgn0030850,FBgn0033926,FBgn0051201,FBgn0262081,FBgn0264959 | 7 | GO:0099177 |
| establishment of planar polarity | 0.0407185 | FBgn0000163,FBgn0000547,FBgn0003391,FBgn0011817,FBgn0014388,FBgn0029082,FBgn0052179 | 7 | GO:0001736 |
| morphogenesis of a polarized epithelium | 0.0407185 | FBgn0000163,FBgn0000547,FBgn0003391,FBgn0011817,FBgn0014388,FBgn0029082,FBgn0052179 | 7 | GO:0001738 |
| establishment of tissue polarity | 0.0407185 | FBgn0000163,FBgn0000547,FBgn0003391,FBgn0011817,FBgn0014388,FBgn0029082,FBgn0052179 | 7 | GO:0007164 |
| detection of chemical stimulus | 0.0027514 | FBgn0033404,FBgn0035806,FBgn0037630,FBgn0040849,FBgn0050081,FBgn0259683 | 6 | GO:0009593 |
| adherens junction organization | 0.003919 | FBgn0000163,FBgn0003391,FBgn0028369,FBgn0262081,FBgn0264959,FBgn0265778 | 6 | GO:0034332 |
| apical junction assembly | 0.0054184 | FBgn0000163,FBgn0003391,FBgn0010238,FBgn0010894,FBgn0033032,FBgn0261284 | 6 | GO:0043297 |
| establishment of ommatidial planar polarity | 0.0083991 | FBgn0000547,FBgn0003391,FBgn0011817,FBgn0014388,FBgn0029082,FBgn0052179 | 6 | GO:0042067 |
| gastrulation | 0.0217839 | FBgn0000163,FBgn0002643,FBgn0003391,FBgn0028292,FBgn0036518,FBgn0085432 | 6 | GO:0007369 |

| | | | | |
|---|---|---|---|---|
| cell fate specification | 0.0320726 | FBgn0000547,FBgn0002732,FBgn0003984,FBgn0011739,FBgn0031461,FBgn0259176 | 6 | GO:0001708 |
| positive regulation of cell population proliferation | 0.0415766 | FBgn0003984,FBgn0031461,FBgn0035626,FBgn0052179,FBgn0259176,FBgn0283499 | 6 | GO:0008284 |
| regulation of tube architecture, open tracheal system | 0.0451 | FBgn0003391,FBgn0010238,FBgn0010894,FBgn0023510,FBgn0033032,FBgn0261284 | 6 | GO:0035152 |
| regulation of oogenesis | 0.0451 | FBgn0003391,FBgn0003655,FBgn0003984,FBgn0004797,FBgn0014073,FBgn0052179 | 6 | GO:1905879 |
| ommatidial rotation | 0.0032684 | FBgn0000547,FBgn0003391,FBgn0011817,FBgn0014388,FBgn0052179 | 5 | GO:0016318 |
| intestinal stem cell homeostasis | 0.0040587 | FBgn0001218,FBgn0032691,FBgn0259176,FBgn0264959,FBgn0283499 | 5 | GO:0036335 |
| homeostasis of number of cells | 0.0040587 | FBgn0001218,FBgn0032691,FBgn0259176,FBgn0264959,FBgn0283499 | 5 | GO:0048872 |
| hippo signaling | 0.0294005 | FBgn0000547,FBgn0004907,FBgn0011739,FBgn0029006,FBgn0262081 | 5 | GO:0035329 |
| regulation of epithelial cell migration | 0.0327878 | FBgn0003391,FBgn0003984,FBgn0014073,FBgn0014135,FBgn0052179 | 5 | GO:0010632 |
| positive regulation of cell migration | 0.0364089 | FBgn0003391,FBgn0003984,FBgn0014073,FBgn0052179,FBgn0266084 | 5 | GO:0030335 |
| regulation of defense response to bacterium | 0.0364089 | FBgn0034647,FBgn0035806,FBgn0035977,FBgn0052133,FBgn0086358 | 5 | GO:1900424 |
| molting cycle, chitin-based cuticle | 0.0443641 | FBgn0000568,FBgn0001112,FBgn0004396,FBgn0043900,FBgn0085432 | 5 | GO:0007591 |
| molting cycle | 0.0443641 | FBgn0000568,FBgn0001112,FBgn0004396,FBgn0043900,FBgn0085432 | 5 | GO:0042303 |
| positive regulation of cell motility | 0.0487023 | FBgn0003391,FBgn0003984,FBgn0014073,FBgn0052179,FBgn0266084 | 5 | GO:2000147 |
| cuticle development involved | 0.0031394 | FBgn0001112,FBgn0004396,FBgn0043900,FBgn0085432 | 4 | GO:0042337 |

| | | | | |
|---|---|---|---|---|
| in chitin-based cuticle molting cycle | | | | |
| adherens junction assembly | 0.0055339 | FBgn0000163,FBgn0003391,FBgn0028369,FBgn0265778 | 4 | GO:0034333 |
| execution phase of apoptosis | 0.0089118 | FBgn0010501,FBgn0015946,FBgn0028406,FBgn0034279 | 4 | GO:0097194 |
| regulation of ERK1 and ERK2 cascade | 0.0191338 | FBgn0003984,FBgn0014135,FBgn0014388,FBgn0264959 | 4 | GO:0070372 |
| circadian sleep/wake cycle | 0.0261696 | FBgn0034136,FBgn0035023,FBgn0053527,FBgn0283499 | 4 | GO:0042745 |
| regulation of compound eye photoreceptor cell differentiation | 0.0261696 | FBgn0000547,FBgn0014388,FBgn0264959,FBgn0265778 | 4 | GO:0110116 |
| feeding behavior | 0.0301997 | FBgn0020258,FBgn0039509,FBgn0040726,FBgn0283499 | 4 | GO:0007631 |
| ERK1 and ERK2 cascade | 0.0301997 | FBgn0003984,FBgn0014135,FBgn0014388,FBgn0264959 | 4 | GO:0070371 |
| syncytium formation by plasma membrane fusion | 0.0345704 | FBgn0011705,FBgn0028369,FBgn0029082,FBgn0261245 | 4 | GO:0000768 |
| syncytium formation | 0.0345704 | FBgn0011705,FBgn0028369,FBgn0029082,FBgn0261245 | 4 | GO:0006949 |
| myoblast fusion | 0.0345704 | FBgn0011705,FBgn0028369,FBgn0029082,FBgn0261245 | 4 | GO:0007520 |
| septate junction assembly | 0.0345704 | FBgn0010238,FBgn0010894,FBgn0033032,FBgn0261284 | 4 | GO:0019991 |
| peptidoglycan recognition protein signaling pathway | 0.0345704 | FBgn0034647,FBgn0035806,FBgn0035977,FBgn0086358 | 4 | GO:0061057 |
| cell-cell fusion | 0.0345704 | FBgn0011705,FBgn0028369,FBgn0029082,FBgn0261245 | 4 | GO:0140253 |
| tight junction assembly | 0.0392924 | FBgn0010238,FBgn0010894,FBgn0033032,FBgn0261284 | 4 | GO:0120192 |
| tight junction organizatio | 0.0392924 | FBgn0010238,FBgn0010894,FBgn0033032,FBgn0261284 | 4 | GO:0120193 |

| | | | | |
|---|---|---|---|---|
| n | | | | |
| positive regulation of border follicle cell migration | 0.0443641 | FBgn0003391,FBgn0003984,FBgn0014073,FBgn0052179 | 4 | GO:1903688 |
| positive regulation of epithelial cell migration | 0.0497853 | FBgn0003391,FBgn0003984,FBgn0014073,FBgn0052179 | 4 | GO:0010634 |
| myotube differentiation | 0.0497853 | FBgn0011705,FBgn0028369,FBgn0029082,FBgn0261245 | 4 | GO:0014902 |
| positive regulation of epithelial cell differentiation | 0.0497853 | FBgn0003391,FBgn0003984,FBgn0014073,FBgn0052179 | 4 | GO:0030858 |
| regulation of border follicle cell migration | 0.0497853 | FBgn0003391,FBgn0003984,FBgn0014073,FBgn0052179 | 4 | GO:1903684 |
| symmetric stem cell division | 0.0001266 | FBgn0003391,FBgn0035626,FBgn0052364 | 3 | GO:0098724 |
| symmetric cell division | 0.0004874 | FBgn0003391,FBgn0035626,FBgn0052364 | 3 | GO:0098725 |
| calcium-dependent cell-cell adhesion via plasma membrane cell adhesion molecules | 0.0038068 | FBgn0003391,FBgn0022800,FBgn0037963 | 3 | GO:0016339 |
| protein polyglycylation | 0.0084735 | FBgn0026147,FBgn0031853,FBgn0034459 | 3 | GO:0018094 |
| response to osmotic stress | 0.0116594 | FBgn0015946,FBgn0030505,FBgn0031885 | 3 | GO:0006970 |
| negative regulation of cell adhesion | 0.0116594 | FBgn0000163,FBgn0025741,FBgn0043900 | 3 | GO:0007162 |
| chitin-based larval cuticle pattern | 0.0116594 | FBgn0004396,FBgn0043900,FBgn0085432 | 3 | GO:0035293 |

| | | | | |
|---|---|---|---|---|
| formation | | | | |
| negative regulation of secretion by cell | 0.0116594 | FBgn0030505,FBgn0032428,FBgn0283499 | 3 | GO:1903531 |
| heterophilic cell-cell adhesion via plasma membrane cell adhesion molecules | 0.015443 | FBgn0015229,FBgn0028369,FBgn0029082 | 3 | GO:0007157 |
| peptidyl-glutamic acid modification | 0.015443 | FBgn0026147,FBgn0031853,FBgn0034459 | 3 | GO:0018200 |
| negative regulation of secretion | 0.015443 | FBgn0030505,FBgn0032428,FBgn0283499 | 3 | GO:0051048 |
| larval chitin-based cuticle development | 0.0198366 | FBgn0004396,FBgn0043900,FBgn0085432 | 3 | GO:0008363 |
| tube fusion | 0.0198366 | FBgn0000547,FBgn0003391,FBgn0024236 | 3 | GO:0035146 |
| branch fusion, open tracheal system | 0.0198366 | FBgn0000547,FBgn0003391,FBgn0024236 | 3 | GO:0035147 |
| negative regulation of imaginal disc growth | 0.0248458 | FBgn0011739,FBgn0036666,FBgn0262081 | 3 | GO:0045571 |
| positive regulation of hippo signaling | 0.0304701 | FBgn0000547,FBgn0004907,FBgn0262081 | 3 | GO:0035332 |
| positive regulation of ERK1 and ERK2 cascade | 0.0304701 | FBgn0003984,FBgn0014135,FBgn0264959 | 3 | GO:0070374 |
| female mating behavior | 0.0367042 | FBgn0028424,FBgn0053527,FBgn0283499 | 3 | GO:0060180 |
| regulation of peptidogly | 0.0367042 | FBgn0034647,FBgn0035806,FBgn0035977 | 3 | GO:0061058 |

| | | | | |
|---|---|---|---|---|
| can recognition protein signaling pathway | | | | |
| histone H4 acetylation | 0.043538 | FBgn0031876,FBgn0032691,FBgn0035624 | 3 | GO:0043967 |
| R8 cell differentiation | 0.043538 | FBgn0000547,FBgn0011739,FBgn0031461 | 3 | GO:0045465 |
| germline stem cell symmetric division | 0.0025308 | FBgn0003391,FBgn0052364 | 2 | GO:0098729 |
| male germline stem cell symmetric division | 0.0025308 | FBgn0003391,FBgn0052364 | 2 | GO:0098730 |
| mesodermal cell fate determination | 0.0073393 | FBgn0002643,FBgn0085432 | 2 | GO:0007500 |
| gonadal mesoderm development | 0.0073393 | FBgn0003391,FBgn0024236 | 2 | GO:0007506 |
| phenol-containing compound catabolic process | 0.0073393 | FBgn0016013,FBgn0037153 | 2 | GO:0019336 |
| response to anoxia | 0.0073393 | FBgn0263316,FBgn0283499 | 2 | GO:0034059 |
| response to light intensity | 0.0141912 | FBgn0033132,FBgn0037163 | 2 | GO:0009642 |
| gonad morphogenesis | 0.0141912 | FBgn0003391,FBgn0024236 | 2 | GO:0035262 |
| histone H2A acetylation | 0.0141912 | FBgn0032691,FBgn0035624 | 2 | GO:0043968 |
| CENP-A containing chromatin organization | 0.0141912 | FBgn0002643,FBgn0037624 | 2 | GO:0061641 |
| negative regulation of feeding behavior | 0.0141912 | FBgn0020258,FBgn0283499 | 2 | GO:2000252 |
| regulation of striated muscle tissue developme | 0.0228698 | FBgn0028369,FBgn0029082 | 2 | GO:0016202 |

| | | | | |
|---|---|---|---|---|
| nt | | | | |
| chromatin remodeling at centromere | 0.0228698 | FBgn0002643,FBgn0037624 | 2 | GO:0031055 |
| CENP-A containing nucleosome assembly | 0.0228698 | FBgn0002643,FBgn0037624 | 2 | GO:0034080 |
| regulation of muscle tissue development | 0.0228698 | FBgn0028369,FBgn0029082 | 2 | GO:1901861 |
| negative regulation of peptide secretion | 0.0331752 | FBgn0032428,FBgn0283499 | 2 | GO:0002792 |
| cell-cell adhesion mediated by cadherin | 0.0331752 | FBgn0003391,FBgn0037963 | 2 | GO:0044331 |
| delamination | 0.0331752 | FBgn0000163,FBgn0043900 | 2 | GO:0060232 |
| mesenchyme development | 0.0331752 | FBgn0003391,FBgn0024236 | 2 | GO:0060485 |
| mesodermal cell fate commitment | 0.0449226 | FBgn0002643,FBgn0085432 | 2 | GO:0001710 |
| DNA replication-independent nucleosome assembly | 0.0449226 | FBgn0002643,FBgn0037624 | 2 | GO:0006336 |
| mechanosensory behavior | 0.0449226 | FBgn0020258,FBgn0267430 | 2 | GO:0007638 |
| response to salt stress | 0.0449226 | FBgn0030505,FBgn0031885 | 2 | GO:0009651 |
| contractile actin filament bundle assembly | 0.0449226 | FBgn0000547,FBgn0266084 | 2 | GO:0030038 |
| centromere complex assembly | 0.0449226 | FBgn0002643,FBgn0037624 | 2 | GO:0034508 |
| mesodermal cell differentiation | 0.0449226 | FBgn0002643,FBgn0085432 | 2 | GO:0048333 |

| | | | | |
|---|---|---|---|---|
| negative regulation of behavior | 0.0449226 | FBgn0020258,FBgn0283499 | 2 | GO:0048521 |

**Table 2.1f: Pathway enrichment for hits differentially upregulated in control males relative to control females**

| p-value | Hits | Gene matches | Pathway ID |
|---|---|---|---|
| 0.002887389 | FBgn0000163,FBgn0000568,FBgn0003984,FBgn0004907,FBgn0011739,FBgn0011817,FBgn0014135,FBgn0014388,FBgn0022800,FBgn0022986,FBgn0023416,FBgn0025741,FBgn0029006,FBgn0030011,FBgn0030505,FBgn0031461,FBgn0031885,FBgn0033205,FBgn0033815,FBgn0034706,FBgn0036290,FBgn0036518,FBgn0039938,FBgn0043900,FBgn0050440,FBgn0050456,FBgn0085432,FBgn0262081,FBgn0264959,FBgn0265778,FBgn0283499 | 31 | R-DME-162582 |
| 0.01914754 | FBgn0004907,FBgn0011817,FBgn0029006,FBgn0030011,FBgn0030505,FBgn0031885,FBgn0039938,FBgn0043900,FBgn0085432 | 9 | R-DME-195721 |
| 0.000383677 | FBgn0010039,FBgn0010040,FBgn0010041,FBgn0026755,FBgn0034335,FBgn0040256,FBgn0063493 | 7 | 980 |
| 0.000383677 | FBgn0010039,FBgn0010040,FBgn0010041,FBgn0026755,FBgn0034335,FBgn0040256,FBgn0063493 | 7 | 982 |
| 0.013554847 | FBgn0010240,FBgn0023416,FBgn0030011,FBgn0034136,FBgn0038752,FBgn0051201,FBgn0266720 | 7 | R-DME-112315 |
| 0.035315175 | FBgn0014135,FBgn0015011,FBgn0024236,FBgn0030638,FBgn0031002,FBgn0034136,FBgn0038752 | 7 | R-DME-425407 |
| 0.004645 | FBgn0003984,FBgn0004907,FBgn0014135,FBgn0022800,FBgn0262081,FBgn0265778 | 6 | R-DME-5673001 |
| 0.005248567 | FBgn0003984,FBgn0004907,FBgn0014135,FBgn0022800,FBgn0262081,FBgn0265778 | 6 | R-DME-5684996 |
| 0.008251417 | FBgn0003984,FBgn0004907,FBgn0014135,FBgn0022800,FBgn0262081,FBgn0265778 | 6 | R-DME-5683057 |
| 0.008251417 | FBgn0003984,FBgn0004907,FBgn0014135,FBgn0022800,FBgn0262081,FBgn0265778 | 6 | R-DME-9607240 |
| 0.030436918 | FBgn0004907,FBgn0029006,FBgn0031885,FBgn0039938,FBgn0043900,FBgn0085432 | 6 | R-DME-201681 |
| 0.005495592 | FBgn0010039,FBgn0010040,FBgn0010041,FBgn0034335,FBgn0063493 | 5 | 480 |
| 0.015090854 | FBgn0024236,FBgn0030638,FBgn0031002,FBgn0034136,FBgn0038752 | 5 | R-DME-425366 |
| 0.009461437 | FBgn0011817,FBgn0030011,FBgn0030505,FBgn0085432 | 4 | R-DME-4086398 |
| 0.009461437 | FBgn0025741,FBgn0030011,FBgn0050440,FBgn0050456 | 4 | R-DME-416482 |
| 0.034465988 | FBgn0026755,FBgn0033294,FBgn0033297,FBgn0040256 | 4 | 500 |
| 0.038070252 | FBgn0010240,FBgn0023416,FBgn0030011,FBgn0051201 | 4 | R-DME-112314 |
| 0.041883273 | FBgn0014135,FBgn0031461,FBgn0031885,FBgn0037772 | 4 | R-DME-381426 |
| 0.041883273 | FBgn0014135,FBgn0031461,FBgn0031885,FBgn0037772 | 4 | R-DME-8957275 |
| 0.009943728 | FBgn0031885,FBgn0043900,FBgn0085432 | 3 | R-DME-201722 |
| 0.01256 | FBgn0000163,FBgn0029006,FBgn0031461 | 3 | R-DME- |

| | | | |
|---|---|---|---|
| 2316 | | | 2173791 |
| 0.01256 2316 | FBgn0003984,FBgn0014135,FBgn0022800 | 3 | R-DME-6811558 |
| 0.02258 2152 | FBgn0004797,FBgn0026755,FBgn0040256 | 3 | 830 |
| 0.02258 2152 | FBgn0003984,FBgn0014135,FBgn0022800 | 3 | R-DME-199418 |
| 0.02258 2152 | FBgn0004907,FBgn0039938,FBgn0085432 | 3 | R-DME-3769402 |
| 0.03109 1166 | FBgn0026755,FBgn0039273,FBgn0040256 | 3 | 514 |
| 0.04656 2625 | FBgn0030367,FBgn0033397,FBgn0036290 | 3 | R-DME-193144 |
| 0.00866 5626 | FBgn0000547,FBgn0028369 | 2 | R-DME-373753 |
| 0.00866 5626 | FBgn0036986,FBgn0037818 | 2 | R-DME-5423646 |
| 0.01407 4039 | FBgn0043900,FBgn0085432 | 2 | R-DME-209421 |
| 0.01407 4039 | FBgn0004907,FBgn0011739 | 2 | R-DME-390098 |
| 0.02057 3844 | FBgn0030011,FBgn0051201 | 2 | R-DME-500657 |
| 0.03648 3803 | FBgn0004907,FBgn0011739 | 2 | R-DME-2028269 |
| 0.03648 3803 | FBgn0014135,FBgn0031461 | 2 | R-DME-3000170 |
| 0.03648 3803 | FBgn0004797,FBgn0035266 | 2 | R-DME-75109 |
| 0.04572 5398 | FBgn0014135,FBgn0031461 | 2 | R-DME-3000171 |
| 0.04572 5398 | FBgn0033205,FBgn0036290 | 2 | R-DME-975634 |
| 0.03916 3624 | FBgn0014135 | 1 | R-DME-190241 |
| 0.03916 3624 | FBgn0014135 | 1 | R-DME-190242 |
| 0.03916 3624 | FBgn0014135 | 1 | R-DME-190370 |
| 0.03916 3624 | FBgn0014135 | 1 | R-DME-190371 |
| 0.03916 3624 | FBgn0014135 | 1 | R-DME-190373 |
| 0.03916 3624 | FBgn0014135 | 1 | R-DME-190374 |
| 0.03916 3624 | FBgn0014135 | 1 | R-DME-190375 |
| 0.03916 3624 | FBgn0014135 | 1 | R-DME-190377 |
| 0.03916 3624 | FBgn0034136 | 1 | R-DME-379401 |

**Table 2.2a: list of genes differentially upregulated in control males relative to 20HE males**

| list of hits>10 raw reads | log2FC edgeR | p-value edgeR | -log10(pvalue) |
|---|---|---|---|

| | | | |
|---|---|---|---|
| AOX2 | -6.5067 | 7.42E-06 | 5.129596095 |
| CG43968 | -6.6688 | 0.0002 | 3.698970004 |
| CG12446 | -5.8271 | 0.0002 | 3.698970004 |
| Pig1 | -3.1216 | 0.0003 | 3.522878745 |
| CG42818 | -6.5236 | 0.0005 | 3.301029996 |
| CG3246 | -3.0039 | 0.0014 | 2.853871964 |
| CG31391 | -4.0215 | 0.0017 | 2.769551079 |
| CG14545 | -2.9623 | 0.0024 | 2.619788758 |
| CG18003 | -3.4764 | 0.0024 | 2.619788758 |
| CG1602 | -1.161 | 0.0032 | 2.494850022 |
| CG14291 | -2.0361 | 0.0036 | 2.443697499 |
| CG3709 | -1.0501 | 0.0039 | 2.408935393 |
| CG31287 | -2.1138 | 0.0039 | 2.408935393 |
| CG7406 | -3.8103 | 0.0043 | 2.366531544 |
| Sr-CIII | -5.6264 | 0.0057 | 2.244125144 |
| CG14837 | -2.4124 | 0.0064 | 2.193820026 |
| Zip88E | -1.4633 | 0.007 | 2.15490196 |
| CR44566 | -1.093 | 0.0075 | 2.124938737 |
| snoRNA:Me28S-C3227b | -1.8774 | 0.008 | 2.096910013 |
| CR43849 | -1.596 | 0.0082 | 2.086186148 |
| CG4462 | -1.0211 | 0.0084 | 2.075720714 |
| CG14238 | -4.2035 | 0.0107 | 1.970616222 |
| CG14695 | -2.7579 | 0.0125 | 1.903089987 |
| CG17681 | -1.6223 | 0.0125 | 1.903089987 |
| CG42364 | -1.5618 | 0.0132 | 1.879426069 |
| snoRNA:Psi28S-2648 | -1.5208 | 0.0135 | 1.869666232 |
| CG14367 | -1.5871 | 0.0138 | 1.860120914 |
| DptA | -6.3191 | 0.0142 | 1.847711656 |
| RpL13A | -1.7022 | 0.0147 | 1.832682665 |
| CG12868 | -1.2714 | 0.016 | 1.795880017 |
| CG42672 | -2.1561 | 0.0161 | 1.793174124 |
| heix | -0.894 | 0.0162 | 1.790484985 |
| CG13843 | -2.2947 | 0.0162 | 1.790484985 |
| CG3335 | -0.8243 | 0.0163 | 1.787812396 |
| tos | -1.4721 | 0.0165 | 1.782516056 |
| Fur2 | -2.0955 | 0.0166 | 1.779891912 |
| CR44833 | -2.7113 | 0.0167 | 1.777283529 |
| GluRS-m | -0.9863 | 0.0173 | 1.761953897 |
| CG10581 | -1.9571 | 0.0174 | 1.759450752 |
| CG6568 | -2.1704 | 0.0177 | 1.752026734 |

| | | | |
|---|---|---|---|
| CG17249 | -0.9304 | 0.0179 | 1.747146969 |
| CG7137 | -0.8816 | 0.021 | 1.677780705 |
| CG10933 | -6.1121 | 0.021 | 1.677780705 |
| CR44611 | -1.5672 | 0.0215 | 1.66756154 |
| snoRNA:Me18S-C419 | -2.2584 | 0.0216 | 1.665546249 |
| snoRNA:Me28S-A982a | -1.8086 | 0.0231 | 1.63638802 |
| Ser7 | -1.24 | 0.0239 | 1.621602099 |
| CG44002 | -0.9024 | 0.024 | 1.619788758 |
| CG8319 | -0.806 | 0.0247 | 1.607303047 |
| CG6712 | -0.7023 | 0.0249 | 1.603800653 |
| CG14252 | -0.9 | 0.0254 | 1.595166283 |
| wor | -1.6041 | 0.0255 | 1.59345982 |
| Tab2 | -1.2721 | 0.0278 | 1.555955204 |
| CG6574 | -1.18 | 0.0296 | 1.528708289 |
| mir-967 | -0.9719 | 0.0296 | 1.528708289 |
| Cyp6a20 | -0.8244 | 0.03 | 1.522878745 |
| CG42258 | -2.6432 | 0.0303 | 1.518557371 |
| CG8072 | -1.7811 | 0.0315 | 1.501689446 |
| CG14971 | -0.7776 | 0.0316 | 1.500312917 |
| CR44138 | -1.6638 | 0.0318 | 1.49757288 |
| snoRNA:Psi28S-2949 | -1.0821 | 0.0321 | 1.493494968 |
| CG16833 | -1.4088 | 0.0324 | 1.48945499 |
| SerRS-m | -1.3166 | 0.0337 | 1.472370099 |
| CG13494 | -1.157 | 0.0348 | 1.458420756 |
| CR44022 | -2.0912 | 0.0354 | 1.450996738 |
| CG33331 | -0.8178 | 0.0363 | 1.440093375 |
| snoRNA:Me28S-A992 | -1.6987 | 0.0367 | 1.435333936 |
| snoRNA:Me28S-G764 | -1.5829 | 0.0379 | 1.42136079 |
| snoRNA:Psi18S-1275 | -1.5073 | 0.038 | 1.420216403 |
| CG10063 | -2.3783 | 0.0411 | 1.386158178 |
| snoRNA:Me28S-G3255b | -1.2316 | 0.0412 | 1.385102784 |
| fray | -2.0595 | 0.0412 | 1.385102784 |
| Arc1 | -0.6566 | 0.0419 | 1.377785977 |
| Kif19A | -5.4692 | 0.0429 | 1.367542708 |
| CG6962 | -0.8724 | 0.0441 | 1.355561411 |
| dsx-c73A | -1.3142 | 0.0448 | 1.348721986 |
| CG34231 | -0.9484 | 0.0449 | 1.347753659 |
| Atxn7 | -1.8506 | 0.045 | 1.346787486 |
| CG31606 | -1.6906 | 0.0455 | 1.341988603 |
| CG32396 | -1.2616 | 0.0457 | 1.3400838 |

| | | | |
|---|---|---|---|
| mthl10 | -1.3117 | 0.0463 | 1.334419009 |
| CG8492 | -3.0693 | 0.0479 | 1.319664487 |
| snoRNA:Psi18S-920 | -1.3085 | 0.048 | 1.318758763 |
| CG12909 | -0.6273 | 0.0481 | 1.317854924 |
| CG7857 | -0.6874 | 0.0486 | 1.313363731 |
| CR46220 | -1.6496 | 0.0491 | 1.308918508 |
| isoQC | -1.074 | 0.0501 | 1.300162274 |
| CG1463 | -4.4261 | 0.0502 | 1.299296283 |
| CG43101 | -0.9784 | 0.0506 | 1.295849483 |
| snoRNA:nop5-x16-a | -1.3274 | 0.0508 | 1.294136288 |
| CG13868 | -1.1543 | 0.051 | 1.292429824 |
| CR46102 | -2.2176 | 0.051 | 1.292429824 |
| SmydA-5 | -1.4836 | 0.0511 | 1.2915791 |
| CR45823 | -4.6824 | 0.0516 | 1.287350298 |
| CG11257 | -0.7572 | 0.0517 | 1.286509457 |
| dpr18 | -0.8827 | 0.0521 | 1.283162277 |
| CG17294 | -0.7187 | 0.0527 | 1.278189385 |
| CG10730 | -1.6359 | 0.0531 | 1.274905479 |
| Rbp4 | -1.6379 | 0.0534 | 1.272458743 |
| Hexo2 | -0.8738 | 0.0538 | 1.269217724 |
| CG43370 | -0.9773 | 0.054 | 1.26760624 |
| TBC1D16 | -0.9783 | 0.054 | 1.26760624 |

**Table 2.2b: list of genes differentially upregulated in 20HE males relative to control males**

| list of hits>10 raw reads | log2FC edgeR | p-value edgeR | -log10(pvalue)2 |
|---|---|---|---|
| CG13813 | 15.064 | 6.06E-26 | 25.21752738 |
| CG11241 | 3.5682 | 5.70E-14 | 13.24412514 |
| alpha-Est7 | 3.0456 | 1.57E-08 | 7.804100348 |
| snoRNA:Me28S-A30 | 3.2883 | 7.11E-08 | 7.148130399 |
| CG5361 | 6.7608 | 7.45E-07 | 6.127843727 |
| CG18180 | 5.1105 | 1.86E-06 | 5.730487056 |
| CG6295 | 3.9842 | 1.45E-05 | 4.838631998 |
| tej | 3.6374 | 1.54E-05 | 4.812479279 |
| CG3344 | 3.414 | 2.80E-05 | 4.552841969 |
| CG18179 | 4.6862 | 2.89E-05 | 4.539102157 |
| CG10910 | 4.6753 | 3.32E-05 | 4.478861916 |
| CG44286 | 4.1695 | 4.07E-05 | 4.390405591 |
| CG30411 | 6.0163 | 4.93E-05 | 4.307153081 |
| CG34026 | 7.9805 | 6.12E-05 | 4.213248578 |
| CR45127 | 3.6236 | 0.0001 | 4 |

| | | | |
|---|---|---|---|
| CG10869 | 3.1314 | 0.0001 | 4 |
| CG32483 | 3.1875 | 0.0002 | 3.698970004 |
| CR45921 | 3.3383 | 0.0002 | 3.698970004 |
| png | 1.6477 | 0.0003 | 3.522878745 |
| Amy-d | 2.7046 | 0.0003 | 3.522878745 |
| CG8952 | 2.8574 | 0.0004 | 3.397940009 |
| CG31690 | 3.8478 | 0.0004 | 3.397940009 |
| Muc68E | 4.0708 | 0.0006 | 3.22184875 |
| CG8299 | 8.1206 | 0.0007 | 3.15490196 |
| CG42825 | 2.9383 | 0.0007 | 3.15490196 |
| CG42846 | 2.8918 | 0.0009 | 3.045757491 |
| CG8568 | 2.3918 | 0.001 | 3 |
| Est-Q | 3.0296 | 0.0011 | 2.958607315 |
| CG14694 | 2.3192 | 0.0011 | 2.958607315 |
| Jon99Cii | 2.8035 | 0.0011 | 2.958607315 |
| Jon99Ci | 2.0867 | 0.0012 | 2.920818754 |
| kappaTry | 2.6034 | 0.0013 | 2.886056648 |
| CG33510 | 1.2647 | 0.0014 | 2.853871964 |
| CR44867 | 3.5541 | 0.0014 | 2.853871964 |
| CG15605 | 3.9996 | 0.0016 | 2.795880017 |
| stg | 2.0629 | 0.0016 | 2.795880017 |
| CG10000 | 6.2272 | 0.0016 | 2.795880017 |
| CR46322 | 6.1148 | 0.0019 | 2.721246399 |
| E(spl)m6-BFM | 1.5074 | 0.002 | 2.698970004 |
| E(spl)m8-HLH | 1.4753 | 0.0021 | 2.677780705 |
| ninaD | 2.811 | 0.0022 | 2.657577319 |
| CAH2 | 3.2068 | 0.0023 | 2.638272164 |
| CG31345 | 3.9613 | 0.0026 | 2.585026652 |
| CG2772 | 1.6162 | 0.0035 | 2.455931956 |
| CG42714 | 2.9918 | 0.0036 | 2.443697499 |
| Ucp4C | 4.1052 | 0.004 | 2.397940009 |
| CG45080 | 4.909 | 0.0041 | 2.387216143 |
| CG5506 | 1.8863 | 0.0041 | 2.387216143 |
| CG7458 | 1.2286 | 0.0046 | 2.337242168 |
| CR44150 | 3.6154 | 0.0051 | 2.292429824 |
| CG4302 | 1.6118 | 0.0062 | 2.207608311 |
| thetaTry | 2.8663 | 0.0064 | 2.193820026 |
| CG33109 | 6.191 | 0.0065 | 2.187086643 |
| Tps1 | 6.1082 | 0.0068 | 2.167491087 |
| CG30339 | 1.087 | 0.0077 | 2.113509275 |

| | | | |
|---|---|---|---|
| Cpr73D | 1.1698 | 0.0079 | 2.102372909 |
| gskt | 2.0345 | 0.0082 | 2.086186148 |
| dgt3 | 1.1599 | 0.0084 | 2.075720714 |
| CG7470 | 1.3092 | 0.0089 | 2.050609993 |
| GstD7 | 2.3818 | 0.0091 | 2.040958608 |
| CG6067 | 1.6202 | 0.0099 | 2.004364805 |
| CG33127 | 1.112 | 0.01 | 2 |
| CG4835 | 5.4578 | 0.0117 | 1.931814138 |
| CG15695 | 3.4705 | 0.0119 | 1.924453039 |
| Jon99Ciii | 3.2062 | 0.0124 | 1.906578315 |
| CR45272 | 3.1296 | 0.0137 | 1.863279433 |
| CG30371 | 5.1978 | 0.0138 | 1.860120914 |
| PGRP-SC2 | 2.1279 | 0.0139 | 1.8569852 |
| CR45908 | 1.5726 | 0.0145 | 1.838631998 |
| CG9396 | 1.6802 | 0.0145 | 1.838631998 |
| CG34347 | 0.9676 | 0.0146 | 1.835647144 |
| Eip78C | 1.2406 | 0.0152 | 1.818156412 |
| CG33301 | 3.7144 | 0.0156 | 1.806875402 |
| fa2h | 3.137 | 0.0159 | 1.798602876 |
| CG11192 | 1.4458 | 0.016 | 1.795880017 |
| Eip75B | 0.9144 | 0.0161 | 1.793174124 |
| CG12780 | 1.2326 | 0.0172 | 1.764471553 |
| Mtp | 0.9393 | 0.0173 | 1.761953897 |
| CG42327 | 2.7127 | 0.0183 | 1.73754891 |
| sut4 | 5.153 | 0.0184 | 1.735182177 |
| lcs | 4.4828 | 0.0187 | 1.728158393 |
| Mdr50 | 1.7958 | 0.0211 | 1.675717545 |
| Gr8a | 5.0115 | 0.0219 | 1.659555885 |
| LysP | 4.9099 | 0.022 | 1.657577319 |
| CG11426 | 1.7413 | 0.0222 | 1.653647026 |
| CG6296 | 4.8824 | 0.023 | 1.638272164 |
| CG32054 | 2.0331 | 0.0232 | 1.634512015 |
| CR44429 | 0.938 | 0.0241 | 1.617982957 |
| CG12766 | 1.5593 | 0.0258 | 1.588380294 |
| CG12219 | 0.7943 | 0.0264 | 1.578396073 |
| CG8642 | 3.2986 | 0.0275 | 1.560667306 |
| CG5804 | 0.992 | 0.0279 | 1.554395797 |
| CG9498 | 2.4184 | 0.0279 | 1.554395797 |
| CR45045 | 2.4959 | 0.0294 | 1.53165267 |
| CR44868 | 0.9162 | 0.0296 | 1.528708289 |

| | | | |
|---|---|---|---|
| CG5254 | 0.7791 | 0.0297 | 1.527243551 |
| CG3739 | 1.673 | 0.0332 | 1.478861916 |
| CG33346 | 2.0919 | 0.0337 | 1.472370099 |
| aay | 0.993 | 0.0338 | 1.4710833 |
| CR45298 | 1.8549 | 0.034 | 1.468521083 |
| lin-28 | 0.7338 | 0.0353 | 1.452225295 |
| CG31300 | 1.5904 | 0.0356 | 1.448550002 |
| Nuf2 | 0.7842 | 0.0369 | 1.432973634 |
| upd2 | 0.8034 | 0.038 | 1.420216403 |
| CR45949 | 1.0705 | 0.038 | 1.420216403 |
| Amyrel | 1.6441 | 0.0392 | 1.406713933 |
| CG14526 | 1.5213 | 0.0401 | 1.396855627 |
| etaTry | 1.6679 | 0.0409 | 1.388276692 |
| CG15497 | 4.5702 | 0.0419 | 1.377785977 |
| Dtg | 0.648 | 0.0426 | 1.370590401 |
| CG15263 | 2.4167 | 0.0494 | 1.306273051 |
| CCHa1-R | 5.2994 | 0.0515 | 1.288192771 |
| CG2254 | 1.3734 | 0.0536 | 1.27083521 |

**Table 2.2c: list of sexually dimorphic hits in reference to Hudry et al,2016 Table S1**

| |
|---|
| alpha-Est7 |
| CG18180 |
| tobi |
| CG6283 |
| CG11155 |
| CG3739 |
| CG33346 |
| aay |
| CG31300 |
| CG13325 |
| Amyrel |
| CG14160 |
| CG11407 |
| CG11899 |
| CG17681 |
| RpL13A |
| CG12868 |
| CG6712 |
| fray |
| CG16833 |

| |
|---|
| Arc1 |
| CG8368 |
| CG4462 |
| CG15263 |
| CG16965 |
| CG42846 |
| Jon99Cii |
| Jon99Ci |
| kappaTry |
| CG33510 |
| CG8299 |
| CG42825 |
| Amy-d |
| CG8952 |
| CG32483 |
| CG34026 |
| CG3344 |
| CG18179 |
| CG10910 |
| ninaD |
| CAH2 |
| CG42714 |
| CG5506 |
| CG3699 |
| CG4363 |
| CG31104 |
| thetaTry |
| CG11878 |
| CG4053 |
| CG7470 |
| GstD7 |
| CG17839 |
| CG13360 |
| Ser8 |
| CG4835 |
| Jon99Ciii |
| CG9396 |
| CG6484 |
| CG33301 |
| Mal-A1 |

| |
|---|
| fa2h |
| CG11898 |
| CG12780 |
| Mal-A4 |
| CG31463 |
| CG6296 |
| CG32054 |
| CG4377 |
| Mdr49 |
| CG10659 |
| CG12766 |
| CG17192 |
| CG17633 |
| CG9498 |
| CG10912 |

**Table 2.2d: Pathway enrichment for hits differentially upregulated in 20HE males relative to control males**

| Pathway enrichment | p-value | Hits | Gene matches | Pathway ID |
|---|---|---|---|---|
| Starch and sucrose metabolism | 8.42E-07 | FBgn0000078,FBgn0002570,FBgn0020506,FBgn0027073,FBgn0027560,FBgn0033294,FBgn0261575 | 7 | 500 |
| Metabolism of lipids | 9.2643E-05 | FBgn0000568,FBgn0010241,FBgn0029994,FBgn0035476,FBgn0036381,FBgn0037166,FBgn0037786,FBgn0039470,FBgn0039471,FBgn0039472,FBgn0039474,FBgn0050502,FBgn0053177 | 13 | R-DME-556833 |
| Galactose metabolism | 0.00014491 | FBgn0002570,FBgn0033294,FBgn0035476,FBgn0261575 | 4 | 52 |
| Synthesis of PA | 0.00021659 | FBgn0037786,FBgn0039470,FBgn0039471,FBgn0039472,FBgn0039474 | 5 | R-DME-1483166 |
| Acyl chain remodelling of PS | 0.00027321 | FBgn0039470,FBgn0039471,FBgn0039472,FBgn0039474 | 4 | R-DME-1482801 |
| Glycerophospholipid biosynthesis | 0.00042991 | FBgn0036381,FBgn0037786,FBgn0039470,FBgn0039471,FBgn0039472,FBgn0039474 | 6 | R-DME-1483206 |
| Metabolic pathways | 0.00159037 | FBgn0000078,FBgn0002570,FBgn0015568,FBgn0015575,FBgn0020506,FBgn0023129,FBgn0027073,FBgn0033294,FBgn0035476,FBgn0037146,FBgn0037166,FBgn0037186,FBgn0037786,FBgn003 | 17 | 1100 |

| | | | | |
|---|---|---|---|---|
| | | 8070,FBgn0039596,FBgn0052220,FBgn0261575 | | |
| Phospholipid metabolism | 0.0017436 | FBgn0036381,FBgn0037786,FBgn0039470,FBgn0039471,FBgn0039472,FBgn0039474 | 6 | R-DME-1483257 |
| Metabolism | 0.00278954 | FBgn0000568,FBgn0010241,FBgn0023129,FBgn0027843,FBgn0029994,FBgn0034200,FBgn0035476,FBgn0036381,FBgn0037146,FBgn0037166,FBgn0037186,FBgn0037786,FBgn0037845,FBgn0039470,FBgn0039471,FBgn0039472,FBgn0039474,FBgn0040383,FBgn0050502,FBgn0053177 | 20 | R-DME-1430728 |
| Lysine catabolism | 0.00381016 | FBgn0036381,FBgn0040383 | 2 | R-DME-71064 |
| Neuroactive ligand-receptor interaction | 0.00429203 | FBgn0003863,FBgn0011554,FBgn0011555 | 3 | 4080 |
| SUMOylation of intracellular receptors | 0.00462862 | FBgn0000568,FBgn0004865 | 2 | R-DME-4090294 |
| Digestion | 0.00502788 | FBgn0000078,FBgn0020506,FBgn0037786 | 3 | R-DME-8935690 |
| Glycerolipid metabolism | 0.00767307 | FBgn0035476,FBgn0037166,FBgn0038070 | 3 | 561 |
| Digestion and absorption | 0.00817995 | FBgn0000078,FBgn0020506,FBgn0037786 | 3 | R-DME-8963743 |
| Digestion of dietary carbohydrate | 0.00862443 | FBgn0000078,FBgn0020506 | 2 | R-DME-189085 |
| Metabolism of amino acids and derivatives | 0.0094115 | FBgn0023129,FBgn0034200,FBgn0036381,FBgn0037146,FBgn0037186,FBgn0040383 | 6 | R-DME-71291 |
| Drug metabolism - other enzymes | 0.0158108 | FBgn0015568,FBgn0015575,FBgn0027073 | 3 | 983 |
| Nuclear Receptor transcription pathway | 0.01663373 | FBgn0000568,FBgn0004865 | 2 | R-DME-383280 |
| Transcriptional regulation of white adipocyte differentiation | 0.01896242 | FBgn0000568 | 1 | R-DME-381340 |

| | | | | |
|---|---|---|---|---|
| Cellular hexose transport | 0.02146927 | FBgn0028560,FBgn0034247 | 2 | R-DME-189200 |
| Glycine, serine and threonine metabolism | 0.02319595 | FBgn0023129,FBgn0037186 | 2 | 260 |
| Keratinization | 0.02319595 | FBgn0031533,FBgn0038070 | 2 | R-DME-6805567 |
| Formation of the cornified envelope | 0.02319595 | FBgn0031533,FBgn0038070 | 2 | R-DME-6809371 |
| Sphingolipid de novo biosynthesis | 0.02681444 | FBgn0037166,FBgn0050502 | 2 | R-DME-1660661 |
| Signaling by Retinoic Acid | 0.02681444 | FBgn0000568,FBgn0029994 | 2 | R-DME-5362517 |
| Transcriptional regulation of granulopoiesis | 0.03757247 | FBgn0000568 | 1 | R-DME-9616222 |
| Serine biosynthesis | 0.03757247 | FBgn0023129 | 1 | R-DME-977347 |
| Collagen degradation | 0.04674736 | FBgn0036381 | 1 | R-DME-1442490 |
| Polo-like kinase mediated events | 0.04674736 | FBgn0003525 | 1 | R-DME-156711 |
| Vitamin B1 (thiamin) metabolism | 0.04674736 | FBgn0037845 | 1 | R-DME-196819 |
| Formation of the activated receptor complex | 0.04674736 | FBgn0030904 | 1 | R-DME-209209 |
| Metabolism of steroids | 0.04929803 | FBgn0010241,FBgn0029994,FBgn0035476 | 3 | R-DME-8957322 |

**Table 2.2g: GO enrichment for hits differentially upregulated in 20HE males relative to control males**

| GO enrichment | p-value | Hits | Gene matches | GO ID |
|---|---|---|---|---|
| proteolysis | 3.502E-05 | FBgn0003356,FBgn0003357,FBgn0003358,FBgn0003863,FBgn0011554,FBgn0011555,FBgn0019928,FBgn0027578,FBgn0029828,FBgn0030688,FBgn0032144,FBgn0034052,FBgn0034507,FBgn0035154,FBgn0036023,FBgn0036024,FBgn0038482,FBgn0038702,FBgn0043471,FBgn0050371,FBgn0051266,FBgn0052483,FBgn0053127 | 23 | GO:0006508 |
| positive regulation of mitotic cell cycle, embryonic | 0.0005896 2 | FBgn0000826,FBgn0003525 | 2 | GO:0045977 |
| positive regulation of embryonic development | 0.0026803 3 | FBgn0000826,FBgn0003525 | 2 | GO:0040019 |
| lipid metabolic process | 0.0038512 1 | FBgn0000568,FBgn0031533,FBgn0037166,FBgn0038070,FBgn0038733,FBgn0039470,FBgn0039471,FBgn0039472,FBgn0039474,FBgn0040349,FBgn0050502,FBgn0053177 | 12 | GO:0006629 |
| carbohydrate metabolic process | 0.0045203 3 | FBgn0000078,FBgn0002570,FBgn0020506,FBgn0027560,FBgn0032387,FBgn0033294,FBgn0039596,FBgn0261575 | 8 | GO:0005975 |
| lipid catabolic process | 0.0063439 1 | FBgn0039470,FBgn0039471,FBgn0039472,FBgn0039474,FBgn0040349 | 5 | GO:0016042 |
| regulation of mitotic cell cycle, embryonic | 0.0083762 1 | FBgn0000826,FBgn0003525 | 2 | GO:0009794 |
| tetraterpenoid transport | 0.0100278 | FBgn0002939 | 1 | GO:0046866 |
| carotenoid transport | 0.0100278 | FBgn0002939 | 1 | GO:0046867 |
| trehalose metabolism in response to stress | 0.0100278 | FBgn0027560 | 1 | GO:0070413 |
| negative regulation of extrinsic apoptotic signaling pathway via death domain receptors | 0.0100278 | FBgn0033985 | 1 | GO:1902042 |
| response to cold | 0.0109026 1 | FBgn0031757,FBgn0034296 | 2 | GO:0009409 |
| glucose import | 0.0152361 7 | FBgn0028560,FBgn0034247 | 2 | GO:0046323 |
| glucose transmembrane transport | 0.0152361 7 | FBgn0028560,FBgn0034247 | 2 | GO:1904659 |
| hexose transmembrane transport | 0.0168195 6 | FBgn0028560,FBgn0034247 | 2 | GO:0008645 |
| monosaccharide | 0.016 | FBgn0028560,FBgn0034247 | 2 | GO:0015749 |

| | | | | |
|---|---|---|---|---|
| transmembrane transport | 81956 | | | |
| carbohydrate transmembrane transport | 0.0184698 | FBgn0028560,FBgn0034247 | 2 | GO:0034219 |
| isoprenoid transport | 0.0199603 | FBgn0002939 | 1 | GO:0046864 |
| terpenoid transport | 0.0199603 | FBgn0002939 | 1 | GO:0046865 |
| regulation of G2/MI transition of meiotic cell cycle | 0.0199603 | FBgn0003525 | 1 | GO:0110030 |
| positive regulation of G2/MI transition of meiotic cell cycle | 0.0199603 | FBgn0003525 | 1 | GO:0110032 |
| positive regulation of meiotic cell cycle phase transition | 0.0199603 | FBgn0003525 | 1 | GO:1901995 |
| regulation of extrinsic apoptotic signaling pathway via death domain receptors | 0.0199603 | FBgn0033985 | 1 | GO:1902041 |
| negative regulation of production of miRNAs involved in gene silencing by miRNA | 0.0199603 | FBgn0035626 | 1 | GO:1903799 |
| regulation of pre-miRNA processing | 0.0199603 | FBgn0035626 | 1 | GO:2000631 |
| negative regulation of pre-miRNA processing | 0.0199603 | FBgn0035626 | 1 | GO:2000632 |
| negative regulation of extrinsic apoptotic signaling pathway | 0.0199603 | FBgn0033985 | 1 | GO:2001237 |
| carbohydrate transport | 0.0219653 8 | FBgn0028560,FBgn0034247 | 2 | GO:0008643 |
| response to insecticide | 0.0238077 | FBgn0010241,FBgn0030108 | 2 | GO:0017085 |
| oligosaccharide biosynthetic process | 0.0257111 8 | FBgn0027560,FBgn0039596 | 2 | GO:0009312 |
| trehalose biosynthetic process | 0.0297856 7 | FBgn0027560 | 1 | GO:0005992 |
| proline biosynthetic | 0.0297856 | FBgn0037146 | 1 | GO:0006561 |

| | | | | |
|---|---|---|---|---|
| process | 7 | | | |
| L-serine biosynthetic process | 0.0297856 7 | FBgn0023129 | 1 | GO:0006564 |
| extrinsic apoptotic signaling pathway via death domain receptors | 0.0297856 7 | FBgn0033985 | 1 | GO:0008625 |
| negative regulation of posttranscriptional gene silencing | 0.0297856 7 | FBgn0035626 | 1 | GO:0060149 |
| negative regulation of gene silencing by miRNA | 0.0297856 7 | FBgn0035626 | 1 | GO:0060965 |
| response to L-canavanine | 0.0297856 7 | FBgn0030108 | 1 | GO:1901354 |
| regulation of production of miRNAs involved in gene silencing by miRNA | 0.0297856 7 | FBgn0035626 | 1 | GO:1903798 |
| lipid localization | 0.0306695 7 | FBgn0002939,FBgn0015575,FBgn0030904,FBgn0266369 | 4 | GO:0010876 |
| fatty acid metabolic process | 0.0349513 3 | FBgn0038733,FBgn0040349,FBgn0050502,FBgn0053177 | 4 | GO:0006631 |
| organic acid biosynthetic process | 0.0367566 4 | FBgn0023129,FBgn0037146,FBgn0038733,FBgn0053177 | 4 | GO:0016053 |
| carboxylic acid biosynthetic process | 0.0367566 4 | FBgn0023129,FBgn0037146,FBgn0038733,FBgn0053177 | 4 | GO:0046394 |
| prostaglandin biosynthetic process | 0.0395176 8 | FBgn0053177 | 1 | GO:0001516 |
| mitochondrial pyruvate transmembrane transport | 0.0395176 8 | FBgn0037714 | 1 | GO:0006850 |
| G2/MI transition of meiotic cell cycle | 0.0395176 8 | FBgn0003525 | 1 | GO:0008315 |
| positive regulation of G2/M transition of mitotic cell cycle | 0.0395176 8 | FBgn0003525 | 1 | GO:0010971 |
| disaccharide biosynthetic process | 0.0395176 8 | FBgn0027560 | 1 | GO:0046351 |
| icosanoid biosynthetic process | 0.0395176 8 | FBgn0053177 | 1 | GO:0046456 |
| prostanoid | 0.039 | FBgn0053177 | 1 | GO:0046457 |

| | | | | |
|---|---|---|---|---|
| biosynthetic process | 5176 8 | | | |
| regulation of meiotic cell cycle phase transition | 0.039 5176 8 | FBgn0003525 | 1 | GO:1901993 |
| positive regulation of cell cycle G2/M phase transition | 0.039 5176 8 | FBgn0003525 | 1 | GO:1902751 |
| regulation of extrinsic apoptotic signaling pathway | 0.039 5176 8 | FBgn0033985 | 1 | GO:2001236 |
| oligosaccharide metabolic process | 0.047 8151 2 | FBgn0027560,FBgn0039596 | 2 | GO:0009311 |
| dephosphorylation | 0.047 8215 5 | FBgn0003525,FBgn0023129,FBgn0037166 ,FBgn0037786,FBgn0259227 | 5 | GO:0016311 |
| L-serine metabolic process | 0.049 1530 3 | FBgn0023129 | 1 | GO:0006563 |
| prostanoid metabolic process | 0.049 1530 3 | FBgn0053177 | 1 | GO:0006692 |
| prostaglandin metabolic process | 0.049 1530 3 | FBgn0053177 | 1 | GO:0006693 |
| phototransduction, UV | 0.049 1530 3 | FBgn0002939 | 1 | GO:0007604 |
| detection of biotic stimulus | 0.049 1530 3 | FBgn0033301 | 1 | GO:0009595 |
| response to symbiont | 0.049 1530 3 | FBgn0283451 | 1 | GO:0009608 |
| xenobiotic transport | 0.049 1530 3 | FBgn0010241 | 1 | GO:0042908 |
| symmetric stem cell division | 0.049 1530 3 | FBgn0035626 | 1 | GO:0098724 |
| pyruvate transmembrane transport | 0.049 1530 3 | FBgn0037714 | 1 | GO:1901475 |

**Table 2.2e: GO enrichment for hits differentially upregulated in control males relative to 20HE males**

| GO enrichment | p-value | Hits | Gene matches | GO ID |
|---|---|---|---|---|
| ï»¿menaquinone metabolic process | 0.0053614 | FBgn0028375 | 1 | GO:0009233 |
| menaquinone biosynthetic process | 0.0053614 | FBgn0028375 | 1 | GO:0009234 |
| lactate oxidation | 0.0053614 | FBgn0061356 | 1 | GO:0019516 |
| proteoglycan | 0.0053614 | FBgn0038660 | 1 | GO:0030167 |

| | | | | |
|---|---|---|---|---|
| catabolic process | | | | |
| heparan sulfate proteoglycan catabolic process | 0.0053614 | FBgn0038660 | 1 | GO:0030200 |
| ubiquinone biosynthetic process via 3,4-dihydroxy-5-polyprenylbenzoate | 0.0053614 | FBgn0028375 | 1 | GO:0032194 |
| positive regulation of histone ubiquitination | 0.0053614 | FBgn0031420 | 1 | GO:0033184 |
| SAGA complex assembly | 0.0053614 | FBgn0031420 | 1 | GO:0036285 |
| cellular response to glucose starvation | 0.0053614 | FBgn0034422 | 1 | GO:0042149 |
| vitamin K biosynthetic process | 0.0053614 | FBgn0028375 | 1 | GO:0042371 |
| regulation of transcription by glucose | 0.0053614 | FBgn0034422 | 1 | GO:0046015 |
| mitochondrial seryl-tRNA aminoacylation | 0.0053614 | FBgn0021750 | 1 | GO:0070158 |
| vesicle-mediated intercellular transport | 0.0053614 | FBgn0033926 | 1 | GO:0110077 |
| positive regulation of histone H2B ubiquitination | 0.0053614 | FBgn0031420 | 1 | GO:2001168 |
| ncRNA metabolic process | 0.00734357 | FBgn0021750,FBgn0030406,FBgn0031227,FBgn0032408,FBgn0033507,FBgn0036629 | 6 | GO:0034660 |
| defense response to bacterium | 0.00827174 | FBgn0004240,FBgn0033980,FBgn0034210,FBgn0035813,FBgn0086358 | 5 | GO:0042742 |
| maturation of LSU-rRNA | 0.01044144 | FBgn0030406,FBgn0032408 | 2 | GO:0000470 |
| chromatin silencing at rDNA | 0.01069458 | FBgn0034422 | 1 | GO:0000183 |
| lactate metabolic process | 0.01069458 | FBgn0061356 | 1 | GO:0006089 |
| glutamyl-tRNA aminoacylation | 0.01069458 | FBgn0036629 | 1 | GO:0006424 |
| seryl-tRNA aminoacylation | 0.01069458 | FBgn0021750 | 1 | GO:0006434 |
| UDP-glucose transmembrane transport | 0.01069458 | FBgn0035449 | 1 | GO:0015786 |
| histone H2B ubiquitination | 0.01069458 | FBgn0031420 | 1 | GO:0033523 |
| fat-soluble vitamin biosynthetic process | 0.01069458 | FBgn0028375 | 1 | GO:0042362 |

| | | | | |
|---|---|---|---|---|
| vitamin K metabolic process | 0.01069458 | FBgn0028375 | 1 | GO:0042373 |
| snoRNA localization | 0.01069458 | FBgn0030406 | 1 | GO:0048254 |
| regulation of histone H2B ubiquitination | 0.01069458 | FBgn0031420 | 1 | GO:2001166 |
| response to bacterium | 0.01425925 | FBgn0004240,FBgn0033980,FBgn0034210,FBgn0035813,FBgn0086358 | 5 | GO:0009617 |
| sphingomyelin catabolic process | 0.01599969 | FBgn0037958 | 1 | GO:0006685 |
| fat-soluble vitamin metabolic process | 0.01599969 | FBgn0028375 | 1 | GO:0006775 |
| tRNA aminoacylation for protein translation | 0.01753328 | FBgn0021750,FBgn0036629 | 2 | GO:0006418 |
| tRNA aminoacylation | 0.01932178 | FBgn0021750,FBgn0036629 | 2 | GO:0043039 |
| amino acid activation | 0.02024368 | FBgn0021750,FBgn0036629 | 2 | GO:0043038 |
| peptidyl-pyroglutamic acid biosynthetic process, using glutaminyl-peptide cyclotransferase | 0.02127688 | FBgn0036999 | 1 | GO:0017186 |
| peptidyl-glutamine modification | 0.02127688 | FBgn0036999 | 1 | GO:0018199 |
| tRNA pseudouridine synthesis | 0.02127688 | FBgn0031227 | 1 | GO:0031119 |
| cardiolipin metabolic process | 0.02127688 | FBgn0067628 | 1 | GO:0032048 |
| cardiolipin biosynthetic process | 0.02127688 | FBgn0067628 | 1 | GO:0032049 |
| tRNA aminoacylation for mitochondrial protein translation | 0.02127688 | FBgn0021750 | 1 | GO:0070127 |
| defense response to Gram-negative bacterium | 0.02412875 | FBgn0004240,FBgn0033980,FBgn0035813 | 3 | GO:0050829 |
| glycoprotein catabolic process | 0.02652629 | FBgn0038660 | 1 | GO:0006516 |
| phosphatidylglycerol biosynthetic process | 0.02652629 | FBgn0067628 | 1 | GO:0006655 |

**Table 2.2f: Pathway enrichment for hits differentially upregulated in control males relative to 20HE males**

| Pathway enrichment | p-value | Hits | Gene matches | Pathway ID |
|---|---|---|---|---|
| Glycosaminoglyca | 0.00114 | FBgn0038660,FBgn0041629 | 2 | 531 |

| | | | | |
|---|---|---|---|---|
| n degradation | 4691 | | | |
| Metabolism of vitamin K | 0.006637902 | FBgn0028375 | 1 | R-DME-6806664 |
| Histidine catabolism | 0.006637902 | FBgn0061356 | 1 | R-DME-70921 |
| Kinesins | 0.006691187 | FBgn0038205,FBgn0052396 | 2 | R-DME-983189 |
| Glycosphingolipid biosynthesis - globo series | 0.013233932 | FBgn0041629 | 1 | 603 |
| Thiamine metabolism | 0.013233932 | FBgn0037046 | 1 | 730 |
| Aminoacyl-tRNA biosynthesis | 0.013304972 | FBgn0021750,FBgn0036629 | 2 | 970 |
| Glycosphingolipid biosynthesis - ganglio series | 0.01978834 | FBgn0041629 | 1 | 604 |
| Removal of aminoterminal propeptides from gamma-carboxylated proteins | 0.01978834 | FBgn0004598 | 1 | R-DME-159782 |
| Gamma-carboxylation, transport, and amino-terminal cleavage of proteins | 0.01978834 | FBgn0004598 | 1 | R-DME-159854 |
| Vitamin B1 (thiamin) metabolism | 0.01978834 | FBgn0037846 | 1 | R-DME-196819 |
| Transport of bile salts and organic acids, metal ions and amine compounds | 0.025511531 | FBgn0038312,FBgn0038752 | 2 | R-DME-425366 |
| Factors involved in megakaryocyte development and platelet production | 0.025511531 | FBgn0038205,FBgn0052396 | 2 | R-DME-983231 |
| COPI-dependent Golgi-to-ER retrograde traffic | 0.032128162 | FBgn0038205,FBgn0052396 | 2 | R-DME-6811434 |
| Activation of Matrix Metalloproteinases | 0.032773283 | FBgn0004598 | 1 | R-DME-1592389 |
| Zinc transporters | 0.032773283 | FBgn0038312 | 1 | R-DME-435354 |
| Zinc influx into cells by the SLC39 gene family | 0.032773283 | FBgn0038312 | 1 | R-DME-442380 |
| Lysosome | 0.036391051 | FBgn0038660,FBgn0041629 | 2 | 4142 |
| SIRT1 negatively regulates rRNA | 0.045594705 | FBgn0034422 | 1 | R-DME-427359 |

| | | | | |
|---|---|---|---|---|
| expression | | | | |
| Negative epigenetic regulation of rRNA expression | 0.045594705 | FBgn0034422 | 1 | R-DME-5250941 |
| Mismatch Repair | 0.045594705 | FBgn0015553 | 1 | R-DME-5358508 |
| Mismatch repair (MMR) directed by MSH2:MSH6 (MutSalpha) | 0.045594705 | FBgn0015553 | 1 | R-DME-5358565 |

**Table 2.3a: list of genes differentially upregulated in 20HE females relative to control males**

| list of hits>10 raw reads | log2FC edgeR | p-value edgeR | -log10(pvalue) |
|---|---|---|---|
| CR44748 | 2.1014 | 0.0007 | 3.15490196 |
| CR43405 | 2.4557 | 0.0008 | 3.096910013 |
| mAChR-C | 6.736 | 0.001 | 3 |
| nvd | 6.6191 | 0.0012 | 2.920818754 |
| CG33160 | 6.0842 | 0.0014 | 2.853871964 |
| CG11656 | 3.2921 | 0.0019 | 2.721246399 |
| CG13894 | 4.1039 | 0.002 | 2.698970004 |
| CG33928 | 6.0018 | 0.0021 | 2.677780705 |
| CG5361 | 7.8665 | 0.0023 | 2.638272164 |
| Tdc1 | 2.5141 | 0.0026 | 2.585026652 |
| CG44405 | 6.1148 | 0.0033 | 2.48148606 |
| CG10337 | 1.394 | 0.0037 | 2.431798276 |
| CG6405 | 2.3727 | 0.0044 | 2.356547324 |
| CR46249 | 2.5628 | 0.005 | 2.301029996 |
| CR44708 | 3.2341 | 0.006 | 2.22184875 |
| Gld | 3.7396 | 0.0067 | 2.173925197 |
| AhcyL2 | 2.7617 | 0.0067 | 2.173925197 |
| CG32055 | 1.7764 | 0.0075 | 2.124938737 |
| Cad96Ca | 2.112 | 0.008 | 2.096910013 |
| rha | 5.7705 | 0.0083 | 2.080921908 |
| snoRNA:Psi18S-1275 | 4.0322 | 0.0084 | 2.075720714 |
| CG6465 | 1.2105 | 0.0093 | 2.031517051 |
| CG14367 | 3.1864 | 0.0095 | 2.022276395 |
| CG31436 | 1.2678 | 0.01 | 2 |
| CG8492 | 5.4687 | 0.0109 | 1.962573502 |
| CG11407 | 5.4687 | 0.0109 | 1.962573502 |
| Arc1 | 1.0416 | 0.0121 | 1.91721463 |
| CG8252 | 2.9416 | 0.016 | 1.795880017 |
| yuri | 3.002 | 0.017 | 1.769551079 |

| | | | |
|---|---|---|---|
| Arc2 | 0.9961 | 0.0173 | 1.761953897 |
| snoRNA:Me28S-A2634b | 2.4565 | 0.0175 | 1.756961951 |
| ninaD | 4.7921 | 0.0177 | 1.752026734 |
| CR45166 | 3.5683 | 0.0192 | 1.716698771 |
| E(spl)mdelta-HLH | 5.5024 | 0.0202 | 1.694648631 |
| CG15865 | 2.8461 | 0.0215 | 1.66756154 |
| CG32040 | 1.5573 | 0.0217 | 1.663540266 |
| Tab2 | 2.1419 | 0.0218 | 1.661543506 |
| PGRP-LF | 1.233 | 0.022 | 1.657577319 |
| CG33258 | 4.0752 | 0.0221 | 1.655607726 |
| CR45824 | 3.3435 | 0.0225 | 1.647817482 |
| CG7387 | 2.6304 | 0.0238 | 1.623423043 |
| cact | 1.492 | 0.0248 | 1.605548319 |
| snoRNA:Me18S-U1356a | 2.2627 | 0.0253 | 1.596879479 |
| CG4676 | 3.3425 | 0.0256 | 1.591760035 |
| CR43832 | 2.3318 | 0.0275 | 1.560667306 |
| Pig1 | 2.0741 | 0.0277 | 1.557520231 |
| CG14740 | 2.9134 | 0.0297 | 1.527243551 |
| CG43101 | 1.8727 | 0.0298 | 1.525783736 |
| BBS8 | 5.5167 | 0.0302 | 1.519993057 |
| CG34401 | 1.5229 | 0.0313 | 1.504455662 |
| CG15818 | 3.6395 | 0.0314 | 1.503070352 |
| bip1 | 3.2594 | 0.0318 | 1.49757288 |
| CR43411 | 5.2125 | 0.0323 | 1.490797478 |
| CR32636 | 2.2817 | 0.0333 | 1.477555766 |
| CG32450 | 5.0165 | 0.034 | 1.468521083 |
| CG43925 | 5.0044 | 0.0352 | 1.453457337 |
| CG5282 | 5.0288 | 0.0363 | 1.440093375 |
| Efhc1.1 | 2.194 | 0.0365 | 1.437707136 |
| Grd | 1.8655 | 0.0376 | 1.424812155 |
| fig | 1.1609 | 0.0381 | 1.419075024 |
| CG8468 | 1.3221 | 0.0384 | 1.415668776 |
| Cbp53E | 2.6048 | 0.0391 | 1.407823243 |
| snoRNA:Me18S-U1356b | 2.4191 | 0.0402 | 1.395773947 |
| Cyp4p3 | 2.4069 | 0.0407 | 1.390405591 |
| Spn42Dd | 1.0623 | 0.0421 | 1.375717904 |
| Atac2 | 0.9165 | 0.0451 | 1.345823458 |
| CG44329 | 5.2286 | 0.0455 | 1.341988603 |
| CG18417 | 1.7246 | 0.0462 | 1.335358024 |

| | | | |
|---|---|---|---|
| CG31897 | 1.7993 | 0.047 | 1.327902142 |
| mthl14 | 0.7291 | 0.0516 | 1.287350298 |
| CG14856 | 1.7005 | 0.0517 | 1.286509457 |
| CR41620 | 4.8367 | 0.0525 | 1.279840697 |
| CR46093 | 1.1195 | 0.0526 | 1.279014256 |
| CG4424 | 1.045 | 0.0532 | 1.274088368 |
| Dcp-1 | 0.9085 | 0.0534 | 1.272458743 |
| AOX2 | 3.9142 | 0.0541 | 1.266802735 |

**Table 2.3b: list of genes differentially upregulated in control females relative to 20HE females**

| Gene name | log2FC edgeR | p-value edgeR | -log10(pvalue) |
|---|---|---|---|
| CG18180 | -4.8605 | 6.61E-20 | 19.17979854 |
| tobi | -5.3313 | 8.83E-10 | 9.054039296 |
| CG18179 | -5.1045 | 4.87E-08 | 7.312471039 |
| CG43055 | -4.4978 | 2.39E-07 | 6.621602099 |
| PGRP-SC2 | -3.8534 | 2.89E-07 | 6.539102157 |
| Amy-d | -2.3118 | 3.66E-07 | 6.436518915 |
| w | -1.9389 | 8.10E-06 | 5.091514981 |
| Jon66Ci | -4.0409 | 1.03E-05 | 4.987162775 |
| CG33109 | -8.0444 | 2.33E-05 | 4.632644079 |
| Jon25Bi | -2.0005 | 2.81E-05 | 4.55129368 |
| CG17633 | -4.1914 | 2.85E-05 | 4.54515514 |
| nerfin-1 | -4.0555 | 3.55E-05 | 4.449771647 |
| CG3739 | -2.5789 | 3.81E-05 | 4.419075024 |
| Jon25Biii | -3.6153 | 4.14E-05 | 4.382999659 |
| Jon65Aiv | -1.4887 | 4.96E-05 | 4.304518324 |
| CG8299 | -4.8541 | 5.47E-05 | 4.262012674 |
| CG6484 | -2.1864 | 7.19E-05 | 4.14327111 |
| Jon65Aiii | -1.461 | 8.74E-05 | 4.058488567 |
| CG18404 | -4.1627 | 0.0001 | 4 |
| CG45080 | -9.0884 | 0.0001 | 4 |
| CG17192 | -1.4986 | 0.0002 | 3.698970004 |
| alphaTry | -1.4007 | 0.0002 | 3.698970004 |
| CG3906 | -4.0425 | 0.0002 | 3.698970004 |
| Cyp28a5 | -3.1808 | 0.0002 | 3.698970004 |
| CG15630 | -6.7813 | 0.0002 | 3.698970004 |
| CG31104 | -2.9523 | 0.0003 | 3.522878745 |
| Jon65Aii | -4.1788 | 0.0003 | 3.522878745 |
| CG5107 | -1.7528 | 0.0004 | 3.397940009 |
| Jon99Ci | -2.0447 | 0.0004 | 3.397940009 |
| CG6067 | -2.4944 | 0.0004 | 3.397940009 |

| | | | |
|---|---|---|---|
| lcs | -9.2652 | 0.0004 | 3.397940009 |
| Jon99Cii | -1.9279 | 0.0005 | 3.301029996 |
| CG10910 | -2.4245 | 0.0005 | 3.301029996 |
| Jon99Fi | -3.8571 | 0.0005 | 3.301029996 |
| CG8834 | -1.791 | 0.0006 | 3.22184875 |
| CG13813 | -3.5184 | 0.0006 | 3.22184875 |
| CG9896 | -2.3041 | 0.0007 | 3.15490196 |
| CG12374 | -1.6431 | 0.0008 | 3.096910013 |
| stv | -1.9563 | 0.0008 | 3.096910013 |
| CG11878 | -2.1455 | 0.0009 | 3.045757491 |
| CG7916 | -4.9286 | 0.0009 | 3.045757491 |
| CG8745 | -2.3306 | 0.001 | 3 |
| CG33346 | -2.516 | 0.0011 | 2.958607315 |
| CG10869 | -3.8835 | 0.0013 | 2.886056648 |
| CG7567 | -6.3309 | 0.0014 | 2.853871964 |
| CG10659 | -2.3237 | 0.0014 | 2.853871964 |
| CG18577 | -2.0732 | 0.0015 | 2.823908741 |
| alpha-Est8 | -3.1631 | 0.0015 | 2.823908741 |
| Jon99Fii | -3.6303 | 0.0015 | 2.823908741 |
| Lrpprc2 | -1.3609 | 0.0016 | 2.795880017 |
| CG4329 | -1.907 | 0.0017 | 2.769551079 |
| CG31041 | -3.2548 | 0.0019 | 2.721246399 |
| mag | -2.6956 | 0.0022 | 2.657577319 |
| Meltrin | -1.6346 | 0.0023 | 2.638272164 |
| Jon66Cii | -4.9687 | 0.0023 | 2.638272164 |
| CG6295 | -1.253 | 0.0024 | 2.619788758 |
| CG3699 | -2.2543 | 0.0024 | 2.619788758 |
| CG3344 | -2.4773 | 0.0026 | 2.585026652 |
| CG16965 | -2.6821 | 0.0026 | 2.585026652 |
| CG3868 | -1.8129 | 0.0027 | 2.568636236 |
| Ag5r2 | -3.3454 | 0.0029 | 2.537602002 |
| CG10911 | -1.1594 | 0.0033 | 2.48148606 |
| CG34345 | -6.0006 | 0.0036 | 2.443697499 |
| Toll-7 | -2.3863 | 0.0037 | 2.431798276 |
| CG5770 | -3.2293 | 0.0039 | 2.408935393 |
| Hsp70Bbb | -1.3497 | 0.0043 | 2.366531544 |
| Muc68E | -2.1028 | 0.0043 | 2.366531544 |
| CG13315 | -1.9901 | 0.0044 | 2.356547324 |
| CG42397 | -2.2297 | 0.0052 | 2.283996656 |
| CG11912 | -4.2693 | 0.0052 | 2.283996656 |

| | | | |
|---|---|---|---|
| CG14780 | -2.7606 | 0.0055 | 2.259637311 |
| CG10912 | -1.4752 | 0.0056 | 2.251811973 |
| CG14688 | -5.7389 | 0.0061 | 2.214670165 |
| epsilonTry | -1.2405 | 0.0064 | 2.193820026 |
| Mur18B | -3.8614 | 0.0068 | 2.167491087 |
| Mal-A3 | -3.105 | 0.0072 | 2.142667504 |
| Listericin | -2.8063 | 0.0077 | 2.113509275 |
| CG6454 | -2.7844 | 0.0077 | 2.113509275 |
| CG6839 | -3.4208 | 0.0078 | 2.107905397 |
| CG1946 | -1.7025 | 0.0081 | 2.091514981 |
| Gr93b | -5.6851 | 0.009 | 2.045757491 |
| CG9396 | -1.4788 | 0.0093 | 2.031517051 |
| CG7024 | -3.3823 | 0.0096 | 2.017728767 |
| CG7091 | -2.566 | 0.01 | 2 |
| CG15605 | -2.3932 | 0.0106 | 1.974694135 |
| CG2652 | -5.5333 | 0.0107 | 1.970616222 |
| LysP | -6.6646 | 0.0119 | 1.924453039 |
| Ing3 | -1.2343 | 0.0119 | 1.924453039 |
| CG42714 | -1.9435 | 0.0119 | 1.924453039 |
| Cyp28d1 | -1.7643 | 0.0124 | 1.906578315 |
| CG13324 | -2.686 | 0.0125 | 1.903089987 |
| CG31077 | -6.4862 | 0.0128 | 1.89279003 |
| CG5892 | -6.6007 | 0.0128 | 1.89279003 |
| Prx2540-1 | -2.1171 | 0.0129 | 1.88941029 |
| CG42826 | -2.733 | 0.0136 | 1.866461092 |
| Jon99Ciii | -2.0618 | 0.0139 | 1.8569852 |
| CR44295 | -2.1387 | 0.0145 | 1.838631998 |
| CG5639 | -5.8025 | 0.0146 | 1.835647144 |
| CG31785 | -1.4184 | 0.0148 | 1.829738285 |
| CG4563 | -1.5862 | 0.0156 | 1.806875402 |
| CG9903 | -1.7253 | 0.0162 | 1.790484985 |
| CG34220 | -1.378 | 0.0171 | 1.76700389 |
| GstE9 | -1.1892 | 0.0172 | 1.764471553 |
| CG43207 | -1.9199 | 0.0172 | 1.764471553 |
| CG30357 | -1.2529 | 0.0178 | 1.749579998 |
| CR45921 | -3.2092 | 0.0184 | 1.735182177 |
| CG30371 | -6.3129 | 0.0188 | 1.725842151 |
| CG10725 | -5.4188 | 0.0194 | 1.71219827 |
| CG11671 | -0.9715 | 0.0196 | 1.707743929 |
| CG42724 | -1.4053 | 0.0198 | 1.70333481 |

| | | | |
|---|---|---|---|
| Mal-A1 | -1.2821 | 0.0199 | 1.701146924 |
| CG10505 | -2.1447 | 0.0199 | 1.701146924 |
| CDC45L | -1.0214 | 0.02 | 1.698970004 |
| CG12896 | -2.0809 | 0.0214 | 1.669586227 |
| Gr64f | -3.5044 | 0.022 | 1.657577319 |
| lectin-24A | -3.955 | 0.0222 | 1.653647026 |
| CG10472 | -1.9923 | 0.0222 | 1.653647026 |
| Inx7 | -1.2924 | 0.0227 | 1.643974143 |
| CG5958 | -1.4071 | 0.023 | 1.638272164 |
| prtp | -2.7135 | 0.0234 | 1.630784143 |
| CG34431 | -1.6441 | 0.0242 | 1.616184634 |
| Sytbeta | -5.5891 | 0.0244 | 1.612610174 |
| CR45962 | -1.169 | 0.0246 | 1.609064893 |
| Pebp1 | -0.8804 | 0.0249 | 1.603800653 |
| CG4267 | -1.7522 | 0.0259 | 1.586700236 |
| lectin-46Cb | -1.7195 | 0.0284 | 1.54668166 |
| CG5767 | -1.758 | 0.0288 | 1.540607512 |
| CG4734 | -1.0377 | 0.0295 | 1.530177984 |
| CheB42b | -3.3329 | 0.0301 | 1.521433504 |
| CG31265 | -3.8124 | 0.0305 | 1.515700161 |
| CG8665 | -2.2354 | 0.0306 | 1.514278574 |
| CG11029 | -1.5351 | 0.0313 | 1.504455662 |
| CR45272 | -3.3745 | 0.0314 | 1.503070352 |
| CG2681 | -1.2706 | 0.0317 | 1.498940738 |
| Trxr-1 | -1.8192 | 0.0318 | 1.49757288 |
| CG13074 | -2.8025 | 0.0325 | 1.488116639 |
| Hsp70Bc | -0.8509 | 0.0327 | 1.485452247 |
| CR43904 | -2.2765 | 0.0329 | 1.482804102 |
| isoQC | -1.5416 | 0.0329 | 1.482804102 |
| Npc1b | -3.1448 | 0.0331 | 1.480172006 |
| AOX1 | -0.8752 | 0.0335 | 1.474955193 |
| CG5010 | -1.5782 | 0.0336 | 1.473660723 |
| CG8258 | -0.8805 | 0.0353 | 1.452225295 |
| E(spl)m6-BFM | -1.0904 | 0.0354 | 1.450996738 |
| bdl | -1.7942 | 0.0358 | 1.446116973 |
| yip7 | -0.814 | 0.0359 | 1.444905551 |
| CG44836 | -3.8514 | 0.0374 | 1.427128398 |
| Pask | -1.4019 | 0.0379 | 1.42136079 |
| Lim1 | -2.0041 | 0.0401 | 1.396855627 |
| CG8952 | -1.0905 | 0.0406 | 1.391473966 |

| | | | |
|---|---|---|---|
| Actbeta | -2.7354 | 0.0407 | 1.390405591 |
| Est-Q | -1.2619 | 0.0412 | 1.385102784 |
| CR44299 | -1.3272 | 0.0418 | 1.378823718 |
| CG9663 | -0.9388 | 0.0427 | 1.369572125 |
| CG31848 | -1.6486 | 0.043 | 1.366531544 |
| CG8642 | -2.4511 | 0.0432 | 1.364516253 |
| CG15439 | -0.9319 | 0.0433 | 1.363512104 |
| CR46214 | -5.5692 | 0.0434 | 1.36251027 |
| CG5157 | -1.9982 | 0.0441 | 1.355561411 |
| Ptpmeg | -2.4651 | 0.0456 | 1.341035157 |
| CG17930 | -1.3686 | 0.0458 | 1.339134522 |
| mus81 | -1.6181 | 0.0458 | 1.339134522 |
| phyl | -1.5518 | 0.0463 | 1.334419009 |
| CG7785 | -0.8683 | 0.0467 | 1.330683119 |
| CCKLR-17D3 | -1.9264 | 0.0469 | 1.328827157 |
| Nurf-38 | -2.0135 | 0.0474 | 1.324221658 |
| CG16749 | -1.4458 | 0.049 | 1.30980392 |
| CR44149 | -2.0322 | 0.0496 | 1.304518324 |
| Vha100-4 | -1.5016 | 0.0501 | 1.300162274 |
| CG7379 | -0.7894 | 0.0506 | 1.295849483 |
| CG15414 | -1.0432 | 0.051 | 1.292429824 |
| CG10592 | -1.0868 | 0.0522 | 1.282329497 |
| CG14262 | -3.2894 | 0.0528 | 1.277366077 |
| CG7458 | -0.9456 | 0.0539 | 1.268411235 |

**Table 2.3c: list of sexually dimorphic hits that are regulated by 20HE feeding in females in reference to Hudry et al,2016 Table S1**

| |
|---|
| Amy-d |
| Arc1 |
| CG10659 |
| CG10910 |
| CG10912 |
| CG11407 |
| CG11878 |
| CG16965 |
| CG17192 |
| CG17633 |
| CG18179 |
| CG18180 |
| CG31104 |

| |
|---|
| CG33346 |
| CG3344 |
| CG3699 |
| CG3739 |
| CG42714 |
| CG6484 |
| CG8299 |
| CG8952 |
| CG9396 |
| Jon99Ci |
| Jon99Cii |
| Jon99Ciii |
| Mal-A1 |
| ninaD |
| tobi |
| Ag5r2 |
| alpha-Est8 |
| Arc2 |
| cact |
| CG10505 |
| CG11912 |
| CG12374 |
| CG13315 |
| CG13324 |
| CG15818 |
| CG16749 |
| CG18577 |
| CG1946 |
| CG31041 |
| CG33258 |
| CG5157 |
| CG5770 |
| CG5958 |
| CG6465 |
| CG7916 |
| CG8258 |
| CG8834 |
| CG9663 |
| CG9896 |
| epsilonTry |

| |
|---|
| GstE9 |
| Jon25Bi |
| Jon25Biii |
| Jon65Aii |
| Jon65Aiii |
| Jon66Ci |
| Jon66Cii |
| Jon99Fi |
| Jon99Fii |
| mag |
| Mal-A3 |
| mthl14 |
| Prx2540-1 |
| Prx2540-2 |
| Ptpmeg |
| Sytbeta |
| w |
| yip7 |

**Table 2.3d:Pathway enrichment for hits differentially upregulated in 20HE females relative to control females**

| Pathway enrichment | p-value | Hits | Gene matches | Pathway ID |
|---|---|---|---|---|
| ï»¿Aflatoxin activation and detoxification | 0.00020088 | FBgn0036986,FBgn0037818 | 2 | R-DME-5423646 |
| Biological oxidations | 0.00311735 | FBgn0033397,FBgn0036986, FBgn0037818 | 3 | R-DME-211859 |
| Synthesis of Leukotrienes (LT) and Eoxins (EX) | 0.01191451 | FBgn0036986 | 1 | R-DME-2142691 |
| Bicarbonate transporters | 0.01782136 | FBgn0015011 | 1 | R-DME-425381 |
| TAK1 activates NFkB by phosphorylation and activation of IKKs complex | 0.01782136 | FBgn0000250 | 1 | R-DME-445989 |
| Insect hormone biosynthesis | 0.02369485 | FBgn0287185 | 1 | 981 |
| BBSome-mediated cargo-targeting to cilium | 0.02369485 | FBgn0031255 | 1 | R-DME-5620922 |

| | | | | |
|---|---|---|---|---|
| Regulation of KIT signaling | 0.02953516 | FBgn0022800 | 1 | R-DME-1433559 |
| DL and DIF homodimers bind to TUB and phosphorylated PLL in the TL receptor 'signalling complex' | 0.02953516 | FBgn0000250 | 1 | R-DME-214842 |
| DL and DIF homodimers complexed with CACT are all phosphorylated in the TL receptor 'signalling complex' | 0.02953516 | FBgn0000250 | 1 | R-DME-214844 |
| Phosphorylated CACT, DL and DIF homodimers dissociate from the TL receptor 'signalling complex' | 0.02953516 | FBgn0000250 | 1 | R-DME-214869 |
| Amine ligand-binding receptors | 0.03534247 | FBgn0029909 | 1 | R-DME-375280 |
| p75NTR signals via NF-kB | 0.04111694 | FBgn0000250 | 1 | R-DME-193639 |
| NF-kB is activated and signals survival | 0.04111694 | FBgn0000250 | 1 | R-DME-209560 |
| Signaling by SCF-KIT | 0.04685875 | FBgn0022800 | 1 | R-DME-1433557 |
| Activation of the IkappaB kinase complex, KEY:IRD5 dimer:KEY | 0.04685875 | FBgn0086358 | 1 | R-DME-209447 |

**Table 2.3e: GO enrichment for hits differentially upregulated in control females relative to 20HE males**

| GO enrichment | p-value | Hits | Gene matches | GO ID |
|---|---|---|---|---|
| ï»¿proteolysis | 4.51E-09 | FBgn0003356,FBgn0003357,FBgn0003358,FBgn0003863,FBgn0010425,FBgn0013725,FBgn0020906,FBgn0024997,FBgn0025383,FBgn0029828,FBgn0 | 33 | GO:0006508 |

| | | | | |
|---|---|---|---|---|
| | | 030688,FBgn0031248,FBgn0031653,FBgn0032144,FBgn0033774,FBgn0034052,FBgn0035154,FBgn0035665,FBgn0035666,FBgn0035670,FBgn0035886,FBgn0035887,FBgn0036023,FBgn0036024,FBgn0037678,FBgn0038702,FBgn0039777,FBgn0039778,FBgn0040060,FBgn0050371,FBgn0051265,FBgn0250815,FBgn0265140 | | |
| cell redox homeostasis | 0.0002664 | FBgn0020653,FBgn0030329,FBgn0033518,FBgn0033520,FBgn0033521 | 5 | GO:0045454 |
| aminoglycan metabolic process | 0.00175486 | FBgn0030999,FBgn0036362,FBgn0043575,FBgn0051077,FBgn0053265,FBgn0085249,FBgn0259748 | 7 | GO:0006022 |
| cofactor catabolic process | 0.00183107 | FBgn0032945,FBgn0033518,FBgn0033520 | 3 | GO:0051187 |
| chitin metabolic process | 0.0030558 | FBgn0030999,FBgn0036362,FBgn0051077,FBgn0053265,FBgn0085249,FBgn0259748 | 6 | GO:0006030 |
| glucosamine-containing compound metabolic process | 0.00451867 | FBgn0030999,FBgn0036362,FBgn0051077,FBgn0053265,FBgn0085249,FBgn0259748 | 6 | GO:1901071 |
| heat shock-mediated polytene chromosome puffing | 0.00472029 | FBgn0013279,FBgn0051354 | 2 | GO:0035080 |
| drug metabolic process | 0.0051005 | FBgn0030999,FBgn0033518,FBgn0033520,FBgn0036362,FBgn0051077,FBgn0053265,FBgn0085249,FBgn0259748,FBgn0267408 | 9 | GO:0017144 |
| amino sugar metabolic process | 0.00522897 | FBgn0030999,FBgn0036362,FBgn0051077,FBgn0053265,FBgn0085249,FBgn0259748 | 6 | GO:0006040 |
| polytene chromosome puffing | 0.00585494 | FBgn0013279,FBgn0051354 | 2 | GO:0035079 |
| hydrogen peroxide catabolic process | 0.00585494 | FBgn0033518,FBgn0033520 | 2 | GO:0042744 |
| double-strand break repair via break-induced replication | 0.00845576 | FBgn0026143,FBgn0040347 | 2 | GO:0000727 |
| hydrogen peroxide metabolic process | 0.00991647 | FBgn0033518,FBgn0033520 | 2 | GO:0042743 |
| guanine nucleotide transport | 0.01181493 | FBgn0003996 | 1 | GO:0001408 |
| innate immune response activating cell | 0.01181493 | FBgn0034476 | 1 | GO:0002220 |

| | | | | |
|---|---|---|---|---|
| surface receptor signaling pathway | | | | |
| immune response-activating cell surface receptor signaling pathway | 0.01181493 | FBgn0034476 | 1 | GO:0002429 |
| cell surface pattern recognition receptor signaling pathway | 0.01181493 | FBgn0034476 | 1 | GO:0002752 |
| 10-formyltetrahydrofolate catabolic process | 0.01181493 | FBgn0032945 | 1 | GO:0009258 |
| folic acid-containing compound catabolic process | 0.01181493 | FBgn0032945 | 1 | GO:0009397 |
| intestinal cholesterol absorption | 0.01181493 | FBgn0261675 | 1 | GO:0030299 |
| negative regulation of epithelial cell differentiation | 0.01181493 | FBgn0261985 | 1 | GO:0030857 |
| pteridine-containing compound catabolic process | 0.01181493 | FBgn0032945 | 1 | GO:0042560 |
| pyridoxal metabolic process | 0.01181493 | FBgn0267408 | 1 | GO:0042817 |
| lipid digestion | 0.01181493 | FBgn0261675 | 1 | GO:0044241 |
| negative regulation of glycogen biosynthetic process | 0.01181493 | FBgn0034950 | 1 | GO:0045719 |
| intestinal absorption | 0.01181493 | FBgn0261675 | 1 | GO:0050892 |
| histamine uptake | 0.01181493 | FBgn0003996 | 1 | GO:0051615 |
| cyclic nucleotide transport | 0.01181493 | FBgn0003996 | 1 | GO:0070729 |

| | | | | |
|---|---|---|---|---|
| cGMP transport | 0.01181493 | FBgn0003996 | 1 | GO:0070731 |
| intestinal lipid absorption | 0.01181493 | FBgn0261675 | 1 | GO:0098856 |
| mitotic DNA replication preinitiation complex assembly | 0.01181493 | FBgn0026143 | 1 | GO:1902977 |
| negative regulation of border follicle cell migration | 0.01181493 | FBgn0261985 | 1 | GO:1903687 |
| amine transport | 0.01314524 | FBgn0003996,FBgn0261090 | 2 | GO:0015837 |
| antibiotic catabolic process | 0.01314524 | FBgn0033518,FBgn0033520 | 2 | GO:0017001 |
| apoptotic DNA fragmentation | 0.01871844 | FBgn0036831,FBgn0053346 | 2 | GO:0006309 |
| cellular component disassembly involved in execution phase of apoptosis | 0.01871844 | FBgn0036831,FBgn0053346 | 2 | GO:0006921 |
| apoptotic nuclear changes | 0.01871844 | FBgn0036831,FBgn0053346 | 2 | GO:0030262 |
| defense response to virus | 0.01997379 | FBgn0033593,FBgn0034476,FBgn0037562 | 3 | GO:0051607 |
| organonitrogen compound metabolic process | 0.02151901 | FBgn0003356,FBgn0003357,FBgn0003358,FBgn0003863,FBgn0003996,FBgn0010425,FBgn0013725,FBgn0020906,FBgn0024913,FBgn0024997,FBgn0025383,FBgn0027794,FBgn0029722,FBgn0029828,FBgn0030688,FBgn0030945,FBgn0030999,FBgn0031248,FBgn0031653,FBgn0032144,FBgn0032945,FBgn0033774,FBgn0034052,FBgn0034950,FBgn0035154,FBgn0035665,FBgn0035666,FBgn0035670,FBgn0035886,FBgn0035887,FBgn0036023,FBgn0036024,FBgn0036362,FBgn0036999,FBgn0037678,FBgn0038702,FBgn0039777,FBgn0039778,FBgn0040060,FBgn0043575,FBgn0050371,FBgn0051077,FBgn0051265,FBgn0053265,FBgn0063491,FBgn0085249,FBgn0085374,FBgn0086708,FBgn0250815,FBgn0259748,FBgn0261985,FBgn0265140,FBgn0267408 | 53 | GO:1901564 |
| regulation of glycogen biosynthetic process | 0.02349143 | FBgn0034950 | 1 | GO:0005979 |
| R1/R6 cell fate commitment | 0.02349143 | FBgn0013725 | 1 | GO:0007462 |

| | | | | |
|---|---|---|---|---|
| coenzyme catabolic process | 0.02349143 | FBgn0032945 | 1 | GO:0009109 |
| negative regulation of epithelial cell migration | 0.02349143 | FBgn0261985 | 1 | GO:0010633 |
| regulation of glucan biosynthetic process | 0.02349143 | FBgn0034950 | 1 | GO:0010962 |
| regulation of polysaccharide biosynthetic process | 0.02349143 | FBgn0034950 | 1 | GO:0032885 |
| induction of bacterial agglutination | 0.02349143 | FBgn0262357 | 1 | GO:0043152 |
| regulation of lipoprotein metabolic process | 0.02349143 | FBgn0086708 | 1 | GO:0050746 |
| positive regulation of lipoprotein metabolic process | 0.02349143 | FBgn0086708 | 1 | GO:0050747 |
| negative regulation of glycogen metabolic process | 0.02349143 | FBgn0034950 | 1 | GO:0070874 |
| DNA replication preinitiation complex assembly | 0.02349143 | FBgn0026143 | 1 | GO:0071163 |
| regulation of protein lipidation | 0.02349143 | FBgn0086708 | 1 | GO:1903059 |
| positive regulation of protein lipidation | 0.02349143 | FBgn0086708 | 1 | GO:1903061 |
| regulation of apoptotic cell clearance | 0.02349143 | FBgn0030329 | 1 | GO:2000425 |
| positive regulation of apoptotic cell clearance | 0.02349143 | FBgn0030329 | 1 | GO:2000427 |
| DNA catabolic process, endonucleolytic | 0.02510873 | FBgn0036831,FBgn0053346 | 2 | GO:0000737 |

| | | | | |
|---|---|---|---|---|
| ammonium transport | 0.02510873 | FBgn0003996,FBgn0261090 | 2 | GO:0015696 |
| response to virus | 0.02832579 | FBgn0033593,FBgn0034476,FBgn0037562 | 3 | GO:0009615 |
| DNA catabolic process | 0.03225301 | FBgn0036831,FBgn0053346 | 2 | GO:0006308 |
| 10-formyltetrahydrofolate metabolic process | 0.03503111 | FBgn0032945 | 1 | GO:0009256 |
| negative regulation of cellular carbohydrate metabolic process | 0.03503111 | FBgn0034950 | 1 | GO:0010677 |
| regulation of chromatin silencing at telomere | 0.03503111 | FBgn0026143 | 1 | GO:0031938 |
| negative regulation of carbohydrate metabolic process | 0.03503111 | FBgn0034950 | 1 | GO:0045912 |
| histamine transport | 0.03503111 | FBgn0003996 | 1 | GO:0051608 |
| regulation of mitochondrial transcription | 0.03503111 | FBgn0027794 | 1 | GO:1903108 |
| response to hypoxia | 0.03674316 | FBgn0013279,FBgn0020653,FBgn0051354 | 3 | GO:0001666 |
| antibiotic metabolic process | 0.03740512 | FBgn0033518,FBgn0033520 | 2 | GO:0016999 |
| cofactor metabolic process | 0.03959033 | FBgn0029722,FBgn0032945,FBgn0033518,FBgn0033520,FBgn0063491,FBgn0267408 | 6 | GO:0051186 |
| organic hydroxy compound transport | 0.04009154 | FBgn0261090,FBgn0261675 | 2 | GO:0015850 |
| regulation of generation of precursor metabolites and energy | 0.0428488 | FBgn0027794,FBgn0034950 | 2 | GO:0043467 |
| response to decreased oxygen levels | 0.0446291 | FBgn0013279,FBgn0020653,FBgn0051354 | 3 | GO:0036293 |
| 'de novo' posttranslational protein folding | 0.04567487 | FBgn0013279,FBgn0051354 | 2 | GO:0051084 |

| | | | | |
|---|---|---|---|---|
| chaperone cofactor-dependent protein refolding | 0.04567487 | FBgn0013279,FBgn0051354 | 2 | GO:0051085 |
| immune response-regulating cell surface receptor signaling pathway | 0.04643555 | FBgn0034476 | 1 | GO:0002768 |
| acetyl-CoA biosynthetic process from pyruvate | 0.04643555 | FBgn0029722 | 1 | GO:0006086 |
| mitochondrial pyruvate transmembrane transport | 0.04643555 | FBgn0037714 | 1 | GO:0006850 |
| eye pigment precursor transport | 0.04643555 | FBgn0003996 | 1 | GO:0006856 |
| peptidyl-pyroglutamic acid biosynthetic process, using glutaminyl-peptide cyclotransferase | 0.04643555 | FBgn0036999 | 1 | GO:0017186 |
| peptidyl-glutamine modification | 0.04643555 | FBgn0036999 | 1 | GO:0018199 |
| regulation of carbohydrate biosynthetic process | 0.04643555 | FBgn0034950 | 1 | GO:0043255 |
| regulation of mitochondrial mRNA stability | 0.04643555 | FBgn0027794 | 1 | GO:0044528 |
| negative regulation of oogenesis | 0.04643555 | FBgn0261985 | 1 | GO:1905880 |
| metabolic process | 0.04784699 | FBgn0000078,FBgn0002570,FBgn0002571,FBgn0003356,FBgn0003357,FBgn0003358,FBgn0003863,FBgn0003996,FBgn0010425,FBgn0013725,FBgn0016687,FBgn0020653,FBgn0020906,FBgn0024913,FBgn0024997,FBgn0025383,FBgn0025838,FBgn0026143,FBgn0026411,FBgn0027794,FBgn0028940,FBgn0028999,FBgn0029722,FBgn0029828,FBgn0030688,FBgn0030945,FBgn0030999,FBgn0031248,FBgn0031653,FBgn0031689,FBgn0031735,FBgn0032144,FBgn0032387,FBgn0032945,FBgn0033518,FBgn0033520,FBgn0033521,FBgn0033733,FBgn0 | 84 | GO:0008152 |

| | | | | |
|---|---|---|---|---|
| | | 033774,FBgn0034052,FBgn0034476,FBgn0034950,FBgn0035006,FBgn0035154,FBgn0035619,FBgn0035665,FBgn0035666,FBgn0035670,FBgn0035886,FBgn0035887,FBgn0036023,FBgn0036024,FBgn0036362,FBgn0036831,FBgn0036996,FBgn0036999,FBgn0037678,FBgn0038546,FBgn0038702,FBgn0039471,FBgn0039472,FBgn0039777,FBgn0039778,FBgn0040060,FBgn0040347,FBgn0040349,FBgn0043575,FBgn0050371,FBgn0051077,FBgn0051265,FBgn0053265,FBgn0053346,FBgn0063491,FBgn0085249,FBgn0085374,FBgn0086708,FBgn0250815,FBgn0259748,FBgn0261575,FBgn0261641,FBgn0261985,FBgn0264979,FBgn0265140,FBgn0267408 | | |
| execution phase of apoptosis | 0.04856777 | FBgn0036831,FBgn0053346 | 2 | GO:0097194 |
| lipid catabolic process | 0.04965137 | FBgn0039471,FBgn0039472,FBgn0040349,FBgn0264979 | 4 | GO:0016042 |

**Table 2.3f: Pathway enrichment for hits differentially upregulated in control females relative to 20HE females**

| Pathway enrichment | p-value | Hits | Gene matches | Pathway ID |
|---|---|---|---|---|
| ï»¿Glycerophospholipid biosynthesis | 1.9399E-05 | FBgn0031735,FBgn0033216,FBgn0035619,FBgn0036381,FBgn0039471,FBgn0039472,FBgn0264979 | 7 | R-DME-1483206 |
| Phospholipid metabolism | 0.0001592 | FBgn0031735,FBgn0033216,FBgn0035619,FBgn0036381,FBgn0039471,FBgn0039472,FBgn0264979 | 7 | R-DME-1483257 |
| Synthesis of PA | 0.0010249 | FBgn0035619,FBgn0039471,FBgn0039472,FBgn0264979 | 4 | R-DME-1483166 |
| Neuroactive ligand-receptor interaction | 0.0010943 | FBgn0003863,FBgn0010425,FBgn0030954 | 3 | 4080 |
| Starch and sucrose metabolism | 0.0017142 | FBgn0000078,FBgn0002570,FBgn0002571,FBgn0261575 | 4 | 500 |
| Galactose metabolism | 0.0020688 | FBgn0002570,FBgn0002571,FBgn0261575 | 3 | 52 |
| Digestion and absorption | 0.0020688 | FBgn0000078,FBgn0035619,FBgn0261675 | 3 | R-DME-8963743 |
| Acyl chain remodelling of PS | 0.0024830 | FBgn0039471,FBgn0039472,FBgn0264979 | 3 | R-DME-1482801 |
| Phenylalanine metabolism | 0.0038803 | FBgn0033518,FBgn0033520 | 2 | 360 |
| Neutrophil degranulation | 0.0073557 | FBgn0013279,FBgn0020508,FBgn0030329,FBgn0038613,FBgn0039527,FBgn0040092,FBgn0051354,FBgn0262357,FBgn0265140,FBgn0284436 | 10 | R-DME-6798695 |
| Degradation of the extracellular matrix | 0.0090207 | FBgn0036381,FBgn0265140 | 2 | R-DME-1474228 |
| Digestion | 0.0160208 | FBgn0000078,FBgn0035619 | 2 | R-DME-8935690 |
| Cytosolic tRNA aminoacylation | 0.0165947 | FBgn0016687 | 1 | R-DME-379716 |

| | | | | |
|---|---|---|---|---|
| tRNA Aminoacylation | 0.01659476 | FBgn0016687 | 1 | R-DME-379724 |
| Mitochondrial tRNA aminoacylation | 0.01659476 | FBgn0016687 | 1 | R-DME-379726 |
| Pyrophosphate hydrolysis | 0.01659476 | FBgn0016687 | 1 | R-DME-71737 |
| GABA synthesis, release, reuptake and degradation | 0.01873476 | FBgn0013279,FBgn0051354 | 2 | R-DME-888590 |
| Metabolism of Angiotensinogen to Angiotensins | 0.02162778 | FBgn0032144,FBgn0033774 | 2 | R-DME-2022377 |
| HSF1-dependent transactivation | 0.02162778 | FBgn0013279,FBgn0051354 | 2 | R-DME-3371571 |
| Innate Immune System | 0.02476815 | FBgn0013279,FBgn0020508,FBgn0030329,FBgn0038613,FBgn0039527,FBgn0040092,FBgn0051354,FBgn0261985,FBgn0262357,FBgn0265140,FBgn0284436 | 11 | R-DME-168249 |
| Regulation of HSF1-mediated heat shock response | 0.02762023 | FBgn0013279,FBgn0051354,FBgn0086708 | 3 | R-DME-3371453 |
| Antagonism of Activin by Follistatin | 0.03291954 | FBgn0024913 | 1 | R-DME-2473224 |
| Intestinal lipid absorption | 0.03291954 | FBgn0261675 | 1 | R-DME-8963678 |
| Cellular response to heat stress | 0.04182323 | FBgn0013279,FBgn0051354,FBgn0086708 | 3 | R-DME-3371556 |
| Peptide hormone metabolism | 0.04637237 | FBgn0032144,FBgn0033774 | 2 | R-DME-2980736 |
| Selenocompound metabolism | 0.04897867 | FBgn0020653 | 1 | 450 |
| Collagen degradation | 0.04897867 | FBgn0036381 | 1 | R-DME-1442490 |
| Cobalamin (Cbl, vitamin B12) transport and metabolism | 0.04897867 | FBgn0031248 | 1 | R-DME-196741 |
| Resolution of D-Loop Structures | 0.04897867 | FBgn0040347 | 1 | R-DME-5693537 |
| Resolution of D-loop Structures through Holliday Junction Intermediates | 0.04897867 | FBgn0040347 | 1 | R-DME-5693568 |

**Table 2.3e: GO enrichment for hits differentially upregulated in 20HE females relative to control females**

| GO enrichment | p-value | Hits | Gene matches | GO ID |
|---|---|---|---|---|
| ï»¿antimicrobial humoral response | 0.00094857 | FBgn0000250,FBgn0028988,FBgn0035977,FBgn0086358 | 4 | GO:0019730 |

| | | | | |
|---|---|---|---|---|
| negative regulation of antimicrobial peptide production | 0.00111074 | FBgn0000250,FBgn0028988 | 2 | GO:0002785 |
| humoral immune response | 0.00120994 | FBgn0000250,FBgn0028988,FBgn0035977,FBgn0086358 | 4 | GO:0006959 |
| negative regulation of immune effector process | 0.00147404 | FBgn0000250,FBgn0028988 | 2 | GO:0002698 |
| negative regulation of production of molecular mediator of immune response | 0.00147404 | FBgn0000250,FBgn0028988 | 2 | GO:0002701 |
| regulation of defense response to fungus | 0.00147404 | FBgn0000250,FBgn0028988 | 2 | GO:1900150 |
| negative regulation of response to biotic stimulus | 0.00148786 | FBgn0000250,FBgn0028988,FBgn0035977 | 3 | GO:0002832 |
| negative regulation of defense response | 0.00148786 | FBgn0000250,FBgn0028988,FBgn0035977 | 3 | GO:0031348 |
| negative regulation of immune response | 0.00148786 | FBgn0000250,FBgn0028988,FBgn0035977 | 3 | GO:0050777 |
| negative regulation of antimicrobial humoral response | 0.00188629 | FBgn0000250,FBgn0028988 | 3 | GO:0008348 |
| negative regulation of Toll signaling pathway | 0.0023468 | FBgn0000250,FBgn0028988 | 2 | GO:0045751 |
| regulation of response to stress | 0.00265316 | FBgn0000250,FBgn0004580,FBgn0022800,FBgn0028988,FBgn0035977,FBgn0086358 | 6 | GO:0080134 |
| negative regulation of multi-organism process | 0.00269392 | FBgn0000250,FBgn0028988,FBgn0035977 | 3 | GO:0043901 |
| negative regulation of humoral immune response | 0.00285486 | FBgn0000250,FBgn0028988 | 2 | GO:0002921 |
| negative regulation of response to external stimulus | 0.00290351 | FBgn0000250,FBgn0028988,FBgn0035977 | 3 | GO:0032102 |
| negative regulation of immune system process | 0.00312289 | FBgn0000250,FBgn0028988,FBgn0035977 | 3 | GO:0002683 |
| antimicrobial peptide production | 0.00437188 | FBgn0000250,FBgn0028988,FBgn0086358 | 3 | GO:0002775 |
| regulation of antimicrobial peptide production | 0.00437188 | FBgn0000250,FBgn0028988,FBgn0086358 | 3 | GO:0002784 |

| | | | | |
|---|---|---|---|---|
| production of molecular mediator of immune response | 0.00465304 | FBgn0000250,FBgn0028988,FBgn0086358 | 3 | GO:0002440 |
| regulation of production of molecular mediator of immune response | 0.00465304 | FBgn0000250,FBgn0028988,FBgn0086358 | 5 | GO:0002700 |
| regulation of response to external stimulus | 0.00472177 | FBgn0000250,FBgn0028988,FBgn0035977,FBgn0085430,FBgn0086358 | 5 | GO:0032101 |
| regulation of antimicrobial humoral response | 0.0052477 | FBgn0000250,FBgn0028988,FBgn0086358 | 3 | GO:0002759 |
| regulation of humoral immune response | 0.00588627 | FBgn0000250,FBgn0028988,FBgn0086358 | 3 | GO:0002920 |
| regulation of defense response | 0.00661344 | FBgn0000250,FBgn0028988,FBgn0035977,FBgn0086358 | 4 | GO:0031347 |
| negative regulation of antifungal peptide production | 0.00745968 | FBgn0000250 | 1 | GO:0002789 |
| G protein-coupled acetylcholine receptor signaling pathway | 0.00745968 | FBgn0029909 | 1 | GO:0007213 |
| cytoplasmic sequestering of NF-kappaB | 0.00745968 | FBgn0000250 | 1 | GO:0007253 |
| phototransduction, UV | 0.00745968 | FBgn0002939 | 1 | GO:0007604 |
| pupal chitin-based cuticle development | 0.00745968 | FBgn0001112 | 1 | GO:0008364 |
| detection of UV | 0.00745968 | FBgn0002939 | 1 | GO:0009589 |
| regulation of ubiquinone biosynthetic process | 0.00745968 | FBgn0039694 | 1 | GO:0010795 |
| negative regulation of nervous system process | 0.00745968 | FBgn0001134 | 1 | GO:0031645 |
| positive regulation of histone acetylation | 0.00745968 | FBgn0032691 | 1 | GO:0035066 |
| negative regulation of action potential | 0.00745968 | FBgn0001134 | 1 | GO:0045759 |
| isoprenoid transport | 0.00745968 | FBgn0002939 | 1 | GO:0046864 |
| terpenoid transport | 0.00745968 | FBgn0002939 | 1 | GO:0046865 |
| tetraterpenoid transport | 0.00745968 | FBgn0002939 | 1 | GO:0046866 |

| | | | | |
|---|---|---|---|---|
| carotenoid transport | 0.00745968 | FBgn0002939 | 1 | GO:0046867 |
| regulation of coenzyme metabolic process | 0.00745968 | FBgn0039694 | 21 | GO:0051196 |
| regulation of transmission of nerve impulse | 0.00745968 | FBgn0001134 | 1 | GO:0051969 |
| negative regulation of transmission of nerve impulse | 0.00745968 | FBgn0001134 | 1 | GO:0051970 |
| synaptic transmission, glycinergic | 0.00745968 | FBgn0001134 | 1 | GO:0060012 |
| positive regulation of histone H4 acetylation | 0.00745968 | FBgn0032691 | 1 | GO:0090240 |
| acetylcholine receptor signaling pathway | 0.00745968 | FBgn0029909 | 1 | GO:0095500 |
| regulation of action potential | 0.00745968 | FBgn0001134 | 1 | GO:0098900 |
| regulation of neuronal action potential | 0.00745968 | FBgn0001134 | 1 | GO:0098908 |
| postsynaptic signal transduction | 0.00745968 | FBgn0029909 | 1 | GO:0098926 |
| vesicle-mediated intercellular transport | 0.00745968 | FBgn0033926 | 1 | GO:0110077 |
| regulation of long-term synaptic potentiation | 0.00745968 | FBgn0004580 | 1 | GO:1900271 |
| positive regulation of protein acetylation | 0.00745968 | FBgn0032691 | 1 | GO:1901985 |
| negative regulation of neuronal action potential | 0.00745968 | FBgn0001134 | 1 | GO:1904456 |
| response to acetylcholine | 0.00745968 | FBgn0029909 | 1 | GO:1905144 |
| cellular response to acetylcholine | 0.00745968 | FBgn0029909 | 1 | GO:1905145 |
| positive regulation of histone H4-K16 acetylation | 0.00745968 | FBgn0032691 | 1 | GO:2000620 |
| positive regulation of peptidyl-lysine acetylation | 0.00745968 | FBgn0032691 | 1 | GO:2000758 |
| regulation of immune response | 0.00756881 | FBgn0000250,FBgn0028988,FBgn0035977,FBgn0086358 | 4 | GO:0050776 |
| regulation of immune effector process | 0.00847882 | FBgn0000250,FBgn0028988,FBgn0086358 | 3 | GO:0002697 |

| | | | | |
|---|---|---|---|---|
| cilium organization | 0.00847882 | FBgn0031255,FBgn0038170,FBgn0045842 | 3 | GO:0044782 |
| regulation of response to wounding | 0.00854911 | FBgn0004580,FBgn0022800 | 2 | GO:1903034 |
| regulation of response to biotic stimulus | 0.00916677 | FBgn0000250,FBgn0028988,FBgn0035977,FBgn0086358 | 4 | GO:0002831 |
| ketone biosynthetic process | 0.00945465 | FBgn0039694,FBgn0287185 | 2 | GO:0042181 |
| regulation of Toll signaling pathway | 0.0145835 | FBgn0000250,FBgn0028988 | 2 | GO:0008592 |
| regulation of synaptic plasticity | 0.0145835 | FBgn0004580,FBgn0033926 | 2 | GO:0048167 |
| peptidoglycan recognition protein signaling pathway | 0.0145835 | FBgn0035977,FBgn0086358 | 2 | GO:0061057 |
| negative regulation of NF-kappaB transcription factor activity | 0.0148652 | FBgn0000250 | 1 | GO:0032088 |
| sperm storage | 0.0148652 | FBgn0001112 | 1 | GO:0046693 |
| regulation of cofactor metabolic process | 0.0148652 | FBgn0039694 | 1 | GO:0051193 |
| antifungal innate immune response | 0.0148652 | FBgn0028988 | 1 | GO:0061760 |
| regulation of antifungal innate immune response | 0.0148652 | FBgn0028988 | 1 | GO:1905034 |
| negative regulation of antifungal innate immune response | 0.0148652 | FBgn0028988 | 1 | GO:1905035 |
| regulation of histone H4-K16 acetylation | 0.0148652 | FBgn0032691 | 1 | GO:2000618 |
| response to external stimulus | 0.01603822 | FBgn0000250,FBgn0002939,FBgn0028988,FBgn0033926,FBgn0035813,FBgn0035977,FBgn0045842,FBgn0085430,FBgn0086358 | 9 | GO:0009605 |
| defense response to fungus | 0.01811977 | FBgn0000250,FBgn0028988 | 2 | GO:0050832 |
| Toll signaling pathway | 0.01937146 | FBgn0000250,FBgn0028988 | 2 | GO:0008063 |
| defense response to other organism | 0.02053956 | FBgn0000250,FBgn0028988,FBgn0035813,FBgn0035977,FBgn0086358 | 5 | GO:0098542 |

| | | | | |
|---|---|---|---|---|
| regulation of immune system process | 0.02140815 | FBgn0000250,FBgn0028988,FBgn0035977,FBgn0086358 | 4 | GO:0002682 |
| neuronal action potential | 0.02221695 | FBgn0001134 | 1 | GO:0019228 |
| negative regulation of protein secretion | 0.02221695 | FBgn0032428 | 1 | GO:0050709 |
| long-term synaptic potentiation | 0.02221695 | FBgn0004580 | 1 | GO:0060291 |
| regulation of histone H4 acetylation | 0.02221695 | FBgn0032691 | 1 | GO:0090239 |
| regulation of presynaptic cytosolic calcium ion concentration | 0.02221695 | FBgn0004580 | 1 | GO:0099509 |
| chloride transmembrane transport | 0.02221695 | FBgn0001134 | 52 | GO:1902476 |
| negative regulation of response to wounding | 0.02221695 | FBgn0004580 | 1 | GO:1903035 |
| defense response | 0.02245378 | FBgn0000250,FBgn0028988,FBgn0035813,FBgn0035977,FBgn0086358 | 5 | GO:0006952 |
| response to fungus | 0.02333727 | FBgn0000250,FBgn0028988 | 2 | GO:0009620 |
| synaptic signaling | 0.02834487 | FBgn0001134,FBgn0004580,FBgn0029909,FBgn0033926 | 4 | GO:0099536 |
| peptidoglycan metabolic process | 0.02951531 | FBgn0035977 | 1 | GO:0000270 |
| peptidoglycan catabolic process | 0.02951531 | FBgn0035977 | 1 | GO:0009253 |
| transmission of nerve impulse | 0.02951531 | FBgn0001134 | 1 | GO:0019226 |
| ciliary basal body organization | 0.02951531 | FBgn0045842 | 1 | GO:0032053 |
| S-adenosylmethionine cycle | 0.02951531 | FBgn0015011 | 1 | GO:0033353 |
| cellular response to UV | 0.02951531 | FBgn0002939 | 1 | GO:0034644 |
| multicellular organismal signaling | 0.02951531 | FBgn0001134 | 1 | GO:0035637 |
| cytoplasmic sequestering of transcription factor | 0.02951531 | FBgn0000250 | 1 | GO:0042994 |
| histone H2A acetylation | 0.02951531 | FBgn0032691 | 1 | GO:0043968 |
| R1/R6 cell differentiation | 0.02951531 | FBgn0002734 | 1 | GO:0048052 |

| | | | | |
|---|---|---|---|---|
| cytoplasmic sequestering of protein | 0.02951531 | FBgn0000250 | 1 | GO:0051220 |
| regulation of defense response to bacterium | 0.030616 | FBgn0035977,FBgn0086358 | 2 | GO:1900424 |
| immune response | 0.033856 | FBgn0000250,FBgn0028988,FBgn0035977,FBgn0086358 | 4 | GO:0006955 |
| response to biotic stimulus | 0.03481612 | FBgn0000250,FBgn0028988,FBgn0035813,FBgn0035977,FBgn0086358 | 5 | GO:0009607 |
| response to external biotic stimulus | 0.03481612 | FBgn0000250,FBgn0028988,FBgn0035813,FBgn0035977,FBgn0086358 | 5 | GO:0043207 |
| response to other organism | 0.03481612 | FBgn0000250,FBgn0028988,FBgn0035813,FBgn0035977,FBgn0086358 | 5 | GO:0051707 |
| cellular ketone metabolic process | 0.03536095 | FBgn0039694,FBgn0287185 | 2 | GO:0042180 |
| regulation of multi-organism process | 0.03649488 | FBgn0000250,FBgn0028988,FBgn0035977,FBgn0086358 | 4 | GO:0043900 |
| action potential | 0.03676066 | FBgn0001134 | 1 | GO:0001508 |
| glycosaminoglycan catabolic process | 0.03676066 | FBgn0035977 | 1 | GO:0006027 |
| intercellular transport | 0.03676066 | FBgn0033926 | 1 | GO:0010496 |
| regulation of ketone biosynthetic process | 0.03676066 | FBgn0039694 | 1 | GO:0010566 |
| behavioral response to starvation | 0.03676066 | FBgn0033926 | 1 | GO:0042595 |
| negative regulation of hemocyte differentiation | 0.03676066 | FBgn0000250 | 1 | GO:0045611 |
| S-adenosylmethionine metabolic process | 0.03676066 | FBgn0015011 | 1 | GO:0046500 |
| signal transduction involved in cellular response to ammonium ion | 0.03676066 | FBgn0029909 | 1 | GO:1903831 |
| immune system process | 0.04145909 | FBgn0000250,FBgn0026263,FBgn0028988,FBgn0035977,FBgn0086358 | 5 | GO:0002376 |
| immune effector | 0.04257944 | FBgn0000250,FBg | 3 | GO:0002252 |

| | | | | |
|---|---|---|---|---|
| process | | n0028988,FBgn0086358 | | |
| antifungal peptide production | 0.04395336 | FBgn0000250 | 1 | GO:0002781 |
| regulation of antifungal peptide production | 0.04395336 | FBgn0000250 | 1 | GO:0002788 |
| negative regulation of peptide secretion | 0.04395336 | FBgn0032428 | 1 | GO:0002792 |
| insemination | 0.04395336 | FBgn0001112 | 1 | GO:0007320 |
| rhodopsin biosynthetic process | 0.04395336 | FBgn0002939 | 1 | GO:0016063 |
| rhodopsin metabolic process | 0.04395336 | FBgn0002939 | 1 | GO:0046154 |
| sperm competition | 0.04395336 | FBgn0001112 | 1 | GO:0046692 |
| inorganic anion transmembrane transport | 0.04395336 | FBgn0001134 | 1 | GO:0098661 |
| aminoglycan metabolic process | 0.04744436 | FBgn0035977,FBgn0053258 | 2 | GO:0006022 |

**Table 2.4a: list of genes differentially upregulated in control females relative to 20HE males**

| list of hits>10 raw reads | log2FC edgeR | p-value edgeR | -log10(pvalue) |
|---|---|---|---|
| pre-rRNA:CR45845 | -6.3651 | 3.96E-23 | 22.40230481 |
| Pebp1 | -5.4311 | 2.77E-14 | 13.55752023 |
| CG5767 | -6.8077 | 2.62E-13 | 12.58169871 |
| CG4563 | -9.2771 | 7.73E-12 | 11.11182051 |
| CG8661 | -4.0981 | 1.05E-10 | 9.978810701 |
| CG8773 | -3.5478 | 5.76E-09 | 8.239577517 |
| Jon25Bi | -4.6617 | 4.70E-08 | 7.327902142 |
| CG10182 | -6.2323 | 5.44E-08 | 7.2644011 |
| CR42767 | -8.2402 | 1.18E-07 | 6.928117993 |
| Jon66Ci | -5.8805 | 2.20E-07 | 6.657577319 |
| CG1946 | -3.1847 | 2.54E-07 | 6.595166283 |
| CG30090 | -2.6413 | 2.59E-07 | 6.586700236 |
| Vha100-4 | -5.4985 | 4.38E-07 | 6.358525889 |
| CG5770 | -10.0087 | 5.40E-07 | 6.26760624 |
| CG14205 | -4.1118 | 5.93E-07 | 6.226945307 |
| CG6296 | -4.3183 | 6.03E-07 | 6.219682688 |
| CG42747 | -2.5566 | 7.37E-07 | 6.132532512 |
| Jon25Biii | -3.7039 | 1.15E-06 | 5.93930216 |
| CG6891 | -4.1297 | 1.69E-06 | 5.772113295 |
| Cht4 | -8.2014 | 1.69E-06 | 5.772113295 |
| CG16775 | -7.5924 | 1.83E-06 | 5.73754891 |

| | | | |
|---|---|---|---|
| CG7298 | -8.1153 | 1.93E-06 | 5.714442691 |
| CG8299 | -7.0528 | 3.77E-06 | 5.42365865 |
| CG8745 | -3.7376 | 6.54E-06 | 5.184422252 |
| CG17192 | -4.2785 | 7.69E-06 | 5.11407366 |
| thetaTry | -3.8037 | 8.58E-06 | 5.066512712 |
| RpS28b | -2.1765 | 9.49E-06 | 5.022733788 |
| CG6277 | -3.8016 | 1.07E-05 | 4.970616222 |
| CG15044 | -7.1295 | 2.01E-05 | 4.696803943 |
| CG18404 | -4.7382 | 2.42E-05 | 4.616184634 |
| Peritrophin-15a | -3.8604 | 3.14E-05 | 4.503070352 |
| CG9686 | -7.6712 | 3.28E-05 | 4.484126156 |
| CG9825 | -7.3528 | 3.45E-05 | 4.462180905 |
| CG33460 | -7.109 | 3.57E-05 | 4.447331784 |
| CG4830 | -3.6388 | 3.57E-05 | 4.447331784 |
| CR45714 | -7.1573 | 4.03E-05 | 4.394694954 |
| pyd3 | -1.9811 | 4.24E-05 | 4.372634143 |
| CG6733 | -5.745 | 4.59E-05 | 4.338187314 |
| CG5958 | -3.5698 | 4.61E-05 | 4.336299075 |
| vanin-like | -2.3955 | 4.76E-05 | 4.322393047 |
| CG33109 | -8.0038 | 4.91E-05 | 4.308918508 |
| Orc1 | -2.3069 | 7.13E-05 | 4.14691047 |
| CG4558 | -6.8057 | 0.0001 | 4 |
| CG32750 | -6.9859 | 0.0001 | 4 |
| bora | -3.8354 | 0.0001 | 4 |
| CG17658 | -4.8365 | 0.0002 | 3.698970004 |
| CG7542 | -4.1347 | 0.0002 | 3.698970004 |
| O-fut2 | -1.7192 | 0.0002 | 3.698970004 |
| CG6839 | -8.0134 | 0.0002 | 3.698970004 |
| yip7 | -3.2953 | 0.0002 | 3.698970004 |
| Cht9 | -4.3142 | 0.0003 | 3.522878745 |
| Fmo-2 | -1.7394 | 0.0003 | 3.522878745 |
| SLC22A | -2.6139 | 0.0003 | 3.522878745 |
| CG7912 | -3.2177 | 0.0003 | 3.522878745 |
| CG15617 | -3.6656 | 0.0003 | 3.522878745 |
| CG15630 | -6.7416 | 0.0004 | 3.397940009 |
| CG5590 | -1.537 | 0.0004 | 3.397940009 |
| CG10914 | -1.9412 | 0.0004 | 3.397940009 |
| CG14820 | -2.9238 | 0.0004 | 3.397940009 |
| CG11068 | -1.7532 | 0.0005 | 3.301029996 |
| CG5804 | -2.2227 | 0.0005 | 3.301029996 |

| | | | |
|---|---|---|---|
| CG6048 | -4.4566 | 0.0006 | 3.22184875 |
| CG8834 | -1.8817 | 0.0006 | 3.22184875 |
| CG3011 | -2.1125 | 0.0006 | 3.22184875 |
| Jon99Fi | -4.2774 | 0.0006 | 3.22184875 |
| Debcl | -1.6166 | 0.0007 | 3.15490196 |
| Mms19 | -1.7071 | 0.0007 | 3.15490196 |
| Pen | -2.009 | 0.0007 | 3.15490196 |
| CG45080 | -6.6695 | 0.0007 | 3.15490196 |
| Fpps | -1.5834 | 0.0008 | 3.096910013 |
| CR43264 | -3.2388 | 0.0008 | 3.096910013 |
| CG10301 | -6.4444 | 0.0009 | 3.045757491 |
| pav | -1.7349 | 0.0009 | 3.045757491 |
| CG9360 | -1.898 | 0.0009 | 3.045757491 |
| Jon66Cii | -7.2096 | 0.001 | 3 |
| CG31266 | -6.7559 | 0.001 | 3 |
| CG13151 | -1.8735 | 0.001 | 3 |
| tos | -2.1576 | 0.001 | 3 |
| CG34198 | -1.6172 | 0.0011 | 2.958607315 |
| CG31344 | -2.04 | 0.0011 | 2.958607315 |
| CG5506 | -3.1168 | 0.0011 | 2.958607315 |
| CG8460 | -1.4618 | 0.0013 | 2.886056648 |
| CG10505 | -2.6599 | 0.0015 | 2.823908741 |
| CG15127 | -2.2121 | 0.0016 | 2.795880017 |
| CG30049 | -1.442 | 0.0017 | 2.769551079 |
| CR44830 | -4.3288 | 0.0018 | 2.744727495 |
| Lrpprc2 | -1.3919 | 0.0018 | 2.744727495 |
| mms4 | -1.8952 | 0.0019 | 2.721246399 |
| CG6310 | -1.5 | 0.002 | 2.698970004 |
| Npc1b | -5.9448 | 0.002 | 2.698970004 |
| Meltrin | -1.7936 | 0.002 | 2.698970004 |
| Mcm6 | -1.7582 | 0.0021 | 2.677780705 |
| CG13300 | -2.2013 | 0.0021 | 2.677780705 |
| CCHa1 | -2.2786 | 0.0022 | 2.657577319 |
| CG18473 | -3.0452 | 0.0022 | 2.657577319 |
| Arc42 | -1.3485 | 0.0024 | 2.619788758 |
| MFS1 | -7.9272 | 0.0024 | 2.619788758 |
| CG7567 | -6.2889 | 0.0027 | 2.568636236 |
| Sr-CIII | -6.0098 | 0.0027 | 2.568636236 |
| CG11700 | -1.6033 | 0.0027 | 2.568636236 |
| Acox57D-d | -2.1186 | 0.0027 | 2.568636236 |

| | | | |
|---|---|---|---|
| CG12926 | -1.859 | 0.0028 | 2.552841969 |
| CG44475 | -2.0327 | 0.0028 | 2.552841969 |
| dmGlut | -1.9304 | 0.0028 | 2.552841969 |
| CG12374 | -3.618 | 0.0029 | 2.537602002 |
| CG7280 | -1.5357 | 0.003 | 2.522878745 |
| CG42329 | -4.1747 | 0.0031 | 2.508638306 |
| bsf | -1.2427 | 0.0031 | 2.508638306 |
| CG12170 | -1.7743 | 0.0032 | 2.494850022 |
| Npc2a | -1.228 | 0.0034 | 2.468521083 |
| CG2781 | -2.1675 | 0.0034 | 2.468521083 |
| CG15126 | -1.7793 | 0.0035 | 2.455931956 |
| CDC45L | -1.4594 | 0.0036 | 2.443697499 |
| Tina-1 | -1.5577 | 0.0037 | 2.431798276 |
| nrv3 | -2.4447 | 0.0037 | 2.431798276 |
| epsilonTry | -3.2273 | 0.0037 | 2.431798276 |
| CG31041 | -4.4018 | 0.0037 | 2.431798276 |
| TyrR | -6.1434 | 0.0038 | 2.420216403 |
| Mst36Fa | -5.9129 | 0.0038 | 2.420216403 |
| CG10137 | -3.0528 | 0.0039 | 2.408935393 |
| CG1671 | -1.3846 | 0.0041 | 2.387216143 |
| gt | -3.0424 | 0.0043 | 2.366531544 |
| l(2)10685 | -1.7053 | 0.0044 | 2.356547324 |
| CG34010 | -1.4232 | 0.0045 | 2.346787486 |
| CG15423 | -1.8733 | 0.0045 | 2.346787486 |
| GILT2 | -1.6841 | 0.0046 | 2.337242168 |
| CG15210 | -2.5549 | 0.0046 | 2.337242168 |
| Jon65Aii | -3.1645 | 0.0046 | 2.337242168 |
| CG14079 | -3.1461 | 0.0048 | 2.318758763 |
| Mcm10 | -2.0607 | 0.0048 | 2.318758763 |
| QC | -2.9766 | 0.0049 | 2.30980392 |
| CG8728 | -1.1915 | 0.0049 | 2.30980392 |
| Ddx1 | -1.7968 | 0.0049 | 2.30980392 |
| psidin | -1.2737 | 0.0051 | 2.292429824 |
| Cbs | -3.1907 | 0.0052 | 2.283996656 |
| CG31198 | -1.8326 | 0.0052 | 2.283996656 |
| SPE | -3.3508 | 0.0054 | 2.26760624 |
| Tsr1 | -1.2907 | 0.0054 | 2.26760624 |
| Zip88E | -1.9368 | 0.0056 | 2.251811973 |
| CG33966 | -2.4914 | 0.0057 | 2.244125144 |
| Fdh | -1.1425 | 0.0058 | 2.236572006 |

| | | | |
|---|---|---|---|
| AdSL | -1.2171 | 0.0061 | 2.214670165 |
| CG8064 | -1.3141 | 0.0064 | 2.193820026 |
| ida | -1.5447 | 0.0064 | 2.193820026 |
| Jon99Fii | -3.32 | 0.0064 | 2.193820026 |
| Ntf-2 | -1.5511 | 0.0065 | 2.187086643 |
| cN-IIIB | -1.3606 | 0.0067 | 2.173925197 |
| CG9903 | -2.1008 | 0.0068 | 2.167491087 |
| Gfat2 | -1.2154 | 0.007 | 2.15490196 |
| CG14036 | -5.7083 | 0.0073 | 2.13667714 |
| CG10184 | -1.2204 | 0.0073 | 2.13667714 |
| Gr94a | -2.9089 | 0.0073 | 2.13667714 |
| CR44873 | -3.8832 | 0.0074 | 2.13076828 |
| CG6962 | -1.4878 | 0.0075 | 2.124938737 |
| CG9568 | -1.9648 | 0.0075 | 2.124938737 |
| Gnmt | -5.8601 | 0.0078 | 2.107905397 |
| CR43989 | -5.8601 | 0.0078 | 2.107905397 |
| CG1371 | -1.189 | 0.0079 | 2.102372909 |
| Pmm45A | -1.1531 | 0.0079 | 2.102372909 |
| CG33514 | -1.4165 | 0.0079 | 2.102372909 |
| amn | -1.1495 | 0.008 | 2.096910013 |
| lectin-24A | -5.3089 | 0.008 | 2.096910013 |
| CG13912 | -2.5162 | 0.0082 | 2.086186148 |
| RnrS | -1.2507 | 0.0089 | 2.050609993 |
| CG3430 | -1.3453 | 0.0089 | 2.050609993 |
| CG31265 | -6.914 | 0.0095 | 2.022276395 |
| Scp2 | -5.7512 | 0.0097 | 2.013228266 |
| AsnRS-m | -1.5104 | 0.0098 | 2.008773924 |
| Jon65Aiv | -2.7792 | 0.0098 | 2.008773924 |
| CG6178 | -1.1543 | 0.0103 | 1.987162775 |
| CG32698 | -1.4959 | 0.0103 | 1.987162775 |
| Oseg6 | -3.0926 | 0.0105 | 1.978810701 |
| Rif1 | -1.3933 | 0.0106 | 1.974694135 |
| CG42826 | -3.0576 | 0.0107 | 1.970616222 |
| CG16736 | -5.5882 | 0.011 | 1.958607315 |
| CG2144 | -1.3111 | 0.0114 | 1.943095149 |
| CG8607 | -1.3361 | 0.0115 | 1.93930216 |
| Ag5r2 | -2.7881 | 0.0116 | 1.935542011 |
| alpha-Est8 | -3.0311 | 0.0117 | 1.931814138 |
| CG6126 | -1.2791 | 0.0119 | 1.924453039 |
| CG6028 | -1.1787 | 0.012 | 1.920818754 |

| | | | |
|---|---|---|---|
| CG3625 | -5.6337 | 0.0123 | 1.910094889 |
| l(3)mbt | -1.3612 | 0.0124 | 1.906578315 |
| Irp-1B | -1.1844 | 0.0126 | 1.899629455 |
| CG7246 | -1.325 | 0.0127 | 1.896196279 |
| PRAS40 | -1.0695 | 0.0129 | 1.88941029 |
| CPT2 | -1.19 | 0.013 | 1.886056648 |
| CG4743 | -1.3586 | 0.013 | 1.886056648 |
| CG12512 | -1.656 | 0.0131 | 1.882728704 |
| CG42728 | -3.6264 | 0.0131 | 1.882728704 |
| CG11598 | -5.4818 | 0.0138 | 1.860120914 |
| CG3520 | -1.4398 | 0.0142 | 1.847711656 |
| Ser6 | -2.1843 | 0.0142 | 1.847711656 |
| CG18765 | -2.7293 | 0.0143 | 1.844663963 |
| CG11123 | -1.3043 | 0.0144 | 1.841637508 |
| CR42491 | -1.0555 | 0.0151 | 1.821023053 |
| CG9143 | -1.1164 | 0.0152 | 1.818156412 |
| Lim1 | -2.9122 | 0.0153 | 1.815308569 |
| xit | -1.12 | 0.0158 | 1.801342913 |
| RecQ4 | -1.8545 | 0.0158 | 1.801342913 |
| DNApol-alpha60 | -1.5519 | 0.0158 | 1.801342913 |
| IP3K2 | -1.6809 | 0.0158 | 1.801342913 |
| CG11103 | -1.2545 | 0.0159 | 1.798602876 |
| CG4053 | -6.5628 | 0.016 | 1.795880017 |
| CG14424 | -3.6028 | 0.0161 | 1.793174124 |
| CG18788 | -2.288 | 0.0161 | 1.793174124 |
| CG17726 | -1.3977 | 0.0163 | 1.787812396 |
| CG12171 | -1.1048 | 0.0164 | 1.785156152 |
| LysP | -6.6245 | 0.0166 | 1.779891912 |
| RfC3 | -1.6405 | 0.017 | 1.769551079 |
| CG7277 | -1.1297 | 0.0171 | 1.76700389 |
| Snm1 | -1.3059 | 0.0175 | 1.756961951 |
| CG31469 | -1.7399 | 0.0175 | 1.756961951 |
| CG34301 | -3.5871 | 0.0177 | 1.752026734 |
| Pex13 | -1.1344 | 0.0178 | 1.749579998 |
| CG32641 | -1.1683 | 0.0178 | 1.749579998 |
| Egm | -1.0441 | 0.0179 | 1.747146969 |
| CG5157 | -2.4948 | 0.0181 | 1.742321425 |
| fa2h | -2.849 | 0.0183 | 1.73754891 |
| heix | -1.218 | 0.0194 | 1.71219827 |
| CG6745 | -1.262 | 0.0196 | 1.707743929 |

| | | | |
|---|---|---|---|
| CG13690 | -1.3186 | 0.0197 | 1.705533774 |
| CG14120 | -1.9371 | 0.0198 | 1.70333481 |
| CG14545 | -2.5358 | 0.0199 | 1.701146924 |
| CG8419 | -3.0404 | 0.0205 | 1.688246139 |
| CR45037 | -2.5396 | 0.0209 | 1.679853714 |
| CR43253 | -3.6744 | 0.0217 | 1.663540266 |
| CG14629 | -1.0631 | 0.0218 | 1.661543506 |
| RtcB | -1.0482 | 0.0219 | 1.659555885 |
| CG10933 | -5.7914 | 0.0226 | 1.645891561 |
| CG5639 | -5.7603 | 0.0226 | 1.645891561 |
| CG7730 | -5.7603 | 0.0226 | 1.645891561 |
| otk2 | -1.6825 | 0.0235 | 1.628932138 |
| Nsun2 | -1.0774 | 0.0236 | 1.627087997 |
| CG15362 | -1.3813 | 0.0242 | 1.616184634 |
| CG31343 | -1.4063 | 0.0245 | 1.610833916 |
| beta-PheRS | -1.1583 | 0.0247 | 1.607303047 |
| Mcm7 | -1.3406 | 0.0247 | 1.607303047 |
| CG10592 | -1.2281 | 0.0249 | 1.603800653 |
| CG14798 | -1.215 | 0.0252 | 1.598599459 |
| AGBE | -1.0353 | 0.0254 | 1.595166283 |
| Ote | -1.1858 | 0.0254 | 1.595166283 |
| Gk1 | -1.2997 | 0.0254 | 1.595166283 |
| CG30371 | -6.273 | 0.0255 | 1.59345982 |
| GILT3 | -2.9457 | 0.026 | 1.585026652 |
| CR45938 | -1.8857 | 0.026 | 1.585026652 |
| CG3663 | -1.0822 | 0.0264 | 1.578396073 |
| CG9577 | -1.0915 | 0.0266 | 1.575118363 |
| lcs | -4.2892 | 0.0267 | 1.573488739 |
| MESK2 | -1.5649 | 0.0269 | 1.57024772 |
| CG1827 | -0.9419 | 0.027 | 1.568636236 |
| ico | -1.1121 | 0.027 | 1.568636236 |
| CG3021 | -1.0484 | 0.0272 | 1.565431096 |
| l(2)dtl | -1.1823 | 0.0272 | 1.565431096 |
| Oatp33Eb | -2.6721 | 0.0272 | 1.565431096 |
| Zip89B | -3.4193 | 0.0278 | 1.555955204 |
| Ssrp | -0.9484 | 0.0281 | 1.55129368 |
| CG7593 | -1.1954 | 0.0282 | 1.549750892 |
| SdhB | -0.9244 | 0.0287 | 1.542118103 |
| CG45061 | -1.024 | 0.0287 | 1.542118103 |
| alpha-Est4 | -5.1983 | 0.0288 | 1.540607512 |

| | | | |
|---|---|---|---|
| CG33116 | -1.0918 | 0.0291 | 1.536107011 |
| Takl1 | -2.8719 | 0.0293 | 1.53313238 |
| CG33080 | -3.0718 | 0.0298 | 1.525783736 |
| CG43207 | -2.146 | 0.0298 | 1.525783736 |
| CG11911 | -2.1631 | 0.0298 | 1.525783736 |
| blw | -0.8956 | 0.0302 | 1.519993057 |
| r-l | -0.9856 | 0.0307 | 1.512861625 |
| CG10470 | -1.0115 | 0.0307 | 1.512861625 |
| Nup107 | -0.961 | 0.031 | 1.508638306 |
| CG6180 | -0.9581 | 0.0311 | 1.507239611 |
| Rrp46 | -1.2152 | 0.0317 | 1.498940738 |
| Syx4 | -1.7451 | 0.0318 | 1.49757288 |
| CG7406 | -3.3421 | 0.0319 | 1.496209317 |
| CG31915 | -1.0831 | 0.0323 | 1.490797478 |
| alphaTub84D | -0.9969 | 0.0325 | 1.488116639 |
| rev7 | -1.1847 | 0.0328 | 1.484126156 |
| Zwilch | -1.2035 | 0.033 | 1.48148606 |
| Cyp6t1 | -1.2044 | 0.0331 | 1.480172006 |
| TBC1D5 | -1.1251 | 0.0336 | 1.473660723 |
| CG32572 | -1.6695 | 0.0337 | 1.472370099 |
| CG9663 | -1.0664 | 0.0339 | 1.469800302 |
| AlaRS-m | -1.0702 | 0.0343 | 1.46470588 |
| CG7137 | -1.1815 | 0.0344 | 1.463441557 |
| CG6271 | -3.7069 | 0.0345 | 1.462180905 |
| cue | -1.0029 | 0.0345 | 1.462180905 |
| upd3 | -0.9525 | 0.0346 | 1.460923901 |
| Thiolase | -0.8613 | 0.036 | 1.443697499 |
| CR44704 | -1.4842 | 0.036 | 1.443697499 |
| CG13704 | -1.5901 | 0.036 | 1.443697499 |
| CG6325 | -1.0797 | 0.037 | 1.431798276 |
| asl | -1.0366 | 0.0371 | 1.43062609 |
| CCKLR-17D3 | -1.8066 | 0.0372 | 1.42945706 |
| spd-2 | -1.2167 | 0.0372 | 1.42945706 |
| CG30377 | -3.2566 | 0.0374 | 1.427128398 |
| CG31097 | -2.7315 | 0.0376 | 1.424812155 |
| LysX | -2.9429 | 0.0376 | 1.424812155 |
| Sytbeta | -5.5508 | 0.0378 | 1.4225082 |
| CG18335 | -1.9689 | 0.0383 | 1.416801226 |
| CG6574 | -1.3936 | 0.0386 | 1.413412695 |
| CG33127 | -1.3018 | 0.0389 | 1.410050399 |

| | | | |
|---|---|---|---|
| CG31391 | -3.3131 | 0.0393 | 1.40560745 |
| Art7 | -0.9828 | 0.0397 | 1.401209493 |
| CR45158 | -2.2982 | 0.0397 | 1.401209493 |
| Tcp-1zeta | -0.9094 | 0.0401 | 1.396855627 |
| Sym | -1.0556 | 0.0403 | 1.394694954 |
| Pi3K59F | -0.992 | 0.0413 | 1.384049948 |
| CG11752 | -0.8841 | 0.0414 | 1.382999659 |
| CG32212 | -0.9485 | 0.0414 | 1.382999659 |
| CG18190 | -1.4024 | 0.0416 | 1.380906669 |
| CR46102 | -2.6128 | 0.0418 | 1.378823718 |
| pont | -0.909 | 0.0418 | 1.378823718 |
| Tao | -1.7571 | 0.0423 | 1.373659633 |
| CG16749 | -1.4462 | 0.0423 | 1.373659633 |
| snoRNA:Me18S-G1189 | -1.4086 | 0.0429 | 1.367542708 |
| NK7.1 | -1.0172 | 0.0436 | 1.360513511 |
| stv | -1.1939 | 0.0436 | 1.360513511 |
| Kif19A | -5.8077 | 0.044 | 1.356547324 |
| RnrL | -0.9965 | 0.0444 | 1.35261703 |
| CG18528 | -1.153 | 0.0446 | 1.350665141 |
| Jon65Aiii | -2.056 | 0.0463 | 1.334419009 |
| CG15629 | -0.9041 | 0.0464 | 1.333482019 |
| Xpd | -0.9409 | 0.0467 | 1.330683119 |
| CG14301 | -3.5842 | 0.0476 | 1.322393047 |
| CG13843 | -2.4964 | 0.0477 | 1.321481621 |
| CNT1 | -1.6745 | 0.05 | 1.301029996 |
| AOX1 | -0.8833 | 0.0502 | 1.299296283 |
| Surf4 | -0.8341 | 0.0503 | 1.298432015 |
| CG12288 | -1.3139 | 0.0503 | 1.298432015 |
| CG6287 | -1.1329 | 0.0505 | 1.296708622 |
| CG17010 | -5.6936 | 0.0507 | 1.294992041 |
| Listericin | -1.9964 | 0.0508 | 1.294136288 |
| Jheh3 | -1.146 | 0.0509 | 1.293282218 |
| fzr2 | -1.3374 | 0.051 | 1.292429824 |
| CG5255 | -1.5677 | 0.051 | 1.292429824 |
| nero | -0.9047 | 0.0519 | 1.284832642 |
| CG17855 | -0.8825 | 0.052 | 1.283996656 |
| snoRNA:Psi28S-1135b | -2.3694 | 0.0527 | 1.278189385 |
| Trxr-1 | -1.6965 | 0.0531 | 1.274905479 |
| CG3987 | -1.0286 | 0.0531 | 1.274905479 |
| Fen1 | -1.0301 | 0.0538 | 1.269217724 |

| | | | |
|---|---|---|---|
| CG43774 | -1.6751 | 0.0539 | 1.268411235 |
| CG7839 | -0.9414 | 0.0549 | 1.260427656 |

**Table 2.4b: list of genes differentially upregulated in 20HE males relative to control females**

| list of hits>10 raw reads | log2FC edgeR | p-value edgeR | -log10(pvalue) |
|---|---|---|---|
| roX2 | 10.6073 | 1.76E-18 | 17.75448733 |
| CR43961 | 9.8493 | 2.07E-15 | 14.68402965 |
| CG12721 | 7.0139 | 6.61E-15 | 14.17979854 |
| hbs | 4.5641 | 2.88E-10 | 9.540607512 |
| CG3739 | 4.9048 | 1.22E-09 | 8.913640169 |
| lin-28 | 2.9282 | 1.47E-09 | 8.832682665 |
| CG42854 | 5.9939 | 5.55E-09 | 8.255707017 |
| CG3703 | 2.6459 | 5.91E-08 | 7.228412519 |
| CG34323 | 8.0601 | 6.89E-08 | 7.161780778 |
| CG31436 | 2.7115 | 1.55E-07 | 6.809668302 |
| CG44006 | 2.8502 | 3.33E-07 | 6.477555766 |
| CG43101 | 3.8771 | 4.07E-07 | 6.390405591 |
| CG15263 | 8.8117 | 5.34E-07 | 6.272458743 |
| CG3568 | 2.8316 | 1.18E-06 | 5.928117993 |
| CR44748 | 3.1285 | 2.32E-06 | 5.634512015 |
| snoRNA:Me28S-A30 | 4.3504 | 6.35E-06 | 5.197226275 |
| Mal-A4 | 3.3322 | 1.12E-05 | 4.950781977 |
| CG13813 | 5.6432 | 1.17E-05 | 4.931814138 |
| CG14196 | 3.7162 | 2.28E-05 | 4.642065153 |
| CG42393 | 2.6649 | 2.46E-05 | 4.609064893 |
| CG11407 | 8.9582 | 2.67E-05 | 4.573488739 |
| Eip75B | 2.441 | 4.18E-05 | 4.378823718 |
| ninaD | 5.0995 | 4.72E-05 | 4.326058001 |
| vilya | 7.0011 | 5.29E-05 | 4.276544328 |
| CG34401 | 2.4342 | 0.0001 | 4 |
| CG15695 | 7.9833 | 0.0001 | 4 |
| gskt | 3.6281 | 0.0002 | 3.698970004 |
| Mal-A8 | 3.5256 | 0.0002 | 3.698970004 |
| CG44286 | 6.8248 | 0.0003 | 3.522878745 |
| CG6465 | 1.7598 | 0.0003 | 3.522878745 |
| CG32040 | 2.1534 | 0.0003 | 3.522878745 |
| sing | 2.4851 | 0.0003 | 3.522878745 |
| CR45522 | 6.5808 | 0.0004 | 3.397940009 |
| E(spl)malpha-BFM | 1.4602 | 0.0004 | 3.397940009 |
| CG12643 | 1.5203 | 0.0004 | 3.397940009 |

| | | | |
|---|---|---|---|
| geko | 4.6019 | 0.0005 | 3.301029996 |
| bip1 | 4.5666 | 0.0005 | 3.301029996 |
| CG5361 | 6.5239 | 0.0005 | 3.301029996 |
| brk | 1.6085 | 0.0005 | 3.301029996 |
| Mal-A1 | 2.8683 | 0.0005 | 3.301029996 |
| CR45824 | 4.5159 | 0.0006 | 3.22184875 |
| Sik2 | 1.7774 | 0.0006 | 3.22184875 |
| mam | 2.0317 | 0.0006 | 3.22184875 |
| Gbeta5 | 3.8145 | 0.0006 | 3.22184875 |
| CG32638 | 1.7381 | 0.0007 | 3.15490196 |
| CG9498 | 5.6766 | 0.0007 | 3.15490196 |
| CG32599 | 3.7467 | 0.0008 | 3.096910013 |
| CG13917 | 1.7188 | 0.0008 | 3.096910013 |
| CR43257 | 1.9416 | 0.0008 | 3.096910013 |
| CG32055 | 2.3407 | 0.0011 | 2.958607315 |
| tobi | 3.9505 | 0.0011 | 2.958607315 |
| CG10257 | 6.2574 | 0.0012 | 2.920818754 |
| TTLL3B | 4.4842 | 0.0012 | 2.920818754 |
| CG6040 | 1.4885 | 0.0013 | 2.886056648 |
| GstD5 | 1.964 | 0.0014 | 2.853871964 |
| CG31808 | 2.7052 | 0.0014 | 2.853871964 |
| Faa | 1.8345 | 0.0015 | 2.823908741 |
| fs(1)Yb | 6.4755 | 0.0016 | 2.795880017 |
| CG4363 | 3.1302 | 0.0016 | 2.795880017 |
| ed | 1.4121 | 0.0018 | 2.744727495 |
| CG11192 | 2.3564 | 0.0019 | 2.721246399 |
| CG3699 | 2.9869 | 0.002 | 2.698970004 |
| Ir40a | 6.1369 | 0.0022 | 2.657577319 |
| E(spl)m6-BFM | 1.6686 | 0.0022 | 2.657577319 |
| CR44429 | 1.9689 | 0.0022 | 2.657577319 |
| tut | 2.2542 | 0.0022 | 2.657577319 |
| br | 6.0958 | 0.0023 | 2.638272164 |
| CG31510 | 1.2895 | 0.0023 | 2.638272164 |
| CR44445 | 2.2644 | 0.0023 | 2.638272164 |
| rha | 7.1366 | 0.0024 | 2.619788758 |
| laccase2 | 1.8044 | 0.0024 | 2.619788758 |
| CG13658 | 1.849 | 0.0025 | 2.602059991 |
| CG30484 | 2.4471 | 0.0025 | 2.602059991 |
| Eip78C | 2.3785 | 0.0026 | 2.585026652 |
| CG13659 | 1.6834 | 0.0027 | 2.568636236 |

| | | | |
|---|---|---|---|
| Gld | 4.2053 | 0.0028 | 2.552841969 |
| GstD8 | 3.9181 | 0.0028 | 2.552841969 |
| CG10559 | 2.1509 | 0.0028 | 2.552841969 |
| Hsromega | 1.2852 | 0.0029 | 2.537602002 |
| CG30324 | 6.3372 | 0.003 | 2.522878745 |
| CG8468 | 1.9052 | 0.003 | 2.522878745 |
| CG8343 | 2.9287 | 0.0032 | 2.494850022 |
| RNaseMRP:RNA | 1.4928 | 0.0032 | 2.494850022 |
| CR45922 | 3.5121 | 0.0033 | 2.48148606 |
| GstD4 | 1.5997 | 0.0033 | 2.48148606 |
| Gbp2 | 5.6621 | 0.0033 | 2.48148606 |
| Paip2 | 1.2468 | 0.0034 | 2.468521083 |
| CR44547 | 1.5687 | 0.0034 | 2.468521083 |
| CG3505 | 2.77 | 0.0038 | 2.420216403 |
| CG10337 | 1.5041 | 0.0039 | 2.408935393 |
| CG30356 | 2.1808 | 0.0039 | 2.408935393 |
| CG13894 | 4.3874 | 0.004 | 2.397940009 |
| Dcp-1 | 1.5625 | 0.004 | 2.397940009 |
| CG3764 | 1.493 | 0.004 | 2.397940009 |
| HP1D3csd | 2.4688 | 0.0041 | 2.387216143 |
| Ect3 | 2.4384 | 0.0041 | 2.387216143 |
| cv-2 | 1.2455 | 0.0042 | 2.37675071 |
| CG32354 | 1.891 | 0.0042 | 2.37675071 |
| CG32523 | 2.8379 | 0.0047 | 2.327902142 |
| CG13893 | 1.9995 | 0.0047 | 2.327902142 |
| CG31370 | 1.4779 | 0.0048 | 2.318758763 |
| CR44380 | 3.1324 | 0.0049 | 2.30980392 |
| CG11275 | 1.4415 | 0.0049 | 2.30980392 |
| CG33160 | 5.9843 | 0.0051 | 2.292429824 |
| CG30197 | 1.5773 | 0.0051 | 2.292429824 |
| pirk | 1.7012 | 0.0054 | 2.26760624 |
| Sirt6 | 1.5188 | 0.0055 | 2.259637311 |
| Ac3 | 2.0016 | 0.0056 | 2.251811973 |
| CR46095 | 1.6041 | 0.0058 | 2.236572006 |
| CG44329 | 6.2133 | 0.006 | 2.22184875 |
| CG11374 | 1.7808 | 0.006 | 2.22184875 |
| CG17111 | 2.046 | 0.0061 | 2.214670165 |
| CG14838 | 3.9156 | 0.0064 | 2.193820026 |
| Tsp42Ej | 1.3247 | 0.0065 | 2.187086643 |
| CG43672 | 3.4032 | 0.0067 | 2.173925197 |

| | | | |
|---|---|---|---|
| Rcd2 | 1.4405 | 0.0067 | 2.173925197 |
| Ir7g | 5.7403 | 0.0069 | 2.161150909 |
| CG15515 | 3.9085 | 0.0072 | 2.142667504 |
| CG43647 | 2.9645 | 0.0073 | 2.13667714 |
| CG12728 | 1.1736 | 0.0073 | 2.13667714 |
| MYPT-75D | 1.4028 | 0.0074 | 2.13076828 |
| CR44538 | 2.7403 | 0.0078 | 2.107905397 |
| alphagamma-element:CR32865 | 1.4048 | 0.0079 | 2.102372909 |
| Cyp6a20 | 1.6509 | 0.0079 | 2.102372909 |
| CR45280 | 3.3498 | 0.008 | 2.096910013 |
| Ir41a | 3.0098 | 0.008 | 2.096910013 |
| CG18745 | 1.1206 | 0.0083 | 2.080921908 |
| CR46250 | 1.9422 | 0.0087 | 2.060480747 |
| CG9422 | 2.3003 | 0.0091 | 2.040958608 |
| CG14141 | 3.8201 | 0.0093 | 2.031517051 |
| Lac | 1.8498 | 0.0093 | 2.031517051 |
| CG5059 | 1.1545 | 0.0096 | 2.017728767 |
| vn | 1.3779 | 0.0096 | 2.017728767 |
| Obp18a | 1.4386 | 0.01 | 2 |
| sprt | 1.4795 | 0.01 | 2 |
| Drep4 | 1.3272 | 0.0101 | 1.995678626 |
| Ddr | 2.1813 | 0.0101 | 1.995678626 |
| E(spl)m7-HLH | 1.3505 | 0.0102 | 1.991399828 |
| CR44608 | 1.361 | 0.0103 | 1.987162775 |
| Vti1a | 1.3318 | 0.0105 | 1.978810701 |
| SIFa | 5.8133 | 0.0106 | 1.974694135 |
| Or45a | 1.8002 | 0.0106 | 1.974694135 |
| kirre | 3.9349 | 0.0107 | 1.970616222 |
| CG4377 | 2.414 | 0.0107 | 1.970616222 |
| mst | 1.5371 | 0.0108 | 1.966576245 |
| CR45082 | 1.5962 | 0.0111 | 1.954677021 |
| Oatp74D | 1.2807 | 0.0113 | 1.946921557 |
| Rad23 | 1.1065 | 0.0115 | 1.93930216 |
| CG43389 | 6.7413 | 0.0117 | 1.931814138 |
| CG4660 | 2.7839 | 0.0118 | 1.928117993 |
| CG17265 | 1.1251 | 0.0119 | 1.924453039 |
| ND-51L1 | 1.9582 | 0.0119 | 1.924453039 |
| snoRNA:Me28S-C437 | 2.0905 | 0.012 | 1.920818754 |
| CR45102 | 1.1325 | 0.0122 | 1.913640169 |
| CR44276 | 2.0229 | 0.0122 | 1.913640169 |

| | | | |
|---|---|---|---|
| CG3262 | 1.2415 | 0.0123 | 1.910094889 |
| Xpac | 1.3311 | 0.0123 | 1.910094889 |
| CG11226 | 2.2916 | 0.0126 | 1.899629455 |
| Cad96Ca | 2.151 | 0.0127 | 1.896196279 |
| CG34040 | 4.4697 | 0.0128 | 1.89279003 |
| CR44784 | 1.3856 | 0.0129 | 1.88941029 |
| CR41257 | 2.4539 | 0.013 | 1.886056648 |
| CG11893 | 1.9762 | 0.013 | 1.886056648 |
| CR32636 | 2.7446 | 0.0133 | 1.876148359 |
| Mal-A2 | 1.8969 | 0.0133 | 1.876148359 |
| CG18467 | 2.581 | 0.0134 | 1.872895202 |
| Mos | 2.8721 | 0.0136 | 1.866461092 |
| daw | 2.6111 | 0.0136 | 1.866461092 |
| krimp | 1.2256 | 0.0137 | 1.863279433 |
| Spn85F | 5.7664 | 0.0138 | 1.860120914 |
| CR44145 | 1.622 | 0.0141 | 1.850780887 |
| CR9162 | 2.1438 | 0.0142 | 1.847711656 |
| CG6683 | 1.2553 | 0.0142 | 1.847711656 |
| Csk | 1.1004 | 0.0143 | 1.844663963 |
| CR45793 | 1.7582 | 0.0144 | 1.841637508 |
| pan | 1.6901 | 0.0145 | 1.838631998 |
| CR44984 | 2.0928 | 0.0146 | 1.835647144 |
| CG14227 | 1.4603 | 0.0146 | 1.835647144 |
| CG5644 | 1.9557 | 0.0146 | 1.835647144 |
| mGluR | 2.8347 | 0.0147 | 1.832682665 |
| CR44564 | 2.6101 | 0.0149 | 1.826813732 |
| CG10910 | 3.3373 | 0.0153 | 1.815308569 |
| Gr47b | 2.0142 | 0.0156 | 1.806875402 |
| Fhos | 2.5471 | 0.0157 | 1.804100348 |
| CG33267 | 1.502 | 0.0163 | 1.787812396 |
| CG32706 | 1.7724 | 0.0169 | 1.772113295 |
| CG12483 | 5.6657 | 0.0171 | 1.76700389 |
| CG9821 | 0.9801 | 0.0171 | 1.76700389 |
| CG31104 | 2.8709 | 0.0172 | 1.764471553 |
| Ptip | 1.0735 | 0.0177 | 1.752026734 |
| CG14626 | 1.0325 | 0.0177 | 1.752026734 |
| sty | 0.9656 | 0.0192 | 1.716698771 |
| CG17186 | 1.2444 | 0.0192 | 1.716698771 |
| Cbp53E | 3.0872 | 0.0194 | 1.71219827 |
| CR43973 | 1.2134 | 0.02 | 1.698970004 |

| | | | |
|---|---|---|---|
| sqz | 1.145 | 0.0201 | 1.696803943 |
| GATAd | 1.1365 | 0.0203 | 1.692503962 |
| CG5281 | 1.6784 | 0.0204 | 1.690369833 |
| snoRNA:Me28S-A3407a | 1.7987 | 0.0204 | 1.690369833 |
| CG34348 | 1.1264 | 0.0207 | 1.684029655 |
| Hsp67Bc | 1.1376 | 0.0209 | 1.679853714 |
| Rbp1 | 1.0379 | 0.0212 | 1.673664139 |
| CHKov2 | 1.1208 | 0.0216 | 1.665546249 |
| noe | 1.1162 | 0.0216 | 1.665546249 |
| CR45625 | 1.7592 | 0.0216 | 1.665546249 |
| CG18368 | 2.8286 | 0.0217 | 1.663540266 |
| CR44723 | 2.4509 | 0.0219 | 1.659555885 |
| VhaSFD | 5.3989 | 0.022 | 1.657577319 |
| CR44404 | 5.3989 | 0.022 | 1.657577319 |
| snoRNA:Psi18S-1854a | 1.97 | 0.0224 | 1.649751982 |
| CR45745 | 2.4539 | 0.0227 | 1.643974143 |
| CR45964 | 3.3242 | 0.0228 | 1.642065153 |
| l(1)G0193 | 1.3413 | 0.0233 | 1.632644079 |
| CR44862 | 6.216 | 0.0237 | 1.625251654 |
| CG12655 | 1.8331 | 0.0237 | 1.625251654 |
| CG14160 | 4.49 | 0.0237 | 1.625251654 |
| olf413 | 2.1822 | 0.0239 | 1.621602099 |
| CR46204 | 1.4381 | 0.024 | 1.619788758 |
| CG30099 | 2.0324 | 0.024 | 1.619788758 |
| Cad87A | 1.1541 | 0.0241 | 1.617982957 |
| CR46093 | 1.4163 | 0.0241 | 1.617982957 |
| CG9328 | 1.2636 | 0.0242 | 1.616184634 |
| CG31300 | 2.0997 | 0.0242 | 1.616184634 |
| scaRNA:MeU5-C46 | 0.976 | 0.0245 | 1.610833916 |
| ntc | 1.3526 | 0.0246 | 1.609064893 |
| laza | 1.168 | 0.0251 | 1.600326279 |
| CG32368 | 1.0242 | 0.0253 | 1.596879479 |
| CG9684 | 0.9432 | 0.0254 | 1.595166283 |
| CG3281 | 1.0923 | 0.0254 | 1.595166283 |
| dos | 1.4552 | 0.0259 | 1.586700236 |
| CG5282 | 6.2688 | 0.0261 | 1.583359493 |
| Traf4 | 1.2 | 0.0262 | 1.581698709 |
| CG10376 | 1.0088 | 0.0264 | 1.578396073 |
| Gycbeta100B | 2.4884 | 0.0265 | 1.576754126 |
| TSG101 | 0.9168 | 0.0265 | 1.576754126 |

| | | | |
|---|---|---|---|
| png | 2.0923 | 0.0269 | 1.57024772 |
| CG13436 | 1.7852 | 0.0269 | 1.57024772 |
| Mnn1 | 1.0997 | 0.0271 | 1.567030709 |
| Ugt37b1 | 3.2953 | 0.0272 | 1.565431096 |
| CR46021 | 5.3113 | 0.0275 | 1.560667306 |
| CG4586 | 1.1636 | 0.0276 | 1.559090918 |
| BtbVII | 2.2912 | 0.0277 | 1.557520231 |
| InR | 1.068 | 0.028 | 1.552841969 |
| CR31451 | 2.9495 | 0.0282 | 1.549750892 |
| grim | 1.9379 | 0.0286 | 1.543633967 |
| TwdlC | 3.1165 | 0.0287 | 1.542118103 |
| CG31288 | 1.6415 | 0.0288 | 1.540607512 |
| Ugt86Dd | 1.3672 | 0.0289 | 1.539102157 |
| CG13739 | 3.3503 | 0.0296 | 1.528708289 |
| CG42816 | 6.0676 | 0.0298 | 1.525783736 |
| kcc | 5.2406 | 0.0298 | 1.525783736 |
| CG7747 | 1.0688 | 0.0299 | 1.524328812 |
| CG45782 | 1.92 | 0.0299 | 1.524328812 |
| CG32795 | 1.2035 | 0.03 | 1.522878745 |
| GstD3 | 0.9395 | 0.0303 | 1.518557371 |
| CG10514 | 3.3346 | 0.0304 | 1.517126416 |
| CR45549 | 1.8994 | 0.0307 | 1.512861625 |
| Eaf6 | 1.0492 | 0.0309 | 1.510041521 |
| cact | 1.1734 | 0.031 | 1.508638306 |
| CG1657 | 1.0623 | 0.0311 | 1.507239611 |
| CR45187 | 1.5706 | 0.0312 | 1.505845406 |
| Sp212 | 3.4438 | 0.0316 | 1.500312917 |
| CR43242 | 1.1103 | 0.0317 | 1.498940738 |
| snoRNA:Me18S-U1356b | 2.6828 | 0.032 | 1.494850022 |
| flfl | 0.9242 | 0.0323 | 1.490797478 |
| CG32625 | 1.3806 | 0.0323 | 1.490797478 |
| CR45234 | 2.421 | 0.0328 | 1.484126156 |
| CG8281 | 1.0712 | 0.0331 | 1.480172006 |
| Arc2 | 0.9756 | 0.0332 | 1.478861916 |
| CR45166 | 3.6136 | 0.0338 | 1.4710833 |
| CR44892 | 1.2216 | 0.0339 | 1.469800302 |
| Gr32a | 2.8891 | 0.0341 | 1.467245621 |
| yuri | 2.8838 | 0.0343 | 1.46470588 |
| CG9425 | 1.5979 | 0.0343 | 1.46470588 |
| CG32444 | 2.0573 | 0.0345 | 1.462180905 |

| | | | |
|---|---|---|---|
| CG9676 | 2.0843 | 0.0345 | 1.462180905 |
| CG33643 | 1.8114 | 0.0345 | 1.462180905 |
| CG11155 | 1.872 | 0.0354 | 1.450996738 |
| PDZ-GEF | 1.0469 | 0.0361 | 1.442492798 |
| Axs | 1.0648 | 0.0361 | 1.442492798 |
| Gr77a | 1.3273 | 0.0361 | 1.442492798 |
| CR44720 | 1.7117 | 0.0364 | 1.438898616 |
| E(spl)m3-HLH | 0.8409 | 0.0366 | 1.436518915 |
| Mal-A6 | 3.5228 | 0.0385 | 1.41453927 |
| CG34160 | 1.1947 | 0.039 | 1.408935393 |
| CG18128 | 2.1524 | 0.0392 | 1.406713933 |
| dop | 1.3293 | 0.0392 | 1.406713933 |
| CG3876 | 1.0554 | 0.0393 | 1.40560745 |
| CG31245 | 3.4138 | 0.0401 | 1.396855627 |
| comm2 | 1.4001 | 0.0406 | 1.391473966 |
| CG7194 | 1.3092 | 0.0409 | 1.388276692 |
| Smyd4-2 | 2.4454 | 0.0411 | 1.386158178 |
| CR41620 | 5.0637 | 0.0413 | 1.384049948 |
| bigmax | 0.8964 | 0.0413 | 1.384049948 |
| mir-4974 | 2.1807 | 0.0415 | 1.381951903 |
| CR45127 | 2.1552 | 0.0417 | 1.379863945 |
| CG8369 | 5.0393 | 0.0418 | 1.378823718 |
| ec | 5.0393 | 0.0418 | 1.378823718 |
| CG4297 | 0.9686 | 0.0424 | 1.372634143 |
| CR43974 | 1.2848 | 0.0428 | 1.368556231 |
| NFAT | 0.9721 | 0.043 | 1.366531544 |
| DJ-1alpha | 2.3331 | 0.0434 | 1.36251027 |
| nvd | 5.7154 | 0.0435 | 1.361510743 |
| CG12224 | 1.0328 | 0.0435 | 1.361510743 |
| fs(1)Ya | 5.7154 | 0.0436 | 1.360513511 |
| omd | 1.5098 | 0.0438 | 1.358525889 |
| insc | 0.8159 | 0.044 | 1.356547324 |
| CR46094 | 2.0502 | 0.0442 | 1.354577731 |
| snoRNA:Psi18S-1854b | 1.1552 | 0.0446 | 1.350665141 |
| CG8568 | 1.8494 | 0.0446 | 1.350665141 |
| swi2 | 1.8474 | 0.0447 | 1.349692477 |
| Ppt2 | 1.001 | 0.0449 | 1.347753659 |
| l(2)35Cc | 2.8217 | 0.0451 | 1.345823458 |
| CG6013 | 0.9736 | 0.0452 | 1.344861565 |
| CG31111 | 1.015 | 0.0456 | 1.341035157 |

| | | | |
|---|---|---|---|
| CG33463 | 2.4061 | 0.0461 | 1.336299075 |
| godzilla | 2.2268 | 0.0463 | 1.334419009 |
| ect | 1.6446 | 0.0463 | 1.334419009 |
| Ucp4C | 2.4212 | 0.0464 | 1.333482019 |
| CR45028 | 1.6695 | 0.0468 | 1.329754147 |
| Vav | 0.8683 | 0.047 | 1.327902142 |
| RhoGAP71E | 1.1549 | 0.0472 | 1.326058001 |
| bowl | 3.4322 | 0.0473 | 1.325138859 |
| Cpr51A | 0.8572 | 0.0473 | 1.325138859 |
| CR46044 | 1.2346 | 0.0474 | 1.324221658 |
| Tsp42El | 0.8205 | 0.0475 | 1.32330639 |
| CG17361 | 1.0572 | 0.0479 | 1.319664487 |
| CG34136 | 2.1762 | 0.0484 | 1.315154638 |
| CG32109 | 0.8844 | 0.0487 | 1.312471039 |
| Tie | 0.9211 | 0.0488 | 1.311580178 |
| CG33510 | 1.3994 | 0.0488 | 1.311580178 |
| baz | 0.9138 | 0.0492 | 1.308034897 |
| Cpr64Ad | 3.4976 | 0.0493 | 1.307153081 |
| kek5 | 0.8218 | 0.0495 | 1.305394801 |
| CG42365 | 1.1459 | 0.0495 | 1.305394801 |
| FASN3 | 2.1101 | 0.0501 | 1.300162274 |
| CG18180 | 2.439 | 0.0504 | 1.297569464 |
| CG31463 | 1.5931 | 0.0506 | 1.295849483 |
| Krn | 0.9266 | 0.0507 | 1.294992041 |
| CG16894 | 3.8045 | 0.0508 | 1.294136288 |
| BBS8 | 5.6118 | 0.0511 | 1.2915791 |
| Gbp1 | 5.7689 | 0.0515 | 1.288192771 |
| Rab2 | 0.8635 | 0.0525 | 1.279840697 |
| glec | 0.806 | 0.0525 | 1.279840697 |
| CG11655 | 1.1328 | 0.053 | 1.27572413 |
| CG10638 | 1.1463 | 0.0532 | 1.274088368 |
| CAH2 | 1.9189 | 0.0535 | 1.271646218 |
| CR44867 | 2.7064 | 0.0538 | 1.269217724 |
| lt | 1.4674 | 0.0541 | 1.266802735 |
| CR44809 | 1.6071 | 0.0546 | 1.262807357 |

**Table 2.4c:**

| threshold p=0.1 in the male control versus male 20HE fed list<br>threshold p=0.05 in the male control versus female control list | | threshold p=0.05 in the male control versus male 20HE fed list<br>threshold p=0.05 in the male control versus female control list | |
|---|---|---|---|
| Genes that are upregulated in control males but were | Genes that are downregulated in control males but were | Genes that are upregulated in control males but were | Genes that are downregulated in control males but were equalized |

| equalized to female levels by 20HE feeding | equalized to female levels by 20HE feeding | equalized to female levels by 20HE feeding | to female levels by 20HE feeding |
|---|---|---|---|
| ave | mus101 | a | Acp53Ea |
| CG6999 | CG4653 | AhcyL2 | Adgf-C |
| Stim | l(2)05287 | AOX2 | AIMP1 |
| CG33107 | mRpL51 | Arc1 | alpha-Est1 |
| snRNA:U7 | rdgBbeta | Atac1 | alpha-Est7 |
| CG8578 | Hsp67Ba | Atf6 | alphaTry |
| FucTC | CG32054 | bnl | Amy-d |
| Pc | CG5346 | bou | AP-1-2beta |
| Ugt86Dj | RfC4 | bun | arx |
| Cyp4ac3 | CG12736 | CG10638 | asp |
| viaf | Spc25 | CG10730 | ATPsynB |
| CG32202 | DNApol-alpha73 | CG11000 | ATPsyndelta |
| crb | Acf | CG11486 | ATPsynE |
| Ugt36Ba | mRpS33 | CG11655 | ATPsynO |
| hebe | CAH1 | CG11656 | aurB |
| CR40611 | CG30280 | CG12398 | Bap60 |
| CG3036 | icln | CG12868 | beg |
| crim | CG30069 | CG13088 | beta'COP |
| CG10324 | Rpn11 | CG14074 | beta4GalT7 |
| CR45753 | CR42874 | CG14252 | Caf1-180 |
| ZIPIC | CG16941 | CG14352 | caix |
| CR42746 | DNA-ligI | CG14367 | CCHa1-R |
| CG11638 | betaggt-II | CG14443 | CCHa2 |
| CG9018 | CG5728 | CG14770 | CG10000 |
| alphaTub67C | FK506-bp2 | CG14837 | CG10472 |
| Mst36Fb | BubR1 | CG14877 | CG10584 |
| ATP7 | CG11060 | CG14965 | CG10869 |
| rgr | CG16985 | CG15084 | CG10911 |
| CR46104 | fng | CG15760 | CG10912 |
| CG5002 | CG14969 | CG16833 | CG10939 |
| CG17977 | m | CG16898 | CG11164 |
| CG6770 | CG33679 | CG17018 | CG11241 |
| CG30385 | CG32278 | CG17684 | CG11403 |
| CG3223 | CG11788 | CG17687 | CG11562 |
| CG33645 | Inx7 | CG17786 | CG11590 |
| CG17765 | tank | CG17929 | CG11777 |
| Gmap | DIP-iota | CG18599 | CG11858 |
| alpha-Man-Ia | Tsp42Ec | CG18635 | CG11878 |
| Fcp3C | mRpL45 | CG2064 | CG11899 |
| Ns2 | Eps-15 | CG30022 | CG11912 |

| | | | |
|---|---|---|---|
| CR45798 | CG11851 | CG30047 | CG11964 |
| CG15461 | babo | CG3008 | CG12129 |
| mbc | GAPcenA | CG30440 | CG12173 |
| CG15879 | ND-13B | CG30441 | CG12204 |
| CG7332 | GstE9 | CG30456 | CG12237 |
| CG2641 | CR44026 | CG31347 | CG12279 |
| nahoda | l(1)G0004 | CG31431 | CG12288 |
| snoRNA:Psi28S-2566 | Bap111 | CG31627 | CG12321 |
| Sin1 | CG33301 | CG31817 | CG1236 |
| CG12025 | Cyp305a1 | CG32371 | CG12825 |
| wake | CG12093 | CG32450 | CG1287 |
| CR44992 | btn | CG32486 | CG13008 |
| Cys | pn | CG32845 | CG13082 |
| CG15611 | CG14757 | CG32855 | CG13324 |
| Sry-delta | crn | CG33468 | CG13364 |
| Aatf | CG7992 | CG33640 | CG13492 |
| CG8713 | CG4332 | CG33710 | CG14104 |
| AspRS-m | CG2233 | CG33928 | CG14270 |
| CG13252 | CG13928 | CG34231 | CG14499 |
| azot | UQCR-C1 | CG3556 | CG14526 |
| CG15818 | CG31546 | CG3709 | CG14543 |
| Ctr1A | Trxr-1 | CG3838 | CG15414 |
| RIOK2 | CG12608 | CG3982 | CG15605 |
| Pde6 | wrapper | CG3995 | CG16700 |
| snoRNA:nop5-x16-a | CG10194 | CG42364 | CG16734 |
| CR43241 | CG13563 | CG42553 | CG16979 |
| zetaCOP | Set | CG42818 | CG17068 |
| Cyp6a13 | CAH2 | CG43646 | CG17145 |
| Grd | CSN7 | CG43925 | CG17278 |
| btv | sc | CG43968 | CG17570 |
| CG5567 | CG16953 | CG4404 | CG17633 |
| CG8036 | CG10425 | CG44405 | CG17660 |
| CG6138 | CG16723 | CG4462 | CG17841 |
| Trim9 | CG17760 | CG45428 | CG17855 |
| scaRNA:PsiU5-44 | CG2533 | CG4676 | CG18179 |
| CG5810 | CG10467 | CG4723 | CG18180 |
| CG1360 | CG6462 | CG5114 | CG18577 |
| CR45979 | Mip | CG6330 | CG1907 |
| CG5071 | CG11880 | CG6405 | CG1942 |
| CG6443 | CG2608 | CG6602 | CG2254 |
| prt | CG8417 | CG6628 | CG2681 |
| CR45035 | lab | CG6791 | CG30001 |

| | | | |
|---|---|---|---|
| bin3 | CG4045 | CG7564 | CG30283 |
| Sodh-2 | Nup75 | CG7706 | CG30287 |
| CG12909 | lds | CG7966 | CG30339 |
| CR32690 | rin | CG8072 | CG30345 |
| CG32814 | Ugt36Bb | CG8223 | CG30411 |
| Cul2 | CR45607 | CG8273 | CG30493 |
| Lrch | Cks30A | CG8319 | CG31076 |
| Gbp1 | Tango4 | CG8492 | CG31126 |
| mir-2b-2 | CG14694 | CG9505 | CG31251 |
| ex | Cdk7 | CG9945 | CG31345 |
| Prx2540-1 | Ube3a | CkIIalpha-i1 | CG31550 |
| da | Fen1 | CR32218 | CG31918 |
| CG14353 | CG11771 | CR41544 | CG32091 |
| Ak6 | CG7156 | CR41583 | CG32201 |
| Su(H) | OstStt3 | CR43405 | CG32284 |
| CG3335 | l(2)35Bd | CR43653 | CG32483 |
| CR44758 | sel | CR43849 | CG32669 |
| CG9951 | Cdc6 | CR43909 | CG33178 |
| CG14562 | ATPsynD | CR44138 | CG3344 |
| Stat92E | rig | CR44440 | CG34026 |
| let-7-C | CG8858 | CR44566 | CG34132 |
| Smr | mus301 | CR44817 | CG34200 |
| noc | Prosalpha4 | CR45054 | CG34288 |
| CG13339 | CG15673 | CR45128 | CG34404 |
| CG11384 | Mulk | CR45148 | CG3706 |
| su(r) | CG6495 | CR45171 | CG3868 |
| CG42450 | SWIP | CR45224 | CG3906 |
| CG3308 | Dhc36C | CR45820 | CG3909 |
| CG10516 | CG8192 | CR45915 | CG4194 |
| ZC3H3 | CG5267 | CR45939 | CG42327 |
| CG5500 | CG34150 | CR46015 | CG42397 |
| CG4022 | CG42239 | CR46249 | CG42714 |
| cnir | Gga | CrebA | CG4278 |
| CG32783 | edl | cwo | CG42825 |
| CG7611 | CR44512 | Cyp311a1 | CG43295 |
| cv-d | CG30344 | Cyp4p3 | CG4557 |
| snoRNA:Me18S-U1356a | mRpS18A | Cyp6d5 | CG4627 |
| snoRNA:684 | GCC88 | Dat | CG4839 |
| CR45188 | ND-B14.5A | dpr1 | CG5010 |
| az2 | Scox | dsx-c73A | CG5107 |
| CR44779 | CG6227 | ebd1 | CG5167 |
| fand | CG15536 | Elp1 | CG5214 |

| | | | |
|---|---|---|---|
| sgl | Prosalpha7 | fidipidine | CG5254 |
| CR45620 | CG14407 | foi | CG5255 |
| CG6665 | Cat | Gk2 | CG5569 |
| smg | CG17059 | glec | CG5724 |
| CG10262 | CG3803 | GluRIIE | CG5892 |
| Tdc2 | CG9065 | GstE1 | CG6067 |
| Su(Tpl) | Tcp-1eta | GstE7 | CG6295 |
| CG33137 | CR46245 | GstE8 | CG6454 |
| CG12007 | Drat | Hexo2 | CG7379 |
| CHKov1 | Pms2 | hog | CG7458 |
| 4EHP | CG15422 | Hsc70-3 | CG7470 |
| Spn42Dd | CG11034 | Ir51b | CG7560 |
| CG30414 | CG34253 | Ir85a | CG7630 |
| scaf6 | mRpS24 | ITP | CG7837 |
| CG17249 | IleRS-m | JhI-26 | CG7889 |
| ymp | CG10877 | Kif3C | CG8258 |
| egl | CG4880 | Krn | CG8311 |
| mthl10 | st | l(3)02640 | CG8323 |
| fs(1)K10 | CG5721 | lace | CG8562 |
| CG32437 | mtSSB | Lap1 | CG8642 |
| CG5705 | CR45804 | lbm | CG8818 |
| CR43899 | CG42763 | Lcch3 | CG8891 |
| CG13108 | CG3902 | lt | CG8952 |
| CG31606 | CR45921 | mdy | CG9344 |
| CG14855 | mys | MFS14 | CG9581 |
| CG43188 | CG31798 | MFS3 | CG9752 |
| Su(z)2 | CG1598 | mir-4968 | Cisd2 |
| Efa6 | GluProRS | mir-967 | Cpr73D |
| fzo | CG4406 | Mrp4 | CR15061 |
| p | CG2680 | mrt | CR44478 |
| CG7794 | CG17646 | mthl14 | CR44692 |
| CG8239 | CG14683 | Muc14A | CR44724 |
| CR43644 | FK506-bp1 | Naam | CR44868 |
| CG6340 | CG10628 | NC2alpha | CR45474 |
| CG32095 | CG12219 | nmo | CR45973 |
| tws | Miro | PGRP-LF | cry |
| Edc3 | CG8132 | PGRP-SD | CstF-50 |
| CR44022 | CG12375 | Pig1 | Ctf4 |
| Spt20 | Amyrel | Pih1D1 | CycE |
| RhoL | CG13365 | pkaap | Cyp1 |
| CG15766 | CG15653 | PlexA | Cyp6d2 |
| CG42258 | CG5589 | ppk | dgt3 |

| | | | |
|---|---|---|---|
| jumu | Rpn1 | ppk27 | dgt6 |
| pwn | CG6428 | Pzl | DNApol-alpha180 |
| CG12003 | l(2)37Bb | Rab2 | DNApol-alpha50 |
| gkt | Oga | Rbcn-3B | DNApol-epsilon58 |
| CG42266 | Tfb4 | ric8a | DNaseII |
| CR43436 | Gr66a | rost | dnd |
| wde | CG43120 | row | dome |
| DptA | CG15247 | shams | E(spl)m2-BFM |
| Eph | l(1)G0045 | shg | E(spl)m8-HLH |
| Or85f | SelG | sima | ecd |
| MED1 | CR32194 | sinu | Eip63F-1 |
| Vps39 | CG34220 | Smurf | Est-Q |
| pcs | COX7A | SmydA-5 | Fadd |
| pygo | GckIII | Snap24 | Fit2 |
| snoRNA:Psi18S-841b | Sas-4 | snoRNA:Psi18S-1086 | Gip |
| CG15563 | mRpL30 | snoRNA:Psi18S-1275 | GlcT-1 |
| CG43192 | CG8311 | Sox102F | Glo1 |
| CG6843 | CG30001 | sstn | glu |
| CR43399 | RpS15Ab | ssx | Gr8a |
| AttD | CG33178 | St3 | Gs1l |
| mir-4964 | CG5255 | stas | Gycalpha99B |
| CR46064 | stg | swa | hdm |
| CG5642 | CG30287 | Tab2 | Hex-C |
| Atac2 | glu | Taf11 | Hsp70Bbb |
| Src42A | CG8323 | Tbc1d15-17 | Hydr1 |
| qkr58E-1 | CG11858 | Tgi | Ibf2 |
| CR44348 | Ptp52F | Tsp42Ef | Ing3 |
| CG3163 | Ibf2 | ttm2 | IntS4 |
| CG16711 | nht | Ugt86Dc | Irp-1A |
| CR45256 | mRpL54 | wts | Jheh3 |
| CG4455 | ATPsynB | | Jon99Ci |
| kune | tex | | Jon99Cii |
| dgt1 | Acp53Ea | | Jon99Ciii |
| CG16716 | Fadd | | kappaTry |
| Lap1 | Pgm | | Klp61F |
| CG9505 | CG11164 | | lectin-46Ca |
| CG33468 | Mgstl | | lectin-46Cb |
| Ir51b | CG7560 | | Lgr3 |
| Tgi | Pdxk | | LysD |
| wts | vls | | LysE |
| foi | CG11590 | | mag |
| CG17018 | Ing3 | | Mcm2 |

| | | | |
|---|---|---|---|
| mrt | CG12204 | | Mcm5 |
| glec | mRpL44 | | Mdh2 |
| CR45224 | CG17068 | | Mdr50 |
| CG30456 | RpS14a | | Mesh1 |
| shg | CG3706 | | Mgstl |
| CR45148 | CG11964 | | mRpL10 |
| pkaap | CG17145 | | mRpL12 |
| CG14877 | CG4278 | | mRpL18 |
| CG43646 | CG3909 | | mRpL20 |
| CR43909 | TyrRS-m | | mRpL34 |
| CG14770 | mRpL18 | | mRpL36 |
| Cyp311a1 | CstF-50 | | mRpL44 |
| CR45054 | Adgf-C | | mRpL47 |
| CG42818 | mRpS35 | | mRpL54 |
| GstE7 | CG16979 | | mRpS11 |
| CR45915 | beg | | mRpS35 |
| CR43849 | Nrk | | msb1l |
| CR43653 | lectin-46Cb | | msd1 |
| CR44817 | CG13492 | | msd5 |
| JhI-26 | p47 | | Muc68Ca |
| Taf11 | CG12279 | | Muc68E |
| CG45428 | CG12173 | | Mur29B |
| CR43405 | Spp | | ND-B15 |
| CR32218 | CG17570 | | Ndc1 |
| CG17684 | tam | | nht |
| fidipidine | Rrp42 | | Npc2f |
| Mrp4 | Caf1-180 | | Nrk |
| lace | Sld5 | | Orc5 |
| CG14965 | CG9752 | | Osbp |
| GluRIIE | mRpL10 | | ox |
| CG16833 | CG18577 | | p47 |
| mthl14 | CR45973 | | pcl |
| CrebA | GlcT-1 | | Pdxk |
| CG8223 | CG31251 | | Pgm |
| Tbc1d15-17 | CG30493 | | PGRP-SC2 |
| nmo | mRpL34 | | phyl |
| GstE1 | CG11562 | | ppk3 |
| CG16898 | arx | | Ptp52F |
| CG14352 | mRpL20 | | rasp |
| SmydA-5 | CG3868 | | Rbf2 |
| cwo | CG17841 | | RpS14a |
| Cyp4p3 | CR45474 | | RpS15Ab |

| | | | |
|---|---|---|---|
| 14-3-3zeta | mRpL47 | | Rrp42 |
| CR41544 | mRpL12 | | Sc2 |
| CG7706 | CG32284 | | schuy |
| bun | Gs1l | | Sdhaf3 |
| CG31817 | Lgr3 | | Sirt2 |
| dsx-c73A | CG11777 | | Sld5 |
| Tsp42Ef | CG4557 | | snoRNA:Psi18S-531 |
| CG7564 | CG14499 | | spdo |
| CG18635 | mRpL36 | | SPH93 |
| PGRP-LF | CG12321 | | Spindly |
| CG14252 | CG8891 | | Spp |
| l(3)02640 | CG4627 | | sqa |
| CG30022 | CG34404 | | Ssb-c31a |
| CR45128 | hdm | | stg |
| Kif3C | Cisd2 | | Surf4 |
| Snap24 | CG8258 | | Taldo |
| ppk | CG11878 | | tam |
| CG34231 | pcl | | tej |
| Rab2 | beta4GalT7 | | tex |
| CG33710 | CG5167 | | Tgt |
| MFS14 | CG2254 | | toy |
| Rbcn-3B | dnd | | Tps1 |
| CG31431 | CG7837 | | TyrRS-m |
| CG4676 | Tgt | | upd2 |
| AhcyL2 | IntS4 | | Vha14-1 |
| mir-967 | Sc2 | | Vha36-1 |
| CG32371 | CG11912 | | vls |
| CkIIalpha-i1 | CG32201 | | w |
| Elp1 | toy | | |
| MFS3 | Gycalpha99B | | |
| CG10638 | Gr8a | | |
| CG17929 | CCHa1-R | | |
| CG17786 | CG8818 | | |
| CG32855 | DNApol-alpha50 | | |
| CG31347 | Irp-1A | | |
| CG9945 | Cyp1 | | |
| CG15760 | CG5569 | | |
| rost | CG31550 | | |
| CG33640 | rasp | | |
| CR44440 | Mdh2 | | |
| CG43925 | Cpr73D | | |
| CG11655 | CG10472 | | |

| | | | |
|---|---|---|---|
| GstE8 | CG32669 | | |
| lbm | Orc5 | | |
| ttm2 | CycE | | |
| CG3995 | CG13008 | | |
| CG11486 | Bap60 | | |
| CG3709 | CG34200 | | |
| row | CG30345 | | |
| CG8273 | CG14270 | | |
| stas | CG5010 | | |
| Pih1D1 | CG31126 | | |
| ric8a | Taldo | | |
| mdy | msb1l | | |
| CG3838 | Hydr1 | | |
| CR45939 | Eip63F-1 | | |
| lt | CG13324 | | |
| snoRNA:Psi18S-1086 | sqa | | |
| Naam | beta'COP | | |
| CG14074 | CG12825 | | |
| CG5114 | ND-B15 | | |
| CG30441 | Sdhaf3 | | |
| CG17687 | CG30283 | | |
| Atf6 | Mcm5 | | |
| CG6791 | Klp61F | | |
| Dat | cry | | |
| St3 | Hsp70Bbb | | |
| CG8492 | CG5214 | | |
| CG32450 | CG7889 | | |
| hog | CG14543 | | |
| CR46015 | aurB | | |
| Atac1 | ATPsynE | | |
| Ugt86Dc | mRpS11 | | |
| Cyp6d5 | snoRNA:Psi18S-531 | | |
| Gk2 | CG1236 | | |
| CG13088 | CG32483 | | |
| Muc14A | CG12129 | | |
| CG10730 | CR44868 | | |
| Smurf | schuy | | |
| CG12398 | Spindly | | |
| dpr1 | Mur29B | | |
| ITP | CG6454 | | |
| Sox102F | CG1907 | | |
| CG32486 | Mdr50 | | |

| | | | |
|---|---|---|---|
| CG6330 | CG17278 | | |
| CG33928 | msd5 | | |
| Hsc70-3 | Zw10 | | |
| CG6602 | Mcm2 | | |
| Pig1 | CG14104 | | |
| CG14443 | alpha-Est1 | | |
| CG32845 | CG13364 | | |
| CG4723 | DNApol-epsilon58 | | |
| PlexA | kappaTry | | |
| sstn | CG11403 | | |
| CG11000 | Vha14-1 | | |
| mir-4968 | ATPsynO | | |
| shams | CG9344 | | |
| bnl | CG7379 | | |
| CG2064 | CG30339 | | |
| CG3008 | spdo | | |
| CG8319 | Ndc1 | | |
| a | Npc2f | | |
| CR45171 | CG10939 | | |
| CG30440 | CR15061 | | |
| ebd1 | CG1942 | | |
| CG4462 | ox | | |
| CG14837 | CR44724 | | |
| CR44138 | CG43295 | | |
| CG3982 | CG17660 | | |
| CG30047 | CG10584 | | |
| ssx | CG17855 | | |
| CG42553 | CR44478 | | |
| CG3556 | caix | | |
| CG7966 | Ssb-c31a | | |
| Lcch3 | Gip | | |
| Ir85a | CG4839 | | |
| NC2alpha | Glo1 | | |
| sima | CG4194 | | |
| CR46249 | AIMP1 | | |
| CG15084 | ecd | | |
| Pzl | CG7470 | | |
| ppk27 | CG32091 | | |
| CR41583 | CG11899 | | |
| PGRP-SD | CG1287 | | |
| CG6628 | CG3906 | | |
| swa | AP-1-2beta | | |

| | | | |
|---|---|---|---|
| CG4404 | phyl | | |
| sinu | lectin-46Ca | | |
| CR44566 | Ctf4 | | |
| CG43968 | CG12237 | | |
| CG31627 | DNApol-alpha180 | | |
| CG42364 | SPH93 | | |
| CG8072 | CG13082 | | |
| CG6405 | CG31918 | | |
| CR45820 | E(spl)m2-BFM | | |
| bou | CG8562 | | |
| AOX2 | Hex-C | | |
| Tab2 | asp | | |
| CG12868 | Muc68Ca | | |
| snoRNA:Psi18S-1275 | CG7630 | | |
| Arc1 | CG16700 | | |
| Hexo2 | CR44692 | | |
| CG18599 | CG42714 | | |
| CG44405 | CCHa2 | | |
| CG14367 | mag | | |
| CG11656 | E(spl)m8-HLH | | |

**Table 2.4d: Pathway enrichment for hits differentially upregulated in 20HE males relative to control females**

| Pathway enrichment | p-value | Hits | Gene matches | Pathway ID |
|---|---|---|---|---|
| Galactose metabolism | 9.47362E-06 | FBgn0002569,FBgn0002570,FBgn0033294,FBgn0033297,FBgn0260746,FBgn0261575 | 6 | 52 |
| Starch and sucrose metabolism | 5.93946E-05 | FBgn0002569,FBgn0002570,FBgn0026755,FBgn0033294,FBgn0033297,FBgn0040256,FBgn0261575 | 7 | 500 |
| PI5P, PP2A and IER3 Regulate PI3K/AKT Signaling | 0.000454317 | FBgn0003984,FBgn0016794,FBgn0022800,FBgn0040068 | 4 | R-DME-6811558 |
| Negative regulation of the PI3K/AKT network | 0.000774174 | FBgn0003984,FBgn0016794,FBgn0022800,FBgn0040068 | 4 | R-DME-199418 |
| Metabolism of xenobiotics by cytochrome P450 | 0.003300173 | FBgn0010039,FBgn0010040,FBgn0010041,FBgn0026755,FBgn0040256 | 5 | 980 |
| Drug metabolism - | 0.003561307 | FBgn0010039,FBg | 5 | 982 |

| | | | | |
|---|---|---|---|---|
| cytochrome P450 | | n0010040,FBgn0010041,FBgn0026755,FBgn0040256 | | |
| PI3K events in ERBB2 signaling | 0.004529543 | FBgn0003984,FBgn0016794 | 2 | R-DME-1963642 |
| Nephrin family interactions | 0.004529543 | FBgn0000547,FBgn0028369 | 2 | R-DME-373753 |
| Signaling by Receptor Tyrosine Kinases | 0.005106565 | FBgn0003984,FBgn0014388,FBgn0016794,FBgn0022800,FBgn0027779,FBgn0040068,FBgn0052055,FBgn0262081,FBgn0283499 | 9 | R-DME-9006934 |
| Signaling by Insulin receptor | 0.005853482 | FBgn0016794,FBgn0022800,FBgn0027779,FBgn0283499 | 4 | R-DME-74752 |
| FLT3 Signaling | 0.009468478 | FBgn0003984,FBgn0016794,FBgn0022800,FBgn0262081,FBgn0265778 | 5 | R-DME-9607240 |
| Signaling by SCF-KIT | 0.010497272 | FBgn0022800,FBgn0040068 | 2 | R-DME-1433557 |
| Signaling by ERBB2 | 0.010688809 | FBgn0003984,FBgn0016794,FBgn0262081 | 3 | R-DME-1227986 |
| Signaling by EGFR | 0.0118715 | FBgn0014388,FBgn0016794,FBgn0052055 | 3 | R-DME-177929 |
| Aflatoxin activation and detoxification | 0.012969919 | FBgn0036986,FBgn0037818 | 2 | R-DME-5423646 |
| SUMOylation of intracellular receptors | 0.015669143 | FBgn0000568,FBgn0004865 | 2 | R-DME-4090294 |
| Signal Transduction | 0.017769782 | FBgn0000163,FBgn0000250,FBgn0000568,FBgn0001229,FBgn0003984,FBgn0014388,FBgn0016794,FBgn0019985,FBgn0022800,FBgn0023416,FBgn0027779,FBgn0030011,FBgn0030505,FBgn0031461,FBgn0031885,FBgn0034706,FBgn0036290,FBgn0036518,FBgn0040068,FBgn0052055,FBgn0085432,FBgn0262081,FBgn0265778,FBgn0283499 | 24 | R-DME-162582 |

| | | | | |
|---|---|---|---|---|
| Glutathione metabolism | 0.021811993 | FBgn0010039,FBgn0010040,FBgn0010041,FBgn0010044 | 4 | 480 |
| Ca2+ pathway | 0.022205774 | FBgn0030011,FBgn0030505,FBgn0085432 | 3 | R-DME-4086398 |
| Downregulation of ERBB2 signaling | 0.025040297 | FBgn0003984,FBgn0262081 | 2 | R-DME-8863795 |
| PI3K Cascade | 0.028560994 | FBgn0016794,FBgn0022800 | 2 | R-DME-109704 |
| Formation of the beta-catenin:TCF transactivating complex | 0.028560994 | FBgn0031885,FBgn0085432 | 2 | R-DME-201722 |
| RAF/MAP kinase cascade | 0.031215951 | FBgn0003984,FBgn0022800,FBgn0262081,FBgn0265778 | 4 | R-DME-5673001 |
| IRS-mediated signalling | 0.032266979 | FBgn0016794,FBgn0022800 | 2 | R-DME-112399 |
| IRS-related events triggered by IGF1R | 0.032266979 | FBgn0016794,FBgn0022800 | 2 | R-DME-2428928 |
| Surfactant metabolism | 0.032266979 | FBgn0032223,FBgn0263747 | 2 | R-DME-5683826 |
| MAPK1/MAPK3 signaling | 0.032726615 | FBgn0003984,FBgn0022800,FBgn0262081,FBgn0265778 | 4 | R-DME-5684996 |
| Transcriptional regulation of white adipocyte differentiation | 0.035453374 | FBgn0000568 | 1 | R-DME-381340 |
| TGF-beta receptor signaling in EMT (epithelial to mesenchymal transition) | 0.03615065 | FBgn0000163,FBgn0031461 | 2 | R-DME-2173791 |
| Signaling by Type 1 Insulin-like Growth Factor 1 Receptor (IGF1R) | 0.03615065 | FBgn0016794,FBgn0022800 | 2 | R-DME-2404192 |
| IGF1R signaling cascade | 0.03615065 | FBgn0016794,FBgn0022800 | 2 | R-DME-2428924 |
| Non-integrin membrane-ECM interactions | 0.040204616 | FBgn0031461,FBgn0053531 | 2 | R-DME-3000171 |
| Insulin receptor signalling cascade | 0.040204616 | FBgn0016794,FBgn0022800 | 2 | R-DME-74751 |
| MAPK family signaling cascades | 0.042682581 | FBgn0003984,FBgn0022800,FBgn0262081,FBgn0265778 | 4 | R-DME-5683057 |
| Presynaptic function of Kainate | 0.044421685 | FBgn0030011,FBgn0039927 | 2 | R-DME-500657 |

| | | | | |
|---|---|---|---|---|
| receptors | | | | |
| Signaling by FGFR4 | 0.048794866 | FBgn0014388,FBgn0016794 | 2 | R-DME-5654743 |

**Table 2.4f: Pathway enrichment for hits differentially upregulated in control females relative to 20HE males**

| p-value | Hits | Gene matches | Pathway ID |
|---|---|---|---|
| 0.007085029 | FBgn0003257,FBgn0011211,FBgn0011703,FBgn0011704,FBgn0011768,FBgn0014028,FBgn0015277,FBgn0025352,FBgn0025373,FBgn0025592,FBgn0028375,FBgn0029823,FBgn0030966,FBgn0031630,FBgn0031703,FBgn0032350,FBgn0033216,FBgn0033377,FBgn0034629,FBgn0034988,FBgn0035383,FBgn0035619,FBgn0036381,FBgn0036575,FBgn0037513,FBgn0037534,FBgn0037846,FBgn0037880,FBgn0037958,FBgn0038074,FBgn0038407,FBgn0038467,FBgn0038542,FBgn0038742,FBgn0039470,FBgn0039472,FBgn0039475,FBgn0039476,FBgn0040069,FBgn0050502,FBgn0052750,FBgn0053116,FBgn0283680 | 43 | R-DME-1430728 |
| 0.015922058 | FBgn0003257,FBgn0011211,FBgn0011703,FBgn0011704,FBgn0011768,FBgn0014028,FBgn0015277,FBgn0015572,FBgn0024957,FBgn0025352,FBgn0025373,FBgn0025592,FBgn0029823,FBgn0029906,FBgn0031703,FBgn0031713,FBgn0032350,FBgn0033377,FBgn0034629,FBgn0035619,FBgn0037356,FBgn0037513,FBgn0037958,FBgn0038467,FBgn0038613,FBgn0038742,FBgn0039094,FBgn0039580,FBgn0040069,FBgn0053116,FBgn0053138,FBgn0259676,FBgn0283680 | 33 | 1100 |
| 0.001805804 | FBgn0015277,FBgn0025352,FBgn0025373,FBgn0025592,FBgn0031630,FBgn0031703,FBgn0033216,FBgn0034629,FBgn0035383,FBgn0035619,FBgn0036381,FBgn0037534,FBgn0037958,FBgn0038407,FBgn0038742,FBgn0039470,FBgn0039472,FBgn0039475,FBgn0039476,FBgn0050502,FBgn0053116 | 21 | R-DME-556833 |
| 0.030596156 | FBgn0011692,FBgn0015553,FBgn0020633,FBgn0025815,FBgn0025832,FBgn0026143,FBgn0027868,FBgn0029856,FBgn0032244,FBgn0032929,FBgn0041147,FBgn0259676,FBgn0259791,FBgn0286788 | 14 | R-DME-1640170 |
| 0.031251957 | FBgn0011692,FBgn0020633,FBgn0025815,FBgn0025832,FBgn0026143,FBgn0027868,FBgn0029856,FBgn0032244,FBgn0032929,FBgn0041147,FBgn0259676,FBgn0259791,FBgn0286788 | 13 | R-DME-69278 |
| 0.001804544 | FBgn0015277,FBgn0025352,FBgn0033216,FBgn0035619,FBgn0036381,FBgn0039470,FBgn0039472,FBgn0039475,FBgn0039476,FBgn0053116 | 10 | R-DME-1483257 |
| 0.003289324 | FBgn0020633,FBgn0025815,FBgn0025832,FBgn0026143,FBgn0029856,FBgn0032244,FBgn0032929,FBgn0041147,FBgn0259676,FBgn0286788 | 10 | R-DME-69306 |
| 0.044828241 | FBgn0013548,FBgn0015553,FBgn0025832,FBgn0029856,FBgn0032244,FBgn0033549,FBgn0037345,FBgn0040078,FBgn0261850,FBgn0267727 | 10 | R-DME-73894 |
| 0.000634202 | FBgn0025352,FBgn0033216,FBgn0035619,FBgn0036381,FBgn0039470,FBgn0039472,FBgn0039475,FBgn0039476,FBgn0053116 | 9 | R-DME-1483206 |
| 0.011319054 | FBgn0015553,FBgn0020633,FBgn0025815,FBgn0026143,FBgn0029856,FBgn0032244,FBgn0032929,FBgn0041147,FBgn0286788 | 9 | R-DME-69620 |
| 0.008223325 | FBgn0025352,FBgn0031703,FBgn0033216,FBgn0034629,FBgn0035383,FBgn0037534,FBgn0038407,FBgn0038742 | 8 | R-DME-8978868 |
| 0.015222878 | FBgn0020633,FBgn0025815,FBgn0025832,FBgn0029856,FBgn0032244,FBgn0041147,FBgn0259676,FBgn0286788 | 8 | R-DME-69239 |
| 0.02764 | FBgn0020633,FBgn0025815,FBgn0025832,FBgn0029856,FBgn0032 | 8 | R-DME- |

| | | | |
|---|---|---|---|
| 311 | 244,FBgn0041147,FBgn0259676,FBgn0286788 | | 69242 |
| 0.00112775 | FBgn0015553,FBgn0020633,FBgn0025815,FBgn0026143,FBgn0032244,FBgn0032929,FBgn0286788 | 7 | R-DME-69481 |
| 0.010713028 | FBgn0020633,FBgn0025815,FBgn0026143,FBgn0029856,FBgn0032929,FBgn0259676,FBgn0286788 | 7 | R-DME-69002 |
| 0.03771378 | FBgn0020633,FBgn0025815,FBgn0026143,FBgn0029856,FBgn0032929,FBgn0259676,FBgn0286788 | 7 | R-DME-69206 |
| 0.000631673 | FBgn0011768,FBgn0025352,FBgn0031703,FBgn0034629,FBgn0035383,FBgn0038742 | 6 | 71 |
| 0.000631673 | FBgn0020633,FBgn0025815,FBgn0026143,FBgn0032929,FBgn0259676,FBgn0286788 | 6 | R-DME-68962 |
| 0.000799516 | FBgn0020633,FBgn0025815,FBgn0026143,FBgn0032244,FBgn0032929,FBgn0286788 | 6 | R-DME-176187 |
| 0.00099984 | FBgn0020633,FBgn0025815,FBgn0025832,FBgn0031252,FBgn0032244,FBgn0259676 | 6 | 3030 |
| 0.009716104 | FBgn0003257,FBgn0011703,FBgn0011704,FBgn0034988,FBgn0037513,FBgn0038467 | 6 | R-DME-15869 |
| 0.044702805 | FBgn0003257,FBgn0011703,FBgn0011704,FBgn0020653,FBgn0037513,FBgn0259676 | 6 | 240 |
| 0.00859338 | FBgn0035619,FBgn0039470,FBgn0039472,FBgn0039475,FBgn0039476 | 5 | R-DME-1483166 |
| 0.030209845 | FBgn0015553,FBgn0025832,FBgn0032244,FBgn0033549,FBgn0267727 | 5 | R-DME-5693532 |
| 0.006791084 | FBgn0039470,FBgn0039472,FBgn0039475,FBgn0039476 | 4 | R-DME-1482801 |
| 0.008419111 | FBgn0029823,FBgn0032350,FBgn0038074,FBgn0039094 | 4 | 260 |
| 0.03080024 | FBgn0022700,FBgn0033377,FBgn0034582,FBgn0039580 | 4 | 520 |
| 0.039263616 | FBgn0013548,FBgn0029856,FBgn0032244,FBgn0037345 | 4 | R-DME-73893 |
| 0.043945631 | FBgn0015553,FBgn0025832,FBgn0032244,FBgn0033549 | 4 | R-DME-5693538 |
| 0.043945631 | FBgn0029856,FBgn0031092,FBgn0033812,FBgn0034629 | 4 | R-DME-9033241 |
| 0.009447184 | FBgn0025352,FBgn0031703,FBgn0038742 | 3 | R-DME-77289 |
| 0.020310018 | FBgn0010425,FBgn0011555,FBgn0030954 | 3 | 4080 |
| 0.020310018 | FBgn0029856,FBgn0032244,FBgn0037345 | 3 | R-DME-110312 |
| 0.020310018 | FBgn0029856,FBgn0032244,FBgn0037345 | 3 | R-DME-5655862 |
| 0.020310018 | FBgn0029856,FBgn0032244,FBgn0037345 | 3 | R-DME-5656121 |
| 0.02497991 | FBgn0025832,FBgn0032244,FBgn0259676 | 3 | R-DME-69186 |
| 0.035898487 | FBgn0025832,FBgn0032244,FBgn0259676 | 3 | R-DME-69190 |
| 0.035898487 | FBgn0022700,FBgn0035619,FBgn0261675 | 3 | R-DME-8963743 |
| 0.002175169 | FBgn0025352,FBgn0038742 | 2 | R-DME-77350 |
| 0.012261509 | FBgn0025352,FBgn0038742 | 2 | R-DME-77286 |

| | | | |
|---|---|---|---|
| 0.01226 1509 | FBgn0038135,FBgn0051343 | 2 | R-DME-983170 |
| 0.01981 1617 | FBgn0031630,FBgn0033216 | 2 | R-DME-2187335 |
| 0.01981 1617 | FBgn0038312,FBgn0038412 | 2 | R-DME-435354 |
| 0.01981 1617 | FBgn0038312,FBgn0038412 | 2 | R-DME-442380 |
| 0.02881 3137 | FBgn0034988,FBgn0037513 | 2 | R-DME-73621 |
| 0.03911 5641 | FBgn0036381,FBgn0053116 | 2 | R-DME-1483213 |
| 0.03911 5641 | FBgn0032244,FBgn0259676 | 2 | R-DME-174411 |
| 0.03911 5641 | FBgn0032244,FBgn0259676 | 2 | R-DME-69091 |
| 0.03911 5641 | FBgn0032244,FBgn0259676 | 2 | R-DME-69109 |
| 0.04679 7212 | FBgn0040069 | 1 | 780 |
| 0.04679 7212 | FBgn0051915 | 1 | R-DME-1474290 |
| 0.04679 7212 | FBgn0051915 | 1 | R-DME-1650814 |
| 0.04679 7212 | FBgn0038542 | 1 | R-DME-392023 |
| 0.04679 7212 | FBgn0028375 | 1 | R-DME-6806664 |
| 0.04679 7212 | FBgn0029823 | 1 | R-DME-71262 |
| 0.04679 7212 | FBgn0011768 | 1 | R-DME-71384 |
| 0.04679 7212 | FBgn0025352 | 1 | R-DME-77285 |
| 0.04679 7212 | FBgn0025352 | 1 | R-DME-77310 |
| 0.04679 7212 | FBgn0038742 | 1 | R-DME-77352 |

**Table 2.4e: GO enrichment for hits differentially upregulated in 20HE males relative to control females**

| GO enrichment | p-value | Hits | Gene matches | GO ID |
|---|---|---|---|---|
| multicellular organismal process | 0.0032011 | FBgn0000152,FBgn0000163,FBgn0000250,FBgn0000395,FBgn0000451,FBgn0000542,FBgn0000547,FBgn0000568,FBgn0000826,FBgn0000928,FBgn0001112,FBgn0001234,FBgn0002566,FBgn0002609,FBgn0002632,FBgn0002633,FBgn0002643,FBgn0002732,FBgn0003984,FBgn0004893,FBgn0010238,FBgn0010501,FBgn0010768,FBgn0011674,FBgn0014073,FBgn0014388,FBgn0015229,FBgn0015946,FBgn0016794,FBgn0019985,FBgn0020300,FBgn0022800,FBgn00 | 89 | GO:0032501 |

| | | | | |
|---|---|---|---|---|
| | | 24250,FBgn0024555,FBgn0026263, FBgn0026319,FBgn0027779,FBgn00 28369,FBgn0029082,FBgn0030985, FBgn0031461,FBgn0031853,FBgn00 31885,FBgn0033404,FBgn0033773, FBgn0033942,FBgn0033985,FBgn00 34098,FBgn0034199,FBgn0034262, FBgn0035461,FBgn0035513,FBgn00 35626,FBgn0036282,FBgn0036518, FBgn0036666,FBgn0036732,FBgn00 36801,FBgn0037802,FBgn0038168, FBgn0038832,FBgn0039469,FBgn00 39509,FBgn0040068,FBgn0040532, FBgn0041160,FBgn0041241,FBgn00 41246,FBgn0045474,FBgn0045842, FBgn0046332,FBgn0052133,FBgn00 52179,FBgn0052354,FBgn0052364, FBgn0053527,FBgn0053531,FBgn00 85430,FBgn0085432,FBgn0259683, FBgn0262081,FBgn0265778,FBgn02 66084,FBgn0267390,FBgn0283451, FBgn0283499,FBgn0283545,FBgn02 86203,FBgn0287185 | | |
| response to stimulus | 0.00265597 | FBgn0000250,FBgn0000395,FBgn00 00547,FBgn0000568,FBgn0001229, FBgn0001234,FBgn0002566,FBgn00 02632,FBgn0002643,FBgn0002732, FBgn0002939,FBgn0003984,FBgn00 04580,FBgn0004832,FBgn0010501, FBgn0010768,FBgn0011674,FBgn00 13973,FBgn0014009,FBgn0014073, FBgn0014388,FBgn0015946,FBgn00 16794,FBgn0019985,FBgn0020300, FBgn0022800,FBgn0023416,FBgn00 24250,FBgn0024555,FBgn0025625, FBgn0026319,FBgn0026777,FBgn00 29082,FBgn0029825,FBgn0029968, FBgn0030011,FBgn0030286,FBgn00 30505,FBgn0031016,FBgn0031461, FBgn0031757,FBgn0031885,FBgn00 33132,FBgn0033404,FBgn0033773, FBgn0033885,FBgn0033980,FBgn00 33985,FBgn0034199,FBgn0034200, FBgn0034262,FBgn0034647,FBgn00 35626,FBgn0036518,FBgn0036732, FBgn0037007,FBgn0037163,FBgn00 37442,FBgn0040068,FBgn0040384, FBgn0040849,FBgn0041160,FBgn00 45842,FBgn0052133,FBgn0052179, FBgn0052638,FBgn0052706,FBgn00 53329,FBgn0053527,FBgn0053531, FBgn0085430,FBgn0085432,FBgn02 59683,FBgn0261794,FBgn0262081, FBgn0265778,FBgn0266084,FBgn02 67390,FBgn0283451,FBgn0283499 | 80 | GO:00 50896 |
| developmental process | 0.01555884 | FBgn0000163,FBgn0000250,FBgn00 00395,FBgn0000451,FBgn0000542, | 78 | GO:00 32502 |

| | | | | |
|---|---|---|---|---|
| | | FBgn0000547,FBgn0000568,FBgn0000826,FBgn0000928,FBgn0001112,FBgn0001234,FBgn0002566,FBgn0002609,FBgn0002632,FBgn0002633,FBgn0002643,FBgn0002732,FBgn0003984,FBgn0004893,FBgn0010238,FBgn0010501,FBgn0010768,FBgn0011674,FBgn0014073,FBgn0014388,FBgn0015229,FBgn0015946,FBgn0016794,FBgn0022800,FBgn0024250,FBgn0024555,FBgn0026263,FBgn0026319,FBgn0027779,FBgn0028369,FBgn0029082,FBgn0031461,FBgn0031853,FBgn0031885,FBgn0032223,FBgn0033773,FBgn0033942,FBgn0033985,FBgn0034098,FBgn0034199,FBgn0034262,FBgn0035461,FBgn0035513,FBgn0035626,FBgn0036282,FBgn0036518,FBgn0036666,FBgn0036732,FBgn0036801,FBgn0037802,FBgn0038168,FBgn0039048,FBgn0039469,FBgn0040068,FBgn0040532,FBgn0041160,FBgn0045842,FBgn0052133,FBgn0052179,FBgn0052354,FBgn0052364,FBgn0053531,FBgn0085430,FBgn0085432,FBgn0261245,FBgn0262081,FBgn0265778,FBgn0266084,FBgn0267390,FBgn0283451,FBgn0283499,FBgn0286203,FBgn0287185 | | |
| anatomical structure development | 0.00650427 | FBgn0000163,FBgn0000250,FBgn0000395,FBgn0000451,FBgn0000542,FBgn0000547,FBgn0000568,FBgn0000826,FBgn0000928,FBgn0001112,FBgn0001234,FBgn0002566,FBgn0002609,FBgn0002632,FBgn0002633,FBgn0002643,FBgn0002732,FBgn0003984,FBgn0004893,FBgn0010238,FBgn0010501,FBgn0010768,FBgn0011674,FBgn0014073,FBgn0014388,FBgn0015229,FBgn0015946,FBgn0016794,FBgn0022800,FBgn0024250,FBgn0024555,FBgn0026263,FBgn0026319,FBgn0027779,FBgn0028369,FBgn0029082,FBgn0031461,FBgn0031853,FBgn0031885,FBgn0033773,FBgn0033942,FBgn0033985,FBgn0034098,FBgn0034262,FBgn0035461,FBgn0035513,FBgn0035626,FBgn0036282,FBgn0036518,FBgn0036666,FBgn0036732,FBgn0036801,FBgn0037802,FBgn0038168,FBgn0039048,FBgn0039469,FBgn0040068,FBgn0040532,FBgn0041160,FBgn0045842,FBgn0052133,FBgn0052179,FBgn0052354,FBgn0052364,FBgn0053531,FBgn0085430,FBgn0085432,FBgn02 | 76 | GO:0048856 |

| | | | | |
|---|---|---|---|---|
| | | 61245,FBgn0262081,FBgn0265778, FBgn0266084,FBgn0267390,FBgn02 83451,FBgn0283499,FBgn0286203, FBgn0287185 | | |
| multicellular organism development | 0.00675677 | FBgn0000163,FBgn0000250,FBgn00 00395,FBgn0000451,FBgn0000542, FBgn0000547,FBgn0000568,FBgn00 00826,FBgn0001112,FBgn0002566, FBgn0002609,FBgn0002632,FBgn00 02633,FBgn0002643,FBgn0002732, FBgn0003984,FBgn0004893,FBgn00 10238,FBgn0010501,FBgn0010768, FBgn0011674,FBgn0014073,FBgn00 14388,FBgn0015229,FBgn0015946, FBgn0016794,FBgn0022800,FBgn00 24250,FBgn0024555,FBgn0026263, FBgn0026319,FBgn0027779,FBgn00 28369,FBgn0029082,FBgn0031461, FBgn0031853,FBgn0031885,FBgn00 33942,FBgn0033985,FBgn0034098, FBgn0034262,FBgn0035461,FBgn00 35513,FBgn0036282,FBgn0036518, FBgn0036666,FBgn0036732,FBgn00 36801,FBgn0037802,FBgn0038168, FBgn0039469,FBgn0040068,FBgn00 40532,FBgn0041160,FBgn0045842, FBgn0052133,FBgn0052179,FBgn00 52354,FBgn0053531,FBgn0085430, FBgn0085432,FBgn0262081,FBgn02 65778,FBgn0266084,FBgn0267390, FBgn0283451,FBgn0283499,FBgn02 86203,FBgn0287185 | 69 | GO:00 07275 |
| cell communication | 0.00251377 | FBgn0000250,FBgn0000395,FBgn00 00547,FBgn0000568,FBgn0001234, FBgn0002566,FBgn0002632,FBgn00 02643,FBgn0002732,FBgn0002939, FBgn0003984,FBgn0004580,FBgn00 10501,FBgn0013973,FBgn0014009, FBgn0014073,FBgn0014388,FBgn00 15946,FBgn0016794,FBgn0019985, FBgn0022800,FBgn0023416,FBgn00 24250,FBgn0025625,FBgn0026319, FBgn0029082,FBgn0030011,FBgn00 30286,FBgn0030505,FBgn0031016, FBgn0031461,FBgn0031885,FBgn00 33773,FBgn0033885,FBgn0033985, FBgn0034199,FBgn0034200,FBgn00 34262,FBgn0034647,FBgn0035626, FBgn0036518,FBgn0036732,FBgn00 37007,FBgn0037163,FBgn0039927, FBgn0040068,FBgn0052179,FBgn00 52638,FBgn0053527,FBgn0053531, FBgn0085432,FBgn0262081,FBgn02 65778,FBgn0267390,FBgn0283499 | 55 | GO:00 07154 |
| signaling | 0.00223074 | FBgn0000250,FBgn0000395,FBgn00 00547,FBgn0000568,FBgn0001234, FBgn0002632,FBgn0002643,FBgn00 | 54 | GO:00 23052 |

| | | | | |
|---|---|---|---|---|
| | | 02732,FBgn0002939,FBgn0003984, FBgn0004580,FBgn0010501,FBgn00 13973,FBgn0014009,FBgn0014073, FBgn0014388,FBgn0015946,FBgn00 16794,FBgn0019985,FBgn0022800, FBgn0023416,FBgn0024250,FBgn00 25625,FBgn0026319,FBgn0029082, FBgn0030011,FBgn0030286,FBgn00 30505,FBgn0031016,FBgn0031461, FBgn0031885,FBgn0033773,FBgn00 33885,FBgn0033985,FBgn0034199, FBgn0034200,FBgn0034262,FBgn00 34647,FBgn0035626,FBgn0036518, FBgn0036732,FBgn0037007,FBgn00 37163,FBgn0039927,FBgn0040068, FBgn0052179,FBgn0052638,FBgn00 53527,FBgn0053531,FBgn0085432, FBgn0262081,FBgn0265778,FBgn02 67390,FBgn0283499 | | |
| cellular response to stimulus | 0.00087659 | FBgn0000250,FBgn0000395,FBgn00 00568,FBgn0001229,FBgn0001234, FBgn0002566,FBgn0002643,FBgn00 02939,FBgn0003984,FBgn0004832, FBgn0010501,FBgn0013973,FBgn00 14009,FBgn0014073,FBgn0014388, FBgn0015946,FBgn0016794,FBgn00 19985,FBgn0022800,FBgn0023416, FBgn0024250,FBgn0024555,FBgn00 25625,FBgn0026319,FBgn0026777, FBgn0029825,FBgn0030011,FBgn00 30286,FBgn0031016,FBgn0031461, FBgn0031885,FBgn0033132,FBgn00 33885,FBgn0033985,FBgn0034199, FBgn0034200,FBgn0034262,FBgn00 35626,FBgn0036518,FBgn0036732, FBgn0037007,FBgn0037163,FBgn00 40068,FBgn0052179,FBgn0052638, FBgn0053527,FBgn0053531,FBgn00 85432,FBgn0261794,FBgn0265778, FBgn0267390,FBgn0283451,FBgn02 83499 | 53 | GO:00 51716 |
| cellular developmental process | 0.01542028 | FBgn0000163,FBgn0000250,FBgn00 00542,FBgn0000547,FBgn0000568, FBgn0000928,FBgn0001234,FBgn00 02609,FBgn0002632,FBgn0002633, FBgn0002643,FBgn0002732,FBgn00 03984,FBgn0010501,FBgn0010768, FBgn0011674,FBgn0014073,FBgn00 14388,FBgn0015946,FBgn0016794, FBgn0024555,FBgn0026319,FBgn00 28369,FBgn0029082,FBgn0031461, FBgn0031853,FBgn0032223,FBgn00 33773,FBgn0033985,FBgn0034098, FBgn0035461,FBgn0035626,FBgn00 36282,FBgn0036518,FBgn0036666, FBgn0038168,FBgn0039048,FBgn00 40068,FBgn0041160,FBgn0045842, | 52 | GO:00 48869 |

| | | | | |
|---|---|---|---|---|
| | | FBgn0052179,FBgn0052354,FBgn0052364,FBgn0085430,FBgn0085432,FBgn0261245,FBgn0262081,FBgn0265778,FBgn0266084,FBgn0267390,FBgn0283451,FBgn0283499 | | |
| cell differentiation | 0.01475489 | FBgn0000163,FBgn0000250,FBgn0000542,FBgn0000547,FBgn0000568,FBgn0000928,FBgn0001234,FBgn0002609,FBgn0002632,FBgn0002633,FBgn0002643,FBgn0002732,FBgn0003984,FBgn0010501,FBgn0010768,FBgn0011674,FBgn0014073,FBgn0014388,FBgn0015946,FBgn0016794,FBgn0024555,FBgn0026319,FBgn0028369,FBgn0029082,FBgn0031461,FBgn0031853,FBgn0032223,FBgn0033773,FBgn0033985,FBgn0034098,FBgn0035461,FBgn0035626,FBgn0036282,FBgn0036518,FBgn0036666,FBgn0038168,FBgn0040068,FBgn0041160,FBgn0045842,FBgn0052179,FBgn0052354,FBgn0052364,FBgn0085430,FBgn0085432,FBgn0261245,FBgn0262081,FBgn0265778,FBgn0266084,FBgn0267390,FBgn0283451,FBgn0283499 | 51 | GO:0030154 |
| signal transduction | 0.00080948 | FBgn0000250,FBgn0000395,FBgn0000547,FBgn0000568,FBgn0001234,FBgn0002632,FBgn0002643,FBgn0002732,FBgn0002939,FBgn0003984,FBgn0013973,FBgn0014009,FBgn0014073,FBgn0014388,FBgn0015946,FBgn0016794,FBgn0019985,FBgn0022800,FBgn0023416,FBgn0024250,FBgn0025625,FBgn0026319,FBgn0029082,FBgn0030011,FBgn0030286,FBgn0031016,FBgn0031461,FBgn0031885,FBgn0033773,FBgn0033885,FBgn0033985,FBgn0034199,FBgn0034200,FBgn0034262,FBgn0034647,FBgn0035626,FBgn0036518,FBgn0036732,FBgn0037007,FBgn0037163,FBgn0040068,FBgn0052179,FBgn0052638,FBgn0053527,FBgn0053531,FBgn0085432,FBgn0262081,FBgn0265778,FBgn0267390,FBgn0283499 | 50 | GO:0007165 |
| multi-organism process | 0.02079769 | FBgn0000152,FBgn0000163,FBgn0000250,FBgn0000547,FBgn0000568,FBgn0000826,FBgn0000927,FBgn0000928,FBgn0001112,FBgn0001234,FBgn0002643,FBgn0003984,FBgn0010501,FBgn0011674,FBgn0014073,FBgn0014388,FBgn0015946,FBgn0019985,FBgn0026319,FBgn0031853,FBgn0033773,FBgn0033980,FBgn0034098,FBgn0034199,FBgn0034647,FBgn0035461,FBgn0035626,FBgn00 | 44 | GO:0051704 |

| | | | | |
|---|---|---|---|---|
| | | 40068,FBgn0040384,FBgn0041246, FBgn0045842,FBgn0046332,FBgn00 52133,FBgn0052179,FBgn0052364, FBgn0052706,FBgn0053329,FBgn00 53527,FBgn0262081,FBgn0265778, FBgn0267390,FBgn0283451,FBgn02 83499,FBgn0283545 | | |
| regulation of cell communication | 0.01419327 | FBgn0000250,FBgn0000395,FBgn00 00547,FBgn0001234,FBgn0002632, FBgn0002732,FBgn0003984,FBgn00 04580,FBgn0010501,FBgn0013973, FBgn0014388,FBgn0016794,FBgn00 19985,FBgn0024250,FBgn0026319, FBgn0029082,FBgn0030286,FBgn00 30505,FBgn0031016,FBgn0031461, FBgn0031885,FBgn0033773,FBgn00 33885,FBgn0033985,FBgn0034199, FBgn0034647,FBgn0035626,FBgn00 39927,FBgn0040068,FBgn0262081, FBgn0283499 | 31 | GO:00 10646 |
| regulation of signaling | 0.01419327 | FBgn0000250,FBgn0000395,FBgn00 00547,FBgn0001234,FBgn0002632, FBgn0002732,FBgn0003984,FBgn00 04580,FBgn0010501,FBgn0013973, FBgn0014388,FBgn0016794,FBgn00 19985,FBgn0024250,FBgn0026319, FBgn0029082,FBgn0030286,FBgn00 30505,FBgn0031016,FBgn0031461, FBgn0031885,FBgn0033773,FBgn00 33885,FBgn0033985,FBgn0034199, FBgn0034647,FBgn0035626,FBgn00 39927,FBgn0040068,FBgn0262081, FBgn0283499 | 31 | GO:00 23051 |
| cell surface receptor signaling pathway | 0.0125462 | FBgn0000250,FBgn0000395,FBgn00 00547,FBgn0002632,FBgn0002643, FBgn0002732,FBgn0003984,FBgn00 14073,FBgn0014388,FBgn0016794, FBgn0019985,FBgn0022800,FBgn00 24250,FBgn0025625,FBgn0026319, FBgn0029082,FBgn0031016,FBgn00 31461,FBgn0033985,FBgn0035626, FBgn0040068,FBgn0052179,FBgn00 53531,FBgn0085432,FBgn0283499 | 25 | GO:00 07166 |
| intracellular signal transduction | 0.01656247 | FBgn0000547,FBgn0001234,FBgn00 03984,FBgn0013973,FBgn0014009, FBgn0014388,FBgn0015946,FBgn00 16794,FBgn0023416,FBgn0025625, FBgn0026319,FBgn0030286,FBgn00 31885,FBgn0033773,FBgn0033885, FBgn0033985,FBgn0034199,FBgn00 34262,FBgn0036518,FBgn0040068, FBgn0262081,FBgn0265778,FBgn02 67390,FBgn0283499 | 24 | GO:00 35556 |
| post-embryonic development | 0.02584292 | FBgn0000395,FBgn0000547,FBgn00 00568,FBgn0001112,FBgn0002643, FBgn0003984,FBgn0004893,FBgn00 14388,FBgn0015946,FBgn0024250, | 24 | GO:00 09791 |

| | | | | |
|---|---|---|---|---|
| | | FBgn0026263,FBgn0026319,FBgn0028369,FBgn0031461,FBgn0031885,FBgn0034262,FBgn0036518,FBgn0036732,FBgn0036801,FBgn0085432,FBgn0265778,FBgn0266084,FBgn0283451,FBgn0287185 | | |
| phosphorylation | 0.02714477 | FBgn0000826,FBgn0001229,FBgn0001234,FBgn0003984,FBgn0014073,FBgn0014388,FBgn0022800,FBgn0025625,FBgn0026319,FBgn0031461,FBgn0031885,FBgn0032702,FBgn0033773,FBgn0033885,FBgn0034199,FBgn0034251,FBgn0040068,FBgn0046332,FBgn0053531,FBgn0262081,FBgn0265778,FBgn0267390,FBgn0283499 | 23 | GO:0016310 |
| morphogenesis of an epithelium | 0.04646577 | FBgn0000163,FBgn0000395,FBgn0000542,FBgn0000547,FBgn0002643,FBgn0003984,FBgn0004893,FBgn0010238,FBgn0014388,FBgn0024250,FBgn0026319,FBgn0029082,FBgn0031461,FBgn0031885,FBgn0036518,FBgn0036666,FBgn0036801,FBgn0040068,FBgn0052179,FBgn0085432,FBgn0265778,FBgn0266084 | 22 | GO:0002009 |
| protein phosphorylation | 0.0038016 | FBgn0000826,FBgn0001229,FBgn0001234,FBgn0003984,FBgn0014073,FBgn0014388,FBgn0022800,FBgn0025625,FBgn0026319,FBgn0031461,FBgn0031885,FBgn0032702,FBgn0033773,FBgn0034199,FBgn0040068,FBgn0046332,FBgn0053531,FBgn0262081,FBgn0265778,FBgn0267390,FBgn0283499 | 21 | GO:0006468 |
| epithelial cell differentiation | 0.027283 | FBgn0000163,FBgn0000250,FBgn0000547,FBgn0000928,FBgn0002643,FBgn0003984,FBgn0014073,FBgn0014388,FBgn0026319,FBgn0029082,FBgn0031461,FBgn0036518,FBgn0040068,FBgn0052179,FBgn0267390,FBgn0283451,FBgn0283499 | 17 | GO:0030855 |
| regulation of cell differentiation | 0.03410763 | FBgn0000250,FBgn0000542,FBgn0000547,FBgn0002609,FBgn0002633,FBgn0003984,FBgn0014073,FBgn0014388,FBgn0028369,FBgn0031461,FBgn0033985,FBgn0038168,FBgn0052179,FBgn0085430,FBgn0265778,FBgn0266084,FBgn0283499 | 17 | GO:0045595 |
| enzyme linked receptor protein signaling pathway | 0.00203711 | FBgn0000395,FBgn0000547,FBgn0003984,FBgn0014073,FBgn0014388,FBgn0016794,FBgn0022800,FBgn0024250,FBgn0025625,FBgn0031016,FBgn0031461,FBgn0035626,FBgn0040068,FBgn0052179,FBgn0053531,FBgn0283499 | 16 | GO:0007167 |
| regulation of catalytic activity | 0.02438309 | FBgn0014073,FBgn0014388,FBgn0015946,FBgn0022800,FBgn0026319, | 16 | GO:0050790 |

| | | | | |
|---|---|---|---|---|
| | | FBgn0029082,FBgn0030286,FBgn0032702,FBgn0035461,FBgn0037772,FBgn0040068,FBgn0040348,FBgn0053531,FBgn0265778,FBgn0267390,FBgn0283499 | | |
| regulation of cell development | 0.03754967 | FBgn0000542,FBgn0000547,FBgn0002609,FBgn0002633,FBgn0003984,FBgn0014073,FBgn0014388,FBgn0031461,FBgn0033985,FBgn0038168,FBgn0052179,FBgn0085430,FBgn0265778,FBgn0266084,FBgn0283499 | 15 | GO:0060284 |
| regulation of phosphorylation | 0.00721047 | FBgn0001234,FBgn0003984,FBgn0014073,FBgn0014388,FBgn0022800,FBgn0026319,FBgn0031461,FBgn0031885,FBgn0032702,FBgn0033773,FBgn0034199,FBgn0040068,FBgn0053531,FBgn0283499 | 14 | GO:0042325 |
| regulation of phosphate metabolic process | 0.01338992 | FBgn0001234,FBgn0003984,FBgn0014073,FBgn0014388,FBgn0022800,FBgn0026319,FBgn0031461,FBgn0031885,FBgn0032702,FBgn0033773,FBgn0034199,FBgn0040068,FBgn0053531,FBgn0283499 | 14 | GO:0019220 |
| regulation of phosphorus metabolic process | 0.01338992 | FBgn0001234,FBgn0003984,FBgn0014073,FBgn0014388,FBgn0022800,FBgn0026319,FBgn0031461,FBgn0031885,FBgn0032702,FBgn0033773,FBgn0034199,FBgn0040068,FBgn0053531,FBgn0283499 | 14 | GO:0051174 |
| cell fate commitment | 0.01527561 | FBgn0000163,FBgn0000547,FBgn0002632,FBgn0002643,FBgn0002732,FBgn0003984,FBgn0011674,FBgn0016794,FBgn0024555,FBgn0026319,FBgn0031461,FBgn0032223,FBgn0085432,FBgn0283451 | 14 | GO:0045165 |
| cellular response to organic substance | 0.04264694 | FBgn0000395,FBgn0000568,FBgn0014388,FBgn0024250,FBgn0025625,FBgn0026319,FBgn0031016,FBgn0031461,FBgn0034199,FBgn0035626,FBgn0036732,FBgn0052638,FBgn0283451,FBgn0283499 | 14 | GO:0071310 |
| transmembrane receptor protein tyrosine kinase signaling pathway | 0.00738567 | FBgn0000547,FBgn0003984,FBgn0014073,FBgn0014388,FBgn0016794,FBgn0022800,FBgn0025625,FBgn0031016,FBgn0035626,FBgn0040068,FBgn0052179,FBgn0053531,FBgn0283499 | 13 | GO:0007169 |
| positive regulation of cellular protein metabolic process | 0.02486577 | FBgn0001229,FBgn0001234,FBgn0003984,FBgn0015946,FBgn0026319,FBgn0029082,FBgn0031461,FBgn0031885,FBgn0033773,FBgn0034199,FBgn0035461,FBgn0040068,FBgn0283499 | 13 | GO:0032270 |
| positive regulation of protein metabolic process | 0.03793025 | FBgn0001229,FBgn0001234,FBgn0003984,FBgn0015946,FBgn0026319,FBgn0029082,FBgn0031461,FBgn0031885,FBgn0033773,FBgn0034199, | 13 | GO:0051247 |

| | | | | |
|---|---|---|---|---|
| | | FBgn0035461,FBgn0040068,FBgn0283499 | | |
| positive regulation of phosphorylation | 0.00021974 | FBgn0001234,FBgn0003984,FBgn0014073,FBgn0022800,FBgn0026319,FBgn0031461,FBgn0031885,FBgn0033773,FBgn0034199,FBgn0040068,FBgn0053531,FBgn0283499 | 12 | GO:0042327 |
| positive regulation of phosphorus metabolic process | 0.00033108 | FBgn0001234,FBgn0003984,FBgn0014073,FBgn0022800,FBgn0026319,FBgn0031461,FBgn0031885,FBgn0033773,FBgn0034199,FBgn0040068,FBgn0053531,FBgn0283499 | 12 | GO:0010562 |
| positive regulation of phosphate metabolic process | 0.00033108 | FBgn0001234,FBgn0003984,FBgn0014073,FBgn0022800,FBgn0026319,FBgn0031461,FBgn0031885,FBgn0033773,FBgn0034199,FBgn0040068,FBgn0053531,FBgn0283499 | 12 | GO:0045937 |
| positive regulation of catalytic activity | 0.00738567 | FBgn0014073,FBgn0015946,FBgn0022800,FBgn0026319,FBgn0029082,FBgn0035461,FBgn0040068,FBgn0040348,FBgn0053531,FBgn0265778,FBgn0267390,FBgn0283499 | 12 | GO:0043085 |
| positive regulation of molecular function | 0.0266796 | FBgn0014073,FBgn0015946,FBgn0022800,FBgn0026319,FBgn0029082,FBgn0035461,FBgn0040068,FBgn0040348,FBgn0053531,FBgn0265778,FBgn0267390,FBgn0283499 | 12 | GO:0044093 |
| embryonic morphogenesis | 0.03242536 | FBgn0000163,FBgn0000547,FBgn0002643,FBgn0004893,FBgn0010238,FBgn0026319,FBgn0036518,FBgn0040068,FBgn0085432,FBgn0265778,FBgn0283499 | 11 | GO:0048598 |
| regulation of protein phosphorylation | 0.035288 | FBgn0001234,FBgn0003984,FBgn0014388,FBgn0026319,FBgn0031461,FBgn0031885,FBgn0032702,FBgn0033773,FBgn0034199,FBgn0040068,FBgn0283499 | 11 | GO:0001932 |
| MAPK cascade | 0.00413587 | FBgn0001234,FBgn0003984,FBgn0014388,FBgn0026319,FBgn0031885,FBgn0033773,FBgn0034199,FBgn0040068,FBgn0265778,FBgn0283499 | 10 | GO:0000165 |
| signal transduction by protein phosphorylation | 0.00640013 | FBgn0001234,FBgn0003984,FBgn0014388,FBgn0026319,FBgn0031885,FBgn0033773,FBgn0034199,FBgn0040068,FBgn0265778,FBgn0283499 | 10 | GO:0023014 |
| cell adhesion | 0.00894071 | FBgn0000163,FBgn0000547,FBgn0010238,FBgn0015229,FBgn0022800,FBgn0028369,FBgn0029082,FBgn0034199,FBgn0037963,FBgn0266084 | 10 | GO:0007155 |
| biological adhesion | 0.00953063 | FBgn0000163,FBgn0000547,FBgn0010238,FBgn0015229,FBgn0022800,FBgn0028369,FBgn0029082,FBgn0034199,FBgn0037963,FBgn0266084 | 10 | GO:0022610 |
| positive regulation of protein modification process | 0.01219293 | FBgn0001229,FBgn0001234,FBgn0003984,FBgn0026319,FBgn0031461,FBgn0031885,FBgn0033773,FBgn0034199,FBgn0040068,FBgn0283499 | 10 | GO:0031401 |

| | | | | |
|---|---|---|---|---|
| positive regulation of intracellular signal transduction | 0.01538287 | FBgn0000547,FBgn0001234,FBgn0003984,FBgn0026319,FBgn0031885,FBgn0033773,FBgn0034199,FBgn0040068,FBgn0262081,FBgn0283499 | 10 | GO:1902533 |
| positive regulation of cell development | 0.0224073 | FBgn0000542,FBgn0002609,FBgn0003984,FBgn0014073,FBgn0031461,FBgn0033985,FBgn0038168,FBgn0052179,FBgn0266084,FBgn0283499 | 10 | GO:0010720 |
| positive regulation of cell differentiation | 0.02604027 | FBgn0000542,FBgn0002609,FBgn0003984,FBgn0014073,FBgn0031461,FBgn0033985,FBgn0038168,FBgn0052179,FBgn0266084,FBgn0283499 | 10 | GO:0045597 |
| cell-cell adhesion | 0.00118625 | FBgn0000163,FBgn0000547,FBgn0010238,FBgn0015229,FBgn0022800,FBgn0028369,FBgn0029082,FBgn0034199,FBgn0037963 | 9 | GO:0098609 |
| positive regulation of protein phosphorylation | 0.00412466 | FBgn0001234,FBgn0003984,FBgn0026319,FBgn0031461,FBgn0031885,FBgn0033773,FBgn0034199,FBgn0040068,FBgn0283499 | 9 | GO:0001934 |
| regulation of MAPK cascade | 0.00666673 | FBgn0001234,FBgn0003984,FBgn0014388,FBgn0026319,FBgn0031885,FBgn0033773,FBgn0034199,FBgn0040068,FBgn0283499 | 9 | GO:0043408 |
| cell-cell adhesion via plasma-membrane adhesion molecules | 1.9281E-05 | FBgn0000163,FBgn0000547,FBgn0010238,FBgn0015229,FBgn0022800,FBgn0028369,FBgn0029082,FBgn0037963 | 8 | GO:0098742 |
| positive regulation of MAPK cascade | 0.00115956 | FBgn0001234,FBgn0003984,FBgn0026319,FBgn0031885,FBgn0033773,FBgn0034199,FBgn0040068,FBgn0283499 | 8 | GO:0043410 |
| positive regulation of programmed cell death | 0.00387376 | FBgn0000542,FBgn0001234,FBgn0015946,FBgn0026319,FBgn0035461,FBgn0037007,FBgn0262081,FBgn0283451 | 8 | GO:0043068 |
| positive regulation of cell death | 0.00611912 | FBgn0000542,FBgn0001234,FBgn0015946,FBgn0026319,FBgn0035461,FBgn0037007,FBgn0262081,FBgn0283451 | 8 | GO:0010942 |
| response to hormone | 0.03226562 | FBgn0000568,FBgn0025625,FBgn0034262,FBgn0035626,FBgn0036732,FBgn0052638,FBgn0283451,FBgn0283499 | 8 | GO:0009725 |
| sensory perception of chemical stimulus | 0.0045763 | FBgn0020300,FBgn0030985,FBgn0033404,FBgn0041241,FBgn0041246,FBgn0045474,FBgn0259683 | 7 | GO:0007606 |
| cuticle development | 0.0045763 | FBgn0000451,FBgn0001112,FBgn0033942,FBgn0035513,FBgn0039469,FBgn0085432,FBgn0286203 | 7 | GO:0042335 |
| cell-cell junction organization | 0.00907956 | FBgn0000163,FBgn0010238,FBgn0026319,FBgn0028369,FBgn0040068,FBgn0262081,FBgn0265778 | 7 | GO:0045216 |
| cell junction organization | 0.00992108 | FBgn0000163,FBgn0010238,FBgn0026319,FBgn0028369,FBgn0040068,FBgn0262081,FBgn0265778 | 7 | GO:0034330 |

| | | | | |
|---|---|---|---|---|
| modulation of chemical synaptic transmission | 0.00992108 | FBgn0004580,FBgn0010501,FBgn0013973,FBgn0019985,FBgn0030505,FBgn0039927,FBgn0262081 | 7 | GO:0050804 |
| regulation of trans-synaptic signaling | 0.00992108 | FBgn0004580,FBgn0010501,FBgn0013973,FBgn0019985,FBgn0030505,FBgn0039927,FBgn0262081 | 7 | GO:0099177 |
| stem cell proliferation | 0.01881843 | FBgn0000163,FBgn0002609,FBgn0011674,FBgn0024555,FBgn0031461,FBgn0035626,FBgn0085432 | 7 | GO:0072089 |
| stem cell division | 0.02327013 | FBgn0000163,FBgn0000928,FBgn0011674,FBgn0024555,FBgn0035626,FBgn0052364,FBgn0283499 | 7 | GO:0017145 |
| cellular response to hormone stimulus | 0.02490298 | FBgn0000568,FBgn0025625,FBgn0035626,FBgn0036732,FBgn0052638,FBgn0283451,FBgn0283499 | 7 | GO:0032870 |
| positive regulation of hydrolase activity | 0.02490298 | FBgn0015946,FBgn0029082,FBgn0035461,FBgn0040068,FBgn0040348,FBgn0265778,FBgn0267390 | 7 | GO:0051345 |
| regulation of proteolysis | 0.04322665 | FBgn0001234,FBgn0015946,FBgn0026777,FBgn0029082,FBgn0034706,FBgn0035461,FBgn0037772 | 7 | GO:0030162 |
| regulation of kinase activity | 0.04568728 | FBgn0014073,FBgn0014388,FBgn0022800,FBgn0026319,FBgn0032702,FBgn0053531,FBgn0283499 | 7 | GO:0043549 |
| homophilic cell adhesion via plasma membrane adhesion molecules | 0.00015927 | FBgn0000547,FBgn0010238,FBgn0022800,FBgn0028369,FBgn0029082,FBgn0037963 | 6 | GO:0007156 |
| adherens junction organization | 0.0011657 | FBgn0000163,FBgn0026319,FBgn0028369,FBgn0040068,FBgn0262081,FBgn0265778 | 6 | GO:0034332 |
| chitin-based cuticle development | 0.00346874 | FBgn0001112,FBgn0033942,FBgn0035513,FBgn0039469,FBgn0085432,FBgn0286203 | 6 | GO:0040003 |
| cellular response to abiotic stimulus | 0.00577872 | FBgn0002939,FBgn0004832,FBgn0014073,FBgn0015946,FBgn0033132,FBgn0261794 | 6 | GO:0071214 |
| cellular response to environmental stimulus | 0.00577872 | FBgn0002939,FBgn0004832,FBgn0014073,FBgn0015946,FBgn0033132,FBgn0261794 | 6 | GO:0104004 |
| positive regulation of cell population proliferation | 0.014778 | FBgn0002609,FBgn0003984,FBgn0031461,FBgn0035626,FBgn0052179,FBgn0283499 | 6 | GO:0008284 |
| striated muscle cell differentiation | 0.014778 | FBgn0014388,FBgn0028369,FBgn0029082,FBgn0040068,FBgn0261245,FBgn0283451 | 6 | GO:0051146 |
| muscle cell differentiation | 0.02088399 | FBgn0014388,FBgn0028369,FBgn0029082,FBgn0040068,FBgn0261245,FBgn0283451 | 6 | GO:0042692 |
| detection of stimulus | 0.0377774 | FBgn0002939,FBgn0029968,FBgn0033404,FBgn0037163,FBgn0040849,FBgn0259683 | 6 | GO:0051606 |
| establishment of planar polarity | 0.04036259 | FBgn0000163,FBgn0000542,FBgn0000547,FBgn0014388,FBgn0029082,FBgn0052179 | 6 | GO:0001736 |
| morphogenesis of a | 0.04036259 | FBgn0000163,FBgn0000542,FBgn00 | 6 | GO:00 |

| | | | | |
|---|---|---|---|---|
| polarized epithelium | | 00547,FBgn0014388,FBgn0029082, FBgn0052179 | | 01738 |
| establishment of tissue polarity | 0.04036259 | FBgn0000163,FBgn0000542,FBgn0000547,FBgn0014388,FBgn0029082, FBgn0052179 | 6 | GO:0007164 |
| establishment of ommatidial planar polarity | 0.01299446 | FBgn0000542,FBgn0000547,FBgn0014388,FBgn0029082,FBgn0052179 | 5 | GO:0042067 |
| phenol-containing compound metabolic process | 0.0180364 | FBgn0015946,FBgn0016013,FBgn0033885,FBgn0037153,FBgn0040068 | 5 | GO:0018958 |
| urogenital system development | 0.02422652 | FBgn0000163,FBgn0011674,FBgn0024250,FBgn0028369,FBgn0029082 | 5 | GO:0001655 |
| renal system development | 0.02422652 | FBgn0000163,FBgn0011674,FBgn0024250,FBgn0028369,FBgn0029082 | 5 | GO:0072001 |
| gastrulation | 0.0290305 | FBgn0000163,FBgn0002643,FBgn0026319,FBgn0036518,FBgn0085432 | 5 | GO:0007369 |
| cell fate specification | 0.04034337 | FBgn0000547,FBgn0002632,FBgn0002732,FBgn0003984,FBgn0031461 | 5 | GO:0001708 |
| positive regulation of apoptotic process | 0.04353597 | FBgn0001234,FBgn0015946,FBgn0026319,FBgn0035461,FBgn0037007 | 5 | GO:0043065 |
| response to osmotic stress | 0.00041991 | FBgn0015946,FBgn0030505,FBgn0031885,FBgn0261794 | 4 | GO:0006970 |
| ommatidial rotation | 0.00848941 | FBgn0000542,FBgn0000547,FBgn0014388,FBgn0052179 | 4 | GO:0016318 |
| syncytium formation by plasma membrane fusion | 0.01585731 | FBgn0028369,FBgn0029082,FBgn0040068,FBgn0261245 | 4 | GO:0000768 |
| syncytium formation | 0.01585731 | FBgn0028369,FBgn0029082,FBgn0040068,FBgn0261245 | 4 | GO:0006949 |
| myoblast fusion | 0.01585731 | FBgn0028369,FBgn0029082,FBgn0040068,FBgn0261245 | 4 | GO:0007520 |
| positive regulation of JNK cascade | 0.01585731 | FBgn0001234,FBgn0026319,FBgn0031885,FBgn0034199 | 4 | GO:0046330 |
| cell-cell fusion | 0.01585731 | FBgn0028369,FBgn0029082,FBgn0040068,FBgn0261245 | 4 | GO:0140253 |
| positive regulation of stress-activated MAPK cascade | 0.01817229 | FBgn0001234,FBgn0026319,FBgn0031885,FBgn0034199 | 4 | GO:0032874 |
| positive regulation of stress-activated protein kinase signaling cascade | 0.01817229 | FBgn0001234,FBgn0026319,FBgn0031885,FBgn0034199 | 4 | GO:0070304 |
| myotube differentiation | 0.02340506 | FBgn0028369,FBgn0029082,FBgn0040068,FBgn0261245 | 4 | GO:0014902 |
| detection of chemical stimulus | 0.02633032 | FBgn0029968,FBgn0033404,FBgn0040849,FBgn0259683 | 4 | GO:0009593 |
| response to ecdysone | 0.03637304 | FBgn0000568,FBgn0034262,FBgn0036732,FBgn0283451 | 4 | GO:0035075 |
| response to sterol | 0.03637304 | FBgn0000568,FBgn0034262,FBgn0036732,FBgn0283451 | 4 | GO:0036314 |
| response to ketone | 0.04014807 | FBgn0000568,FBgn0034262,FBgn0036732,FBgn0283451 | 4 | GO:1901654 |
| regulation of stem | 0.04413795 | FBgn0002609,FBgn0031461,FBgn00 | 4 | GO:00 |

| | | | | |
|---|---|---|---|---|
| cell proliferation | | 35626,FBgn0085432 | | 72091 |
| response to salt stress | 0.00191883 | FBgn0030505,FBgn0031885,FBgn0261794 | 3 | GO:0009651 |
| basal protein localization | 0.00298069 | FBgn0000163,FBgn0011674,FBgn0024555 | 3 | GO:0045175 |
| heterophilic cell-cell adhesion via plasma membrane cell adhesion molecules | 0.00803979 | FBgn0015229,FBgn0028369,FBgn0029082 | 3 | GO:0007157 |
| asymmetric protein localization involved in cell fate determination | 0.01314246 | FBgn0000163,FBgn0011674,FBgn0026319 | 3 | GO:0045167 |
| adherens junction assembly | 0.01972316 | FBgn0000163,FBgn0028369,FBgn0265778 | 3 | GO:0034333 |
| execution phase of apoptosis | 0.02781216 | FBgn0010501,FBgn0015946,FBgn0028406 | 3 | GO:0097194 |
| positive regulation of stem cell proliferation | 0.02781216 | FBgn0002609,FBgn0031461,FBgn0035626 | 3 | GO:2000648 |
| positive regulation of endopeptidase activity | 0.03740398 | FBgn0015946,FBgn0029082,FBgn0035461 | 3 | GO:0010950 |
| positive regulation of peptidase activity | 0.03740398 | FBgn0015946,FBgn0029082,FBgn0035461 | 3 | GO:0010952 |
| sensory perception of taste | 0.04275372 | FBgn0041241,FBgn0041246,FBgn0045474 | 3 | GO:0050909 |
| nucleotide-excision repair, DNA damage recognition | 0.00156981 | FBgn0004832,FBgn0026777 | 2 | GO:0000715 |
| mesodermal cell fate determination | 0.00458594 | FBgn0002643,FBgn0085432 | 2 | GO:0007500 |
| phenol-containing compound catabolic process | 0.00458594 | FBgn0016013,FBgn0037153 | 2 | GO:0019336 |
| symmetric stem cell division | 0.00458594 | FBgn0035626,FBgn0052364 | 2 | GO:0098724 |
| response to light intensity | 0.00893217 | FBgn0033132,FBgn0037163 | 2 | GO:0009642 |
| cellular response to UV | 0.00893217 | FBgn0002939,FBgn0004832 | 2 | GO:0034644 |
| symmetric cell division | 0.00893217 | FBgn0035626,FBgn0052364 | 2 | GO:0098725 |
| regulation of striated muscle tissue development | 0.01449913 | FBgn0028369,FBgn0029082 | 2 | GO:0016202 |
| cellular response to osmotic stress | 0.01449913 | FBgn0015946,FBgn0261794 | 2 | GO:0071470 |
| regulation of muscle tissue development | 0.01449913 | FBgn0028369,FBgn0029082 | 2 | GO:1901861 |
| mesodermal cell fate commitment | 0.02889002 | FBgn0002643,FBgn0085432 | 2 | GO:0001710 |

| | | | | |
|---|---|---|---|---|
| I-kappaB kinase/NF-kappaB signaling | 0.02889002 | FBgn0026319,FBgn0033985 | 2 | GO:0007249 |
| calcium-dependent cell-cell adhesion via plasma membrane cell adhesion molecules | 0.02889002 | FBgn0022800,FBgn0037963 | 2 | GO:0016339 |
| contractile actin filament bundle assembly | 0.02889002 | FBgn0000547,FBgn0266084 | 2 | GO:0030038 |
| dopamine metabolic process | 0.02889002 | FBgn0033885,FBgn0037153 | 2 | GO:0042417 |
| mesodermal cell differentiation | 0.02889002 | FBgn0002643,FBgn0085432 | 2 | GO:0048333 |
| cyclic purine nucleotide metabolic process | 0.02889002 | FBgn0013973,FBgn0023416 | 2 | GO:0052652 |
| RNA 5'-end processing | 0.03752647 | FBgn0033092,FBgn0052706 | 2 | GO:0000966 |
| epithelial cell morphogenesis involved in gastrulation | 0.03752647 | FBgn0026319,FBgn0036518 | 2 | GO:0003381 |
| catecholamine metabolic process | 0.03752647 | FBgn0033885,FBgn0037153 | 2 | GO:0006584 |
| cyclic nucleotide biosynthetic process | 0.03752647 | FBgn0013973,FBgn0023416 | 2 | GO:0009190 |
| catechol-containing compound metabolic process | 0.03752647 | FBgn0033885,FBgn0037153 | 2 | GO:0009712 |
| peptide hormone secretion | 0.03752647 | FBgn0034199,FBgn0283499 | 2 | GO:0030072 |
| ncRNA 5'-end processing | 0.03752647 | FBgn0033092,FBgn0052706 | 2 | GO:0034471 |
| regulation of peptide hormone secretion | 0.03752647 | FBgn0034199,FBgn0283499 | 2 | GO:0090276 |
| apical constriction involved in gastrulation | 0.04700803 | FBgn0026319,FBgn0036518 | 2 | GO:0003384 |
| endosome organization | 0.04700803 | FBgn0036666,FBgn0267390 | 2 | GO:0007032 |
| regulation of muscle organ development | 0.04700803 | FBgn0028369,FBgn0029082 | 2 | GO:0048634 |
| endonucleolytic cleavage of tetracistronic rRNA transcript (SSU-rRNA, 5.8S rRNA, 2S rRNA, LSU-rRNA) | 0.03971774 | FBgn0065098 | 1 | GO:0000483 |
| negative regulation of antifungal | 0.03971774 | FBgn0000250 | 1 | GO:0002789 |

| | | | | |
|---|---|---|---|---|
| peptide production | | | | |
| tyrosine catabolic process | 0.03971774 | FBgn0016013 | 1 | GO:0006572 |
| hypotonic response | 0.03971774 | FBgn0261794 | 1 | GO:0006971 |
| activation of NF-kappaB-inducing kinase activity | 0.03971774 | FBgn0026319 | 1 | GO:0007250 |
| cytoplasmic sequestering of NF-kappaB | 0.03971774 | FBgn0000250 | 1 | GO:0007253 |
| phototransduction, UV | 0.03971774 | FBgn0002939 | 1 | GO:0007604 |
| pupal chitin-based cuticle development | 0.03971774 | FBgn0001112 | 1 | GO:0008364 |
| detection of UV | 0.03971774 | FBgn0002939 | 1 | GO:0009589 |
| response to high light intensity | 0.03971774 | FBgn0033132 | 1 | GO:0009644 |
| regulation of translational initiation by eIF2 alpha phosphorylation | 0.03971774 | FBgn0001229 | 1 | GO:0010998 |
| keratinocyte differentiation | 0.03971774 | FBgn0031461 | 1 | GO:0030216 |
| positive regulation of homotypic cell-cell adhesion | 0.03971774 | FBgn0034199 | 1 | GO:0034112 |
| nuclear speck organization | 0.03971774 | FBgn0001234 | 1 | GO:0035063 |
| negative regulation of fusion cell fate specification | 0.03971774 | FBgn0000547 | 1 | GO:0035157 |
| angiotensin-activated signaling pathway | 0.03971774 | FBgn0052638 | 1 | GO:0038166 |
| hypotonic salinity response | 0.03971774 | FBgn0261794 | 1 | GO:0042539 |
| regulation of translational initiation in response to stress | 0.03971774 | FBgn0001229 | 1 | GO:0043558 |
| skin development | 0.03971774 | FBgn0031461 | 1 | GO:0043588 |
| histone H4-K5 acetylation | 0.03971774 | FBgn0035624 | 1 | GO:0043981 |
| histone H3-K14 acetylation | 0.03971774 | FBgn0035624 | 1 | GO:0044154 |
| metaphase/anaphase transition of meiotic cell cycle | 0.03971774 | FBgn0033773 | 1 | GO:0044785 |
| regulation of R8 cell differentiation | 0.03971774 | FBgn0000547 | 1 | GO:0045679 |

| | | | | |
|---|---|---|---|---|
| negative regulation of R8 cell differentiation | 0.03971774 | FBgn0000547 | 1 | GO:0045680 |
| isoprenoid transport | 0.03971774 | FBgn0002939 | 1 | GO:0046864 |
| terpenoid transport | 0.03971774 | FBgn0002939 | 1 | GO:0046865 |
| tetraterpenoid transport | 0.03971774 | FBgn0002939 | 1 | GO:0046866 |
| carotenoid transport | 0.03971774 | FBgn0002939 | 1 | GO:0046867 |
| protein heterotetramerization | 0.03971774 | FBgn0283499 | 1 | GO:0051290 |
| protein heterooligomerization | 0.03971774 | FBgn0283499 | 1 | GO:0051291 |
| establishment of centrosome localization | 0.03971774 | FBgn0000163 | 1 | GO:0051660 |
| garland nephrocyte differentiation | 0.03971774 | FBgn0028369 | 1 | GO:0061321 |
| positive regulation of fat cell proliferation | 0.03971774 | FBgn0283499 | 1 | GO:0070346 |
| cellular hypotonic response | 0.03971774 | FBgn0261794 | 1 | GO:0071476 |
| cellular hypotonic salinity response | 0.03971774 | FBgn0261794 | 1 | GO:0071477 |
| cellular response to high light intensity | 0.03971774 | FBgn0033132 | 1 | GO:0071486 |
| regulation of actin cytoskeleton organization by cell-cell adhesion | 0.03971774 | FBgn0000547 | 1 | GO:0090138 |
| cell-cell adhesion involved in establishment of planar polarity | 0.03971774 | FBgn0000163 | 1 | GO:0090250 |
| synaptic signaling by nitric oxide | 0.03971774 | FBgn0013973 | 1 | GO:0099163 |
| trans-synaptic signaling by soluble gas | 0.03971774 | FBgn0013973 | 1 | GO:0099543 |
| trans-synaptic signaling by nitric oxide | 0.03971774 | FBgn0013973 | 1 | GO:0099548 |
| trans-synaptic signaling, modulating synaptic transmission | 0.03971774 | FBgn0013973 | 1 | GO:0099550 |
| trans-synaptic signaling by soluble gas, modulating | 0.03971774 | FBgn0013973 | 1 | GO:0099554 |

| | | | | |
|---|---|---|---|---|
| synaptic transmission | | | | |
| trans-synaptic signaling by nitric oxide, modulating synaptic transmission | 0.03971774 | FBgn0013973 | 1 | GO:0099555 |
| regulation of glutamate receptor clustering | 0.03971774 | FBgn0014009 | 1 | GO:0106104 |
| negative regulation of imaginal disc-derived wing vein specification | 0.03971774 | FBgn0014388 | 1 | GO:0110109 |
| regulation of long-term synaptic potentiation | 0.03971774 | FBgn0004580 | 1 | GO:1900271 |
| positive regulation of NIK/NF-kappaB signaling | 0.03971774 | FBgn0026319 | 1 | GO:1901224 |
| negative regulation of meiotic cell cycle phase transition | 0.03971774 | FBgn0033773 | 1 | GO:1901994 |
| homogentisate metabolic process | 0.03971774 | FBgn0016013 | 1 | GO:1901999 |
| homogentisate catabolic process | 0.03971774 | FBgn0016013 | 1 | GO:1902000 |
| regulation of extrinsic apoptotic signaling pathway via death domain receptors | 0.03971774 | FBgn0033985 | 1 | GO:1902041 |
| negative regulation of extrinsic apoptotic signaling pathway via death domain receptors | 0.03971774 | FBgn0033985 | 1 | GO:1902042 |
| regulation of metaphase/anaphase transition of meiotic cell cycle | 0.03971774 | FBgn0033773 | 1 | GO:1902102 |
| negative regulation of metaphase/anaphase transition of meiotic cell cycle | 0.03971774 | FBgn0033773 | 1 | GO:1902103 |
| regulation of receptor clustering | 0.03971774 | FBgn0014009 | 1 | GO:1903909 |
| cellular response to angiotensin | 0.03971774 | FBgn0052638 | 1 | GO:1904385 |
| regulation of meiotic chromosome separation | 0.03971774 | FBgn0033773 | 1 | GO:1905132 |
| negative regulation | 0.03971774 | FBgn0033773 | 1 | GO:19 |

| | | | | |
|---|---|---|---|---|
| of meiotic chromosome separation | | | | 05133 |
| negative regulation of morphogenesis of an epithelium | 0.03971774 | FBgn0014388 | 1 | GO:1905331 |
| response to angiotensin | 0.03971774 | FBgn0052638 | 1 | GO:1990776 |
| regulation of ATP-dependent microtubule motor activity, minus-end-directed | 0.03971774 | FBgn0267390 | 1 | GO:2000577 |
| positive regulation of ATP-dependent microtubule motor activity, minus-end-directed | 0.03971774 | FBgn0267390 | 1 | GO:2000579 |
| negative regulation of extrinsic apoptotic signaling pathway | 0.03971774 | FBgn0033985 | 1 | GO:2001237 |
| muscle fiber development | 0.04700803 | FBgn0014388,FBgn0283451 | GO:0048747 | |
| negative regulation of synaptic transmission | 0.04700803 | FBgn0010501,FBgn0030505 | GO:0050805 | |
| cellular response to endogenous stimulus | 0.04807654 | FBgn0000568,FBgn0025625,FBgn0031461,FBgn0034199,FBgn0035626,FBgn0036732,FBgn0052638,FBgn0283451,FBgn0283499 | GO:0071495 | |
| regulation of endopeptidase activity | 0.04834249 | FBgn0015946,FBgn0029082,FBgn0035461,FBgn0037772 | GO:0052548 | |
| cell population proliferation | 0.04844707 | FBgn0000163,FBgn0002609,FBgn0003984,FBgn0011674,FBgn0024555,FBgn0031461,FBgn0031885,FBgn0035626,FBgn0051111,FBgn0052179,FBgn0085432,FBgn0262081,FBgn0283499 | GO:0008283 | |
| negative regulation of epidermal growth factor receptor signaling pathway | 0.04846444 | FBgn0000547,FBgn0014388,FBgn0031016,FBgn0040068 | GO:0042059 | |
| regulation of ERK1 and ERK2 cascade | 0.04846444 | FBgn0003984,FBgn0014388,FBgn0040068 | GO:0070372 | |
| cellular response to light stimulus | 0.04846444 | FBgn0002939,FBgn0004832,FBgn0033132 | GO:0071482 | |
| negative regulation of ERBB signaling pathway | 0.04846444 | FBgn0000547,FBgn0014388,FBgn0031016,FBgn0040068 | GO:1901185 | |

**Table 2.4g: GO enrichment for hits differentially upregulated in control females relative to 20HE males**

| GO | p- | Hits | Gene | GO ID |
|---|---|---|---|---|

| enrichment | value | | matches | |
|---|---|---|---|---|
| metabolic process | 0.03099917 | FBgn0001150,FBgn0002441,FBgn0003257,FBgn0010278,FBgn0010425,FBgn0011211,FBgn0011555,FBgn0011703,FBgn0011704,FBgn0011768,FBgn0011834,FBgn0014028,FBgn0015075,FBgn0015277,FBgn0015553,FBgn0020633,FBgn0020653,FBgn0020906,FBgn0022700,FBgn0024321,FBgn0024957,FBgn0025352,FBgn0025373,FBgn0025592,FBgn0025815,FBgn0025832,FBgn0026079,FBgn0026143,FBgn0026411,FBgn0027791,FBgn0027794,FBgn0027868,FBgn0028375,FBgn0028962,FBgn0029131,FBgn0029823,FBgn0029827,FBgn0029856,FBgn0029906,FBgn0030081,FBgn0030136,FBgn0030966,FBgn0031030,FBgn0031092,FBgn0031145,FBgn0031182,FBgn0031249,FBgn0031252,FBgn0031381,FBgn0031653,FBgn0031703,FBgn0031713,FBgn0031875,FBgn0031996,FBgn0031999,FBgn0032244,FBgn0032350,FBgn0032424,FBgn0032781,FBgn0032929,FBgn0033079,FBgn0033187,FBgn0033235,FBgn0033377,FBgn0033431,FBgn0033454,FBgn0033549,FBgn0033733,FBgn0033774,FBgn0034052,FBgn0034177,FBgn0034422,FBgn0034582,FBgn0034629,FBgn0034817,FBgn0034937,FBgn0034988,FBgn0035006,FBgn0035383,FBgn0035619,FBgn0035665,FBgn0035666,FBgn0035718,FBgn0035886,FBgn0035887,FBgn0035901,FBgn0036321,FBgn0036738,FBgn0036831,FBgn0036948,FBgn0037073,FBgn0037301,FBgn0037338,FBgn0037345,FBgn0037356,FBgn0037371,FBgn0037513,FBgn0037534,FBgn0037678,FBgn0037683,FBgn0037814,FBgn0037815,FBgn0037958,FBgn0037996,FBgn0038067,FBgn0038074,FBgn0038135,FBgn0038467,FBgn0038482,FBgn0038485,FBgn0038597,FBgn0038632,FBgn0038742,FBgn0039052,FBgn0039094,FBgn0039099,FBgn0039102,FBgn0039156,FBgn0039175,FBgn0039189,FBgn0039470,FBgn0039472,FBgn0039475,FBgn0039476,FBgn0039580,FBgn0039687,FBgn0039777,FBgn0039778,FBgn0040060,FBgn0040069,FBgn0040078,FBgn0040290,FBgn0040337,FBgn0040959,FBgn0041147,FBgn0046689,FBgn0050049,FBgn0050085,FBgn0050090,FBgn0050371,FBgn0050502,FBgn0051198,FBgn0051265,FBgn0051266,FBgn0051343,FBgn0051391,FBgn0051469,FBgn0052412,FBgn0052750,FBgn0053080,FBgn0053116,FBgn0053127,FBgn0053138,FBgn0053460,FBgn0086708,FBgn0086712,FBgn0243511,FBgn0250815,FBgn0259676,FBgn0259791,FBgn0261479,FBgn0261681,FBgn0261850,FBgn0263133,FBgn0265140,FBgn0266420,FBgn0267408,FBgn0267824,FBgn0283525,FBgn0283680,FBgn0284256,FBgn0286788 | 172 | GO:0008152 |
| organic substance metabolic process | 0.03835981 | FBgn0001150,FBgn0002441,FBgn0003257,FBgn0010278,FBgn0010425,FBgn0011211,FBgn0011555,FBgn0011703,FBgn0011704,FBgn0011768,FBgn0011834,FBgn0015075,FBgn0015277,FBgn0015553,FBgn0020633,FBgn0020906,FBgn0022700,FBgn0024321,FBgn0024957,FBgn0025352,FBgn0025373,FBgn0025592,FBgn0025815,FBgn0025832,FBgn0026079,FBgn0026143,FBgn0026411,FBgn0027791,FBgn0027794,FBgn0027868,FBgn0028375,FBgn0028962,FBgn0029823,FBgn0029827,FBgn0029856,FBgn0029906,FBgn0030081,FBgn0030136,FBgn0030966,FBgn0031030,FBgn0031092,FBgn0031145,FBgn0031249,F | 161 | GO:0071704 |

| | | | | |
|---|---|---|---|---|
| | | Bgn0031252,FBgn0031381,FBgn0031653,FBgn0031703,FBgn0031713,FBgn0031875,FBgn0031996,FBgn0031999,FBgn0032244,FBgn0032350,FBgn0032424,FBgn0032781,FBgn0032929,FBgn0033187,FBgn0033235,FBgn0033377,FBgn0033431,FBgn0033454,FBgn0033549,FBgn0033733,FBgn0033774,FBgn0034052,FBgn0034177,FBgn0034422,FBgn0034582,FBgn0034629,FBgn0034817,FBgn0034937,FBgn0034988,FBgn0035006,FBgn0035383,FBgn0035665,FBgn0035666,FBgn0035718,FBgn0035886,FBgn0035887,FBgn0035901,FBgn0036321,FBgn0036738,FBgn0036831,FBgn0036948,FBgn0037073,FBgn0037301,FBgn0037338,FBgn0037345,FBgn0037356,FBgn0037371,FBgn0037513,FBgn0037534,FBgn0037678,FBgn0037814,FBgn0037815,FBgn0037958,FBgn0037996,FBgn0038067,FBgn0038074,FBgn0038135,FBgn0038467,FBgn0038482,FBgn0038485,FBgn0038597,FBgn0038632,FBgn0038742,FBgn0039052,FBgn0039094,FBgn0039102,FBgn0039156,FBgn0039175,FBgn0039189,FBgn0039470,FBgn0039472,FBgn0039475,FBgn0039476,FBgn0039580,FBgn0039687,FBgn0039777,FBgn0039778,FBgn0040060,FBgn0040078,FBgn0040290,FBgn0040337,FBgn0040959,FBgn0041147,FBgn0046689,FBgn0050049,FBgn0050085,FBgn0050090,FBgn0050371,FBgn0050502,FBgn0051198,FBgn0051265,FBgn0051266,FBgn0051343,FBgn0051469,FBgn0052412,FBgn0053080,FBgn0053116,FBgn0053127,FBgn0053138,FBgn0053460,FBgn0086708,FBgn0086712,FBgn0243511,FBgn0250815,FBgn0259676,FBgn0259791,FBgn0261479,FBgn0261681,FBgn0261850,FBgn0263133,FBgn0265140,FBgn0266420,FBgn0267408,FBgn0267824,FBgn0283525,FBgn0283680,FBgn0284256,FBgn0286788 | | |
| small molecule metabolic process | 1.2133E-05 | FBgn0003257,FBgn0011211,FBgn0011703,FBgn0011704,FBgn0011768,FBgn0024957,FBgn0025352,FBgn0025592,FBgn0028375,FBgn0028962,FBgn0029823,FBgn0030966,FBgn0031092,FBgn0031381,FBgn0031703,FBgn0031713,FBgn0032350,FBgn0032424,FBgn0033733,FBgn0034177,FBgn0034629,FBgn0034988,FBgn0035006,FBgn0035383,FBgn0037356,FBgn0037513,FBgn0037534,FBgn0037996,FBgn0038074,FBgn0038467,FBgn0038742,FBgn0039052,FBgn0039094,FBgn0039156,FBgn0039175,FBgn0039580,FBgn0050502,FBgn0086712,FBgn0267408,FBgn0283680 | 40 | GO:0044281 |
| proteolysis | 5.6745E-05 | FBgn0010425,FBgn0011555,FBgn0011703,FBgn0011704,FBgn0011834,FBgn0020906,FBgn0029827,FBgn0029856,FBgn0031249,FBgn0031653,FBgn0033235,FBgn0033774,FBgn0034052,FBgn0034937,FBgn0035665,FBgn0035666,FBgn0035718,FBgn0035886,FBgn0035887,FBgn0036738,FBgn0037678,FBgn0038135,FBgn0038482,FBgn0038485,FBgn0039102,FBgn0039777,FBgn0039778,FBgn0040060,FBgn0041147,FBgn0050049,FBgn0050090,FBgn0050371,FBgn0051198,FBgn0051265,FBgn0051266,FBgn0051343,FBgn0053127,FBgn0053460,FBgn0250815,FBgn0265140 | 40 | GO:0006508 |
| organic substance catabolic process | 0.03882098 | FBgn0011768,FBgn0022700,FBgn0025352,FBgn0027794,FBgn0029823,FBgn0029856,FBgn0031092,FBgn0031252,FBgn0034582,FBgn0034629,FBgn0034937,FBgn0034988,FBgn0035383,FBgn0036321,FBgn0036831,FBgn0037 | 31 | GO:1901575 |

| | | | | |
|---|---|---|---|---|
| | | 513,FBgn0037815,FBgn0037958,FBgn0038074,FBgn0038135,FBgn0038742,FBgn0039094,FBgn0039470,FBgn0039472,FBgn0039475,FBgn0039476,FBgn0041147,FBgn0051198,FBgn0051343,FBgn0086712,FBgn0284256 | | |
| lipid metabolic process | 0.00013624 | FBgn0015277,FBgn0025352,FBgn0025373,FBgn0025592,FBgn0029906,FBgn0031092,FBgn0031381,FBgn0031703,FBgn0033187,FBgn0033733,FBgn0034629,FBgn0035006,FBgn0035383,FBgn0037356,FBgn0037534,FBgn0037958,FBgn0037996,FBgn0038067,FBgn0038742,FBgn0039156,FBgn0039470,FBgn0039472,FBgn0039475,FBgn0039476,FBgn0050502,FBgn0053116,FBgn0086712 | 27 | GO:0006629 |
| organic acid metabolic process | 2.8548E-05 | FBgn0024957,FBgn0025352,FBgn0028962,FBgn0029823,FBgn0030966,FBgn0031092,FBgn0031703,FBgn0032350,FBgn0033733,FBgn0034177,FBgn0034629,FBgn0035006,FBgn0035383,FBgn0037356,FBgn0037513,FBgn0037534,FBgn0037996,FBgn0038074,FBgn0038742,FBgn0039052,FBgn0039094,FBgn0039156,FBgn0039175,FBgn0050502,FBgn0086712 | 25 | GO:0006082 |
| oxoacid metabolic process | 2.8548E-05 | FBgn0024957,FBgn0025352,FBgn0028962,FBgn0029823,FBgn0030966,FBgn0031092,FBgn0031703,FBgn0032350,FBgn0033733,FBgn0034177,FBgn0034629,FBgn0035006,FBgn0035383,FBgn0037356,FBgn0037513,FBgn0037534,FBgn0037996,FBgn0038074,FBgn0038742,FBgn0039052,FBgn0039094,FBgn0039156,FBgn0039175,FBgn0050502,FBgn0086712 | 25 | GO:0043436 |
| carboxylic acid metabolic process | 3.8053E-05 | FBgn0024957,FBgn0025352,FBgn0028962,FBgn0029823,FBgn0031092,FBgn0031703,FBgn0032350,FBgn0033733,FBgn0034177,FBgn0034629,FBgn0035006,FBgn0035383,FBgn0037356,FBgn0037513,FBgn0037534,FBgn0037996,FBgn0038074,FBgn0038742,FBgn0039052,FBgn0039094,FBgn0039156,FBgn0039175,FBgn0050502,FBgn0086712 | 24 | GO:0019752 |
| oxidation-reduction process | 0.03433962 | FBgn0011211,FBgn0011703,FBgn0011704,FBgn0011768,FBgn0014028,FBgn0020653,FBgn0024957,FBgn0025352,FBgn0030966,FBgn0031092,FBgn0031182,FBgn0031713,FBgn0032350,FBgn0033079,FBgn0034629,FBgn0035383,FBgn0038742,FBgn0039099,FBgn0050502,FBgn0053138,FBgn0086712,FBgn0267408 | 22 | GO:0055114 |
| DNA metabolic process | 0.00051279 | FBgn0015075,FBgn0015553,FBgn0020633,FBgn0025815,FBgn0025832,FBgn0026143,FBgn0027868,FBgn0031252,FBgn0032244,FBgn0032929,FBgn0033549,FBgn0036321,FBgn0036831,FBgn0037301,FBgn0037338,FBgn0037345,FBgn0040290,FBgn0050085,FBgn0259676,FBgn0261850,FBgn0286788 | 21 | GO:0006259 |
| cellular lipid metabolic process | 0.00129471 | FBgn0015277,FBgn0025352,FBgn0025373,FBgn0025592,FBgn0029906,FBgn0031092,FBgn0031703,FBgn0033187,FBgn0033733,FBgn0034629,FBgn0035006,FBgn0035383,FBgn0037356,FBgn0037534,FBgn0037958,FBgn0037996,FBgn0038742,FBgn0039156,FBgn0050502,FBgn0053116,FBgn0086712 | 21 | GO:0044255 |
| transmembrane transport | 0.02522501 | FBgn0010497,FBgn0011211,FBgn0031516,FBgn0032435,FBgn0032946,FBgn0033371,FBgn0033812,FBgn0034612,FBgn0034783,FBgn0037140,FBgn0037668,FBgn0037846,FBgn0038312,FBgn0038407,FBgn0038412,FBgn0038613,FBgn0039357,FBgn0039736,FBgn0042126,FBgn0050272,FBgn0262008 | 21 | GO:0055085 |

| | | | | |
|---|---|---|---|---|
| homeostatic process | 0.03806386 | FBgn0011204,FBgn0015277,FBgn0020653,FBgn0024957,FBgn0029131,FBgn0031030,FBgn0031381,FBgn0031677,FBgn0032746,FBgn0032946,FBgn0034629,FBgn0035383,FBgn0037338,FBgn0038074,FBgn0038613,FBgn0050085,FBgn0050377,FBgn0053542,FBgn0086712,FBgn0266420 | 20 | GO:0042592 |
| carbohydrate derivative metabolic process | 0.03806386 | FBgn0003257,FBgn0011211,FBgn0011703,FBgn0011704,FBgn0022700,FBgn0025592,FBgn0027791,FBgn0029906,FBgn0033187,FBgn0033431,FBgn0034582,FBgn0034988,FBgn0036948,FBgn0038074,FBgn0038467,FBgn0038632,FBgn0039156,FBgn0039580,FBgn0040959,FBgn0261681 | 20 | GO:1901135 |
| cellular response to DNA damage stimulus | 0.00187823 | FBgn0015075,FBgn0015553,FBgn0020633,FBgn0025815,FBgn0025832,FBgn0026143,FBgn0027868,FBgn0029131,FBgn0029588,FBgn0031030,FBgn0031252,FBgn0032244,FBgn0033549,FBgn0037301,FBgn0037338,FBgn0040290,FBgn0050085,FBgn0261850 | 18 | GO:0006974 |
| small molecule biosynthetic process | 0.00011852 | FBgn0028375,FBgn0029823,FBgn0031381,FBgn0031703,FBgn0031713,FBgn0033733,FBgn0034988,FBgn0035006,FBgn0035383,FBgn0037356,FBgn0037513,FBgn0037534,FBgn0037996,FBgn0038074,FBgn0039094,FBgn0039156,FBgn0283680 | 17 | GO:0044283 |
| drug metabolic process | 0.00045547 | FBgn0011211,FBgn0011768,FBgn0022700,FBgn0024957,FBgn0029823,FBgn0034582,FBgn0035383,FBgn0036948,FBgn0038074,FBgn0038467,FBgn0038632,FBgn0039094,FBgn0040959,FBgn0261681,FBgn0267408 | 15 | GO:0017144 |
| fatty acid metabolic process | 4.2887E-06 | FBgn0025352,FBgn0031092,FBgn0031703,FBgn0033733,FBgn0034629,FBgn0035006,FBgn0035383,FBgn0037356,FBgn0037534,FBgn0037996,FBgn0038742,FBgn0039156,FBgn0050502,FBgn0086712 | 14 | GO:0006631 |
| monocarboxylic acid metabolic process | 0.00029901 | FBgn0025352,FBgn0031092,FBgn0031703,FBgn0033733,FBgn0034629,FBgn0035006,FBgn0035383,FBgn0037356,FBgn0037534,FBgn0037996,FBgn0038742,FBgn0039156,FBgn0050502,FBgn0086712 | 14 | GO:0032787 |
| DNA repair | 0.00278036 | FBgn0015075,FBgn0015553,FBgn0020633,FBgn0025815,FBgn0025832,FBgn0026143,FBgn0027868,FBgn0031252,FBgn0032244,FBgn0033549,FBgn0037301,FBgn0037338,FBgn0040290,FBgn0261850 | 14 | GO:0006281 |
| lipid biosynthetic process | 0.0029862 | FBgn0015277,FBgn0025373,FBgn0031381,FBgn0031703,FBgn0033187,FBgn0033733,FBgn0035006,FBgn0037356,FBgn0037534,FBgn0037958,FBgn0037996,FBgn0039156,FBgn0050502,FBgn0053116 | 14 | GO:0008610 |
| DNA replication | 0.00029309 | FBgn0011703,FBgn0020633,FBgn0025815,FBgn0026143,FBgn0031875,FBgn0032244,FBgn0032929,FBgn0033549,FBgn0040290,FBgn0050085,FBgn0259676,FBgn0286788 | 12 | GO:0006260 |
| organophosphate biosynthetic process | 0.01780335 | FBgn0003257,FBgn0011211,FBgn0011703,FBgn0011704,FBgn0015277,FBgn0025373,FBgn0025592,FBgn0033187,FBgn0038467,FBgn0039156,FBgn0053116,FBgn0283680 | 12 | GO:0090407 |
| chemical homeostasis | 0.04513263 | FBgn0011204,FBgn0024957,FBgn0031381,FBgn0031677,FBgn0032746,FBgn0032946,FBgn0034629,FBgn0035383,FBgn0038074,FBgn0038613,FBgn0050377,FBgn0086712 | 12 | GO:0048878 |
| lipid catabolic process | 0.00034632 | FBgn0025352,FBgn0031092,FBgn0034629,FBgn0035383,FBgn0037958,FBgn0038742,FBgn0039470,FBgn0039472,FBgn0039475,FBgn0039476,FBgn0086712 | 11 | GO:0016042 |

| | | | | |
|---|---|---|---|---|
| organic acid biosynthetic process | 0.00034632 | FBgn0029823,FBgn0031703,FBgn0033733,FBgn0035006,FBgn0037356,FBgn0037513,FBgn0037534,FBgn0037996,FBgn0038074,FBgn0039094,FBgn0039156 | 11 | GO:0016053 |
| carboxylic acid biosynthetic process | 0.00034632 | FBgn0029823,FBgn0031703,FBgn0033733,FBgn0035006,FBgn0037356,FBgn0037513,FBgn0037534,FBgn0037996,FBgn0038074,FBgn0039094,FBgn0039156 | 11 | GO:0046394 |
| DNA-dependent DNA replication | 0.00044532 | FBgn0020633,FBgn0025815,FBgn0026143,FBgn0031875,FBgn0032244,FBgn0032929,FBgn0033549,FBgn0040290,FBgn0050085,FBgn0259676,FBgn0286788 | 11 | GO:0006261 |
| small molecule catabolic process | 0.00496955 | FBgn0011768,FBgn0025352,FBgn0029823,FBgn0031092,FBgn0034629,FBgn0034988,FBgn0035383,FBgn0038742,FBgn0039094,FBgn0086712 | 10 | GO:0044282 |
| response to drug | 0.02870394 | FBgn0010497,FBgn0029823,FBgn0031030,FBgn0031182,FBgn0036381,FBgn0037140,FBgn0037668,FBgn0039357,FBgn0086782,FBgn0261090 | 10 | GO:0042493 |
| double-strand break repair | 0.0036555 | FBgn0015075,FBgn0020633,FBgn0025815,FBgn0026143,FBgn0027868,FBgn0033549,FBgn0037301,FBgn0037338,FBgn0040290 | 9 | GO:0006302 |
| DNA recombination | 0.00492357 | FBgn0015553,FBgn0020633,FBgn0025815,FBgn0026143,FBgn0027868,FBgn0033549,FBgn0037301,FBgn0040290,FBgn0261850 | 9 | GO:0006310 |
| cellular amino acid metabolic process | 0.01957051 | FBgn0028962,FBgn0029823,FBgn0032350,FBgn0034177,FBgn0037513,FBgn0038074,FBgn0039052,FBgn0039094,FBgn0039175 | 9 | GO:0006520 |
| organic acid catabolic process | 0.00513011 | FBgn0025352,FBgn0029823,FBgn0031092,FBgn0034629,FBgn0035383,FBgn0038742,FBgn0039094,FBgn0086712 | 8 | GO:0016054 |
| carboxylic acid catabolic process | 0.00513011 | FBgn0025352,FBgn0029823,FBgn0031092,FBgn0034629,FBgn0035383,FBgn0038742,FBgn0039094,FBgn0086712 | 8 | GO:0046395 |
| fatty acid biosynthetic process | 0.0013821 | FBgn0031703,FBgn0033733,FBgn0035006,FBgn0037356,FBgn0037534,FBgn0037996,FBgn0039156 | 7 | GO:0006633 |
| amino sugar metabolic process | 0.00296798 | FBgn0022700,FBgn0034582,FBgn0036948,FBgn0038632,FBgn0039580,FBgn0040959,FBgn0261681 | 7 | GO:0006040 |
| monocarboxylic acid biosynthetic process | 0.00296798 | FBgn0031703,FBgn0033733,FBgn0035006,FBgn0037356,FBgn0037534,FBgn0037996,FBgn0039156 | 7 | GO:0072330 |
| cellular lipid catabolic process | 0.00891742 | FBgn0025352,FBgn0031092,FBgn0034629,FBgn0035383,FBgn0037958,FBgn0038742,FBgn0086712 | 7 | GO:0044242 |
| DNA replication initiation | 0.0002188 | FBgn0020633,FBgn0025815,FBgn0026143,FBgn0032929,FBgn0050085,FBgn0286788 | 6 | GO:0006270 |

| | | | | |
|---|---|---|---|---|
| fatty acid catabolic process | 0.0012 6835 | FBgn0025352,FBgn0031092,FBgn0034629,FBgn0035383 ,FBgn0038742,FBgn0086712 | 6 | GO:0009 062 |
| monocarbo xylic acid catabolic process | 0.0026 97 | FBgn0025352,FBgn0031092,FBgn0034629,FBgn0035383 ,FBgn0038742,FBgn0086712 | 6 | GO:0072 329 |
| chitin metabolic process | 0.0031 9207 | FBgn0022700,FBgn0034582,FBgn0036948,FBgn0038632 ,FBgn0040959,FBgn0261681 | 6 | GO:0006 030 |
| double-strand break repair via homologou s recombinat ion | 0.0087 4888 | FBgn0020633,FBgn0025815,FBgn0026143,FBgn0027868 ,FBgn0037301,FBgn0040290 | 6 | GO:0000 724 |
| recombinat ional repair | 0.0087 4888 | FBgn0020633,FBgn0025815,FBgn0026143,FBgn0027868 ,FBgn0037301,FBgn0040290 | 6 | GO:0000 725 |
| glucosamin e-containing compound metabolic process | 0.0087 4888 | FBgn0022700,FBgn0034582,FBgn0036948,FBgn0038632 ,FBgn0040959,FBgn0261681 | 6 | GO:1901 071 |
| lipid homeostasi s | 0.0191 5643 | FBgn0011204,FBgn0031381,FBgn0034629,FBgn0035383 ,FBgn0038074,FBgn0086712 | 6 | GO:0055 088 |
| aminoglyc an metabolic process | 0.0211 2945 | FBgn0022700,FBgn0034582,FBgn0036948,FBgn0038632 ,FBgn0040959,FBgn0261681 | 6 | GO:0006 022 |
| lipid modificatio n | 0.0388 4904 | FBgn0015277,FBgn0025352,FBgn0031092,FBgn0034629 ,FBgn0035383,FBgn0086712 | 6 | GO:0030 258 |
| DNA duplex unwinding | 0.0003 0339 | FBgn0015075,FBgn0020633,FBgn0025815,FBgn0040290 ,FBgn0261850 | 5 | GO:0032 508 |
| DNA geometric change | 0.0004 3786 | FBgn0015075,FBgn0020633,FBgn0025815,FBgn0040290 ,FBgn0261850 | 5 | GO:0032 392 |
| drug transport | 0.0023 5624 | FBgn0010497,FBgn0037140,FBgn0037668,FBgn0039357 ,FBgn0261090 | 5 | GO:0015 893 |
| fatty acid beta-oxidation | 0.0029 3478 | FBgn0025352,FBgn0031092,FBgn0034629,FBgn0035383 ,FBgn0086712 | 5 | GO:0006 635 |
| fatty acid oxidation | 0.0043 8844 | FBgn0025352,FBgn0031092,FBgn0034629,FBgn0035383 ,FBgn0086712 | 5 | GO:0019 395 |
| lipid oxidation | 0.0052 8033 | FBgn0025352,FBgn0031092,FBgn0034629,FBgn0035383 ,FBgn0086712 | 5 | GO:0034 440 |
| maturation of SSU-rRNA | 0.0305 2081 | FBgn0030081,FBgn0030136,FBgn0033454,FBgn0037073 ,FBgn0038597 | 5 | GO:0030 490 |
| neurotrans mitter | 0.0042 325 | FBgn0011768,FBgn0029823,FBgn0037513,FBgn0039094 | 4 | GO:0042 133 |

| | | | | |
|---|---|---|---|---|
| metabolic process | | | | |
| DNA amplification | 0.00543906 | FBgn0025815,FBgn0026143,FBgn0040290,FBgn0286788 | 4 | GO:0006277 |
| cellular amino acid biosynthetic process | 0.02720496 | FBgn0029823,FBgn0037513,FBgn0038074,FBgn0039094 | 4 | GO:0008652 |
| positive regulation of mitotic cell cycle | 0.02720496 | FBgn0026143,FBgn0032929,FBgn0040290,FBgn0041147 | 4 | GO:0045931 |
| regulation of DNA metabolic process | 0.03950524 | FBgn0037301,FBgn0037345,FBgn0050085,FBgn0261850 | 4 | GO:0051052 |
| positive regulation of DNA metabolic process | 0.000942 | FBgn0037301,FBgn0037345,FBgn0261850 | 3 | GO:0051054 |
| double-strand break repair via break-induced replication | 0.00307374 | FBgn0020633,FBgn0025815,FBgn0026143 | 3 | GO:0000727 |
| DNA unwinding involved in DNA replication | 0.00474912 | FBgn0020633,FBgn0025815,FBgn0040290 | 3 | GO:0006268 |
| vitamin metabolic process | 0.00687967 | FBgn0028375,FBgn0029823,FBgn0267408 | 3 | GO:0006766 |
| neurotransmitter biosynthetic process | 0.00687967 | FBgn0029823,FBgn0037513,FBgn0039094 | 3 | GO:0042136 |
| nucleobase biosynthetic process | 0.00687967 | FBgn0003257,FBgn0029823,FBgn0037513 | 3 | GO:0046112 |
| sulfur compound transport | 0.00687967 | FBgn0037668,FBgn0039357,FBgn0039736 | 3 | GO:0072348 |
| peptide catabolic process | 0.01623751 | FBgn0038135,FBgn0051198,FBgn0051343 | 3 | GO:0043171 |
| organic hydroxy compound transport | 0.02039263 | FBgn0031381,FBgn0261090,FBgn0261675 | 3 | GO:0015850 |
| nucleobase metabolic process | 0.02507592 | FBgn0003257,FBgn0029823,FBgn0037513 | 3 | GO:0009112 |

| | | | | |
|---|---|---|---|---|
| ribonucleoside monophosphate metabolic process | 0.02507592 | FBgn0003257,FBgn0034988,FBgn0038467 | 3 | GO:0009161 |
| eggshell chorion gene amplification | 0.03028677 | FBgn0025815,FBgn0040290,FBgn0286788 | 3 | GO:0007307 |
| nucleoside monophosphate metabolic process | 0.03028677 | FBgn0003257,FBgn0034988,FBgn0038467 | 3 | GO:0009123 |
| defense response to Gram-positive bacterium | 0.03028677 | FBgn0033593,FBgn0038973,FBgn0039102 | 3 | GO:0050830 |
| acylglycerol homeostasis | 0.03028677 | FBgn0011204,FBgn0035383,FBgn0038074 | 3 | GO:0055090 |
| triglyceride homeostasis | 0.03028677 | FBgn0011204,FBgn0035383,FBgn0038074 | 3 | GO:0070328 |
| inorganic anion transport | 0.03602086 | FBgn0010497,FBgn0037668,FBgn0039736 | 3 | GO:0015698 |
| nuclear DNA replication | 0.03602086 | FBgn0020633,FBgn0025815,FBgn0026143 | 3 | GO:0033260 |
| positive regulation of mitotic cell cycle phase transition | 0.04227057 | FBgn0026143,FBgn0040290,FBgn0041147 | 3 | GO:1901992 |
| detoxification | 0.04902542 | FBgn0011768,FBgn0031182,FBgn0038412 | 3 | GO:0098754 |
| chromatin silencing at rDNA | 0.00217883 | FBgn0034422,FBgn0039687 | 2 | GO:0000183 |
| positive regulation of DNA recombination | 0.00217883 | FBgn0037301,FBgn0261850 | 2 | GO:0045911 |
| glycine biosynthetic process | 0.00633435 | FBgn0029823,FBgn0039094 | 2 | GO:0006545 |
| deoxyribonucleotide biosynthetic process | 0.00633435 | FBgn0011703,FBgn0011704 | 2 | GO:0009263 |

| | | | | |
|---|---|---|---|---|
| response to nicotine | 0.00633435 | FBgn0031030,FBgn0036381 | 2 | GO:0035094 |
| regulation of mitochondrial mRNA stability | 0.00633435 | FBgn0027794,FBgn0284256 | 2 | GO:0044528 |
| protein homotetramerization | 0.00633435 | FBgn0029823,FBgn0038074 | 2 | GO:0051289 |
| regulation of mitochondrial transcription | 0.00633435 | FBgn0027794,FBgn0284256 | 2 | GO:1903108 |
| reactive nitrogen species metabolic process | 0.00633435 | FBgn0011768,FBgn0030966 | 2 | GO:2001057 |
| pre-replicative complex assembly involved in nuclear cell cycle DNA replication | 0.01227841 | FBgn0020633,FBgn0025815 | 2 | GO:0006267 |
| deoxyribonucleotide metabolic process | 0.01227841 | FBgn0011703,FBgn0011704 | 2 | GO:0009262 |
| pre-replicative complex assembly | 0.01227841 | FBgn0020633,FBgn0025815 | 2 | GO:0036388 |
| pre-replicative complex assembly involved in cell cycle DNA replication | 0.01227841 | FBgn0020633,FBgn0025815 | 2 | GO:1902299 |
| chitin catabolic process | 0.01983602 | FBgn0022700,FBgn0034582 | 2 | GO:0006032 |
| N-terminal protein amino acid acetylation | 0.01983602 | FBgn0039687,FBgn0243511 | 2 | GO:0006474 |
| sulfate transport | 0.01983602 | FBgn0037668,FBgn0039736 | 2 | GO:0008272 |
| regulation of mitochondr | 0.01983602 | FBgn0029131,FBgn0029588 | 2 | GO:0046902 |

| | | | | |
|---|---|---|---|---|
| ial membrane permeability | | | | |
| protein tetramerization | 0.01983602 | FBgn0029823,FBgn0038074 | 2 | GO:0051262 |
| necrotic cell death | 0.01983602 | FBgn0029131,FBgn0029588 | 2 | GO:0070265 |
| regulation of membrane permeability | 0.01983602 | FBgn0029131,FBgn0029588 | 2 | GO:0090559 |
| 'de novo' pyrimidine nucleobase biosynthetic process | 0.02884451 | FBgn0003257,FBgn0037513 | 2 | GO:0006207 |
| glycine metabolic process | 0.02884451 | FBgn0029823,FBgn0039094 | 2 | GO:0006544 |
| phosphate ion transport | 0.02884451 | FBgn0010497,FBgn0037668 | 2 | GO:0006817 |
| serine family amino acid biosynthetic process | 0.02884451 | FBgn0029823,FBgn0039094 | 2 | GO:0009070 |
| cholesterol transport | 0.02884451 | FBgn0031381,FBgn0261675 | 2 | GO:0030301 |
| amino sugar catabolic process | 0.02884451 | FBgn0022700,FBgn0034582 | 2 | GO:0046348 |
| glucosamine-containing compound catabolic process | 0.02884451 | FBgn0022700,FBgn0034582 | 2 | GO:1901072 |
| regulation of oxidative phosphorylation | 0.03915282 | FBgn0027794,FBgn0284256 | 2 | GO:0002082 |
| digestion | 0.03915282 | FBgn0053542,FBgn0261675 | 2 | GO:0007586 |
| sterol transport | 0.03915282 | FBgn0031381,FBgn0261675 | 2 | GO:0015918 |
| pyrimidine nucleobase biosynthetic process | 0.03915282 | FBgn0003257,FBgn0037513 | 2 | GO:0019856 |
| RNA exon ligation | 0.04677419 | FBgn0032781 | 1 | GO:0000378 |

| | | | | |
|---|---|---|---|---|
| nucleotide-excision repair, DNA duplex unwinding | 0.0467 7419 | FBgn0261850 | 1 | GO:0000 717 |
| tRNA exon ligation | 0.0467 7419 | FBgn0032781 | 1 | GO:0000 968 |
| tRNA exon ligation utilizing 2',3' cyclic phosphate of 5'-exon as source of linkage phosphate | 0.0467 7419 | FBgn0032781 | 1 | GO:0000 971 |
| biosynthetic process of antibacterial peptides active against Gram-positive bacteria | 0.0467 7419 | FBgn0039102 | 1 | GO:0002 815 |
| regulation of biosynthetic process of antibacterial peptides active against Gram-positive bacteria | 0.0467 7419 | FBgn0039102 | 1 | GO:0002 816 |
| L-serine catabolic process | 0.0467 7419 | FBgn0029823 | 1 | GO:0006 565 |
| fat-soluble vitamin metabolic process | 0.0467 7419 | FBgn0028375 | 1 | GO:0006 775 |
| positive regulation of biosynthetic process of antibacterial peptides active against Gram- | 0.0467 7419 | FBgn0039102 | 1 | GO:0006 965 |

| | | | | |
|---|---|---|---|---|
| positive bacteria | | | | |
| regulation of preblastoderm mitotic cell cycle | 0.04677419 | FBgn0002441 | 1 | GO:0007347 |
| specification of segmental identity, labial segment | 0.04677419 | FBgn0001150 | 1 | GO:0007381 |
| peptidyl-lysine modification to peptidyl-hypusine | 0.04677419 | FBgn0261479 | 1 | GO:0008612 |
| menaquinone metabolic process | 0.04677419 | FBgn0028375 | 1 | GO:0009233 |
| menaquinone biosynthetic process | 0.04677419 | FBgn0028375 | 1 | GO:0009234 |
| response to amine | 0.04677419 | FBgn0038542 | 1 | GO:0014075 |
| S-adenosyl-L-methionine transport | 0.04677419 | FBgn0039357 | 1 | GO:0015805 |
| nucleoside transport | 0.04677419 | FBgn0033371 | 1 | GO:0015858 |
| acetylcholine transport | 0.04677419 | FBgn0037140 | 1 | GO:0015870 |
| protein nitrosylation | 0.04677419 | FBgn0011768 | 1 | GO:0017014 |
| peptidyl-cysteine S-nitrosylation | 0.04677419 | FBgn0011768 | 1 | GO:0018119 |
| glycine biosynthetic process from serine | 0.04677419 | FBgn0029823 | 1 | GO:0019264 |
| intestinal cholesterol absorption | 0.04677419 | FBgn0261675 | 1 | GO:0030299 |
| protection from non-homologous end | 0.04677419 | FBgn0037338 | 1 | GO:0031848 |

| | | | | |
|---|---|---|---|---|
| joining at telomere | | | | |
| regulation of deoxyribonuclease activity | 0.04677419 | FBgn0037345 | 1 | GO:0032070 |
| positive regulation of nuclease activity | 0.04677419 | FBgn0037345 | 1 | GO:0032075 |
| positive regulation of deoxyribonuclease activity | 0.04677419 | FBgn0037345 | 1 | GO:0032077 |
| ubiquinone biosynthetic process via 3,4-dihydroxy-5-polyprenyl benzoate | 0.04677419 | FBgn0028375 | 1 | GO:0032194 |
| negative regulation of synaptic transmission, cholinergic | 0.04677419 | FBgn0037140 | 1 | GO:0032223 |
| geranyl diphosphate metabolic process | 0.04677419 | FBgn0025373 | 1 | GO:0033383 |
| geranyl diphosphate biosynthetic process | 0.04677419 | FBgn0025373 | 1 | GO:0033384 |
| beta-alanine biosynthetic process via 3-ureidopropionate | 0.04677419 | FBgn0037513 | 1 | GO:0033396 |
| internal genitalia morphogenesis | 0.04677419 | FBgn0267728 | 1 | GO:0035260 |
| neurotrophin signaling pathway | 0.04677419 | FBgn0267824 | 1 | GO:0038179 |
| nitrate metabolic | 0.04677419 | FBgn0030966 | 1 | GO:0042126 |

| | | | | |
|---|---|---|---|---|
| process | | | | |
| nitrate assimilation | 0.04677419 | FBgn0030966 | 1 | GO:0042128 |
| cellular response to glucose starvation | 0.04677419 | FBgn0034422 | 1 | GO:0042149 |
| fat-soluble vitamin biosynthetic process | 0.04677419 | FBgn0028375 | 1 | GO:0042362 |
| vitamin K biosynthetic process | 0.04677419 | FBgn0028375 | 1 | GO:0042371 |
| vitamin K metabolic process | 0.04677419 | FBgn0028375 | 1 | GO:0042373 |
| pyridoxal metabolic process | 0.04677419 | FBgn0267408 | 1 | GO:0042817 |
| telomere maintenance in response to DNA damage | 0.04677419 | FBgn0037338 | 1 | GO:0043247 |
| 'de novo' UMP biosynthetic process | 0.04677419 | FBgn0003257 | 1 | GO:0044205 |
| lipid digestion | 0.04677419 | FBgn0261675 | 1 | GO:0044241 |
| regulation of transcription involved in anterior/posterior axis specification | 0.04677419 | FBgn0001150 | 1 | GO:0044324 |
| sodium-dependent phosphate transport | 0.04677419 | FBgn0010497 | 1 | GO:0044341 |
| positive regulation of mitotic recombination | 0.04677419 | FBgn0261850 | 1 | GO:0045951 |
| regulation of transcription by glucose | 0.04677419 | FBgn0034422 | 1 | GO:0046015 |

| | | | | |
|---|---|---|---|---|
| formaldehyde metabolic process | 0.04677419 | FBgn0011768 | 1 | GO:0046292 |
| formaldehyde catabolic process | 0.04677419 | FBgn0011768 | 1 | GO:0046294 |
| folic acid metabolic process | 0.04677419 | FBgn0029823 | 1 | GO:0046655 |
| ketone body biosynthetic process | 0.04677419 | FBgn0035383 | 1 | GO:0046951 |
| neurotrophin TRK receptor signaling pathway | 0.04677419 | FBgn0267824 | 1 | GO:0048011 |
| S-adenosylmethionine catabolic process | 0.04677419 | FBgn0038074 | 1 | GO:0050843 |
| intestinal absorption | 0.04677419 | FBgn0261675 | 1 | GO:0050892 |
| coenzyme transport | 0.04677419 | FBgn0039357 | 1 | GO:0051182 |
| L-glutamate import | 0.04677419 | FBgn0010497 | 1 | GO:0051938 |
| apoptotic process involved in morphogenesis | 0.04677419 | FBgn0029131 | 1 | GO:0060561 |
| regulation of chromatin silencing at rDNA | 0.04677419 | FBgn0039687 | 1 | GO:0061187 |
| cellular response to amine stimulus | 0.04677419 | FBgn0038542 | 1 | GO:0071418 |
| replication fork arrest involved in DNA replication termination | 0.04677419 | FBgn0050085 | 1 | GO:0071807 |
| tyramine signaling pathway | 0.04677419 | FBgn0038542 | 1 | GO:0071928 |
| nitrogen cycle | 0.04677419 | FBgn0030966 | 1 | GO:0071941 |

| | | | | |
|---|---|---|---|---|
| metabolic process | | | | |
| regulation of nitric oxide metabolic process | 0.0467 7419 | FBgn0011768 | 1 | GO:0080 164 |
| peptidyl-N-phospho-arginine dephosphorylation | 0.0467 7419 | FBgn0051469 | 1 | GO:0098 628 |
| intestinal lipid absorption | 0.0467 7419 | FBgn0261675 | 1 | GO:0098 856 |
| cellular detoxification of aldehyde | 0.0467 7419 | FBgn0011768 | 1 | GO:0110 095 |
| cellular response to aldehyde | 0.0467 7419 | FBgn0011768 | 1 | GO:0110 096 |
| regulation of phospholipase C-activating G protein-coupled receptor signaling pathway | 0.0467 7419 | FBgn0038542 | 1 | GO:1900 736 |
| positive regulation of phospholipase C-activating G protein-coupled receptor signaling pathway | 0.0467 7419 | FBgn0038542 | 1 | GO:1900 738 |
| sarcosine metabolic process | 0.0467 7419 | FBgn0038074 | 1 | GO:1901 052 |
| sarcosine biosynthetic process | 0.0467 7419 | FBgn0038074 | 1 | GO:1901 054 |
| acetate ester transport | 0.0467 7419 | FBgn0037140 | 1 | GO:1901 374 |
| nucleoside transmembrane transport | 0.0467 7419 | FBgn0033371 | 1 | GO:1901 642 |

| | | | | |
|---|---|---|---|---|
| negative regulation of compound eye retinal cell apoptotic process | 0.04677419 | FBgn0032929 | 1 | GO:1901693 |
| regulation of exodeoxyribonuclease activity | 0.04677419 | FBgn0037345 | 1 | GO:1902392 |
| positive regulation of exodeoxyribonuclease activity | 0.04677419 | FBgn0037345 | 1 | GO:1902394 |
| mitotic DNA replication preinitiation complex assembly | 0.04677419 | FBgn0026143 | 1 | GO:1902977 |
| regulation of tRNA metabolic process | 0.04677419 | FBgn0032781 | 1 | GO:1903326 |
| positive regulation of tRNA metabolic process | 0.04677419 | FBgn0032781 | 1 | GO:1903328 |
| microtubule bundle formation involved in mitotic spindle midzone assembly | 0.04677419 | FBgn0011692 | 1 | GO:1903562 |
| regulation of cytoplasmic transport | 0.04677419 | FBgn0015277 | 1 | GO:1903649 |
| response to tetrahydrofolate | 0.04677419 | FBgn0029823 | 1 | GO:1904481 |
| cellular response to tetrahydrofolate | 0.04677419 | FBgn0029823 | 1 | GO:1904482 |
| positive regulation of double-strand | 0.04677419 | FBgn0037301 | 1 | GO:1905168 |

| | | | | |
|---|---|---|---|---|
| break repair via homologous recombination | | | | |
| regulation of exonuclease activity | 0.04677419 | FBgn0037345 | 1 | GO:1905777 |
| positive regulation of exonuclease activity | 0.04677419 | FBgn0037345 | 1 | GO:1905779 |
| regulation of peptidyl-cysteine S-nitrosylation | 0.04677419 | FBgn0011768 | 1 | GO:2000169 |
| regulation of tRNA processing | 0.04677419 | FBgn0032781 | 1 | GO:2000235 |
| positive regulation of tRNA processing | 0.04677419 | FBgn0032781 | 1 | GO:2000237 |
| regulation of early endosome to late endosome transport | 0.04677419 | FBgn0015277 | 1 | GO:2000641 |
| positive regulation of double-strand break repair | 0.04677419 | FBgn0037301 | 1 | GO:2000781 |

**Table 2.4h: GO enrichment for hits equalized in control females relative to 20HE males**

| GO enrichment | p-value | Hits | Gene matches | GO ID |
|---|---|---|---|---|
| ï»¿mitochondrial translation | 4.82E-07 | FBgn0011787,FBgn0014023,FBgn0026741,FBgn0029718,FBgn0031231,FBgn0032053,FBgn0032486,FBgn0033184,FBgn0034579,FBgn0035064,FBgn0035374,FBgn0036335,FBgn0036569,FBgn0037330,FBgn0038426,FBgn0038474,FBgn0039159,FBgn0042112,FBgn0051450,FBgn0083983,FBgn0263863 | 21 | GO:0032543 |
| DNA-dependent DNA replication | 1.2254E-06 | FBgn0002878,FBgn0003116,FBgn0004406,FBgn0005696,FBgn0010438,FBgn0011762,FBgn0014861,FBgn0015271,FBgn0017577,FBgn0030054,FBgn0032290,FBgn0032813,FBgn0033890,FBgn0035644,FBgn0035918,FBgn0039403,FBgn0259113,FBgn0260985,FBgn0262619 | 19 | GO:0006261 |

| | | | | |
|---|---|---|---|---|
| DNA replication | 1.2492E-06 | FBgn0002878,FBgn0003116,FBgn0004406,FBgn0005696,FBgn0010382,FBgn0010438,FBgn0011762,FBgn0014861,FBgn0015271,FBgn0017577,FBgn0030054,FBgn0032290,FBgn0032813,FBgn0033890,FBgn0034495,FBgn0035644,FBgn0035918,FBgn0039403,FBgn0259113,FBgn0260985,FBgn0262619 | 21 | GO:0006260 |
| mitochondrial gene expression | 7.7436E-06 | FBgn0011787,FBgn0014023,FBgn0026741,FBgn0029718,FBgn0031231,FBgn0032053,FBgn0032486,FBgn0033184,FBgn0034579,FBgn0035064,FBgn0035374,FBgn0036335,FBgn0036569,FBgn0037330,FBgn0038426,FBgn0038474,FBgn0039159,FBgn0042112,FBgn0051450,FBgn0083983,FBgn0263863 | 21 | GO:0140053 |
| DNA replication initiation | 0.00029005 | FBgn0002878,FBgn0005696,FBgn0014861,FBgn0015271,FBgn0017577,FBgn0035918,FBgn0259113 | 7 | GO:0006270 |
| heterocycle metabolic process | 0.00052487 | FBgn0000377,FBgn0000477,FBgn0000543,FBgn0000562,FBgn0000591,FBgn0001187,FBgn0002522,FBgn0002542,FBgn0002566,FBgn0002878,FBgn0002899,FBgn0003042,FBgn0003044,FBgn0003116,FBgn0003512,FBgn0003515,FBgn0003996,FBgn0004170,FBgn0004396,FBgn0004403,FBgn0004406,FBgn0004837,FBgn0004907,FBgn0005674,FBgn0005696,FBgn0005771,FBgn0010382,FBgn0010786,FBgn0011291,FBgn0011660,FBgn0011762,FBgn0011787,FBgn0013972,FBgn0014037,FBgn0014861,FBgn0014949,FBgn0015271,FBgn0015299,FBgn0015396,FBgn0015778,FBgn0016070,FBgn0016120,FBgn0016691,FBgn0016917,FBgn0017577,FBgn0019644,FBgn0019650,FBgn0022986,FBgn0023214,FBgn0024987,FBgn0025185,FBgn0025463,FBgn0025629,FBgn0025680,FBgn0025741,FBgn0025832,FBgn0026679,FBgn0026702,FBgn0026876,FBgn0027499,FBgn0027620,FBgn0028342,FBgn0029006,FBgn0029079,FBgn0029977,FBgn0030054,FBgn0030085,FBgn0030093,FBgn0030365,FBgn0030432,FBgn0030507,FBgn0030631,FBgn0030683,FBgn0030699,FBgn0031227,FBgn0031309,FBgn0031321,FBgn0031643,FBgn0031663,FBgn0031851,FBgn0032130,FBgn0032290,FBgn0032400,FBgn0032813,FBgn0032956,FBgn0033010,FBgn0033507,FBgn0033859,FBgn0033890,FBgn0033921,FBgn0033998,FBgn0034065,FBgn0034310,FBgn0034564,FBgn0034614,FBgn0034650,FBgn0034938,FBgn0035064,FBgn0035153,FBgn0035246,FBgn0035318,FBgn0035397,FBgn0035644,FBgn0035900,FBgn0035918,FBgn0035986,FBgn0036018,FBgn0036157,FBgn0036373,FBgn0036374,FBgn0036569,FBgn0036734,FBgn0036735,FBgn0036754,FBgn0036771,FBgn0036826,FBgn0036827,FBgn0037109,FBgn0037146,FBgn0037330,FBgn0037607,FBgn0037669,FBgn0037716,FBgn0037722,FBgn0037822,FBgn0037918,FBgn0037926,FBgn0038173,FBgn0038224,FBgn0038237,FBgn0038390,FBgn0038474,FBgn0038546,FBgn0038592,FBgn0039182,FBgn0039306,FBgn0039403,FBgn0039404,FBgn0039462,FBgn0039464,FBgn0039650,FBgn0039740,FBgn0039938,FBgn0039972,FBgn0041103,FBgn0043796,FBgn0043900,FBgn0051126,FBgn0051550,FBgn0051739,FBgn0053504,FBgn0061469,FBgn0085484,FBgn0086450,FBgn0086679,FBgn0250850,FBgn0259113,FBgn0259176,FBgn0259938,FBgn0260817,FBgn | 177 | GO:0046483 |

| | | | | |
|---|---|---|---|---|
| | | 0260985,FBgn0261287,FBgn0261872,FBgn0262467,FBgn0262619,FBgn0263144,FBgn0263237,FBgn0263855,FBgn0265048,FBgn0265523,FBgn0265623,FBgn0266411,FBgn0266917,FBgn0267792,FBgn0267821,FBgn0286027,FBgn0286506 | | |
| mitotic DNA replication | 0.00053522 | FBgn0014861,FBgn0032290,FBgn0035644,FBgn0259113,FBgn0262619 | 5 | GO:1902969 |
| cellular aromatic compound metabolic process | 0.00101431 | FBgn0000377,FBgn0000477,FBgn0000543,FBgn0000562,FBgn0000591,FBgn0001187,FBgn0002522,FBgn0002542,FBgn0002566,FBgn0002878,FBgn0002899,FBgn0003042,FBgn0003044,FBgn0003116,FBgn0003512,FBgn0003515,FBgn0003996,FBgn0004170,FBgn0004396,FBgn0004403,FBgn0004406,FBgn0004837,FBgn0004907,FBgn0005674,FBgn0005696,FBgn0005771,FBgn0010382,FBgn0010786,FBgn0011291,FBgn0011660,FBgn0011762,FBgn0011787,FBgn0013972,FBgn0014037,FBgn0014380,FBgn0014861,FBgn0014949,FBgn0015271,FBgn0015299,FBgn0015396,FBgn0015778,FBgn0016070,FBgn0016120,FBgn0016691,FBgn0016917,FBgn0017577,FBgn0019644,FBgn0019650,FBgn0022986,FBgn0023214,FBgn0024987,FBgn0025185,FBgn0025463,FBgn0025629,FBgn0025680,FBgn0025741,FBgn0025832,FBgn0025936,FBgn0026679,FBgn0026702,FBgn0026876,FBgn0027499,FBgn0027620,FBgn0028342,FBgn0029006,FBgn0029079,FBgn0029977,FBgn0030054,FBgn0030085,FBgn0030093,FBgn0030365,FBgn0030432,FBgn0030507,FBgn0030631,FBgn0030683,FBgn0030699,FBgn0031227,FBgn0031309,FBgn0031321,FBgn0031643,FBgn0031663,FBgn0031851,FBgn0032130,FBgn0032290,FBgn0032400,FBgn0032813,FBgn0032956,FBgn0033010,FBgn0033507,FBgn0033859,FBgn0033890,FBgn0033921,FBgn0033998,FBgn0034065,FBgn0034310,FBgn0034564,FBgn0034614,FBgn0034650,FBgn0034938,FBgn0035064,FBgn0035153,FBgn0035246,FBgn0035318,FBgn0035397,FBgn0035644,FBgn0035900,FBgn0035918,FBgn0035986,FBgn0036018,FBgn0036157,FBgn0036373,FBgn0036374,FBgn0036569,FBgn0036734,FBgn0036735,FBgn0036754,FBgn0036771,FBgn0036826,FBgn0036827,FBgn0037109,FBgn0037330,FBgn0037607,FBgn0037669,FBgn0037716,FBgn0037722,FBgn0037822,FBgn0037918,FBgn0037926,FBgn0038173,FBgn0038224,FBgn0038237,FBgn0038390,FBgn0038474,FBgn0038546,FBgn0038592,FBgn0039182,FBgn0039306,FBgn0039403,FBgn0039404,FBgn0039462,FBgn0039464,FBgn0039650,FBgn0039740,FBgn0039938,FBgn0039972,FBgn0041103,FBgn0043796,FBgn0043900,FBgn0051126,FBgn0051550,FBgn0051739,FBgn0053504,FBgn0061469,FBgn0085484,FBgn0086450,FBgn0086679,FBgn0250850,FBgn0259113,FBgn0259176,FBgn0259938,FBgn0260817,FBgn0260985,FBgn0261287,FBgn0261872,FBgn0262467,FBgn0262619,FBgn0263144,FBgn0263237,FBgn0263855,FBgn0265048,FBgn0265523,FBgn0265623,FBgn0266411,FBgn0266917,FBgn0267792,FBgn0267821,FBgn0286027,FBgn0286506 | 178 | GO:0006725 |
| copper ion transport | 0.00107248 | FBgn0030343,FBgn0030610,FBgn0062413,FBgn0262467 | 4 | GO:0006825 |

| | | | | |
|---|---|---|---|---|
| nuclear DNA replication | 0.00117708 | FBgn0014861,FBgn0017577,FBgn0032290,FBgn0035644,FBgn0259113,FBgn0262619 | 6 | GO:0033260 |
| organic cyclic compound metabolic process | 0.00118241 | FBgn0000377,FBgn0000477,FBgn0000543,FBgn0000562,FBgn0000591,FBgn0001187,FBgn0002522,FBgn0002542,FBgn0002566,FBgn0002878,FBgn0002899,FBgn0003042,FBgn0003044,FBgn0003116,FBgn0003512,FBgn0003515,FBgn0003996,FBgn0004170,FBgn0004396,FBgn0004403,FBgn0004406,FBgn0004837,FBgn0004907,FBgn0005674,FBgn0005696,FBgn0005771,FBgn0010382,FBgn0010786,FBgn0011291,FBgn0011660,FBgn0011762,FBgn0011787,FBgn0013972,FBgn0014037,FBgn0014380,FBgn0014861,FBgn0014949,FBgn0015271,FBgn0015299,FBgn0015396,FBgn0015778,FBgn0016070,FBgn0016120,FBgn0016691,FBgn0016917,FBgn0017577,FBgn0019644,FBgn0019650,FBgn0022986,FBgn0023214,FBgn0024987,FBgn0025185,FBgn0025463,FBgn0025629,FBgn0025680,FBgn0025741,FBgn0025832,FBgn0025936,FBgn0026679,FBgn0026702,FBgn0026876,FBgn0027499,FBgn0027620,FBgn0028342,FBgn0029006,FBgn0029079,FBgn0029977,FBgn0030054,FBgn0030085,FBgn0030093,FBgn0030365,FBgn0030432,FBgn0030507,FBgn0030596,FBgn0030631,FBgn0030683,FBgn0030699,FBgn0031227,FBgn0031309,FBgn0031321,FBgn0031643,FBgn0031663,FBgn0031851,FBgn0032130,FBgn0032290,FBgn0032400,FBgn0032813,FBgn0032956,FBgn0033010,FBgn0033507,FBgn0033859,FBgn0033890,FBgn0033921,FBgn0033998,FBgn0034065,FBgn0034310,FBgn0034564,FBgn0034614,FBgn0034650,FBgn0034938,FBgn0035064,FBgn0035153,FBgn0035246,FBgn0035318,FBgn0035397,FBgn0035644,FBgn0035900,FBgn0035918,FBgn0035986,FBgn0036018,FBgn0036157,FBgn0036373,FBgn0036374,FBgn0036569,FBgn0036734,FBgn0036735,FBgn0036754,FBgn0036771,FBgn0036826,FBgn0036827,FBgn0037109,FBgn0037146,FBgn0037330,FBgn0037607,FBgn0037669,FBgn0037716,FBgn0037722,FBgn0037822,FBgn0037918,FBgn0037926,FBgn0038173,FBgn0038224,FBgn0038237,FBgn0038390,FBgn0038474,FBgn0038546,FBgn0038592,FBgn0039182,FBgn0039306,FBgn0039403,FBgn0039404,FBgn0039462,FBgn0039464,FBgn0039650,FBgn0039740,FBgn0039938,FBgn0039972,FBgn0041103,FBgn0043796,FBgn0043900,FBgn0051126,FBgn0051550,FBgn0051739,FBgn0053100,FBgn0053504,FBgn0061469,FBgn0085484,FBgn0086450,FBgn0086679,FBgn0250850,FBgn0259113,FBgn0259176,FBgn0259938,FBgn0260817,FBgn0260985,FBgn0261287,FBgn0261872,FBgn0262467,FBgn0262619,FBgn0263144,FBgn0263237,FBgn0263855,FBgn0265048,FBgn0265523,FBgn0265623,FBgn0266411,FBgn0266917,FBgn0267792,FBgn0267821,FBgn0286027,FBgn0286506 | 181 | GO:1901360 |
| maturation of SSU-rRNA | 0.00165345 | FBgn0002899,FBgn0004403,FBgn0030085,FBgn0031643,FBgn0034564,FBgn0036754,FBgn0038474,FBgn0039306,FBgn0039404 | 9 | GO:0030490 |
| mitochondrial DNA replication | 0.00172323 | FBgn0003116,FBgn0004406,FBgn0010438 | 3 | GO:0006264 |

| | | | | |
|---|---|---|---|---|
| aminergic neurotransmitter loading into synaptic vesicle | 0.00172323 | FBgn0003515,FBgn0003996,FBgn0043005 | 3 | GO:0015842 |
| cell cycle DNA replication | 0.00233396 | FBgn0014861,FBgn0017577,FBgn0030054,FBgn0032290,FBgn0033890,FBgn0035644,FBgn0259113,FBgn0262619 | 8 | GO:0044786 |
| nucleobase-containing compound metabolic process | 0.00269511 | FBgn0000377,FBgn0000477,FBgn0000543,FBgn0000562,FBgn0000591,FBgn0001187,FBgn0002522,FBgn0002542,FBgn0002878,FBgn0002899,FBgn0003042,FBgn0003044,FBgn0003512,FBgn0004170,FBgn0004396,FBgn0004403,FBgn0004406,FBgn0004837,FBgn0004907,FBgn0005674,FBgn0005696,FBgn0005771,FBgn0010382,FBgn0011291,FBgn0011660,FBgn0011762,FBgn0011787,FBgn0013972,FBgn0014037,FBgn0014861,FBgn0014949,FBgn0015271,FBgn0015299,FBgn0015396,FBgn0015778,FBgn0016070,FBgn0016120,FBgn0016691,FBgn0016917,FBgn0017577,FBgn0019644,FBgn0019650,FBgn0022986,FBgn0023214,FBgn0024987,FBgn0025185,FBgn0025463,FBgn0025629,FBgn0025680,FBgn0025741,FBgn0025832,FBgn0026679,FBgn0026702,FBgn0026876,FBgn0027499,FBgn0027620,FBgn0028342,FBgn0029006,FBgn0029079,FBgn0029977,FBgn0030054,FBgn0030085,FBgn0030093,FBgn0030365,FBgn0030432,FBgn0030507,FBgn0030631,FBgn0030683,FBgn0030699,FBgn0031227,FBgn0031309,FBgn0031321,FBgn0031643,FBgn0031663,FBgn0031851,FBgn0032130,FBgn0032290,FBgn0032400,FBgn0032813,FBgn0032956,FBgn0033010,FBgn0033507,FBgn0033859,FBgn0033890,FBgn0033921,FBgn0033998,FBgn0034065,FBgn0034310,FBgn0034564,FBgn0034614,FBgn0034650,FBgn0035064,FBgn0035153,FBgn0035246,FBgn0035318,FBgn0035397,FBgn0035644,FBgn0035900,FBgn0035918,FBgn0035986,FBgn0036018,FBgn0036373,FBgn0036374,FBgn0036569,FBgn0036734,FBgn0036735,FBgn0036754,FBgn0036771,FBgn0036826,FBgn0036827,FBgn0037109,FBgn0037330,FBgn0037607,FBgn0037669,FBgn0037716,FBgn0037722,FBgn0037822,FBgn0037918,FBgn0037926,FBgn0038173,FBgn0038224,FBgn0038237,FBgn0038390,FBgn0038474,FBgn0038546,FBgn0038592,FBgn0039182,FBgn0039306,FBgn0039403,FBgn0039404,FBgn0039462,FBgn0039464,FBgn0039650,FBgn0039740,FBgn0039938,FBgn0039972,FBgn0041103,FBgn0043796,FBgn0043900,FBgn0051126,FBgn0051550,FBgn0051739,FBgn0053504,FBgn0061469,FBgn0086450,FBgn0250850,FBgn0259113,FBgn0259176,FBgn0259938,FBgn0260817,FBgn0260985,FBgn0261287,FBgn0261872,FBgn0262467,FBgn0262619,FBgn0263144,FBgn0263237,FBgn0263855,FBgn0265048,FBgn0265523,FBgn0265623,FBgn0266411,FBgn0266917,FBgn0267792,FBgn0267821,FBgn0286027,FBgn0286506 | 167 | GO:0006139 |
| mitochondrial respiratory | 0.00316855 | FBgn0002021,FBgn0011227,FBgn0030610,FBgn0031247,FBgn0033274,FBgn0034919,FBgn0038437,FBgn0262467 | 8 | GO:0033108 |

| | | | | |
|---|---|---|---|---|
| chain complex assembly | | | | |
| regulation of helicase activity | 0.00328788 | FBgn0010438,FBgn0014861 | 2 | GO:0051095 |
| ATP biosynthetic process | 0.00365611 | FBgn0016120,FBgn0016691,FBgn0019644,FBgn0028342,FBgn0038224,FBgn0262467 | 6 | GO:0006754 |
| mitotic cell cycle phase transition | 0.00413304 | FBgn0002878,FBgn0003525,FBgn0004583,FBgn0004643,FBgn0004837,FBgn0004889,FBgn0010382,FBgn0011739,FBgn0024227,FBgn0031549,FBgn0032047,FBgn0035918,FBgn0038390,FBgn0039403,FBgn0263855 | 15 | GO:0044772 |
| mitotic cell cycle | 0.00437591 | FBgn0000140,FBgn0002878,FBgn0003042,FBgn0003525,FBgn0004170,FBgn0004378,FBgn0004583,FBgn0004643,FBgn0004837,FBgn0004889,FBgn0004907,FBgn0010314,FBgn0010382,FBgn0011020,FBgn0011739,FBgn0014861,FBgn0015271,FBgn0015391,FBgn0024227,FBgn0028292,FBgn0031549,FBgn0032047,FBgn0032290,FBgn0033890,FBgn0034495,FBgn0034569,FBgn0035249,FBgn0035644,FBgn0035918,FBgn0038390,FBgn0038565,FBgn0039403,FBgn0039638,FBgn0087021,FBgn0087040,FBgn0259113,FBgn0262619,FBgn0263237,FBgn0263855,FBgn0265523,FBgn0266418,FBgn0266465,FBgn0266917 | 43 | GO:0000278 |
| regulation of mitotic cell cycle phase transition | 0.00456763 | FBgn0002878,FBgn0003525,FBgn0004583,FBgn0004643,FBgn0004837,FBgn0004889,FBgn0010382,FBgn0024227,FBgn0031549,FBgn0035918,FBgn0038390,FBgn0039403,FBgn0263855 | 13 | GO:1901990 |
| mitotic cell cycle process | 0.00484144 | FBgn0000140,FBgn0002878,FBgn0003525,FBgn0004378,FBgn0004583,FBgn0004643,FBgn0004837,FBgn0004889,FBgn0010382,FBgn0011739,FBgn0014861,FBgn0015271,FBgn0015391,FBgn0024227,FBgn0028292,FBgn0031549,FBgn0032047,FBgn0032290,FBgn0034495,FBgn0034569,FBgn0035249,FBgn0035644,FBgn0035918,FBgn0038390,FBgn0039403,FBgn0039638,FBgn0087021,FBgn0087040,FBgn0259113,FBgn0262619,FBgn0263855,FBgn0266418 | 32 | GO:1903047 |
| cellular copper ion homeostasis | 0.00552936 | FBgn0030343,FBgn0062413,FBgn0262467 | 3 | GO:0006878 |
| neurotransmitter loading into synaptic vesicle | 0.00552936 | FBgn0003515,FBgn0003996,FBgn0043005 | 3 | GO:0098700 |
| peripheral nervous system development | 0.00607998 | FBgn0004170,FBgn0010382,FBgn0025936,FBgn0051721,FBgn0061469,FBgn0087040,FBgn0259938,FBgn0260440,FBgn0267821 | 9 | GO:0007422 |
| nucleic acid metabolic | 0.00625836 | FBgn0000377,FBgn0000477,FBgn0000543,FBgn0000591,FBgn0002522,FBgn0002542,FBgn0002878,FBgn0002899,FBgn0003042,FBgn0003044,FBgn0003512,FBgn0 | 148 | GO:0090304 |

| | | | | |
|---|---|---|---|---|
| process | | 004170,FBgn0004396,FBgn0004403,FBgn0004406,FBgn0004837,FBgn0004907,FBgn0005674,FBgn0005696,FBgn0005771,FBgn0010382,FBgn0011291,FBgn0011660,FBgn0011762,FBgn0011787,FBgn0014037,FBgn0014861,FBgn0014949,FBgn0015271,FBgn0015299,FBgn0015396,FBgn0015778,FBgn0016070,FBgn0016917,FBgn0017577,FBgn0019650,FBgn0022986,FBgn0023214,FBgn0024987,FBgn0025185,FBgn0025463,FBgn0025629,FBgn0025680,FBgn0025832,FBgn0026679,FBgn0026702,FBgn0027499,FBgn0027620,FBgn0029006,FBgn0029079,FBgn0029977,FBgn0030054,FBgn0030085,FBgn0030093,FBgn0030365,FBgn0030432,FBgn0030507,FBgn0030631,FBgn0030699,FBgn0031227,FBgn0031309,FBgn0031321,FBgn0031643,FBgn0031851,FBgn0032130,FBgn0032290,FBgn0032400,FBgn0032813,FBgn0032956,FBgn0033010,FBgn0033507,FBgn0033859,FBgn0033890,FBgn0033921,FBgn0033998,FBgn0034065,FBgn0034310,FBgn0034564,FBgn0034614,FBgn0034650,FBgn0035064,FBgn0035153,FBgn0035246,FBgn0035318,FBgn0035397,FBgn0035644,FBgn0035900,FBgn0035918,FBgn0035986,FBgn0036018,FBgn0036373,FBgn0036374,FBgn0036569,FBgn0036734,FBgn0036735,FBgn0036754,FBgn0036771,FBgn0036826,FBgn0036827,FBgn0037109,FBgn0037330,FBgn0037607,FBgn0037669,FBgn0037716,FBgn0037722,FBgn0037822,FBgn0037918,FBgn0037926,FBgn0038390,FBgn0038474,FBgn0038546,FBgn0038592,FBgn0039182,FBgn0039306,FBgn0039403,FBgn0039404,FBgn0039462,FBgn0039740,FBgn0039938,FBgn0039972,FBgn0041103,FBgn0043796,FBgn0043900,FBgn0051126,FBgn0051550,FBgn0051739,FBgn0053504,FBgn0061469,FBgn0250850,FBgn0259113,FBgn0259176,FBgn0259938,FBgn0260817,FBgn0260985,FBgn0261287,FBgn0261872,FBgn0262619,FBgn0263144,FBgn0263237,FBgn0263855,FBgn0265048,FBgn0265523,FBgn0265623,FBgn0266411,FBgn0266917,FBgn0267792,FBgn0267821,FBgn0286027 | | |
| regulation of cell cycle phase transition | 0.0069118 | FBgn0002878,FBgn0003525,FBgn0004583,FBgn0004643,FBgn0004837,FBgn0004889,FBgn0010382,FBgn0024227,FBgn0031549,FBgn0035918,FBgn0038390,FBgn0039403,FBgn0263855 | 13 | GO:1901987 |
| nucleoside triphosphate metabolic process | 0.0070387 | FBgn0016120,FBgn0016691,FBgn0019644,FBgn0028342,FBgn0031663,FBgn0038224,FBgn0262467 | 7 | GO:0009141 |
| cell cycle phase transition | 0.0074546 | FBgn0002878,FBgn0003525,FBgn0004583,FBgn0004643,FBgn0004837,FBgn0004889,FBgn0010382,FBgn0011739,FBgn0024227,FBgn0031549,FBgn0032047,FBgn0035918,FBgn0038390,FBgn0039403,FBgn0263855 | 15 | GO:0044770 |
| purine nucleoside triphosphate biosynthetic process | 0.0074854 | FBgn0016120,FBgn0016691,FBgn0019644,FBgn0028342,FBgn0038224,FBgn0262467 | 6 | GO:0009145 |
| purine | 0.00748 | FBgn0016120,FBgn0016691,FBgn0019644,FBgn00283 | 6 | GO:0009 |

| | | | | |
|---|---|---|---|---|
| ribonucleoside triphosphate metabolic process | 54 | 42,FBgn0038224,FBgn0262467 | | 205 |
| purine ribonucleoside triphosphate biosynthetic process | 0.0074854 | FBgn0016120,FBgn0016691,FBgn0019644,FBgn0028342,FBgn0038224,FBgn0262467 | 6 | GO:0009206 |
| negative regulation of Notch signaling pathway | 0.00807882 | FBgn0004837,FBgn0013725,FBgn0035060,FBgn0039273,FBgn0259685,FBgn0260440,FBgn0265523 | 7 | GO:0045746 |
| metabolic process | 0.00812459 | FBgn0000078,FBgn0000261,FBgn0000377,FBgn0000477,FBgn0000543,FBgn0000562,FBgn0000591,FBgn0000810,FBgn0001187,FBgn0001218,FBgn0002021,FBgn0002522,FBgn0002524,FBgn0002542,FBgn0002566,FBgn0002878,FBgn0002899,FBgn0003042,FBgn0003044,FBgn0003076,FBgn0003116,FBgn0003356,FBgn0003357,FBgn0003358,FBgn0003512,FBgn0003515,FBgn0003525,FBgn0003863,FBgn0003996,FBgn0004066,FBgn0004170,FBgn0004396,FBgn0004403,FBgn0004406,FBgn0004432,FBgn0004797,FBgn0004837,FBgn0004889,FBgn0004907,FBgn0005674,FBgn0005696,FBgn0005771,FBgn0010314,FBgn0010380,FBgn0010382,FBgn0010438,FBgn0010786,FBgn0011227,FBgn0011291,FBgn0011300,FBgn0011336,FBgn0011591,FBgn0011660,FBgn0011739,FBgn0011762,FBgn0011770,FBgn0011787,FBgn0011817,FBgn0013269,FBgn0013725,FBgn0013954,FBgn0013972,FBgn0014023,FBgn0014037,FBgn0014135,FBgn0014380,FBgn0014427,FBgn0014861,FBgn0014949,FBgn0015011,FBgn0015271,FBgn0015299,FBgn0015396,FBgn0015513,FBgn0015778,FBgn0016070,FBgn0016120,FBgn0016691,FBgn0016917,FBgn0017577,FBgn0019644,FBgn0019650,FBgn0020391,FBgn0020506,FBgn0020653,FBgn0022359,FBgn0022986,FBgn0023175,FBgn0023214,FBgn0023477,FBgn0023545,FBgn0024194,FBgn0024227,FBgn0024958,FBgn0024987,FBgn0024995,FBgn0024997,FBgn0025185,FBgn0025463,FBgn0025629,FBgn0025680,FBgn0025741,FBgn0025814,FBgn0025832,FBgn0025839,FBgn0025936,FBgn0026147,FBgn0026679,FBgn0026702,FBgn0026741,FBgn0026876,FBgn0026879,FBgn0027499,FBgn0027560,FBgn0027578,FBgn0027620,FBgn0027843,FBgn0027844,FBgn0028342,FBgn0028694,FBgn0028695,FBgn0028836,FBgn0028970,FBgn0028988,FBgn0029006,FBgn0029079,FBgn0029689,FBgn0029718,FBgn0029828,FBgn0029977,FBgn0030054,FBgn0030085,FBgn0030093,FBgn0030365,FBgn0030367,FBgn0030432,FBgn0030507,FBgn0030596,FBgn0030631,FBgn0030683,FBgn0030688,FBgn0030699,FBgn0030776,FBgn0030945,FBgn0031003,FBgn0031227,FBgn0031231,FBgn0031248,FBgn003126 | 283 | GO:0008152 |

| | | | | |
|---|---|---|---|---|
| | | 0,FBgn0031309,FBgn0031321,FBgn0031635,FBgn0031643,FBgn0031663,FBgn0031678,FBgn0031695,FBgn0031741,FBgn0031805,FBgn0031851,FBgn0031876,FBgn0032047,FBgn0032053,FBgn0032130,FBgn0032144,FBgn0032187,FBgn0032290,FBgn0032400,FBgn0032486,FBgn0032638,FBgn0032691,FBgn0032813,FBgn0032956,FBgn0033010,FBgn0033061,FBgn0033179,FBgn0033184,FBgn0033188,FBgn0033274,FBgn0033304,FBgn0033382,FBgn0033397,FBgn0033507,FBgn0033520,FBgn0033527,FBgn0033555,FBgn0033815,FBgn0033859,FBgn0033890,FBgn0033921,FBgn0033935,FBgn0033961,FBgn0033988,FBgn0033998,FBgn0034030,FBgn0034065,FBgn0034085,FBgn0034141,FBgn0034199,FBgn0034310,FBgn0034335,FBgn0034459,FBgn0034495,FBgn0034527,FBgn0034564,FBgn0034579,FBgn0034614,FBgn0034650,FBgn0034756,FBgn0034938,FBgn0035064,FBgn0035124,FBgn0035153,FBgn0035154,FBgn0035246,FBgn0035266,FBgn0035318,FBgn0035374,FBgn0035397,FBgn0035471,FBgn0035644,FBgn0035663,FBgn0035670,FBgn0035679,FBgn0035779,FBgn0035806,FBgn0035900,FBgn0035918,FBgn0035977,FBgn0035986,FBgn0036018,FBgn0036023,FBgn0036157,FBgn0036237,FBgn0036258,FBgn0036290,FBgn0036335,FBgn0036373,FBgn0036374,FBgn0036512,FBgn0036549,FBgn0036569,FBgn0036671,FBgn0036691,FBgn0036713,FBgn0036734,FBgn0036735,FBgn0036754,FBgn0036760,FBgn0036771,FBgn0036824,FBgn0036826,FBgn0036827,FBgn0036910,FBgn0036953,FBgn0036996,FBgn0037045,FBgn0037109,FBgn0037146,FBgn0037293,FBgn0037305,FBgn0037330,FBgn0037370,FBgn0037538,FBgn0037569,FBgn0037607,FBgn0037669,FBgn0037687,FBgn0037716,FBgn0037722,FBgn0037822,FBgn0037891,FBgn0037918,FBgn0037926,FBgn0038038,FBgn0038173,FBgn0038194,FBgn0038224,FBgn0038237,FBgn0038271,FBgn0038348,FBgn0038390,FBgn0038426,FBgn0038437,FBgn0038474,FBgn0038485,FBgn0038546,FBgn0038588,FBgn0038592,FBgn0038593,FBgn0038788,FBgn0038870,FBgn0038928,FBgn0038981,FBgn0039023,FBgn0039159,FBgn0039182,FBgn0039252,FBgn0039258,FBgn0039273,FBgn0039304,FBgn0039306,FBgn0039347,FBgn0039403,FBgn0039404,FBgn0039462,FBgn0039464,FBgn0039471,FBgn0039507,FBgn0039596,FBgn0039650,FBgn0039740,FBgn0039938,FBgn0039972,FBgn0040529,FBgn0040754,FBgn0041103,FBgn0041629,FBgn0042112,FBgn0043471,FBgn0043575,FBgn0043796,FBgn0043900,FBgn0044872,FBgn0047038,FBgn0050022,FBgn0050047,FBgn0050287,FBgn0050414,FBgn0050446,FBgn0050493,FBgn0051126,FBgn0051450,FBgn0051550,FBgn0051721,FBgn0051739,FBgn0052201,FBgn0052284,FBgn0052483,FBgn0053100,FBgn0053178,FBgn0053265,FBgn0053504,FBgn0061469,FBgn0063491,FBgn0063492,FBgn0063493,FBgn0067102,FBgn0083983,FBgn0085249,FBgn0085484,FBgn0086358,FBgn0086450,FBgn0086679,FBgn0250850,FBgn0259113,FBgn0259170,FBgn0259176,FBgn0259227,FBgn0259678,FBgn0259685,FBgn0259748,FBgn0259938,FBgn0260477,FBgn0260750,FBgn0260817,FBgn0260985,FBgn02 | | |

| | | | | |
|---|---|---|---|---|
| | | 61287,FBgn0261445,FBgn0261872,FBgn0262449,FBgn0262467,FBgn0262559,FBgn0262619,FBgn0263144,FBgn0263237,FBgn0263260,FBgn0263780,FBgn0263855,FBgn0263863,FBgn0264494,FBgn0264959,FBgn0265048,FBgn0265052,FBgn0265523,FBgn0265623,FBgn0266411,FBgn0266465,FBgn0266917,FBgn0267792,FBgn0267821,FBgn0286027,FBgn0286506 | | |
| leading strand elongation | 0.00847253 | FBgn0032813,FBgn0259113,FBgn0260985 | 3 | GO:0006272 |
| purine nucleoside triphosphate metabolic process | 0.00877658 | FBgn0016120,FBgn0016691,FBgn0019644,FBgn0028342,FBgn0038224,FBgn0262467 | 6 | GO:0009144 |
| tRNA-guanine transglycosylation | 0.0094875 | FBgn0031321,FBgn0034614 | 2 | GO:0101030 |
| response to L-canavanine | 0.0094875 | FBgn0030108,FBgn0035870 | 2 | GO:1901354 |
| regulation of mitotic cell cycle | 0.01028673 | FBgn0002878,FBgn0003525,FBgn0004170,FBgn0004583,FBgn0004643,FBgn0004837,FBgn0004889,FBgn0010314,FBgn0010382,FBgn0024227,FBgn0031549,FBgn0034569,FBgn0035249,FBgn0035918,FBgn0038390,FBgn0039403,FBgn0039638,FBgn0263855,FBgn0265523,FBgn0266465 | 20 | GO:0007346 |
| energy coupled proton transport, down electrochemical gradient | 0.01046341 | FBgn0016120,FBgn0016691,FBgn0019644,FBgn0028342,FBgn0038224 | 5 | GO:0015985 |
| ATP synthesis coupled proton transport | 0.01046341 | FBgn0016120,FBgn0016691,FBgn0019644,FBgn0028342,FBgn0038224 | 5 | GO:0015986 |
| cellular transition metal ion homeostasis | 0.01046341 | FBgn0024236,FBgn0024958,FBgn0030343,FBgn0062413,FBgn0262467 | 5 | GO:0046916 |
| ribonucleoside triphosphate metabolic process | 0.01182359 | FBgn0016120,FBgn0016691,FBgn0019644,FBgn0028342,FBgn0038224,FBgn0262467 | 6 | GO:0009199 |
| ribonucleoside triphosphate | 0.01182359 | FBgn0016120,FBgn0016691,FBgn0019644,FBgn0028342,FBgn0038224,FBgn0262467 | 6 | GO:0009201 |

| | | | | |
|---|---|---|---|---|
| biosynthetic process | | | | |
| positive regulation of Ras protein signal transduction | 0.01187745 | FBgn0004907,FBgn0015513,FBgn0034194,FBgn0050440,FBgn0050456,FBgn0050476,FBgn0051158 | 7 | GO:0046579 |
| positive regulation of small GTPase mediated signal transduction | 0.01187745 | FBgn0004907,FBgn0015513,FBgn0034194,FBgn0050440,FBgn0050456,FBgn0050476,FBgn0051158 | 7 | GO:0051057 |
| one-carbon metabolic process | 0.01217255 | FBgn0027843,FBgn0027844,FBgn0036157 | 3 | GO:0006730 |
| protein stabilization | 0.01359687 | FBgn0004889,FBgn0004907,FBgn0028292,FBgn0028836,FBgn0259685,FBgn0267821 | 6 | GO:0050821 |
| ribosomal small subunit biogenesis | 0.0138091 | FBgn0002899,FBgn0004403,FBgn0030085,FBgn0031643,FBgn0034564,FBgn0036754,FBgn0038474,FBgn0039306,FBgn0039404 | 9 | GO:0042274 |
| DNA strand elongation involved in DNA replication | 0.01403523 | FBgn0032813,FBgn0259113,FBgn0260985,FBgn0262619 | 4 | GO:0006271 |
| DNA strand elongation | 0.01403523 | FBgn0032813,FBgn0259113,FBgn0260985,FBgn0262619 | 4 | GO:0022616 |
| determination of adult lifespan | 0.0144596 | FBgn0000261,FBgn0002566,FBgn0004657,FBgn0011300,FBgn0015575,FBgn0016120,FBgn0020653,FBgn0030350,FBgn0033127,FBgn0033448,FBgn0035132,FBgn0035977,FBgn0038788,FBgn0051216,FBgn0259170,FBgn0259176,FBgn0263316 | 17 | GO:0008340 |
| apical junction assembly | 0.01503664 | FBgn0003391,FBgn0010894,FBgn0033032,FBgn0036198,FBgn0259685,FBgn0261284,FBgn0266465 | 7 | GO:0043297 |
| chromosome separation | 0.01540763 | FBgn0004643,FBgn0004889,FBgn0015391,FBgn0017577,FBgn0024227,FBgn0029977,FBgn0031549,FBgn0263855 | 8 | GO:0051304 |
| positive regulation of G1/S transition of mitotic cell cycle | 0.0166579 | FBgn0004837,FBgn0010382,FBgn0039403 | 3 | GO:1900087 |
| multicellular organism aging | 0.0170086 | FBgn0000261,FBgn0002566,FBgn0004657,FBgn0011300,FBgn0015575,FBgn0016120,FBgn0020653,FBgn0030350,FBgn0033127,FBgn0033448,FBgn0035132,FBgn0035977,FBgn0038788,FBgn0051216,FBgn0259170,FBg | 17 | GO:0010259 |

| | | | | |
|---|---|---|---|---|
| | | n0259176,FBgn0263316 | | |
| copper ion homeostasis | 0.01724405 | FBgn0030343,FBgn0033274,FBgn0062413,FBgn0262467 | 4 | GO:0055070 |
| nucleoside triphosphate biosynthetic process | 0.01768425 | FBgn0016120,FBgn0016691,FBgn0019644,FBgn0028342,FBgn0038224,FBgn0262467 | 6 | GO:0009142 |
| prostaglandin biosynthetic process | 0.01825495 | FBgn0025814,FBgn0053178 | 2 | GO:0001516 |
| lagging strand elongation | 0.01825495 | FBgn0259113,FBgn0262619 | 2 | GO:0006273 |
| eye pigment precursor transport | 0.01825495 | FBgn0003515,FBgn0003996 | 2 | GO:0006856 |
| ocellus development | 0.01825495 | FBgn0005771,FBgn0019650 | 2 | GO:0008056 |
| regulation of nucleotide biosynthetic process | 0.01825495 | FBgn0025741,FBgn0262467 | 2 | GO:0030808 |
| positive regulation of nucleotide biosynthetic process | 0.01825495 | FBgn0025741,FBgn0262467 | 2 | GO:0030810 |
| copper ion transmembrane transport | 0.01825495 | FBgn0030343,FBgn0062413 | 2 | GO:0035434 |
| DNA replication proofreading | 0.01825495 | FBgn0004406,FBgn0035644 | 2 | GO:0045004 |
| positive regulation of nucleotide metabolic process | 0.01825495 | FBgn0025741,FBgn0262467 | 2 | GO:0045981 |
| icosanoid biosynthetic process | 0.01825495 | FBgn0025814,FBgn0053178 | 2 | GO:0046456 |
| prostanoid biosynthetic process | 0.01825495 | FBgn0025814,FBgn0053178 | 2 | GO:0046457 |
| regulation of purine | 0.01825495 | FBgn0025741,FBgn0262467 | 2 | GO:1900371 |

| | | | | |
|---|---|---|---|---|
| nucleotide biosynthetic process | | | | |
| positive regulation of purine nucleotide biosynthetic process | 0.01825495 | FBgn0025741,FBgn0262467 | 2 | GO:1900373 |
| positive regulation of purine nucleotide metabolic process | 0.01825495 | FBgn0025741,FBgn0262467 | 2 | GO:1900544 |
| cell cycle DNA replication initiation | 0.01825495 | FBgn0014861,FBgn0259113 | 2 | GO:1902292 |
| nuclear cell cycle DNA replication initiation | 0.01825495 | FBgn0014861,FBgn0259113 | 2 | GO:1902315 |
| mitotic DNA replication initiation | 0.01825495 | FBgn0014861,FBgn0259113 | 2 | GO:1902975 |
| positive regulation of chromatin organization | 0.02083228 | FBgn0016917,FBgn0025463,FBgn0027499,FBgn0032691,FBgn0037669,FBgn0263855,FBgn0265623 | 7 | GO:1905269 |
| ommochrome biosynthetic process | 0.0208748 | FBgn0002566,FBgn0003515,FBgn0003996,FBgn0086679 | 4 | GO:0006727 |
| ocellus pigment biosynthetic process | 0.0208748 | FBgn0002566,FBgn0003515,FBgn0003996,FBgn0086679 | 4 | GO:0008055 |
| ocellus pigmentation | 0.0208748 | FBgn0002566,FBgn0003515,FBgn0003996,FBgn0086679 | 4 | GO:0033060 |
| ommochrome metabolic process | 0.0208748 | FBgn0002566,FBgn0003515,FBgn0003996,FBgn0086679 | 4 | GO:0046152 |
| ocellus pigment metabolic process | 0.0208748 | FBgn0002566,FBgn0003515,FBgn0003996,FBgn0086679 | 4 | GO:0046158 |
| regulation of exit from mitosis | 0.02194419 | FBgn0004583,FBgn0010382,FBgn0263855 | 3 | GO:0007096 |

| | | | | |
|---|---|---|---|---|
| intestinal stem cell homeostasis | 0.02310798 | FBgn0000261,FBgn0001218,FBgn0032691,FBgn0259176,FBgn0264959 | 5 | GO:0036335 |
| aging | 0.02313687 | FBgn0000261,FBgn0002566,FBgn0004657,FBgn0011300,FBgn0015575,FBgn0016120,FBgn0020653,FBgn0030350,FBgn0033127,FBgn0033448,FBgn0035132,FBgn0035977,FBgn0038788,FBgn0051216,FBgn0259170,FBgn0259176,FBgn0263316 | 17 | GO:0007568 |
| regulation of mitotic nuclear division | 0.02511586 | FBgn0004583,FBgn0004643,FBgn0004889,FBgn0010382,FBgn0024227,FBgn0031549,FBgn0034569,FBgn0039638,FBgn0263855 | 9 | GO:0007088 |
| organic substance metabolic process | 0.02523394 | FBgn0000078,FBgn0000377,FBgn0000477,FBgn0000543,FBgn0000562,FBgn0000591,FBgn0000810,FBgn0001187,FBgn0001218,FBgn0002522,FBgn0002524,FBgn0002542,FBgn0002566,FBgn0002878,FBgn0002899,FBgn0003042,FBgn0003044,FBgn0003076,FBgn0003116,FBgn0003356,FBgn0003357,FBgn0003358,FBgn0003512,FBgn0003515,FBgn0003525,FBgn0003863,FBgn0003996,FBgn0004066,FBgn0004170,FBgn0004396,FBgn0004403,FBgn0004406,FBgn0004432,FBgn0004797,FBgn0004837,FBgn0004889,FBgn0004907,FBgn0005674,FBgn0005696,FBgn0005771,FBgn0010314,FBgn0010382,FBgn0010438,FBgn0010786,FBgn0011291,FBgn0011300,FBgn0011336,FBgn0011591,FBgn0011660,FBgn0011739,FBgn0011762,FBgn0011770,FBgn0011787,FBgn0011817,FBgn0013725,FBgn0013954,FBgn0013972,FBgn0014023,FBgn0014037,FBgn0014135,FBgn0014380,FBgn0014427,FBgn0014861,FBgn0014949,FBgn0015011,FBgn0015271,FBgn0015299,FBgn0015396,FBgn0015513,FBgn0015778,FBgn0016070,FBgn0016120,FBgn0016691,FBgn0016917,FBgn0017577,FBgn0019644,FBgn0019650,FBgn0020391,FBgn0020506,FBgn0022986,FBgn0023175,FBgn0023214,FBgn0023477,FBgn0023545,FBgn0024194,FBgn0024227,FBgn0024958,FBgn0024987,FBgn0024995,FBgn0024997,FBgn0025185,FBgn0025463,FBgn0025629,FBgn0025680,FBgn0025741,FBgn0025814,FBgn0025832,FBgn0025936,FBgn0026147,FBgn0026679,FBgn0026702,FBgn0026741,FBgn0026876,FBgn0026879,FBgn0027499,FBgn0027560,FBgn0027578,FBgn0027620,FBgn0028342,FBgn0028694,FBgn0028695,FBgn0028836,FBgn0028970,FBgn0028988,FBgn0029006,FBgn0029079,FBgn0029689,FBgn0029718,FBgn0029828,FBgn0029977,FBgn0030054,FBgn0030085,FBgn0030093,FBgn0030365,FBgn0030432,FBgn0030507,FBgn0030596,FBgn0030631,FBgn0030683,FBgn0030688,FBgn0030699,FBgn0030776,FBgn0030945,FBgn0031003,FBgn0031227,FBgn0031231,FBgn0031248,FBgn0031260,FBgn0031309,FBgn0031321,FBgn0031643,FBgn0031663,FBgn0031678,FBgn0031741,FBgn0031805,FBgn0031851,FBgn0031876,FBgn0032047,FBgn0032053,FBgn0032130,FBgn0032144,FBgn0032187,FBgn0032290,FBgn0032400,FBgn0032486,FBgn0032638,FBgn0032691,FBgn0032813,FBgn0032956,FBgn0033010,FBgn0033061,FBgn0033179,FBgn0033184,FBgn0033188,FBgn0033274,FBgn0033382,FBgn0033507,FBgn0033527, | 283 | GO:0071704 |

| | | | | |
|---|---|---|---|---|
| | | FBgn0033555,FBgn0033815,FBgn0033859,FBgn0033890,FBgn0033921,FBgn0033935,FBgn0033988,FBgn0033998,FBgn0034030,FBgn0034065,FBgn0034085,FBgn0034141,FBgn0034199,FBgn0034310,FBgn0034335,FBgn0034459,FBgn0034495,FBgn0034527,FBgn0034564,FBgn0034579,FBgn0034614,FBgn0034650,FBgn0034938,FBgn0035064,FBgn0035124,FBgn0035153,FBgn0035154,FBgn0035246,FBgn0035266,FBgn0035318,FBgn0035374,FBgn0035397,FBgn0035471,FBgn0035644,FBgn0035663,FBgn0035670,FBgn0035679,FBgn0035779,FBgn0035806,FBgn0035900,FBgn0035918,FBgn0035977,FBgn0035986,FBgn0036018,FBgn0036023,FBgn0036157,FBgn0036237,FBgn0036258,FBgn0036335,FBgn0036373,FBgn0036374,FBgn0036512,FBgn0036549,FBgn0036569,FBgn0036671,FBgn0036691,FBgn0036713,FBgn0036734,FBgn0036735,FBgn0036754,FBgn0036760,FBgn0036771,FBgn0036826,FBgn0036827,FBgn0036953,FBgn0036996,FBgn0037045,FBgn0037109,FBgn0037146,FBgn0037293,FBgn0037305,FBgn0037330,FBgn0037538,FBgn0037569,FBgn0037607,FBgn0037669,FBgn0037687,FBgn0037716,FBgn0037722,FBgn0037822,FBgn0037918,FBgn0037926,FBgn0038038,FBgn0038173,FBgn0038224,FBgn0038237,FBgn0038271,FBgn0038348,FBgn0038390,FBgn0038426,FBgn0038437,FBgn0038474,FBgn0038485,FBgn0038546,FBgn0038588,FBgn0038592,FBgn0038788,FBgn0038870,FBgn0038928,FBgn0039023,FBgn0039159,FBgn0039182,FBgn0039252,FBgn0039258,FBgn0039273,FBgn0039304,FBgn0039306,FBgn0039347,FBgn0039403,FBgn0039404,FBgn0039462,FBgn0039464,FBgn0039471,FBgn0039507,FBgn0039596,FBgn0039650,FBgn0039740,FBgn0039938,FBgn0039972,FBgn0040754,FBgn0041103,FBgn0041629,FBgn0042112,FBgn0043471,FBgn0043575,FBgn0043796,FBgn0043900,FBgn0044872,FBgn0050022,FBgn0050047,FBgn0050287,FBgn0050414,FBgn0050446,FBgn0050493,FBgn0051126,FBgn0051450,FBgn0051550,FBgn0051721,FBgn0051739,FBgn0052201,FBgn0052284,FBgn0052483,FBgn0053100,FBgn0053178,FBgn0053265,FBgn0053504,FBgn0061469,FBgn0063491,FBgn0063492,FBgn0063493,FBgn0067102,FBgn0083983,FBgn0085249,FBgn0085484,FBgn0086358,FBgn0086450,FBgn0086679,FBgn0250850,FBgn0259113,FBgn0259170,FBgn0259176,FBgn0259227,FBgn0259678,FBgn0259685,FBgn0259748,FBgn0259938,FBgn0260477,FBgn0260750,FBgn0260817,FBgn0260985,FBgn0261287,FBgn0261445,FBgn0261872,FBgn0262449,FBgn0262467,FBgn0262559,FBgn0262619,FBgn0263144,FBgn0263237,FBgn0263260,FBgn0263780,FBgn0263855,FBgn0263863,FBgn0264494,FBgn0264959,FBgn0265048,FBgn0265523,FBgn0265623,FBgn0266411,FBgn0266465,FBgn0266917,FBgn0267792,FBgn0267821,FBgn0286027,FBgn0286506 | | |
| nitrogen compound metabolic process | 0.0272728 6 | FBgn0000377,FBgn0000477,FBgn0000543,FBgn0000562,FBgn0000591,FBgn0000810,FBgn0001187,FBgn0001218,FBgn0002522,FBgn0002524,FBgn0002542,FBgn0002566,FBgn0002878,FBgn0002899,FBgn0003042,FBgn0003044,FBgn0003116,FBgn0003356,FBgn0003357,F | 283 | GO:0006807 |

| | | | | |
|---|---|---|---|---|
| | | Bgn0003358,FBgn0003512,FBgn0003525,FBgn0003863,FBgn0003996,FBgn0004066,FBgn0004170,FBgn0004396,FBgn0004403,FBgn0004406,FBgn0004432,FBgn0004837,FBgn0004889,FBgn0004907,FBgn0005674,FBgn0005696,FBgn0005771,FBgn0010314,FBgn0010382,FBgn0010786,FBgn0011291,FBgn0011300,FBgn0011336,FBgn0011591,FBgn0011660,FBgn0011739,FBgn0011762,FBgn0011787,FBgn0011817,FBgn0013725,FBgn0013954,FBgn0013972,FBgn0014023,FBgn0014037,FBgn0014135,FBgn0014427,FBgn0014861,FBgn0014949,FBgn0015271,FBgn0015299,FBgn0015396,FBgn0015513,FBgn0015778,FBgn0016070,FBgn0016120,FBgn0016691,FBgn0016917,FBgn0017577,FBgn0019644,FBgn0019650,FBgn0020391,FBgn0022986,FBgn0023175,FBgn0023214,FBgn0023545,FBgn0024194,FBgn0024227,FBgn0024987,FBgn0024995,FBgn0024997,FBgn0025185,FBgn0025463,FBgn0025629,FBgn0025680,FBgn0025741,FBgn0025832,FBgn0025936,FBgn0026147,FBgn0026679,FBgn0026702,FBgn0026741,FBgn0026876,FBgn0026879,FBgn0027499,FBgn0027578,FBgn0027620,FBgn0028342,FBgn0028694,FBgn0028695,FBgn0028836,FBgn0028970,FBgn0028988,FBgn0029006,FBgn0029079,FBgn0029689,FBgn0029718,FBgn0029828,FBgn0029977,FBgn0030054,FBgn0030085,FBgn0030093,FBgn0030365,FBgn0030432,FBgn0030507,FBgn0030631,FBgn0030683,FBgn0030688,FBgn0030699,FBgn0030776,FBgn0030945,FBgn0031003,FBgn0031227,FBgn0031231,FBgn0031248,FBgn0031260,FBgn0031309,FBgn0031321,FBgn0031643,FBgn0031663,FBgn0031678,FBgn0031741,FBgn0031805,FBgn0031851,FBgn0031876,FBgn0032047,FBgn0032053,FBgn0032130,FBgn0032144,FBgn0032187,FBgn0032290,FBgn0032400,FBgn0032486,FBgn0032638,FBgn0032691,FBgn0032813,FBgn0032956,FBgn0033010,FBgn0033179,FBgn0033184,FBgn0033274,FBgn0033507,FBgn0033527,FBgn0033555,FBgn0033815,FBgn0033859,FBgn0033890,FBgn0033921,FBgn0033935,FBgn0033988,FBgn0033998,FBgn0034030,FBgn0034065,FBgn0034085,FBgn0034199,FBgn0034310,FBgn0034335,FBgn0034459,FBgn0034527,FBgn0034564,FBgn0034579,FBgn0034614,FBgn0034650,FBgn0034938,FBgn0035064,FBgn0035124,FBgn0035153,FBgn0035154,FBgn0035246,FBgn0035318,FBgn0035374,FBgn0035397,FBgn0035644,FBgn0035663,FBgn0035670,FBgn0035779,FBgn0035806,FBgn0035900,FBgn0035918,FBgn0035977,FBgn0035986,FBgn0036018,FBgn0036023,FBgn0036157,FBgn0036237,FBgn0036258,FBgn0036335,FBgn0036373,FBgn0036374,FBgn0036512,FBgn0036549,FBgn0036569,FBgn0036671,FBgn0036734,FBgn0036735,FBgn0036754,FBgn0036760,FBgn0036771,FBgn0036826,FBgn0036827,FBgn0036953,FBgn0037045,FBgn0037109,FBgn0037146,FBgn0037293,FBgn0037305,FBgn0037330,FBgn0037538,FBgn0037607,FBgn0037669,FBgn0037687,FBgn0037716,FBgn0037722,FBgn0037822,FBgn0037918,FBgn0037926,FBgn0038173,FBgn0038224,FBgn0038237,FBgn0038271,FBgn0038390,FBgn0038426,FBgn0038474,FBgn0038485,FBgn0038546,FBgn0038588,FBgn0038592,FBgn0038788,FBgn0038 | | |

| | | | | |
|---|---|---|---|---|
| | | 870,FBgn0038928,FBgn0039023,FBgn0039159,FBgn0039182,FBgn0039252,FBgn0039258,FBgn0039273,FBgn0039304,FBgn0039306,FBgn0039347,FBgn0039403,FBgn0039404,FBgn0039462,FBgn0039464,FBgn0039650,FBgn0039740,FBgn0039938,FBgn0039972,FBgn0040754,FBgn0041103,FBgn0042112,FBgn0043471,FBgn0043575,FBgn0043796,FBgn0043900,FBgn0044872,FBgn0050022,FBgn0050047,FBgn0050287,FBgn0050414,FBgn0050446,FBgn0051126,FBgn0051450,FBgn0051550,FBgn0051721,FBgn0051739,FBgn0052201,FBgn0052284,FBgn0052483,FBgn0053100,FBgn0053178,FBgn0053265,FBgn0053504,FBgn0061469,FBgn0063491,FBgn0063492,FBgn0063493,FBgn0067102,FBgn0083983,FBgn0085249,FBgn0085484,FBgn0086358,FBgn0086450,FBgn0250850,FBgn0259113,FBgn0259170,FBgn0259176,FBgn0259227,FBgn0259678,FBgn0259685,FBgn0259748,FBgn0259938,FBgn0260477,FBgn0260750,FBgn0260817,FBgn0260985,FBgn0261287,FBgn0261445,FBgn0261872,FBgn0262449,FBgn0262467,FBgn0262559,FBgn0262619,FBgn0263144,FBgn0263237,FBgn0263260,FBgn0263780,FBgn0263855,FBgn0263863,FBgn0264959,FBgn0265048,FBgn0265523,FBgn0265623,FBgn0266411,FBgn0266465,FBgn0266917,FBgn0267792,FBgn0267821,FBgn0286027,FBgn0286506 | | |
| double-strand break repair via break-induced replication | 0.02803595 | FBgn0014861,FBgn0017577,FBgn0039403 | 3 | GO:0000727 |
| positive regulation of defense response to virus by host | 0.02803595 | FBgn0016917,FBgn0038928,FBgn0086358 | 3 | GO:0002230 |
| regulation of defense response to virus by host | 0.02803595 | FBgn0016917,FBgn0038928,FBgn0086358 | 3 | GO:0050691 |
| prostanoid metabolic process | 0.0292761 | FBgn0025814,FBgn0053178 | 2 | GO:0006692 |
| prostaglandin metabolic process | 0.0292761 | FBgn0025814,FBgn0053178 | 2 | GO:0006693 |
| protein-cofactor linkage | 0.0292761 | FBgn0010786,FBgn0033274 | 2 | GO:0018065 |
| respiratory chain complex II assembly | 0.0292761 | FBgn0033274,FBgn0038437 | 2 | GO:0034552 |

| | | | | |
|---|---|---|---|---|
| mitochondrial respiratory chain complex II assembly | 0.0292761 | FBgn0033274,FBgn0038437 | 2 | GO:0034553 |
| regulation of Notch signaling pathway | 0.0292927 | FBgn0002592,FBgn0004837,FBgn0011591,FBgn0013725,FBgn0035060,FBgn0039273,FBgn0259685,FBgn0260440,FBgn0265523 | 9 | GO:0008593 |
| nuclear-transcribed mRNA poly(A) tail shortening | 0.0294497 | FBgn0016070,FBgn0035246,FBgn0035397,FBgn0039972 | 4 | GO:0000289 |
| protein peptidyl-prolyl isomerization | 0.0294497 | FBgn0004432,FBgn0013954,FBgn0033527,FBgn0039347 | 4 | GO:0000413 |
| sensory organ development | 0.0297520 | FBgn0000008,FBgn0000543,FBgn0000591,FBgn0002592,FBgn0003116,FBgn0003174,FBgn0003391,FBgn0004170,FBgn0004583,FBgn0004837,FBgn0004889,FBgn0005771,FBgn0010380,FBgn0010382,FBgn0011300,FBgn0011591,FBgn0011739,FBgn0011817,FBgn0013725,FBgn0014135,FBgn0015396,FBgn0015778,FBgn0019650,FBgn0020391,FBgn0023214,FBgn0033179,FBgn0034243,FBgn0043903,FBgn0045073,FBgn0050476,FBgn0051158,FBgn0051721,FBgn0259176,FBgn0259685,FBgn0260440,FBgn0264959,FBgn0267821 | 37 | GO:0007423 |
| regulation of mitotic metaphase/anaphase transition | 0.0301115 | FBgn0004643,FBgn0004889,FBgn0024227,FBgn0031549,FBgn0263855 | 5 | GO:0030071 |
| regulation of chromosome organization | 0.0308107 | FBgn0004643,FBgn0004889,FBgn0014861,FBgn0016917,FBgn0024227,FBgn0025463,FBgn0027499,FBgn0027620,FBgn0031549,FBgn0032691,FBgn0037607,FBgn0037669,FBgn0039507,FBgn0043796,FBgn0263855,FBgn0265623,FBgn0267792 | 17 | GO:0033044 |
| ncRNA metabolic process | 0.0313941 | FBgn0002899,FBgn0004403,FBgn0005674,FBgn0025629,FBgn0026679,FBgn0026702,FBgn0030085,FBgn0031227,FBgn0031321,FBgn0031643,FBgn0033507,FBgn0033921,FBgn0034065,FBgn0034564,FBgn0034614,FBgn0035064,FBgn0035986,FBgn0036569,FBgn0036754,FBgn0037330,FBgn0037822,FBgn0037926,FBgn0038474,FBgn0039306,FBgn0039404,FBgn0051739,FBgn0263144 | 27 | GO:0034660 |
| mitotic cell cycle, embryonic | 0.0313946 | FBgn0003042,FBgn0003525,FBgn0004907,FBgn0010314,FBgn0011020,FBgn0033890 | 6 | GO:0045448 |
| cell cycle process | 0.0320394 | FBgn0000140,FBgn0002542,FBgn0002878,FBgn0002899,FBgn0003525,FBgn0004378,FBgn0004583,FBgn0004643,FBgn0004837,FBgn0004889,FBgn0010314,FBgn0010382,FBgn0011020,FBgn0011739,FBgn0014861,FBg | 45 | GO:0022402 |

| | | | | |
|---|---|---|---|---|
| | | n0015271,FBgn0015391,FBgn0017577,FBgn0024227,FBgn0026876,FBgn0028292,FBgn0029977,FBgn0030054,FBgn0031549,FBgn0032047,FBgn0032290,FBgn0033890,FBgn0033921,FBgn0034495,FBgn0034569,FBgn0035249,FBgn0035644,FBgn0035918,FBgn0038390,FBgn0039403,FBgn0039638,FBgn0052371,FBgn0087021,FBgn0087040,FBgn0259113,FBgn0259685,FBgn0260985,FBgn0262619,FBgn0263855,FBgn0266418 | | |
| cellular metal ion homeostasis | 0.032973 | FBgn0024236,FBgn0024958,FBgn0030343,FBgn0030350,FBgn0034136,FBgn0034199,FBgn0045073,FBgn0062413,FBgn0261872,FBgn0262467 | 10 | GO:0006875 |
| homeostasis of number of cells | 0.03406246 | FBgn0000261,FBgn0001218,FBgn0032691,FBgn0259176,FBgn0264959 | 5 | GO:0048872 |
| regulation of metaphase/anaphase transition of cell cycle | 0.03406246 | FBgn0004643,FBgn0004889,FBgn0024227,FBgn0031549,FBgn0263855 | 5 | GO:1902099 |
| exit from mitosis | 0.03492824 | FBgn0004583,FBgn0010382,FBgn0263855 | 3 | GO:0010458 |
| regulation of heterochromatin assembly | 0.03492824 | FBgn0016917,FBgn0025463,FBgn0027620 | 3 | GO:0031445 |
| bicoid mRNA localization | 0.03492824 | FBgn0000562,FBgn0003512,FBgn0003655 | 3 | GO:0045450 |
| negative regulation of behavior | 0.03492824 | FBgn0020258,FBgn0033257,FBgn0036713 | 3 | GO:0048521 |
| regulation of nuclear-transcribed mRNA poly(A) tail shortening | 0.03492824 | FBgn0016070,FBgn0035246,FBgn0039972 | 3 | GO:0060211 |
| positive regulation of nuclear-transcribed mRNA poly(A) tail shortening | 0.03492824 | FBgn0016070,FBgn0035246,FBgn0039972 | 3 | GO:0060213 |
| positive regulation of cell cycle G1/S phase | 0.03492824 | FBgn0004837,FBgn0010382,FBgn0039403 | 3 | GO:1902808 |

| | | | | |
|---|---|---|---|---|
| transition | | | | |
| cellular metabolic process | 0.0356041 | FBgn0000261,FBgn0000377,FBgn0000477,FBgn0000543,FBgn0000562,FBgn0000591,FBgn0000810,FBgn0001187,FBgn0001218,FBgn0002522,FBgn0002524,FBgn0002542,FBgn0002566,FBgn0002878,FBgn0002899,FBgn0003042,FBgn0003044,FBgn0003076,FBgn0003116,FBgn0003512,FBgn0003515,FBgn0003525,FBgn0003996,FBgn0004066,FBgn0004170,FBgn0004396,FBgn0004403,FBgn0004406,FBgn0004432,FBgn0004797,FBgn0004837,FBgn0004889,FBgn0004907,FBgn0005674,FBgn0005696,FBgn0005771,FBgn0010314,FBgn0010380,FBgn0010382,FBgn0010438,FBgn0010786,FBgn0011227,FBgn0011291,FBgn0011300,FBgn0011336,FBgn0011591,FBgn0011660,FBgn0011739,FBgn0011762,FBgn0011770,FBgn0011787,FBgn0011817,FBgn0013269,FBgn0013725,FBgn0013954,FBgn0013972,FBgn0014023,FBgn0014037,FBgn0014135,FBgn0014380,FBgn0014427,FBgn0014861,FBgn0014949,FBgn0015011,FBgn0015271,FBgn0015299,FBgn0015396,FBgn0015513,FBgn0015778,FBgn0016070,FBgn0016120,FBgn0016691,FBgn0016917,FBgn0017577,FBgn0019644,FBgn0019650,FBgn0020391,FBgn0022986,FBgn0023175,FBgn0023214,FBgn0023477,FBgn0023545,FBgn0024194,FBgn0024227,FBgn0024958,FBgn0024987,FBgn0024995,FBgn0024997,FBgn0025185,FBgn0025463,FBgn0025629,FBgn0025680,FBgn0025741,FBgn0025814,FBgn0025832,FBgn0025839,FBgn0025936,FBgn0026147,FBgn0026679,FBgn0026702,FBgn0026741,FBgn0026876,FBgn0026879,FBgn0027499,FBgn0027560,FBgn0027620,FBgn0027843,FBgn0027844,FBgn0028342,FBgn0028694,FBgn0028695,FBgn0028836,FBgn0028970,FBgn0028988,FBgn0029006,FBgn0029079,FBgn0029689,FBgn0029718,FBgn0029977,FBgn0030054,FBgn0030085,FBgn0030093,FBgn0030365,FBgn0030432,FBgn0030507,FBgn0030596,FBgn0030631,FBgn0030683,FBgn0030699,FBgn0030945,FBgn0031003,FBgn0031227,FBgn0031231,FBgn0031260,FBgn0031309,FBgn0031321,FBgn0031635,FBgn0031643,FBgn0031663,FBgn0031851,FBgn0031876,FBgn0032047,FBgn0032053,FBgn0032130,FBgn0032187,FBgn0032290,FBgn0032400,FBgn0032486,FBgn0032691,FBgn0032813,FBgn0032956,FBgn0033010,FBgn0033179,FBgn0033184,FBgn0033274,FBgn0033382,FBgn0033507,FBgn0033520,FBgn0033527,FBgn0033555,FBgn0033815,FBgn0033859,FBgn0033890,FBgn0033921,FBgn0033935,FBgn0033961,FBgn0033988,FBgn0033998,FBgn0034030,FBgn0034065,FBgn0034085,FBgn0034141,FBgn0034199,FBgn0034310,FBgn0034335,FBgn0034459,FBgn0034495,FBgn0034527,FBgn0034564,FBgn0034579,FBgn0034614,FBgn0034650,FBgn0034938,FBgn0035064,FBgn0035124,FBgn0035153,FBgn0035154,FBgn0035246,FBgn0035266,FBgn0035318,FBgn0035374,FBgn0035397,FBgn0035471,FBgn0035644,FBgn0035900,FBgn0035918,FBgn0035977,FBgn0035986,FBgn0036018,FBgn0036157,FBgn0036258,FBgn0036335,FBgn0036373,FBgn0036374,FBgn0036549,FBgn0036569,FBgn0036671,FBgn0036691,FBgn0036713,FBgn0036734,FBgn0036735,FBgn0036754,FBgn0036760,FBgn00367 | 283 | GO:0044237 |

| | | | | |
|---|---|---|---|---|
| | | 71,FBgn0036826,FBgn0036827,FBgn0036953,FBgn0037045,FBgn0037109,FBgn0037146,FBgn0037293,FBgn0037305,FBgn0037330,FBgn0037538,FBgn0037607,FBgn0037669,FBgn0037687,FBgn0037716,FBgn0037722,FBgn0037822,FBgn0037891,FBgn0037918,FBgn0037926,FBgn0038038,FBgn0038173,FBgn0038224,FBgn0038237,FBgn0038271,FBgn0038348,FBgn0038390,FBgn0038426,FBgn0038437,FBgn0038474,FBgn0038546,FBgn0038588,FBgn0038592,FBgn0038593,FBgn0038788,FBgn0038870,FBgn0038928,FBgn0039159,FBgn0039182,FBgn0039252,FBgn0039258,FBgn0039273,FBgn0039304,FBgn0039306,FBgn0039347,FBgn0039403,FBgn0039404,FBgn0039462,FBgn0039464,FBgn0039650,FBgn0039740,FBgn0039938,FBgn0039972,FBgn0040529,FBgn0040754,FBgn0041103,FBgn0042112,FBgn0043575,FBgn0043796,FBgn0043900,FBgn0044872,FBgn0047038,FBgn0050022,FBgn0050446,FBgn0050493,FBgn0051126,FBgn0051450,FBgn0051550,FBgn0051721,FBgn0051739,FBgn0052201,FBgn0052284,FBgn0052483,FBgn0053100,FBgn0053178,FBgn0053265,FBgn0053504,FBgn0061469,FBgn0063491,FBgn0063492,FBgn0063493,FBgn0067102,FBgn0083983,FBgn0085249,FBgn0085484,FBgn0086358,FBgn0086450,FBgn0086679,FBgn0250850,FBgn0259113,FBgn0259170,FBgn0259176,FBgn0259227,FBgn0259678,FBgn0259685,FBgn0259748,FBgn0259938,FBgn0260750,FBgn0260817,FBgn0260985,FBgn0261287,FBgn0261445,FBgn0261872,FBgn0262449,FBgn0262467,FBgn0262559,FBgn0262619,FBgn0263144,FBgn0263237,FBgn0263855,FBgn0263863,FBgn0264494,FBgn0264959,FBgn0265048,FBgn0265052,FBgn0265523,FBgn0265623,FBgn0266411,FBgn0266465,FBgn0266917,FBgn0267792,FBgn0267821,FBgn0286027,FBgn0286506 | | |
| asymmetric cell division | 0.03580441 | FBgn0000140,FBgn0003391,FBgn0004837,FBgn0004889,FBgn0010382,FBgn0011020,FBgn0024227,FBgn0028292,FBgn0028836,FBgn0260440,FBgn0266418 | 11 | GO:0008356 |
| regulation of nuclear division | 0.03643352 | FBgn0004583,FBgn0004643,FBgn0004889,FBgn0010382,FBgn0024227,FBgn0031549,FBgn0034569,FBgn0039638,FBgn0263855 | 9 | GO:0051783 |
| wing disc dorsal/ventral pattern formation | 0.03673362 | FBgn0004837,FBgn0010651,FBgn0011591,FBgn0011817,FBgn0014037,FBgn0259685,FBgn0263316 | 7 | GO:0048190 |
| rRNA processing | 0.03678627 | FBgn0002899,FBgn0004403,FBgn0026702,FBgn0030085,FBgn0031643,FBgn0033507,FBgn0034065,FBgn0034564,FBgn0035986,FBgn0036754,FBgn0037822,FBgn0038474,FBgn0039306,FBgn0039404 | 14 | GO:0006364 |
| mRNA transport | 0.03840119 | FBgn0000562,FBgn0033926,FBgn0034310,FBgn0035900,FBgn0037569,FBgn0087040 | 6 | GO:0051028 |
| transition metal ion homeostasis | 0.03840119 | FBgn0024236,FBgn0024958,FBgn0030343,FBgn0033274,FBgn0062413,FBgn0262467 | 6 | GO:0055076 |
| response to oxygen levels | 0.03905725 | FBgn0004240,FBgn0010651,FBgn0020653,FBgn0033188,FBgn0038437,FBgn0038530,FBgn0051354,FBgn0263316,FBgn0266411 | 9 | GO:0070482 |

| | | | | |
|---|---|---|---|---|
| cell cycle | 0.0394661 | FBgn0000140,FBgn0002542,FBgn0002878,FBgn0002899,FBgn0003042,FBgn0003525,FBgn0004170,FBgn0004378,FBgn0004583,FBgn0004643,FBgn0004837,FBgn0004889,FBgn0004907,FBgn0010314,FBgn0010382,FBgn0011020,FBgn0011739,FBgn0014861,FBgn0015271,FBgn0015391,FBgn0017577,FBgn0024227,FBgn0026876,FBgn0028292,FBgn0029977,FBgn0030054,FBgn0031549,FBgn0032047,FBgn0032290,FBgn0032400,FBgn0033890,FBgn0033921,FBgn0034495,FBgn0034569,FBgn0035249,FBgn0035644,FBgn0035918,FBgn0037716,FBgn0038390,FBgn0038565,FBgn0039403,FBgn0039638,FBgn0052371,FBgn0087021,FBgn0087040,FBgn0259113,FBgn0259685,FBgn0260985,FBgn0262619,FBgn0263237,FBgn0263855,FBgn0265523,FBgn0266418,FBgn0266465,FBgn0266917 | 55 | GO:0007049 |
| cellular chemical homeostasis | 0.03951186 | FBgn0001187,FBgn0011300,FBgn0023510,FBgn0024236,FBgn0024958,FBgn0030343,FBgn0030350,FBgn0034136,FBgn0034199,FBgn0045073,FBgn0062413,FBgn0261872,FBgn0262467 | 13 | GO:0055082 |
| DNA endoreduplication | 0.0398265 | FBgn0017577,FBgn0030054,FBgn0033890,FBgn0035644 | 4 | GO:0042023 |
| cellular nitrogen compound metabolic process | 0.0421574 | FBgn0000377,FBgn0000477,FBgn0000543,FBgn0000562,FBgn0000591,FBgn0000810,FBgn0001187,FBgn0002522,FBgn0002542,FBgn0002878,FBgn0002899,FBgn0003042,FBgn0003044,FBgn0003512,FBgn0003996,FBgn0004170,FBgn0004396,FBgn0004403,FBgn0004406,FBgn0004837,FBgn0004907,FBgn0005674,FBgn0005696,FBgn0005771,FBgn0010382,FBgn0010786,FBgn0011291,FBgn0011660,FBgn0011762,FBgn0011787,FBgn0013972,FBgn0014023,FBgn0014037,FBgn0014861,FBgn0014949,FBgn0015271,FBgn0015299,FBgn0015396,FBgn0015778,FBgn0016070,FBgn0016120,FBgn0016691,FBgn0016917,FBgn0017577,FBgn0019644,FBgn0019650,FBgn0022986,FBgn0023214,FBgn0024987,FBgn0025185,FBgn0025463,FBgn0025629,FBgn0025680,FBgn0025741,FBgn0025832,FBgn0026679,FBgn0026702,FBgn0026741,FBgn0026876,FBgn0026879,FBgn0027499,FBgn0027620,FBgn0028342,FBgn0029006,FBgn0029079,FBgn0029689,FBgn0029718,FBgn0029977,FBgn0030054,FBgn0030085,FBgn0030093,FBgn0030365,FBgn0030432,FBgn0030507,FBgn0030631,FBgn0030683,FBgn0030699,FBgn0031227,FBgn0031231,FBgn0031260,FBgn0031309,FBgn0031321,FBgn0031643,FBgn0031663,FBgn0031851,FBgn0032053,FBgn0032130,FBgn0032290,FBgn0032400,FBgn0032486,FBgn0032813,FBgn0032956,FBgn0033010,FBgn0033184,FBgn0033507,FBgn0033555,FBgn0033859,FBgn0033890,FBgn0033921,FBgn0033998,FBgn0034065,FBgn0034310,FBgn0034335,FBgn0034564,FBgn0034579,FBgn0034614,FBgn0034650,FBgn0034938,FBgn0035064,FBgn0035153,FBgn0035246,FBgn0035318,FBgn0035374,FBgn0035397,FBgn0035644,FBgn0035900,FBgn0035918,FBgn0035986,FBgn0036018,FBgn0036157,FBgn0036258,FBgn0036335,FBgn0036373,FBgn0036374,FBgn0036569,FBgn0036734,FBgn0036735,FBgn0036754,FBgn0036771,FBgn0036826,FBgn0036827,FBgn0037109,FBgn0037330,FBgn003 | 209 | GO:0034641 |

| | | | | |
|---|---|---|---|---|
| | | 7607,FBgn0037669,FBgn0037687,FBgn0037716,FBgn0037722,FBgn0037822,FBgn0037918,FBgn0037926,FBgn0038173,FBgn0038224,FBgn0038237,FBgn0038390,FBgn0038426,FBgn0038474,FBgn0038546,FBgn0038592,FBgn0038928,FBgn0039159,FBgn0039182,FBgn0039252,FBgn0039306,FBgn0039403,FBgn0039404,FBgn0039462,FBgn0039464,FBgn0039650,FBgn0039740,FBgn0039938,FBgn0039972,FBgn0041103,FBgn0042112,FBgn0043575,FBgn0043796,FBgn0043900,FBgn0050022,FBgn0051126,FBgn0051450,FBgn0051550,FBgn0051739,FBgn0053100,FBgn0053178,FBgn0053504,FBgn0061469,FBgn0063491,FBgn0063492,FBgn0063493,FBgn0067102,FBgn0083983,FBgn0085484,FBgn0086358,FBgn0086450,FBgn0250850,FBgn0259113,FBgn0259176,FBgn0259938,FBgn0260750,FBgn0260817,FBgn0260985,FBgn0261287,FBgn0261872,FBgn0262449,FBgn0262467,FBgn0262619,FBgn0263144,FBgn0263237,FBgn0263855,FBgn0263863,FBgn0265048,FBgn0265523,FBgn0265623,FBgn0266411,FBgn0266917,FBgn0267792,FBgn0267821,FBgn0286027,FBgn0286506 | | |
| neurotransmitter uptake | 0.04226429 | FBgn0003996,FBgn0034136 | 2 | GO:0001504 |
| regulation of nucleotide metabolic process | 0.04226429 | FBgn0025741,FBgn0262467 | 2 | GO:0006140 |
| icosanoid metabolic process | 0.04226429 | FBgn0025814,FBgn0053178 | 2 | GO:0006690 |
| polarity specification of dorsal/ventral axis | 0.04226429 | FBgn0002899,FBgn0263260 | 2 | GO:0009951 |
| protein geranylgeranylation | 0.04226429 | FBgn0028970,FBgn0037293 | 2 | GO:0018344 |
| translesion synthesis | 0.04226429 | FBgn0032813,FBgn0035644 | 2 | GO:0019985 |
| regulation of purine nucleotide metabolic process | 0.04226429 | FBgn0025741,FBgn0262467 | 2 | GO:1900542 |
| organic substance biosynthetic process | 0.0423717 | FBgn0000543,FBgn0000562,FBgn0000591,FBgn0000810,FBgn0002522,FBgn0002524,FBgn0002542,FBgn0002566,FBgn0002878,FBgn0002899,FBgn0003042,FBgn0003044,FBgn0003076,FBgn0003116,FBgn0003512,FBgn0003515,FBgn0003996,FBgn0004170,FBgn0004396,FBgn0004403,FBgn0004406,FBgn0004797,FBgn0004837,FBgn0004907,FBgn0005674,FBgn0005696,FBgn0005771,FBgn0010382,FBgn0010438,FBgn0010786,FBgn0011291,FBgn0011336,FBgn0011591,FBgn0011762,FBgn0011787,FBgn0013972,FBgn0014023,FBgn0014037,FBgn0014427,FBgn0014861,FBgn0014949,FBgn0015271, | 182 | GO:1901576 |

| | | | | |
|---|---|---|---|---|
| | | FBgn0015299,FBgn0015396,FBgn0016070,FBgn0016120,FBgn0016691,FBgn0016917,FBgn0017577,FBgn0019644,FBgn0019650,FBgn0023214,FBgn0023545,FBgn0024194,FBgn0025185,FBgn0025463,FBgn0025680,FBgn0025741,FBgn0025814,FBgn0026741,FBgn0026879,FBgn0027499,FBgn0027560,FBgn0027620,FBgn0028342,FBgn0029006,FBgn0029718,FBgn0030054,FBgn0030093,FBgn0030432,FBgn0030683,FBgn0030699,FBgn0031231,FBgn0031309,FBgn0031663,FBgn0031851,FBgn0032053,FBgn0032130,FBgn0032290,FBgn0032400,FBgn0032486,FBgn0032813,FBgn0032956,FBgn0033010,FBgn0033184,FBgn0033507,FBgn0033555,FBgn0033815,FBgn0033890,FBgn0033998,FBgn0034141,FBgn0034310,FBgn0034495,FBgn0034579,FBgn0034650,FBgn0034938,FBgn0035064,FBgn0035153,FBgn0035246,FBgn0035266,FBgn0035374,FBgn0035471,FBgn0035644,FBgn0035918,FBgn0036157,FBgn0036258,FBgn0036335,FBgn0036373,FBgn0036374,FBgn0036569,FBgn0036691,FBgn0036713,FBgn0036771,FBgn0036826,FBgn0036827,FBgn0037109,FBgn0037146,FBgn0037305,FBgn0037330,FBgn0037607,FBgn0037669,FBgn0037722,FBgn0037918,FBgn0038038,FBgn0038173,FBgn0038224,FBgn0038390,FBgn0038426,FBgn0038474,FBgn0038546,FBgn0038592,FBgn0038870,FBgn0038928,FBgn0039159,FBgn0039258,FBgn0039273,FBgn0039304,FBgn0039403,FBgn0039462,FBgn0039464,FBgn0039596,FBgn0039650,FBgn0039740,FBgn0039938,FBgn0041103,FBgn0042112,FBgn0043575,FBgn0043796,FBgn0043900,FBgn0044872,FBgn0050493,FBgn0051126,FBgn0051450,FBgn0051739,FBgn0053100,FBgn0053178,FBgn0061469,FBgn0067102,FBgn0083983,FBgn0085484,FBgn0086358,FBgn0086450,FBgn0086679,FBgn0259113,FBgn0259176,FBgn0259938,FBgn0260985,FBgn0261445,FBgn0262449,FBgn0262467,FBgn0262619,FBgn0263144,FBgn0263237,FBgn0263855,FBgn0263863,FBgn0265048,FBgn0265523,FBgn0265623,FBgn0266411,FBgn0267792,FBgn0267821,FBgn0286506 | | |
| mechanosensory behavior | 0.04260806 | FBgn0020258,FBgn0023096,FBgn0267430 | 3 | GO:0007638 |
| response to amino acid | 0.04260806 | FBgn0030108,FBgn0034199,FBgn0035870 | 3 | GO:0043200 |
| response to hyperoxia | 0.04260806 | FBgn0004240,FBgn0038437,FBgn0038530 | 3 | GO:0055093 |
| positive regulation of small molecule metabolic process | 0.04260806 | FBgn0025741,FBgn0053100,FBgn0262467 | 3 | GO:0062013 |
| regulation of nuclear-transcribed mRNA catabolic process, deadenylati | 0.04260806 | FBgn0016070,FBgn0035246,FBgn0039972 | 3 | GO:1900151 |

| | | | | |
|---|---|---|---|---|
| on-dependent decay | | | | |
| positive regulation of nuclear-transcribed mRNA catabolic process, deadenylation-dependent decay | 0.04260806 | FBgn0016070,FBgn0035246,FBgn0039972 | 3 | GO:1900153 |
| hindgut morphogenesis | 0.0434344 | FBgn0000377,FBgn0000543,FBgn0016917,FBgn0029006,FBgn0033859,FBgn0043903,FBgn0259685 | 7 | GO:0007442 |
| hindgut development | 0.0434344 | FBgn0000377,FBgn0000543,FBgn0016917,FBgn0029006,FBgn0033859,FBgn0043903,FBgn0259685 | 7 | GO:0061525 |
| negative regulation of organ growth | 0.04569919 | FBgn0004583,FBgn0011739,FBgn0015778,FBgn0259685 | 4 | GO:0046621 |
| RNA metabolic process | 0.04650811 | FBgn0000377,FBgn0000543,FBgn0000591,FBgn0002522,FBgn0002542,FBgn0002899,FBgn0003042,FBgn0003044,FBgn0003512,FBgn0004170,FBgn0004396,FBgn0004403,FBgn0004837,FBgn0004907,FBgn0005674,FBgn0005771,FBgn0011291,FBgn0011762,FBgn0011787,FBgn0014037,FBgn0014949,FBgn0015299,FBgn0015396,FBgn0015778,FBgn0016070,FBgn0016917,FBgn0019650,FBgn0022986,FBgn0023214,FBgn0024987,FBgn0025185,FBgn0025463,FBgn0025629,FBgn0025680,FBgn0026679,FBgn0026702,FBgn0027499,FBgn0027620,FBgn0029006,FBgn0029079,FBgn0030085,FBgn0030093,FBgn0030365,FBgn0030432,FBgn0030507,FBgn0030631,FBgn0030699,FBgn0031227,FBgn0031309,FBgn0031321,FBgn0031643,FBgn0031851,FBgn0032130,FBgn0032400,FBgn0032956,FBgn0033010,FBgn0033507,FBgn0033859,FBgn0033921,FBgn0033998,FBgn0034065,FBgn0034310,FBgn0034564,FBgn0034614,FBgn0034650,FBgn0035064,FBgn0035153,FBgn0035246,FBgn0035318,FBgn0035397,FBgn0035900,FBgn0035986,FBgn0036018,FBgn0036373,FBgn0036374,FBgn0036569,FBgn0036734,FBgn0036735,FBgn0036754,FBgn0036771,FBgn0036826,FBgn0036827,FBgn0037109,FBgn0037330,FBgn0037607,FBgn0037669,FBgn0037716,FBgn0037722,FBgn0037822,FBgn0037918,FBgn0037926,FBgn0038390,FBgn0038474,FBgn0038546,FBgn0038592,FBgn0039182,FBgn0039306,FBgn0039404,FBgn0039462,FBgn0039740,FBgn0039938,FBgn0039972,FBgn0041103,FBgn0043796,FBgn0043900,FBgn0051126,FBgn0051550,FBgn0051739,FBgn0053504,FBgn0061469,FBgn0250850,FBgn0259176,FBgn0259938,FBgn0261287,FBgn0261872,FBgn0263144,FBgn0263237,FBgn0263855,FBgn0265048,FBgn0265523,FBgn0265623,FBgn0266411,FBgn0266917,FBgn0267792,FBgn0267821,FBgn0286027 | 126 | GO:0016070 |

| | | | | |
|---|---|---|---|---|
| cellular biosynthetic process | 0.04693523 | FBgn0000543,FBgn0000562,FBgn0000591,FBgn0000810,FBgn0002522,FBgn0002524,FBgn0002542,FBgn0002566,FBgn0002878,FBgn0002899,FBgn0003042,FBgn0003044,FBgn0003076,FBgn0003116,FBgn0003512,FBgn0003515,FBgn0003996,FBgn0004170,FBgn0004396,FBgn0004403,FBgn0004406,FBgn0004797,FBgn0004837,FBgn0004907,FBgn0005674,FBgn0005696,FBgn0005771,FBgn0010382,FBgn0010438,FBgn0010786,FBgn0011291,FBgn0011336,FBgn0011591,FBgn0011762,FBgn0011787,FBgn0013972,FBgn0014023,FBgn0014037,FBgn0014427,FBgn0014861,FBgn0014949,FBgn0015271,FBgn0015299,FBgn0015396,FBgn0016070,FBgn0016120,FBgn0016691,FBgn0016917,FBgn0017577,FBgn0019644,FBgn0019650,FBgn0023214,FBgn0023545,FBgn0024194,FBgn0025185,FBgn0025463,FBgn0025680,FBgn0025741,FBgn0025814,FBgn0026741,FBgn0026879,FBgn0027499,FBgn0027560,FBgn0027620,FBgn0028342,FBgn0029006,FBgn0029718,FBgn0030054,FBgn0030093,FBgn0030432,FBgn0030683,FBgn0030699,FBgn0031231,FBgn0031309,FBgn0031663,FBgn0031851,FBgn0032053,FBgn0032130,FBgn0032290,FBgn0032400,FBgn0032486,FBgn0032813,FBgn0032956,FBgn0033010,FBgn0033184,FBgn0033507,FBgn0033555,FBgn0033815,FBgn0033890,FBgn0033998,FBgn0034141,FBgn0034310,FBgn0034495,FBgn0034579,FBgn0034650,FBgn0034938,FBgn0035064,FBgn0035153,FBgn0035246,FBgn0035374,FBgn0035471,FBgn0035644,FBgn0035918,FBgn0036157,FBgn0036258,FBgn0036335,FBgn0036373,FBgn0036374,FBgn0036569,FBgn0036691,FBgn0036713,FBgn0036771,FBgn0036826,FBgn0036827,FBgn0037109,FBgn0037146,FBgn0037305,FBgn0037330,FBgn0037607,FBgn0037669,FBgn0037722,FBgn0037918,FBgn0038038,FBgn0038173,FBgn0038224,FBgn0038390,FBgn0038426,FBgn0038474,FBgn0038546,FBgn0038592,FBgn0038870,FBgn0038928,FBgn0039159,FBgn0039258,FBgn0039273,FBgn0039304,FBgn0039403,FBgn0039462,FBgn0039464,FBgn0039650,FBgn0039740,FBgn0039938,FBgn0041103,FBgn0042112,FBgn0043575,FBgn0043796,FBgn0043900,FBgn0044872,FBgn0050493,FBgn0051126,FBgn0051450,FBgn0051739,FBgn0053100,FBgn0053178,FBgn0061469,FBgn0067102,FBgn0083983,FBgn0085484,FBgn0086358,FBgn0086450,FBgn0086679,FBgn0259113,FBgn0259176,FBgn0259938,FBgn0260985,FBgn0261445,FBgn0262449,FBgn0262467,FBgn0262619,FBgn0263144,FBgn0263237,FBgn0263855,FBgn0263863,FBgn0265048,FBgn0265523,FBgn0265623,FBgn0266411,FBgn0267792,FBgn0267821,FBgn0286506 | 180 | GO:0044249 |
| G1/S transition of mitotic cell cycle | 0.04777039 | FBgn0004837,FBgn0010382,FBgn0011739,FBgn0038390,FBgn0039403 | 5 | GO:0000082 |
| regulation of cell cycle | 0.04881975 | FBgn0002878,FBgn0003525,FBgn0004170,FBgn0004583,FBgn0004643,FBgn0004837,FBgn0004889,FBgn0010314,FBgn0010382,FBgn0024227,FBgn0031549,FBgn0032047,FBgn0032400,FBgn0034569,FBgn0035249,FBgn0035644,FBgn0035918,FBgn0037716,FBgn0038390,F | 26 | GO:0051726 |

| | | | | |
|---|---|---|---|---|
| | | Bgn0039403,FBgn0039638,FBgn0260985,FBgn0263237,FBgn0263855,FBgn0265523,FBgn0266465 | | |
| rRNA metabolic process | 0.04913521 | FBgn0002899,FBgn0004403,FBgn0026702,FBgn0030085,FBgn0031643,FBgn0033507,FBgn0034065,FBgn0034564,FBgn0035986,FBgn0036754,FBgn0037822,FBgn0038474,FBgn0039306,FBgn0039404 | 14 | GO:0016072 |

**Table 2.4i:Pathway enrichment for hits differentially upregulated in control females relative to 20HE males**

| Pathway enrichment | p-value | Hits | Gene matches | Pathway ID |
|---|---|---|---|---|
| DNA replication | 8.09E-07 | FBgn0005696,FBgn0010438,FBgn0011762,FBgn0014861,FBgn0017577,FBgn0025832,FBgn0030507,FBgn0032813,FBgn0035644,FBgn0259113,FBgn0260985,FBgn0262619 | 12 | 3030 |
| Mitochondrial translation termination | 2.0637E-05 | FBgn0011787,FBgn0014023,FBgn0026741,FBgn0029718,FBgn0031231,FBgn0032053,FBgn0032486,FBgn0034579,FBgn0035374,FBgn0037330,FBgn0038426,FBgn0038474,FBgn0039159,FBgn0042112,FBgn0051450,FBgn0083983,FBgn0263863 | 17 | R-DME-5419276 |
| Mitochondrial translation | 2.4345E-05 | FBgn0011787,FBgn0014023,FBgn0026741,FBgn0029718,FBgn0031231,FBgn0032053,FBgn0032486,FBgn0034579,FBgn0035374,FBgn0037330,FBgn0038426,FBgn0038474,FBgn0039159,FBgn0042112,FBgn0051450,FBgn0083983,FBgn0263863 | 17 | R-DME-5368287 |
| G1/S Transition | 4.1676E-05 | FBgn0003525,FBgn0004066,FBgn0005696,FBgn0010314,FBgn0010382,FBgn0011762,FBgn0014861,FBgn0015271,FBgn0017577,FBgn0023175,FBgn0028694,FBgn0028695,FBgn0032047,FBgn0035644,FBgn0035918,FBgn0038390,FBgn0259113,FBgn0263237 | 18 | R-DME-69206 |
| Mitotic G1 phase and G1/S transition | 5.6144E-05 | FBgn0003525,FBgn0004066,FBgn0004889,FBgn0005696,FBgn0010314,FBgn0010382,FBgn0011762,FBgn0014861,FBgn0015271,FBgn0017577,FBgn0023175,FBgn0028694,FBgn0028695,FBgn0032047,FBgn0035644,FBgn0035918,FBgn0038390,FBgn0259113,FBgn0263237 | 19 | R-DME-453279 |
| Mitochondrial translation elongation | 5.7761E-05 | FBgn0011787,FBgn0014023,FBgn0026741,FBgn0029718,FBgn0031231,FBgn0032053,FBgn0034579,FBgn0035374,FBgn0037330,FBgn0038426,FBgn0038474,FBgn0039159,FBgn0042112,FBgn0051450,FBgn0083983,FBgn0263863 | 16 | R-DME-5389840 |
| DNA strand elongation | 0.00036464 | FBgn0005696,FBgn0011762,FBgn0025832,FBgn0039403,FBgn0259113,FBgn0260985,FBgn0262619 | 7 | R-DME-69190 |
| Synthesis of DNA | 0.00054656 | FBgn0004066,FBgn0005696,FBgn0010382,FBgn0011762,FBgn0014861,FBgn0017577,FBgn0023175,FBgn0025832,FBgn0028694,FBgn0028695,FBgn0032047,FBgn0035644,FBgn0035918,FBgn0039403,FBgn0259113,FBgn0260985,FBgn0262619 | 17 | R-DME-69239 |
| S Phase | 0.0006263 | FBgn0004066,FBgn0005696,FBgn0010314,FBgn0010382,FBgn0011762,FBgn0014861,FBgn0017577,FBgn0023175,FBgn0025832,FBgn0028694,FBgn0028695,FBgn0032047,FBgn0035644,FBgn0035918,FBgn0039403,FBgn0259113,FBgn0260985,FBgn0262619 | 18 | R-DME-69242 |
| Activation of the pre-replicative complex | 0.00067525 | FBgn0005696,FBgn0011762,FBgn0014861,FBgn0015271,FBgn0017577,FBgn0035644,FBgn0035918,FBgn0259113 | 8 | R-DME-68962 |

| | | | | |
|---|---|---|---|---|
| Lagging Strand Synthesis | 0.00073792 | FBgn0005696,FBgn0011762,FBgn0025832,FBgn0259113,FBgn0260985,FBgn0262619 | 6 | R-DME-69186 |
| DNA Replication | 0.00076884 | FBgn0004066,FBgn0005696,FBgn0010382,FBgn0011762,FBgn0014861,FBgn0015271,FBgn0017577,FBgn0023175,FBgn0025832,FBgn0028694,FBgn0028695,FBgn0032047,FBgn0035644,FBgn0035918,FBgn0039403,FBgn0259113,FBgn0260985,FBgn0262619 | 18 | R-DME-69306 |
| Processive synthesis on the lagging strand | 0.00099917 | FBgn0005696,FBgn0011762,FBgn0025832,FBgn0259113,FBgn0262619 | 5 | R-DME-69183 |
| Telomere C-strand synthesis initiation | 0.00104899 | FBgn0005696,FBgn0011762,FBgn0035644,FBgn0259113 | 4 | R-DME-174430 |
| DNA replication initiation | 0.00104899 | FBgn0005696,FBgn0011762,FBgn0035644,FBgn0259113 | 4 | R-DME-68952 |
| Inhibition of replication initiation of damaged DNA by RB1/E2F1 | 0.00179059 | FBgn0005696,FBgn0011762,FBgn0038390,FBgn0259113 | 4 | R-DME-113501 |
| E2F mediated regulation of DNA replication | 0.00179059 | FBgn0005696,FBgn0011762,FBgn0038390,FBgn0259113 | 4 | R-DME-113510 |
| Formation of ATP by chemiosmotic coupling | 0.00208883 | FBgn0016120,FBgn0016691,FBgn0019644,FBgn0028342,FBgn0038224 | 5 | R-DME-163210 |
| Cristae formation | 0.00208883 | FBgn0016120,FBgn0016691,FBgn0019644,FBgn0028342,FBgn0038224 | 5 | R-DME-8949613 |
| Vitamin B6 metabolism | 0.00256753 | FBgn0014427,FBgn0031048,FBgn0085484 | 3 | 750 |
| Polymerase switching on the C-strand of the telomere | 0.00283042 | FBgn0005696,FBgn0011762,FBgn0259113,FBgn0260985 | 4 | R-DME-174411 |
| Polymerase switching | 0.00283042 | FBgn0005696,FBgn0011762,FBgn0259113,FBgn0260985 | 4 | R-DME-69091 |
| Leading Strand Synthesis | 0.00283042 | FBgn0005696,FBgn0011762,FBgn0259113,FBgn0260985 | 4 | R-DME-69109 |
| Cell Cycle | 0.00349065 | FBgn0002878,FBgn0003525,FBgn0004066,FBgn0004889,FBgn0004907,FBgn0005696,FBgn0010314,FBgn0010382,FBgn0011762,FBgn0014009,FBgn0014861,FBgn0014879,FBgn0015271,FBgn0015391,FBgn0017577,FBgn0023175,FBgn0024227,FBgn0025463,FBgn0025832,FBgn0028694,FBgn0028695,FBgn0032047,FBgn0034310,FBgn0035644,FBgn0035918,FBgn0038390,FBgn0039125,FBgn0039403,FBgn0259113,FBgn0260985,FBgn0262619,FBgn0263237,FBgn0263855 | 33 | R-DME-1640170 |

| | | | | |
|---|---|---|---|---|
| NOTCH4 Activation and Transmission of Signal to the Nucleus | 0.00433111 | FBgn0004907,FBgn0259685 | 2 | R-DME-9013700 |
| Formation of the activated STAT92E dimer and transport to the nucleus | 0.00488501 | FBgn0016917,FBgn0030904,FBgn0043903 | 3 | R-DME-209228 |
| DNA Replication Pre-Initiation | 0.00511388 | FBgn0004066,FBgn0005696,FBgn0011762,FBgn0014861,FBgn0015271,FBgn0017577,FBgn0023175,FBgn0028694,FBgn0028695,FBgn0035644,FBgn0035918,FBgn0259113 | 12 | R-DME-69002 |
| Removal of the Flap Intermediate | 0.00600359 | FBgn0005696,FBgn0011762,FBgn0025832,FBgn0259113 | 4 | R-DME-69166 |
| Mismatch repair | 0.00650023 | FBgn0010438,FBgn0011660,FBgn0032813,FBgn0260985,FBgn0262619 | 5 | 3430 |
| Cyclin E associated events during G1/S transition | 0.00669738 | FBgn0003525,FBgn0004066,FBgn0010314,FBgn0010382,FBgn0023175,FBgn0028694,FBgn0028695,FBgn0032047,FBgn0038390,FBgn0263237 | 10 | R-DME-69202 |
| Cell Cycle, Mitotic | 0.00717698 | FBgn0003525,FBgn0004066,FBgn0004889,FBgn0005696,FBgn0010314,FBgn0010382,FBgn0011762,FBgn0014009,FBgn0014861,FBgn0014879,FBgn0015271,FBgn0015391,FBgn0017577,FBgn0023175,FBgn0024227,FBgn0025832,FBgn0028694,FBgn0028695,FBgn0032047,FBgn0034310,FBgn0035644,FBgn0035918,FBgn0038390,FBgn0039125,FBgn0039403,FBgn0259113,FBgn0260985,FBgn0262619,FBgn0263237,FBgn0263855 | 30 | R-DME-69278 |
| Dephosphorylation by PTP61F phosphatases | 0.0081339 | FBgn0016917,FBgn0030904,FBgn0043903 | 3 | R-DME-210688 |
| Telomere Maintenance | 0.00820811 | FBgn0005696,FBgn0011762,FBgn0035644,FBgn0259113,FBgn0260985 | 5 | R-DME-157579 |
| Mitochondrial biogenesis | 0.00820811 | FBgn0016120,FBgn0016691,FBgn0019644,FBgn0028342,FBgn0038224 | 5 | R-DME-1592230 |
| Telomere C-strand (Lagging Strand) Synthesis | 0.00820811 | FBgn0005696,FBgn0011762,FBgn0035644,FBgn0259113,FBgn0260985 | 5 | R-DME-174417 |
| Extension of Telomeres | 0.00820811 | FBgn0005696,FBgn0011762,FBgn0035644,FBgn0259113,FBgn0260985 | 5 | R-DME-180786 |
| Chromosome Maintenanc | 0.00820811 | FBgn0005696,FBgn0011762,FBgn0035644,FBgn0259113,FBgn0260985 | 5 | R-DME-73886 |

| | | | | |
|---|---|---|---|---|
| e | | | | |
| Starch and sucrose metabolism | 0.01135767 | FBgn0000078,FBgn0001187,FBgn0003076,FBgn0020506,FBgn0027560,FBgn0040250,FBgn0040261,FBgn0040262,FBgn0261445 | 9 | 500 |
| Insulin effects increased synthesis of Xylulose-5-Phosphate | 0.01242561 | FBgn0023477,FBgn0037607 | 2 | R-DME-163754 |
| TP53 regulates transcription of several additional cell death genes whose specific roles in p53-dependent apoptosis remain uncertain | 0.01242561 | FBgn0028970,FBgn0037293 | 2 | R-DME-6803205 |
| Phosphorylation of proteins involved in G1/S transition by active Cyclin E:Cdk2 complexes | 0.01242561 | FBgn0010382,FBgn0038390 | 2 | R-DME-69200 |
| Signaling by NOTCH4 | 0.01242561 | FBgn0004907,FBgn0259685 | 2 | R-DME-9013694 |
| G2/M Checkpoints | 0.01724178 | FBgn0002878,FBgn0003525,FBgn0004907,FBgn0014861,FBgn0015271,FBgn0017577,FBgn0035918,FBgn0260985 | 8 | R-DME-69481 |
| Reversible hydration of carbon dioxide | 0.01768199 | FBgn0027843,FBgn0027844,FBgn0039486 | 3 | R-DME-1475029 |
| JAK/STAT pathway | 0.01768199 | FBgn0016917,FBgn0030904,FBgn0043903 | 3 | R-DME-209405 |
| Triglyceride biosynthesis | 0.01768199 | FBgn0004797,FBgn0033215,FBgn0035266 | 3 | R-DME-75109 |
| PCNA-Dependent Long Patch Base Excision Repair | 0.01790198 | FBgn0025832,FBgn0035644,FBgn0260985,FBgn0262619 | 4 | R-DME-5651801 |
| Metabolism | 0.01892694 | FBgn0001187,FBgn0002524,FBgn0003076,FBgn0004066,FBgn0004797,FBgn0010241,FBgn0010786,FBgn0011227,FBgn0014427,FBgn0016120,FBgn0016691,FBgn0019644,FBgn0019982,FBgn0020626,FBgn0022359,FBgn002 | 92 | R-DME-1430728 |

| | | | | |
|---|---|---|---|---|
| | | 3175,FBgn0023477,FBgn0025463,FBgn0025814,FBgn0025839,FBgn0027843,FBgn0027844,FBgn0028342,FBgn0028694,FBgn0028695,FBgn0029689,FBgn0029708,FBgn0029994,FBgn0030367,FBgn0030584,FBgn0030638,FBgn0030683,FBgn0030816,FBgn0031048,FBgn0031248,FBgn0031663,FBgn0031695,FBgn0032790,FBgn0033205,FBgn0033215,FBgn0033238,FBgn0033382,FBgn0033397,FBgn0033754,FBgn0033756,FBgn0033815,FBgn0033961,FBgn0034919,FBgn0034938,FBgn0035266,FBgn0035471,FBgn0036157,FBgn0036290,FBgn0036691,FBgn0036824,FBgn0037109,FBgn0037146,FBgn0037186,FBgn0037305,FBgn0037370,FBgn0037607,FBgn0037845,FBgn0037891,FBgn0038224,FBgn0038260,FBgn0038271,FBgn0038752,FBgn0039258,FBgn0039304,FBgn0039464,FBgn0039471,FBgn0039486,FBgn0039637,FBgn0039674,FBgn0040250,FBgn0040257,FBgn0040383,FBgn0044872,FBgn0047038,FBgn0050022,FBgn0050344,FBgn0050345,FBgn0052669,FBgn0053178,FBgn0067102,FBgn0085484,FBgn0086450,FBgn0260750,FBgn0261445,FBgn0262559,FBgn0265523,FBgn0283450 | | |
| Respiratory electron transport, ATP synthesis by chemiosmotic coupling, and heat production by uncoupling proteins. | 0.01936936 | FBgn0011227,FBgn0016120,FBgn0016691,FBgn0019644,FBgn0025839,FBgn0028342,FBgn0033961,FBgn0034919,FBgn0038224,FBgn0038271,FBgn0047038 | 11 | R-DME-163200 |
| Phosphorylation-independent inhibition of YKI | 0.02377146 | FBgn0004583,FBgn0011739 | 2 | R-DME-451806 |
| Activation of ATR in response to replication stress | 0.02501701 | FBgn0003525,FBgn0014861,FBgn0015271,FBgn0017577,FBgn0035918,FBgn0260985 | 6 | R-DME-176187 |
| Cyclin D associated events in G1 | 0.0251819 | FBgn0004889,FBgn0010314,FBgn0032047,FBgn0038390,FBgn0263237 | 5 | R-DME-69231 |
| G1 Phase | 0.0251819 | FBgn0004889,FBgn0010314,FBgn0032047,FBgn0038390,FBgn0263237 | 5 | R-DME-69236 |
| Metabolic pathways | 0.02636559 | FBgn0000078,FBgn0000261,FBgn0001187,FBgn0002524,FBgn0003076,FBgn0004406,FBgn0004797,FBgn0005674,FBgn0005696,FBgn0010786,FBgn0011227,FBgn0011336,FBgn0011762,FBgn0011770,FBgn0014427,FBgn0015011,FBgn0015568,FBgn0015575,FBgn0016120,FBgn0016691,FBgn0019644,FBgn0020506,FBgn0022097,FBgn0022359,FBgn0023477,FBgn0023545,FBgn0024958,FBgn0025839,FBgn0028342,FBgn0030596,FBgn0030610,FBgn0030683,FBgn0031048,FBgn0031663,FBgn0033520,FBgn0033961,FBgn0034141,FBgn0034938,FBgn0035266,F | 70 | 1100 |

| | | | | |
|---|---|---|---|---|
| | | Bgn0035644,FBgn0036157,FBgn0036691,FBgn0036824,FBgn0037146,FBgn0037186,FBgn0037607,FBgn0037891,FBgn0038080,FBgn0038224,FBgn0039258,FBgn0039293,FBgn0039304,FBgn0039464,FBgn0039596,FBgn0040250,FBgn0040261,FBgn0040262,FBgn0041629,FBgn0047038,FBgn0052201,FBgn0067102,FBgn0085484,FBgn0086450,FBgn0259113,FBgn0259170,FBgn0260750,FBgn0261445,FBgn0262512,FBgn0262559,FBgn0286506 | | |
| Resolution of AP sites via the multiple-nucleotide patch replacement pathway | 0.02712762 | FBgn0025832,FBgn0035644,FBgn0260985,FBgn0262619 | 4 | R-DME-110373 |
| Cell Cycle Checkpoints | 0.02875638 | FBgn0002878,FBgn0003525,FBgn0004066,FBgn0004907,FBgn0014861,FBgn0015271,FBgn0017577,FBgn0023175,FBgn0025463,FBgn0028694,FBgn0028695,FBgn0035918,FBgn0260985,FBgn0263855 | 14 | R-DME-69620 |
| Drug metabolism - other enzymes | 0.02894952 | FBgn0015568,FBgn0015575,FBgn0031663,FBgn0039464,FBgn0040250,FBgn0040261,FBgn0040262,FBgn0086450 | 8 | 983 |
| Nucleotide excision repair | 0.03210262 | FBgn0031309,FBgn0032813,FBgn0035644,FBgn0260985,FBgn0262619,FBgn0263237 | 6 | 3420 |
| Oxidative phosphorylation | 0.03449947 | FBgn0011227,FBgn0016120,FBgn0016691,FBgn0019644,FBgn0022097,FBgn0025839,FBgn0028342,FBgn0030610,FBgn0033961,FBgn0034938,FBgn0038224,FBgn0040529,FBgn0047038,FBgn0262512 | 14 | 190 |
| Formation of the activated receptor complex | 0.03790741 | FBgn0030904,FBgn0043903 | 2 | R-DME-209209 |
| Synthesis of Dolichyl-phosphate | 0.03790741 | FBgn0030683,FBgn0034141 | 2 | R-DME-446199 |
| Base excision repair | 0.03873329 | FBgn0025832,FBgn0032813,FBgn0035644,FBgn0262619 | 4 | 3410 |
| Metabolism of folate and pterines | 0.03873329 | FBgn0036157,FBgn0037845,FBgn0050344,FBgn0050345 | 4 | R-DME-196757 |
| Circadian Clock pathway | 0.04895275 | FBgn0004066,FBgn0004889,FBgn0023175,FBgn0025680,FBgn0028694,FBgn0028695,FBgn0050476,FBgn0259938,FBgn0264959 | 9 | R-DME-432626 |
| Synthesis of PC | 0.04949968 | FBgn0031048,FBgn0033382,FBgn0039637 | 3 | R-DME-1483191 |
| Regulation of lipid metabolism by PPARalpha | 0.04949968 | FBgn0025463,FBgn0037109,FBgn0265523 | 3 | R-DME-400206 |
| Triglyceride metabolism | 0.04949968 | FBgn0004797,FBgn0033215,FBgn0035266 | 3 | R-DME-8979227 |